

World Journal of *Gastroenterology*

World J Gastroenterol 2023 May 28; 29(20): 3048-3221



REVIEW

- 3048 *Hericium erinaceus*, a medicinal fungus with a centuries-old history: Evidence in gastrointestinal diseases
Gravina AG, Pellegrino R, Auletta S, Palladino G, Brandimarte G, D'Onofrio R, Arboretto G, Imperio G, Ventura A, Cipullo M, Romano M, Federico A

MINIREVIEWS

- 3066 Machine perfusion and the prevention of ischemic type biliary lesions following liver transplant: What is the evidence?
Durán M, Calleja R, Hann A, Clarke G, Ciria R, Nutu A, Sanabria-Mateos R, Ayllón MD, López-Cillero P, Mergental H, Briceño J, Perera MTPR

ORIGINAL ARTICLE**Basic Study**

- 3084 Metronomic capecitabine inhibits liver transplant rejection in rats by triggering recipients' T cell ferroptosis
Wang H, Wang ZL, Zhang S, Kong DJ, Yang RN, Cao L, Wang JX, Yoshida S, Song ZL, Liu T, Fan SL, Ren JS, Li JH, Shen ZY, Zheng H
- 3103 Dihydroergotamine ameliorates liver fibrosis by targeting transforming growth factor β type II receptor
Zheng KX, Yuan SL, Dong M, Zhang HL, Jiang XX, Yan CL, Ye RC, Zhou HQ, Chen L, Jiang R, Cheng ZY, Zhang Z, Wang Q, Jin WZ, Xie W

Retrospective Study

- 3119 Malignancy risk factors and prognostic variables of pancreatic mucinous cystic neoplasms in Chinese patients
Xia Q, Li F, Min R, Sun S, Han YX, Feng ZZ, Li N

Clinical Trials Study

- 3133 Safety and effectiveness of vonoprazan-based rescue therapy for *Helicobacter pylori* infection
Yu J, Lv YM, Yang P, Jiang YZ, Qin XR, Wang XY

Observational Study

- 3145 Determination of esophageal squamous cell carcinoma and gastric adenocarcinoma on raw tissue using Raman spectroscopy
Ito H, Uragami N, Miyazaki T, Shimamura Y, Ikeda H, Nishikawa Y, Onimaru M, Matsuo K, Isozaki M, Yang W, Issha K, Kimura S, Kawamura M, Yokoyama N, Kushima M, Inoue H
- 3157 Real-time continuous image guidance for endoscopic retrograde cholangiopancreatography based on 3D/2D registration and respiratory compensation
Zhang DY, Yang S, Geng HX, Yuan YJ, Ding CJ, Yang J, Li MY

- 3168** Inflammation-related nomogram for predicting survival of patients with unresectable hepatocellular carcinoma received conversion therapy

Wu JL, Luo JY, Jiang ZB, Huang SB, Chen GR, Ran HY, Liang QY, Huang MS, Lai LS, Chen JW

META-ANALYSIS

- 3185** Fecal microbiota transplantation for the treatment of irritable bowel syndrome: A systematic review and meta-analysis

Halkjær SI, Lo B, Cold F, Højer Christensen A, Holster S, König J, Brummer RJ, Aroniadis OC, Lahtinen P, Holvoet T, Gluud LL, Petersen AM

SCIENTOMETRICS

- 3203** Global research trends on diet and nutrition in Crohn's disease

Shakhshir M, Zyoud SH

CASE REPORT

- 3216** Inflammatory myofibroblastic tumor of the pancreatic neck misdiagnosed as neuroendocrine tumor: A case report

Liu JB, Gu QB, Liu P

ABOUT COVER

Editorial Board Member of *World Journal of Gastroenterology*, Toshimi Chiba, AGAF, MD, PhD, Professor, Department of Internal Medicine, Iwate Medical University, Morioka 020-8505, Japan. toschiba@iwate-med.ac.jp

AIMS AND SCOPE

The primary aim of *World Journal of Gastroenterology* (WJG, *World J Gastroenterol*) is to provide scholars and readers from various fields of gastroenterology and hepatology with a platform to publish high-quality basic and clinical research articles and communicate their research findings online. WJG mainly publishes articles reporting research results and findings obtained in the field of gastroenterology and hepatology and covering a wide range of topics including gastroenterology, hepatology, gastrointestinal endoscopy, gastrointestinal surgery, gastrointestinal oncology, and pediatric gastroenterology.

INDEXING/ABSTRACTING

The WJG is now abstracted and indexed in Science Citation Index Expanded (SCIE, also known as SciSearch®), Current Contents/Clinical Medicine, Journal Citation Reports, Index Medicus, MEDLINE, PubMed, PubMed Central, Scopus, Reference Citation Analysis, China National Knowledge Infrastructure, China Science and Technology Journal Database, and Superstar Journals Database. The 2022 edition of Journal Citation Reports® cites the 2021 impact factor (IF) for WJG as 5.374; IF without journal self cites: 5.187; 5-year IF: 5.715; Journal Citation Indicator: 0.84; Ranking: 31 among 93 journals in gastroenterology and hepatology; and Quartile category: Q2. The WJG's CiteScore for 2021 is 8.1 and Scopus CiteScore rank 2021: Gastroenterology is 18/149.

RESPONSIBLE EDITORS FOR THIS ISSUE

Production Editor: *Yu-Xi Chen*; Production Department Director: *Xu Guo*; Editorial Office Director: *Jia-Ru Fan*.

NAME OF JOURNAL

World Journal of Gastroenterology

ISSN

ISSN 1007-9327 (print) ISSN 2219-2840 (online)

LAUNCH DATE

October 1, 1995

FREQUENCY

Weekly

EDITORS-IN-CHIEF

Andrzej S Tarnawski

EDITORIAL BOARD MEMBERS

<http://www.wjgnet.com/1007-9327/editorialboard.htm>

PUBLICATION DATE

May 28, 2023

COPYRIGHT

© 2023 Baishideng Publishing Group Inc

INSTRUCTIONS TO AUTHORS

<https://www.wjgnet.com/bpg/gerinfo/204>

GUIDELINES FOR ETHICS DOCUMENTS

<https://www.wjgnet.com/bpg/GerInfo/287>

GUIDELINES FOR NON-NATIVE SPEAKERS OF ENGLISH

<https://www.wjgnet.com/bpg/gerinfo/240>

PUBLICATION ETHICS

<https://www.wjgnet.com/bpg/GerInfo/288>

PUBLICATION MISCONDUCT

<https://www.wjgnet.com/bpg/gerinfo/208>

ARTICLE PROCESSING CHARGE

<https://www.wjgnet.com/bpg/gerinfo/242>

STEPS FOR SUBMITTING MANUSCRIPTS

<https://www.wjgnet.com/bpg/GerInfo/239>

ONLINE SUBMISSION

<https://www.f6publishing.com>

***Hericium erinaceus*, a medicinal fungus with a centuries-old history: Evidence in gastrointestinal diseases**

Antonietta Gerarda Gravina, Raffaele Pellegrino, Salvatore Auletta, Giovanna Palladino, Giovanni Brandimarte, Rossella D'Onofrio, Giusi Arboretto, Giuseppe Imperio, Andrea Ventura, Marina Cipullo, Marco Romano, Alessandro Federico

Specialty type: Gastroenterology and hepatology

Provenance and peer review: Invited article; Externally peer reviewed.

Peer-review model: Single blind

Peer-review report's scientific quality classification

Grade A (Excellent): 0
Grade B (Very good): B
Grade C (Good): C
Grade D (Fair): 0
Grade E (Poor): 0

P-Reviewer: Liu J, China; Sun SY, China

Received: March 3, 2023

Peer-review started: March 3, 2023

First decision: March 21, 2023

Revised: March 22, 2023

Accepted: April 21, 2023

Article in press: April 21, 2023

Published online: May 28, 2023



Antonietta Gerarda Gravina, Raffaele Pellegrino, Salvatore Auletta, Giovanna Palladino, Rossella D'Onofrio, Giusi Arboretto, Giuseppe Imperio, Andrea Ventura, Marina Cipullo, Marco Romano, Alessandro Federico, Department of Precision Medicine, University of Campania "Luigi Vanvitelli", Naples 80138, Italy

Giovanni Brandimarte, Division of Internal Medicine and Gastroenterology, Cristo Re Hospital, Rome 00167, Italy

Corresponding author: Antonietta Gerarda Gravina, MD, MSc, PhD, Assistant Professor, Department of Precision Medicine, University of Campania "Luigi Vanvitelli", Via L. de Crechio, Naples 80138, Italy. antoniettagerarda.gravina@unicampania.it

Abstract

Hericium erinaceus is an edible and medicinal mushroom commonly used in traditional Chinese medicine for centuries. Several studies have highlighted its therapeutic potential for gastrointestinal disorders such as gastritis and inflammatory bowel diseases. In addition, some components of this mushroom appear to possess strong antineoplastic capabilities against gastric and colorectal cancer. This review aims to analyse all available evidence on the digestive therapeutic potential of this fungus as well as the possible underlying molecular mechanisms.

Key Words: *Hericium erinaceus*; Fungus; Gastritis; Inflammatory bowel diseases; Gastric cancer; Colorectal cancer

©The Author(s) 2023. Published by Baishideng Publishing Group Inc. All rights reserved.

Core Tip: Various natural and non-pharmacological principles have been used to treat gastrointestinal disorders. *Hericium erinaceus* is a Chinese mushroom with a centuries-old medicinal tradition. Several preclinical studies have demonstrated their anti-inflammatory and antineoplastic potential. The therapeutic activity of this mushroom also targets inflammatory bowel diseases, as demonstrated in several animal experiments. However, evidence from *in vivo* studies is not generally available for patients with gastrointestinal disorders. It is also unclear which component of this mushroom has the greatest potency and the best safety profile.

Citation: Gravina AG, Pellegrino R, Auletta S, Palladino G, Brandimarte G, D’Onofrio R, Arboretto G, Imperio G, Ventura A, Cipullo M, Romano M, Federico A. *Hericium erinaceus*, a medicinal fungus with a centuries-old history: Evidence in gastrointestinal diseases. *World J Gastroenterol* 2023; 29(20): 3048-3065

URL: <https://www.wjgnet.com/1007-9327/full/v29/i20/3048.htm>

DOI: <https://dx.doi.org/10.3748/wjg.v29.i20.3048>

INTRODUCTION

Gastrointestinal disorders are one of the most prevalent diseases in the general population. They are associated with a significant epidemiological and economic burden, with an estimated annual cost of over a hundred and thirty billion in the United States alone[1]. Many gastrointestinal disorders require a pharmacological approach; however, the possibility of adopting naturally derived complementary therapies whenever possible is emerging[2,3].

Among the abundant natural compounds studied, there is a Chinese mushroom, *Herichium erinaceus* (*H. erinaceus*) that has shown the potential to prevent and treat digestive diseases, such as gastric ulcers [4]. Furthermore, its therapeutic potential has been demonstrated in several conditions, including diabetes, hyperlipidaemia, neurodegenerative disorders, and cancer[5-8]. In addition, mild cognitive impairment is another disorder in which *H. erinaceus* has shown encouraging results in randomised clinical trials[9,10].

Therefore, *H. erinaceus* has traditionally and historically been used as a natural remedy for epigastric pain caused by chronic gastritis, gastric ulcers, or even atrophic gastritis[8].

Despite the strong need for clinical studies, several experiments, mainly preclinical and mouse model-based, have been conducted on the beneficial effects of many *H. erinaceus* extracts and components on gastrointestinal diseases. Therefore, this narrative review aimed to provide overall evidence of the therapeutic potential of *H. erinaceus* in gastrointestinal tract diseases.

H. ERINACEUS: GENERAL CONSIDERATIONS

H. erinaceus, also known as Yamabushitake (in the Japanese language), Houtou (in the Chinese language), or also as “lion’s mane” is a fungus that belongs to the class *Basidiomycetes*, subclass *Holobasidiomycetidae*, order *Hericiales*, and family *Hericiaceae*[4]. This fungus is mainly distributed in European, Asian, and American regions[11]. It is a saprophytic fungus or weak parasite that typically grows on hardwoods, such as beech, chestnut, and cherry[12].

Many active metabolites of *H. erinaceus* that are structurally different from each other and potentially bioactive have been discovered[13].

The main constituents of *H. erinaceus* are erinacines (cyathane-type diterpenoid aromatic compounds as erinacines A-I), steroids (such as ergosterol, erinarols A-F, and ergostane-type steroids), alkaloids (such as hericirine, 12 β -hydroxyverruculogenTR-2, fumitremorgin, methylthioglioto, pseurotin A, and FD-838), and lactones such as vitamin B₁₂-c-lactone (Figure 1)[13].

In addition, each 100 g of dried *H. erinaceus* contains approximately 61.3-77.5 g of total sugars, of which β -glucans, α -glucans, and glucan-protein complexes are the most abundant[14,15]. Among these, the β -glucans in the fungal cell wall have known and marked anti-inflammatory and anti-cancer potency and can positively modify the gut microbiota[16].

Much of the research devoted to the chemical characterisation of *H. erinaceus* has focused on its polysaccharide components, which are generally obtained from its fruiting body, and various extraction methods have been developed[17-19].

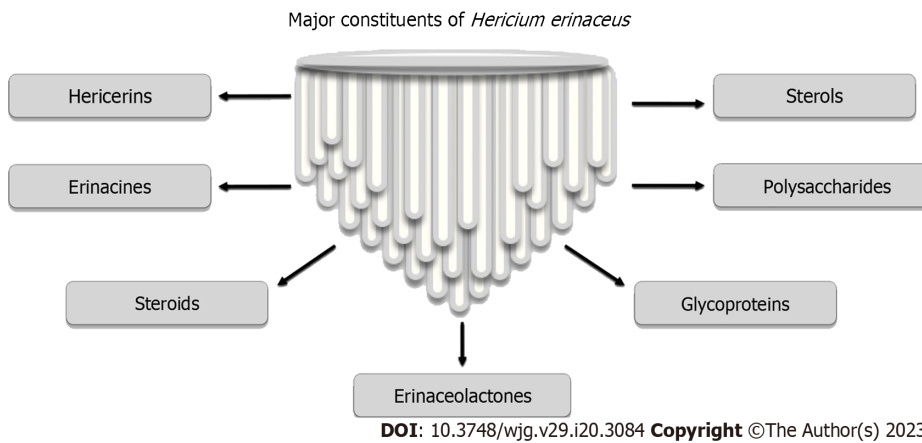


Figure 1 Several constituents can be obtained from *Hericium erinaceus* by different means of extraction (for example, by alcohol, chloroform, or petroleum). However, fractions such as erinacines and polysaccharides are those most commonly used in studies conducted in the gastrointestinal setting.

H. ERINACEUS IN UPPER GASTROINTESTINAL TRACT DISEASES: THE EVIDENCE

The role of H. erinaceus in non-infectious gastric diseases: Gastroprotective effects and therapeutic potential in repairing gastric mucosal damage

Gastric ulcers are a significant epidemiological burden[20]. Among the most common forms of gastric ulcers, those caused by non-steroidal anti-inflammatory drugs are also included. This is due to the pharmacological inhibition of cyclooxygenases 1 and 2, which are responsible for producing proinflammatory cytokines and prostaglandins, which help maintain the integrity of the gastric mucosal barrier [21]. An adequate balance between proinflammatory and anti-inflammatory cytokines is necessary for maintaining gastric mucosal integrity, such that polymorphisms in genes encoding proinflammatory cytokines can increase the risk of peptic ulcer and gastric cancer[22].

As anticipated, *H. erinaceus* has shown various anti-inflammatory, antioxidative, and gastroprotective properties. Boddy *et al*[23] showed, for example, that the action of several polysaccharides of *H. erinaceus* inhibits the secretion of proinflammatory cytokines interleukin 6 (IL-6), IL-8, and IL-12 and promotes the secretion of the anti-inflammatory cytokine IL-10 in a co-culture system of Cancer coli 2 (Caco-2) cells and Caco-2/RAW264.7 cells under bacterial lipopolysaccharide stimulation. This emphasises how this fungus can intervene in cytokine imbalance in an inflamed environment by shifting the balance toward an anti-inflammatory cytokine pattern.

To evaluate the gastroprotective, antioxidant, and anti-inflammatory activities *in vivo*, Wang *et al*[24] conducted experiments in a mouse model in which ethanol or ligation of the pylorus induced gastric ulcers. The study involved two polysaccharides, namely the crude polysaccharide of *H. erinaceus*, [*i.e.*, crude polysaccharide (HECP)] and the refined polysaccharide of *H. erinaceus* [*i.e.*, refined polysaccharide (HERP)], obtained from the fruiting body using water extraction and ethanol precipitation methods[25]. The mice were divided into several groups, including control groups and those receiving *H. erinaceus* polysaccharides at different dosages (100 mg/kg, 200 mg/kg, and 400 mg/kg). In the ethanol-induced gastric ulcer model, there was a reduction in the severity of the ulcers in a dose-dependent manner in the HERP/HECP-*treated* groups, with a significant reduction when pre-treatment with 400 mg/kg of HERP/HECP was performed. In contrast, in the pylorus-ligation-induced ulcer model, significant ulcer-inhibiting power was achieved when mice were administered HERP or HECP in a 200 mg/kg dosage. Nevertheless, the ulcers appeared to be more mitigated by HECP polysaccharide than HERP.

These results generally indicate a marked gastroprotective effect of HERP/HECP polysaccharides in ethanol-induced and pylorus-ligated gastric ulcers. However, the authors also showed results related to the control of gastric secretions. HERP/HECP administration provided a regulatory advantage over the imbalance in acid secretion induced by pylorus ligation.

Once the gastric mucosa has been damaged, the inflammatory process is activated, thereby increasing the mediators of inflammation, including tumor necrosis factor α (TNF- α), IL-1 β , and IL-6[26]. TNF- α stimulates neutrophil infiltration and apoptosis of epithelial cells, reduces gastric microcirculation around the ulcer region, and delays its healing[27]. Leucocyte infarction in the gastric mucosa is generally assessed using myeloperoxidase (MPO) activity[28]. IL-1 β significantly promotes ulcer formation[29]. Another defensive element that protects against gastric ulceration is the mucus-carbonate barrier. The mucus is a gel that adheres to the mucosa, preventing gastric acid penetration and injury. Mucus typically works in conjunction with nitric oxide (NO), prostaglandin E₂ (PGE₂), and epidermal growth factor (EGF) to maintain mucosal integrity[30]. NO protects the mucosal barrier and integrity of the gastric epithelium by inducing the inactivation of gastric parietal cells that secrete

hydrochloric acid, thereby reducing acidity[31]. PEG₂ increases mucus and bicarbonate production, leading to a decrease in gastric epithelial permeability[32]. EGF induces the proliferation of epithelial cells, thereby promoting tissue healing[30].

Wang *et al*[24] discovered that rats administered with HERP or HECF had lower serum TNF- α and IL-1 β levels and lower gastric tissue MPO activity than in the control group, indicating that these polysaccharides reduced the inflammatory response. In addition, the mucus content in the stomach was higher in the *H. erinaceus* polysaccharides-treated group than in the control group, suggesting that polysaccharides may protect the integrity of the gastric mucosa. The latter was also promoted by the increased release of NO, PGE₂ and EGF in the *H. erinaceus* polysaccharides-treated group. HERP/HECF also showed scavenging effects for 2,2-diphenyl-1-picrylhydrazyl, chelating capacity for Fe²⁺ and OH *in vitro*, antioxidant activity, and increased superoxide dismutase (SOD) and glutathione peroxidase (GPx) activities. It is known that SOD can rapidly convert peroxy radicals into biologically safe and inactive substances[33].

Furthermore, GPx protects the gastric mucosa from reactive oxygen species (ROS)-induced injury and reduces lipid peroxidation[34]. Phenolic compounds appear to be the main contributors to the antioxidant capacity of *H. erinaceus*[35]. The antioxidant and scavenger properties of *H. erinaceus* exerted through its polysaccharide component have also been confirmed by other studies, in which it was shown to prevent H₂O₂-induced apoptotic cell death in gastric epithelial cell lines (*i.e.*, GES-1 cells)[25].

In general, there are several studies on the use of *H. erinaceus* in ethanol-induced ulcers[36-38], with some focusing on acetic acid-induced ulcers[39]. Mao *et al*[36] also highlighted a possible therapeutic mechanism for ethanol-induced ulceration in mice *via* epidermal differentiation by studying the differences in the expression of several keratins, including 16, 6b, and transglutaminase E, in mucosa treated with *H. erinaceus* and untreated mucosa.

In addition to its multidimensional gastroprotective properties, *H. erinaceus* can regulate chaperonins, including HSP70. For example, in a model of ethanol-induced ulcers in Sprague Dawley mice, immunohistochemical studies have demonstrated an increased presence of HSP70 and downregulation of proapoptotic Bcl-2-associated X proteins[40]. Heat shock proteins (as, for example, HSP70) have a well-defined role in the pathogenesis of gastric ulcers. They are among the key players in the intracellular defence mechanisms of gastric cells. Some maintain protein integrity under homeostatic and non-stressful conditions, while others are activated after noxious stimuli[41].

However, the literature on this fungus has focused on both the erosive and atrophic patterns of gastric mucosal damage. Wang *et al*[42] examined the EP-1 fraction obtained from *H. erinaceus* mycelium in chronic atrophic gastritis. They found the potential to reduce the proliferation of MC cells (a model of atrophic gastritis) by arresting them in the G₀/G₁ phase of the cell cycle. However, there is a clinical, double-blinded, preliminary Chinese report for atrophic gastritis, although it was conducted in 1985 on 25 patients with atrophic gastritis who were administered *H. erinaceus* orally for three months. Clinical and histological improvements were observed in 63% and 52% of treated patients[43].

Although there is a considerable amount of preclinical experience, there is a substantial lack of clinical trials that have evaluated this mushroom as a pharmacological intervention in erosive gastritis, gastric ulcers, and atrophic gastritis.

***H. erinaceus* properties against *Helicobacter pylori* infection**

Helicobacter pylori (*H. pylori*) is a gram-negative spiral-shaped bacillus that contributes to several gastrointestinal disorders, including chronic gastritis, peptic ulcer, gastric adenocarcinoma, and gastric mucosa-associated lymphoid tissue lymphoma[44]. In addition, it is associated (to varying degrees) with several extra-gastric disorders, including vitamin B₁₂ deficiency anemia, primary immune thrombocytopenia, as well as ophthalmic conditions (such as glaucoma and central serous chorioretinopathy), dermatological disorders (such as rosacea and psoriasis), inflammatory bowel diseases (IBD), metabolic and neurological disorders[45]. The International Agency for Research on Cancer has designated *H. pylori* as a Group I carcinogen for gastric cancer[46]. Therefore, eradication is imperative when an infection is diagnosed[47]. However, we frequently encounter this bacterium's substantial antibiotic resistance; therefore, the guidelines suggest an algorithm based on several successive lines of treatment until eradication is achieved[48,49]. In addition to standard drug therapy, probiotics have been proposed to reduce adverse events associated with drug therapy[48]. *H. erinaceus* components (obtained by various extraction techniques) have shown marked antimicrobial properties against *H. pylori*[50-54]; however, the significant available evidence is preclinical. The minimum inhibitory concentrations (MIC) of the various components of *H. erinaceus* against *H. pylori* are shown in Table 1. MIC values fluctuate by varying the extractive, qualitative, and quantitative characteristics of the extracted components while reaching interesting values in some cases, as in the experience of Liu *et al*[52].

Therefore, it would be desirable to determine through clinical trials whether supplementation with *H. erinaceus* can have an additive effect on the anti-*H. pylori* efficacy of available antibiotic therapies, and whether such supplementation can reduce the adverse events associated with these antibiotic therapies.

***H. erinaceus* antineoplastic properties concerning gastric cancer**

Gastric cancer is now the fourth leading cause of cancer-related deaths, based on its incidence and prevalence[55]. Surgical and medical therapy take the lead in managing this neoplasm[56]; however,

Table 1 Preclinical studies evaluating the antimicrobial activity of several *Hericium erinaceus* fraction toward *Helicobacter pylori*

Ref.	<i>H. erinaceus</i> fraction employed	Extraction method	Anti- <i>H. pylori</i> MIC (µg/mL)
Shang et al[50], 2013	Ethyl acetate fractions		62.5-250.0 ¹
Zhu et al[51], 2014	HEP25 (197 kDa)	Ethanol precipitation (ethanol concentration 25%)	320 ²
	HEP75 (20 kDa)	Ethanol precipitation (ethanol concentration 75%)	160 ²
	Bi ³⁺ plus HEP25	Complexation of peptides with bismuth[54]	20 ²
	Bi ³⁺ plus HEP75		20 ²
Liu et al[52], 2016	PE2s (4 g)	Petroleum ether extract	250-500 ³
	II-14-18 (311.000 mg)	Methyl alcohol elution from PE2s	12.5-50 ³
	II-19-30 (355.100 mg)		12.5-25 ³
	II-10-13 (306.100 mg)		25-100 ³
	II-54-58 (96.000 mg)		100-400 + ³
	II-31-45 (363.900 mg)		25-50 ³
	II-46-53 (184.500 mg)		25-100 ³
	II-59-63 (78.100 mg)		50-100 ³
	II-64-78 (425.400 mg)		100-400 + ³
	II-1-6 (215.700 mg)		50-200 ³
	II-7-9 (319.900 mg)		25-200 ³
	1-(5-chloro-2-hydroxyphenyl)-3-methyl-1-butanone)	Recrystallized from II-10-13 and II-54-58	12.5-50 ³
	2,5-bis(methoxycarbonyl)terephthalic acid	Recrystallized from II-10-13 and II-54-58	6.25-25 ³
	Thi My Ngan et al[53], 2021	fEtOAc (11.040 g)	Culture filtrate-derived ethyl acetate fraction
mEtOAc (0.091 g)		Mycelium-derived Ethyl acetate fraction	1.5 ⁴
mHexane (0.162 g)		Mycelium-derived hexane fraction	7.5 ⁴
PS (26.400 g)		Culture filtrate-derived polysaccharide	7.5 ⁴
fHexane (0.120 g)		Culture filtrate-derived hexane fraction	10 ⁴
mWater (0.509 g)		Mycelium-derived water fraction	10 + ⁴
fWater (72.480 g)		Culture filtrate-derived water fraction	10 + ⁴

¹Nine clinical isolates are the employed strain of *Helicobacter pylori* (*H. pylori*).

²Colloidal bismuth subcitrate with a minimum inhibitory concentration (MIC) of 20 µg/mL was used as the comparison reference. NTCC11637 is the employed strain of *H. pylori*.

³The comparison references were metronidazole (MIC range 0.7800-1.5625 µg/mL) and tetracycline (MIC range 0.780-3.125 µg/mL). In addition, different isolates of *H. pylori* were used (*i.e.*, ATCC 43504, SS1, *H. pylori* W₂504, *H. pylori* 9, *H. pylori* 64, *H. pylori* 78, and *H. pylori* 83). Therefore, the results are presented as MIC ranges.

⁴The reference comparison was amoxicillin, with a MIC of 0.032 µg/mL.

ATCC43504 is the employed strain of *H. pylori*. Bi³⁺: Bismuth; *H. pylori*: *Helicobacter pylori*; MIC: Minimum inhibitory concentration.

while not changing this premise, several natural substances have been studied as complementary treatments[57-59].

Potential applications of *H. erinaceus* also extend in this context with a specific component of this fungus named in connection with these properties (*i.e.*, erinacines). They are diterpenoids with known neuroprotective properties, of which erinacine A is obtained from the ethanol extract of *H. erinaceus* mycelium[13]. With its exact origin, it is possible to obtain another extract, a sesterterpene, erinacine S [60].

Tung *et al*[61] demonstrated a unique mechanism by which erinacine S could intervene in gastric carcinogenesis through epigenetic regulation. This molecule can induce selective apoptosis in gastric cancer cell lines (*i.e.*, AGS) mediated by ROS toxicity while sparing normal cells. A mouse model of AGS-xenografts in which erinacine S suppressed tumour growth also confirmed this phenomenon[61]. In general, erinacine S may promote apoptosis in gastric carcinoma cells by inducing a specific pathway involving several molecules, such as TNF-related apoptosis-inducing ligand T (TRAIL), Fas ligand (Fas-L), and caspases 3,8,9 which are known to be involved in apoptotic death. At the same time, erinacine S suppressed the expression of anti-apoptotic molecules (*i.e.*, Bcl-2 and Bcl-XL). In addition, cell arrest is promoted in the G₁ phase of the cell cycle by the inactivation of specific cyclins and cyclin-dependent kinases[61]. Furthermore, erinacine S promotes the expression of Fas-L and TRAIL in gastric cancer cells undergoing apoptosis by trimethylation of histone H3 in the promoter regions of the Fas-L and TRAIL genes[61].

Erinacine A exhibits characteristics similar to erinacine S with respect to apoptosis induction. Several studies have shown that erinacine S can inhibit the growth of colorectal cancer both *in vitro* and *in vivo*, which could be attributed to the inhibition of proliferation and induction of the apoptosis signalling pathway, such as the generation of ROS *via* the phosphatidylinositol 3-kinase (PI3K)/mechanistic target of rapamycin (mTOR)/ribosomal protein S6 kinase beta-1 (p70S6K) pathway[62,63].

Proteomic analyses have confirmed that erinacine A reduces the growth and invasiveness of TSGH9201 gastric cancer cells *via* ROS-mediated phosphorylation of focal adhesion kinase (FAK)/protein kinase B (also known as AKT)/p70S6K and p21-activated kinase 1 (PAK1)[64]. Previous studies have shown that erinacine A-mediated apoptosis involves the actin depolymerisation pathway[65]. Furthermore, several PAK partners can phosphorylate or activate mitogen-activated protein kinases. The kinases PI3-kinase/AKT and LIM are involved in the regulation of the cytoskeleton[66,67]. In addition, erinacine A is believed to induce upregulation of the onco-suppressive proteins microtubule-associated scaffold protein 2 (MTUS2) and 14-3-3 protein sigma (1433S), associated with antitumour activity in gastric cancer cells[63]. Recent studies have shown that the 1433S protein appears to intervene in gastric cancer by exerting G₂/M checkpoint regulation in the cell cycle[68,69].

Furthermore, the MTUS2 gene plays a central role in controlling microtubule plus-end-tracking proteins (also known as +TIPs) by regulating cell division and migration through its mitotic kinesin-associated centromere, a microtubule depolymerase[70,71]. Moreover, the cytoskeleton depolymerisation pathway has been recognised as a critical cellular response that controls apoptosis and inhibits Rho GTPase-activated cell migration through its effector kinases, Rho-associated coiled-coil containing protein kinases 1 and 2[72]. These findings are significant and imply that phosphorylation of the FAK/AKT/p70S6K and PAK1 pathways determines the downstream expression of the MTUS2 and 1433S genes, the execution of cancer cell apoptosis, and the role of erinacine A as an anti-invasive agent. This effect most likely reflects cytoskeleton rearrangement, reducing erinacine A-dependent cell motility[63, 73,74]. Figure 2 summarises the primary antineoplastic mechanisms of erinacines.

An additional polysaccharide protein extracted from the fermented mycelia of *H. erinaceus* (HEG-5) was studied in SGC-7901 gastric cancer lines. Again, positive regulation of apoptosis and the cell cycle appears to be the mechanisms underlying this antineoplastic action. Indeed, it seems that HEG-5 blocks the development of SGC-7901 cells in the S phase of the cell cycle by promoting the opposite regulation of anti- and pro-apoptotic genes. That is, predictably, the downregulation of anti-apoptotic molecules (such as Bcl-2, PI3K, and AKT) and, conversely, by upregulating caspases 3,8, p53, the bcl-2-associated X-protein, and the bcl-2-associated death promoter. Thus, caspase 3,8-dependent, p53-dependent, and PI3K/AKT-mediated apoptotic pathways are activated[75].

A synergy between doxorubicin and *H. erinaceus* was also observed in their pro-apoptotic action toward SGC-7901 cells *via* ROS-induced stress and caspase activation[76].

Moreover, two extracts of *H. erinaceus* (*i.e.*, HTH5 and HTJ5A) have been shown in an experiment conducted in NCI-87 gastric carcinoma cells to possess both *in vitro* and *in vivo* (in xenograft models including severe combined immunodeficient bearing mice) concentration-dependent cytotoxicity toward such cells, lower toxicity, and more efficacy than 5-fluorouracil[77].

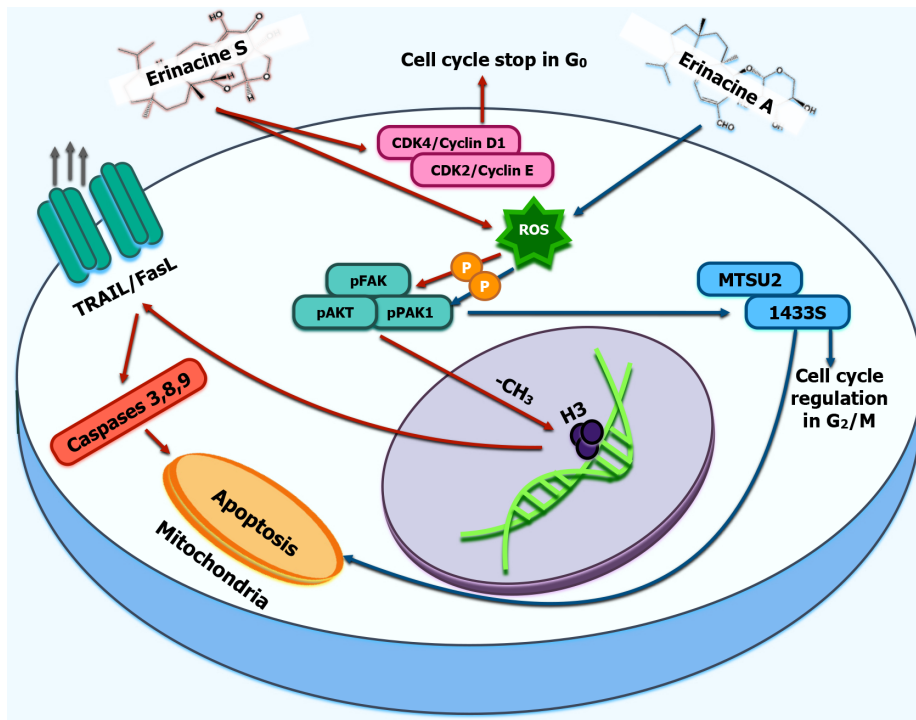
Finally, *H. erinaceus* (via the EP-1 polysaccharide) targets not only cancer cells but also precancerous cell lines by promoting their arrest in the G₀/G₁ phase of the cell cycle[78].

H. ERINACEUS IN LOWER GASTROINTESTINAL TRACT DISEASES: THE EVIDENCE

H. erinaceus and IBD

IBD is a chronic digestive disease that results in sustained gastrointestinal inflammation and consists mainly of ulcerative colitis (UC) and Crohn's disease[79].

Available evidence related to *H. erinaceus* primarily focuses on UC. Wang *et al*[80] evaluated three polysaccharides (*i.e.*, wHEP-1, wHEP-2, and wHEP-3) and proposed the third as the one showing the greatest anti-inflammatory action in a UC-like model in Caco-2 cells inflamed by bacterial lipopolysaccharide.



DOI: 10.3748/wjg.v29.i20.3084 Copyright ©The Author(s) 2023.

Figure 2 Main antineoplastic molecular mechanisms of erinacines S and A from *Hericium erinaceus* in gastric cancer cell models.

Erinacine S (in AGS gastric cancer cells) can activate a pathway (red arrows) with reactive oxygen species (ROS) mediated phosphorylation of focal adhesion kinase (FAK)/protein kinase B (also known as AKT)/p21-activated kinase 1 (PAK1). Subsequently, by trimethylation of histone H3, the latter pathway can induce the increased expression of TNF-related apoptosis-inducing ligand T and Fas ligand receptors by the cancer cell with the subsequent activation of apoptosis by initiating caspases 3, 8, and 9. Erinacine A (in TSGH9201 gastric cancer cells), once activated (blue arrows), the FAK/AKT/PAK1 pathway, in a similar manner as previously described, upregulates microtubule-associated scaffold protein 2/14-3-3 protein sigma proteins with subsequent activation of caspases-mediated apoptosis. In addition, erinacines can also modulate cell cycle regulation by preventing cell cycle continuation through the blockade at checkpoints, *i.e.*, blocking cyclin-dependent kinases. ROS: Reactive oxygen species; FAK: Focal adhesion kinase; PAK: Activated kinase 1; MTUS2: Microtubule-associated scaffold protein 2; TRAIL: TNF-related apoptosis-inducing ligand T; Fas-L: Fas ligand; CDKs: Cyclin-dependent kinases; 1433S: 14-3-3 protein sigma.

A more complete *in vivo* model has been reported by Diling *et al*[81]. The authors experimentally induced UC-like colitis in mice using trinitrobenzene-sulfonic acid enemas. They were then treated with mixed extracts of *H. erinaceus* (polysaccharide, alcoholic, and cumulative fractions) for 14 d. Significant clinical improvements were observed in the treated mice compared with the untreated control mice. Also, histologically, the treated group had significantly less severe lesions. They recorded reduced MPO levels in the treated mice to verify tissue infiltration of neutrophils. This was accompanied by a modulation of cytokines in the treated group with the restoration of proinflammatory and anti-inflammatory cytokines to pre-treatment levels with trinitro-benzene-sulfonic acid.

Further study has confirmed the anti-UC properties of ethanolic extracts of *H. erinaceus* in C57BL/6 mice exposed to dextran sulphate sodium orally to induce experimental UC-like colitis. The dosage used by the authors was 250/500 mg/kg/d[82]. This study showed as much clinical improvement as histologic (including neutrophil infiltration by MPO dosing) and cytokine improvement. However, these authors also stigmatised antioxidant potential by upregulating NO, malondialdehyde, and SOD. Wang *et al*[83] also focused on the antioxidant potential of *H. erinaceus* polysaccharides as a therapeutic mechanism in UC experimental colitis and discovered the positive regulation of SOD and reduced ROS production. It is no coincidence that combating oxidative stress is part of the therapeutic proposals for IBD[84].

UC pathogenesis remains largely unclear, but bowel inflammation and oxidative stress are considered fundamental mechanisms underlying its pathophysiology. During the active phase of UC, activated leukocytes generate many proinflammatory cytokines and pro-oxidative stress reactions. The joint deterioration caused by inflammation and oxidative stress significantly alters the redox balance within the intestinal mucosa, which accelerates the apoptosis of intestinal epithelial cells[85,86]. Excessive ROS production directly leads to tissue damage and induces an inflammatory cascade[87]. When mitochondria are damaged by oxidative stress, they enter a vicious cycle in which the loss of respiration disrupts redox homeostasis and, in turn, increases intracellular oxygen availability, resulting in increased ROS formation and subsequent oxidative damage to DNA[88]. Several studies have shown that UC onset and course are related to changes in mitochondrial structure and function[89,90].

Finally, in the context of *H. erinaceus* polysaccharides, Ren et al[91] confirmed this finding in C57BL/6 mice with experimental UC-like colitis induced by dextran sulphate sodium. Furthermore, the authors recorded (as also done by Diling et al[81]) an anti-inflammatory downregulation of nuclear factor kappa B (NF- κ B).

NF- κ B is part of several pathways (i.e., the canonical and noncanonical pathways) that have been extensively studied in IBD, upon which the mainstay of biological therapy for IBD, namely anti-TNF- α agents, has been built[92].

However, another mechanism by which the anti-IBD effect of *H. erinaceus* has been studied is the modulation of the gut microbiota, as described in the last section of this review.

Colonic diverticulosis and *H. erinaceus*

Diverticular disease has acquired several modifications of its nomenclature over time, including the concept of symptomatic uncomplicated diverticular disease (SUDD) in its nosological entity. SUDD is characterised by colonic diverticulosis associated with chronic abdominal pain without signs, symptoms, or evidence of underlying diverticulitis or colitis[93]. Several pathogenetic mechanisms have been implicated, including visceral hypersensitivity and a reduction in the interstitial Cajal cells, resulting in slowed colonic motility[94]. SUDD therapy includes poorly absorbable antibiotics (such as rifaximin[95]), mesalamine[96], or probiotics[97], as well as modification of habits with increased physical activity[94]. However, definitive medical therapy for SUDD has not yet been defined.

Paradoxically, in the case of diverticular disease, the *H. erinaceus* research trend was reversed with the availability of clinical studies and the absence of preclinical studies.

Brandimarte et al[98], in a single study, evaluated a combination nutraceutical compound mainly consisting of polysaccharide extracts of *H. erinaceus* in 305 patients with SUDD. The authors recorded clinical remission rates (defined by them as the disappearance of all symptoms) of 9.34% and 17.64% at three and six months of treatment, respectively. Beyond clinical remission, it is interesting to note that the clinical response rate (defined as symptom reduction) was > 90% at three months and approximately 85% at six months. Furthermore, at three and six months, the authors recorded a significant decrease in faecal calprotectin values from baseline. However, these data should be interpreted within the limitations of a single study and the lack of clarification regarding the actual mechanism underlying this clinical improvement.

Nevertheless, it is clear how the inflammatory process plays a role in the pathogenesis of diverticular disease[99]. In addition, TNF- α levels appear to increase progressively with the severity of diverticular disease in both diverticulitis and SUDD[100]. Therefore, as in the other gastrointestinal disorders already discussed in this review, *H. erinaceus* might potentially intervene in diverticular disease through the regulation of the local inflammatory load; however, as already mentioned, there is currently no evidence.

***H. erinaceus* and irritable bowel syndrome: A potential ally in this brain-gut interaction disorder?**

Unlike IBD, where *H. erinaceus* has been extensively studied in preclinical models, no evidence is available regarding its role in irritable bowel syndrome (IBS). However, it is becoming increasingly clear that IBS is coded within functional gastrointestinal disorders and how ROME IV has now defined these disorders as “disorders of brain-gut interaction”, stigmatising the decisive role that the gut-brain axis has acquired in the pathogenesis and clinical features of IBS and other similar functional disorders[101]. Indeed, it is also clear how many brain-derived factors (from neurotransmitters to psychological disorders) are directly involved in IBS pathogenesis[101]. Patients with IBS experience a notably higher prevalence of anxiety-depressive disorders than the healthy population[102]. *H. erinaceus* has been widely studied in clinical settings in patients with anxiety and depression. One randomised controlled trial provided results in favour of positive regulation of psychiatric disorders[103]. Moreover, several pathogenetic mechanisms have been suggested in studies on mood disorders. In mice, *H. erinaceus* appears to exert anti-inflammatory effects (negative regulation of proinflammatory cytokines and positive regulation of anti-inflammatory cytokines), stimulate hippocampal neurogenesis, and increase neurotransmitters such as 5-hydroxytryptamine, dopamine, and noradrenaline. However, in humans, it appears to increase salivary levels of free 3-methoxy-4-hydroxyphenylethylene glycol and circulating levels of pro-brain-derived neurotrophic factor. These molecular changes are associated with an improved anxiety-depressive effect[104-107].

Beyond that, the potential of *H. erinaceus* to intervene in the gut-brain axis could also be explored in patients with IBD, where the prevalence and impact on the disease course of anxiety-depressive disorders are not negligible[108,109]. In addition, factors leading to anxiety-depressive disorders can impact therapeutic adherence, as observed during the COVID-19 pandemic[110,111].

IBS therapy is challenging, and much more needs to be added to the research field[112]. In addition, naturally derived substances have repeatedly been considered possible therapies for IBS[113-115]. Ultimately, despite the interesting prospect of the impact of *H. erinaceus* on the dysregulation of the gut-brain axis in IBS, studies evaluating the effects of this fungus on both the gastrointestinal clinical features and the impact of modulation of anxiety and depression on the latter are still awaited.

***H. erinaceus* and the colorectal cancer**

As observed for gastric cancer, even in the case of colorectal cancer, studies have been conducted regarding the antineoplastic potential of *H. erinaceus*. Table 2 summarises the main pathophysiological mechanisms identified.

Liu *et al*[116] focused on two polysaccharides from the fruiting body of *H. erinaceus* extracted by hot water and ferrocyanide-zinc acetate (HEFP-1 and HEFP-2). These polysaccharides showed the ability in their assay to selectively inhibit the growth of colonic cancer cells (*i.e.*, HCT-116) while sparing normal colonic cells. Furthermore, the HEFP polysaccharide 2b fraction (HEFP-2b) was determined to be responsible for this action. In other words, HEFP-2b induced S-phase cell cycle arrest of such cells through the downregulation of CDK1,2 and cyclin A2 and concomitant inhibition of mini-chromosomal maintenance protein 5 (MCM5), a protein essential for the transition from the S-phase to the M-phase [117].

Using the exact extraction mechanism, Hou *et al*[118] obtained and characterised another polysaccharide fraction of the mushroom fruiting body with antineoplastic properties in colonic cancer. The model was similar to the cellular model employing both the same cells as the previous authors (*i.e.*, HCT-116) but with the addition of the DLD1 cell group. They showed an upregulation of cleaved caspase-9 and cleaved caspase-3 without a change in the cleavage of caspase-8, confirming that the apoptotic mechanism was mitochondrial and not extrinsic with relative inhibition of the Bcl-2 protein and stimulation of the pro-apoptotic Bax protein. Confirming this evidence, the authors identified that ROS production might be one of the triggers of this apoptotic phenomenon.

Another study examined fungal extracts obtained by boiling water, microwave extraction in ethanol, and acid or alkaline extracts with hydrochloric acid or sodium hydroxide, respectively[119]. These extracts specifically demonstrated inhibitory effects on implanted tumours in mice (using CT-26 murine cancer cells). Furthermore, intraperitoneal administration of the extracts obtained by boiling water and microwaving in ethanol reduced tumour growth by 38% and 41%, respectively. These extracts increased the cytolytic activity of natural killer cells and phagocytic activity of macrophages and blocked tumour angiogenesis.

In addition, as in gastric cancer, HTJ5 and HTJ5A extracts were shown to block the growth of HT-29 colon cancer cell implants in mice with severe combined immunodeficiency[77]. Another study also confirmed the antineoplastic action of *H. erinaceus* in HT-29 cells by evaluating its anti-tyrosinase and α -glucosidase activities[120].

As previously described, erinacines are the principal antineoplastic components of *H. erinaceus* in gastric cancer. However, erinacine A showed marked antineoplastic effects against colon cancer. In detail, Lee *et al*[65] highlighted this in HCT-116 and DLD-1 cells by demonstrating how erinacine A was able to exert its cytotoxic action similar to that observed in gastric cancer by increasing ROS production and decreasing cancer cell proliferation through upregulation of the PI3K/mTOR/p70S6K pathway.

H. ERINACEUS AND GUT MICROBIOTA MODULATION

***H. erinaceus* may promote a shift in the gut microbiota phenotype toward the increased selection of short-chain fatty acids-producing bacteria**

The gut microbiota, although not fully detailed and understood, plays a crucial role in the development, progression, and treatment of several gastrointestinal pathological conditions, including IBS and IBD [121].

H. erinaceus is closely related to the modulation of the gut microbiota. In general, it seems to be able to change the gut microbiota's quantitative and qualitative phenotypes in a health-promoting manner. Therefore, it has often been defined as a prebiotic or probiotic[81,122-124]. It appears that *H. erinaceus* selects certain beneficial bacterial strains from the gut microbiota at the expense of pathogenic strains. For example, Xie *et al*[124] studied the fourteen days administration of 1 g of *H. erinaceus* dry powder in submerged cultures in 13 healthy young volunteers and recorded an increase in the alpha diversity of the gut microbiota. They recorded an increase in *Bifidobacterium* and *Bacteroides* and an increase in short-chain fatty acid (SCFAs) production (*i.e.*, *Roseburia faecis*, *Faecalibacterium prausnitzii*, *Eubacterium rectale*, *Fusicatenibacter saccharivorans*, *Kineothrix alysooides*, *Gemmiger formicilis*, and *Dorea longicatena*). Confirming the modulation of the microbiota, in addition to this whole series of beneficial bacterial species, *H. erinaceus* resulted in a reduction in the relative abundance of pathogenic bacteria (*Streptococcus thermophilus*, *Roseburia intestinalis*, *Bacteroides caccae*, and *Anaerostipes hadrus*).

SCFA-producing bacteria may intervene in immune homeostasis through the regulation of lymphocyte chemotaxis and phagocytosis and possess anti-inflammatory and anti-tumourigenic properties[125]. In addition, SCFAs produced mainly in the colon from indigestible polysaccharides are associated with a reduced risk of IBD and IBD-associated dysbiosis[126]. Not surprisingly, they regulate the immune response by suppressing TNF- α production in neutrophils, contributing to intestinal barrier integrity by inducing secretion of IL-18, mucin, and antimicrobial peptides by intestinal epithelial cells and impacting the ability of dendritic cells to bind to T lymphocytes[126].

Table 2 Main studies examining antineoplastic mechanisms of *Hericium erinaceus* against colorectal cancer

Ref.	<i>H. erinaceus</i> fraction employed	Colonic cancer model	Identified mechanism
Kim et al[119], 2011	Hot water/ microwave ethanol extraction extracts	CT-26 cancer cells graft in mice	NK cells activity ↑; macrophages activity ↑; angiogenesis ↓
Li et al[77], 2014	Polysaccharides	HT-29 cancer cells graft in mice	-
Lee et al[65], 2017	Erinacine A	Cancer cells (HCT-116, DLD1)	PI3K/AKT/mTOR/; p70S6K pathway; ROS ↑
Sharif et al[120], 2018	Ethanol and methanolic extracts	Cancer cells (HT-29)	α-glucosidase activity ↑; anti-tyrosinase activity ↓
Liu et al[116], 2020	Polysaccharides	Cancer cells (HCT-116)	CDK1 ↓; CDK2 ↓; Cyclin A2 ↓; MCM5 ↓
Hou et al[118], 2020	Polysaccharides	Cancer cells (HCT-116, DLD1)	Clived caspases 3,9 ↑; ROS ↑; Bax ↑; Bcl-2 ↓

NK: Natural killer; PI3K: Phosphatidylinositol 3-Kinase; AKT: Protein kinase B; mTOR: Mechanistic target of rapamycin; p70S6K: Ribosomal protein S6 kinase beta-1; CDK: Cyclin-dependent kinase; MCM5: Mini-chromosomal maintenance protein 5; ROS: Reactive oxygen species; Bax: Bcl-2-like protein 4; Bcl-2: B-cell lymphoma 2.

Moreover, the authors posited the impact of such changes in the gut microbiota with a shift in several hematochemical parameters by observing a beneficial correlation with several analytes (*i.e.*, alkaline phosphatase, low-density lipoprotein, creatinine, and uric acid). These data suggest a possible clinical impact of *H. erinaceus*-driven modulation of the gut microbiota.

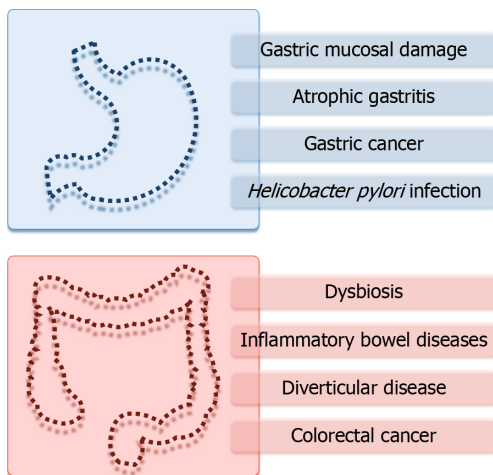
A further study recreated some experimental conditions of digestion to evaluate whether some polysaccharides of *H. erinaceus* could overcome the digestive barrier of the upper digestive tract and influence gut microbiota composition.

Following this experimental model, several *H. erinaceus* polysaccharides obtained by alcohol precipitation (*i.e.*, HEP30, HEP50, and HEP70) increased the relative abundance of SCFA-producing bacteria and reduced pathobiont concentrations (*i.e.*, *Escherichia-Shigella*, *Klebsiella*, and *Enterobacter* in this experience), stigmatised the role of such polysaccharides as possible functional foods[127]. Therefore, they set up an experimental *in vitro* digestion model, as previously described. First, they suggested the likely passage of polysaccharides through the gastrointestinal tract without being digested by the saliva of healthy donors or gastric and small intestinal juices (simulated in the laboratory). Therefore, they may reach the distal tract of the intestine. Second, at that level, the authors demonstrated how the gut microbiota utilised HEP50 for fermentation by increasing the levels of SCFAs and decreasing the pH of the faecal fermentation broth.

Furthermore, Yang et al[127] examined the impact of a polysaccharide from the mycelium of *H. erinaceus* on the quality of murine gut microbiota. The authors observed a change in the relative abundance of different bacteria depending on the age of the mice used for the microbiota analysis. In both the control and experimental groups of adult and middle-aged mice, there was an increase in the relative abundance of *Lachnospiraceae*, *Ruminococcaceae*, and *Akkermansiaceae* and a decrease in the relative abundance of *Muribaculaceae*, *Rikenellaceae*, *Lactobacillaceae*, and *Bacteroidaceae*. On the other hand, only the treated adult mice showed an increase in *Erysipelotrichaceae*, *Enterobacteriaceae*, *Christensenellaceae*, and *Coriobacteriaceae* and a decrease in *Bifidobacteriaceae* and *Peptostreptococcaceae*. Finally, in the group of middle-aged and old mice, the increased bacterial species were *Rhizobiaceae*, *Desulfovibrionaceae*, and *Lachnospiraceae*, while the decreased species were *Corynebacteriaceae* and *Rikenellaceae*. Among the many modified families of bacteria, the relevant ones are the butyrate-producing bacteria (*i.e.*, *Lachnospiraceae* and *Ruminococcaceae*). Butyrate is an SCFA used as an energy source by the intestinal mucosa to promote gut health and protect against colorectal cancer[128-130]. These two species of bacteria are among the leading producers of butyrate[131]. Further *in vitro* studies have shown the beneficial effects of *H. erinaceus* in modulating SCFA-producing bacteria[132]. Positive *H. erinaceus*-driven modulation of the gut microbiota has also been confirmed in elderly dogs, with ameliorative effects on immunity and obesity[133].

***H. erinaceus* in restoring the gut microbiota after dysbiosis induced by antineoplastic drug therapy: The evidence**

Cancer therapy is associated with significant adverse events, including gastrointestinal complications. The latter includes dysbiosis induced by antineoplastic treatments[134]. However, while the microbiota may be impacted by antineoplastic therapy, it is also true that several reports suggest an opposite mechanism whereby the gut microbiota may modulate the response to treatment, specifically immunotherapy[135]. In this context, *H. erinaceus* showed some preclinical results, demonstrating its potential in cancer therapy-induced toxicity. For this purpose, an investigation based on polysaccharides was conducted in mice treated with cyclophosphamide[136]. This brought the composition of the gut microbiota of chemotherapy-treated mice closer to that of control and healthy mice through increased



DOI: 10.3748/wjg.v29.i20.3084 Copyright ©The Author(s) 2023.

Figure 3 The potential of *Hericium erinaceus* in upper and lower gastrointestinal tract diseases. *Hericium erinaceus* is a promising candidate as a therapeutic modality or functional food in the treatment of various diseases of the gastrointestinal tract. This evidence stems from several experiences, largely preclinical, that have shown that this mushroom possesses anti-inflammatory and antineoplastic capabilities concerning the gastrointestinal tract.

alpha and beta diversity. Similar results were reported in another study[123]. Moreover, these data are also available for 5-fluorouracil toxicity. Wang *et al*[137] examined the proteins of *H. erinaceus* in a xenograft cancer model in mice successfully treated with 5-fluorouracil and revealed an anti-dysbiosis action.

***H. erinaceus* may intervene in IBD through the gut microbiota**

Although a therapy based on the direct modification of the gut microbiota is not yet recommended in the current guidelines for managing IBD, it is clear that the potential of this option has been extensively studied and is currently under investigation[138-141].

Ren *et al*[142] studied whether the administration of *H. erinaceus* to Cynomolgus monkeys affected the clinical features of spontaneous UC by exerting an anti-inflammatory effect through modulation of the gut microbiota. They recorded an increase in the abundance of bacteria, such as *Lactobacillus reuteri* (already implicated in improving the clinical features of IBS, acute gastrointestinal infections, and IBD in children and adults). In contrast, *Streptococcus lutetiensis* is negatively modulated and is known to cause sepsis in newborns[143].

In addition, Diling *et al*[81], in the above cited model of murine colitis induced by trinitro-benzene-sulfonic acid, demonstrated how the administration of extracts (*i.e.*, polysaccharide, alcoholic extracts, and whole extracts) of *H. erinaceus* improved both the clinical and histological picture but, more importantly, the gut microbiota by promoting a switch to a microbial composition similar to that of the controls. In other words, a reduction in proinflammatory strains (*Corynebacterium*, *Staphylococcus*, *Ruminococcus*, *Roseburia*, *Dorea*, and *Sutterella*) and an increase in anti-inflammatory strains (*Bacteroides*, *Bifidobacterium*, *Prevotella*, *Parabacteroides*, *Coprococcus*, *Desulfovibrio*, and *Lactobacillus*) were observed.

In a similar study, in an acetic acid-induced murine colitis model, the mycelium polysaccharide EP-1 drastically improved the gut microbiota of mice by increasing SCFA-producing populations while suppressing the expression of G protein-coupled receptor 41 (GPR41) and GPR43[144]. SCFAs can bind to GPR41 and GPR43 and increase the production of inflammatory cytokines and chemokines in the intestine[145].

Finally, positive microbiota modulation was observed in mice with dextran sulphate sodium-induced colitis[91].

Despite the possibility that *H. erinaceus* may have intervened in the pathogenesis of IBD through the gut microbiota, studies conducted in humans as well as those exploring the clinical impact of such microbiota modification, are still awaited, especially with clinical tools and scores that are widely validated and used in clinical and IBD research practise[146,147].

CONCLUSION

H. erinaceus is a mushroom with a long tradition of use as a medicinal product. Numerous preclinical studies have probed its gastrointestinal anti-inflammatory and antineoplastic properties and its impact on the composition of the intestinal microbiota (Figure 3). In the face of a large body of evidence, there is a strong need for clinical studies conducted on humans, especially considering the promising results of previous studies. Furthermore, it is necessary to determine whether this fungus can represent an

excellent nutritional supplement in gastrointestinal pathologies, the patients who may benefit from it, and whether there is a possible therapeutic role for the compounds extracted from *H. erinaceus*. Finally, various technical processes for such fungi yield many extracts and fractions. Therefore, it is essential to understand which of these presents the best safety and efficacy profiles.

FOOTNOTES

Author contributions: Gravina AG, Pellegrino R, Romano M, and Federico A collected the literature, wrote the initial manuscript, conceptualised the tables and figures, and contributed equally to this work; Gravina AG, Pellegrino R, Auletta S, Palladino G, Brandimarte G, D'Onofrio R, Arboretto G, Imperio G, Ventura A, Cipullo M, Romano M, and Federico A conceptualised the structure of the text, critically revised the manuscript for important intellectual content, and read and approved the final version of the manuscript.

Conflict-of-interest statement: The authors declare no conflicts of interest for this article.

Open-Access: This article is an open-access article that was selected by an in-house editor and fully peer-reviewed by external reviewers. It is distributed in accordance with the Creative Commons Attribution NonCommercial (CC BY-NC 4.0) license, which permits others to distribute, remix, adapt, build upon this work non-commercially, and license their derivative works on different terms, provided the original work is properly cited and the use is non-commercial. See: <https://creativecommons.org/licenses/by-nc/4.0/>

Country/Territory of origin: Italy

ORCID number: Antonietta Gerarda Gravina 0000-0001-8049-0115; Raffaele Pellegrino 0000-0001-5074-230X; Salvatore Auletta 0009-0008-8565-0120; Giovanna Palladino 0000-0002-7367-4175; Rossella D'Onofrio 0009-0002-4761-0028; Giusi Arboretto 0009-0000-7938-8949; Giuseppe Imperio 0000-0002-4182-2858; Andrea Ventura 0009-0005-5735-7195; Marina Cipullo 0000-0003-4938-5805; Marco Romano 0000-0002-3271-349X; Alessandro Federico 0000-0002-0885-0793.

S-Editor: Chen YL

L-Editor: A

P-Editor: Zhao S

REFERENCES

- 1 Peery AF, Crockett SD, Murphy CC, Lund JL, Dellon ES, Williams JL, Jensen ET, Shaheen NJ, Barritt AS, Lieber SR, Kochar B, Barnes EL, Fan YC, Pate V, Galanko J, Baron TH, Sandler RS. Burden and Cost of Gastrointestinal, Liver, and Pancreatic Diseases in the United States: Update 2018. *Gastroenterology* 2019; **156**: 254-272.e11 [PMID: 30315778 DOI: 10.1053/j.gastro.2018.08.063]
- 2 Deutsch JK, Levitt J, Hass DJ. Complementary and Alternative Medicine for Functional Gastrointestinal Disorders. *Am J Gastroenterol* 2020; **115**: 350-364 [PMID: 32079860 DOI: 10.14309/ajg.0000000000000539]
- 3 Cheifetz AS, Gianotti R, Luber R, Gibson PR. Complementary and Alternative Medicines Used by Patients With Inflammatory Bowel Diseases. *Gastroenterology* 2017; **152**: 415-429.e15 [PMID: 27743873 DOI: 10.1053/j.gastro.2016.10.004]
- 4 Thongbai B, Rapior S, Hyde KD, Wittstein K, Stadler M. *Heridium erinaceus*, an amazing medicinal mushroom. *Mycol Progress* 2015; **14**: 91 [DOI: 10.1007/s11557-015-1105-4]
- 5 Cheng JH, Tsai CL, Lien YY, Lee MS, Sheu SC. High molecular weight of polysaccharides from *Heridium erinaceus* against amyloid beta-induced neurotoxicity. *BMC Complement Altern Med* 2016; **16**: 170 [PMID: 27266872 DOI: 10.1186/s12906-016-1154-5]
- 6 Lee JS, Hong EK. *Heridium erinaceus* enhances doxorubicin-induced apoptosis in human hepatocellular carcinoma cells. *Cancer Lett* 2010; **297**: 144-154 [PMID: 20554107 DOI: 10.1016/j.canlet.2010.05.006]
- 7 Shang HM, Song H, Xing YL, Niu SL, Ding GD, Jiang YY, Liang F. Effects of dietary fermentation concentrate of *Heridium caput-medusae* (Bull.:Fr.) Pers. on growth performance, digestibility, and intestinal microbiology and morphology in broiler chickens. *J Sci Food Agric* 2016; **96**: 215-222 [PMID: 25582752 DOI: 10.1002/jsfa.7084]
- 8 Zhang Z, Lv G, Pan H, Pandey A, He W, Fan L. Antioxidant and hepatoprotective potential of endo-polysaccharides from *Heridium erinaceus* grown on tofu whey. *Int J Biol Macromol* 2012; **51**: 1140-1146 [PMID: 22982810 DOI: 10.1016/j.ijbiomac.2012.09.002]
- 9 Saito Y, Nishide A, Kikushima K, Shimizu K, Ohnuki K. Improvement of cognitive functions by oral intake of *Heridium erinaceus*. *Biomed Res* 2019; **40**: 125-131 [PMID: 31413233 DOI: 10.2220/biomedres.40.125]
- 10 Mori K, Inatomi S, Ouchi K, Azumi Y, Tuchida T. Improving effects of the mushroom Yamabushitake (*Heridium erinaceus*) on mild cognitive impairment: a double-blind placebo-controlled clinical trial. *Phytother Res* 2009; **23**: 367-372 [PMID: 18844328 DOI: 10.1002/ptr.2634]
- 11 Miles PG, Chang S-T. *Mushrooms*. 0 ed. CRC Press, Taylor & Francis Group, 2004 [DOI: 10.1201/9780203492086]
- 12 Boddy L, Crockatt ME, Ainsworth AM. Ecology of *Heridium cirrhatum*, *H. coralloides* and *H. erinaceus* in the UK. *Fungal Ecology* 2011; **4**: 163-173 [DOI: 10.1016/j.funeco.2010.10.001]
- 13 Friedman M. *Chemistry, Nutrition, and Health-Promoting Properties of Heridium erinaceus (Lion's Mane) Mushroom*

- Fruiting Bodies and Mycelia and Their Bioactive Compounds. *J Agric Food Chem* 2015; **63**: 7108-7123 [PMID: 26244378 DOI: 10.1021/acs.jafc.5b02914]
- 14 **Li W**, Gu Z, Yang Y, Zhou S, Liu Y, Zhang J. Non-volatile taste components of several cultivated mushrooms. *Food Chem* 2014; **143**: 427-431 [PMID: 24054262 DOI: 10.1016/j.foodchem.2013.08.006]
 - 15 **Rodrigues DMF**, Freitas AC, Rocha-Santos TAP, Vasconcelos MW, Roriz M, Rodríguez-Alcalá LM, Gomes AMP, Duarte AC. Chemical composition and nutritive value of *Pleurotus citrinopileatus* var *cornucopiae*, *P. eryngii*, *P. salmoneo stramineus*, *Pholiota nameko* and *Hericium erinaceus*. *J Food Sci Technol* 2015; **52**: 6927-6939 [DOI: 10.1007/s13197-015-1826-z]
 - 16 **Jayachandran M**, Chen J, Chung SSM, Xu B. A critical review on the impacts of β -glucans on gut microbiota and human health. *J Nutr Biochem* 2018; **61**: 101-110 [PMID: 30196242 DOI: 10.1016/j.jnutbio.2018.06.010]
 - 17 **Zhu F**, Du B, Xu B. Preparation and Characterization of Polysaccharides from Mushrooms. In: Ramawat KG, Mérillon J-M, editors. *Polysaccharides*. Cham: Springer International Publishing, 2014: 1-16
 - 18 **Liu J**, Wang W, Hu Q, Wu X, Xu H, Su A, Xie M, Yang W. Bioactivities and molecular mechanisms of polysaccharides from *Hericium erinaceus*. *J Future Foods* 2022; **2**: 103-111 [DOI: 10.1016/j.jfutfo.2022.03.007]
 - 19 **Lubek-Nguyen A**, Ziemichód W, Olech M. Application of Enzyme-Assisted Extraction for the Recovery of Natural Bioactive Compounds for Nutraceutical and Pharmaceutical Applications. *Appl Sci* 2022; **12**: 3232 [DOI: 10.3390/app12073232]
 - 20 **Lanas A**, Chan FKL. Peptic ulcer disease. *Lancet* 2017; **390**: 613-624 [PMID: 28242110 DOI: 10.1016/S0140-6736(16)32404-7]
 - 21 **Takeuchi K**. Pathogenesis of NSAID-induced gastric damage: importance of cyclooxygenase inhibition and gastric hypermotility. *World J Gastroenterol* 2012; **18**: 2147-2160 [PMID: 22611307 DOI: 10.3748/wjg.v18.i18.2147]
 - 22 **Sugimoto M**, Yamaoka Y, Furuta T. Influence of interleukin polymorphisms on development of gastric cancer and peptic ulcer. *World J Gastroenterol* 2010; **16**: 1188-1200 [PMID: 20222161 DOI: 10.3748/wjg.v16.i10.1188]
 - 23 **Boddy L**, Wald P. *Creolophus* (*Hericium*) *cirrhatum*, *Hericium erinaceus* and *H. coralloides* in England (English nature research report 492). *English Nature* 2003; 168-169
 - 24 **Wang XY**, Yin JY, Zhao MM, Liu SY, Nie SP, Xie MY. Gastroprotective activity of polysaccharide from *Hericium erinaceus* against ethanol-induced gastric mucosal lesion and pylorus ligation-induced gastric ulcer, and its antioxidant activities. *Carbohydr Polym* 2018; **186**: 100-109 [PMID: 29455967 DOI: 10.1016/j.carbpol.2018.01.004]
 - 25 **Wang M**, Kanako N, Zhang Y, Xiao X, Gao Q, Tetsuya K. A unique polysaccharide purified from *Hericium erinaceus* mycelium prevents oxidative stress induced by H₂O₂ in human gastric mucosa epithelium cell. *PLoS One* 2017; **12**: e0181546 [PMID: 28742114 DOI: 10.1371/journal.pone.0181546]
 - 26 **Liu J**, Wang F, Luo H, Liu A, Li K, Li C, Jiang Y. Protective effect of butyrate against ethanol-induced gastric ulcers in mice by promoting the anti-inflammatory, anti-oxidant and mucosal defense mechanisms. *Int Immunopharmacol* 2016; **30**: 179-187 [PMID: 26604089 DOI: 10.1016/j.intimp.2015.11.018]
 - 27 **Roza AL**, Meira de Faria F, Souza Brito AR, Pellizzon CH. The gastroprotective effect of menthol: involvement of anti-apoptotic, antioxidant and anti-inflammatory activities. *PLoS One* 2014; **9**: e86686 [PMID: 24466200 DOI: 10.1371/journal.pone.0086686]
 - 28 **Amirshahrokhi K**, Khalili AR. The effect of thalidomide on ethanol-induced gastric mucosal damage in mice: involvement of inflammatory cytokines and nitric oxide. *Chem Biol Interact* 2015; **225**: 63-69 [PMID: 25478868 DOI: 10.1016/j.cbi.2014.11.019]
 - 29 **Moezi L**, Heidari R, Amirghofran Z, Nekooeian AA, Monabati A, Dehpour AR. Enhanced anti-ulcer effect of pioglitazone on gastric ulcers in cirrhotic rats: the role of nitric oxide and IL-1 β . *Pharmacol Rep* 2013; **65**: 134-143 [PMID: 23563031 DOI: 10.1016/s1734-1140(13)70971-x]
 - 30 **Bi WP**, Man HB, Man MQ. Efficacy and safety of herbal medicines in treating gastric ulcer: a review. *World J Gastroenterol* 2014; **20**: 17020-17028 [PMID: 25493014 DOI: 10.3748/wjg.v20.i45.17020]
 - 31 **Yandrapu H**, Sarosiek J. Protective Factors of the Gastric and Duodenal Mucosa: An Overview. *Curr Gastroenterol Rep* 2015; **17**: 24 [PMID: 26109006 DOI: 10.1007/s11894-015-0452-2]
 - 32 **Sofidiya MO**, Orisaremi CO, Sansaliyu I, Adetunde TO. Gastroprotective and antioxidant potentials of ethanolic stem bark extract of *Margaritaria discoidea* (Euphorbiaceae) in rats. *J Ethnopharmacol* 2015; **171**: 240-246 [PMID: 26068431 DOI: 10.1016/j.jep.2015.05.059]
 - 33 **deFoneska A**, Kaunitz JD. Gastroduodenal mucosal defense. *Curr Opin Gastroenterol* 2010; **26**: 604-610 [PMID: 20948371 DOI: 10.1097/MOG.0b013e32833f1222]
 - 34 **Sidahmed HM**, Hashim NM, Amir J, Abdulla MA, Hadi AH, Abdelwahab SI, Taha MM, Hassandarvish P, Teh X, Loke MF, Vadivelu J, Rahmani M, Mohan S. Pyranocycloartobioxanthone A, a novel gastroprotective compound from *Artocarpus obtusus* Jarret, against ethanol-induced acute gastric ulcer in vivo. *Phytomedicine* 2013; **20**: 834-843 [PMID: 23570997 DOI: 10.1016/j.phymed.2013.03.002]
 - 35 **Guo YJ**, Deng GF, Xu XR, Wu S, Li S, Xia EQ, Li F, Chen F, Ling WH, Li HB. Antioxidant capacities, phenolic compounds and polysaccharide contents of 49 edible macro-fungi. *Food Funct* 2012; **3**: 1195-1205 [PMID: 22868715 DOI: 10.1039/c2fo30110e]
 - 36 **Mao X**, Lu ZM, Gong TT, Wang KL, Geng Y, Xu HY, Xu GH, Shi JS, Xu ZH. Therapeutic Effect and Potential Mechanisms of Lion's Mane Medicinal Mushroom, *Hericium erinaceus* (Agaricomycetes), Mycelia in Submerged Culture on Ethanol-Induced Chronic Gastric Injury. *Int J Med Mushrooms* 2019; **21**: 1137-1150 [PMID: 32450023 DOI: 10.1615/IntJMedMushrooms.2019032885]
 - 37 **Chen W**, Wu D, Jin Y, Li Q, Liu Y, Qiao X, Zhang J, Dong G, Li Z, Li T, Yang Y. Pre-protective effect of polysaccharides purified from *Hericium erinaceus* against ethanol-induced gastric mucosal injury in rats. *Int J Biol Macromol* 2020; **159**: 948-956 [PMID: 32450327 DOI: 10.1016/j.ijbiomac.2020.05.163]
 - 38 **Hou C**, Liu L, Ren J, Huang M, Yuan E. Structural characterization of two *Hericium erinaceus* polysaccharides and their protective effects on the alcohol-induced gastric mucosal injury. *Food Chem* 2022; **375**: 131896 [PMID: 34954576 DOI: 10.1016/j.foodchem.2021.131896]

- 39 **Wang XY**, Wang M, Yin JY, Song YH, Wang YX, Nie SP, Xie MY. Gastroprotective activity of polysaccharide from the fruiting body of *Herichium erinaceus* against acetic acid-induced gastric ulcer in rats and structure of one bioactive fraction. *Int J Biol Macromol* 2022; **210**: 455-464 [PMID: 35483513 DOI: 10.1016/j.ijbiomac.2022.04.153]
- 40 **Wong JY**, Abdulla MA, Raman J, Phan CW, Kuppusamy UR, Golbabapour S, Sabaratnam V. Gastroprotective Effects of Lion's Mane Mushroom *Herichium erinaceus* (Bull.:Fr.) Pers. (Aphyllophoromycetidae) Extract against Ethanol-Induced Ulcer in Rats. *Evid Based Complement Alternat Med* 2013; **2013**: 492976 [PMID: 24302966 DOI: 10.1155/2013/492976]
- 41 **Choi SR**, Lee SA, Kim YJ, Ok CY, Lee HJ, Hahm KB. Role of heat shock proteins in gastric inflammation and ulcer healing. *J Physiol Pharmacol* 2009; **60** Suppl 7: 5-17 [PMID: 20388941]
- 42 **Wang M**, Gao Y, Xu D, Gao Q. A polysaccharide from cultured mycelium of *Herichium erinaceus* and its anti-chronic atrophic gastritis activity. *Int J Biol Macromol* 2015; **81**: 656-661 [PMID: 26314904 DOI: 10.1016/j.ijbiomac.2015.08.043]
- 43 **Xu CP**, Liu WW, Liu FX, Chen SS, Liao FQ, Xu Z, Jiang LG, Wang CA, Lu XH. A double-blind study of effectiveness of hericium erinaceus pers therapy on chronic atrophic gastritis. A preliminary report. *Chin Med J (Engl)* 1985; **98**: 455-456 [PMID: 3932005]
- 44 **Gravina AG**, Zagari RM, De Musis C, Romano L, Loguercio C, Romano M. Helicobacter pylori and extragastric diseases: A review. *World J Gastroenterol* 2018; **24**: 3204-3221 [PMID: 30090002 DOI: 10.3748/wjg.v24.i29.3204]
- 45 **Gravina AG**, Priadko K, Ciarrarra P, Granata L, Facchiano A, Miranda A, Dallio M, Federico A, Romano M. Extra-Gastric Manifestations of Helicobacter pylori Infection. *J Clin Med* 2020; **9** [PMID: 33265933 DOI: 10.3390/jcm9123887]
- 46 **Wang F**, Meng W, Wang B, Qiao L. Helicobacter pylori-induced gastric inflammation and gastric cancer. *Cancer Lett* 2014; **345**: 196-202 [PMID: 23981572 DOI: 10.1016/j.canlet.2013.08.016]
- 47 **Flores-Treviño S**, Mendoza-Olazarán S, Bocanegra-Ibarias P, Maldonado-Garza HJ, Garza-González E. Helicobacter pylori drug resistance: therapy changes and challenges. *Expert Rev Gastroenterol Hepatol* 2018; **12**: 819-827 [PMID: 29976092 DOI: 10.1080/17474124.2018.1496017]
- 48 **Romano M**, Gravina AG, Eusebi LH, Pellegrino R, Palladino G, Frazzoni L, Dajti E, Gasbarrini A, Di Mario F, Zagari RM; Members of SIGE; Members of SIED National Council. Management of Helicobacter pylori infection: Guidelines of the Italian Society of Gastroenterology (SIGE) and the Italian Society of Digestive Endoscopy (SIED). *Dig Liver Dis* 2022; **54**: 1153-1161 [PMID: 35831212 DOI: 10.1016/j.dld.2022.06.019]
- 49 **Malfertheiner P**, Megraud F, Rokkas T, Gisbert JP, Liou JM, Schulz C, Gasbarrini A, Hunt RH, Leja M, O'Morain C, Rugge M, Suerbaum S, Tilg H, Sugano K, El-Omar EM; European Helicobacter and Microbiota Study group. Management of Helicobacter pylori infection: the Maastricht VI/Florence consensus report. *Gut* 2022 [PMID: 35944925 DOI: 10.1136/gutjnl-2022-327745]
- 50 **Shang X**, Tan Q, Liu R, Yu K, Li P, Zhao GP. In vitro anti-Helicobacter pylori effects of medicinal mushroom extracts, with special emphasis on the Lion's Mane mushroom, *Herichium erinaceus* (higher Basidiomycetes). *Int J Med Mushrooms* 2013; **15**: 165-174 [PMID: 23557368 DOI: 10.1615/intjmedmushr.v15.i2.50]
- 51 **Zhu Y**, Chen Y, Li Q, Zhao T, Zhang M, Feng W, Takase M, Wu X, Zhou Z, Yang L. Preparation, characterization, and anti-Helicobacter pylori activity of Bi³⁺-*Herichium erinaceus* polysaccharide complex. *Carbohydr Polym* 2014; **110**: 231-237 [PMID: 24906751 DOI: 10.1016/j.carbpol.2014.03.081]
- 52 **Liu JH**, Li L, Shang XD, Zhang JL, Tan Q. Anti-Helicobacter pylori activity of bioactive components isolated from *Herichium erinaceus*. *J Ethnopharmacol* 2016; **183**: 54-58 [PMID: 26364939 DOI: 10.1016/j.jep.2015.09.004]
- 53 **Thi My Ngan L**, Thien Vi N, Thi Mong Tham D, Thi Thanh Loan L, Thanh Ho P, Trung Hieu T. Antioxidant and anti-Helicobacter pylori activities of *Herichium erinaceus* mycelium and culture filtrate. *Biomed Res Ther* 2021; **8**: 4266-4275 [DOI: 10.15419/bmrat.v8i3.665]
- 54 **Jin Y**, Ling P, He Y, Chen L, Chen J, Zhang T. Preparation, characterization and anti-Helicobacter pylori activity of Bi³⁺-hyaluronate complex. *Carbohydr Polym* 2008; **74**: 50-58 [DOI: 10.1016/j.carbpol.2008.01.014]
- 55 **Machlowska J**, Baj J, Sitarz M, Maciejewski R, Sitarz R. Gastric Cancer: Epidemiology, Risk Factors, Classification, Genomic Characteristics and Treatment Strategies. *Int J Mol Sci* 2020; **21** [PMID: 32512697 DOI: 10.3390/ijms21114012]
- 56 **Sexton RE**, Al Hallak MN, Diab M, Azmi AS. Gastric cancer: a comprehensive review of current and future treatment strategies. *Cancer Metastasis Rev* 2020; **39**: 1179-1203 [PMID: 32894370 DOI: 10.1007/s10555-020-09925-3]
- 57 **Ju HM**, Yu KW, Cho SD, Cheong SH, Kwon KH. Anti-cancer effects of traditional Korean wild vegetables in complementary and alternative medicine. *Complement Ther Med* 2016; **24**: 47-54 [PMID: 26860801 DOI: 10.1016/j.ctim.2015.11.004]
- 58 **Jain A**, Tiwari A, Verma A, Jain SK. Vitamins for Cancer Prevention and Treatment: An Insight. *Curr Mol Med* 2017; **17**: 321-340 [PMID: 29210648 DOI: 10.2174/1566524018666171205113329]
- 59 **Hassanalilou T**, Ghavamzadeh S, Khalili L. Curcumin and Gastric Cancer: a Review on Mechanisms of Action. *J Gastrointest Cancer* 2019; **50**: 185-192 [PMID: 30725357 DOI: 10.1007/s12029-018-00186-6]
- 60 **Chen CC**, Tzeng TT, Chen CC, Ni CL, Lee LY, Chen WP, Shiao YJ, Shen CC. Erinacine S, a Rare Sesterterpene from the Mycelia of *Herichium erinaceus*. *J Nat Prod* 2016; **79**: 438-441 [PMID: 26807743 DOI: 10.1021/acs.jnatprod.5b00474]
- 61 **Tung SY**, Lee KC, Lee KF, Yang YL, Huang WS, Lee LY, Chen WP, Chen CC, Teng CC, Shen CH, Hsieh MC, Huang CY, Sheen JM, Kuo HC. Apoptotic mechanisms of gastric cancer cells induced by isolated erinacine S through epigenetic histone H3 methylation of FasL and TRAIL. *Food Funct* 2021; **12**: 3455-3468 [PMID: 33900313 DOI: 10.1039/d0fo03089a]
- 62 **Kallergi G**, Agelaki S, Markomanolaki H, Georgoulis V, Stournaras C. Activation of FAK/PI3K/Rac1 signaling controls actin reorganization and inhibits cell motility in human cancer cells. *Cell Physiol Biochem* 2007; **20**: 977-986 [PMID: 17982280 DOI: 10.1159/000110458]
- 63 **Kuo HC**, Kuo YR, Lee KF, Hsieh MC, Huang CY, Hsieh YY, Lee KC, Kuo HL, Lee LY, Chen WP, Chen CC, Tung SY. A Comparative Proteomic Analysis of Erinacine A's Inhibition of Gastric Cancer Cell Viability and Invasiveness. *Cell Physiol Biochem* 2017; **43**: 195-208 [PMID: 28854418 DOI: 10.1159/000480338]
- 64 **Loo G**. Redox-sensitive mechanisms of phytochemical-mediated inhibition of cancer cell proliferation (review). *J Nutr*

- Biochem* 2003; **14**: 64-73 [PMID: 12667597 DOI: 10.1016/s0955-2863(02)00251-6]
- 65 **Lee KC**, Kuo HC, Shen CH, Lu CC, Huang WS, Hsieh MC, Huang CY, Kuo YH, Hsieh YY, Teng CC, Lee LY, Tung SY. A proteomics approach to identifying novel protein targets involved in erinacine A-mediated inhibition of colorectal cancer cells' aggressiveness. *J Cell Mol Med* 2017; **21**: 588-599 [PMID: 27709782 DOI: 10.1111/jcmm.13004]
- 66 **Thomas GM**, Huganir RL. MAPK cascade signalling and synaptic plasticity. *Nat Rev Neurosci* 2004; **5**: 173-183 [PMID: 14976517 DOI: 10.1038/nrn1346]
- 67 **Johannessen M**, Delghandi MP, Moens U. What turns CREB on? *Cell Signal* 2004; **16**: 1211-1227 [PMID: 15337521 DOI: 10.1016/j.cellsig.2004.05.001]
- 68 **Luk SC**, Siu SW, Lai CK, Wu YJ, Pang SF. Cell Cycle Arrest by a Natural Product via G2/M Checkpoint. *Int J Med Sci* 2005; **2**: 64-69 [PMID: 15968342 DOI: 10.7150/ijms.2.64]
- 69 **Tsukamoto Y**, Nakada C, Noguchi T, Tanigawa M, Nguyen LT, Uchida T, Hijiya N, Matsuura K, Fujioka T, Seto M, Moriyama M. MicroRNA-375 is downregulated in gastric carcinomas and regulates cell survival by targeting PDK1 and 14-3-3zeta. *Cancer Res* 2010; **70**: 2339-2349 [PMID: 20215506 DOI: 10.1158/0008-5472.CAN-09-2777]
- 70 **Adams G Jr**, Zhou J, Wang W, Wu H, Quan J, Liu Y, Xia P, Wang Z, Zhou S, Jiang J, Mo F, Zhuang X, Thomas K, Hill DL, Aikhionbare FO, He P, Liu X, Ding X, Yao X. The Microtubule Plus End Tracking Protein TIP150 Interacts with Cortactin to Steer Directional Cell Migration. *J Biol Chem* 2016; **291**: 20692-20706 [PMID: 27451391 DOI: 10.1074/jbc.M116.732719]
- 71 **Jiang K**, Wang J, Liu J, Ward T, Wordeman L, Davidson A, Wang F, Yao X. TIP150 interacts with and targets MCAK at the microtubule plus ends. *EMBO Rep* 2009; **10**: 857-865 [PMID: 19543227 DOI: 10.1038/embor.2009.94]
- 72 **Croft DR**, Olson MF. Transcriptional regulation of Rho GTPase signaling. *Transcription* 2011; **2**: 211-215 [PMID: 22231116 DOI: 10.4161/trns.2.5.16904]
- 73 **Gu S**, Kounenidakis M, Schmidt EM, Deshpande D, Alkahtani S, Alarifi S, Föller M, Alevizopoulos K, Lang F, Stournaras C. Rapid activation of FAK/mTOR/p70S6K/PAK1-signaling controls the early testosterone-induced actin reorganization in colon cancer cells. *Cell Signal* 2013; **25**: 66-73 [PMID: 23316499 DOI: 10.1016/j.cellsig.2012.08.005]
- 74 **Papakonstanti EA**, Kampa M, Castanas E, Stournaras C. A rapid, nongenomic, signaling pathway regulates the actin reorganization induced by activation of membrane testosterone receptors. *Mol Endocrinol* 2003; **17**: 870-881 [PMID: 12554777 DOI: 10.1210/me.2002-0253]
- 75 **Zan X**, Cui F, Li Y, Yang Y, Wu D, Sun W, Ping L. *Hericium erinaceus* polysaccharide-protein HEG-5 inhibits SGC-7901 cell growth via cell cycle arrest and apoptosis. *Int J Biol Macromol* 2015; **76**: 242-253 [PMID: 25703932 DOI: 10.1016/j.ijbiomac.2015.01.060]
- 76 **Yang W**, Han D, Wu L, Huang Y, Li J, Guo H, Liu Y. *Hericium erinaceus* synergizing with doxorubicin induced SGC7901 cell apoptosis. *Int J Clin Exp Med* 2016; **9**: 1447-1457
- 77 **Li G**, Yu K, Li F, Xu K, Li J, He S, Cao S, Tan G. Anticancer potential of *Hericium erinaceus* extracts against human gastrointestinal cancers. *J Ethnopharmacol* 2014; **153**: 521-530 [PMID: 24631140 DOI: 10.1016/j.jep.2014.03.003]
- 78 **Wang M**, Zhang Y, Xiao X, Xu D, Gao Y, Gao Q. A Polysaccharide Isolated from Mycelia of the Lion's Mane Medicinal Mushroom *Hericium erinaceus* (Agaricomycetes) Induced Apoptosis in Precancerous Human Gastric Cells. *Int J Med Mushrooms* 2017; **19**: 1053-1060 [PMID: 29431066 DOI: 10.1615/IntJMedMushrooms.2017024975]
- 79 **Chang JT**. Pathophysiology of Inflammatory Bowel Diseases. *N Engl J Med* 2020; **383**: 2652-2664 [PMID: 33382932 DOI: 10.1056/NEJMra2002697]
- 80 **Wang D**, Xu D, Zhao D, Wang M. Screening and Comparison of Anti-Intestinal Inflammatory Activities of Three Polysaccharides from the Mycelium of Lion's Mane Culinary-Medicinal Mushroom, *Hericium erinaceus* (Agaricomycetes). *Int J Med Mushrooms* 2021; **23**: 63-71 [PMID: 34591399 DOI: 10.1615/IntJMedMushrooms.2021039951]
- 81 **Diling C**, Xin Y, Chaoqun Z, Jian Y, Xiaocui T, Jun C, Ou S, Yizhen X. Extracts from *Hericium erinaceus* relieve inflammatory bowel disease by regulating immunity and gut microbiota. *Oncotarget* 2017; **8**: 85838-85857 [PMID: 29156761 DOI: 10.18632/oncotarget.20689]
- 82 **Qin M**, Geng Y, Lu Z, Xu H, Shi JS, Xu X, Xu ZH. Anti-Inflammatory Effects of Ethanol Extract of Lion's Mane Medicinal Mushroom, *Hericium erinaceus* (Agaricomycetes), in Mice with Ulcerative Colitis. *Int J Med Mushrooms* 2016; **18**: 227-234 [PMID: 27481156 DOI: 10.1615/IntJMedMushrooms.v18.i3.50]
- 83 **Wang D**, Zhang Y, Yang S, Zhao D, Wang M. A polysaccharide from cultured mycelium of *Hericium erinaceus* relieves ulcerative colitis by counteracting oxidative stress and improving mitochondrial function. *Int J Biol Macromol* 2019; **125**: 572-579 [PMID: 30543884 DOI: 10.1016/j.ijbiomac.2018.12.092]
- 84 **Moura FA**, de Andrade KQ, Dos Santos JCF, Araújo ORP, Goulart MOF. Antioxidant therapy for treatment of inflammatory bowel disease: Does it work? *Redox Biol* 2015; **6**: 617-639 [PMID: 26520808 DOI: 10.1016/j.redox.2015.10.006]
- 85 **Watt DG**, Horgan PG, McMillan DC. Routine clinical markers of the magnitude of the systemic inflammatory response after elective operation: a systematic review. *Surgery* 2015; **157**: 362-380 [PMID: 25616950 DOI: 10.1016/j.surg.2014.09.009]
- 86 **Biasi F**, Leonarduzzi G, Oteiza PI, Poli G. Inflammatory bowel disease: mechanisms, redox considerations, and therapeutic targets. *Antioxid Redox Signal* 2013; **19**: 1711-1747 [PMID: 23305298 DOI: 10.1089/ars.2012.4530]
- 87 **Morcillo EJ**, Estrela J, Cortijo J. Oxidative stress and pulmonary inflammation: pharmacological intervention with antioxidants. *Pharmacol Res* 1999; **40**: 393-404 [PMID: 10527653 DOI: 10.1006/phrs.1999.0549]
- 88 **Sung HJ**, Ma W, Wang PY, Hynes J, O'Riordan TC, Combs CA, McCoy JP Jr, Bunz F, Kang JG, Hwang PM. Mitochondrial respiration protects against oxygen-associated DNA damage. *Nat Commun* 2010; **1**: 5 [PMID: 20975668 DOI: 10.1038/ncomms1003]
- 89 **Roediger WE**. The colonic epithelium in ulcerative colitis: an energy-deficiency disease? *Lancet* 1980; **2**: 712-715 [PMID: 6106826 DOI: 10.1016/s0140-6736(80)91934-0]
- 90 **Santhanam S**, Rajamanickam S, Motamarry A, Ramakrishna BS, Amirtharaj JG, Ramachandran A, Pulimood A, Venkatraman A. Mitochondrial electron transport chain complex dysfunction in the colonic mucosa in ulcerative colitis.

- Inflamm Bowel Dis* 2012; **18**: 2158-2168 [PMID: 22374887 DOI: 10.1002/ibd.22926]
- 91 **Ren Y**, Geng Y, Du Y, Li W, Lu ZM, Xu HY, Xu GH, Shi JS, Xu ZH. Polysaccharide of *Hericium erinaceus* attenuates colitis in C57BL/6 mice via regulation of oxidative stress, inflammation-related signaling pathways and modulating the composition of the gut microbiota. *J Nutr Biochem* 2018; **57**: 67-76 [PMID: 29677563 DOI: 10.1016/j.jnutbio.2018.03.005]
 - 92 **Wang B**, Shen J. NF- κ B Inducing Kinase Regulates Intestinal Immunity and Homeostasis. *Front Immunol* 2022; **13**: 895636 [PMID: 35833111 DOI: 10.3389/fimmu.2022.895636]
 - 93 **Piscopo N**, Ellul P. Diverticular Disease: A Review on Pathophysiology and Recent Evidence. *Ulster Med J* 2020; **89**: 83-88 [PMID: 33093692]
 - 94 **Rezapour M**, Ali S, Stollman N. Diverticular Disease: An Update on Pathogenesis and Management. *Gut Liver* 2018; **12**: 125-132 [PMID: 28494576 DOI: 10.5009/gnl16552]
 - 95 **Colecchia A**, Vestito A, Pasqui F, Mazzella G, Roda E, Pistoia F, Brandimarte G, Festi D. Efficacy of long term cyclic administration of the poorly absorbed antibiotic Rifaximin in symptomatic, uncomplicated colonic diverticular disease. *World J Gastroenterol* 2007; **13**: 264-269 [PMID: 17226906 DOI: 10.3748/wjg.v13.i2.264]
 - 96 **Floch MH**, White JA. Management of diverticular disease is changing. *World J Gastroenterol* 2006; **12**: 3225-3228 [PMID: 16718843 DOI: 10.3748/wjg.v12.i20.3225]
 - 97 **Lahner E**, Esposito G, Zullo A, Hassan C, Cannaviello C, Paolo MC, Pallotta L, Garbagna N, Grossi E, Annibale B. High-fibre diet and *Lactobacillus paracasei* B21060 in symptomatic uncomplicated diverticular disease. *World J Gastroenterol* 2012; **18**: 5918-5924 [PMID: 23139608 DOI: 10.3748/wjg.v18.i41.5918]
 - 98 **Brandimarte G**, Frajese GV, Bargiggia S, Castellani D, Cocco A, Colucci R, Evangelista E, Gravina AG, Napoletano D, Nardi E, Maisto T, Morabito A, Pianese G, Romano A, Sacco R, Sediari L, Sinnona N, Tifi L, D'Avino A, Elisei W, Tursi A. Performance of a multicomponents nutraceutical formulation in patients with symptomatic uncomplicated diverticular disease. *Minerva Gastroenterol (Torino)* 2022; **68**: 216-222 [PMID: 35262307 DOI: 10.23736/S2724-5985.22.03132-1]
 - 99 **Kupcinskis J**, Strate LL, Bassotti G, Torti G, Herszényi L, Malfertheiner P, Cassieri C, Walker MM, Tursi A. Pathogenesis of Diverticulosis and Diverticular Disease. *J Gastrointest Liver Dis* 2019; **28**: 7-10 [PMID: 31930230 DOI: 10.15403/jgld-551]
 - 100 **Tursi A**, Elisei W, Brandimarte G, Giorgetti GM, Inchingolo CD, Nenna R, Picchio M, Giorgio F, Ierardi E. Musosal tumour necrosis factor α in diverticular disease of the colon is overexpressed with disease severity. *Colorectal Dis* 2012; **14**: e258-e263 [PMID: 22469482 DOI: 10.1111/j.1463-1318.2012.02926.x]
 - 101 **Fukudo S**, Okumura T, Inamori M, Okuyama Y, Kanazawa M, Kamiya T, Sato K, Shiotani A, Naito Y, Fujikawa Y, Hokari R, Masaoka T, Fujimoto K, Kaneko H, Torii A, Matsueda K, Miwa H, Enomoto N, Shimosegawa T, Koike K. Evidence-based clinical practice guidelines for irritable bowel syndrome 2020. *J Gastroenterol* 2021; **56**: 193-217 [PMID: 33538894 DOI: 10.1007/s00535-020-01746-z]
 - 102 **Fond G**, Loundou A, Hamdani N, Boukouaci W, Dargel A, Oliveira J, Roger M, Tamouza R, Leboyer M, Boyer L. Anxiety and depression comorbidities in irritable bowel syndrome (IBS): a systematic review and meta-analysis. *Eur Arch Psychiatry Clin Neurosci* 2014; **264**: 651-660 [PMID: 24705634 DOI: 10.1007/s00406-014-0502-z]
 - 103 **Nagano M**, Shimizu K, Kondo R, Hayashi C, Sato D, Kitagawa K, Ohnuki K. Reduction of depression and anxiety by 4 weeks *Herichium erinaceus* intake. *Biomed Res* 2010; **31**: 231-237 [PMID: 20834180 DOI: 10.2220/biomedres.31.231]
 - 104 **Chong PS**, Fung ML, Wong KH, Lim LW. Therapeutic Potential of *Herichium erinaceus* for Depressive Disorder. *Int J Mol Sci* 2019; **21** [PMID: 31881712 DOI: 10.3390/ijms21010163]
 - 105 **Fijalkowska A**, Jędrejko K, Sułkowska-Ziaja K, Ziaja M, Kała K, Muszyńska B. Edible Mushrooms as a Potential Component of Dietary Interventions for Major Depressive Disorder. *Foods* 2022; **11** [PMID: 35627059 DOI: 10.3390/foods11101489]
 - 106 **Rodriguez MN**, Lippi SLP. Lion's Mane (*Herichium erinaceus*) Exerts Anxiolytic Effects in the rTg4510 Tau Mouse Model. *Behav Sci (Basel)* 2022; **12** [PMID: 35877305 DOI: 10.3390/bs12070235]
 - 107 **Chou MY**, Ho JH, Huang MJ, Chen YJ, Yang MD, Lin LH, Chi CH, Yeh CH, Tsao TY, Tzeng JK, Hsu RJ, Huang PH, Lu WC, Li PH, Wang MF. Potential antidepressant effects of a dietary supplement from the chlorella and lion's mane mushroom complex in aged SAMP8 mice. *Front Nutr* 2022; **9**: 977287 [PMID: 36118772 DOI: 10.3389/fnut.2022.977287]
 - 108 **Spina A**, Mazzarella C, Dallio M, Romeo M, Pellegrino R, Durante T, Romano M, Loguercio C, Di Mauro M, Federico A, Gravina AG. The Lesson from the First Italian Lockdown: Impacts on Anxiety and Depressive Symptoms and Sleep Quality in Patients with Remission of Inflammatory Bowel Disease. *Rev Recent Clin Trials* 2022; **17**: 109-119 [PMID: 35346015 DOI: 10.2174/1574887117666220328125720]
 - 109 **Barberio B**, Zamani M, Black CJ, Savarino EV, Ford AC. Prevalence of symptoms of anxiety and depression in patients with inflammatory bowel disease: a systematic review and meta-analysis. *Lancet Gastroenterol Hepatol* 2021; **6**: 359-370 [PMID: 33721557 DOI: 10.1016/S2468-1253(21)00014-5]
 - 110 **Ryu JE**, Kang SG, Jung SH, Lee SH, Kang SB. Psychological Effects and Medication Adherence among Korean Patients with Inflammatory Bowel Disease during the Coronavirus Disease 2019 Pandemic: A Single-Center Survey. *J Clin Med* 2022; **11** [PMID: 35683421 DOI: 10.3390/jcm11113034]
 - 111 **Pellegrino R**, Pellino G, Selvaggi F, Federico A, Romano M, Gravina AG. Therapeutic adherence recorded in the outpatient follow-up of inflammatory bowel diseases in a referral center: Damages of COVID-19. *Dig Liver Dis* 2022; **54**: 1449-1451 [PMID: 35973931 DOI: 10.1016/j.dld.2022.07.016]
 - 112 **Barbara G**, Cremon C, Bellini M, Corsetti M, Di Nardo G, Falangone F, Fuccio L, Galeazzi F, Iovino P, Sarnelli G, Savarino EV, Stanghellini V, Staiano A, Stasi C, Tosetti C, Turco R, Ubaldi E, Zagari RM, Zenzeri L, Marasco G. Italian guidelines for the management of irritable bowel syndrome: Joint Consensus from the Italian Societies of: Gastroenterology and Endoscopy (SIGE), Neurogastroenterology and Motility (SINGEM), Hospital Gastroenterologists and Endoscopists (AIGO), Digestive Endoscopy (SIED), General Medicine (SIMG), Gastroenterology, Hepatology and Pediatric Nutrition (SIGENP) and Pediatrics (SIP). *Dig Liver Dis* 2023; **55**: 187-207 [PMID: 36517261 DOI: 10.1016/j.dld.2022.11.015]

- 113 **Chumpitazi BP**, Kearns GL, Shulman RJ. Review article: the physiological effects and safety of peppermint oil and its efficacy in irritable bowel syndrome and other functional disorders. *Aliment Pharmacol Ther* 2018; **47**: 738-752 [PMID: 29372567 DOI: 10.1111/apt.14519]
- 114 **Currò D**, Ianiro G, Pecere S, Bibbò S, Cammarota G. Probiotics, fibre and herbal medicinal products for functional and inflammatory bowel disorders. *Br J Pharmacol* 2017; **174**: 1426-1449 [PMID: 27696378 DOI: 10.1111/bph.13632]
- 115 **Lu Q**, Tan D, Luo J, Ye Y, Zuo M, Wang S, Li C. Potential of natural products in the treatment of irritable bowel syndrome. *Phytomedicine* 2022; **106**: 154419 [PMID: 36087525 DOI: 10.1016/j.phymed.2022.154419]
- 116 **Liu JY**, Hou XX, Li ZY, Shan SH, Chang MC, Feng CP, Wei Y. Isolation and structural characterization of a novel polysaccharide from *Herichium erinaceus* fruiting bodies and its arrest of cell cycle at S-phase in colon cancer cells. *Int J Biol Macromol* 2020; **157**: 288-295 [PMID: 32339580 DOI: 10.1016/j.ijbiomac.2020.04.162]
- 117 **Giaginis C**, Georgiadou M, Dimakopoulou K, Tsourouflis G, Gatzidou E, Kouraklis G, Theocharis S. Clinical significance of MCM-2 and MCM-5 expression in colon cancer: association with clinicopathological parameters and tumor proliferative capacity. *Dig Dis Sci* 2009; **54**: 282-291 [PMID: 18465232 DOI: 10.1007/s10620-008-0305-z]
- 118 **Hou XX**, Liu JY, Li ZY, Chang MC, Guo M, Feng CP, Shi JY. Fruiting body polysaccharides of *Herichium erinaceus* induce apoptosis in human colorectal cancer cells via ROS generation mediating caspase-9-dependent signaling pathways. *Food Funct* 2020; **11**: 6128-6138 [PMID: 32573644 DOI: 10.1039/d0fo00916d]
- 119 **Kim SP**, Kang MY, Kim JH, Nam SH, Friedman M. Composition and mechanism of antitumor effects of *Herichium erinaceus* mushroom extracts in tumor-bearing mice. *J Agric Food Chem* 2011; **59**: 9861-9869 [PMID: 21846141 DOI: 10.1021/jf201944n]
- 120 **Sharif S**, Atta A, Huma T, Shah AA, Afzal G, Rashid S, Shahid M, Mustafa G. Anticancer, antithrombotic, antityrosinase, and anti- α -glucosidase activities of selected wild and commercial mushrooms from Pakistan. *Food Sci Nutr* 2018; **6**: 2170-2176 [PMID: 30510718 DOI: 10.1002/fsn3.781]
- 121 **Hills RD Jr**, Pontefract BA, Mishcon HR, Black CA, Sutton SC, Theberge CR. Gut Microbiome: Profound Implications for Diet and Disease. *Nutrients* 2019; **11** [PMID: 31315227 DOI: 10.3390/nu11071613]
- 122 **Yang Y**, Zhao C, Diao M, Zhong S, Sun M, Sun B, Ye H, Zhang T. The Prebiotic Activity of Simulated Gastric and Intestinal Digesta of Polysaccharides from the *Herichium erinaceus*. *Molecules* 2018; **23** [PMID: 30513668 DOI: 10.3390/molecules23123158]
- 123 **Diling C**, Chaoqun Z, Jian Y, Jian L, Jiyan S, Yizhen X, Guoxiao L. Immunomodulatory Activities of a Fungal Protein Extracted from *Herichium erinaceus* through Regulating the Gut Microbiota. *Front Immunol* 2017; **8**: 666 [PMID: 28713364 DOI: 10.3389/fimmu.2017.00666]
- 124 **Xie XQ**, Geng Y, Guan Q, Ren Y, Guo L, Lv Q, Lu ZM, Shi JS, Xu ZH. Influence of Short-Term Consumption of *Herichium erinaceus* on Serum Biochemical Markers and the Changes of the Gut Microbiota: A Pilot Study. *Nutrients* 2021; **13** [PMID: 33800983 DOI: 10.3390/nu13031008]
- 125 **Tan J**, McKenzie C, Potamitis M, Thorburn AN, Mackay CR, Macia L. The role of short-chain fatty acids in health and disease. *Adv Immunol* 2014; **121**: 91-119 [PMID: 24388214 DOI: 10.1016/B978-0-12-800100-4.00003-9]
- 126 **Sun M**, Wu W, Liu Z, Cong Y. Microbiota metabolite short chain fatty acids, GPCR, and inflammatory bowel diseases. *J Gastroenterol* 2017; **52**: 1-8 [PMID: 27448578 DOI: 10.1007/s00535-016-1242-9]
- 127 **Yang Y**, Ye H, Zhao C, Ren L, Wang C, Georgiev MI, Xiao J, Zhang T. Value added immunoregulatory polysaccharides of *Herichium erinaceus* and their effect on the gut microbiota. *Carbohydr Polym* 2021; **262**: 117668 [PMID: 33838836 DOI: 10.1016/j.carbpol.2021.117668]
- 128 **Dmitrieva-Posocco O**, Wong AC, Lundgren P, Golos AM, Descamps HC, Dohnalová L, Cramer Z, Tian Y, Yueh B, Eskiocak O, Egervari G, Lan Y, Liu J, Fan J, Kim J, Madhu B, Schneider KM, Khoziainova S, Andreeva N, Wang Q, Li N, Furth EE, Bailis W, Kelsen JR, Hamilton KE, Kaestner KH, Berger SL, Epstein JA, Jain R, Li M, Beyaz S, Lengner CJ, Katona BW, Grivennikov SI, Thaiss CA, Levy M. β -Hydroxybutyrate suppresses colorectal cancer. *Nature* 2022; **605**: 160-165 [PMID: 35477756 DOI: 10.1038/s41586-022-04649-6]
- 129 **Louis P**, Hold GL, Flint HJ. The gut microbiota, bacterial metabolites and colorectal cancer. *Nat Rev Microbiol* 2014; **12**: 661-672 [PMID: 25198138 DOI: 10.1038/nrmicro3344]
- 130 **Bultman SJ**. Interplay between diet, gut microbiota, epigenetic events, and colorectal cancer. *Mol Nutr Food Res* 2017; **61** [PMID: 27138454 DOI: 10.1002/mnfr.201500902]
- 131 **Louis P**, Flint HJ. Formation of propionate and butyrate by the human colonic microbiota. *Environ Microbiol* 2017; **19**: 29-41 [PMID: 27928878 DOI: 10.1111/1462-2920.13589]
- 132 **Mitsou EK**, Saxami G, Stamoulou E, Kerezoudi E, Terzi E, Koutrotsios G, Bekiaris G, Zervakis GI, Mountzouris KC, Pletsas V, Kyriacou A. Effects of Rich in B-Glucans Edible Mushrooms on Aging Gut Microbiota Characteristics: An In Vitro Study. *Molecules* 2020; **25** [PMID: 32570735 DOI: 10.3390/molecules25122806]
- 133 **Cho HW**, Choi S, Seo K, Kim KH, Jeon JH, Kim CH, Lim S, Jeong S, Chun JL. Gut microbiota profiling in aged dogs after feeding pet food contained *Herichium erinaceus*. *J Anim Sci Technol* 2022; **64**: 937-949 [PMID: 36287790 DOI: 10.5187/jast.2022.e66]
- 134 **Helmink BA**, Khan MAW, Hermann A, Gopalakrishnan V, Wargo JA. The microbiome, cancer, and cancer therapy. *Nat Med* 2019; **25**: 377-388 [PMID: 30842679 DOI: 10.1038/s41591-019-0377-7]
- 135 **Khan MAW**, Ologun G, Arora R, McQuade JL, Wargo JA. Gut Microbiome Modulates Response to Cancer Immunotherapy. *Dig Dis Sci* 2020; **65**: 885-896 [PMID: 32067144 DOI: 10.1007/s10620-020-06111-x]
- 136 **Tian B**, Liu R, Xu T, Cai M, Mao R, Huang L, Yang K, Zeng X, Peilong S. Modulating effects of *Herichium erinaceus* polysaccharides on the immune response by regulating gut microbiota in cyclophosphamide-treated mice. *J Sci Food Agric* 2023; **103**: 3050-3064 [PMID: 36546454 DOI: 10.1002/jsfa.12404]
- 137 **Wang D**, Zhu X, Tang X, Li H, Yizhen X, Chen D. Auxiliary antitumor effects of fungal proteins from *Herichium erinaceus* by target on the gut microbiota. *J Food Sci* 2020; **85**: 1872-1890 [PMID: 32460371 DOI: 10.1111/1750-3841.15134]
- 138 **Larussa T**, Abenavoli L, Fabiano G, Mancuso MA, Polimeni N, Dumitrascu DL, Luzzo F. Gut microbiota in inflammatory bowel disease: a target for therapy not to be missed. *Minerva Gastroenterol (Torino)* 2021; **67**: 357-368

- [PMID: 35040302 DOI: 10.23736/S2724-5985.21.02907-7]
- 139 **Wallace KL**, Zheng LB, Kanazawa Y, Shih DQ. Immunopathology of inflammatory bowel disease. *World J Gastroenterol* 2014; **20**: 6-21 [PMID: 24415853 DOI: 10.3748/wjg.v20.i1.6]
- 140 **Jandhyala SM**, Talukdar R, Subramanyam C, Vuyyuru H, Sasikala M, Nageshwar Reddy D. Role of the normal gut microbiota. *World J Gastroenterol* 2015; **21**: 8787-8803 [PMID: 26269668 DOI: 10.3748/wjg.v21.i29.8787]
- 141 **Wang WL**, Xu SY, Ren ZG, Tao L, Jiang JW, Zheng SS. Application of metagenomics in the human gut microbiome. *World J Gastroenterol* 2015; **21**: 803-814 [PMID: 25624713 DOI: 10.3748/wjg.v21.i3.803]
- 142 **Ren Z**, Xu Z, Amakye WK, Liu W, Zhao Z, Gao L, Wang M, Ren J. *Hericium erinaceus* mycelium-Derived Polysaccharide Alleviates Ulcerative Colitis and Modulates Gut Microbiota in Cynomolgus Monkeys. *Mol Nutr Food Res* 2023; **67**: e2200450 [PMID: 36443636 DOI: 10.1002/mnfr.202200450]
- 143 **Yu AT**, Shapiro K, Beneri CA, Wilks-Gallo LS. *Streptococcus lutetiensis* neonatal meningitis with empyema. *Access Microbiol* 2021; **3**: 000264 [PMID: 34712909 DOI: 10.1099/acmi.0.000264]
- 144 **Shao S**, Wang D, Zheng W, Li X, Zhang H, Zhao D, Wang M. A unique polysaccharide from *Herichium erinaceus* mycelium ameliorates acetic acid-induced ulcerative colitis rats by modulating the composition of the gut microbiota, short chain fatty acids levels and GPR41/43 receptors. *Int Immunopharmacol* 2019; **71**: 411-422 [PMID: 31059977 DOI: 10.1016/j.intimp.2019.02.038]
- 145 **Kim MH**, Kang SG, Park JH, Yanagisawa M, Kim CH. Short-chain fatty acids activate GPR41 and GPR43 on intestinal epithelial cells to promote inflammatory responses in mice. *Gastroenterology* 2013; **145**: 396-406.e1 [PMID: 23665276 DOI: 10.1053/j.gastro.2013.04.056]
- 146 **Kishi M**, Hirai F, Takatsu N, Hisabe T, Takada Y, Beppu T, Takeuchi K, Naganuma M, Ohtsuka K, Watanabe K, Matsumoto T, Esaki M, Koganei K, Sugita A, Hata K, Futami K, Ajioka Y, Tanabe H, Iwashita A, Shimizu H, Arai K, Suzuki Y, Hisamatsu T. A review on the current status and definitions of activity indices in inflammatory bowel disease: how to use indices for precise evaluation. *J Gastroenterol* 2022; **57**: 246-266 [PMID: 35235037 DOI: 10.1007/s00535-022-01862-y]
- 147 **Lamb CA**, Kennedy NA, Raine T, Hendy PA, Smith PJ, Limdi JK, Hayee B, Lomer MCE, Parkes GC, Selinger C, Barrett KJ, Davies RJ, Bennett C, Gittens S, Dunlop MG, Faiz O, Fraser A, Garrick V, Johnston PD, Parkes M, Sanderson J, Terry H; IBD guidelines eDelphi consensus group, Gaya DR, Iqbal TH, Taylor SA, Smith M, Brookes M, Hansen R, Hawthorne AB. British Society of Gastroenterology consensus guidelines on the management of inflammatory bowel disease in adults. *Gut* 2019; **68**: s1-s106 [PMID: 31562236 DOI: 10.1136/gutjnl-2019-318484]

Machine perfusion and the prevention of ischemic type biliary lesions following liver transplant: What is the evidence?

Manuel Durán, Rafael Calleja, Angus Hann, George Clarke, Ruben Ciria, Anisa Nutu, Rebeca Sanabria-Mateos, María Dolores Ayllón, Pedro López-Cillero, Hynek Mergental, Javier Briceño, M Thamara P R Perera

Specialty type: Gastroenterology and hepatology

Provenance and peer review: Invited article; Externally peer reviewed.

Peer-review model: Single blind

Peer-review report's scientific quality classification

Grade A (Excellent): 0
Grade B (Very good): B, B
Grade C (Good): 0
Grade D (Fair): 0
Grade E (Poor): 0

P-Reviewer: Dabbous H, Egypt; Xu X, China

Received: January 26, 2023

Peer-review started: January 26, 2023

First decision: February 16, 2023

Revised: March 1, 2023

Accepted: April 28, 2023

Article in press: April 28, 2023

Published online: May 28, 2023



Manuel Durán, Rafael Calleja, Ruben Ciria, María Dolores Ayllón, Pedro López-Cillero, Javier Briceño, Department of Liver Transplantation, Reina Sofía University Hospital, Córdoba 14004, Spain

Angus Hann, George Clarke, Anisa Nutu, Rebeca Sanabria-Mateos, Hynek Mergental, M Thamara P R Perera, The Liver Unit, Queen Elizabeth Hospital Birmingham, Birmingham B15 2TH, United Kingdom

Angus Hann, George Clarke, Hynek Mergental, M Thamara P R Perera, Centre for Liver and Gastrointestinal Research, Institute of Immunology and Immunotherapy, University of Birmingham, Birmingham B15 2TH, United Kingdom

Corresponding author: M Thamara P R Perera, FEBS, FRCS, MBBS, MD, MS, Chairman, Professor, Surgeon, The Liver Unit, Queen Elizabeth Hospital Birmingham, Mindelsohn Way, Birmingham B15 2TH, United Kingdom. thamara.perera@uhb.nhs.uk

Abstract

The widespread uptake of different machine perfusion (MP) strategies for liver transplant has been driven by an effort to minimize graft injury. Damage to the cholangiocytes during the liver donation, preservation, or early posttransplant period may result in stricturing of the biliary tree and inadequate biliary drainage. This problem continues to trouble clinicians, and may have catastrophic consequences for the graft and patient. Ischemic injury, as a result of compromised hepatic artery flow, is a well-known cause of biliary strictures, sepsis, and graft failure. However, very similar lesions can appear with a patent hepatic artery and these are known as ischemic type biliary lesions (ITBL) that are attributed to microcirculatory dysfunction rather than main hepatic arterial compromise. Both the warm and cold ischemic period duration appear to influence the onset of ITBL. All of the commonly used MP techniques deliver oxygen to the graft cells, and therefore may minimize the cholangiocyte injury and subsequently reduce the incidence of ITBL. As clinical experience and published evidence grows for these modalities, the impact they have on ITBL rates is important to consider. In this review, the evidence for the three commonly used MP strategies (abdominal normothermic regional perfusion [A-NRP], hypothermic oxygenated perfusion [HOPE], and normothermic machine perfusion [NMP] for ITBL prevention has been critically reviewed. Inconsistencies with ITBL definitions used in trials, coupled with variations in techniques of MP, make interpretation challenging.

Overall, the evidence suggests that both HOPE and A-NRP prevent ITBL in donated after circulatory death grafts compared to cold storage. The evidence for ITBL prevention in donor after brain death grafts with any MP technique is weak.

Key Words: Liver transplant; Ischemic type biliary lesions; Hypothermic oxygenated machine perfusion; Normothermic machine perfusion; Abdominal normothermic regional perfusion; Donation after circulatory death

©The Author(s) 2023. Published by Baishideng Publishing Group Inc. All rights reserved.

Core Tip: In recent years, the development of different machine perfusion (MP) strategies has generated interest in their use for both the assessment of grafts and optimization during the preservation period. The different mechanisms behind the diverse array of MP strategies may reduce the extent of cholangiocyte and may have the subsequent clinical effect of preventing the development of ischemic type biliary lesions (ITBL). This review summarizes the strength and limitations of clinical studies that have been undertaken, their results, and provides a summary of the available literature on MP and the prevention of ITBL.

Citation: Durán M, Calleja R, Hann A, Clarke G, Ciria R, Nutu A, Sanabria-Mateos R, Ayllón MD, López-Cillero P, Mergental H, Briceño J, Perera MTPR. Machine perfusion and the prevention of ischemic type biliary lesions following liver transplant: What is the evidence? *World J Gastroenterol* 2023; 29(20): 3066-3083

URL: <https://www.wjgnet.com/1007-9327/full/v29/i20/3066.htm>

DOI: <https://dx.doi.org/10.3748/wjg.v29.i20.3066>

INTRODUCTION

In recent decades, liver transplantation has made several forward strides. These have been in the area of surgical technique, immunosuppressive drug strategies, treatment and prevention of recurrent viral infections, and the increasing use of alternative preservation techniques. Consequently, recipient and graft survival are greater than 90% at 1 year and long-term survival is considered the norm[1]. A longstanding problem that liver transplantation has faced is the mismatch between the number of donors and the higher number of patients listed for transplant. This has led to long waiting lists for a graft, and up to 20% of patients do not survive until transplantation[2,3]. Furthermore, the recent expansion of transplant indications to include certain oncological scenarios may further aggravate this issue[4]. As a response to this shortage in supply, living donor liver transplantation and using more marginal organs, including those donated after circulatory death (DCD) are strategies that have been used to increase the donor pool[5]. Improving long-term graft survival is vital, as the need for retransplantation creates additional demand on a scarce resource.

Adequate biliary drainage is paramount for the success of a liver transplant, and was previously labeled the 'Achilles heel' of this procedure[6]. Although vascular complications have the largest impact on short-term graft outcomes, biliary complications are the main source of long-term morbidity. These conditions often require costly interventions, cause suffering, and adversely affect patients' quality of life[7]. The incidence of these complications is increasing as a result of the growing utilization of extended criteria donor organs, mainly from DCD donors[8].

In recent years, the development of numerous machine perfusion (MP) strategies has generated interest in their use for both the assessment of grafts and optimization during the preservation period [9]. Different techniques of MP have been described and vary in their application, with *in situ* MP occurring during organ procurement while the graft is within the donor and *ex situ* MP which occurs after the donor hepatectomy is completed. Both hepatocytes and cholangiocytes are vulnerable to ischemia-reperfusion injury (IRI), and injury to the latter during organ procurement and preservation lies behind the pathogenesis for biliary dysfunction[10]. Consequently, a current trend of research in the MP field is focused on how these different MP perfusion regimens influence post-transplant biliary complications and more specifically, ischemic type biliary lesions (ITBL).

This narrative literature review describes the strength and limitations of clinical studies that have been undertaken, their results, and provides a summary of the available literature on MP and the prevention of ITBL.

Nonanastomotic biliary strictures and ischemic type biliary lesions

Postliver transplantation biliary complications can comprise one (or both) of the following entities; strictures (anastomotic and non-anastomotic), and biliary leaks[11]. Anastomotic biliary strictures occur

at the site of biliary reconstruction and the surgical technique, and/or local tissue ischemia likely play a role. These strictures are usually managed with endoscopic or radiological procedures, however surgical revision may be required depending on the timing and type of anastomosis[12]. Nonanastomotic strictures (NAS), as the name implies, occur at a site away from the anastomosis and are most common within the initial 12 mo posttransplant. NAS are one of most feared late complications due to it being associated with high rates of graft loss and mortality, and minimal treatment options except re-transplantation[8,13].

NAS is characterized by diffuse fibrotic strictures and dilatation of the biliary tree at any location from the liver periphery to the main extrahepatic ducts (Figure 1). In addition, with the disease evolution, the formation of biliary casts and intrahepatic bilomas may occur in its severest form[14]. The radiological manifestations of NAS are highly variable and range from a peripheral abscess, individual or multiple strictures around the hilum and first order biliary branches, to vanishing ducts seen along the entire biliary tree[15]. NAS can occur as a direct result of ischemia from an identifiable hepatic artery stenosis or thrombosis (HAT). However, very similar lesions can develop in the setting of an entirely patent hepatic artery and this specific situation is termed ITBL, given its similarity to an actual ischemic cholangiopathy (Figure 1).

In a seminal paper by authors from Groningen which excluded patients with HAT, ITBL was classified according to the affected area of the biliary tree[16]. In this study, they demonstrated that the anatomical location of ITBL varied between those that presented early (< 1 year) as opposed to late (> 1 year). In those presenting late, the peripheral liver (zone D) was involved more frequently and there was an association with immunological risk factors. By contrast, patients with an early presentation had lesions around the bifurcation and the common bile duct (zone A). This early group had a longer period of both cold and warm ischemia; therefore, hypoxia is thought to be one of the underlying mechanisms. More recently, a United States group from the Mayo Clinic proposed a radiologic classification of ITBL into four distinct patterns that correlate with a distinct natural evolution and prognosis[17]. In this case, those patients with diffuse necrosis and multifocal progressive patterns experienced more episodes of cholangitis and almost all required stents and eventual retransplant.

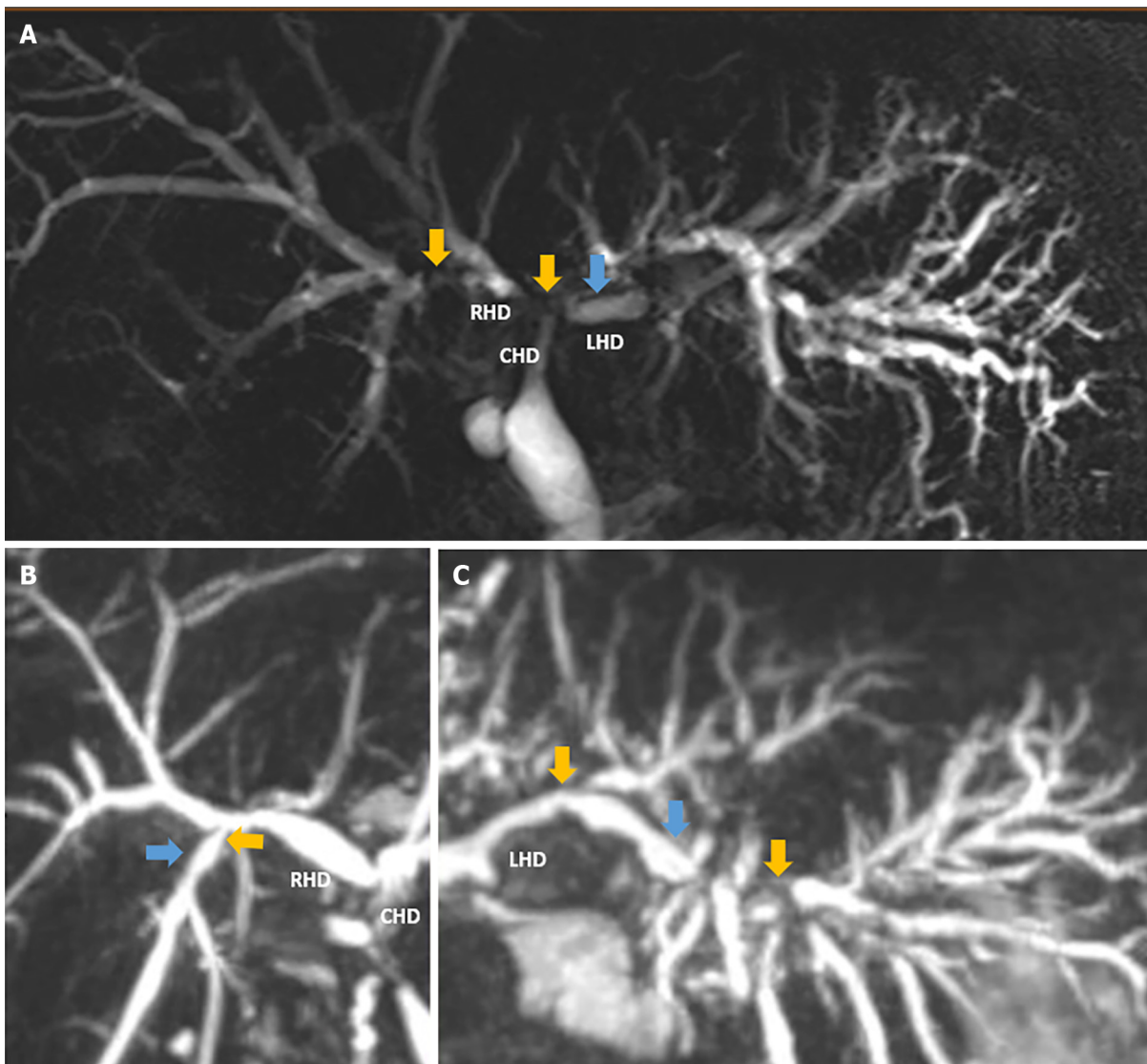
Multiple factors have been associated with ITBL development and are generally divided into three categories: ischemia-related injury; bile salt mediated injury; and immune-mediated injury[18,19]. The cold ischemia time (CIT) and donor warm ischemia time (dWIT), and inadequate microvasculature preservation predispose cholangiocytes to a subsequent IRI[10,18]. The increased incidence of ITBL in DCD grafts, which are characterized by a period of dWIT is well established, with ITBL rates of up to 39% following controlled DCD liver transplantation[13,20,21]. The toxic effect of bile salts on cholangiocytes at low temperatures during preservation is well known. Certain bile acids have been shown to promote the secretion of inflammatory mediators, and others are directly cytotoxic to cholangiocytes [22]. In addition, new bile after implantation and its altered bile salt/phospholipid ratio have detrimental effects on biliary epithelium and induce NAS[23-25]. An immune-mediated component to the cholangiocyte injury has also been proposed due to several clinical associations, but the mechanism remains under investigation. ITBL has been demonstrated in association with ABO incompatibility, recurrence of immune-mediated liver diseases, cytomegalovirus infection, presence of C-C chemokine receptor type 5, polymorphism, and acute or chronic rejection[18].

The pathogenesis of ITBL is multifactorial. Both the cold and warm ischemic periods induce the formation of reactive oxygen species (ROS). These ROS are generated as a result of Kupffer and polymorphonuclear cells activation, mitochondrial permeability transition production, oxidative changes in the structure of the biliary canaliculus and adenosine triphosphate adenosine triphosphate (ATP) depletion. These all lead to the apoptosis and/or necrosis of the cholangiocytes. This mechanism is interrelated with the cytotoxic effect of bile salts, the cholestasis status induced by ischemia-reperfusion and different immune-mediated mechanisms, which all further propagate the biliary injury. Appropriate donor selection, the use of preservation fluids and MP are just some of the strategies which are thought to prevent this condition[26].

The different mechanisms behind the diverse array of MP strategies may reduce the extent of cholangiocyte injury during the transplantation process, in comparison with static cold storage (SCS). This may have the subsequent clinical effect of preventing the development of ITBL. The number of clinical studies on MP strategies continues to increase. With only a few exceptions, the primary outcomes focus mainly on graft and patient survival. In this review, we focus on the available clinical evidence for abdominal normothermic regional perfusion (A-NRP), and *ex situ* hypothermic oxygenated perfusion (HOPE), and normothermic MP (NMP) in relation to the outcome of ITBL.

PREVENTION OF ITBL VIA MP

The incidence of ITBL posttransplant varies considerably between institution and nations. These differences likely relate to the type of organ donation permitted, ranging from donor after brain death (DBD) donors only in some parts of the world, to uncontrolled DCD donors in others. Different national laws regarding the donor age and the 'no-touch' period following asystole in DCD donors likely



DOI: 10.3748/wjg.v29.i20.3066 Copyright ©The Author(s) 2023.

Figure 1 Magnetic resonance cholangiopancreatography reconstruction images of ischemic type biliary lesions in donated after circulatory death graft recipients. A: Significant structuring and confluence of right and left ducts, in addition to the right posterior duct (yellow arrows). Upstream dilation on left indicated by blue arrow; B: Structuring at a second order duct on the right (yellow arrow) with upstream dilation; C: Strictures in periphery of left biliary system. Figure created with biorender.com, accessed on January 2023. LHD: Left ducts; RHD: Right ducts; CHD: Common hepatic duct.

influences outcome, and these matters also complicate the results and interpretation of clinical trials on MP. In addition, it should be noted that the lack of clear and consistent definitions of ITBL in the currently available literature makes the assessment of the true impact challenging. Many studies either do not differentiate between anastomotic, ischemic NAS and ITBL; furthermore they may include both symptomatic and nonsymptomatic cases[27]. With these limitations in mind, a literature search was performed in October 2022 using PUBMED®, Embase®, and Medline®. Publications were restricted to those in English, however no further search filters were applied. The following search terms were used (in different combinations with Boolean operators): Liver, transplant, biliary stricture, ITBL, MP, machine preservation, normothermic, hypothermic, and NRP. Both prospective and retrospective studies were included if they included outcome data pertaining to biliary strictures. Studies without a control (or comparator) group were excluded. A pooled analysis was not performed due to a significant variation in study methodology, MP application technique, and outcome definitions. Institutional ethical approval was not required.

A-NRP and ITBL

A-NRP is an *in situ* preservation technique using an extracorporeal oxygenated membrane, restoring the perfusion of abdominal organs after the donor is declared deceased. This technique may lead to a reduction in the dWIT depending on the timing of cannulation; however, it provides a period of resuscitation immediately after the cellular injury incurred from the dWIT. The provision of near physiological conditions during A-NRP provides a period in which cells can recover their energy stores,

therefore they tolerate the CIT with minimal additional injury. It can also provide information about graft viability and reduce the effects of the IRI process[28].

In recent years, countries such as Spain, France, United Kingdom, and Italy have developed different A-NRP protocols as a strategy to improve the outcomes of DCD grafts[29-33]. These protocols differ in the liver viability criteria utilized “no-touch” periods required, pre-mortem substance administration, and vessel cannulation. All countries aforementioned have a mandatory no-touch period of 5 min except Italy, which requires 20 min. This inevitably lengthens the dWIT. Sedative analgesia administration is not allowed in the United Kingdom, in contrast to other countries. In Spain, pre-mortem cannulation is allowed while in Italy and France only the identification of femoral vessels to ease cannulation is permitted. The obvious benefit of pre-mortem cannulation is that it minimizes the dWIT and could achieve better outcomes as a result[34]. During A-NRP, certain viability parameters are measured, the most common among the different protocols are transaminase levels. Despite transaminase levels being widely accepted, it only reflects hepatocyte injury and not cholangiocytes. Other viability criteria employed include A-NRP duration[31], lactate clearance[30], and/or the presence of macrosteatosis[30,31]. However, some of these parameters are considered controversial[28].

To date, there has been no randomized controlled trial (RCT) comparing A-NRP to the standard retrieval method, known as the super rapid retrieval (SRR) technique. The clinical studies investigating A-NRP that include a comparator group, and provide data on biliary strictures are summarized in Table 1. The definition of ITBL used in these studies is relatively homogeneous as most authors have considered ITBL to have occurred when NAS developed in the context of a patent hepatic artery. However, two studies did not include an ITBL definition[35,36] and two authors[31,37] considered NAS regardless of the presence of concomitant HAT. Other limitations of these studies include variation in the A-NRP protocols, small sample size, and variability in follow-up periods. These trials can be put into three categories, according to the comparator groups: DCD-A-NRP *vs* DBD-SCS; DCD-A-NRP *vs* DCD-SRR; and DCD-A-NRP *vs* DCD with other MP.

In the first group of studies[31,35,38-40] that compared DCD-NRP-A grafts *vs* DBD-SCS grafts, these authors aimed to demonstrate that DCD grafts after NRP could have similar results of DBD grafts and therefore should not be considered marginal. These studies showed a similar incidence of ITBL between both groups, and the results in regard to early allograft dysfunction were promising. However, they had small sample sizes[35,38,39], differences in follow-up periods[31,35,38,39], and a high proportion of uncontrolled DCD donors[38]. Other authors have assessed the outcomes of DCD NRP grafts *vs* DCDs grafts recovered by *via* the SRR technique and subsequent SCS[33,34,36,41]. Watson *et al*[33] compared two groups, DCD-A-NRP ($n = 43$) *vs* DCD-SRR ($n = 187$), and reported both early allograft dysfunction and biliary complication rates. A significantly lower rate of early allograft dysfunction (12% *vs* 32%) and ischemic cholangiopathy (IC) (0% *vs* 27%) occurred in the DCD-A-NRP group. Similar comparisons have been performed by Spanish transplant groups. Muñoz *et al*[36] did not demonstrate significant differences in their cohort, probably due to the short follow-up period in the A-NRP group and the low number of patients. However, Hessheimer *et al*[41] subsequently found an ITBL incidence of 2% in the NRP group ($n = 95$) *vs* 13% in the SRR group ($n = 117$). These findings were repeated in a second study [34] with a larger sample size (545 NRP *vs* 258 SRR). In this second study the ITBL incidence was 1% *vs* 9% in favor of A-NRP, and this is at present the largest cohort of patients with A-NRP with pre-mortem cannulation in the literature. Recently, Schurink *et al*[42] have reported the safety of NRP to rescue DCD grafts that were declined by the Eurotransplant region for transplantation, with no differences in primary nonfunction or IC compared to DBD and standard, non-NRP DCD grafts[42].

Finally, other authors[37,43-45] have compared A-NRP with *ex situ* preservation techniques such as NMP or HOPE. However, in many of these trials, accurate data on ITBL are lacking. The only study comparing HOPE *vs* NRP was conducted by Muller *et al*[37]. These authors reported the incidence of NAS regardless of hepatic artery status, rather than ITBL specifically. The rate of NAS was reported to be 6.3% in the NRP group and 12.5% in the HOPE group, but was not significantly different. DCD grafts that underwent A-NRP have been compared to DCD grafts undergoing *ex situ* NMP in a study by Gaurav *et al*[44]. This study showed significantly lower rates of ITBL in the NRP group (6.3% *vs* 12.5%) after propensity score matching (PSM)[44]. However, in another study that used PSM analysis[45] (34 NMP *vs* 68 NRP), there were no significant differences in the ITBL rate of both groups (2.9% NRP *vs* 8.8% NMP). In this latter study, NMP was applied at source as opposed to the study by Gaurav *et al* [44], which applied it at the recipient hospital in the majority of cases[44].

A-NRP is a widely used *in situ* perfusion technique that has improved outcomes and graft utilization in DCD grafts. Protocol aspects such as the “no-touch” period or pre-mortem cannulation may impact in these results, due to its association with WIT. Despite the differences between the protocols adopted in different countries, NRP has still achieved superior outcomes in comparison to SRR in regards to ITBL.

HOPE and ITBL

Hypothermic MP (HMP) was first introduced in clinical practice in 2010 by Guarrera *et al*[46], who demonstrate in their pilot case-controlled series that it was a feasible and safe preservation method[46]. Subsequently, in preclinical studies that investigated the active oxygenation of the hypothermic perfusate over a short period, it demonstrated restored mitochondrial integrity. This indicated a reduction of oxygen free radicals and damage-associated molecular patterns after transplantation[47-

Table 1 Clinical studies assessing the impact of abdominal normothermic regional perfusion on ischemic type biliary lesions after liver transplantation

Ref.	Study design	Groups (n)	Control group	NRP protocol and viability criteria	Definition of ITBL	Follow up	ITBL in intervention (DCD NRP)	ITBL in control (DCD)	ITBL in control (DBD)
Schurink <i>et al</i> [42], 2022	Cohort	NRP ¹ (20) <i>vs</i> DCD (49) <i>vs</i> DBD (81)	DCD/DBD	Dutch protocol ²	Symptomatic radiologically NAS without the presence of a HAT	Median-NRP 23 mo, DCD 25 mo and DBD 26 mo	1/15 (7%); 1/5 (20%) ³	8/30 (26%)	6/78 (7%)
Mohkam <i>et al</i> [45], 2022	Cohort	NRP (157) <i>vs</i> NMP (34)	DCD	France protocol ⁴	NAS that were unrelated to any hepatic artery complications	Median-NRP 22 mo; NMP 24 mo	2/68 (2.9%) ⁵	3/34 (8.8%) ⁵	NA
Gaurav <i>et al</i> [44], 2022	Cohort	NRP (69) <i>vs</i> NMP (67) <i>vs</i> SCS (97)	DCD	United Kingdom protocol ⁶	Presence of any biliary stricture, dilatation, or irregularity of the intra- or extrahepatic bile ducts and/or cast on MRCP away from the biliary anastomosis in the presence of patent arterial vasculature	Median-54 mo (SCS), 28 mo (NRP) and 24 mo (NMP)	0/69 (0%) ⁷	7/67 (11%) ⁷ NMP and 12/97 (14%) ⁷ SCS	NA
Hessheimer <i>et al</i> [34], 2022	Cohort	NRP (545) <i>vs</i> SRR (258)	DCD	Spain protocol ⁸	Patient with patent hepatic artery, signs or symptoms of cholestasis, and direct or indirect cholangiographic imaging reflecting strictures of the intra- and/or extrahepatic biliary tree proximal to the transplant anastomosis	Median-31 mo	6/545 (1%)	24/258 (9%)	NA
Ruiz <i>et al</i> [40], 2021	Cohort	NRP (100) <i>vs</i> DBD (200)	DBD	Spain protocol ⁸	Non-anastomotic biliary stricture in the presence of a patent hepatic artery and confirmed based on cholangiographic evidence (T-tube cholangiogram or magnetic resonance)	Mean-36 mo	0/100 (0%)	NA	0/200 (0%)
Muñoz <i>et al</i> [36], 2020	Cohort	NRP (23) <i>vs</i> SRR (22)	DCD	Spain protocol ⁸	NR	Mean-33.9 mo (SRR) and 14.2 mo (NRP)	0/23 (0%)	3/22 (13.6%)	NA
Savier <i>et al</i> [31], 2020	Cohort	NRP (50) <i>vs</i> DBD (100)	DBD	France protocol ⁴	Presence of any disseminated biliary stricture on magnetic resonance and endoscopic retrograde cholangiopancreatography, regardless of the presence or absence of arterial thrombosis or stenosis	Mean-34.8 mo (cDCD NRP) and 51.7 mo (DBD)	1/50 (2%)	NA	1/100 (1%)
Miñambres <i>et al</i> [35], 2020	Cohort	NRP (16) <i>vs</i> DBD (29)	DBD	Spain protocol ⁸	NR	Median-6 mo (cDCD) and 16 mo (DBD)	0/16 (0%)	NA	0/29 (0%)
De carlis <i>et al</i> [43], 2021	Cohort	DCD NRP + D-HOPE (37) <i>vs</i> DCD SRR SCS (37)	DCD	Italy protocol ⁹	Cholangiographic evidence of diffuse intrahepatic, hilar, or extrahepatic biliary strictures in the presence of a patent hepatic artery. Isolated anastomotic strictures were excluded from IC	Median-17 mo (NRP + D-HOPE) and all transplants were followed at least 1 yr	1/37 (3%)	3/37 (8%)	NA
Muller <i>et al</i> [37], 2020	Cohort	NRP (132) <i>vs</i> HOPE (93)	DCD	France protocol ⁴	NAS was defined as either multifocal, unifocal intrahepatic, or hilar strictures with or without the presence of concomitant HAT or arterial complications. NAS was detected clinically and confirmed by magnetic resonance cholangiography	Median-20 mo (NRP) and 28 mo (HOPE)	2/32 (6.3%) ⁵	4/32 (12.5%) ⁵	NA
Hessheimer <i>et al</i> [41], 2019	Cohort	NRP (95) <i>vs</i> SRR (117)	DCD	Spain protocol ⁸	Cholestasis and confirmed based on cholangiographic evidence (typically coming from magnetic resonance cholangiopancreatography) of diffuse non-anastomotic biliary strictures, with or without prestenotic dilatations, in the presence of a patent hepatic artery	Median-20 mo	2/95 (2%)	15/117 (13%)	NA
Rodríguez-	Cohort	NRP (11) <i>vs</i> DBD	DBD	Spain	Diffuse stenosis of the intrahepatic biliary tree-suspected by jaundice,	Ranges between 7-27	2/11 (13.3%)	NA	13/51 (27.7%)

Sanjuán <i>et al</i> [39], 2019	(51)	protocol ⁸			cholangitis, abnormal biochemical liver test, or abnormal findings on ultrasound or T-tube cholangiography- provided there is no hepatic artery thrombosis	mo. Minimum follow-up of 3 mo			
Watson <i>et al</i> [33], 2019	Cohort	NRP (43) vs SRR (187)	DCD	United Kingdom protocol ⁶	Presence of any non-anastomotic biliary stricture on ERCP or MRCP in the absence of arterial thrombosis or stenosis	Up to 5 yr of follow-up	0/42 (0%)	47/171 (27%)	NA
De Carlis <i>et al</i> [38], 2018	Cohort	NRP (20) vs DBD ECMO SCS (17) vs DBD non-ECMO SCS (52)	DBD-ECMO DBD-non-ECMO	Italy protocol ⁹	Strictures, irregularities, or dilatations of the intrahepatic bile duct. Isolated anastomotic biliary strictures were not included in the definition of IC. The diagnosis of IC was confirmed with at least 1 adequate imaging study of the biliary tree, and concomitant hepatic artery thrombosis was excluded by Doppler ultrasound or computed tomography	Median-14 mo (cDCD), 20 mo (DBD-ECMO) and 17 mo (DBD-non-ECMO)	2/20 (10%)	NA	DBD-ECMO 0/17 0%; DBD-non-ECMO 2/52 (4%)

¹For logistic reasons, 5 patients received additional consecutive dual hypothermic machine perfusion (DHOPE) anticipating a longer cold ischemia time (CIT) due to difficulties in recipient hepatectomy.

²Viability criteria used: Assessment 60 min of perfusion, with stable alanine transaminase (ALT) levels < 200 U/L, a plasma glucose peak > 10 mmol/L, and decreasing lactate level, around < 5 mmol/L. Adequate bile quality was defined as a pH > 7.45 and glucose < 3.0 mmol/L. Macroscopy of the liver did not influence. Postmortem cannulation. 5 No touch period. No antemortem interventions are allowed in Netherlands.

³Normothermic Regional Perfusion (NRP) + DHOPE patients.

⁴Viability criteria used: (1) serum ALT < 1000 IU/L at the end of NRP; (2) macroscopic appearance; (3) decrease in lactate levels; and (4) presence of macrosteatosis < 30% or fibrosis Ishak score < 2; Ante mortem cannulation not allowed but identification of femoral vessels to facilitate cannulation is permitted; No touch period: 5 min; Ante mortem substances administration allowed.

⁵After propensity score matching.

⁶Viability criteria used: (1) ALT levels stabilized between the first and second hour; and (2) macroscopic appearance. Ante mortem cannulation not allowed; No touch period: 5 min; Ante mortem substances administration not allowed.

⁷Clinically significant nonanastomotic biliary strictures defined as strictures requiring endoscopic or/and surgical intervention.

⁸Viability criteria used: (1) Baseline aspartate aminotransferase (AST) and ALT < 3-4 times normal value and/or AST and ALT < 4-5 times normal value at the end of NRP; and (2) macroscopic appearance; Ante mortem cannulation allowed; No touch period: 5 min; Ante mortem substances administration allowed.

⁹Viability criteria used: (1) AST and ALT > 200 IU/L; (2) macrosteatosis < 20%; and (3) More than 60 min of NRP; Ante mortem cannulation not allowed but identification of femoral vessels to facilitate cannulation is permitted; No touch period: 20 min; Ante mortem substances administration allowed.

BS: Biliary strictures; DBD: Donor after Brain Death; DCD: Donated after circulatory death; ERCP: Endoscopic retrograde cholangiopancreatography; HA: Hepatic artery; HAT: Hepatic artery thrombosis; ITBL: Ischemic type biliary lesions; MRCP: Magnetic resonance cholangiopancreatography; NAS: Nonanastomotic biliary strictures; NR: Not reported; NRP: Normothermic Regional Perfusion; SRR: Super rapid retrieval technique.

49]. Clinical studies have also reported promising results in preventing biliary complication and graft function compared to standard SCS[50,51].

HOPE is employed as an end-ischemic treatment after SRR or standard procurement in the case of DCD and DBD livers respectively, followed by a variable period of SCS. The devices available are not portable and HOPE needs to be applied at the recipient hospital. Its use limits the CIT and extends graft preservation time, avoiding the damage associated with extended periods of preservation. Two main perfusion strategies are currently employed which combine hypothermia with a highly oxygenated perfusate: (1) Single HOPE or 'HOPE', which consists of single perfusion through the portal vein; and (2) dual or 'D-HOPE' consisting of dual perfusion through the portal vein and the hepatic artery[15,52]. Currently, there are no clinical studies comparing the two strategies, although preclinical studies performed on pigs did not find differences regarding the preservation of hepatobiliary or endothelial function when comparing both strategies[53]. Advocates of D-HOPE emphasize that dominant vasculature of the bile ducts comes from arterial supply and single portal perfusion may not provide optimal preservation of the biliary tree. On the other hand, many argue the potential risk of mechanical damage to the hepatic artery intima that may occur during cannulation could cause a higher incidence of acute HAT following liver transplant[51]. Researchers from Zurich have proposed methods for liver

graft assessment during HOPE using real-time quantification of flavin mononucleotide (FMN) in the perfusate[54]. FMN is a molecule part of complex I of the mitochondrial respiratory chain[37]. Its concentration is determined by fluorescence spectroscopy and levels in perfusate correlate with graft function, complications, and graft survival in DCD livers[54].

The available studies on the use of HOPE as a preservation method, with a control group and reporting data on biliary strictures are summarized in Table 2. At present, these include four RCTs and five retrospective cohort studies with an appropriate control group of SCS grafts, and a single study comparing HOPE against NRP. The influence of HOPE on ITBL prevention has been studied only to a limited extent because in the majority, the primary endpoint was not related to biliary complications.

The relationship between ITBL and DCD livers is well established[20]. However, only 4/10 published cohort studies and 1 RCT have studied the influence of HOPE on DCD graft outcomes[51,52,55]. Thus, most published studies included only DBD livers so there is little or no ITBL incidence, and are not powered for this endpoint[56-60]. The most relevant study on ITBL prevention by *ex situ* MP was the multicenter clinical trial led by the Groningen group[52]. This European trial had symptomatic NAS within 6 mo after transplantation as the primary outcome. The study included a clear definition of NAS, which included the presence of a patent hepatic artery and therefore the NAS in this study were all ITBL. The authors demonstrated that two hours of end-ischemic D-HOPE led to a lower risk of symptomatic NAS after liver transplantation of grafts from DCD donors. NAS occurred in 5/78 (6%) of the patients in the HOPE group compared to 14/78 (18%) of SCS grafts with 2 patients from the SCS group requiring a retransplant because of severe NAS. Furthermore, the D-HOPE group showed a reduction by a factor of almost four in treatment interventions required for NAS.

Trials published by Italian and German groups have reported the efficacy of HOPE for the prevention of complications and a shorter intensive care unit stay[56,57]. There was no mention of ITBL in both trials, and grafts studied were from DBD donors so one could assume that most of the biliary complications were from an anastomotic origin. While the primary endpoint in the German[57] study was the peak alanine transaminase within 1 wk after transplantation and demonstrated a 47% reduction in the serum peak of this enzyme in the HOPE group, the authors did not find any difference in biliary complication rate (4/23, 17% vs 26% 6/23). A trial[56] demonstrated benefits of HOPE, with a reduction in EAD and better graft survival rates. This study did provide a clear definition of biliary complications, although reported a rate of biliary complication different from bile leak of 5/55 (9%) in the HOPE group compared to 6/55 (11%). Two patients in each group (4%) had biliary strictures, but it was unclear if these were ITBL. A recent multicenter trial on DBD livers from the Zurich group[61] reported the effects of HOPE on preventing postoperative complications. Although the primary endpoint was not reached, and the proportion of patients with at least one Clavien³ III complication did not differ, findings suggested that HOPE may decrease the risk of severe liver graft related events. The study did not include a clear definition of NAS and state if hepatic artery patency was required. In this study the NAS incidence was 1/85 (1.2%) in the HOPE group compared to 3/85 (3.5%) in the SCS group.

The only study comparing A-NRP and HOPE for liver grafts from DCD donors included an A-NRP cohort from six high-volume French centers and the HOPE cohort from the Zurich group[37]. In the A-NRP cohort, femoral artery cannulas were introduced post-mortem after a “no-touch” period of 5 min. NAS was defined as strictures with or without the presence of concomitant HAT or arterial complications and both groups showed similar rates of HAT, PNF and NAS (6/132 in the A-NRP group vs 8/93 in the HOPE group). D-HOPE has an encouraging role in preventing symptomatic ITBL in liver transplants from DCD grafts, due to mitochondrial injury prevention and ATP recovery under the hypothermic aerobic conditions.

NMP and ITBL

NMP provides oxygenated blood at a physiological temperature *via* both the hepatic artery and portal vein, whilst the liver graft is *ex situ*[62]. Several different NMP devices are commercially available, and the majority are transportable even with graft connected. The only major differences between the devices are the nature of the arterial flow (pulsatile or non-pulsatile) and the caval outflow (open or closed). Since the phase 1 first-in-man study that demonstrated safety and feasibility of NMP, there has been a significant uptake in this preservation modality around the world and two large RCTs[63-65]. In contrast to *ex situ* HMP, the more physiological nature of NMP allows cellular function to continue and this can be assessed *via* surrogate parameters[66,67]. Numerous biochemical parameters within the NMP perfusate or bile have been used to predict hepatocellular and cholangiocyte function respectively, in an effort to identify the grafts destined to demonstrate severe EAD or biliary complications[68]. Therefore, an accurate discussion of the impact NMP on ITBL posttransplant needs to consist of two components: (1) The incidence of ITBL in NMP preserved grafts in comparison to other modalities; and (2) the accuracy of NMP parameters to identify livers destined to develop clinically significant ITBL.

Published outcomes for NMP are confounded by the fact that this preservation modality is more frequently applied to organs of marginal quality to facilitate transplantation[69], and it may be applied for the entirety of the preservation period from the donor hospital (“at source”) or following a period of cold storage during transport to the recipient center (“back to base”). The early clinical trials of NMP included both DBD and DCD grafts, with a focus on its feasibility, safety, and impact on the IRI as indicated by markers of early graft function[63,64]. These multicenter trials included standard risk

Table 2 Clinical studies assessing the impact of hypothermic machine perfusion on ischemic type biliary lesions after liver transplantation

Ref.	Study design	Group (n)	DBD/DCD	HOPE duration (median)	Definition of ITBL	Follow up	ITBL-intervention		ITBL-control	
							DCD	DBD	DCD	DBD
Schlegel <i>et al</i> [61], 2023	RCT	HOPE (85) vs SCS (85)	DBD	95.5 min	NR	12 mo	NA	1/85 (1.2%)	NA	3/85 (3.5%)
Ravaioli <i>et al</i> [56], 2022	RCT	HOPE (66) vs SCS (69)	DBD	145 min	Nonspecifically provided: Biliary strictures; Biliary others	12 mo	NA	5/55 (9%)	NA	6/55 (11%)
van Rijn <i>et al</i> [52], 2021	RCT	D-HOPE (78) vs SCS (78)	DCD	132 min	Symptomatic NAS diagnosed with the use of 6-mo cholangiography in the presence of a patent HA	6 mo	5/78 (6%)	NA	14/78 (18%)	NA
Czigany <i>et al</i> [57], 2021	RCT	HOPE (23) vs SCS (23)	DBD	145 min	Biliary complications (clinical; radiological)	12 mo	NA	4/23 (17%)	NA	6/23 (26%)
Patrono <i>et al</i> [60], 2022	Cohort	D-HOPE (121) vs SCS (723)	DBD	138 min	Biliary complications 3-mo cholangiography if clinically indicated	Median 21.6 (D-HOPE) and 51.1 (SCS) mo	NA	5/121 (4%)	NA	35/723 (5%)
Rayar <i>et al</i> [58], 2021	Cohort	HOPE (25) vs SCS (69)	DBD	117 min	NR	12 mo	NA	0/25 (0%)	NA	1/69 (1.5%) ¹
Muller <i>et al</i> [37], 2020	Cohort	NRP (132) vs HOPE (93)	DCD	132 min	NAS was defined as strictures with or without HA thrombosis or arterial complications.	Median 20 (NRP) 28 mo (HOPE) mo	2/32 (6.3%)	NA	4/32 (12.5%)	NA
Ravaioli <i>et al</i> [59], 2020	Cohort	HOPE (10) vs SCS (30)	DBD	132 min	NR	12 mo	NA	NP	NA	NP
Schlegel <i>et al</i> [55], 2019	Cohort	HOPE (50) vs SCS DBD (50) vs SCS DCD (50)	Both	120 min	Ischemic cholangiopathy defined radiologically, as intrahepatic or hilar BS and dilatations with patent HA	5 yr	4/50 (8%)	NA	11/50 (22%)	1/50 (2%)
van Rijn <i>et al</i> [51], 2017	Cohort	D-HOPE (10) vs SCS (20)	DCD	126 min	NAS was defined as bile duct stenosis in the biliary tree as detected by ERCP or MRCP with clinical signs of cholestasis and/or cholangitis in the presence of a patent HA	12 mo	1/10 (10%)	NA	9/20 (45%) ²	NA

¹Ischemic necrosis.

²Biliary necrosis 2/9.

BS: Biliary strictures; DBD: Donor after Brain Death; DCD: Donated after circulatory death; ERCP: Endoscopic retrograde cholangiopancreatography; HA: Hepatic artery; ITBL: Ischemic type biliary lesions; MRCP: Magnetic resonance cholangiopancreatography; NAS: Nonanastomotic biliary strictures; NR: Not reported; NA: Not available.

donors that were accepted for transplant regardless of the preservation modality (NMP or SCS). Subsequently, clinical practice and research shifted to investigate the ability of NMP to resuscitate poor quality grafts that were otherwise deemed untransplantable with SCS[70-72]. Complicating matters further, supposedly untransplantable livers are a heterogenous group with a varying overall risk of ITBL[71,73]. As an example, a DBD graft with severe macrosteatosis has a different risk of ITBL than a DCD graft with 60 min of dWIT, but both will fall into the declined group due to differing clinical concerns. The increased utilization of NMP for livers otherwise deemed to high risk for transplant following SCS has pragmatic consequences for trial design. This loss in equipoise over the safety of randomizing high-risk livers to SCS results in a greater reliance on cohort studies.

The trials that have investigated NMP in the clinical setting, *via* either an RCT or cohort study with a representative control group, are listed in Table 3. Many of these trials unfortunately lacked clear definitions of what was considered ITBL, and whether complete artery patency was required for the diagnosis. To date, three RCTs of NMP have been completed[64,65,74] (Table 3). The first multicenter RCT published by Nasralla *et al*[64] in 2018 included standard risk grafts from both DBD and DCD donors and applied NMP at source. This study included a protocol magnetic resonance cholangiopancreatography at 6 mo to assess for biliary complications of which only a small proportion of subjects

Table 3 Clinical studies assessing the impact of normothermic machine perfusion on ischemic type biliary lesions after liver transplantation

Ref.	Study design	Intervention group (n)	Control group (n)	DBD, DCD intervention	DBD, DCD control	NMP duration ¹	Viability testing	Definition of ITBL	Follow up	ITBL-intervention		ITBL-control		
										DCD	DBD	DCD	DBD	
Markmann <i>et al</i> [65], 2022	RCT	NMP at source (153)	SCS (146)	125, 28	133, 13	4.5 h	NR	IBC defined as NAS or bile leaks, confirmed with ERCP or MRCP	12 mo	4/153 (2.6%) (DBD and DCD)	14/146 (9.5%) (DBD and DCD)			
Nasralla <i>et al</i> [64], 2018	RCT	NMP at source (121)	SCS (101)	87, 34	80, 21	9.1 h	No viability testing	Protocol MRCP at 6 mo. No distinction between IC and ITBL	6 mo	3/27 (11.1%) ²	4/54 (7.4%) ²	5/19 (26.3%) ²	3/55 (5.5%) ²	
Ghinolfi <i>et al</i> [74], 2019	RCT	NMP back-to-base (10)	SCS (10)	All DBD	All DBD	4.2 h	NR	NR	6 mo	NA	1/10 (10%)	NA	0/10	
Gaurav <i>et al</i> [44], 2022	Cohort	NMP back to base OR at-source (67)	SCS (97); NRP (69)	All DCD	All DCD	7.6 h	Cambridge criteria	NAS defined as any BS, dilatation, or irregularity of the bile ducts and/or cast on MRCP away from the anastomosis with patent HA	6 mo minimum	12/67 (17.9%) [7/67, 10.4% ³]	NA	NRP-4/69 (5.7%) [0 ³]	SCS-22/97 (22.6%) [12/97, 12.3% ³]	NA
Hann <i>et al</i> [82], 2022	Cohort	NMP back to base (26)	SCS (56)	All DBD	All DBD	12 h	Birmingham criteria	Not reported	6 mo minimum	NA	1/26 (3.8%)	NA	6/56 (10.7%)	
Fodor <i>et al</i> [75], 2021	Cohort	NMP back to base (59)	SCS (59)	49, 9	55, 4	15 h	Certain parameters signs of "good organ function", others considered "warning" signs	ITBL was defined as BS, dilatation or irregularity of the intra- or extrahepatic bile ducts with or without biliary cast formation in the absence of HAS or HAT	3 mo minimum	0/9	2/49 (4%)	1/4 (25%)	7/55 (12.7%)	
Mohkam <i>et al</i> [45], 2022	Cohort	NMP at source (34)	NRP (68)	All DCDs	All DCD	8.8 h	Not applied	Refers to BS requiring a specific treatment or resulting to graft loss and/or death	23 mo	1/34 (2.9%)	NA	1/68 (1.5%)	NA	
Mergental <i>et al</i> [71], 2020	Cohort	NMP back-to-base (22)	SCS (44)	12, 10	24, 20 ⁴	9.8 h	Birmingham criteria	NR	6 mo	7/10 (70%)	0/12	NR	NR	
Bral <i>et al</i> [83], 2019	Cohort	NMP back-to-base (26)	NMP at source (17)	20, 6	13, 4	7.8 h (back-to-base) 10.3 h (at-source)	Parameters included opening lactate level, lactate clearance, necessity of bicarbonate supplementation, and bile production	IC defined as diffuse BS in the absence of significant arterial stenosis	6 mo	0/6	0/20	0/4	0/13	
Ceresa <i>et al</i> [62], 2019	Cohort	NMP back-to-base (31)	NMP at-source (104)	23, 8	73, 31	8.4 h (mean)	No viability criteria	NR	12 mo	0/8	0/23	NR	NR	
Liu <i>et al</i> [84], 2019	Cohort	NMP back to base OR at-source (21)	SCS (84)	13, 8	52, 32	4 h 52	No viability testing	NR	12 mo minimum	0/8	0/13	NR	NR	
Bral <i>et al</i> [85], 2017	Cohort	NMP at-source (9)	SCS (30)	6, 3	22, 8	11.5 h	No viability testing	NR	6 mo	0/3	0/6	NR	NR	

Ravikumar <i>et al</i> [63], 2016	Cohort	NMP at-source (20)	SCS (40)	16, 4	32, 8	9.3 h	No viability testing	NR	30 d	0/4	0/16	NR	NR
--------------------------------------	--------	-----------------------	----------	-------	-------	-------	----------------------	----	------	-----	------	----	----

¹Median duration unless otherwise stated.

²Numerator represents the number of patients that completed the 6 mo protocol magnetic resonance cholangiopancreatography.

³Number of clinically significant strictures, defined as those requiring intervention.

⁴Presumed based on propensity matching.

BS: Biliary strictures; DBD: Donor after Brain Death; DCD: Donated after circulatory death; ERCP: Endoscopic retrograde cholangiopancreatography; IC: Ischemic cholangiopathy; HA: Hepatic artery; HAS: Hepatic artery stenosis; HAT: Hepatic artery thrombosis; IBC: Ischemic biliary complication; ITBL: Ischemic type biliary lesions; NAS: Nonanastomotic biliary strictures; NR: Not reported; NRP: Normothermic Regional Perfusion; MRCP: Magnetic resonance cholangiopancreatography; RCT: Randomized controlled trials; NA: Not available.

completed. The difference in stricture incidence was greatest in the DCD subgroup, with a rate of 26.3% in the DCD-SCS group as opposed to 11.1% in the DCD-NMP group. Whether these ischemic strictures were ITBL or the result of a vascular lesion is unclear, as HA patency was not possible to determine from the data provided[64]. The smaller RCT conducted by Ghinolfi *et al*[74] comprised a sample of elderly DBD donors (≥ 70 years) and applied NMP in a back-to-base approach[74]. However, the small sample size and lower overall risk of ITBL in DBD grafts makes the findings of this study less informative. In this study, only one patient developed a biliary stricture, and they were in the NMP group. A recent large RCT from the United States randomized nearly 300 livers (both DBD and DCD) to either at-source NMP or SCS[65]. These authors did provide a definition of what they considered an ischemic biliary complication (Table 3) and this occurred in 4 and 14 of the NMP and SCS livers respectively. Once again, the granularity of the data presented does not allow determination of the proportion of patients with ischemic biliary complications that were truly ITBL. It should be noted that none of these RCTs performed any formal viability testing of the grafts prior to transplant and were not powered appropriately to assess for biliary complications.

Both prospective and retrospective cohort studies have investigated biliary complications following NMP (Table 3). In the VITAL trial, Mergental *et al*[71] reported the outcomes of a prospective cohort of 22 livers (12 DBD, 10 DCD) destined for discard that were transplanted following back-to-base NMP. After 6 mo follow-up, 3/10 of the DCD livers had developed symptomatic nonanastomotic biliary strictures. Requiring retransplantation[71]. Fodor *et al*[75] subsequently reported a retrospective cohort study of predominantly DBD grafts (49 DBD and 9 DCD) preserved *via* back-to-base NMP and reported both a lower incidence and severity of ITBL in the NMP group in comparison to SCS[75]. This study had a clear definition of ITBL and applied viability testing, which included bile output and pH, however specific parameters for these were not reported. Recently, Gaurav *et al*[44] published a single center retrospective cohort study of DCD grafts preserved by NMP (back-to-base and at-source), NRP and CS with the primary outcome being NAS[44]. These authors also provided a clear definition of NAS and this required hepatic artery patency. In the NMP group, 12/69 developed NAS and in 7/12 it was clinically significant. This was comparable to the SCS group (22/97, 12/22 clinically significant) but higher than the NRP group (4/69, 0/4 clinically significant). It must be noted that this study applied biliary viability testing to NMP preserved livers and 77% of these NMP preserved DCD livers proceeded to transplant.

Utilizing NMP perfusate and bile parameters to predict (and avoid) certain outcomes remains controversial. The risks associated with liberal use of NMP preserved livers is associated morbidity and mortality. The risks associated with being too stringent on the NMP viability criteria, when predictive accuracy is less than perfect, is the discard of a liver that would have resulted in acceptable outcomes. NMP indicators of biliary injury and/or function have been studied by several groups in human livers [76,77]. The early experience of associating bile pH, bicarbonate and glucose with cholangiopathies was reported by Watson *et al*[77] in 2018, from 16 transplanted livers. In this group of livers, a biliary pH < 7.4 occurred in 3/16, and all three of these developed a cholangiopathy. A lower biliary bicarbonate and higher biliary glucose concentration was also associated with subsequent cholangiopathy. Recently, the same group have reported outcomes in a much larger cohort of 144 transplanted livers[78]. Interestingly, 15 of these transplanted livers did not meet their previously reported cholangiocyte viability criteria and in a further three livers no bile was produced which precluded this assessment. Clinically significant NAS developed in 9/144 recipients and all of these had a bile pH > 7.5. Matton *et al* [76] investigated biliary NMP parameters in both the laboratory and a small clinical trial ($n = 6$)[76]. These authors did not have any cases of ITBL in the recipients within the trial, but demonstrated an inverse correlation between bile pH and bicarbonate concentration with histological evidence of biliary injury in a group of non-transplanted livers. A pH and bicarbonate concentration of < 7.48 and < 18 mmol/L had a positive predictive value of 75% and 91% for significant biliary injury. In summary, the prediction (and avoidance) of ITBL using NMP requires further research. This will undoubtedly be of assistance to the transplant community, however at present the accuracy remains sub-optimal and it must be improved to avoid the unnecessary discard of grafts.

Machine combination approaches

In theory, the different rationale behind the various MP strategies could work synergistically to prevent ITBL. A-NRP abbreviates the dWIT induced damage and provides in-situ resuscitation prior to the cold ischemic period, whereas the *ex situ* techniques may dampen IRI. Conversely, the application of sequential MP strategies may follow the rule of diminishing returns and the resources may not be justified. Despite the report that individual grafts had the combination of A-NRP and NMP, clarity in the ITBL rate with this combination is lacking as they were excluded from the analysis of this study[44, 79]. The Groningen group have also reported their experience with sequential *ex-situ* end-ischemic D-HOPE, controlled oxygenated rewarming and NMP for high-risk livers (mostly DCD grafts)[80]. The application of this protocol is proposed to protect these livers against IRI (D-HOPE phase) and enables viability assessment (NMP phase) prior to transplantation, resulting in promising outcomes.

In Italy, as aforementioned circulatory death during DCD procurement is declared after a stand-off period of 20 min. This prolonged dWIT time has been a general reluctance to use such DCD grafts for transplantation due to the probable high risk of graft failure. The combination of A-NRP and D-HOPE has contributed to increase the donor pool in this high-risk donor context. In a retrospective cohort study, this combination has reported satisfactory outcomes in terms of ITBL when compared with relatively low-risk donor control group (A-NRP + D-HOPE 3% *vs* SCS 8%)[43]. Recently, a new procedure called ischemia-free liver transplantation has been proposed, during which liver grafts are procured, preserved and implanted under continuous NMP. Its applicability and clinical impact are yet to be determined[81]. Further studies are required to determine if additional benefits are achieved by combining different techniques.

EVIDENCE SUMMARY

The volume of data on MP and its impact on the development of ITBL following liver transplant is growing. However, with only a few exceptions, ITBL was not the primary outcome under investigation in these studies and therefore were not designed and reported with this entity in mind. It is difficult in many published studies to tease out what biliary complications represent the development of ITBL, as opposed to strictures of another cause. With this considered, the evidence for prevention of ITBL with MP is distinctly different for DCD as opposed to DBD grafts.

The highest quality evidence for ITBL prevention with MP in DCD grafts is D-HOPE, in comparison to SRR and SCS. This is based on finding from a RCT[52]. However, a larger quantity of lower quality evidence supports A-NRP in comparison to both SRR with SCS, and NMP *via* a 'back to base' approach. At present, there is no evidence that D-HOPE is superior to A-NRP or that the combination of these two MP techniques results in a further reduction of ITBL than each one in isolation. Based on the DCD subgroup from one randomized trial[64], there is a suggestion that NMP applied 'at source' reduces ITBL in comparison to SRR and SCS[64]. There is no good quality evidence that NMP applied in a 'back to base' approach for DCD grafts prevents ITBL. In DBD donors, the incidence of ITBL is lower and therefore studies with a large sample size will be required to demonstrate a noticeable effect. The available evidence to suggest that either NMP 'at source' or 'back to base' for DBD grafts is weak, and consists of only one cohort study[75]. There is no trial evidence to support a reduction in ITBL for DBD grafts with HMP strategies.

CONCLUSION

ITBL remains an ongoing issue and the notion that biliary complications are the ‘achilles heel’ of liver transplantation remains true. However, with the introduction of MP technology, gains are being made in the prevention of this highly morbid condition. The greatest area of improvement is for DCD grafts with RCT evidence for D-HOPE, and large cohort studies supporting A-NRP. Given the demonstrated benefits these modalities have over SCS for DCD grafts, a loss of equipoise within the transplant community is diminishing the opportunity for further RCTs that include a SCS group. As an organ donor often generously gives numerous organs, the impact A-NRP has on other abdominal viscera may influence the decision regarding the most appropriate MP strategies. Multiple factors likely interact to cause ITBL, and a greater understanding of these will undoubtedly help refine both preventative and treatment interventions.

ACKNOWLEDGEMENTS

Angus Hann would like to acknowledge the funding received in the form of the Catherine Marie Enright research scholarship from the Royal Australasian College of Surgeons to support his program of research. Figure created with biorender.com, accessed on January 2023.

FOOTNOTES

Author contributions: Perera MTPR and Hann A contributed to the conceptualization; Durán M, Hann A, Calleja R, and Clarke G performed the literature review; Durán M, Hann A, Clarke G, and Calleja R wrote the original draft; Perera MTPR, Hann A, Briceño J, Calleja R, Nutu A, Ayllón MD, López-Cillero P, Sanabria-Mateos R, and Mergental H wrote the review and performed the editing; All authors have read and agreed to the published version of the manuscript.

Conflict-of-interest statement: The funding provided for normothermic machine perfusion consumables generously donated by the Ann Fox Foundation, under the umbrella of University Hospital Birmingham Charities.

Open-Access: This article is an open-access article that was selected by an in-house editor and fully peer-reviewed by external reviewers. It is distributed in accordance with the Creative Commons Attribution NonCommercial (CC BY-NC 4.0) license, which permits others to distribute, remix, adapt, build upon this work non-commercially, and license their derivative works on different terms, provided the original work is properly cited and the use is non-commercial. See: <https://creativecommons.org/licenses/by-nc/4.0/>

Country/Territory of origin: United Kingdom

ORCID number: Manuel Durán 0000-0003-1161-2195; Rafael Calleja 0000-0003-0048-0756; Angus Hann 0000-0003-4431-3642; George Clarke 0000-0002-8913-398X; Ruben Ciria 0000-0002-7839-2329; Anisa Nutu 0000-0003-4699-0970; Rebeca Sanabria-Mateos 0000-0002-1431-6386; María Dolores Ayllón 0000-0003-2493-3756; Pedro López-Cillero 0000-0002-2568-6438; Hynek Mergental 0000-0001-5480-9380; Javier Briceño 0000-0001-7027-7898; M Thamara P R Perera 0000-0002-5417-3850.

S-Editor: Fan JR

L-Editor: Filipodia

P-Editor: Yu HG

REFERENCES

- Muller X, Marcon F, Sapisochin G, Marquez M, Dondero F, Rayar M, Doyle MMB, Callans L, Li J, Nowak G, Allard MA, Jochmans I, Jacsikon K, Beltrame MC, van Reeve M, Iesari S, Cucchetti A, Sharma H, Staiger RD, Raptis DA, Petrowsky H, de Oliveira M, Hernandez-Alejandro R, Pinna AD, Lerut J, Polak WG, de Santibañes E, de Santibañes M, Cameron AM, Pirenne J, Cherqui D, Adam RA, Ericzon BG, Nashan B, Olthoff K, Shaked A, Chapman WC, Boudjema K, Soubrane O, Paugam-Burtz C, Greig PD, Grant DR, Carvalheiro A, Muiesan P, Dutkowski P, Puhon M, Clavien PA. Defining Benchmarks in Liver Transplantation: A Multicenter Outcome Analysis Determining Best Achievable Results. *Ann Surg* 2018; **267**: 419-425 [PMID: 28885508 DOI: 10.1097/SLA.0000000000002477]
- MacConmara M, Hanish SI, Hwang CS, De Gregorio L, Desai DM, Feizpour CA, Tanriover B, Markmann JF, Zeh H 3rd, Vagefi PA. Making Every Liver Count: Increased Transplant Yield of Donor Livers Through Normothermic Machine Perfusion. *Ann Surg* 2020; **272**: 397-401 [PMID: 32694447 DOI: 10.1097/SLA.0000000000004198]
- Briceño J, Ciria R, de la Mata M. Donor-recipient matching: myths and realities. *J Hepatol* 2013; **58**: 811-820 [PMID: 23104164 DOI: 10.1016/j.jhep.2012.10.020]

- 4 **Panayotova G**, Lunsford KE, Latt NL, Paterno F, Guarrera JV, Pylsopoulos N. Expanding indications for liver transplantation in the era of liver transplant oncology. *World J Gastrointest Surg* 2021; **13**: 392-405 [PMID: 34122730 DOI: 10.4240/wjgs.v13.i5.392]
- 5 **Kollmann D**, Sapisochin G, Goldaracena N, Hansen BE, Rajakumar R, Selzner N, Bhat M, McCluskey S, Cattral MS, Greig PD, Lilly L, McGilvray ID, Ghanekar A, Grant DR, Selzner M. Expanding the donor pool: Donation after circulatory death and living liver donation do not compromise the results of liver transplantation. *Liver Transpl* 2018; **24**: 779-789 [PMID: 29604237 DOI: 10.1002/lt.25068]
- 6 **Calne RY**. A new technique for biliary drainage in orthotopic liver transplantation utilizing the gall bladder as a pedicle graft conduit between the donor and recipient common bile ducts. *Ann Surg* 1976; **184**: 605-609 [PMID: 791164 DOI: 10.1097/0000658-197611000-00012]
- 7 **Boteon YL**, Boteon AP, Attard J, Wallace L, Bhogal RH, Afford SC. Impact of machine perfusion of the liver on post-transplant biliary complications: A systematic review. *World J Transplant* 2018; **8**: 220-231 [PMID: 30370232 DOI: 10.5500/wjt.v8.i6.220]
- 8 **Hessheimer AJ**, Cárdenas A, García-Valdecasas JC, Fondevila C. Can we prevent ischemic-type biliary lesions in donation after circulatory determination of death liver transplantation? *Liver Transpl* 2016; **22**: 1025-1033 [PMID: 27082839 DOI: 10.1002/lt.24460]
- 9 **Durán M**, Hann A, Lembach H, Nutu A, Clarke G, Patel I, Sneiders D, Hartog H, Mirza DF, Perera MTPR. Normothermic Machine Perfusion as a Tool for Safe Transplantation of High-Risk Recipients. *Transplantology* 2022; **3**: 169-183 [DOI: 10.3390/transplantology3020018]
- 10 **Noack K**, Bronk SF, Kato A, Gores GJ. The greater vulnerability of bile duct cells to reoxygenation injury than to anoxia. Implications for the pathogenesis of biliary strictures after liver transplantation. *Transplantation* 1993; **56**: 495-500 [PMID: 8212138 DOI: 10.1097/00007890-199309000-00001]
- 11 **Kochhar G**, Parungao JM, Hanouneh IA, Parsi MA. Biliary complications following liver transplantation. *World J Gastroenterol* 2013; **19**: 2841-2846 [PMID: 23704818 DOI: 10.3748/wjg.v19.i19.2841]
- 12 **Verdonk RC**, Buis CI, Porte RJ, van der Jagt EJ, Limburg AJ, van den Berg AP, Slooff MJ, Peeters PM, de Jong KP, Kleibeuker JH, Haagsma EB. Anastomotic biliary strictures after liver transplantation: causes and consequences. *Liver Transpl* 2006; **12**: 726-735 [PMID: 16628689 DOI: 10.1002/Lt.20714]
- 13 **Jay CL**, Lyuksemburg V, Ladner DP, Wang E, Caicedo JC, Holl JL, Abecassis MM, Skaro AI. Ischemic cholangiopathy after controlled donation after cardiac death liver transplantation: a meta-analysis. *Ann Surg* 2011; **253**: 259-264 [PMID: 21245668 DOI: 10.1097/SLA.0b013e318204e658]
- 14 **Foley DP**, Fernandez LA, Levenson G, Anderson M, Mezrich J, Sollinger HW, D'Alessandro A. Biliary complications after liver transplantation from donation after cardiac death donors: an analysis of risk factors and long-term outcomes from a single center. *Ann Surg* 2011; **253**: 817-825 [PMID: 21475025 DOI: 10.1097/SLA.0b013e3182104784]
- 15 **Schlegel A**, Porte R, Dutkowski P. Protective mechanisms and current clinical evidence of hypothermic oxygenated machine perfusion (HOPE) in preventing post-transplant cholangiopathy. *J Hepatol* 2022; **76**: 1330-1347 [PMID: 35589254 DOI: 10.1016/j.jhep.2022.01.024]
- 16 **Buis CI**, Verdonk RC, Van der Jagt EJ, van der Hilst CS, Slooff MJ, Haagsma EB, Porte RJ. Nonanastomotic biliary strictures after liver transplantation, part 1: Radiological features and risk factors for early vs. late presentation. *Liver Transpl* 2007; **13**: 708-718 [PMID: 17457932 DOI: 10.1002/Lt.21166]
- 17 **Croome KP**, Mathur AK, Aqel B, Yang L, Taner T, Heimbach JK, Rosen CB, Paz-Fumagalli R, Taner CB. Classification of Distinct Patterns of Ischemic Cholangiopathy Following DCD Liver Transplantation: Distinct Clinical Courses and Long-term Outcomes From a Multicenter Cohort. *Transplantation* 2022; **106**: 1206-1214 [PMID: 34468429 DOI: 10.1097/TP.0000000000003928]
- 18 **Op den Dries S**, Sutton ME, Lisman T, Porte RJ. Protection of bile ducts in liver transplantation: looking beyond ischemia. *Transplantation* 2011; **92**: 373-379 [PMID: 21629175 DOI: 10.1097/TP.0b013e318223a384]
- 19 **de Vries Y**, von Meijenfeldt FA, Porte RJ. Post-transplant cholangiopathy: Classification, pathogenesis, and preventive strategies. *Biochim Biophys Acta Mol Basis Dis* 2018; **1864**: 1507-1515 [PMID: 28645651 DOI: 10.1016/j.bbadis.2017.06.013]
- 20 **O'Neill S**, Roebuck A, Khoo E, Wigmore SJ, Harrison EM. A meta-analysis and meta-regression of outcomes including biliary complications in donation after cardiac death liver transplantation. *Transpl Int* 2014; **27**: 1159-1174 [PMID: 25052036 DOI: 10.1111/tri.12403]
- 21 **Laing RW**, Scaleria I, Isaac J, Mergental H, Mirza DF, Hodson J, Wilkin RJ, Perera MT, Muiesan P. Liver Transplantation Using Grafts From Donors After Circulatory Death: A Propensity Score-Matched Study From a Single Center. *Am J Transplant* 2016; **16**: 1795-1804 [PMID: 26725645 DOI: 10.1111/ajt.13699]
- 22 **Lamireau T**, Zoltowska M, Levy E, Yousef I, Rosenbaum J, Tuchweber B, Desmoulière A. Effects of bile acids on biliary epithelial cells: proliferation, cytotoxicity, and cytokine secretion. *Life Sci* 2003; **72**: 1401-1411 [PMID: 12527037 DOI: 10.1016/s0024-3205(02)02408-6]
- 23 **Knoop M**, Schnoy N, Keck H, Neuhaus P. Morphological changes of human common bile ducts after extended cold preservation. *Transplantation* 1993; **56**: 1572-1573 [PMID: 8279043]
- 24 **Buis CI**, Geuken E, Visser DS, Kuipers F, Haagsma EB, Verkade HJ, Porte RJ. Altered bile composition after liver transplantation is associated with the development of nonanastomotic biliary strictures. *J Hepatol* 2009; **50**: 69-79 [PMID: 19012987 DOI: 10.1016/j.jhep.2008.07.032]
- 25 **Geuken E**, Visser D, Kuipers F, Blokzijl H, Leuvenink HG, de Jong KP, Peeters PM, Jansen PL, Slooff MJ, Gouw AS, Porte RJ. Rapid increase of bile salt secretion is associated with bile duct injury after human liver transplantation. *J Hepatol* 2004; **41**: 1017-1025 [PMID: 15582136 DOI: 10.1016/j.jhep.2004.08.023]
- 26 **Cursio R**, Gugenheim J. Ischemia-Reperfusion Injury and Ischemic-Type Biliary Lesions following Liver Transplantation. *J Transplant* 2012; **2012**: 164329 [PMID: 22530107 DOI: 10.1155/2012/164329]
- 27 **Ramírez-Del Val A**, Guarrera J, Porte RJ, Selzner M, Spiro M, Raptis DA, Friend PJ, Nasralla D; ERAS4OLT. org Working Group. Does machine perfusion improve immediate and short-term outcomes by enhancing graft function and

- recipient recovery after liver transplantation? A systematic review of the literature, meta-analysis and expert panel recommendations. *Clin Transplant* 2022; **36**: e14638 [PMID: 35279883 DOI: 10.1111/ctr.14638]
- 28 **Melandro F**, Basta G, Torri F, Biancofiore G, Del Turco S, Orlando F, Guarracino F, Maremmi P, Lazzeri C, Peris A, De Simone P, Ghinolfi D. Normothermic regional perfusion in liver transplantation from donation after cardiocirculatory death: Technical, biochemical, and regulatory aspects and review of literature. *Artif Organs* 2022; **46**: 1727-1740 [PMID: 35733227 DOI: 10.1111/aor.14330]
- 29 **Abdel-Misih SR**, Wei L, Benson AB 3rd, Cohen S, Lai L, Skibber J, Wilkinson N, Weiser M, Schrag D, Bekaii-Saab T. Neoadjuvant Therapy for Rectal Cancer Affects Lymph Node Yield and Status Without Clear Implications on Outcome: The Case for Eliminating a Metric and Using Preoperative Staging to Guide Therapy. *J Natl Compr Canc Netw* 2016; **14**: 1528-1534 [PMID: 27956537 DOI: 10.6004/jnccn.2016.0164]
- 30 **De Carlis L**, De Carlis R, Lauterio A, Di Sandro S, Ferla F, Zanierato M. Sequential Use of Normothermic Regional Perfusion and Hypothermic Machine Perfusion in Donation After Cardiac Death Liver Transplantation With Extended Warm Ischemia Time. *Transplantation* 2016; **100**: e101-e102 [PMID: 27495774 DOI: 10.1097/TP.0000000000001419]
- 31 **Saviez E**, Lim C, Rayar M, Orlando F, Boudjema K, Mohkam K, Lesurtel M, Mabrut JY, Pittau G, Begdadi N, Cherqui D, Adam R, Dondero F, Sepulveda A, Soubrane O, Bucur P, Barbier L, Salame E, Jasseron C, Antoine C, Riou B, Scatton O. Favorable Outcomes of Liver Transplantation from Controlled Circulatory Death Donors Using Normothermic Regional Perfusion Compared to Brain Death Donors. *Transplantation* 2020; **104**: 1943-1951 [PMID: 32639402 DOI: 10.1097/TP.0000000000003372]
- 32 **Trasplantes ONT**. Protocolo nacional de donación y trasplante hepático en donación en asistolia controlada. 2015. Available from: <https://www.enfermeria21.com/revistas/metad/articulo/81185/>
- 33 **Watson CJE**, Hunt F, Messer S, Currie I, Large S, Sutherland A, Crick K, Wigmore SJ, Fear C, Cornateanu S, Randle LV, Terrace JD, Upponi S, Taylor R, Allen E, Butler AJ, Oniscu GC. In situ normothermic perfusion of livers in controlled circulatory death donation may prevent ischemic cholangiopathy and improve graft survival. *Am J Transplant* 2019; **19**: 1745-1758 [PMID: 30589499 DOI: 10.1111/ajt.15241]
- 34 **Hessheimer AJ**, de la Rosa G, Gastaca M, Ruiz P, Otero A, Gómez M, Alconchel F, Ramírez P, Bosca A, López-Andújar R, Atutxa L, Royo-Villanova M, Sánchez B, Santoyo J, Marín LM, Gómez-Bravo MÁ, Mosteiro F, Villegas Herrera MT, Villar Del Moral J, González-Abos C, Vidal B, López-Domínguez J, Lladó L, Roldán J, Justo I, Jiménez C, López-Monclús J, Sánchez-Turrión V, Rodríguez-Laíz G, Velasco Sánchez E, López-Baena JA, Caralt M, Charco R, Tomé S, Varo E, Martí-Cruchaga P, Rotellar F, Varona MA, Barrera M, Rodríguez-Sanjuan JC, Briceño J, López D, Blanco G, Nuño J, Pacheco D, Coll E, Domínguez-Gil B, Fondevila C. Abdominal normothermic regional perfusion in controlled donation after circulatory determination of death liver transplantation: Outcomes and risk factors for graft loss. *Am J Transplant* 2022; **22**: 1169-1181 [PMID: 34856070 DOI: 10.1111/ajt.16899]
- 35 **Miñambres E**, Ruiz P, Ballesteros MA, Álvarez C, Cifrián JM, Atutxa L, Ventoso A, Castillo F, Gastaca M. Combined lung and liver procurement in controlled donation after circulatory death using normothermic abdominal perfusion. Initial experience in two Spanish centers. *Am J Transplant* 2020; **20**: 231-240 [PMID: 31265753 DOI: 10.1111/ajt.15520]
- 36 **Muñoz DC**, Pérez BS, Martínez MP, León Díaz FJ, Fernández Aguilar JL, Pérez Daga JA, Santoyo J. Does Normothermic Regional Perfusion Improve the Results of Donation After Circulatory Death Liver Transplantation? *Transplant Proc* 2020; **52**: 1477-1480 [PMID: 32252997 DOI: 10.1016/j.transproceed.2020.01.088]
- 37 **Muller X**, Mohkam K, Mueller M, Schlegel A, Dondero F, Sepulveda A, Saviez E, Scatton O, Bucur P, Salame E, Jeddou H, Sulpice L, Pittau G, Allard MA, Mabrut JY, Dutkowsky P, Clavien PA, Lesurtel M. Hypothermic Oxygenated Perfusion Versus Normothermic Regional Perfusion in Liver Transplantation From Controlled Donation After Circulatory Death: First International Comparative Study. *Ann Surg* 2020; **272**: 751-758 [PMID: 32833758 DOI: 10.1097/SLA.0000000000004268]
- 38 **De Carlis R**, Di Sandro S, Lauterio A, Botta F, Ferla F, Andorno E, Bagnardi V, De Carlis L. Liver Grafts From Donors After Circulatory Death on Regional Perfusion With Extended Warm Ischemia Compared With Donors After Brain Death. *Liver Transpl* 2018; **24**: 1523-1535 [PMID: 30022597 DOI: 10.1002/lt.25312]
- 39 **Rodríguez-Sanjuán JC**, Ruiz N, Miñambres E, Toledo E, González-Noriega M, Fernández-Santiago R, Castillo F. Liver Transplant From Controlled Cardiac Death Donors Using Normothermic Regional Perfusion: Comparison With Liver Transplants From Brain Dead Donors. *Transplant Proc* 2019; **51**: 12-19 [PMID: 30655135 DOI: 10.1016/j.transproceed.2018.04.067]
- 40 **Ruiz P**, Valdivieso A, Palomares I, Prieto M, Ventoso A, Salvador P, Senosiain M, Fernandez JR, Testillano M, Bustamante FJ, Gastaca M. Similar Results in Liver Transplantation From Controlled Donation After Circulatory Death Donors With Normothermic Regional Perfusion and Donation After Brain Death Donors: A Case-Matched Single-Center Study. *Liver Transpl* 2021; **27**: 1747-1757 [PMID: 34455694 DOI: 10.1002/lt.26281]
- 41 **Hessheimer AJ**, Coll E, Torres F, Ruiz P, Gastaca M, Rivas JI, Gómez M, Sánchez B, Santoyo J, Ramírez P, Parrilla P, Marín LM, Gómez-Bravo MÁ, García-Valdecasas JC, López-Monclús J, Bosca A, López-Andújar R, Fundora-Suárez J, Villar J, García-Sesma Á, Jiménez C, Rodríguez-Laíz G, Lladó L, Rodríguez JC, Barrera M, Charco R, López-Baena JA, Briceño J, Pardo F, Blanco G, Pacheco D, Domínguez-Gil B, Sánchez Turrión V, Fondevila C. Normothermic regional perfusion vs. super-rapid recovery in controlled donation after circulatory death liver transplantation. *J Hepatol* 2019; **70**: 658-665 [PMID: 30582980 DOI: 10.1016/j.jhep.2018.12.013]
- 42 **Schurink IJ**, de Goeij FHC, Habets LJM, van de Leemkolk FEM, van Dun CAA, Oniscu GC, Alwayn IPJ, Polak WG, Huurman VAL, de Jonge J. Salvage of Declined Extended-criteria DCD Livers Using In Situ Normothermic Regional Perfusion. *Ann Surg* 2022; **276**: e223-e230 [PMID: 35861530 DOI: 10.1097/SLA.0000000000005611]
- 43 **De Carlis R**, Schlegel A, Frassoni S, Olivieri T, Ravaioli M, Camagni S, Patrono D, Bassi D, Pagano D, Di Sandro S, Lauterio A, Bagnardi V, Gruttadauria S, Cillo U, Romagnoli R, Colledan M, Cescon M, Di Benedetto F, Muiesan P, De Carlis L. How to Preserve Liver Grafts From Circulatory Death With Long Warm Ischemia? A Retrospective Italian Cohort Study With Normothermic Regional Perfusion and Hypothermic Oxygenated Perfusion. *Transplantation* 2021; **105**: 2385-2396 [PMID: 33617211 DOI: 10.1097/TP.0000000000003595]
- 44 **Gaurav R**, Butler AJ, Kosmoliaptis V, Mumford L, Fear C, Swift L, Fedotovs A, Upponi S, Khwaja S, Richards J,

- Allison M, Watson CJE. Liver Transplantation Outcomes From Controlled Circulatory Death Donors: SCS vs in situ NRP vs ex situ NMP. *Ann Surg* 2022; **275**: 1156-1164 [PMID: 35258511 DOI: 10.1097/SLA.0000000000005428]
- 45 **Mohkam K**, Nasralla D, Mergental H, Muller X, Butler A, Jassem W, Imber C, Monbaliu D, Perera MTPR, Laing RW, García-Valdecasas JC, Paul A, Dondero F, Cauchy F, Savier E, Scatton O, Robin F, Sulpice L, Bucur P, Salamé E, Pittau G, Allard MA, Pradat P, Rossignol G, Mabrut JY, Ploeg RJ, Friend PJ, Mirza DF, Lesurtel M; Consortium for Organ Preservation in Europe (COPE). In situ normothermic regional perfusion versus ex situ normothermic machine perfusion in liver transplantation from donation after circulatory death. *Liver Transpl* 2022; **28**: 1716-1725 [PMID: 35662403 DOI: 10.1002/lt.26522]
- 46 **Guarrera JV**, Henry SD, Samstein B, Odeh-Ramadan R, Kinkhabwala M, Goldstein MJ, Ratner LE, Renz JF, Lee HT, Brown RS Jr, Emond JC. Hypothermic machine preservation in human liver transplantation: the first clinical series. *Am J Transplant* 2010; **10**: 372-381 [PMID: 19958323 DOI: 10.1111/j.1600-6143.2009.02932.x]
- 47 **Schlegel A**, Kron P, Graf R, Clavien PA, Dutkowski P. Hypothermic Oxygenated Perfusion (HOPE) downregulates the immune response in a rat model of liver transplantation. *Ann Surg* 2014; **260**: 931-7; discussion 937 [PMID: 25243553 DOI: 10.1097/SLA.0000000000000941]
- 48 **Dutkowski P**, Furrer K, Tian Y, Graf R, Clavien PA. Novel short-term hypothermic oxygenated perfusion (HOPE) system prevents injury in rat liver graft from non-heart beating donor. *Ann Surg* 2006; **244**: 968-76; discussion 976 [PMID: 17122622 DOI: 10.1097/01.sla.0000247056.85590.6b]
- 49 **de Rougemont O**, Breitenstein S, Leskosek B, Weber A, Graf R, Clavien PA, Dutkowski P. One hour hypothermic oxygenated perfusion (HOPE) protects nonviable liver allografts donated after cardiac death. *Ann Surg* 2009; **250**: 674-683 [PMID: 19806056 DOI: 10.1097/SLA.0b013e3181bcb1ee]
- 50 **Dutkowski P**, Polak WG, Muiesan P, Schlegel A, Verhoeven CJ, Scalera I, DeOliveira ML, Kron P, Clavien PA. First Comparison of Hypothermic Oxygenated Perfusion Versus Static Cold Storage of Human Donation After Cardiac Death Liver Transplants: An International-matched Case Analysis. *Ann Surg* 2015; **262**: 764-70; discussion 770 [PMID: 26583664 DOI: 10.1097/SLA.0000000000001473]
- 51 **van Rijn R**, Karimian N, Matton APM, Burlage LC, Westerkamp AC, van den Berg AP, de Kleine RHJ, de Boer MT, Lisman T, Porte RJ. Dual hypothermic oxygenated machine perfusion in liver transplants donated after circulatory death. *Br J Surg* 2017; **104**: 907-917 [PMID: 28394402 DOI: 10.1002/bjs.10515]
- 52 **van Rijn R**, Schurink IJ, de Vries Y, van den Berg AP, Cortes Cerisuelo M, Darwish Murad S, Erdmann JI, Gilbo N, de Haas RJ, Heaton N, van Hoek B, Huurman VAL, Jochmans I, van Leeuwen OB, de Meijer VE, Monbaliu D, Polak WG, Slangen JGG, Troisi RI, Vanlander A, de Jonge J, Porte RJ; DHOPE-DCD Trial Investigators. Hypothermic Machine Perfusion in Liver Transplantation - A Randomized Trial. *N Engl J Med* 2021; **384**: 1391-1401 [PMID: 33626248 DOI: 10.1056/NEJMoa2031532]
- 53 **de Vries Y**, Brüggewirth IMA, Karangwa SA, von Meijenfeldt FA, van Leeuwen OB, Burlage LC, de Jong IEM, Gouw ASH, de Meijer VE, Lisman T, Porte RJ. Dual Versus Single Oxygenated Hypothermic Machine Perfusion of Porcine Livers: Impact on Hepatobiliary and Endothelial Cell Injury. *Transplant Direct* 2021; **7**: e741 [PMID: 34386578 DOI: 10.1097/TXD.0000000000001184]
- 54 **Muller X**, Schlegel A, Kron P, Eshmunov D, Würdinger M, Meierhofer D, Clavien PA, Dutkowski P. Novel Real-time Prediction of Liver Graft Function During Hypothermic Oxygenated Machine Perfusion Before Liver Transplantation. *Ann Surg* 2019; **270**: 783-790 [PMID: 31592808 DOI: 10.1097/SLA.0000000000003513]
- 55 **Schlegel A**, Muller X, Kalisvaart M, Muellhaupt B, Perera MTPR, Isaac JR, Clavien PA, Muiesan P, Dutkowski P. Outcomes of DCD liver transplantation using organs treated by hypothermic oxygenated perfusion before implantation. *J Hepatol* 2019; **70**: 50-57 [PMID: 30342115 DOI: 10.1016/j.jhep.2018.10.005]
- 56 **Ravaioli M**, Germinario G, Dajti G, Sessa M, Vasuri F, Siniscalchi A, Morelli MC, Serenari M, Del Gaudio M, Zanfi C, Odaldi F, Bertuzzo VR, Maroni L, Laurenzi A, Cescon M. Hypothermic oxygenated perfusion in extended criteria donor liver transplantation-A randomized clinical trial. *Am J Transplant* 2022; **22**: 2401-2408 [PMID: 35671067 DOI: 10.1111/ajt.17115]
- 57 **Czigany Z**, Pratschke J, Froněk J, Guba M, Schöning W, Raptis DA, Andrassy J, Kramer M, Strnad P, Tolba RH, Liu W, Keller T, Miller H, Pavicevic S, Uluk D, Kocik M, Lurje I, Trautwein C, Mehrabi A, Popescu I, Vondran FWR, Ju C, Tacke F, Neumann UP, Lurje G. Hypothermic Oxygenated Machine Perfusion Reduces Early Allograft Injury and Improves Post-transplant Outcomes in Extended Criteria Donation Liver Transplantation From Donation After Brain Death: Results From a Multicenter Randomized Controlled Trial (HOPE ECD-DBD). *Ann Surg* 2021; **274**: 705-712 [PMID: 34334635 DOI: 10.1097/SLA.0000000000005110]
- 58 **Rayar M**, Beaupaire JM, Bajoux E, Hamonic S, Renard T, Locher C, Desfourneaux V, Merdignac A, Bergate D, Lakehal M, Sulpice L, Housset-Debry P, Jezequel C, Camus C, Bardou-Jacquet E, Meunier B. Hypothermic Oxygenated Perfusion Improves Extended Criteria Donor Liver Graft Function and Reduces Duration of Hospitalization Without Extra Cost: The PERPHO Study. *Liver Transpl* 2021; **27**: 349-362 [PMID: 33237618 DOI: 10.1002/lt.25955]
- 59 **Ravaioli M**, De Pace V, Angeletti A, Comai G, Vasuri F, Baldassarre M, Maroni L, Odaldi F, Fallani G, Caraceni P, Germinario G, Donadei C, Malvi D, Del Gaudio M, Bertuzzo VR, Siniscalchi A, Ranieri VM, D'Errico A, Pasquinelli G, Morelli MC, Pinna AD, Cescon M, La Manna G. Hypothermic Oxygenated New Machine Perfusion System in Liver and Kidney Transplantation of Extended Criteria Donors: First Italian Clinical Trial. *Sci Rep* 2020; **10**: 6063 [PMID: 32269237 DOI: 10.1038/s41598-020-62979-9]
- 60 **Patrono D**, Cussa D, Sciannameo V, Montanari E, Panconesi R, Berchiolla P, Lepore M, Gambella A, Rizza G, Catalano G, Mirabella S, Tandoi F, Lupo F, Balagna R, Salizzoni M, Romagnoli R. Outcome of liver transplantation with grafts from brain-dead donors treated with dual hypothermic oxygenated machine perfusion, with particular reference to elderly donors. *Am J Transplant* 2022; **22**: 1382-1395 [PMID: 35150050 DOI: 10.1111/ajt.16996]
- 61 **Schlegel A**, Mueller M, Muller X, Eden J, Panconesi R, von Felten S, Steigmüller K, Sousa Da Silva RX, de Rougemont O, Mabrut JY, Lesurtel M, Cerisuelo MC, Heaton ND, Allard MA, Adam R, Monbaliu D, Jochmans I, Haring MPD, Porte RJ, Parente A, Muiesan P, Kron P, Attia M, Kollmann D, Berlakovich G, Rogiers X, Petterson K, Kranich AL, Amberg S, Müllhaupt B, Clavien PA, Dutkowski P. A multicenter randomized-controlled trial of hypothermic oxygenated perfusion

- (HOPE) for human liver grafts before transplantation. *J Hepatol* 2023; **78**: 783-793 [PMID: 36681160 DOI: 10.1016/j.jhep.2022.12.030]
- 62 **Ceresa CDL**, Nasralla D, Coussios CC, Friend PJ. The case for normothermic machine perfusion in liver transplantation. *Liver Transpl* 2018; **24**: 269-275 [PMID: 29272051 DOI: 10.1002/lt.25000]
- 63 **Ravikumar R**, Jassem W, Mergental H, Heaton N, Mirza D, Perera MT, Quaglia A, Holroyd D, Vogel T, Coussios CC, Friend PJ. Liver Transplantation After Ex Vivo Normothermic Machine Preservation: A Phase 1 (First-in-Man) Clinical Trial. *Am J Transplant* 2016; **16**: 1779-1787 [PMID: 26752191 DOI: 10.1111/ajt.13708]
- 64 **Nasralla D**, Coussios CC, Mergental H, Akhtar MZ, Butler AJ, Ceresa CDL, Chiocchia V, Dutton SJ, García-Valdecasas JC, Heaton N, Imber C, Jassem W, Jochmans I, Karani J, Knight SR, Kocabayoglu P, Malagò M, Mirza D, Morris PJ, Pallan A, Paul A, Pavel M, Perera MTPR, Pirenne J, Ravikumar R, Russell L, Upponi S, Watson CJE, Weissenbacher A, Ploeg RJ, Friend PJ; Consortium for Organ Preservation in Europe. A randomized trial of normothermic preservation in liver transplantation. *Nature* 2018; **557**: 50-56 [PMID: 29670285 DOI: 10.1038/s41586-018-0047-9]
- 65 **Markmann JF**, Abouljoud MS, Ghobrial RM, Bhati CS, Pelletier SJ, Lu AD, Ottmann S, Klair T, Eymard C, Roll GR, Magliocca J, Prueett TL, Reyes J, Black SM, Marsh CL, Schnickel G, Kinkhabwala M, Florman SS, Merani S, Demetris AJ, Kimura S, Rizzari M, Saharia A, Levy M, Agarwal A, Cigarroa FG, Eason JD, Syed S, Washburn WK, Parekh J, Moon J, Maskin A, Yeh H, Vagefi PA, MacConmara MP. Impact of Portable Normothermic Blood-Based Machine Perfusion on Outcomes of Liver Transplant: The OCS Liver PROTECT Randomized Clinical Trial. *JAMA Surg* 2022; **157**: 189-198 [PMID: 34985503 DOI: 10.1001/jamasurg.2021.6781]
- 66 **Hann A**, Lembach H, Nutu A, Mergental H, Isaac JL, Isaac JR, Oo YH, Armstrong MJ, Rajoriya N, Afford S, Bartlett D, Mirza DF, Hartog H, Perera MTPR. Assessment of Deceased Brain Dead Donor Liver Grafts via Normothermic Machine Perfusion: Lactate Clearance Time Threshold Can Be Safely Extended to 6 Hours. *Liver Transpl* 2022; **28**: 493-496 [PMID: 34606663 DOI: 10.1002/lt.26317]
- 67 **Mergental H**, Stephenson BTF, Laing RW, Kirkham AJ, Neil DAH, Wallace LL, Boteon YL, Widmer J, Bhogal RH, Perera MTPR, Smith A, Reynolds GM, Yap C, Hübscher SG, Mirza DF, Afford SC. Development of Clinical Criteria for Functional Assessment to Predict Primary Nonfunction of High-Risk Livers Using Normothermic Machine Perfusion. *Liver Transpl* 2018; **24**: 1453-1469 [PMID: 30359490 DOI: 10.1002/lt.25291]
- 68 **Hann A**, Nutu A, Clarke G, Patel I, Sneider D, Oo YH, Hartog H, Perera MTPR. Normothermic Machine Perfusion-Improving the Supply of Transplantable Livers for High-Risk Recipients. *Transpl Int* 2022; **35**: 10460 [PMID: 35711320 DOI: 10.3389/ti.2022.10460]
- 69 **Hann A**, Raza SS, Sneider D, Nutu A, Mergental H, Mirza DF, Hartog H, Perera MTP. Comment on: Static cold storage compared with normothermic machine perfusion of the liver and effect on ischaemic-type biliary lesions after transplantation: a propensity-score matched study. *Br J Surg* 2021; **109**: e12-e13 [PMID: 34672319 DOI: 10.1093/bjs/znab349]
- 70 **Mergental H**, Perera MT, Laing RW, Muiesan P, Isaac JR, Smith A, Stephenson BT, Cilliers H, Neil DA, Hübscher SG, Afford SC, Mirza DF. Transplantation of Declined Liver Allografts Following Normothermic Ex-Situ Evaluation. *Am J Transplant* 2016; **16**: 3235-3245 [PMID: 27192971 DOI: 10.1111/ajt.13875]
- 71 **Mergental H**, Laing RW, Kirkham AJ, Perera MTPR, Boteon YL, Attard J, Barton D, Curbishley S, Wilkhu M, Neil DAH, Hübscher SG, Muiesan P, Isaac JR, Roberts KJ, Abradelo M, Schlegel A, Ferguson J, Cilliers H, Bion J, Adams DH, Morris C, Friend PJ, Yap C, Afford SC, Mirza DF. Transplantation of discarded livers following viability testing with normothermic machine perfusion. *Nat Commun* 2020; **11**: 2939 [PMID: 32546694 DOI: 10.1038/s41467-020-16251-3]
- 72 **Reiling J**, Butler N, Simpson A, Hodgkinson P, Campbell C, Lockwood D, Bridle K, Santrampurwala N, Britton L, Crawford D, Dejong CHC, Fawcett J. Assessment and Transplantation of Orphan Donor Livers: A Back-to-Base Approach to Normothermic Machine Perfusion. *Liver Transpl* 2020; **26**: 1618-1628 [PMID: 32682340 DOI: 10.1002/lt.25850]
- 73 **Marcon F**, Schlegel A, Bartlett DC, Kalisvaart M, Bishop D, Mergental H, Roberts KJ, Mirza DF, Isaac J, Muiesan P, Perera MT. Utilization of Declined Liver Grafts Yields Comparable Transplant Outcomes and Previous Decline Should Not Be a Deterrent to Graft Use. *Transplantation* 2018; **102**: e211-e218 [PMID: 29702538 DOI: 10.1097/TP.0000000000002127]
- 74 **Ghinolfi D**, Rreka E, De Tata V, Franzini M, Pezzati D, Fierabracci V, Masini M, Cacciatoinsilla A, Bindi ML, Marselli L, Mazzotti V, Morganti R, Marchetti P, Biancofiore G, Campani D, Paolicchi A, De Simone P. Pilot, Open, Randomized, Prospective Trial for Normothermic Machine Perfusion Evaluation in Liver Transplantation From Older Donors. *Liver Transpl* 2019; **25**: 436-449 [PMID: 30362649 DOI: 10.1002/lt.25362]
- 75 **Fodor M**, Cardini B, Peter W, Weissenbacher A, Oberhuber R, Hautz T, Otashvili G, Margreiter C, Maglione M, Resch T, Krendl F, Meszaros AT, Bogensperger C, Gasteiger S, Messner F, Henninger B, Zoller H, Tilg H, Öfner D, Schneeberger S. Static cold storage compared with normothermic machine perfusion of the liver and effect on ischaemic-type biliary lesions after transplantation: a propensity score-matched study. *Br J Surg* 2021; **108**: 1082-1089 [PMID: 34027968 DOI: 10.1093/bjs/znab118]
- 76 **Matton APM**, de Vries Y, Burlage LC, van Rijn R, Fujiyoshi M, de Meijer VE, de Boer MT, de Kleine RHJ, Verkade HJ, Gouw ASH, Lisman T, Porte RJ. Biliary Bicarbonate, pH, and Glucose Are Suitable Biomarkers of Biliary Viability During Ex Situ Normothermic Machine Perfusion of Human Donor Livers. *Transplantation* 2019; **103**: 1405-1413 [PMID: 30395120 DOI: 10.1097/TP.0000000000002500]
- 77 **Watson CJE**, Kosmoliaptis V, Pley C, Randle L, Fear C, Crick K, Gimson AE, Allison M, Upponi S, Brais R, Jochmans I, Butler AJ. Observations on the ex situ perfusion of livers for transplantation. *Am J Transplant* 2018; **18**: 2005-2020 [PMID: 29419931 DOI: 10.1111/ajt.14687]
- 78 **Watson CJE**, Gaurav R, Fear C, Swift L, Selves L, Ceresa CDL, Upponi SS, Brais R, Allison M, Macdonald-Wallis C, Taylor R, Butler AJ. Predicting Early Allograft Function After Normothermic Machine Perfusion. *Transplantation* 2022; **106**: 2391-2398 [PMID: 36044364 DOI: 10.1097/TP.0000000000004263]
- 79 **Ghinolfi D**, Dondossola D, Rreka E, Lonati C, Pezzati D, Cacciatoinsilla A, Kersik A, Lazzeri C, Zanella A, Peris A, Maggioni M, Biancofiore G, Reggiani P, Morganti R, De Simone P, Rossi G. Sequential Use of Normothermic Regional and Ex Situ Machine Perfusion in Donation After Circulatory Death Liver Transplant. *Liver Transpl* 2021; **27**: 385-402

- [PMID: 32949117 DOI: 10.1002/lt.25899]
- 80 **van Leeuwen OB**, Bodewes SB, Lantinga VA, Haring MPD, Thorne AM, Brüggewirth IMA, van den Berg AP, de Boer MT, de Jong IEM, de Kleine RHJ, Lascaris B, Nijsten MWN, Reijntjens KMEM, de Meijer VE, Porte RJ. Sequential hypothermic and normothermic machine perfusion enables safe transplantation of high-risk donor livers. *Am J Transplant* 2022; **22**: 1658-1670 [PMID: 35286759 DOI: 10.1111/ajt.17022]
- 81 **Guo Z**, Zhao Q, Huang S, Huang C, Wang D, Yang L, Zhang J, Chen M, Wu L, Zhang Z, Zhu Z, Wang L, Zhu C, Zhang Y, Tang Y, Sun C, Xiong W, Shen Y, Chen X, Xu J, Wang T, Ma Y, Hu A, Chen Y, Zhu X, Rong J, Cai C, Gong F, Guan X, Huang W, Ko DS, Li X, Tullius SG, Huang J, Ju W, He X. Ischaemia-free liver transplantation in humans: a first-in-human trial. *Lancet Reg Health West Pac* 2021; **16**: 100260 [PMID: 34590063 DOI: 10.1016/j.lanwpc.2021.100260]
- 82 **Hann A**, Lembach H, Nutu A, Dassanayake B, Tillakaratne S, McKay SC, Boteon APCS, Boteon YL, Mergental H, Murphy N, Bangash MN, Neil DAH, Issac JL, Javed N, Faulkner T, Bennet D, Moore R, Vasanth S, Subash G, Cuell J, Rao R, Cilliers H, Russel S, Haydon G, Mutimer D, Roberts KJ, Mirza DF, Ferguson J, Bartlett D, Isaac JR, Rajoriya N, Armstrong MJ, Hartog H, Perera MTPR. Outcomes of normothermic machine perfusion of liver grafts in repeat liver transplantation (NAPLES initiative). *Br J Surg* 2022; **109**: 372-380 [PMID: 35170730 DOI: 10.1093/bjs/znab475]
- 83 **Bral M**, Dajani K, Leon Izquierdo D, Bigam D, Kneteman N, Ceresa CDL, Friend PJ, Shapiro AMJ. A Back-to-Base Experience of Human Normothermic Ex Situ Liver Perfusion: Does the Chill Kill? *Liver Transpl* 2019; **25**: 848-858 [PMID: 30938039 DOI: 10.1002/lt.25464]
- 84 **Liu Q**, Hassan A, Pezzati D, Soliman B, Lomaglio L, Grady P, Del Angel Diaz L, Simioni A, Maikhor S, Etterling J, D'Amico G, Iuppa G, Diago Uso T, Hashimoto K, Aucejo F, Fujiki M, Eghtesad B, Sasaki K, Kwon CHD, Cywinski J, Irefin S, Bennett A, Baldwin W, Miller C, Quintini C. Ex Situ Liver Machine Perfusion: The Impact of Fresh Frozen Plasma. *Liver Transpl* 2020; **26**: 215-226 [PMID: 31642164 DOI: 10.1002/lt.25668]
- 85 **Bral M**, Gala-Lopez B, Bigam D, Kneteman N, Malcolm A, Livingstone S, Andres A, Emamaullee J, Russell L, Coussios C, West LJ, Friend PJ, Shapiro AM. Preliminary Single-Center Canadian Experience of Human Normothermic Ex Vivo Liver Perfusion: Results of a Clinical Trial. *Am J Transplant* 2017; **17**: 1071-1080 [PMID: 27639262 DOI: 10.1111/ajt.14049]

Basic Study

Metronomic capecitabine inhibits liver transplant rejection in rats by triggering recipients' T cell ferroptosis

Hao Wang, Zheng-Lu Wang, Sai Zhang, De-Jun Kong, Rui-Ning Yang, Lei Cao, Jian-Xi Wang, Sei Yoshida, Zhuo-Lun Song, Tao Liu, Shun-Li Fan, Jia-Shu Ren, Jiang-Hong Li, Zhong-Yang Shen, Hong Zheng

Specialty type: Gastroenterology and hepatology

Provenance and peer review: Unsolicited article; Externally peer reviewed.

Peer-review model: Single blind

Peer-review report's scientific quality classification

Grade A (Excellent): 0
Grade B (Very good): B
Grade C (Good): C, C
Grade D (Fair): 0
Grade E (Poor): 0

P-Reviewer: Boteon YL, Brazil;
Chun JW, Korea

Received: January 21, 2023

Peer-review started: January 21, 2023

First decision: February 7, 2023

Revised: February 19, 2023

Accepted: April 28, 2023

Article in press: April 28, 2023

Published online: May 28, 2023



Hao Wang, Rui-Ning Yang, Jia-Shu Ren, Jiang-Hong Li, The First Central Clinical School, Tianjin Medical University, Tianjin 300190, China

Zheng-Lu Wang, Zhuo-Lun Song, Shun-Li Fan, Zhong-Yang Shen, Hong Zheng, Department of Organ Transplant, Tianjin First Central Hospital, School of Medicine, Nankai University, Tianjin 300190, China

Zheng-Lu Wang, Zhong-Yang Shen, Hong Zheng, Key Laboratory of Transplant Medicine, Chinese Academy of Medical Sciences, Tianjin 300190, China

Sai Zhang, De-Jun Kong, School of Medicine, Nankai University, Tianjin 300190, China

Lei Cao, Jian-Xi Wang, Sei Yoshida, Zhong-Yang Shen, Hong Zheng, Research Institute of Transplant Medicine, Nankai University, Tianjin 300071, China

Lei Cao, Jian-Xi Wang, Zhong-Yang Shen, Hong Zheng, Tianjin Key Laboratory for Organ Transplantation, Tianjin First Central Hospital, School of Medicine, Nankai University, Tianjin 300071, China

Tao Liu, Zhong-Yang Shen, Hong Zheng, National Health Commission's Key Laboratory for Critical Care Medicine, Tianjin First Central Hospital, Tianjin 300071, China

Corresponding author: Hong Zheng, PhD, Professor, Department of Organ Transplant, Tianjin First Central Hospital, School of Medicine, Nankai University, No. 24 Fukang Road, Nankai District, Tianjin 300190, China. zhenghongyx@139.com

Abstract

BACKGROUND

Capecitabine (CAP) is a classic antimetabolic drug and has shown potential antirejection effects after liver transplantation (LT) in clinical studies. Our previous study showed that metronomic CAP can cause the programmed death of T cells by inducing oxidative stress in healthy mice. Ferroptosis, a newly defined non-apoptotic cell death that occurs in response to iron overload and lethal levels of lipid peroxidation, is an important mechanism by which CAP induces cell death. Therefore, ferroptosis may also play an important role in CAP-induced T cell death and play an immunosuppressive role in acute rejection after transplantation.

AIM

To investigate the functions and underlying mechanisms of antirejection effects of metronomic CAP.

METHODS

A rat LT model of acute rejection was established, and the effect of metronomic CAP on splenic hematopoietic function and acute graft rejection was evaluated 7 d after LT. *In vitro*, primary CD3⁺ T cells were sorted from rat spleens and human peripheral blood, and co-cultured with or without 5-fluorouracil (5-FU) (active agent of CAP). The levels of ferroptosis-related proteins, ferrous ion concentration, and oxidative stress-related indicators were observed. The changes in mitochondrial structure were observed using electron microscopy.

RESULTS

With no significant myelotoxicity, metronomic CAP alleviated graft injury (Banff score 9 *vs* 7.333, $P < 0.001$), prolonged the survival time of the recipient rats (11.5 d *vs* 16 d, $P < 0.01$), and reduced the infiltration rate of CD3⁺ T cells in peripheral blood (6.859 *vs* 3.735, $P < 0.001$), liver graft (7.459 *vs* 3.432, $P < 0.001$), and spleen (26.92 *vs* 12.9, $P < 0.001$), thereby inhibiting acute rejection after LT. *In vitro*, 5-FU, an end product of CAP metabolism, induced the degradation of the ferritin heavy chain by upregulating nuclear receptor coactivator 4, which caused the accumulation of ferrous ions. It also inhibited nuclear erythroid 2 p45-related factor 2, heme oxygenase-1, and glutathione peroxidase 4, eventually leading to oxidative damage and ferroptosis of T cells.

CONCLUSION

Metronomic CAP can suppress acute allograft rejection in rats by triggering CD3⁺ T cell ferroptosis, which makes it an effective immunosuppressive agent after LT.

Key Words: Capecitabine; Ferroptosis; T Lymphocytes; Immunosuppressive agents; Graft rejection; Liver transplantation

©The Author(s) 2023. Published by Baishideng Publishing Group Inc. All rights reserved.

Core Tip: Our studies proved that metronomic capecitabine (CAP) alleviated the acute rejection after transplantation in rats without the common side effect of myelosuppression. T cell ferroptosis is the underlying mechanism behind the antirejection effect of CAP, which can induce cell ferrous ions overload and suppress the nuclear erythroid 2 p45-related factor 2, heme oxygenase-1/glutathione peroxidase 4 antioxidant systems, thereby directly increasing the levels of intracellular reactive oxygen species, and leading to severe oxidative damage in T cells. These results revealed a new mechanism of CAP-induced T cell programmed death and suggested the possibility of using CAP as an immunosuppressant after transplantation.

Citation: Wang H, Wang ZL, Zhang S, Kong DJ, Yang RN, Cao L, Wang JX, Yoshida S, Song ZL, Liu T, Fan SL, Ren JS, Li JH, Shen ZY, Zheng H. Metronomic capecitabine inhibits liver transplant rejection in rats by triggering recipients' T cell ferroptosis. *World J Gastroenterol* 2023; 29(20): 3084-3102

URL: <https://www.wjgnet.com/1007-9327/full/v29/i20/3084.htm>

DOI: <https://dx.doi.org/10.3748/wjg.v29.i20.3084>

INTRODUCTION

Recurrence of hepatocellular carcinoma (HCC) represents a serious issue after liver transplantation (LT), and is closely related to the usage of immunosuppressant drugs[1-3]. As a classic antimetabolic chemotherapeutic agent, capecitabine (CAP) is widely used in the treatment of cancers and has also shown good effects on HCC[4,5]. Metronomic CAP is suitable for long-term oral administration with low adverse effects and without sacrificing treatment efficacy[6,7]. In patients with recurrent liver cancer after LT, Ravaoli *et al*[8] showed that metronomic CAP achieved similar efficacy to sorafenib, a protein kinase inhibitor approved for HCC but with a high incidence of adverse effects[9]. Interestingly, no acute rejection was seen, suggesting that CAP may have both immunosuppressive and anticarcinogenic effects. CAP is a fluoropyrimidine prodrug that is metabolized in a three-step process to 5-fluorouracil (5-FU)[10]. The last step requires thymidine phosphorylase (TP), the distribution of which determines CAP distribution. This partially explains its different pharmacological characteristics

compared to 5-FU. Because TP is highly expressed in cancer cells and lymphocytes[11,12], the administration of CAP to LT patients with HCC may increase tumor killing while preventing graft rejection. In preliminary work, we found that the differential expression of TP avoided CAP's side effects of myelosuppression and suppressed normal mouse immune responses by inducing T cell apoptosis[13]. However, it is not clear what effect CAP has during the immune activation that follows transplantation, which is key to its use as an immunosuppressant.

Ferroptosis is a newly defined nonapoptotic cell death that occurs with iron overload and lethal levels of lipid peroxidation[14-16]. Ferroptosis is tightly regulated by iron metabolism, while ferritin is the major intracellular iron storage protein complex. Ferritinophagy activation depends on nuclear receptor coactivator 4 (NCOA4) to transport ferritin to the autophagosome and degrade ferritin to increase intracellular iron levels[17,18]. Subsequently, free ferrous ions overload results in oxidative injury by the Fenton reaction. Although the regulatory mechanisms of ferroptosis are poorly understood, some molecules with antioxidant effects may be implicated, such as nuclear erythroid 2 p45-related factor 2 (Nrf2)[19,20], heme oxygenase-1 (HO-1)[21], and glutathione peroxidase 4 (GPX4)[22]. Overall, free ferrous ions result in reactive oxygen species (ROS) generation and oxidative injury, whereas the Nrf2-HO-1/GPX4 antioxidative system protects cells from oxidative damage induced by ferroptosis[23]. In mouse models and *in vitro*, 5-FU mediates injuries in intestinal mucosal cells, such as those occurring during chemotherapy, by reducing Nrf2 expression and increasing ferroptosis[24]. 5-FU also leads to ROS and iron homeostasis-dependent ferroptosis in myocardial cells by reducing the expression of GPX4 and ferritin heavy chain (FTH1) but enhancing the expression of transferrin receptor 1[25]. Thus, mechanistically, ferroptosis plays an important role in the cell-killing effect of 5-FU.

Our previous study indicated that metronomic CAP can increase ROS levels and reduce mitochondrial membrane potential (MMP), thus affecting the immune system of mice[13]. Those results prompted us to further explore whether ferroptosis plays a significant role in 5-FU-induced immunosuppression. In this study, we investigated the effect of metronomic CAP on acute rejection in a rat model of LT, and determined how ferroptosis affects 5-FU-induced immunosuppression. Elucidating the possible mechanism of CAP as an immunosuppressant with anticancer effects is of great relevance to optimize drug regimens for HCC patients after LT in the future.

MATERIALS AND METHODS

Animals

Specific-pathogen-free male Lewis rats (donors) and male Brown Norway rats (recipients) aged 8–10 wk and weighing 250–300 g were obtained from Beijing Vital River Laboratory Animal Technology Co. Ltd. (Beijing, China). The rats were housed in a standard room, and fed filtered clean water and standard laboratory food. To acclimatize, the rats were housed 1 wk before transplantation. According to different postoperative medication regimens, the rats were randomized to untreated control group (CON) (0.9% saline, ig) and metronomic capecitabine-treated (MET) groups (CAP 100 mg/kg/d, ig). A total of 12 recipients (6 rats/group) were used for postoperative specimen collection at 7 d after transplantation, and another 12 recipients (6 rats/group) were used to observe survival. All invasive procedures and specimen collection were performed under isoflurane anesthesia to minimize pain or discomfort.

Orthotopic LT in rats

Anesthesia was induced with isoflurane and orthotopic LT was performed based on Kamada's two-cuff method. The anhepatic phase was controlled within 26 min[26,27]. After transplantation, the rats received 2 mL Ringer's lactate to replenish blood volume and were rewarmed in an incubator at 37 °C for 30 min. On day 7 after LT, an overdose of pentobarbital (150 mg/kg) was injected intraperitoneally for euthanasia. Femur, blood, spleen, and the transplanted liver were collected for further examination.

Routine blood tests

Whole blood was used for blood routine tests 7 d after LT. These were performed with an automatic hematology analyzer (BC-2800Vet; Mindray, Shenzhen, China).

Peripheral blood lymphocyte CD3⁺ T cell count

Peripheral blood lymphocyte CD3⁺ T cell count was obtained based on peripheral blood lymphocyte count and flow cytometric analysis of the CD3⁺ T cell ratio.

Liver function assay

Serum levels of aspartate aminotransferase (AST), alanine aminotransferase (ALT), total bilirubin (TBIL), and direct bilirubin (DBIL) were measured using kits (Mindray, Shenzhen, China) and read with an automatic biochemical analyzer (BS-240VET; Mindray, Shenzhen, China).

Flow cytometric analysis

Rat peripheral blood mononuclear cells were isolated by gradient centrifugation with a rat peripheral blood mononuclear cell separation solution (Solarbio, Beijing, China). Anti-CD3 antibodies (APC anti-rat CD3 Antibody, Cat# 201414; RRID: AB_2563366 BioLegend, San Diego, CA, United States) were used for extracellular staining to identify CD3-positive lymphocytes. Flow cytometry was performed using the Accuri C6 Plus flow cytometry (BD Biosciences, Palo Alto, CA, United States), and FlowJo software (TreeStar, Woodburn, OR, United States) was used for data analysis.

The ferrous levels in T cells were measured using FerroOrange (Cat# MX4559, Maokang Biotechnology, Shanghai, China). Cells were incubated with FerroOrange (37 °C, 20 min) for fluorescence detection. To measure intracellular ROS, cells were resuspended in phosphate-buffered saline (PBS) containing DCFH-DA (Cat# CA1410, Solarbio, Beijing, China) at 37 °C for 30 min and washed twice with PBS for fluorescence detection. To measure the lipid ROS of T cells, C11-BODIPY 581/591 (Cat# MX5211, Maokang Biotechnology, Shanghai, China) was added and incubated at 37 °C with 5% CO₂ for 30 min. Cells were then washed twice before fluorescence detection. The MMP Assay Kit (Cat# M8650, Solarbio, Beijing, China) was used to measure the MMP in T cells. Cells were incubated with JC-1 working solution at 37 °C for 20 min, then washed twice with JC-1 buffer for fluorescence detection. BODIPY emission was recorded on an oxidized C11 signal (FITC channel).

Luminex assay

The rat sera were analyzed for cytokine concentrations [interleukin (IL)-10, IL-2, IL-1 α , IL-4, interferon gamma (IFN- γ), tumor necrosis factor alpha (TNF- α), IL-5, IL-6, growth-regulated oncogene (GRO)/keratinocyte chemoattractant (KC), IL-12p70] using the Millipore Luminex 200 instrument (Luminex Corporation, Austin, TX, United States), after incubation of the samples with beads according to the manufacturer's instructions. The quantification was performed with Luminex xPonent version 3.1 software.

Cell culture

Healthy mononuclear cells from the spleen of rats and peripheral blood of humans were collected by gradient centrifugation with respectively, rat tissue mononuclear cell separation solution (Solarbio, Beijing, China) and human peripheral blood mononuclear cell separation solution (Solarbio, Beijing, China). T cells were purified through positive magnetic selection using microbeads (Miltenyi Biotec, Bergisch Gladbach, Germany) and cultivated at 2.0×10^6 cells/well in 6-well plates with RPMI-1640 with 5% fetal bovine serum and 100 IU/mL IL-2. Within the first 72 h, the anti-CD3/CD28 antibody (Cat# 201401, RRID: AB_893302; 2 μ g/mL and Cat# 200902, RRID: AB_313891; 1 μ g/mL) were used to stimulate the T cells.

Cell proliferation assay

The Cell Counting Kit-8 (CCK-8) assay (Boster, Hubei, China) was used to evaluate T cell proliferation *in vitro*. The CON group ($n = 3$), 5-FU group (5-FU 15 μ mol/L, MCE, Shanghai, China; $n = 3$); ferrostatin-1 (Fer-1) group (Fer-1 2 μ mol/L, MCE, Shanghai, China; $n = 3$); 5-FU+fer-1 group (5-FU 15 μ mol/L + fer-1 2 μ mol/L) were included. After 72 h of culture, CCK-8 solution was added to each well of the 96-well plates and allowed to incubate for 2 h at 37 °C, and the optical density value at 450 nm was recorded.

Histopathology

The femurs and grafts ($n = 6$ for each group) were removed on postoperative day 7. The femurs were decalcified with EDTA decalcifying solution (Solarbio, Beijing, China). Then both femurs and grafts were fixed in 10% paraformaldehyde, dehydrated, paraffin-embedded, cut into 4 μ m slides, and stained with hematoxylin and eosin (H&E; G1120; Solarbio, Beijing, China).

Immunohistochemistry

CD3⁺ cell infiltration was assessed on spleen and liver graft sections as follows: Tissue sections were heated for 15 min in EDTA (pH 8.0) in a microwave for antigen retrieval, incubated in 3% hydrogen peroxide for 30 min to eliminate endogenous peroxidase activity, and blocked in normal goat serum. Then the sections were incubated overnight at 4 °C with a rat anti-CD3 antibody (CD3-12, Cat# ab11089, RRID: AB_2889189; Abcam, Cambridge, MA, United States) and incubated with a secondary antibody (Goat Anti-Rat IgG H&L, Cat# ab97057, RRID: AB_10680316; Abcam, Cambridge, MA, United States) or 30 min at room temperature the next day. Finally, the sections were stained with freshly prepared diaminobenzidine solution and counterstained with hematoxylin. ImageJ software was applied to 200 \times images to quantify the CD3-positive fields.

Transmission electron microscopy

Cells were collected after centrifugation and fixed in 2.5% glutaraldehyde. After dehydration through graded ethanol, the cells were embedded in epoxy resins and cut into ultrathin sections. The

morphologic changes in mitochondrial ultrastructure were observed using a transmission electron microscope (HT7800; Hitachi, Tokyo, Japan).

Western blot analysis

Total protein was extracted using RIPA buffer containing protease and phosphatase inhibitors. The mixture was placed on ice for 30 min for cell lysis, and then centrifuged at 12000 g for 15 min at 4 °C to discard the cell debris. Total protein concentration was quantified by the BCA Protein Assay Kit (Beyotime Biotechnology, Beijing, China). The proteins were resolved by sodium dodecyl sulfate-polyacrylamide gel electrophoresis, electrotransferred to polyvinylidene fluoride membranes, and blocked in 5% skimmed milk for 1 h. Then the membranes were incubated overnight at 4 °C with primary antibodies against FTH1 (EPR18878, Cat# ab183781; Abcam, Cambridge, MA, United States), NCOA4 (Cat# PA5-96398, RRID: AB_2808200; Thermo Fisher Scientific, Waltham, MA, United States), Nrf2 (E5F1A, Cat# 20733S, Cell Signaling Technology, Danvers, MA, United States), HO-1 (EPR1390Y, Cat# ab68477, RRID: AB_11156457; Abcam, Cambridge, MA, United States), and GPX4 (EPNCIR144, Cat# ab125066, RRID: AB_10973901; Abcam, Cambridge, MA, United States). β -actin (SP124, Cat# ab115777, RRID: AB_10899528; Abcam, Cambridge, MA, United States) antibody served as the internal control. The membranes were washed and then incubated with a secondary antibody (Goat anti-Rabbit IgG H+L, Cat# A16110; Thermo Fisher Scientific, Shanghai, China) for 1 h at RT. Proteins were detected with an imaging system (Bio-Rad, Hercules, CA, United States), and band intensities were analyzed with ImageJ software (National Institutes of Health, Bethesda, MD, United States).

Statistical analyses

The statistical analyses were performed with SPSS 23.0 (IBM Analytics) and GraphPad 8.0 (GraphPad Software). The statistical methods of this study were reviewed by Yuan Wang from the Department of Biostatistics and Epidemiology, The First Central Clinical School, Tianjin Medical University. Data are presented as the mean \pm standard error of the mean. The unpaired *t*-test was used to assess the differences between the two groups, and a one-way analysis of variance was used to assess the differences among three or more groups. $P < 0.05$ was considered statistically significant.

RESULTS

Metronomic CAP exerts a marginal myelosuppressive effect, compatible with continuous administration

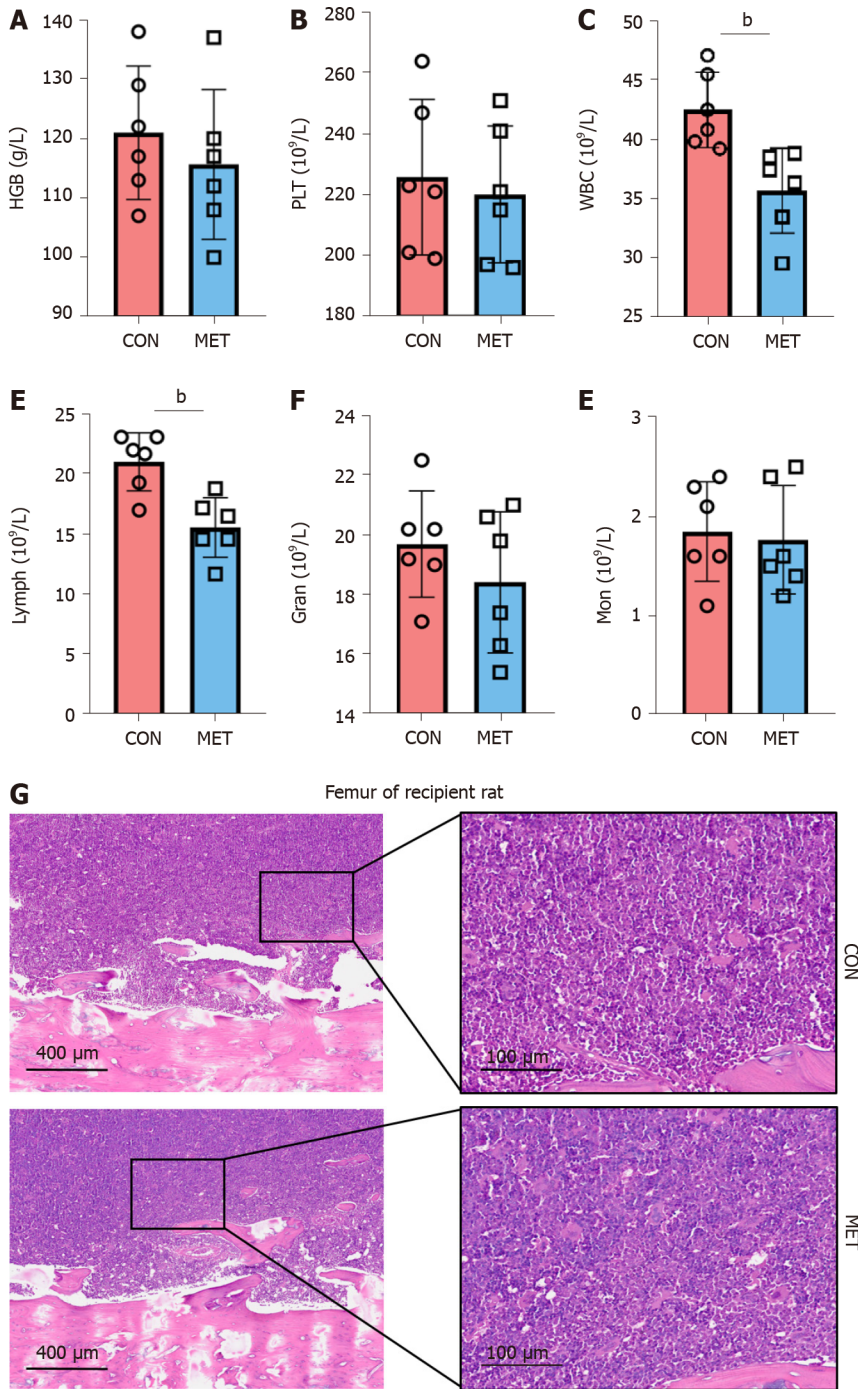
5-FU, the end product of CAP, may induce myelotoxicity. Thus, we first evaluated metronomic CAP's myelotoxicity on peripheral blood hemoglobin (HGB), platelets (PLTs), and leukocytes in a rat model of orthotopic LT, where recipient Brown-Norway rats received the livers from Lewis rats. Seven days after LT, there was no significant difference in the index of HGB and PLTs between the CON group and the MET group (Figure 1A and B). However, leukopenia with a reduced number of lymphocytes was found in the MET group, while the number of other leukocyte subsets (granulocytes and mononuclear cells) was not significantly different (Figure 1C-F). These results suggest that CAP had a relatively targeted killing effect on lymphocytes, but no obvious effect on PLTs, erythrocytes, monocytes, or granulocytes. In the bone marrow, the rats in the MET group had no pathological manifestation of myelosuppression (Figure 1G), suggesting that the lymphocytopenia caused by CAP did not result from myelosuppression.

Metronomic CAP reduces acute rejection and alleviates graft injury

To evaluate the effect of metronomic CAP during acute rejection, the grafted livers were harvested on day 7 after LT for histopathological examination. As shown in Figure 2A, prominent acute rejection with severe bile duct damage, endothelitis, and hepatocyte vacuolation occurred in the grafts of the CON group. Portal areas were infiltrated by inflammatory cells, hepatic sinusoids were greatly expanded, and the sinusoidal endothelial cells were markedly swollen. Compared with the CON group, acute rejection in the MET group was ameliorated, as evidenced by inflammatory cell infiltration being confined to only some of the portal areas and the degeneration of a few bile duct epithelia. The Banff scores [28] decreased in the MET group compared with the CON group (Figure 2B). On day 7 after LT, liver damage was assessed by measuring serum levels of AST and ALT (Figure 2C and D). Compared with the CON group, CAP significantly decreased the serum levels of ALT and AST. However, TBIL and DBIL in both groups showed an increasing trend after the operation, but there was no significant difference between the two groups (Figure 2E and F). In the survival analysis, a log-rank (Mantel Cox) test was conducted. Rats in the MET group had a longer survival time compared with the CON group (Figure 2G, median survival time: 16.5 and 11.5 d; $P < 0.01$).

Metronomic CAP reduces the number of CD3⁺ T cells in graft recipients

Next, to investigate whether the inhibition of acute rejection by metronomic CAP involved an effect on



DOI: 10.3748/wjg.v29.i20.3084 Copyright ©The Author(s) 2023.

Figure 1 Metronomic capecitabine showed no significant myelosuppression. A and B: Hemoglobin level and platelets count in the peripheral blood; C-F: White blood cells, lymphocytes, granulocytes, and monocytes counts in the peripheral blood; G: Bone marrow tissue was stained with hematoxylin and eosin (50 × and 200 ×). Statistical analysis was done by unpaired *t*-test, *n* = 6. Data are shown as mean ± SD; ^b*P* < 0.01 vs the control group. CON: Untreated control groups, rats received 0.9% normal saline for 7 d; MET: Metronomic capecitabine (CAP)-treated groups, rats received metronomic CAP (100 mg/kg/d) treated for 7 d; HGB: Hemoglobin; PLT: Platelets; WBC: White blood cells; lymph: Lymphocytes; Gran: Granulocytes; Mon: Monocytes.

T cells, CD3⁺ T cells in the peripheral blood, grafts, and spleens were analyzed. Compared to the CON group, the CD3⁺ T cells in the peripheral blood were significantly lower in the MET group (Figure 3A and B). In addition, a large number of CD3⁺ T cells was localized in the portal canal area of the CON group. Infiltrated CD3⁺ T cells in both the liver and spleen were significantly reduced in the MET group (Figure 3C and D). These results indicate that metronomic CAP can decrease the number of CD3⁺ T cells in the peripheral blood, liver, and spleen of the recipient rats.

Metronomic CAP regulates serum cytokine levels

Cytokines are an important reflection of immune cell function and immune status. Thus, the levels of

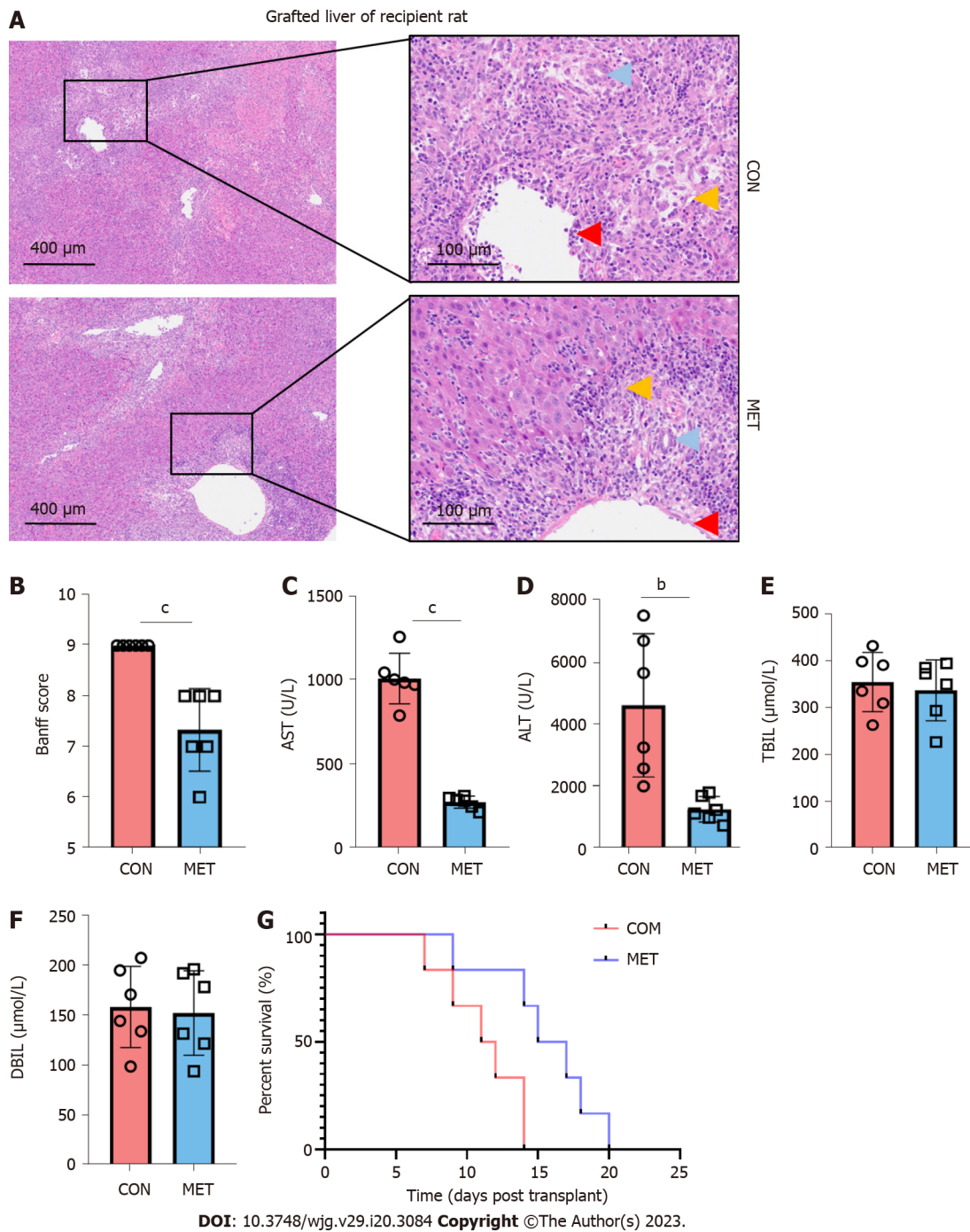


Figure 2 Metronomic capecitabine improves liver function and ameliorates liver allograft rejection. A: Liver allograft tissue was stained with hematoxylin and eosin (50 × and 200 ×). Liver tissue, portal vein, and bile duct were significantly injured in the untreated control group (CON), with a large number of inflammatory cells infiltrated. In the metronomic capecitabine-treated groups (MET), liver tissue destruction was relatively mild, with limited infiltration of inflammatory cells (yellow arrows), relatively little degeneration of portal vein endothelium (red arrows), and bile duct epithelium (blue arrows); B: The severity of acute rejection was graded according to the Banff liver rejection criteria; C-F: Alanine transaminase, aspartate transaminase, total bilirubin, and direct bilirubin levels in the peripheral blood; G: Survival analysis of rats after liver transplantation. The median survival time of the CON and MET groups were 11.5 d and 16 d, respectively ($P < 0.01$). The survival analysis was done by log-rank (Mantel Cox) test, $n = 6$. Statistical analysis was done by unpaired *t*-test, $n = 6$. Data are shown as mean ± SD; ^b $P < 0.01$ vs the control group, ^c $P < 0.001$ vs the control group. CON: Untreated control groups, rats received 0.9% normal saline for 7 d; MET: Metronomic capecitabine (CAP)-treated groups, rats received metronomic CAP (100 mg/kg/d) treated for 7 d; ALT: Alanine transaminase; AST: Aspartate transaminase; TBIL: Total bilirubin; DBIL: Direct bilirubin.

IFN- γ , TNF- α , human GRO/KC, IL-1 β , IL-2, IL-4, IL-5, IL-6, IL-10, and IL-12p70 in peripheral blood and graft were quantified by Luminex assay. As shown in Figure 4, the levels of pro-inflammatory IFN- γ , TNF- α , IL-2, and IL-12p70 in the MET group were significantly lower than those in the CON group. Other cytokines (IL-1 β , IL-5, IL-6, IL-4, IL-10, and GRO/KC) did not show significant changes (Supplementary Figure 1). The results showed that metronomic CAP plays an immunosuppressive role by downregulating the concentration of pro-inflammatory cytokines.

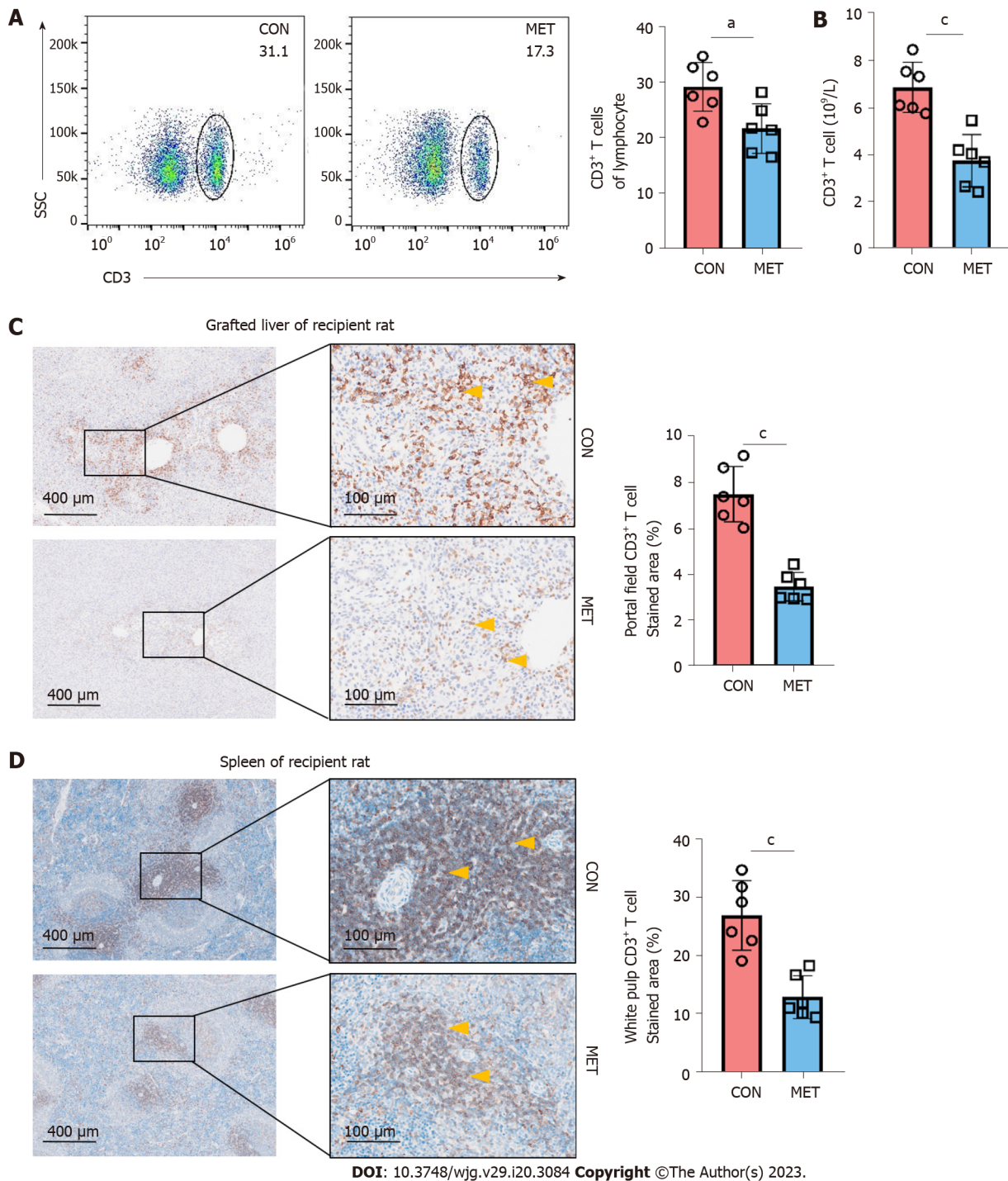


Figure 3 Metronomic capecitabine decreased the infiltration of CD3⁺ T cells in peripheral blood, liver allografts, and spleen. A: The percentage of CD3⁺ T cells among lymphocytes in the peripheral blood at postoperative day 7; B: The number of CD3⁺ T cells in the peripheral blood at postoperative day 7; C and D: Grafted liver (C) and spleen (D) sections were stained for CD3. The samples from each group were collected on postoperative day 7. The arrows show positive staining (50 × and 200 ×). Quantification of the proportion of CD3⁺ positive area within a given section (%). Statistical analysis was done by unpaired *t*-test, *n* = 6. Data are shown as mean ± SD; ^a*P* < 0.05 vs the control group, ^c*P* < 0.001 vs the control group. CON: Untreated control groups, rats received 0.9% normal saline for 7 d; MET: Metronomic capecitabine (CAP)-treated groups, rats received metronomic CAP (100 mg/kg/d) treated for 7 d.

Metronomic CAP increases T cell free ferrous ions and induces lipid peroxidation in vivo

The immune activation of T cells is particularly important in the acute rejection of organ transplants. Similar to many commonly used immunosuppressants, the killing effect of CAP on T cells is also key to its immunosuppressive activity [13]. Therefore, we further explored the mechanism of T cell killing by metronomic CAP. Ferroptosis is a new form of ROS-dependent programmed cell death that may play an important role in CAP-mediated cytotoxicity. Thus, we measured by flow cytometry the concentration of free ferrous ions, ROS level, and lipid ROS level in peripheral blood CD3⁺ T cells from transplanted rats of both groups at day 7. Compared with the CON group, free ferrous ion concen-

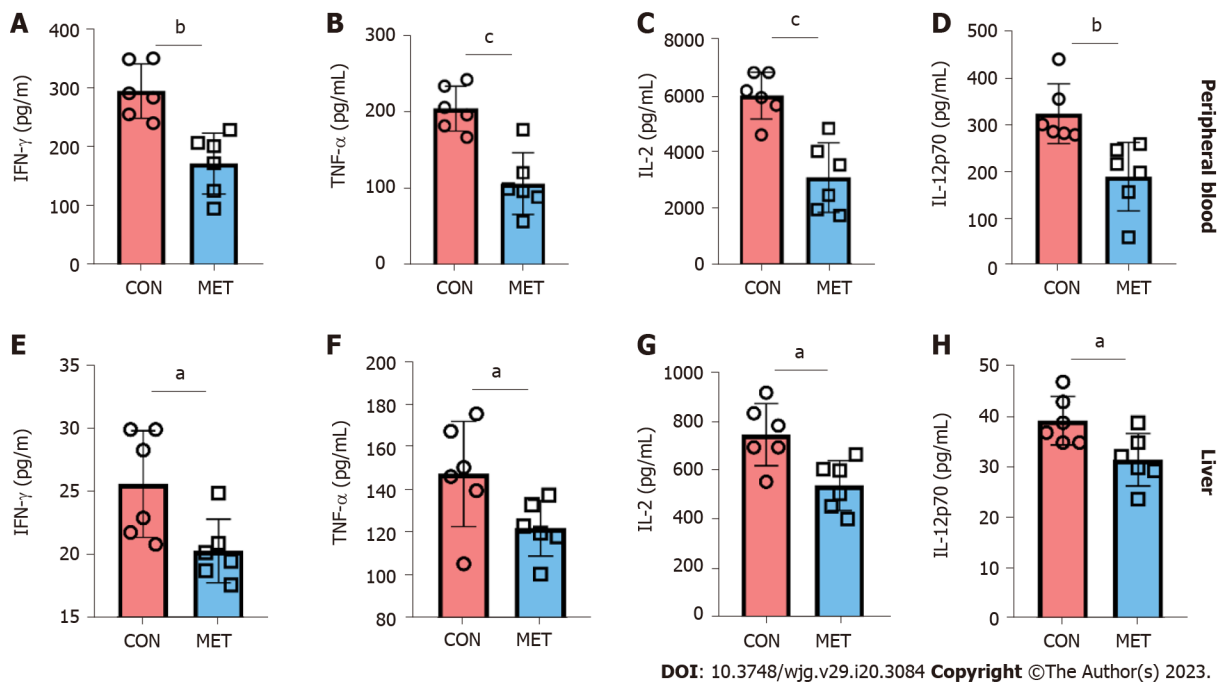


Figure 4 Cytokine concentrations of peripheral blood and liver graft in transplanted rats. Use Luminex assay to detect the concentrations of interferon gamma (IFN- γ), tumor necrosis factor alpha (TNF- α), interleukin (IL)-2 and IL-12 in peripheral blood and graft. A and E: IFN- γ ; B and F: TNF- α ; C and G: IL-2; D and H: IL-12. Statistical analysis was done by unpaired Students *t*-test, $n = 6$. Data are shown as mean \pm SD; ^a $P < 0.05$ vs the control group, ^b $P < 0.01$ vs the control group, ^c $P < 0.001$ vs the control group. CON: Untreated control groups, rats received 0.9% normal saline for 7 d; MET: Metronomic capecitabine (CAP)-treated groups, rats received metronomic CAP (100 mg/kg/d) treated for 7 d; IFN- γ : Interferon gamma; TNF- α : Tumor necrosis factor alpha; IL: Interleukin.

tration (Figure 5A), total ROS (Figure 5B), and lipid ROS (Figure 5C) levels were increased in the MET group. At the same time, the detection of the MMP showed a decreasing trend in the MET group (Figure 5D). These results indicated that metronomic CAP leads to the generation of ferrous ions and results in lipid peroxidation, which conforms to the typical characteristics of ferroptosis.

5-FU triggers ferritinophagy and ferroptosis in T cells *in vitro*

To further explore *in vitro* the mechanism underlying the CAP-mediated ferroptosis linked to immunosuppression observed *in vivo*, primary CD3⁺ T cells were sorted from rat spleens and human peripheral blood (Supplementary Figure 2). Both primary CD3⁺ T cells were treated with 5-FU *in vitro* (Supplementary Figure 3). This treatment significantly inhibited cell viability, which was attenuated by the ferroptosis inhibitor Fer-1 (Figure 6A). Transmission electron microscopy revealed typical characteristics of ferroptosis in 5-FU-treated group, namely, smaller mitochondria with increased membrane density, and diminished mitochondrial cristae (Figure 6B). Free ferrous ions concentration was increased in the 5-FU-treated group, whereas Fer-1 partially reversed the increase of ferrous ions induced by 5-FU (Figure 6C). As a selective cargo receptor, NCOA4 mediates the transport of ferritin into lysosomes, inducing ferroptosis. Western blot analysis revealed that 5-FU treatment induced FTH1 decrease, but a tendency toward increasing NCOA4 expression was observed (Figure 6D), consistent with the *in vivo* studies (Supplementary Figure 4). These results confirmed that the cytotoxicity of 5-FU is at least partly related to the induction of T cell ferroptosis, in which the increase of free ferrous ions caused by NCOA4-mediated ferritinophagy plays an important role.

5-FU-triggered ferroptosis is associated with the inhibition of the Nrf2-HO-1/GPX4 antioxidative pathway

To evaluate the effect of 5-FU on the antioxidant system, antioxidant-related proteins were measured in rat and human primary CD3⁺ T cells treated with 5-FU. The expression of Nrf-2, HO-1, and GPX4 was evaluated in both groups and compared, and treatment with 5-FU was found to be associated with a marked decrease (Figure 7A), consistent with the *in vivo* studies (Supplementary Figure 4). The results showed that 5-FU treatment increased total ROS and lipid ROS levels and decreased MMP (Figure 7B-D). It also decreased glutathione (GSH) levels and increased the oxidative stress biomarker malondialdehyde (MDA) (Figure 7E and F). Fer-1 inhibits ferroptosis partly by activating Nrf2[29]. Accordingly, it reversed 5-FU-mediated inhibition of Nrf-2, HO-1, and GPX4, increased GSH level, and decreased MDA content, thereby alleviating cell peroxidation induced by 5-FU (Figure 7A-D). These results suggest that 5-FU inhibits the antioxidant system of T cells, inducing the T cells damaged by lipid peroxidation, which results in ferroptosis.

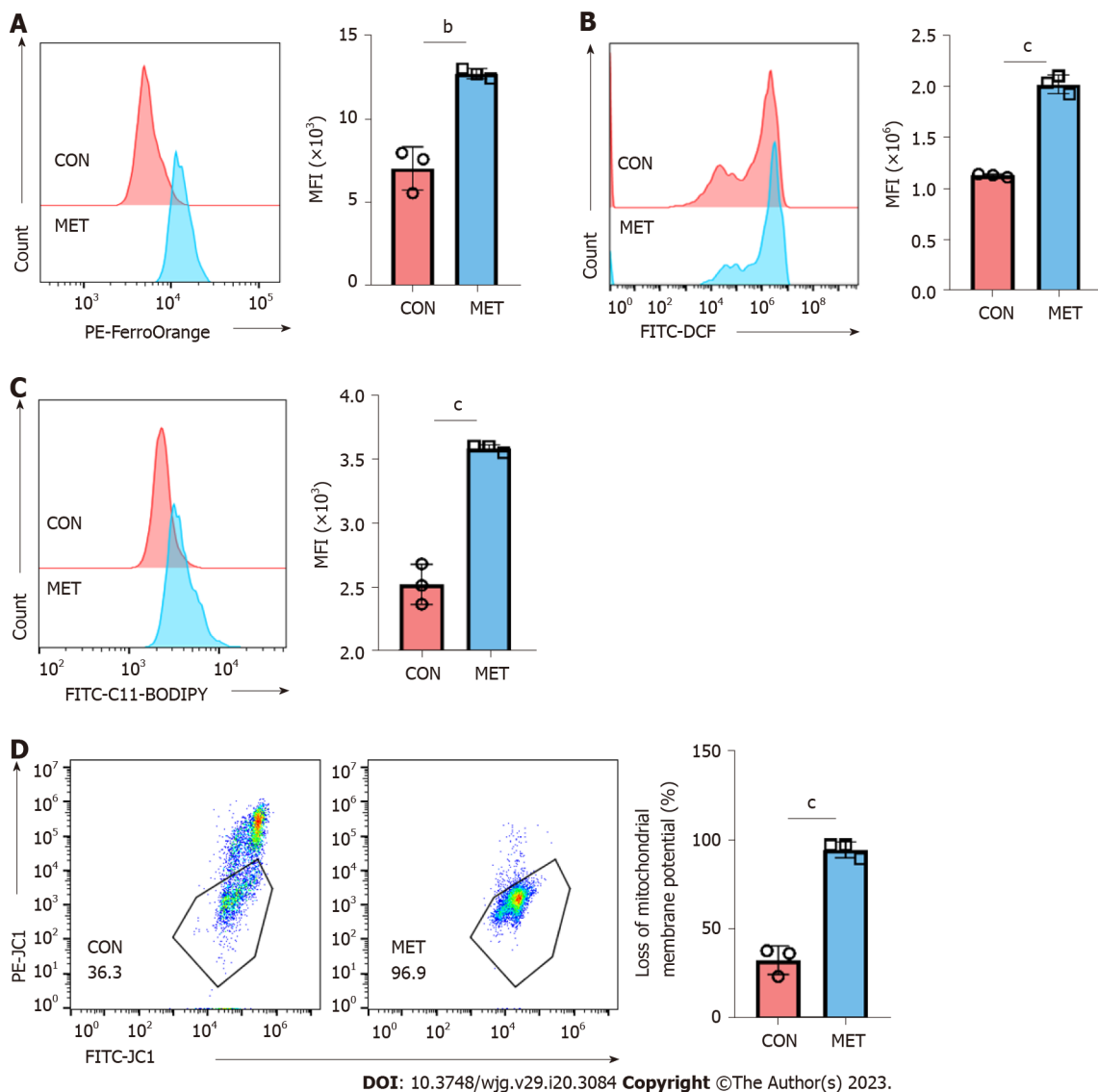


Figure 5 Metronomic capecitabine caused the increase of free ferrous ions and oxidative stress in peripheral blood CD3⁺ T cells of transplanted rats. A: Representative FACS data showing differential FerroOrange staining reflecting different cytoplasmic labile iron concentrations in control groups and metronomic capecitabine-treated rats, followed by statistical analysis of mean fluorescence intensity (MFI); B and C: Reactive oxygen species (ROS) and lipid ROS detected by FACS using DCFH-DA and C11-BODIPY respectively, BODIPY emission was recorded on oxidized C11 (FITC channel) signal. The graph shows the statistical analysis of differential MFIs in the two groups; D: The proportion of cells with reduced mitochondrial membrane potential was assessed by flow cytometry. Statistical analysis was done by unpaired *t*-test, *n* = 3. Data are shown as mean ± SD; ^b*P* < 0.01 vs the control group, ^c*P* < 0.001 vs the control group. CON: Untreated control groups, rats received 0.9% normal saline for 7 d; MET: Metronomic capecitabine (CAP)-treated groups, rats received metronomic CAP (100 mg/kg/d) treated for 7 d; MFI: Mean fluorescence intensity.

DISCUSSION

The conflict between the risk of tumor formation and immune rejection after transplantation has always been a concern. Therefore, it is of great clinical value to identify a drug with both immunosuppressive and anticancer effects. CAP is a classic chemotherapy drug for HCC[4,6], which has been shown to have immunosuppressive effects in a previous study[8], suggesting that metronomic CAP can be used as an immunosuppressant after transplantation and bring long-term benefits to LT patients with HCC. In our previous study, we found that metronomic CAP exerts immunosuppressive effects on normal mice by inducing T cell apoptosis[13]; however, the effect of CAP on the immune system in the context of organ transplantation was unclear. Therefore, we explored the safety, availability, and mechanism of metronomic CAP as an immunosuppressant in a model of rat orthotopic LT. Our results suggest that metronomic CAP can inhibit the acute rejection of LT by inhibiting T cells while avoiding the main side effects of 5-FU. Its mechanism is related to the induction of ferritin degradation and the inhibition of antioxidant-related proteins, which ultimately leads to the death of T cells (Figure 8).

The main effects of 5-FU are on rapidly proliferating tissues, specifically bone marrow. 5-FU suppressed bone marrow hematopoiesis including a significant decrease in the number of erythrocytes,

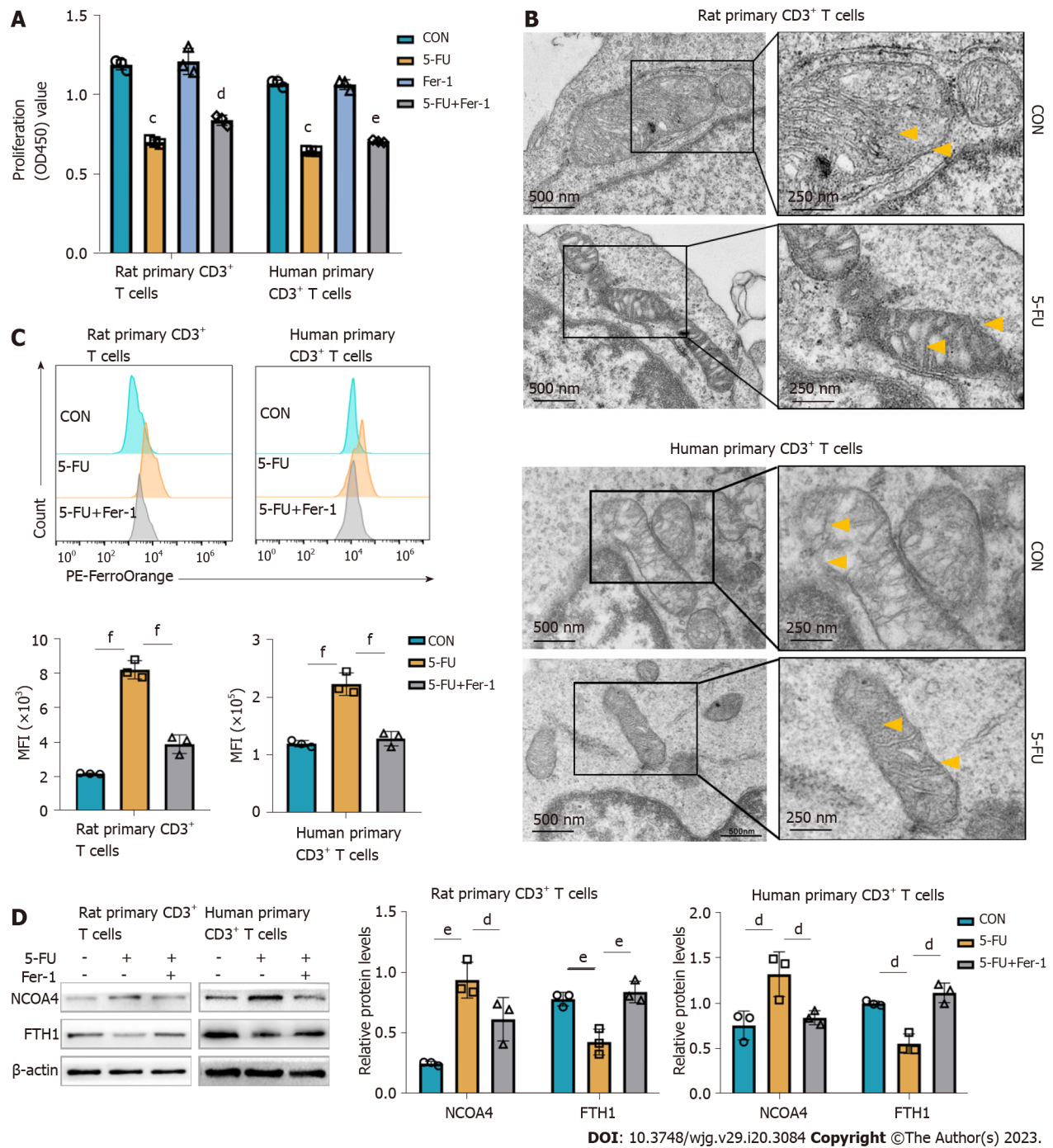
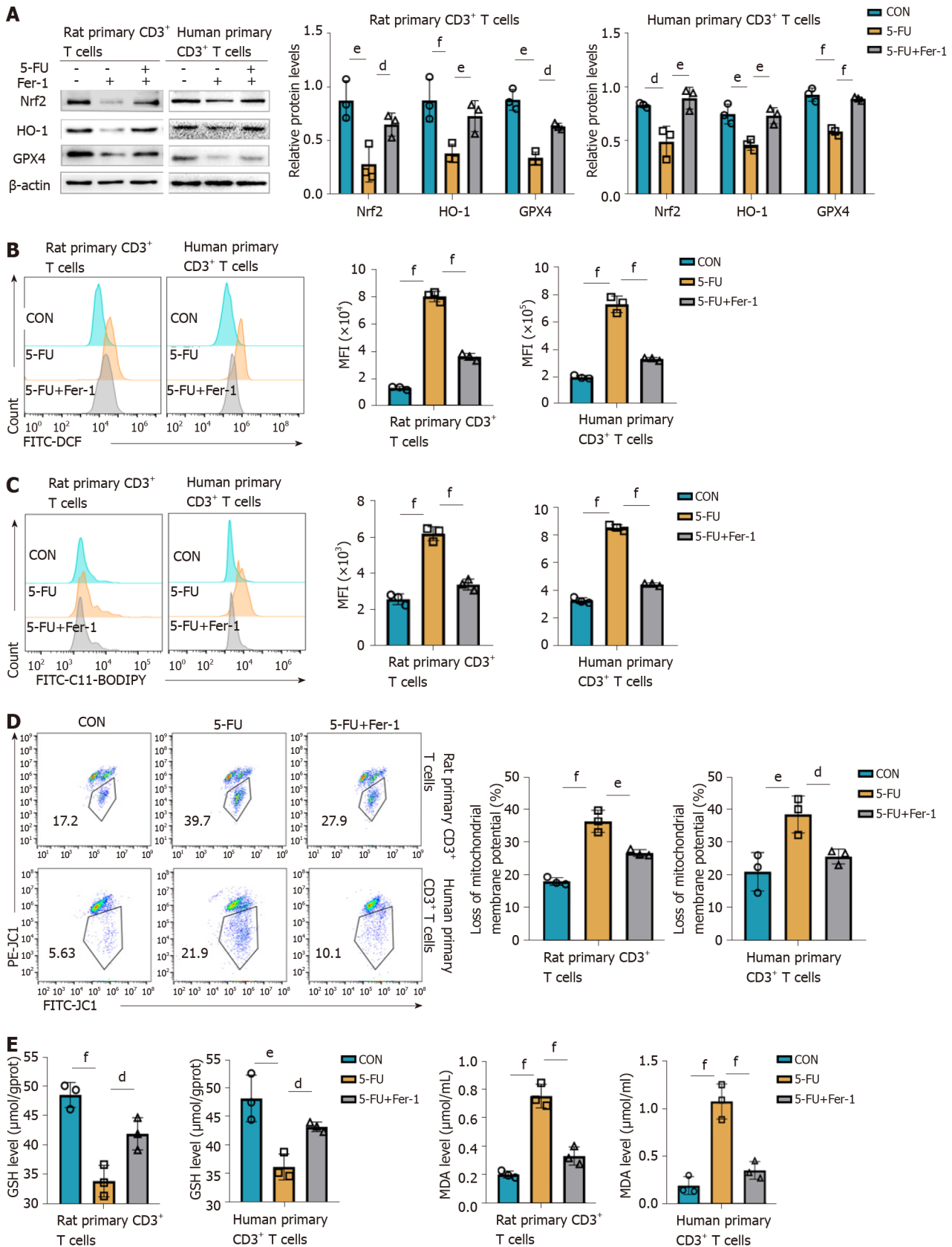


Figure 6 5-fluorouracil increases the pool of labile iron and contributes to ferroptosis in CD3⁺ T cells. *Vitro* experiments were conducted on rat splenic and human peripheral blood CD3⁺ T cells, which were sorted by immunomagnetic beads. According to predetermined IC50, the rat, and human primary CD3⁺ T cells were treated with 5-fluorouracil (5-FU) (15 μmol/L) and ferrostatin-1 (Fer-1) (2 μmol/L) for 48 h. A: Cell viability was assessed with a Cell Counting Kit-8 kit; the results are expressed as optical density read at 450 nm; B: Transmission electron microscopy images of mitochondria in T cells show increased membrane density (yellow arrows) and a shrunk morphology (Scale bar, 500 nm, and 250 nm); C: Representative FACS data showing FerroOrange staining as the measurement of the level of cytoplasmic labile iron in primary CD3⁺ T cells. The graph shows the statistical analysis of mean fluorescence intensity in the different groups; D: Levels of ferritinophagy-related proteins nuclear receptor coactivator 4 and ferritin heavy chain 1 were assessed by western blot. CON groups: T cells were treated with DMSO for 48 h; 5-FU groups: T cells were treated with 5-FU (15 μmol/L) for 48 h; 5-FU+ Fer-1 groups: T cells were treated with 5-FU (15 μmol/L) and Fer-1 (2 μmol/L) for 48 h. Statistical analysis was done by one-way ANOVA, *n* = 3. Data are shown as mean ± SD. Data are shown as mean ± SD. **P* < 0.001 vs the control group, ^o*P* < 0.05 vs the 5-FU group, ^e*P* < 0.01 vs the 5-FU group, ^f*P* < 0.001 vs the 5-FU group. CON: Untreated control groups; 5-FU: 5-fluorouracil; NCOA4: Nuclear receptor coactivator 4; FTH1: Ferritin heavy chain 1; Fer-1: Ferrostatin-1.

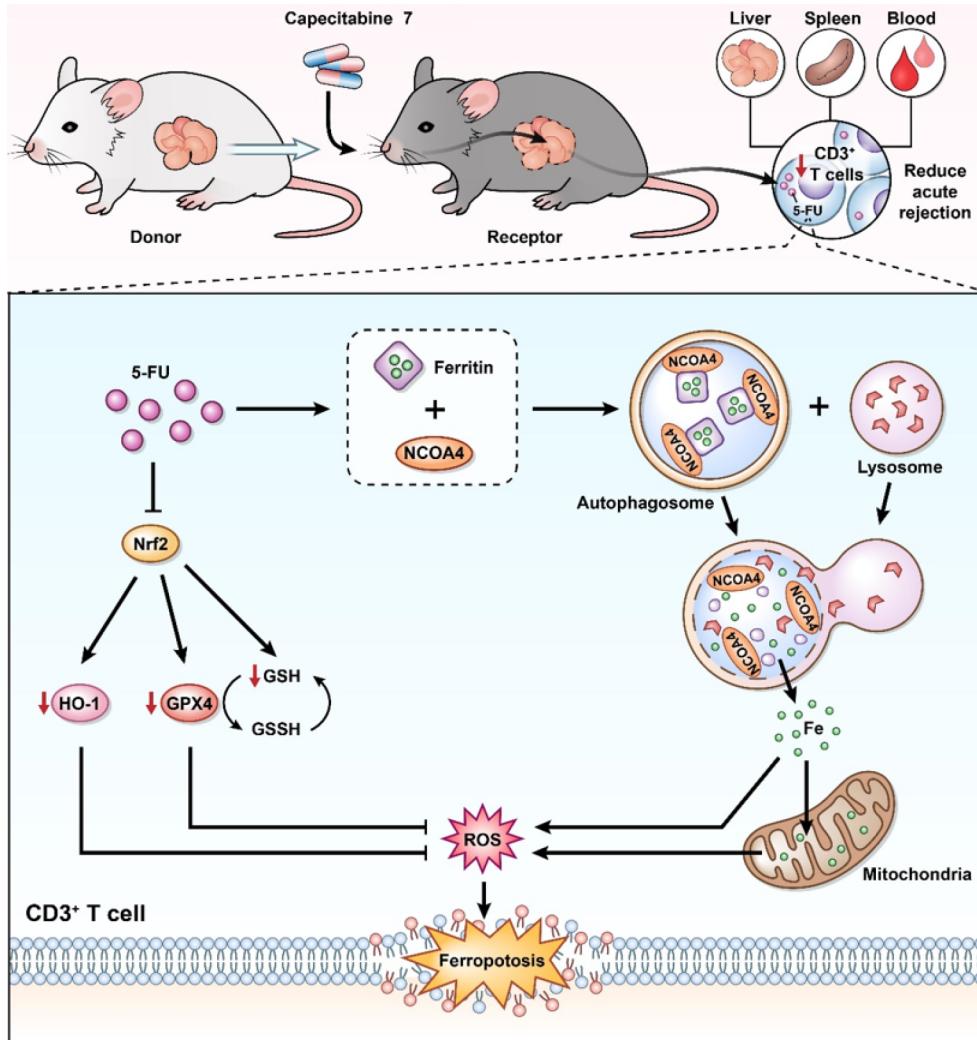
platelet, and leukocyte in the peripheral blood[30,31]. As the prodrug of 5-FU, it is of high clinical relevance to show the safety of the medication of CAP. Overall, metronomic CAP is considered safe, with fewer side effects than traditional chemotherapy regimens. Metronomic CAP is well tolerated and safe in clinical practice, including for patients with HCC or patients after LT[8,32-34]. In mice, there was also no obvious myelosuppression in the MET group 7 d after taking CAP, though the related studies



DOI: 10.3748/wjg.v29.i20.3084 Copyright ©The Author(s) 2023.

Figure 5 5-fluorouracil disturbs the antioxidative/oxidative balance, resulting in CD3⁺ T cells ferroptosis. A: Levels of antioxidant proteins nuclear erythroid 2 p45-related factor 2, heme oxygenase-1, and glutathione peroxidase 4 assessed by western blot, and corresponding graphs showing the statistical comparison between groups; B and C: Reactive oxygen species (ROS) and lipid ROS of rat and human CD3⁺ T cells were detected by FACS using DCFH-DA and C11-BODIPY fluorescent conjugates, BODIPY emission was recorded on oxidized C11 (FITC channel) signal; the graphs display the comparison of mean fluorescence intensity levels in the different groups; D: Proportion of cells with reduced mitochondrial membrane potential assessed by flow cytometry; E and F:

Glutathione and malondialdehyde content T cells after treatment for 48 h. CON groups: T cells were treated with DMSO for 48 h; 5-fluorouracil (5-FU) groups: T cells were treated with 5-FU (15 $\mu\text{mol/L}$) for 48 h; 5-FU+ferrostatin-1 (Fer-1) groups: T cells were treated with 5-FU (15 $\mu\text{mol/L}$) and Fer-1 (2 $\mu\text{mol/L}$) for 48 h. Statistical analysis was done by one-way ANOVA, $n = 3$. $^{\text{a}}P < 0.05$ vs the 5-FU group, $^{\text{b}}P < 0.01$ vs the 5-FU group, $^{\text{c}}P < 0.001$ vs the 5-FU group. Nrf2: Nuclear erythroid 2 p45-related factor 2; HO-1: Heme oxygenase-1; GPX4: Glutathione peroxidase 4; GSH: Glutathione; MDA: Malondialdehyde; CON: Untreated control groups; 5-FU: 5-fluorouracil; Fer-1: Ferrostatin-1; MFI: Mean fluorescence intensity.



DOI: 10.3748/wjg.v29.i20.3084 Copyright ©The Author(s) 2023.

Figure 8 Possible immunosuppressive mechanisms of metronomic capecitabine on T cells by ferroptosis induction. In the rat model of acute rejection after liver transplantation, metronomic capecitabine (CAP) exerts an immunosuppressive effect by decreasing T cell numbers in peripheral blood, liver graft, and spleen. Metronomic CAP increases the concentration of free ferrous ions by inducing ferritin degradation while inhibiting the expression of antioxidant proteins. Eventually, these effects lead to peroxidation damage and iron toxicity, which induce T cell death. 5-FU: 5-fluorouracil; Nrf2: Nuclear erythroid 2 p45-related factor 2; NCOA4: Nuclear receptor coactivator 4; HO-1: Heme oxygenase-1; GPX4: Glutathione peroxidase 4; GSH: Glutathione; GSSH: Oxidized glutathione; ROS: Reactive oxygen species.

showed that 5-FU could cause severe myelosuppression after 7 d of administration[35]. TP is a key enzyme in the metabolism of CAP[36]. The lack of TP in bone marrow may explain the lack of bone marrow suppression of CAP[11,13]. In a past study, we established the safety of CAP in CAP-fed mice, which did not cause significant myelosuppression after 21 d of administration[13]. However, the depletion of lymphocytes is not related to bone marrow suppression, and the high expression of TP in lymphocytes directly leads to the killing effect of CAP[11]. CAP is safe for long-term use because it can circumvent the inhibitory effect of 5-FU on bone marrow hematopoietic function.

When acute rejection occurs, immune cells mainly infiltrate the hilar region of the grafted liver, inducing pericentral inflammation, damaging the vascular and bile duct endothelium, damaging hepatocytes, and destroying the lobular structure[37,38]. CAP can preserve the function and structure of the transplanted liver by inhibiting acute rejection. Compared with the CON group, the Banff score was significantly lower in the MET group at 7 d after transplantation while the elevation of ALT and AST in

the MET group was significantly less pronounced than that in the CON group. ALT and AST are primarily expressed in liver cells, and liver allograft destruction caused by rejection is positively associated with ALT and AST expression[39,40]. However, TBIL and DBIL in both groups showed an increasing trend after surgery with no significant difference between the two groups. It may be related to biliary tract injury and bilirubin stasis caused by the lack of hepatic artery reconstruction and the use of cannula reconstruction of the bile duct in the traditional rat “two-cuff method” orthotopic LT[41].

Antigen presentation and T cell activation are key steps in rejection. Donor-derived antigen-presenting cells provide immune stimulation to recipient naive CD4⁺ T cells, known as the direct antigen presentation pathway, which is the main mode of activation in acute rejection[42,43]. Once rejection is initiated, CD8⁺ T cells mainly differentiate into cytotoxic T cells, which directly cause graft injury. CD4⁺ T cells can differentiate into many subtypes, mainly helper T cells (Th1, Th2, and Th17) and regulatory T cells (Treg). In acute rejection, T cells differentiate mainly to Th1, driven by pro-inflammatory cytokines such as IL-12 and IFN- γ . Th1 cells secrete IL-2 and IFN- γ , providing a positive feedback loop to stimulate Th1 cells to proliferate further. IFN- γ is usually associated with proinflammatory and immune activation processes while IL-2 is necessary for survival and effects of activated T cells. T cell activation, proliferation, differentiation, and migration are the immune basis of acute rejection after organ transplantation, and are often used as the targets of clinical immunosuppression[42, 44,45]. The results of our study showed that IL-2 and IFN- γ were decreased in CAP treated rats. The changes in cytokines suggest that in addition to decreasing the number of T cells, CAP may also target Th0 cells' differentiation. Since IFN- γ has a stimulatory effect on the secretion of TNF- α by M1 macrophages[46], the decrease in TNF- α may be related to the inhibition of IL-2 secretion in T cells by CAP. By inducing the programmed death of T cells, CAP mitigates transplant rejection and protects graft function. Moreover, cytokines associated with rejection were also affected by CAP treatment. Metronomic CAP significantly reduced the levels of pro-inflammatory cytokines (IFN- γ , TNF- α , IL-2, and IL-12p70), which are mainly secreted by immune cells and contributing to rejection[47-50].

The data from our study demonstrated that the selective cytotoxic effect of the T cells of metronomic CAP is crucial for the prevention of acute organ transplant rejection. Next, we further explored the mechanism underlying the immunosuppressive effect of metronomic CAP by studying CD3⁺ T cells in more details. Mitochondria is a main source of ROS and mitochondria ROS is a critical component of T cell activation, proliferation, and effector function of T cells[51-53]. However, excessive ROS production, inducible by a high level of iron, leads to ROS-mediated membrane phospholipid peroxidation and T cell death upon activation[54]. Thus, we investigated the effect of CAP on the level of CD3⁺ T cell ferrous ions with a ferrous probe and found that CAP treatment induced ferrous ion accumulation, accompanied by increased ROS and lipid ROS and decreased MMP. Mitochondrial ROS production and MMP reduction are two important parameters of mitochondrial damage, and lipid peroxidation following ROS generation plays an important role in ROS-induced cellular damage[55-57]. These results indicate that metronomic CAP increased ferrous ion accumulation and oxidative damage in the CD3⁺ T cells of rats after transplantation, which may be the mechanism behind CAP-induced T cell reduction. Next, we used rat and human primary CD3⁺ T cells to further explore the role of ferroptosis in CAP-induced immunosuppression *in vitro*. Free ferrous iron overload, lipid peroxide accumulation, and specific mitochondrial morphological changes are three key characteristics that distinguish ferroptosis from other programmed cell deaths[14]. In this study, typical mitochondrial changes were observed in T cells of the 5-FU group under transmission electron microscopy. Ferrous ion in rat primary CD3⁺ T cells of the 5-FU group was increased with the downregulation of FTH1 and upregulation of NCOA4, revealing the occurrence of ferritinophagy. That is, the autophagic degradation of ferritin, contributed to rat T cell ferrous overload, excessive lipid peroxidation, and eventually ferroptosis in the 5-FU group. Nrf2 is a core player in the regulation of antioxidant molecules in cells, which can induce the synthesis of HO-1 and GPX4[20,58]. The Nrf2-HO-1/GPX4 antioxidative system, which participates in the regulation of oxidative damage and inhibits erastin-induced ferroptosis[59], was suppressed by 5-FU *in vitro*. It also reduced GSH levels, indicative of impairment of antioxidant capacity, and improved the levels of MDA, an end-product of lipid peroxidation.

In this study, we showed that metronomic CAP alleviated rat LT rejection without the common side effect (myelosuppression) of antitumor drugs. T cell ferroptosis plays an important role in the antirejection effect of CAP, which can induce cell iron overload and suppress the Nrf2-HO-1/GPX4 antioxidant systems, directly increasing the levels of intracellular ROS, leading to severe mitochondrial damage in T cells. These results revealed a new mechanism of CAP-induced T cell programmed death and suggested the possibility of using CAP as an immunosuppressant after transplantation. As a traditional antitumor drug, CAP has immunosuppressive effects, that may kill tumor cells and induce T cell death at the same time. CAP may have both antirejection and antitumor effects on patients with HCC after LT, thereby having broad clinical application prospects. In light of our findings, CAP alone as an immunosuppressive agent does not achieve satisfactory therapeutic effects. Therefore, the combination and interaction of CAP with other immunosuppressive agents is an important research direction in the future. In addition, we observed interesting effects of CAP on different cytokines, but further observations were lacking. The effects of CAP on T cell subsets and other immune cells are worth further attention. In the future, we plan to establish tumor-bearing animal models for allotransplantation, to clarify the dual antirejection and antitumor effects of CAP. In conclusion, the immunosup-

pressive effect of CAP should be further explored to optimize the drug treatment regimen for LT patients with liver cancer.

CONCLUSION

Metronomic CAP can alleviate liver graft injury and reduce the proliferation and infiltration of CD3⁺ T cells in peripheral blood, graft, and spleen, thereby inhibiting acute rejection after LT. T cell ferroptosis plays an important role in the antirejection effect of CAP, which can induce cell iron overload and suppress the Nrf2-HO-1/GPX4 antioxidant systems, thereby directly increasing the levels of intracellular ROS and leading to severe oxidative damage in T cells.

ARTICLE HIGHLIGHTS

Research background

As a classical antimetabolite, capecitabine (CAP) has shown potential antirejection effects after liver transplantation (LT) in clinical trials. Our previous study showed that metronomic CAP can cause programmed T cell death in healthy mice by inducing oxidative stress, which is also the key step in ferroptosis. Thus, ferroptosis may play an important role in CAP-induced T cell death and an immunosuppressive role in acute rejection after transplantation.

Research motivation

This study investigated the immunosuppressive effect of metronomic CAP in rat LT and its mechanism, which may be used as an immunosuppressive agent after LT to improve the prognosis of liver transplant patients with hepatocellular carcinoma.

Research objectives

The objective of this study was to investigate the possibility of using CAP as an anti-rejection agent after transplantation. The results showed that metronomic CAP could exert an immunosuppressive effect by inducing T cell ferroptosis, which provided a basis for investigating CAP as part of an immunosuppressive regimen.

Research methods

A rat LT model of acute rejection was established, and the effect of metronomic CAP on splenic hematopoietic function and acute graft rejection was evaluated 7 d after transplantation. *In vitro*, primary CD3⁺ T cells were sorted and co-cultured with or without 5-fluorouracil (5-FU) (active agent of CAP). The levels of ferroptosis-related proteins, ferrous ion concentration, and oxidative stress-related indicators were observed. The changes in mitochondrial structure were observed using electron microscopy.

Research results

With no significant myelotoxicity, metronomic CAP alleviated graft injury, prolonged the survival time of the recipient rats, and reduced the infiltration rate of CD3⁺ T cells in peripheral blood, liver graft, and spleen, thereby inhibiting acute rejection after LT. *In vitro*, 5-FU, an end product of CAP metabolism, induced the degradation of the ferritin heavy chain by upregulating nuclear receptor coactivator 4, which caused the accumulation of ferrous ions. It also inhibited nuclear erythroid 2 p45-related factor 2, heme oxygenase-1, and glutathione peroxidase 4, eventually leading to oxidative damage and ferroptosis of T cells.

Research conclusions

Metronomic CAP can alleviate liver graft injury and reduce the proliferation and infiltration of CD3⁺ T cells in peripheral blood, graft, and spleen by inducing T cell oxidative damage and ferroptosis, thereby inhibiting acute rejection after LT.

Research perspectives

The combination and interaction of CAP with other immunosuppressive agents is an important research direction in the future. In addition, the effects of CAP on T cell subsets and other immune cells are worth further attention. Besides, we plan to establish tumor-bearing animal models for allotransplantation, to clarify the dual antirejection and antitumor effects of CAP.

FOOTNOTES

Author contributions: Wang H conceived the study, performed the experiments, analyzed the data, generated the figures, and wrote the manuscript; Wang ZL, Zhang S, and Kong DJ provided technical help and assisted with the experiments; Zhang S, Kong DJ, Yang RN, Cao L, and Wang JX helped with the data analyses; Wang ZL, Yoshida S, Zhang S, Liu T, Shen ZY, and Zheng H performed critical reading of the manuscript; Fan SL, Ren JS, Li JH, and Zheng H assisted with the editing and writing of the manuscript; Zheng H supervised the study and edited the manuscript.

Supported by National Key Research and Development Program of China, No. 2020YFA0710802; The Youth Science Fund of the Nature Science Foundation of Tianjin, No. 20JCQNJC01370; The Key Projects of Tianjin Science and Technology Project, No. 21JCZDJC00160; and The Science Foundation of Tianjin Health Commission, No. ZC20065 and No. ZC20089.

Institutional review board statement: The studies involving human participants were conducted in accordance with the Declaration of Helsinki (1964) and were reviewed and approved by the Tianjin First Hospital clinical research ethics committee, No. 2022N150KY. The participants provided written informed consent to participate in this study.

Institutional animal care and use committee statement: The animal study was reviewed and approved by the ethics committee of the Institute of Radiation Medicine of the Chinese Academy of Medical Sciences, No. IRM-DWLL-2021184.

Informed consent statement: All study participants or their legal guardian provided informed written consent about personal and medical data collection prior to study enrolment.

Conflict-of-interest statement: All the authors report no relevant conflicts of interest for this article.

Data sharing statement: No additional data are available.

ARRIVE guidelines statement: The authors have read the ARRIVE guidelines, and the manuscript was prepared and revised according to the ARRIVE guidelines.

Open-Access: This article is an open-access article that was selected by an in-house editor and fully peer-reviewed by external reviewers. It is distributed in accordance with the Creative Commons Attribution NonCommercial (CC BY-NC 4.0) license, which permits others to distribute, remix, adapt, build upon this work non-commercially, and license their derivative works on different terms, provided the original work is properly cited and the use is non-commercial. See: <https://creativecommons.org/licenses/by-nc/4.0/>

Country/Territory of origin: China

ORCID number: Hao Wang 0000-0002-2841-8834; Zheng-Lu Wang 0000-0003-0463-1080; Sai Zhang 0000-0002-4046-5385; De-Jun Kong 0000-0002-6878-9293; Rui-Ning Yang 0000-0002-3676-733X; Lei Cao 0000-0001-5982-4264; Jian-Xi Wang 0000-0003-3220-9717; Sei Yoshida 0000-0002-4771-3900; Zhuo-Lun Song 0000-0001-5101-3950; Tao Liu 0000-0002-0931-7288; Shun-Li Fan 0000-0002-3848-7905; Jia-Shu Ren 0000-0002-0186-1297; Jiang-Hong Li 0000-0001-5642-2040; Zhong-Yang Shen 0000-0003-0045-4355; Hong Zheng 0000-0001-7386-7084.

S-Editor: Fan JR

L-Editor: A

P-Editor: Liu JH

REFERENCES

- 1 **Vivarelli M**, Cucchetti A, La Barba G, Ravaoli M, Del Gaudio M, Lauro A, Grazi GL, Pinna AD. Liver transplantation for hepatocellular carcinoma under calcineurin inhibitors: reassessment of risk factors for tumor recurrence. *Ann Surg* 2008; **248**: 857-862 [PMID: 18948815 DOI: 10.1097/SLA.0b013e3181896278]
- 2 **Gish RG**. Hepatocellular carcinoma: overcoming challenges in disease management. *Clin Gastroenterol Hepatol* 2006; **4**: 252-261 [PMID: 16527686 DOI: 10.1016/j.cgh.2006.01.001]
- 3 **Kawahara T**, Asthana S, Kneteman NM. m-TOR inhibitors: what role in liver transplantation? *J Hepatol* 2011; **55**: 1441-1451 [PMID: 21781947 DOI: 10.1016/j.jhep.2011.06.015]
- 4 **Pelizzaro F**, Sammarco A, Dadduzio V, Pastorelli D, Giovanis P, Soldà C, Rizzato MD, Lombardi G, Lonardi S, Peserico G, Imondi A, Sartori A, Maddalo G, Farinati F. Capecitabine in advanced hepatocellular carcinoma: A multicenter experience. *Dig Liver Dis* 2019; **51**: 1713-1719 [PMID: 31320302 DOI: 10.1016/j.dld.2019.06.015]
- 5 **Changou CA**, Shiah HS, Chen LT, Liu S, Luh F, Liu SH, Cheng YC, Yen Y. A Phase II Clinical Trial on the Combination Therapy of PHY906 Plus Capecitabine in Hepatocellular Carcinoma. *Oncologist* 2021; **26**: e367-e373 [PMID: 33140457 DOI: 10.1002/onco.13582]
- 6 **Bocci G**, Kerbel RS. Pharmacokinetics of metronomic chemotherapy: a neglected but crucial aspect. *Nat Rev Clin Oncol*

- 2016; **13**: 659-673 [PMID: [27184418](#) DOI: [10.1038/nrclinonc.2016.64](#)]
- 7 **Kerbel RS**, Shaked Y. The potential clinical promise of 'multimodality' metronomic chemotherapy revealed by preclinical studies of metastatic disease. *Cancer Lett* 2017; **400**: 293-304 [PMID: [28202353](#) DOI: [10.1016/j.canlet.2017.02.005](#)]
 - 8 **Ravaioli M**, Cucchetti A, Pinna AD, De Pace V, Neri F, Barbera MA, Maroni L, Frega G, Palloni A, De Lorenzo S, Ripoli MC, Pantaleo MA, Cescon M, Del Gaudio M, Brandi G. The role of metronomic capecitabine for treatment of recurrent hepatocellular carcinoma after liver transplantation. *Sci Rep* 2017; **7**: 11305 [PMID: [28900245](#) DOI: [10.1038/s41598-017-11810-z](#)]
 - 9 **Keating GM**, Santoro A. Sorafenib: a review of its use in advanced hepatocellular carcinoma. *Drugs* 2009; **69**: 223-240 [PMID: [19228077](#) DOI: [10.2165/00003495-200969020-00006](#)]
 - 10 **Ishikawa T**, Utoh M, Sawada N, Nishida M, Fukase Y, Sekiguchi F, Ishitsuka H. Tumor selective delivery of 5-fluorouracil by capecitabine, a new oral fluoropyrimidine carbamate, in human cancer xenografts. *Biochem Pharmacol* 1998; **55**: 1091-1097 [PMID: [9605432](#) DOI: [10.1016/s0006-2952\(97\)00682-5](#)]
 - 11 **Yoshimura A**, Kuwazuru Y, Furukawa T, Yoshida H, Yamada K, Akiyama S. Purification and tissue distribution of human thymidine phosphorylase; high expression in lymphocytes, reticulocytes and tumors. *Biochim Biophys Acta* 1990; **1034**: 107-113 [PMID: [2328255](#) DOI: [10.1016/0304-4165\(90\)90160-x](#)]
 - 12 **Schüller J**, Cassidy J, Dumont E, Roos B, Durston S, Banken L, Utoh M, Mori K, Weidekamm E, Reigner B. Preferential activation of capecitabine in tumor following oral administration to colorectal cancer patients. *Cancer Chemother Pharmacol* 2000; **45**: 291-297 [PMID: [10755317](#) DOI: [10.1007/s002800050043](#)]
 - 13 **Zhang S**, Wang Z, Fan S, Liu T, Yoshida S, Yang S, Liu L, Hou W, Cao L, Wang J, Song Z, Li S, Zhang S, Wang H, Li J, Zheng H, Shen Z. Capecitabine Can Induce T Cell Apoptosis: A Potential Immunosuppressive Agent With Anti-Cancer Effect. *Front Immunol* 2021; **12**: 737849 [PMID: [34557199](#) DOI: [10.3389/fimmu.2021.737849](#)]
 - 14 **Dixon SJ**, Lemberg KM, Lamprecht MR, Skouta R, Zaitsev EM, Gleason CE, Patel DN, Bauer AJ, Cantley AM, Yang WS, Morrison B 3rd, Stockwell BR. Ferroptosis: an iron-dependent form of nonapoptotic cell death. *Cell* 2012; **149**: 1060-1072 [PMID: [22632970](#) DOI: [10.1016/j.cell.2012.03.042](#)]
 - 15 **Xie Y**, Hou W, Song X, Yu Y, Huang J, Sun X, Kang R, Tang D. Ferroptosis: process and function. *Cell Death Differ* 2016; **23**: 369-379 [PMID: [26794443](#) DOI: [10.1038/cdd.2015.158](#)]
 - 16 **Li J**, Cao F, Yin HL, Huang ZJ, Lin ZT, Mao N, Sun B, Wang G. Ferroptosis: past, present and future. *Cell Death Dis* 2020; **11**: 88 [PMID: [32015325](#) DOI: [10.1038/s41419-020-2298-2](#)]
 - 17 **Truman-Rosentsvit M**, Berenbaum D, Spektor L, Cohen LA, Belizowsky-Moshe S, Lifshitz L, Ma J, Li W, Kesselman E, Abutbul-Ionita I, Danino D, Gutierrez L, Li H, Li K, Lou H, Regoni M, Poli M, Glaser F, Rouault TA, Meyron-Holtz EG. Ferritin is secreted via 2 distinct nonclassical vesicular pathways. *Blood* 2018; **131**: 342-352 [PMID: [29074498](#) DOI: [10.1182/blood-2017-02-768580](#)]
 - 18 **Fuhrmann DC**, Mondorf A, Beifuß J, Jung M, Brüne B. Hypoxia inhibits ferritinophagy, increases mitochondrial ferritin, and protects from ferroptosis. *Redox Biol* 2020; **36**: 101670 [PMID: [32810738](#) DOI: [10.1016/j.redox.2020.101670](#)]
 - 19 **Dodson M**, Castro-Portuguez R, Zhang DD. NRF2 plays a critical role in mitigating lipid peroxidation and ferroptosis. *Redox Biol* 2019; **23**: 101107 [PMID: [30692038](#) DOI: [10.1016/j.redox.2019.101107](#)]
 - 20 **Song X**, Long D. Nrf2 and Ferroptosis: A New Research Direction for Neurodegenerative Diseases. *Front Neurosci* 2020; **14**: 267 [PMID: [32372896](#) DOI: [10.3389/fnins.2020.00267](#)]
 - 21 **Kwon MY**, Park E, Lee SJ, Chung SW. Heme oxygenase-1 accelerates erastin-induced ferroptotic cell death. *Oncotarget* 2015; **6**: 24393-24403 [PMID: [26405158](#) DOI: [10.18632/oncotarget.5162](#)]
 - 22 **Seibt TM**, Proneth B, Conrad M. Role of GPX4 in ferroptosis and its pharmacological implication. *Free Radic Biol Med* 2019; **133**: 144-152 [PMID: [30219704](#) DOI: [10.1016/j.freeradbiomed.2018.09.014](#)]
 - 23 **Deng HF**, Yue LX, Wang NN, Zhou YQ, Zhou W, Liu X, Ni YH, Huang CS, Qiu LZ, Liu H, Tan HL, Tang XL, Wang YG, Ma ZC, Gao Y. Mitochondrial Iron Overload-Mediated Inhibition of Nrf2-HO-1/GPX4 Assisted ALI-Induced Nephrotoxicity. *Front Pharmacol* 2020; **11**: 624529 [PMID: [33584308](#) DOI: [10.3389/fphar.2020.624529](#)]
 - 24 **Deng S**, Wu D, Li L, Li J, Xu Y. TBHQ attenuates ferroptosis against 5-fluorouracil-induced intestinal epithelial cell injury and intestinal mucositis via activation of Nrf2. *Cell Mol Biol Lett* 2021; **26**: 48 [PMID: [34794379](#) DOI: [10.1186/s11658-021-00294-5](#)]
 - 25 **Li D**, Song C, Zhang J, Zhao X. ROS and iron homeostasis dependent ferroptosis play a vital role in 5-Fluorouracil induced cardiotoxicity in vitro and in vivo. *Toxicology* 2022; **468**: 153113 [PMID: [35101590](#) DOI: [10.1016/j.tox.2022.153113](#)]
 - 26 **Xu HS**, Rosenlof LK, Pruett TL, Jones RS. Prostaglandin E1 increases survival with extended anhepatic phase during liver transplantation. *Ann Surg* 1994; **220**: 53-58 [PMID: [8024359](#) DOI: [10.1097/0000658-199407000-00009](#)]
 - 27 **Kamada N**, Calne RY. Orthotopic liver transplantation in the rat. Technique using cuff for portal vein anastomosis and biliary drainage. *Transplantation* 1979; **28**: 47-50 [PMID: [377595](#)]
 - 28 Banff schema for grading liver allograft rejection: an international consensus document. *Hepatology* 1997; **25**: 658-663 [PMID: [9049215](#) DOI: [10.1002/hep.510250328](#)]
 - 29 **Li X**, Chen J, Yuan S, Zhuang X, Qiao T. Activation of the P62-Keap1-NRF2 Pathway Protects against Ferroptosis in Radiation-Induced Lung Injury. *Oxid Med Cell Longev* 2022; **2022**: 8973509 [PMID: [35847598](#) DOI: [10.1155/2022/8973509](#)]
 - 30 **Ishibashi M**, Ishii M, Yamamoto S, Mori Y, Shimizu S. Possible involvement of TRPM2 activation in 5-fluorouracil-induced myelosuppression in mice. *Eur J Pharmacol* 2021; **891**: 173671 [PMID: [33131720](#) DOI: [10.1016/j.ejphar.2020.173671](#)]
 - 31 **Numazawa S**, Sugihara K, Miyake S, Tomiyama H, Hida A, Hatsuno M, Yamamoto M, Yoshida T. Possible involvement of oxidative stress in 5-fluorouracil-mediated myelosuppression in mice. *Basic Clin Pharmacol Toxicol* 2011; **108**: 40-45 [PMID: [20722640](#) DOI: [10.1111/j.1742-7843.2010.00621.x](#)]
 - 32 **Brandi G**, de Rosa F, Agostini V, di Girolamo S, Andreone P, Bolondi L, Serra C, Sama C, Golfieri R, Gramenzi A, Cucchetti A, Pinna AD, Trevisani F, Biasco G; Italian Liver Cancer (ITA. LI.CA) Group. Metronomic capecitabine in advanced hepatocellular carcinoma patients: a phase II study. *Oncologist* 2013; **18**: 1256-1257 [PMID: [24232581](#) DOI: [10.1093/oncol/okt011](#)]

- 10.1634/theoncologist.2013-0093]
- 33 **Granito A**, Marinelli S, Terzi E, Piscaglia F, Renzulli M, Venerandi L, Benevento F, Bolondi L. Metronomic capecitabine as second-line treatment in hepatocellular carcinoma after sorafenib failure. *Dig Liver Dis* 2015; **47**: 518-522 [PMID: 25861840 DOI: 10.1016/j.dld.2015.03.010]
 - 34 **Casadei Gardini A**, Foca F, Scartozzi M, Silvestris N, Tamburini E, Faloppi L, Brunetti O, Rudnas B, Pisconti S, Valgiusti M, Marisi G, Foschi FG, Ercolani G, Tassinari D, Cascinu S, Frassinetti GL. Metronomic capecitabine versus best supportive care as second-line treatment in hepatocellular carcinoma: a retrospective study. *Sci Rep* 2017; **7**: 42499 [PMID: 28211921 DOI: 10.1038/srep42499]
 - 35 **Kojima S**, Takaba K, Kimoto N, Takeda T, Kakuni M, Mizutani M, Suzuki K, Sato H, Hara T. Protective effects of glutathione on 5-fluorouracil-induced myelosuppression in mice. *Arch Toxicol* 2003; **77**: 285-290 [PMID: 12734643 DOI: 10.1007/s00204-003-0448-9]
 - 36 **Lam SW**, Guchelaar HJ, Boven E. The role of pharmacogenetics in capecitabine efficacy and toxicity. *Cancer Treat Rev* 2016; **50**: 9-22 [PMID: 27569869 DOI: 10.1016/j.ctrv.2016.08.001]
 - 37 **Fels Elliott DR**, Tavakol M, Lucas CH, Sheahon K, Kakar S, Hameed B, Ferrell LD, Gill RM. Clinicopathological features and outcomes of parenchymal rejection in liver transplant biopsies. *Histopathology* 2020; **76**: 822-831 [PMID: 31894595 DOI: 10.1111/his.14058]
 - 38 **Demirhan B**, Bilezikçi B, Haberal AN, Sevmiş S, Arat Z, Haberal M. Hepatic parenchymal changes and histologic eosinophilia as predictors of subsequent acute liver allograft rejection. *Liver Transpl* 2008; **14**: 214-219 [PMID: 18236397 DOI: 10.1002/lt.21360]
 - 39 **De Lorenzo S**, Tovoli F, Barbera MA, Garuti F, Palloni A, Frega G, Garajová I, Rizzo A, Trevisani F, Brandi G. Metronomic capecitabine vs. best supportive care in Child-Pugh B hepatocellular carcinoma: a proof of concept. *Sci Rep* 2018; **8**: 9997 [PMID: 29968763 DOI: 10.1038/s41598-018-28337-6]
 - 40 **Vionnet J**, Miquel R, Abalde JG, Wall J, Kodala E, Lozano JJ, Ruiz P, Navasa M, Marshall A, Nevens F, Gelson W, Leithead J, Masson S, Jaeckel E, Taubert R, Tachtatzis P, Eurich D, Simpson KJ, Bonaccorsi-Riani E, Feng S, Bucuvalas J, Ferguson J, Quaglia A, Sidorova J, Elstad M, Douiri A, Sánchez-Fueyo A. Non-invasive alloimmune risk stratification of long-term liver transplant recipients. *J Hepatol* 2021; **75**: 1409-1419 [PMID: 34437910 DOI: 10.1016/j.jhep.2021.08.007]
 - 41 **Li GL**, Lin HM, Long TZ, Lv LH, Yu JD, Huang YH, Min J, Wan YL. High incidence of biliary complications in rat liver transplantation: can we avoid it? *World J Gastroenterol* 2011; **17**: 3140-3144 [PMID: 21912457 DOI: 10.3748/wjg.v17.i26.3140]
 - 42 **Ronca V**, Wootton G, Milani C, Cain O. The Immunological Basis of Liver Allograft Rejection. *Front Immunol* 2020; **11**: 2155 [PMID: 32983177 DOI: 10.3389/fimmu.2020.02155]
 - 43 **Safinia N**, Vaikunthanathan T, Lechler RI, Sanchez-Fueyo A, Lombardi G. Advances in Liver Transplantation: where are we in the pursuit of transplantation tolerance? *Eur J Immunol* 2021; **51**: 2373-2386 [PMID: 34375446 DOI: 10.1002/eji.202048875]
 - 44 **Kumar BV**, Connors TJ, Farber DL. Human T Cell Development, Localization, and Function throughout Life. *Immunity* 2018; **48**: 202-213 [PMID: 29466753 DOI: 10.1016/j.immuni.2018.01.007]
 - 45 **Wong TC**, Lo CM, Fung JY. Emerging drugs for prevention of T-cell mediated rejection in liver and kidney transplantation. *Expert Opin Emerg Drugs* 2017; **22**: 123-136 [PMID: 28503959 DOI: 10.1080/14728214.2017.1330884]
 - 46 **Sun G**, Yang S, Cao G, Wang Q, Hao J, Wen Q, Li Z, So KF, Liu Z, Zhou S, Zhao Y, Yang H, Zhou L, Yin Z. $\gamma\delta$ T cells provide the early source of IFN- γ to aggravate lesions in spinal cord injury. *J Exp Med* 2018; **215**: 521-535 [PMID: 29282251 DOI: 10.1084/jem.20170686]
 - 47 **Li S**, Yu J, Guo C, Jie Y, Pan Z. The Balance of Th1/Th2 and LAP+Tregs/Th17 Cells Is Crucial for Graft Survival in Allogeneic Corneal Transplantation. *J Ophthalmol* 2018; **2018**: 5404989 [PMID: 29576879 DOI: 10.1155/2018/5404989]
 - 48 **Newstead CG**, Lamb WR, Brenchley PE, Short CD. Serum and urine IL-6 and TNF-alpha in renal transplant recipients with graft dysfunction. *Transplantation* 1993; **56**: 831-835 [PMID: 8212202 DOI: 10.1097/00007890-199310000-00010]
 - 49 **Ma L**, Zhang H, Hu K, Lv G, Fu Y, Ayana DA, Zhao P, Jiang Y. The imbalance between Tregs, Th17 cells and inflammatory cytokines among renal transplant recipients. *BMC Immunol* 2015; **16**: 56 [PMID: 26400627 DOI: 10.1186/s12865-015-0118-8]
 - 50 **Assadiasl S**, Mooney N, Nicknam MH. Cytokines in Liver Transplantation. *Cytokine* 2021; **148**: 155705 [PMID: 34564024 DOI: 10.1016/j.cyto.2021.155705]
 - 51 **Sena LA**, Li S, Jairaman A, Prakriya M, Ezponda T, Hildeman DA, Wang CR, Schumacker PT, Licht JD, Perlman H, Bryce PJ, Chandel NS. Mitochondria are required for antigen-specific T cell activation through reactive oxygen species signaling. *Immunity* 2013; **38**: 225-236 [PMID: 23415911 DOI: 10.1016/j.immuni.2012.10.020]
 - 52 **Pearce EL**, Poffenberger MC, Chang CH, Jones RG. Fueling immunity: insights into metabolism and lymphocyte function. *Science* 2013; **342**: 1242454 [PMID: 24115444 DOI: 10.1126/science.1242454]
 - 53 **Gerriets VA**, Kishton RJ, Nichols AG, Macintyre AN, Inoue M, Ilkayeva O, Winter PS, Liu X, Priyadarshini B, Slawinska ME, Haeblerli L, Huck C, Turka LA, Wood KC, Hale LP, Smith PA, Schneider MA, MacIver NJ, Locasale JW, Newgard CB, Shinohara ML, Rathmell JC. Metabolic programming and PDHK1 control CD4+ T cell subsets and inflammation. *J Clin Invest* 2015; **125**: 194-207 [PMID: 25437876 DOI: 10.1172/JCI76012]
 - 54 **Matsushita M**, Freigang S, Schneider C, Conrad M, Bornkamm GW, Kopf M. T cell lipid peroxidation induces ferroptosis and prevents immunity to infection. *J Exp Med* 2015; **212**: 555-568 [PMID: 25824823 DOI: 10.1084/jem.20140857]
 - 55 **Ogando DG**, Choi M, Shyam R, Li S, Bonanno JA. Ammonia sensitive SLC4A11 mitochondrial uncoupling reduces glutamine induced oxidative stress. *Redox Biol* 2019; **26**: 101260 [PMID: 31254733 DOI: 10.1016/j.redox.2019.101260]
 - 56 **Zhang J**, Wang X, Vikash V, Ye Q, Wu D, Liu Y, Dong W. ROS and ROS-Mediated Cellular Signaling. *Oxid Med Cell Longev* 2016; **2016**: 4350965 [PMID: 26998193 DOI: 10.1155/2016/4350965]
 - 57 **Zorov DB**, Juhaszova M, Sollott SJ. Mitochondrial reactive oxygen species (ROS) and ROS-induced ROS release. *Physiol Rev* 2014; **94**: 909-950 [PMID: 24987008 DOI: 10.1152/physrev.00026.2013]

- 58 **Kerins MJ**, Milligan J, Wohlschlegel JA, Ooi A. Fumarate hydratase inactivation in hereditary leiomyomatosis and renal cell cancer is synthetic lethal with ferroptosis induction. *Cancer Sci* 2018; **109**: 2757-2766 [PMID: [29917289](#) DOI: [10.1111/cas.13701](#)]
- 59 **Xu C**, Sun S, Johnson T, Qi R, Zhang S, Zhang J, Yang K. The glutathione peroxidase Gpx4 prevents lipid peroxidation and ferroptosis to sustain Treg cell activation and suppression of antitumor immunity. *Cell Rep* 2021; **35**: 109235 [PMID: [34133924](#) DOI: [10.1016/j.celrep.2021.109235](#)]

Basic Study

Dihydroergotamine ameliorates liver fibrosis by targeting transforming growth factor β type II receptor

Ke-Xin Zheng, Shou-Li Yuan, Meng Dong, Han-Lin Zhang, Xiao-Xiao Jiang, Chun-Long Yan, Rong-Cai Ye, Hui-Qiao Zhou, Li Chen, Rui Jiang, Zi-Yu Cheng, Zhi Zhang, Qi Wang, Wan-Zhu Jin, Wen Xie

Specialty type: Gastroenterology and hepatology

Provenance and peer review: Unsolicited article; Externally peer reviewed.

Peer-review model: Single blind

Peer-review report's scientific quality classification

Grade A (Excellent): 0
Grade B (Very good): B, B
Grade C (Good): 0
Grade D (Fair): 0
Grade E (Poor): 0

P-Reviewer: Jena MK, India; Shrewsbury SB, United States

Received: February 6, 2023

Peer-review started: February 6, 2023

First decision: March 21, 2023

Revised: April 1, 2023

Accepted: April 24, 2023

Article in press: April 24, 2023

Published online: May 28, 2023



Ke-Xin Zheng, Qi Wang, Wen Xie, Center of Liver Diseases, Beijing Ditan Hospital, Capital Medical University, Beijing 100015, China

Shou-Li Yuan, Meng Dong, Han-Lin Zhang, Xiao-Xiao Jiang, Chun-Long Yan, Rong-Cai Ye, Hui-Qiao Zhou, Li Chen, Rui Jiang, Zi-Yu Cheng, Zhi Zhang, Wan-Zhu Jin, Key Laboratory of Animal Ecology and Conservation Biology, Institute of Zoology, Chinese Academy of Sciences, Beijing 100101, China

Shou-Li Yuan, Han-Lin Zhang, Xiao-Xiao Jiang, Rong-Cai Ye, Hui-Qiao Zhou, Li Chen, Rui Jiang, Zi-Yu Cheng, Zhi Zhang, Graduate School, University of the Chinese Academy of Sciences, Beijing 100049, China

Chun-Long Yan, Graduate School, Agriculture College of Yanbian University, Yanji 133002, Jilin Province, China

Corresponding author: Wen Xie, MD, Doctor, Center of Liver Diseases, Beijing Ditan Hospital, Capital Medical University, No. 8 Jingshun East Street, Chaoyang District, Beijing 100015, China. xiewen6218@163.com

Abstract

BACKGROUND

The transforming growth factor β (TGF β) signaling pathway plays a crucial role in the development of liver fibrosis by activating TGF β type II receptor (TGF β R2), followed by the recruitment of TGF β R1 finally triggering downstream signaling pathway.

AIM

To find drugs targeting TGF β R2 that inhibit TGF β R1/TGF β R2 complex formation, theoretically inhibit TGF β signaling pathway, and thereby ameliorate liver fibrosis.

METHODS

Food and Drug Administration-approved drugs were screened for binding affinity with TGF β R2 by virtual molecular docking. We identified 6 candidates and further explored their potential by Cell Counting Kit-8 (CCK-8) cell cytotoxic experiment to validate toxicity and titrated the best cellular working concentrations. Next, we further demonstrated the detailed molecular working

mechanisms using mutagenesis analysis. Finally, we used a mouse model to investigate its potential anti-liver fibrosis effect.

RESULTS

We identified 6 drug candidates. Among these 6 drugs, dihydroergotamine (DHE) shows great ability in reducing fibrotic gene expressions such as collagen, p-SMAD3, and α -SMA in TGF β induced cellular model of liver fibrosis in LX-2 cells. Furthermore, we demonstrated that DHE binds to TGF β R2. Moreover, mutation of Leu27, Phe30, Thr51, Ser52, Ile53, and Glu55 of TGF β R2 disrupted the binding of TGF β R2 with DHE. In addition, DHE significantly improved liver fibrosis, as evidenced by Masson's trichrome staining of liver sections. This is further supported by the width and the velocity of the portal vein, and serum markers of liver function. In line with those observations, DHE also decreased macrophages infiltration and extracellular matrix deposition in the liver.

CONCLUSION

DHE alleviates liver fibrosis by binding to TGF β R2 thereby suppressing TGF β signaling pathway. We show here that as far as drug repurposing, DHE has great potential to treat liver fibrosis.

Key Words: Liver fibrosis; Transforming growth factor β (TGF β) signaling pathway; TGF β type II receptor (TGF β R2); Virtual screening; Drug-repurposing; Dihydroergotamine

©The Author(s) 2023. Published by Baishideng Publishing Group Inc. All rights reserved.

Core Tip: An effective and safe drug for treating liver fibrosis is urgently needed in current clinical practice. Here, we investigated and discovered that dihydroergotamine (DHE) could alleviate liver fibrosis by specific binding of transforming growth factor β type II receptor (TGF β R2) to disrupt the binding of TGF β R2 with TGF β 1, and ultimately suppressing its downstream TGF β signaling pathway. DHE may be an effective anti-liver fibrosis drug, which could be employed in liver cirrhotic patients.

Citation: Zheng KX, Yuan SL, Dong M, Zhang HL, Jiang XX, Yan CL, Ye RC, Zhou HQ, Chen L, Jiang R, Cheng ZY, Zhang Z, Wang Q, Jin WZ, Xie W. Dihydroergotamine ameliorates liver fibrosis by targeting transforming growth factor β type II receptor. *World J Gastroenterol* 2023; 29(20): 3103-3118

URL: <https://www.wjgnet.com/1007-9327/full/v29/i20/3103.htm>

DOI: <https://dx.doi.org/10.3748/wjg.v29.i20.3103>

INTRODUCTION

Liver fibrosis is the consequence of various chronic pathogenic factors[1], it is a dynamic process that is characterized by an excessive accumulation of extracellular matrix[2]. Early liver fibrosis can be reversed to a normal architecture by removal of underlying causes[2], but liver fibrosis could further develop into cirrhosis without effective treatment[3]. Liver cirrhosis can be complicated by variceal bleeding, hepatic encephalopathy, ascites, bacterial peritonitis, and hepatocellular carcinoma, which has high mortality[4]. Liver cirrhosis can regress to early stage of disease, but it cannot be reversed to a normal liver[5]. Therefore, it is very important to control the disease progression in the early reversible stage of liver fibrosis.

Etiological treatment of liver fibrosis is most important and effective, such as antivirals, quitting alcohol consumption, and weight loss[1]. However, effects of etiological treatment are limited and insufficient, and difficult to prevent the development of liver fibrosis into cirrhosis. At present, liver transplantation is a radical cure for cirrhosis but is associated with a high cost, organ shortages, and the risk of immune rejection[6]. In addition, almost all current clinical trials targeting fibrosis are focused on non-alcoholic steatohepatitis, specifically focusing on hepatic stellate cell (HSC) activation and/or fibrogenesis[7]. However, there are still no approved antifibrotic therapies for liver fibrosis[7]. Therefore, it is urgent to develop new effective drugs.

Developing new drugs is a difficult, high-cost, and extremely low success rate procedure[8]. A good strategy to address this problem is to investigate new indications of old drugs, a process called "drug repurposing"[9]. Scientists have repurposed many old drugs such as propranolol[10], cimetidine[11], sildenafil[12], and thalidomide[13]. Thus, drug repurposing is an attractive approach and has been widely employed. Drugs that have been approved by Food and Drug Administration (FDA) have passed preliminary clinical trials and are considered extremely safe. Therefore, FDA-approved drugs may be good candidates for developing new indications. Molecular docking, a fast, efficient, and widely

used technique in drug repurposing, is a computational strategy to predict binding sites between ligands and targets based on their structures[9,14].

The activation of HSCs is considered the central effector of liver fibrosis[15]. There are many associated signaling molecules, including transforming growth factor β (TGF β), platelet-derived growth factor, and connective tissue growth factor[16]. The TGF β signaling pathway plays a crucial role in the development of liver fibrosis[17]. A review paper illustrated that TGF β 1 activates TGF β type II receptor (TGF β R2), followed by the recruitment of TGF β R1. Afterward, TGF β R2 phosphorylates TGF β R1 thereby triggering down-stream signaling pathway to regulate the expression of collagens and extracellular matrix (ECM)[18]. Therefore, TGF β R2 is considered an important target for developing drugs against liver fibrosis. Consistently, our group and others demonstrated that both inhibiting the expression of TGF β R2 and exogenous extracellular domain of TGF β R2 supplement effectively alleviated liver fibrosis [19,20].

In the current study, FDA-approved drugs were screened for binding affinity with the TGF β R2 by virtual molecular docking. We used cellular and mouse models to investigate its potential anti-liver fibrosis effect. In addition, by using mutagenesis analysis we further demonstrated detailed molecular working mechanism.

MATERIALS AND METHODS

Molecular docking of FDA-approved drugs and TGF β R2

The structures of FDA-approved drugs were downloaded from the ZINC database (<https://zinc12.docking.org/>). Then, the files of each small molecular structures were generated using Open Babel GUI (3.1.1). The TGF β R2-TGF β 1 complex (PDB: 3KFD) was downloaded from the Protein Data Bank (<https://www.rcsb.org/>). The TGF β R2 structure was derived from the TGF β R2-TGF β 1 complex using AutoDock Vina software (<https://vina.scripps.edu/>). AutoDock Vina software was employed to screen for the lowest energy complex among complexes of the extracellular TGF β R2 domain and the FDA-approved drugs.

Cell culture and viability experiments

The human HSC line LX-2 was purchased from the BeNa Culture Collection (Beijing, China) and cultured in Dulbecco's modified Eagle medium (DMEM, Gibco, United States) with 10% fetal bovine serum (FBS, Gibco, United States) at 37 °C in a 5% CO₂ atmosphere. LX-2 was activated by human recombinant protein TGF β 1 (5 ng/mL) for 24 h, followed by drug treatment for 24 h. The expression of fibrosis-related genes was analyzed.

Cell Counting Kit-8 (CCK-8, Beyotime Biotechnology, Shanghai, China) test was used to test the cytotoxicity of a series of working concentrations of the candidate drugs on LX-2 cell. After 24 h of treatment, the CCK-8 solution was added to each well for an additional 1 h of incubation (37 °C in a 5% CO₂ atmosphere). A microplate analyzer was used to measure the optical density of each well at 450 nm. Cell vitality was expressed as a percentage of optical density between the treatment wells and the negative control cells.

Determination of K_d value between TGF β R2 and dihydroergotamine

The K_d value of the small molecules and the TGF β R2 protein was measured using a microscale thermophoresis (MST)-Nanotemper instrument (Nanotemper, Germany). Micro thermophoresis is the directional movement of particles in the micro temperature gradient. The affinity is determined by measuring the change of micro thermophoresis caused by the change of hydration layer (usually caused by the change of biomolecular structure/conformation). First, 100 μ L each of 10 μ M TGF β R2 and different concentrations of the small molecules (diluted from 400 μ M stock) were prepared. Second, TGF β R2 was labeled with a fluorescent dye and mixed with the small molecules. Third, fluorescence was measured to assess the binding behavior of the small molecule-TGF β R2 complex.

Molecular dynamics simulation

Molecular dynamics simulations were performed using Gromacs 2020.1, in which a charm36-mar2019 force field was chosen. The TGF β R2 or TGF β R2-small molecule complex was solved with TIP3P water and immersed in a dodecahedron box extending to at least 1 nm of the solvent on all sides. The system was neutralized with Na⁺ and Cl⁻ by adding 0.15 M NaCl. It was energy-minimized using the steepest descent algorithm for 5000 steps and creating a maximum force of < 1000 kJ/mol/nm. After energy minimization, the system was equilibrated with a constrained "number of particles, volume, and temperature" (NVT) and "number of particles, pressure, and temperature" (NPT) running for 100 ps. Through NVT and NPT equilibration, the system was well-equilibrated at 300 K and 1 bar. Finally, MD simulations of the TGF β R2 or complex were carried out for 200 ns; trajectories were saved every 10 ps for analysis. The Verlet cut-off scheme and a Leap-frog integrator with a step size of 2 fs were applied. The modified Berendsen thermostat was used for temperature coupling, the Parrinello-Rahman barostat was used for pressure coupling, and the Particle Mesh Ewald method was used to determine long-range

electrostatic interactions.

The root-mean-square displacement (RMSD) and root-mean-square fluctuation (RMSF) of TGF β R2 and the complex were calculated using GROMACS 2020.1. The content of the secondary structure was calculated using DSSP software. The last MD simulation frame of the complex was extracted using GROMACS 2020.1. LigPlot+ software (<https://www.ebi.ac.uk/thornton-srv/software/LigPlus/>) was used to analyze the detailed interactions between the extracellular TGF β R2 domain and small molecule. PyMOL (<http://www.pymol.org/>) was used to prepare the structural images.

Production and purification of site-directed mutagenesis of TGF β R2

The binding sites of TGF β R2 and small molecule were established using the molecular docking results. The amino acids at the binding sites were mutated to alanine whose nucleotide sequence was GCG. The sequences of mutated extracellular TGF β R2 and a 6X His-tag were inserted into a pMAL-c5x plasmid that was synthesized by GenScript Biotech Corporation.

The mutated plasmid was transformed into BL21 (DE3) bacteria and induced with 0.8 mmol/L IPTG for 16 h at 28 °C. Then, bacteria were collected and resuspended in phosphate buffered saline (PBS). The mutated TGF β R2 protein was purified by HisTrap FF affinity chromatography and eluted with PBS containing gradient concentrations of imidazole. Finally, the eluted proteins were concentrated and the imidazole was removed by dialysis.

CCl₄ injury mouse model

Six-week-old male C57BL/6N mice were purchased from Vital River Laboratory Animal Technology Co. Ltd. to induce a liver fibrosis model. The animal protocol was designed to minimize pain or discomfort to the animals. The animals were acclimatized to laboratory conditions (23 °C, 12 h/12 h light/dark, 50% humidity, ad libitum access to food and water) for 2 wk prior to experimentation. After being transferred to our institute, the animals were randomly and evenly divided into four groups (eight mice per group) according to their body weight: Corn oil, carbon tetrachloride (CCl₄), low-concentration treatment, and high-concentration treatment groups. The same volume of CCl₄ (0.5 μ L/g of body weight, Sigma-Aldrich, St. Louis, MO, United States) and corn oil were intraperitoneally injected three times a week to induce a liver fibrosis model and in control animals for four weeks, respectively. Intra-gastric gavage administration was carried out with conscious animals, using straight gavage needles appropriate for the animal size. Then, the small molecule aqueous solution and water was administered orally once a day as treatment and control for eight weeks, respectively. All animals were euthanized for tissue collection. All animal studies were performed following the National Institutes of Health's Guide for the Care and Use of Laboratory Animals and conducted with the approval of the Institutional Animal Care and Use Committee of the Institute of Zoology, Chinese Academy of Sciences.

B-mode ultrasonography

Small-animal B-ultrasound was used to inspect the portal veins. A high-resolution ultrasound imaging system (Vevo LAZR, VisualSonics, Canada) was used to measure the width and velocity of the portal vein. Mice were fasted for 12 h and shaved before the ultrasonic examination. Then, the mice were fixed on the platform and examined after being anesthetized with Avertin. After coating the mouse's abdomen with the coupling gel, the probe was used to inspect the mouse's portal vein.

Masson's trichrome staining

Mouse liver tissues were fixed in 4% paraformaldehyde, embedded in paraffin, and sectioned at 5 μ m thickness. Then, the liver paraffin-embedded tissue sections were stained with a Masson's trichrome kit (G1281, Solarbio, Beijing, China) and observed under a 10x objective lens. Masson's trichrome staining is used to distinguish collagen fibrosis from muscle fibers. Muscle fibers were stained red and collagen fibrosis was stained green or blue. The collagen area was quantified using ImageJ 1.52a software. And one liver section was taken from each mouse for analysis.

Western blot analysis

Total proteins were extracted from the LX-2 cells or liver tissues using radioimmunoprecipitation assay lysis buffer (50 mmol/L Tris-HCl, pH 7.4; 1% NP-40; 0.25% sodium deoxycholate; 150 mmol/L NaCl; and 1 mmol/L ethylene diamine tetraacetic acid (EDTA)) containing a protease and phosphatase inhibitor mixture (Roche Diagnostics). The proteins were separated on 10% sodium dodecyl sulfate (SDS) polyacrylamide gels and transferred onto polyvinylidene fluoride membranes (Millipore). After blocking with 5% skim milk in Tris-buffered saline-Tween 20 (0.02 M Tris base, 0.1% Tween 20, 0.14 M NaCl, pH 7.4) for 1 h, the membranes were incubated with primary antibodies overnight at 4 °C. The membranes were then incubated with horseradish-peroxidase (HRP)-conjugated secondary antibodies for 1 h at room temperature. [Supplementary Table 1](#) lists the antibodies.

Real-time quantitative PCR (RT-PCR) analysis

Total RNA was extracted from the LX-2 cells or liver tissues using TRIzol™ Reagent (Thermo Fisher Scientific, United States) according to the manufacturer's instructions. Complementary DNA (cDNA)

was obtained from the reverse-transcribed RNA using a high-capacity cDNA reverse-transcription kit (Promega, United States). The relative expression of genes was analyzed by RT-PCR (Light Cycler 480, Roche, Sweden) with SYBR Green Master Mix (Promega, United States). [Supplementary Table 2](#) lists the primer sequences.

Isolation of liver mononuclear cells and flow cytometry analysis

Liver mononuclear cells (MNCs), including Kupffer cells, were isolated from mouse liver tissues. Liver samples were collected from mice under deep anesthesia. The liver samples were cut into pieces, transferred into 5 mL of enzyme mix [RPMI 1640 containing 1 mg/mL collagen IV (Sigma) and 20 U/mL DNase I (Roche, Burgess Hill, United Kingdom)], and digested in a water bath at 37 °C for 30 min. RPMI 1640 containing 10% FBS was added to arrest the digestion. The digested mixture was filtered through a 70 µm strainer, centrifuged at 4 °C for 10 min at 1000 × g, and the pellet was washed in PBS twice. Liver immune cells were subsequently isolated using a 33% Percoll cell separation solution after centrifuging for 25 min at 2200 × g at room temperature. The red blood cells were removed using a red blood cell lysis buffer (YESEN, Shanghai, China). Finally, liver immune cells were counted and stained with anti-F4/80 antibody eFluor® 450 (eBioscience, San Diego, CA), brilliant violet 510™-conjugated anti-CD45 antibody (Biolegend, San Diego, CA), and percp-cyanine5.5-conjugated anti-CD11b antibody (eBioscience, San Diego, CA), which were then filtered into flow tubes through a 0.45 µm strainer. The result of flow cytometry was analyzed using a BD Fortessa instrument (BD, NY, United States).

Plasma biochemical markers

Mouse blood samples were collected from the tail vein, collected into EDTA-containing tubes, and gently shaken. Plasma was collected after centrifuging at 3000 × g for 15 min at 4 °C. Plasma alanine aminotransferase (ALT) and aspartate aminotransferase (AST) levels were measured using a biochemistry analyzer (Cobas c 501, Roche, Sweden).

Statistical analyses

Data are expressed as mean ± standard error of the mean. The statistical significance between groups was analyzed using one-way ANOVA test. Statistical significance was set at $P < 0.05$ and $P < 0.05$, $P < 0.01$, $P < 0.001$, and $P < 0.0001$ were denoted as a, b, c, and d, respectively. GraphPad Prism software was used to perform all statistical analyses.

RESULTS

The docking analysis of FDA-approved small molecule drugs and TGFβR2

AutoDock Vina software was employed to dock drugs with the extracellular domain of TGFβR2 and output the complex structures. The complex and the binding sites of TGFβR2 and TGFβ1 were shown ([Figure 1A](#)), and the structure of TGFβR2 was split from the complex ([Figure 1B](#)). The binding affinity of each FDA-approved drug was evaluated ([Figure 1C](#)). Among those, darifenacin, cyproheptadine, lifitegrast, difenoxin, phenytoin, dihydroergotamine (DHE), naldemedine, and irinotecan showed higher scores out of 1615 drugs ([Figure 1C](#)). Darifenacin is a competitive muscarinic M receptor antagonist used to treat urinary frequency, urgency, and incontinence caused by bladder hyperstimulation[21]. Cyproheptadine is an antihistamine used to treat allergies[22]. Lifitegrast is a small molecule integrin inhibitor primarily used to treat symptoms and signs of dry eye[23]. Difenoxin is a human metabolite of diphenoxylate, which is a derivative of pethidine and can be used to treat functional diarrhea and chronic enteritis[24]. Phenytoin is an effective voltage-gated Na⁺ channel blocker used to treat epilepsy, neuralgia, and arrhythmia[25]. DHE is an adrenergic receptor antagonist used to treat severe orthostatic hypotension, migraine, and headache[26], which can bind with various receptors. DHE is also an agonist at 5-HT1B, 5-HT1D, and 5-HT1F receptors, but it also binds to 5-HT1A and 5-HT2A receptors. Naldemedine is an opioid receptor antagonist used to treat non-cancerous pain and opioid-induced constipation[27]. Irinotecan is a semi-synthesis of water-soluble camptothecin derivatives used to treat advanced colorectal cancer and postoperative adjuvant chemotherapy[28] ([Table 1](#)). All the above drugs were purchased from Selleck Chemicals, except for difenoxin and naldemedine which are banned from purchase as they are under management control. Therefore, we performed the following experiments using the rest 6 small molecule drugs.

Cytotoxicity of candidate drugs

To investigate the cytotoxicity of these drugs, LX-2 cells were treated with 20 µM of each candidate for 24 h. The results demonstrated that irinotecan and cyproheptadine were cytotoxic to LX-2 cells at this concentration ([Figure 1D](#)). Therefore, irinotecan and cyproheptadine were regarded as cytotoxic drugs and excluded from subsequent experiments. Next, to identify the best range of concentrations that would not influence the viability of these cells, LX-2 cells were treated with different concentrations of the remaining drugs for 24 h. The results demonstrated that neither lifitegrast nor phenytoin was

Table 1 The drugs with the highest affinity of transforming growth factor β type II receptor

Name	ZINC_ID	Affinity (kcal/mol)	Indications
Darifenacin	ZINC000001996117	-7.6	Urinary frequency, urgency, and incontinence caused by bladder hyperstimulation
Cyproheptadine	ZINC000000968264	-7.4	Allergy
Lifitegrast	ZINC000084668739	-7.4	Symptoms and signs of dry eye
Difenoxin	ZINC000000601317	-7.3	Functional diarrhea and chronic enteritis
Phenytoin	ZINC000002510358	-7.3	Epilepsy, neuralgia, and arrhythmia
DHE	ZINC000003978005	-7.3	Severe orthostatic hypotension, migraine, and headache
Naldemedine	ZINC000100378061	-7.3	Non-cancerous pain and opioid induced constipation
Irinotecan	ZINC000001612996	-7.3	Advanced colorectal cancer and postoperative adjuvant chemotherapy

DHE: Dihydroergotamine.

cytotoxic to LX-2 cells when concentrations were up to 100 μ M and 150 μ M, respectively (Figure 1E and F). Darifenacin and DHE were cytotoxic to LX-2 cells when concentrations were beyond 50 μ M and 20 μ M, respectively (Figure 1G and H). Therefore, to avoid interference on fibrosis-related gene expression due to the cytotoxicity of candidate drugs, lifitegrast and phenytoin concentrations below 100 μ M and darifenacin and DHE concentrations below 20 μ M were used to treat LX-2 cells.

Anti-fibrotic effect of candidate drugs in cellular model

Increased expression of collagen and alpha-smooth muscle actin (α -SMA) are principal markers of HSC activation[29]. LX-2 cells were treated with different concentrations of drugs for 24 h after TGF β 1 stimulation. The results demonstrated that lifitegrast and phenytoin did not decrease the protein levels of collagen III and α -SMA after TGF β 1 stimulation (Figure 2A and B). Moreover, darifenacin did not decrease the protein levels of collagen III, p-SMAD3, and α -SMA as much as DHE (Figure 2C and D). Consistently, DHE significantly decreased the mRNA expression of collagen I alpha 1 (COL1A1), collagen I alpha 2 (COL1A2), collagen III alpha 1 (COL3A1), and α -SMA compared with darifenacin (Figure 2E and F). Taken together, DHE (PubChem CID: 10531) was the most effective small molecule drug that suppressed the TGF β 1 induced LX-2 activation.

The binding affinity of DHE to TGF β 2

We further verified the molecular docking result by MST-Nanotemper. The results demonstrated that the fluorescence intensity of TGF β 2 changed gradually in proportion to the DHE concentration (Figure 3A). The affinity is determined by measuring the change of micro thermophoresis caused by the change of hydration layer, and results showed the binding affinity of DHE to TGF β 2 with a Kd value of 17.64 μ M.

Molecular dynamics simulation of DHE and TGF β 2

To identify the specific binding mode of DHE and TGF β 2, we used the complex structure obtained from AutoDock vina to perform the molecular dynamics simulation with GROMACS 2020.1 software for 200 ns. The results demonstrated that the RMSD of the backbone atoms of TGF β 2 and TGF β 2 \square DHE in the simulation system reached equilibrium after 100 ns (Figure 3B). The RMSFs of the TGF β 2 skeleton carbon atoms in the two simulated systems were almost identical (Figure 3C). The secondary structural elements of TGF β 2 in the complex simulation were only slightly changed (Figure 3D and Table 2). The coil and 3-helix components of TGF β 2 decreased in the complex simulation system (Table 2). Finally, we extracted the simulated complex structure and analyzed the amino acid sites of TGF β 2 bound to DHE by Ligplot+ software (Figure 3E and F). In conclusion, our molecular dynamics simulations showed that the binding of DHE to TGF β 2 has little effect on the structure of TGF β 2. We also obtained the binding sites of TGF β 2 to DHE by stimulations.

Leu27, Phe30, Thr51, Ser52, Ile53, and Glu55 of TGF β 2 bind with DHE

Molecule docking demonstrated that Leu27, Phe30, Thr51, Ser52, Ile53, and Glu55 of TGF β 2 were binding sites for DHE (Figure 3F). To verify these binding sites, we mutated the above-mentioned amino acids to alanine. The DNA sequences of mutated extracellular TGF β 2 were synthesized (Table 3) and the binding affinity was measured. The results demonstrated that the mutated TGF β 2 no longer bound to DHE (Figure 3G). Thus, the above-mentioned binding sites of TGF β 2 predicted by molecule docking were the exact binding sites of TGF β 2 and DHE, and this further verified the binding of TGF β 2 and DHE. Therefore, we inferred that the binding of TGF β 1 and TGF β 2 was

Table 2 Content of secondary structural analysis from DSSP method

Structure	Coil	β -Sheet	β -Bridge	Bend	Turn	3-Helix
TGF β R2	0.58	0.3	0.42	0.02	0.12	0.13
TGF β R2-DHE	0.56	0.3	0.42	0.02	0.12	0.12

TGF β R2: Transforming growth factor β type II receptor; DHE: Dihydroergotamine.

Table 3 DNA sequence of extracellular transforming growth factor β type II receptor before and after mutation

	Before mutation	After mutation
DNA sequence of TGF β R2 extracellular domain	ACGATCCCACCGCACGTCAGAAAGTCGGTTAATAACGACA TGATAGTCACTGACAACAACGGTGCAGTCAAGTTTCCACA ACTGTGTAATTTGTGATGTGAGATTTCCACCTGTGACA ACCAGAAATCCTGCATGAGCAACTGCAGCATCACCTCCA TCGTGAGAAGCCACAGGAAGTCTGTGTGGCTGTATGGA GAAAGAATGACGAGAACATAAACAAGTACAGAGCAGTTTGC ATGACCCCAAGCTCCCCTACCATGACTTTATTTCTGGAAGAT GCTGCTTCTCCAAAGTGCATTATGAAGGAAAAAAAAAAGC CTGGTGAGACTTCTTCATGTGTTCTGTAGCTCTGATGAG TGCAATGACAACATCATCTTCTCAGAAGAATAAACACCA GCAATCTGACTGTGTGCTAGTCATATTTCAA	ACGATCCCACCGCACGTCAGAAAGTCGGTTAATAACGACA TGATAGTCACTGACAACAACGGTGCAGTCAAGTTTCCACA AGCGTGTAAGCGTGTGATGTGAGATTTCCACCTGTGACA ACCAGAAATCCTGCATGAGCAACTGCAGCATCGCGGGG CGTGTGCGAAGCCACAGGAAGTCTGTGTGGCTGTATGGA GAAAGAATGACGAGAACATAAACAAGTACAGAGCAGTTTGC ATGACCCCAAGCTCCCCTACCATGACTTTATTTCTGGAAGAT GCTGCTTCTCCAAAGTGCATTATGAAGGAAAAAAAAAAGC CTGGTGAGACTTCTTCATGTGTTCTGTAGCTCTGATGAG TGCAATGACAACATCATCTTCTCAGAAGAATAAACACCA GCAATCTGACTGTGTGCTAGTCATATTTCAA

TGF β R2: Transforming growth factor β type II receptor.

blocked by the binding of DHE and TGF β R2, further preventing the TGF β signaling cascade.

DHE alleviated liver fibrosis in mouse

To explore whether DHE could alleviate fibrosis in vivo, we used two different concentrations of DHE to treat a CCl₄-induced mouse fibrosis model. Six-week-old C57BL/6N mice were intraperitoneally injected three-time per week with CCl₄ and corn oil (control group) during the whole experimental periods (Supplementary Figure 1). After four weeks, the mice intraperitoneally injected with CCl₄ were randomly divided into three groups: CCl₄ and the 2 and 5 mg/kg DHE treatment groups. The aqueous solution of DHE was orally gavaged to the mice in the treatment groups. For vehicle treatment, water was provided by oral gavage to the mice in the corn oil and CCl₄ group (disease group).

It is well known that more serious the degree of liver fibrosis, the wider the portal vein and the slower its velocity. The results demonstrated that the portal vein in the CCl₄ group was significantly wider than that in the corn oil group. Interestingly, the width of the portal vein in the 2 mg/kg DHE treatment group was significantly decreased (Figure 4A). Furthermore, the velocity of the portal vein in the treatment groups was also improved (Figure 4B). After eight weeks of treatment, there were no significant differences in body weight, liver weight, spleen weight, or the ratio of liver weight to body weight among the four groups (Figure 4C and Supplementary Figure 2A). Gross liver specimens of the CCl₄ group were paler and had a rough appearance. However, it was back to normal appearance by DHE treatment compared to the CCl₄ group (Figure 4D). The level of plasma ALT of the CCl₄ group mice was significantly higher than corn oil group. Whereas, DHE treatment significantly decreased the level of ALT compared with CCl₄ group mice. In addition, the level of plasma AST was significantly decreased after 2 mg/kg DHE treatment (Figure 4E). Collagen area were visualized by Masson's trichrome and quantified by using ImageJ 1.52a software. DHE treatment in both dosages significantly reduced collagen accumulation compared with those of the CCl₄ group (Figure 4F and G). Taken together, these results demonstrated that DHE significantly protected from liver fibrosis in CCl₄-induced mouse fibrosis model.

DHE decreased the liver macrophages infiltration and ECM deposition

The infiltration of macrophages reflects the severity of liver inflammation. To investigate the degree of macrophages infiltration, the liver immune cells were extracted and labeled with CD45⁺, F4/80⁺, and CD11b⁺ antibodies followed by flow-cytometric analysis. The results demonstrated that the DHE treatment at both dosages significantly reduced proportion of CD11b⁺ cells (Figure 5A and B, and Supplementary Figure 2B-F). Consistent with the result of flow cytometry, the mRNA levels of tumor necrosis factor alpha (TNF α) and F4/80 which are two important indicators of liver inflammation significantly decreased upon DHE treatment (Figure 5C). On the other hand, the accumulation of ECM is another important sign of liver fibrosis. The results demonstrated that the mRNA levels of COL1A1, COL1A2, and α -SMA significantly decreased in the DHE treatment group more than those of the CCl₄ group (Figure 5D). The mRNA levels of COL3A1 also decreased in the DHE treatment groups

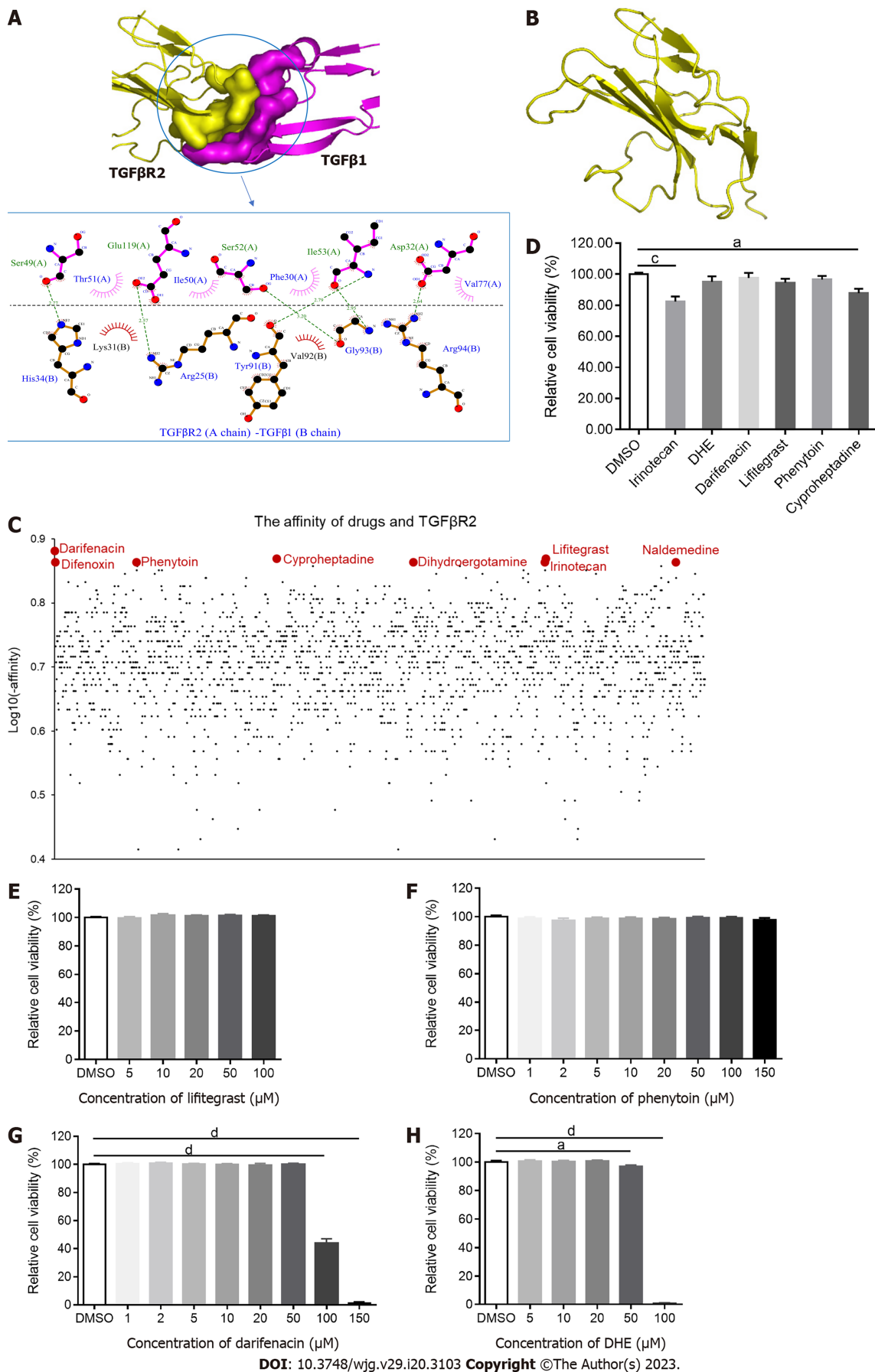
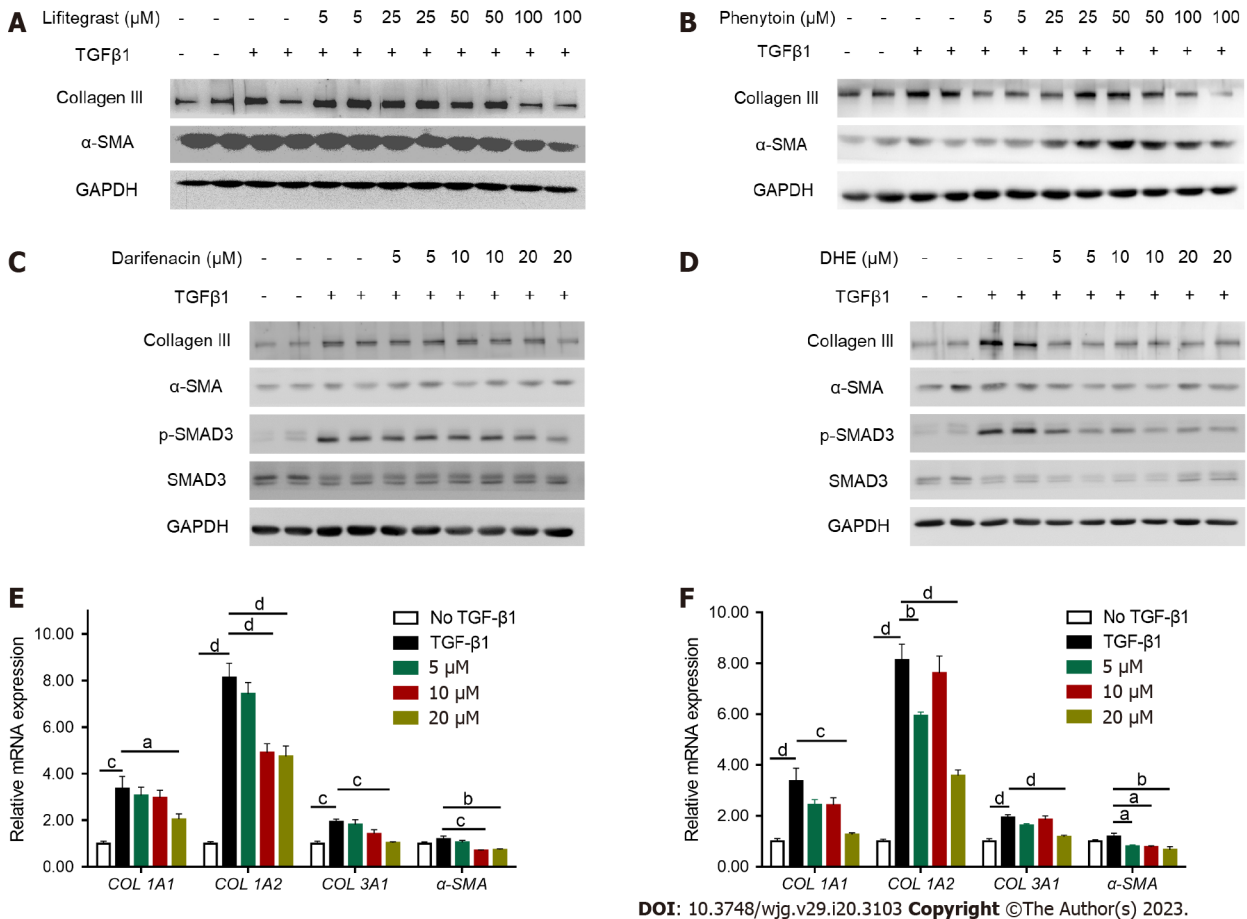


Figure 1 Screening Food and Drug Administration-approved drugs for binding to transforming growth factor β type II receptor. A: The combination of transforming growth factor β type II receptor (TGF β 2) and transforming growth factor β 1 (TGF β 1); B: The structure of TGF β 2; C: The affinity of

each Food and Drug Administration-approved drug and TGF β R2. The affinity of TGF β R2 and darifenacin, cyproheptadine, lifitegrast, difenoxin, phenytoin, dihydroergotamine (DHE), naldemedine, and irinotecan was -7.6, -7.4, -7.4, -7.3, -7.3, -7.3, and -7.3 kcal/mol, respectively; D: Cell viability of LX-2 treated with 20 μ M of the drugs for 24 h ($n = 5$); E-H: Cell viability following LX-2 treatment with different concentrations of darifenacin, DHE, lifitegrast, and phenytoin for 24 h ($n = 6$). All data are presented as mean \pm standard error of the mean. One-way ANOVA test was performed. ^a $P < 0.05$, ^b $P < 0.01$, ^c $P < 0.001$, and ^d $P < 0.0001$. TGF β : Transforming growth factor β ; TGF β R: Transforming growth factor β receptor; DHE: Dihydroergotamine.



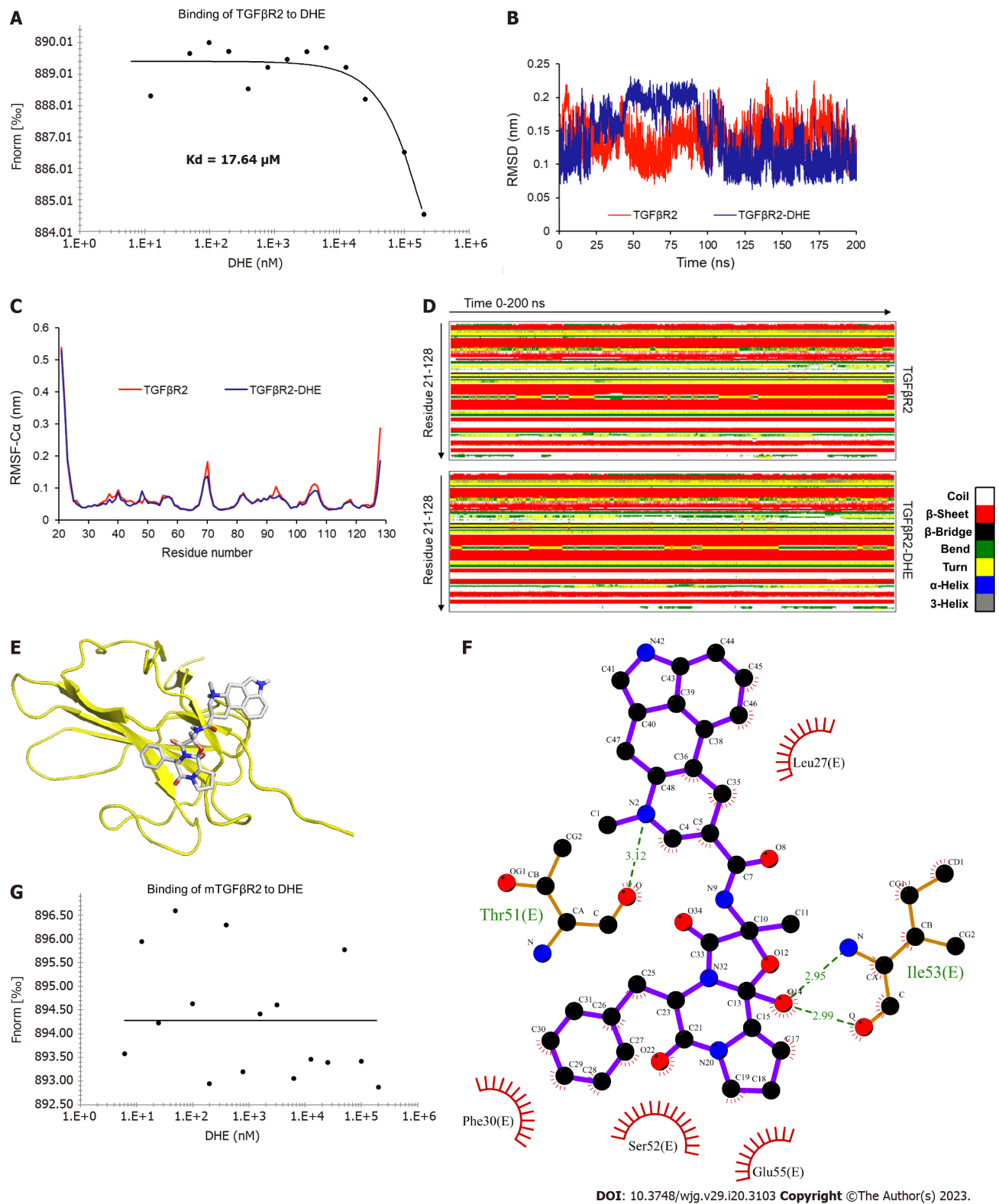
DOI: 10.3748/wjg.v29.i20.3103 Copyright ©The Author(s) 2023.

Figure 2 Treatment inhibiting the activation of LX-2 cells. A and B: After LX-2 cell was activated with transforming growth factor β 1 (TGF β 1) (5 ng/mL) for 24 h, different concentrations of lifitegrast and phenytoin were added for 24 h, and the protein levels of collagen III and α -SMA were detected by western blot; C and D: After LX-2 was activated with TGF β 1 (5 ng/mL) for 24 h, different concentrations of darifenacin and dihydroergotamine (DHE) were added for further treatment for 24 h, and the protein levels of collagen III, α -SMA, and p-SMAD3 were detected by western blot; E: Real-time polymerase chain reaction (RT-PCR) was performed to detect the expression of COL1A1, COL1A2, COL3A1, and α -SMA of LX-2 after different concentrations of darifenacin treatment ($n = 6$); F: RT-PCR was performed to detect the expression of COL1A1, COL1A2, COL3A1, and α -SMA of LX-2 after different concentrations of DHE treatment ($n = 5-6$). All data are presented as means \pm standard error of the mean. One-way ANOVA test was performed. ^a $P < 0.05$, ^b $P < 0.01$, ^c $P < 0.001$, and ^d $P < 0.0001$. TGF β : Transforming growth factor β ; TGF β R: Transforming growth factor β receptor; DHE: Dihydroergotamine.

(Figure 5D). Meanwhile, the protein levels of α -SMA and p-SMAD3 were significantly decreased in the DHE treatment group compared to those of the CCl₄ group (Figure 5E and F). Thus, we demonstrated here that, DHE significantly decreased the liver macrophages infiltration and ECM deposition.

DISCUSSION

TGF β 1 is regarded as the most potent fibrogenic cytokine, which activates TGF β R2, followed by the recruitment of TGF β R1, therefore triggers HSC activation[30]. In the current study, we aimed to screen drugs targeting TGF β R2 and further blocking TGF β down-stream signaling pathway from FDA-approved small molecule library. Among these 6 candidate drugs, DHE significantly decreased the protein and mRNA expression of fibrotic-related genes in LX-2 cells. The results of the affinity experiment demonstrated that DHE binds with TGF β R2 at Leu27, Phe30, Thr51, Ser52, Ile53, and Glu55. DHE also significantly alleviated liver fibrosis by decreasing macrophages infiltration and ECM accumulation in CCl₄-induced mouse fibrosis model. Thus, we demonstrate here for the first time that

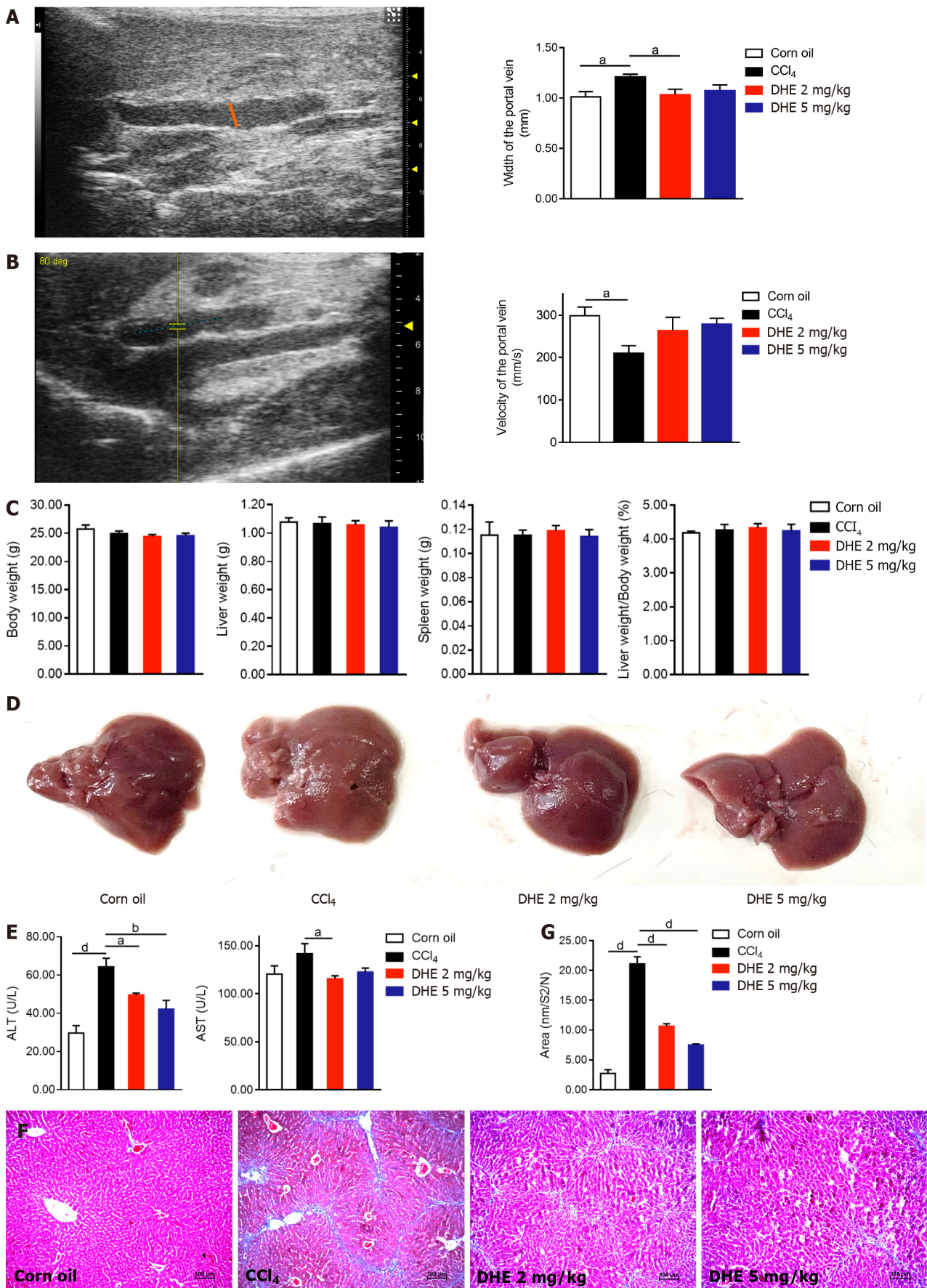


DOI: 10.3748/wjg.v29.i20.3103 Copyright ©The Author(s) 2023.

Figure 3 The binding affinity and sites of dihydroergotamine and transforming growth factor β type II receptor. A: Transforming growth factor β type II receptor (TGF β R2) bound to dihydroergotamine (DHE) with a K_d of 17.64 μM ; B: Molecular dynamics simulation results of DHE and TGF β R2. Root-mean-square deviation of TGF β R2 skeleton atom; C: Root-mean-square fluctuation of backbone C α atoms of TGF β R2 skeleton atom; D: The secondary structure components of TGF β R2 and complex simulation systems in 0-200 ns; E and F: The binding sites of DHE and TGF β R2; G: The binding affinity of TGF β R2 mutants with DHE. TGF β : Transforming growth factor β ; TGF β R: Transforming growth factor β receptor; DHE: Dihydroergotamine.

DHE, an anti-headache agent, is used in the treatment of liver fibrosis.

Developing a new drug needs more than a decade and significant investment[8]. Drug repurposing is a potential tool to accelerate the drug discovery process, which has been employed to develop therapies for coronavirus disease 2019[31], antimicrobials[32], and rare diseases[33]. The chemical structure of DHE is similar to that of many natural neurotransmitters, including epinephrine, norepinephrine,



DOI: 10.3748/wjg.v29.i20.3103 Copyright ©The Author(s) 2023.

Figure 4 Dihydroergotamine alleviated fibrosis in CCl₄-induced liver fibrosis model mice. A: The width of the portal vein (left panel); portal vein width of mice in each group (right panel, n = 7); B: The velocity of the portal vein (left panel); the velocity of mice in each group (right panel, n = 7); C: Body weight,

liver weight, spleen weight, and liver weight/body weight of mice in each group ($n = 6-8$); D: Gross liver specimens of the mice in each group; E: An automated biochemistry analyzer determined the enzymatic activities of serum levels of alanine aminotransferase and aspartate aminotransferase ($n = 6-7$); F: Masson's trichrome staining was performed on liver sections; G: Collagen area in Masson's trichrome staining ($n = 7-8$). All data were presented as means \pm standard error of the mean. One-way ANOVA test was performed. ^a $P < 0.05$, ^b $P < 0.01$, ^c $P < 0.001$, and ^d $P < 0.0001$. TGF β : Transforming growth factor β ; TGF β R: Transforming growth factor β receptor; DHE: Dihydroergotamine.

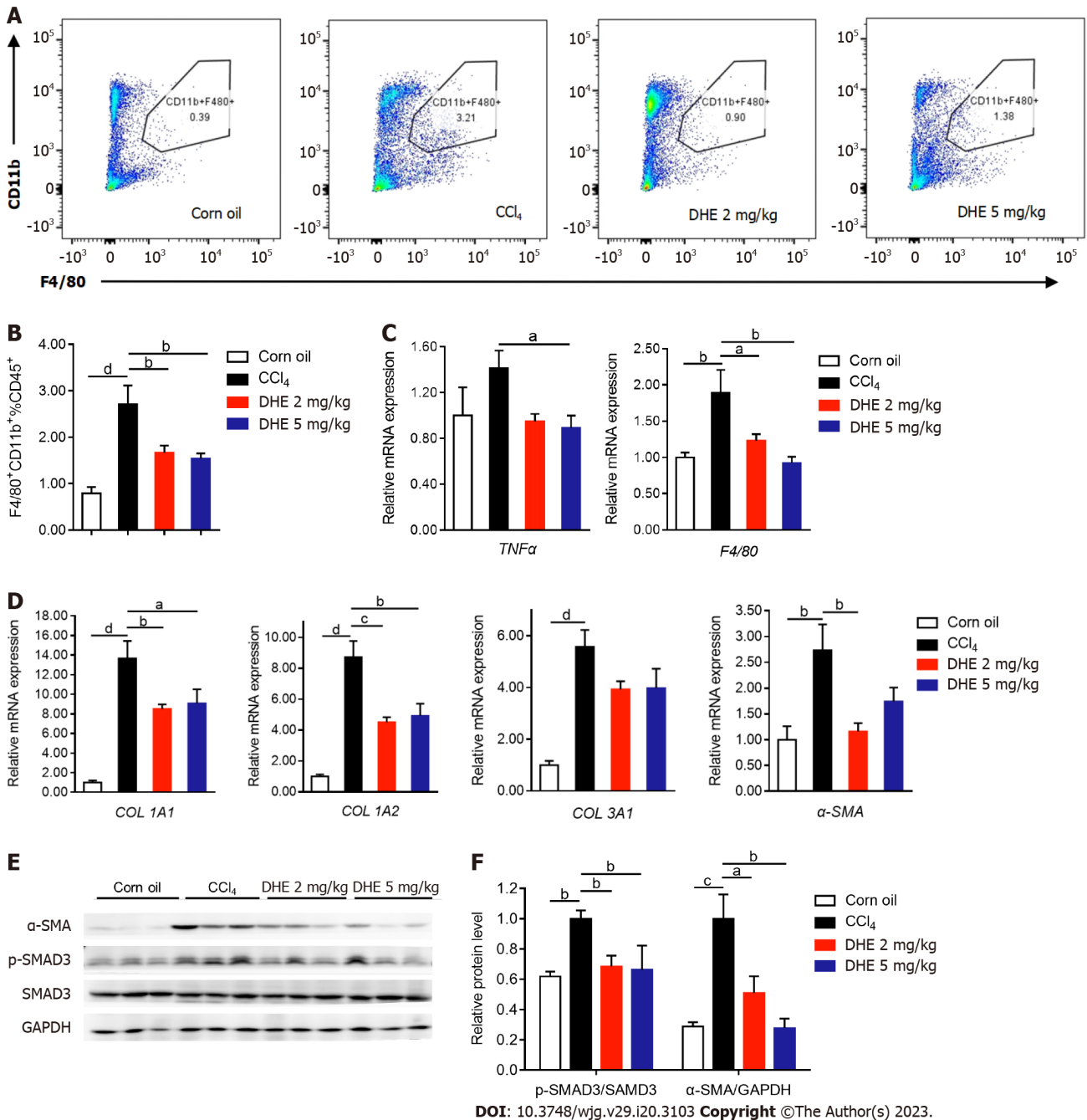


Figure 5 Dihydroergotamine decreased the inflammatory infiltration of macrophages and extracellular matrix deposition in the liver. A and B: The flow cytometric analysis of CD11b⁺ cells ($n = 6-8$); C: The effects of dihydroergotamine (DHE) treatment on the mRNA expression levels of inflammation-related genes ($n = 6-8$); D: The effects of DHE treatment on the mRNA expression levels of extracellular matrix-related genes ($n = 6-8$); E: The protein levels of p-SMAD3 and α -SMA in liver tissues of mice in each group were detected by western blot ($n = 3$). All data are presented as means \pm standard error of the mean. One-way ANOVA test was performed. ^a $P < 0.05$, ^b $P < 0.01$, ^c $P < 0.001$, and ^d $P < 0.0001$. TGF β : Transforming growth factor β ; TGF β R: Transforming growth factor β receptor; DHE: Dihydroergotamine.

dopamine, and serotonin[26]. It can modulate noradrenergic, serotonergic, and dopaminergic neurotransmission[34]. DHE is an adrenergic receptor antagonist used to treat severe orthostatic hypotension, migraine, and headache[26], which can bind with various receptors. DHE is also an

agonist of 5-HT1B, 5-HT1D, and 5-HT1F receptors, but it also binds to 5-HT1A and 5-HT2A receptors [26]. In the current study, surprisingly, we found that DHE also bind with TGF β R2 at reasonable affinity. Furthermore, we also identified specific binding sites by mutagenesis analysis. These results imply that DHE not only specifically targets 5-HT, but also TGF β R2. It further highlights wide-spread function of DHE in physiology/pathophysiology.

Continuous local and systemic inflammation aggravates liver injury, which is a critical factor in liver fibrosis. The innate immune system plays a pivotal role from the onset to the end stage of chronic liver disease[35]. Hepatic macrophages are considered as the first line of defense against pathogens, are a key cellular determinant in the process of fibrosis[36]. Bone marrow monocyte-derived macrophages and Kupffer cells are two distinct subsets of macrophages in the liver, which have been identified as key regulators of liver inflammation and key to the progression or regression of liver fibrosis. Kupffer cells, which are resident macrophages in liver tissue, exert anti-inflammatory effects[37]. Activated macrophages produce large amounts of TGF β , which activates HSC into myofibroblast-like cells and synthesizes ECM[38]. This inflammatory response is also evident in the CCl₄-induced mouse model, especially in the increased number of macrophages in liver. Consistent with previous results, we also found that the macrophages infiltration was significantly increased after CCl₄ treatment. We speculate that, upon binding to TGF β R2, DHE prevents recruitment of TGF β R1 to TGF β R2, thereby inhibiting TGF β down-stream signaling pathway. Consistently, F4/80 and TNF α mRNA expression also significantly decreased upon DHE treatment. Taken together, DHE might reduce macrophages infiltration and finally prevent liver inflammation.

Activated HSCs secreting ECM represent a critical event in development of liver fibrosis[37]. In the fibrotic liver, type I and III collagens are deposited instead of laminins, type IV collagen, and proteoglycans in the normal liver[17]. Various mechanisms of HSC activation have been postulated, including TGF β /SMAD pathway, Notch, Wnt/ β -catenin, Hedgehog, and Hippo signaling[16]. In the current study, we revealed that DHE significantly reduced TGF β induced HSCs activation in LX-2 cellular model through specific blocking of TGF β signaling pathway. It explained clearly the significant reduction of ECM by DHE treatment. Taken together, our data show that DHE alleviated liver fibrosis by binding to TGF β R2, preventing the binding of TGF β 1 and TGF β R2, and blocking TGF β 1 signaling to reduce liver inflammation.

CONCLUSION

Our study demonstrated that DHE alleviated liver fibrosis while decreasing inflammation-related gene expression and HSC activation. The mechanism of its action is likely to be associated with decreased macrophages infiltration and ECM accumulation. Considering that liver fibrosis can be reversed, DHE might open-up new avenue to treat liver fibrosis in the future.

ARTICLE HIGHLIGHTS

Research background

The transforming growth factor β (TGF β) signaling pathway plays a crucial role in the development of liver fibrosis by activating TGF β type II receptor (TGF β R2), followed by the recruitment of TGF β R1 finally triggering downstream signaling pathway.

Research motivation

TGF β R2 is considered an important target for developing drugs against liver fibrosis. Previous studies demonstrated that both inhibiting the expression of TGF β R2 and exogenous extracellular domain of TGF β R2 supplement effectively alleviated liver fibrosis.

Research objectives

To find drugs targeting TGF β R2 that inhibit TGF β R1/TGF β R2 complex formation, theoretically inhibit its downstream TGF β signaling pathway, and thereby ameliorate liver fibrosis, we screened drugs approved by the Food and Drug Administration (FDA) to identify potential TGF β R2 blockers.

Research methods

FDA-approved drugs were screened for binding affinity with TGF β R2 by virtual molecular docking. We identified 6 candidates and further explored their potential by Cell Counting Kit-8 cell cytotoxic experiment to validate toxicity and titrated the best cellular working concentrations. Next, we further demonstrated the detailed molecular working mechanisms using mutagenesis analysis. Finally, we used a mouse model to investigate its potential anti-liver fibrosis effect.

Research results

Dihydroergotamine (DHE) shows great ability in reducing fibrotic gene expressions such as collagen, p-SMAD3, and α -SMA in TGF β induced cellular model of liver fibrosis in LX-2 cells. Furthermore, we demonstrated that DHE binds to TGF β R2 with a Kd value of 17.64 μ M. In addition, DHE significantly improved liver fibrosis, as evidenced by Masson's trichrome staining of liver sections, the width and the velocity of the portal vein, and serum markers of liver function. In line with those observations, DHE also decreased macrophages infiltration and extracellular matrix deposition in the liver.

Research conclusions

DHE could alleviate liver fibrosis by binding to TGF β R2 thereby suppressing its downstream TGF β signaling pathway. We show here that as far as drug repurposing, DHE has great potential to treat liver fibrosis.

Research perspectives

Considering that liver fibrosis can be reversed, DHE might open-up new avenue to treat liver fibrosis in the future.

FOOTNOTES

Author contributions: Xie W designed experiments and revised the manuscript; Jin WZ and Wang Q reversed the manuscript; Zheng KX and Yuan SL performed experiments, analyzed data, and wrote the manuscript; Dong M and Zhang HL performed experiments, analyzed data, and revised the manuscript; Other authors helped with the experiments; All authors read and approved the final version of the article.

Supported by the Special Research Project for Capital Health Development, No. 2022-2-2174; and the Beijing Municipal Science and Technology Commission, No. Z191100007619037.

Institutional animal care and use committee statement: All procedures involving animals were reviewed and approved by the Institutional Animal Care and Use Committee the Institute of Zoology, Chinese Academy of Sciences, IACUC protocol No. IOZ-IACUC-2020-114.

Conflict-of-interest statement: Dr. Xie reports in addition, Dr. Xie has a patent Application of dihydroergotamine in the treatment of liver fibrosis issued.

Data sharing statement: No additional data are available.

ARRIVE guidelines statement: The authors have read the ARRIVE guidelines, and the manuscript was prepared and revised according to the ARRIVE guidelines.

Open-Access: This article is an open-access article that was selected by an in-house editor and fully peer-reviewed by external reviewers. It is distributed in accordance with the Creative Commons Attribution NonCommercial (CC BY-NC 4.0) license, which permits others to distribute, remix, adapt, build upon this work non-commercially, and license their derivative works on different terms, provided the original work is properly cited and the use is non-commercial. See: <https://creativecommons.org/licenses/by-nc/4.0/>

Country/Territory of origin: China

ORCID number: Ke-Xin Zheng 0000-0002-8252-1170; Shou-Li Yuan 0000-0002-4733-9891; Zhi Zhang 0000-0002-2471-1494; Qi Wang 0000-0002-0269-1568; Wen Xie 0000-0002-7314-8175.

S-Editor: Li L

L-Editor: A

P-Editor: Yuan YY

REFERENCES

- 1 Parola M, Pinzani M. Liver fibrosis: Pathophysiology, pathogenetic targets and clinical issues. *Mol Aspects Med* 2019; **65**: 37-55 [PMID: 30213667 DOI: 10.1016/j.mam.2018.09.002]
- 2 Pellicoro A, Ramachandran P, Iredale JP, Fallowfield JA. Liver fibrosis and repair: immune regulation of wound healing in a solid organ. *Nat Rev Immunol* 2014; **14**: 181-194 [PMID: 24566915 DOI: 10.1038/nri3623]
- 3 Karsdal MA, Nielsen SH, Leeming DJ, Langholm LL, Nielsen MJ, Manon-Jensen T, Siebuhr A, Gudmann NS, Rønnow S, Sand JM, Daniels SJ, Mortensen JH, Schuppan D. The good and the bad collagens of fibrosis - Their role in signaling and organ function. *Adv Drug Deliv Rev* 2017; **121**: 43-56 [PMID: 28736303 DOI: 10.1016/j.addr.2017.07.014]

- 4 **Ginès P**, Krag A, Abrales JG, Solà E, Fabrellas N, Kamath PS. Liver cirrhosis. *Lancet* 2021; **398**: 1359-1376 [PMID: 34543610 DOI: 10.1016/S0140-6736(21)01374-X]
- 5 **Marcellin P**, Gane E, Buti M, Afdhal N, Sievert W, Jacobson IM, Washington MK, Germanidis G, Flaherty JF, Aguilar Schall R, Bornstein JD, Kitrinou KM, Subramanian GM, McHutchison JG, Heathcote EJ. Regression of cirrhosis during treatment with tenofovir disoproxil fumarate for chronic hepatitis B: a 5-year open-label follow-up study. *Lancet* 2013; **381**: 468-475 [PMID: 23234725 DOI: 10.1016/S0140-6736(12)61425-1]
- 6 **Sapisochin G**, Bruix J. Liver transplantation for hepatocellular carcinoma: outcomes and novel surgical approaches. *Nat Rev Gastroenterol Hepatol* 2017; **14**: 203-217 [PMID: 28053342 DOI: 10.1038/nrgastro.2016.193]
- 7 **Friedman SL**, Pinzani M. Hepatic fibrosis 2022: Unmet needs and a blueprint for the future. *Hepatology* 2022; **75**: 473-488 [PMID: 34923653 DOI: 10.1002/hep.32285]
- 8 **Parvathaneni V**, Kulkarni NS, Muth A, Gupta V. Drug repurposing: a promising tool to accelerate the drug discovery process. *Drug Discov Today* 2019; **24**: 2076-2085 [PMID: 31238113 DOI: 10.1016/j.drudis.2019.06.014]
- 9 **Pushpakom S**, Iorio F, Eyers PA, Escott KJ, Hopper S, Wells A, Doig A, Guillelliams T, Latimer J, McNamee C, Norris A, Sanseau P, Cavalla D, Pirmohamed M. Drug repurposing: progress, challenges and recommendations. *Nat Rev Drug Discov* 2019; **18**: 41-58 [PMID: 30310233 DOI: 10.1038/nrd.2018.168]
- 10 **Knight JM**, Kerswill SA, Hari P, Cole SW, Logan BR, D'Souza A, Shah NN, Horowitz MM, Stolley MR, Sloan EK, Giles KE, Costanzo ES, Hamadani M, Chhabra S, Dhakal B, Rizzo JD. Repurposing existing medications as cancer therapy: design and feasibility of a randomized pilot investigating propranolol administration in patients receiving hematopoietic cell transplantation. *BMC Cancer* 2018; **18**: 593 [PMID: 29793446 DOI: 10.1186/s12885-018-4509-0]
- 11 **Ramos-Arancibia N**, Varas C, Rozas-Muñoz E. Severe and recalcitrant periungual warts in a child successfully treated with cimetidine. *Dermatol Ther* 2021; **34**: e15154 [PMID: 34623743 DOI: 10.1111/dth.15154]
- 12 **Galiè N**, Ghofrani HA, Torbicki A, Barst RJ, Rubin LJ, Badesch D, Fleming T, Parpia T, Burgess G, Branzi A, Grimminger F, Kurzyna M, Simonneau G; Sildenafil Use in Pulmonary Arterial Hypertension (SUPER) Study Group. Sildenafil citrate therapy for pulmonary arterial hypertension. *N Engl J Med* 2005; **353**: 2148-2157 [PMID: 16291984 DOI: 10.1056/NEJMoa050010]
- 13 **Franks ME**, Macpherson GR, Figg WD. Thalidomide. *Lancet* 2004; **363**: 1802-1811 [PMID: 15172781 DOI: 10.1016/S0140-6736(04)16308-3]
- 14 **Yang J**, Roy A, Zhang Y. Protein-ligand binding site recognition using complementary binding-specific substructure comparison and sequence profile alignment. *Bioinformatics* 2013; **29**: 2588-2595 [PMID: 23975762 DOI: 10.1093/bioinformatics/btt447]
- 15 **Higashi T**, Friedman SL, Hoshida Y. Hepatic stellate cells as key target in liver fibrosis. *Adv Drug Deliv Rev* 2017; **121**: 27-42 [PMID: 28506744 DOI: 10.1016/j.addr.2017.05.007]
- 16 **Yan Y**, Zeng J, Xing L, Li C. Extra- and Intra-Cellular Mechanisms of Hepatic Stellate Cell Activation. *Biomedicines* 2021; **9** [PMID: 34440218 DOI: 10.3390/biomedicines9081014]
- 17 **Tsuchida T**, Friedman SL. Mechanisms of hepatic stellate cell activation. *Nat Rev Gastroenterol Hepatol* 2017; **14**: 397-411 [PMID: 28487545 DOI: 10.1038/nrgastro.2017.38]
- 18 **Fabregat I**, Moreno-Càceres J, Sánchez A, Dooley S, Dewidar B, Giannelli G, Ten Dijke P; IT-LIVER Consortium. TGF- β signalling and liver disease. *FEBS J* 2016; **283**: 2219-2232 [PMID: 26807763 DOI: 10.1111/febs.13665]
- 19 **Liu Y**, Wang Z, Wang J, Lam W, Kwong S, Li F, Friedman SL, Zhou S, Ren Q, Xu Z, Wang X, Ji L, Tang S, Zhang H, Lui EL, Ye T. A histone deacetylase inhibitor, largazole, decreases liver fibrosis and angiogenesis by inhibiting transforming growth factor- β and vascular endothelial growth factor signalling. *Liver Int* 2013; **33**: 504-515 [PMID: 23279742 DOI: 10.1111/liv.12034]
- 20 **Yuan S**, Dong M, Zhang H, Xu H, Wang Q, Yan C, Ye R, Jiang X, Zhou H, Chen L, Cheng J, Xie W, Jin W. Oral delivery of a Lactococcus lactis expressing extracellular TGF β R2 alleviates hepatic fibrosis. *Appl Microbiol Biotechnol* 2021; **105**: 6007-6018 [PMID: 34390354 DOI: 10.1007/s00253-021-11485-7]
- 21 **Haab F**, Stewart L, Dwyer P. Darifenacin, an M3 selective receptor antagonist, is an effective and well-tolerated once-daily treatment for overactive bladder. *Eur Urol* 2004; **45**: 420-9; discussion 429 [PMID: 15041104 DOI: 10.1016/j.eururo.2004.01.008]
- 22 **Goudie AJ**, Cooper GD, Cole JC, Sumnall HR. Cyproheptadine resembles clozapine in vivo following both acute and chronic administration in rats. *J Psychopharmacol* 2007; **21**: 179-190 [PMID: 17329298 DOI: 10.1177/0269881107067076]
- 23 **Haber SL**, Benson V, Buckway CJ, Gonzales JM, Romanet D, Scholes B. Lifitegrast: a novel drug for patients with dry eye disease. *Ther Adv Ophthalmol* 2019; **11**: 2515841419870366 [PMID: 31489402 DOI: 10.1177/2515841419870366]
- 24 **Scarlett Y**. Medical management of fecal incontinence. *Gastroenterology* 2004; **126**: S55-S63 [PMID: 14978639 DOI: 10.1053/j.gastro.2003.10.007]
- 25 **Patočka J**, Wu Q, Nepovimova E, Kuca K. Phenytoin - An anti-seizure drug: Overview of its chemistry, pharmacology and toxicology. *Food Chem Toxicol* 2020; **142**: 111393 [PMID: 32376339 DOI: 10.1016/j.fct.2020.111393]
- 26 **Silberstein SD**, Shrewsbury SB, Hoekman J. Dihydroergotamine (DHE) - Then and Now: A Narrative Review. *Headache* 2020; **60**: 40-57 [PMID: 31737909 DOI: 10.1111/head.13700]
- 27 **Blair HA**. Naldemedine: A Review in Opioid-Induced Constipation. *Drugs* 2019; **79**: 1241-1247 [PMID: 31267482 DOI: 10.1007/s40265-019-01160-7]
- 28 **Kciuk M**, Marciniak B, Kontek R. Irinotecan-Still an Important Player in Cancer Chemotherapy: A Comprehensive Overview. *Int J Mol Sci* 2020; **21** [PMID: 32664667 DOI: 10.3390/ijms21144919]
- 29 **Kisseleva T**, Brenner D. Molecular and cellular mechanisms of liver fibrosis and its regression. *Nat Rev Gastroenterol Hepatol* 2021; **18**: 151-166 [PMID: 33128017 DOI: 10.1038/s41575-020-00372-7]
- 30 **Dufton NP**, Peghaire CR, Osuna-Almagro L, Raimondi C, Kalna V, Chauhan A, Webb G, Yang Y, Birdsey GM, Lalor P, Mason JC, Adams DH, Randi AM. Dynamic regulation of canonical TGF β signalling by endothelial transcription factor ERG protects from liver fibrogenesis. *Nat Commun* 2017; **8**: 895 [PMID: 29026072 DOI: 10.1038/s41467-017-01169-0]
- 31 **Ng YL**, Salim CK, Chu JJH. Drug repurposing for COVID-19: Approaches, challenges and promising candidates.

- Pharmacol Ther* 2021; **228**: 107930 [PMID: 34174275 DOI: 10.1016/j.pharmthera.2021.107930]
- 32 **Farha MA**, Brown ED. Drug repurposing for antimicrobial discovery. *Nat Microbiol* 2019; **4**: 565-577 [PMID: 30833727 DOI: 10.1038/s41564-019-0357-1]
- 33 **Roessler HI**, Knoers NVAM, van Haelst MM, van Haaften G. Drug Repurposing for Rare Diseases. *Trends Pharmacol Sci* 2021; **42**: 255-267 [PMID: 33563480 DOI: 10.1016/j.tips.2021.01.003]
- 34 **Piechal A**, Blecharz-Klin K, Joniec-Maciejak I, Pyrzanowska J, Krzysztoforska K, Mirowska-Guzel D, Widy-Tyszkiewicz E. Dihydroergotamine affects spatial behavior and neurotransmission in the central nervous system of Wistar rats. *Ann Agric Environ Med* 2021; **28**: 437-445 [PMID: 34558267 DOI: 10.26444/aaem/126020]
- 35 **Bernsmeier C**, van der Merwe S, Périanin A. Innate immune cells in cirrhosis. *J Hepatol* 2020; **73**: 186-201 [PMID: 32240716 DOI: 10.1016/j.jhep.2020.03.027]
- 36 **Campana L**, Iredale JP. Regression of Liver Fibrosis. *Semin Liver Dis* 2017; **37**: 1-10 [PMID: 28201843 DOI: 10.1055/s-0036-1597816]
- 37 **Cheng D**, Chai J, Wang H, Fu L, Peng S, Ni X. Hepatic macrophages: Key players in the development and progression of liver fibrosis. *Liver Int* 2021; **41**: 2279-2294 [PMID: 33966318 DOI: 10.1111/liv.14940]
- 38 **Binatti E**, Gerussi A, Barisani D, Invernizzi P. The Role of Macrophages in Liver Fibrosis: New Therapeutic Opportunities. *Int J Mol Sci* 2022; **23** [PMID: 35743092 DOI: 10.3390/ijms23126649]

Retrospective Study

Malignancy risk factors and prognostic variables of pancreatic mucinous cystic neoplasms in Chinese patients

Qing Xia, Fan Li, Rui Min, Shuai Sun, Yue-Xin Han, Zhen-Zhong Feng, Nan Li

Specialty type: Gastroenterology and hepatology**Provenance and peer review:** Unsolicited article; Externally peer reviewed.**Peer-review model:** Single blind**Peer-review report's scientific quality classification**Grade A (Excellent): 0
Grade B (Very good): B
Grade C (Good): C
Grade D (Fair): 0
Grade E (Poor): 0**P-Reviewer:** Tenreiro N, Portugal; Zimmitti G, Italy**Received:** March 3, 2023**Peer-review started:** March 3, 2023**First decision:** April 12, 2023**Revised:** April 21, 2023**Accepted:** May 4, 2023**Article in press:** May 4, 2023**Published online:** May 28, 2023**Qing Xia, Rui Min, Nan Li**, Department of Pathology, The First Affiliated Hospital of Bengbu Medical College, Bengbu Medical College, Bengbu 233004, Anhui Province, China**Fan Li, Shuai Sun**, Department of Pathology, Bengbu Medical College, Bengbu 233030, Anhui Province, China**Yue-Xin Han**, School of Clinical Medicine, Bengbu Medical College, Bengbu 233030, Anhui Province, China**Zhen-Zhong Feng, Nan Li**, Department of Pathology, The Second Affiliated Hospital of Anhui Medical University, Hefei 230601, Anhui Province, China**Corresponding author:** Nan Li, Doctor, MD, PhD, Chief Doctor, Professor, Department of Pathology, The First Affiliated Hospital of Bengbu Medical College, No. 287 Changhuai Road, Bengbu 233004, Anhui Province, China. linanangel100@sina.com**Abstract****BACKGROUND**

Pancreatic mucinous cystic neoplasms (MCNs) represent one of the precursor lesions of pancreatic ductal adenocarcinoma, and their detection has been facilitated by advances in preoperative imaging. Due primarily to the rarity of MCNs, however, there is limited knowledge regarding the prognostic variables and high-risk factors for malignant transformation. A more comprehensive and nuanced approach is necessary to fill this gap and provide a basis for improved treatment decisions and patient outcomes.

AIM

To investigate the high-risk factors associated with malignant MCNs and to explore the prognostic factors of MCN with associated invasive carcinoma (MCN-AIC).

METHODS

All cases of resected MCNs from a single high-volume institution between January 2012 and January 2022 were retrospectively reviewed. Only cases with ovarian-type stroma verified by progesterone receptor staining were included. Preoperative features, histological findings and postoperative course were documented. Multivariate logistic regression was employed to investigate variables related to malignancy. Survival analysis was performed using the

Kaplan-Meier curve, and the prognostic factors were assessed to evaluate the postoperative course of patients with MCN-AIC.

RESULTS

Among the 48 patients, 36 had benign MCNs, and 12 had malignant MCNs (1 high-grade atypical hyperplasia and 11 MCN-AIC). Age, tumour size, presence of solid components or mural nodules and pancreatic duct dilatation were identified as independent risk factors associated with malignancy. The follow-up period ranged from 12 mo to 120 mo, with a median overall survival of 58.2 mo. Only three patients with MCN-AIC died, and the 5-year survival rate was 70.1%. All 11 cases of MCN-AIC were stage I, and extracapsular invasion was identified as a prognostic factor for poorer outcomes.

CONCLUSION

The risk factors independently associated with malignant transformation of MCNs included age, tumour size, presence of solid components or mural nodules, and pancreatic duct dilatation. Our study also revealed that encapsulated invasion was a favourable prognostic factor in MCN-AIC patients.

Key Words: Mucinous cystic neoplasms; Pancreatic adenocarcinoma; Invasive carcinoma; Risk of malignancy; Prognostic factor; Retrospective study

©The Author(s) 2023. Published by Baishideng Publishing Group Inc. All rights reserved.

Core Tip: Pancreatic mucinous cystic neoplasms (MCNs) are a rare tumour with a low incidence and one of the precursor lesions of pancreatic ductal adenocarcinoma. The detection of MCN has been increasing by advances in imaging technology. MCNs associated risk factors, clinicopathological manifestations, and prognosis must be explored to improve our understanding of this rare tumour type and optimize clinical treatment.

Citation: Xia Q, Li F, Min R, Sun S, Han YX, Feng ZZ, Li N. Malignancy risk factors and prognostic variables of pancreatic mucinous cystic neoplasms in Chinese patients. *World J Gastroenterol* 2023; 29(20): 3119-3132

URL: <https://www.wjgnet.com/1007-9327/full/v29/i20/3119.htm>

DOI: <https://dx.doi.org/10.3748/wjg.v29.i20.3119>

INTRODUCTION

Pancreatic mucinous cystic neoplasm (MCN) is a rare sporadic tumour with a low incidence, accounting for 10%-45% of all resected primary pancreatic cystic neoplasms and 2.5% of exocrine pancreatic tumours[1,2]. With the increasing popularity of imaging evaluation and advances in radiological technology, the rate of MCN identification is on the rise. Pancreatic ductal adenocarcinoma (PDAC) is the leading cause of cancer-related death globally, and its incidence has been consistently increasing[3]. However, the majority of PDAC cases are detected at an advanced stage, highlighting the importance of early diagnosis and treatment of associated precancerous lesions to improve survival rates. MCN is a precancerous lesion of PDAC and evolves from benign adenoma to invasive carcinoma similarly to intraductal papillary mucinous neoplasm (IPMN) and pancreatic intraepithelial neoplasia (Pan IN)[4].

However, MCNs have not been studied in sufficient detail or breadth owing to their infrequency. The risk factors associated with malignancy have not been well characterized, and physicians have not been unanimous in adopting an optimal management profile. Discrepancies in recommendations offered by several medical associations may contribute to further challenges in managing the disease. Moreover, despite PDAC being the most common histopathological type of invasive MCN, notable differences exist in prognosis. However, the precise prognostic determinants of MCNs have yet to be fully elucidated.

Therefore, we conducted a retrospective study of the clinicopathological, radiological and survival data of a sizable cohort of patients. The findings of this study were intended to help identify key risk factors of malignant transformation in MCNs as well as the prognostic determinants of MCN with associated invasive carcinoma (MCN-AIC). The insights gained from this study may be used to inform the development of more effective management strategies for patients with MCNs, ultimately improving their clinical outcomes.

MATERIALS AND METHODS

Patient identification and ethics statement

All cases of MCN identified at the Department of Pathology of the First Affiliated Hospital of Bengbu Medical College from January 2012 to January 2022 were retrospectively retrieved. A total of 48 patients who fit the diagnostic criteria were included in the study. This study was approved by the Ethics Committee of the First Affiliated Hospital of Bengbu Medical College. Written informed consent was obtained from all patients for the use of their clinical data.

Inclusion and exclusion criteria

The inclusion criteria were patients who had been confirmed by surgical pathology to have MCN, underwent imaging examinations, and did not receive preoperative radiotherapy or chemotherapy. The exclusion criteria included poor-quality radiographic images, insufficient pathological diagnostic data, the presence of other pancreatic diseases, and a history of other malignant tumours. These criteria were carefully selected to ensure the accuracy and reliability of the study's findings.

Methods

All patients underwent preoperative imaging examinations, and the imaging data were uploaded to the Picture Archiving and Communication System. After reviewing and interpreting the data, two radiologists evaluated the radiographic tumour size, location, calcification, separation, solid composition or mural nodule status and duct dilatation of the lesion. Clinical information, including patient age and sex, symptoms, and serum tumour marker levels, was obtained through the analysis of medical records. The tumour tissues were paraffin-embedded and stained with haematoxylin-eosin staining (H&E) after being fixed in 10% neutral formaldehyde. MCN is classified by the World Health Organization (2019) as either atypical hyperplasia or MCN-AIC[5]. Low-grade atypical hyperplasia (LGD) and high-grade atypical hyperplasia (HGD, carcinoma in situ) have replaced the former three-tiered classification of atypical hyperplasia in MCN. All slides were reassessed by two senior pathologists who were uninformed of the patients' clinical diagnoses. All tissues were analysed immunohistochemically using the EnVision technique, and the progesterone receptor (PR) primary antibody was purchased from Fuzhou Maixin Biotechnology Co., Ltd., China. Expression of PR was restricted to the subepithelial ovarian-type stroma.

Patient outcomes

From the date of diagnosis to January 31, 2022, 48 patients were followed up by reviewing their medical records, interviewing them *via* phone, or sending emails to acquire follow-up data, including post-operative recurrence, overall survival (OS), and therapy. OS was measured from the date of surgery until the date of death or the end of follow-up.

Statistical analysis

The data were analyzed statistically using IBM SPSS Statistics (version 25.0) and R (version 4.0.0). The χ^2 test or Fisher's exact test was used to compare categorical data. The preoperative risk variables associated with malignant MCNs were evaluated using a multivariate binary logistic regression model. The cumulative survival rate was calculated using the Kaplan-Meier method, and the log rank test was performed to analyse the association between clinicopathological data and survival rate. $P < 0.05$ was regarded as indicating statistical significance.

RESULTS

Clinicopathological and radiological information of patients

A total of 48 patients diagnosed with MCN were included in accordance with strict inclusion and exclusion criteria. MCNs accounted for 2.8% (48/1685) of all pancreatic lesions resected over the same period. The median age of the patients was 47.2 years \pm 13.1 years (range, 27-72 years), and 16 patients (33.3%) were more than 50 years old. There were 34 females and 14 males, with a female-to-male ratio of 2.2:1.0. Approximately 41.7% of patients were asymptomatic, including 18 patients whose disease was detected incidentally by imaging evaluation and 2 patients whose disease was identified by elevated preoperative carbohydrate antigen 19-9 (CA19-9) serology. The remaining 28 patients presented with nonspecific clinical symptoms, such as stomach pain, abdominal distension, abdominal discomfort, and jaundice. Serologic CA19-9 Levels were elevated in 16 patients (33.3%).

Imaging revealed oval-shaped, lobulated hypodense masses that were well circumscribed, separated linearly, and surrounded by egg-shell-like foci of calcification. The contents of the cyst were also visible. The average radiological diameter of the tumour was 5.8 cm \pm 3.7 cm (1.2-14.5 cm), and in 23 patients (47.9%), the tumour measured more than 4 cm. Thirty-five patients (72.9%) had tumours that were located in the distal pancreas. Solid components or mural nodules were identified in 14 patients (29.2%),

septations in 21 (43.85%), calcification in 13 (27.1%) and duct dilatation in 18 (37.5%) (Figure 1). Detailed data on the imaging findings and clinicopathological information of MCN patients are shown in Table 1.

MCN was correctly diagnosed using preoperative imaging in 35 patients (72.9%). The most common misdiagnoses involved other subtypes of pancreatic cystic lesions (PCLs) and the use of imprecise terms such as pancreatic cystic or solid masses. The preoperative imaging modalities employed in this study comprised computed tomography (CT), magnetic resonance imaging (MRI), and endoscopic ultrasound (EUS). Of the 48 patients, all underwent CT, 33 underwent MRI, and 21 underwent EUS. The corresponding detection accuracy rates were 64.6%, 87.9%, and 71.4%, respectively. Nevertheless, there was no significant difference in diagnostic accuracy among the three methods ($P = 0.64$).

Microscopic and immunohistochemical features

Postoperative pathological diagnosis revealed 36 cases of LGD, 1 case of HGD, and 11 cases of MCN-AIC (the histological type of the invasive component was PDAC in all cases). All cases were solitary without multiple foci. The morphology of the cysts generally manifested as unilocular or multilocular with septa, and the fluid aspirated from the cystic cavity was frequently viscous.

Microscopically, the cyst walls were found to be coated with mucinous columnar epithelium (Figure 2A and B). Subepithelial tissue in the MCN consisted of ovarian-type stroma (OTS) characterized by dense spindle cells expressing PR and possessing round or elongated nuclei with scant cytoplasm. Positive PR staining was observed in all tumours (Figure 2D). The mucin-producing columnar epithelial cells exhibited varying degrees of dysplasia. In cases of LGD, mild to moderate structural and cellular atypia was observed with occasional micropapillae (Figure 2A and B). HGD showed obvious atypia of both structures and cells, including multilayered cell arrangement, nuclear enlargement, loss of alignment polarity, and emergence of aberrant mitotic figures. In cases of MCN-AIC, interstitial infiltration was noted in comparison to HGD, with invasive components growing interspersed in the stroma (Figure 2C). Solid components, mural nodules, or nipple protrusion were also occasionally visible. Notably, 5 cases of MCN-AIC showed atypical hyperplasia adjacent to invasive components.

Risk factors for malignant MCNs and the prediction probability

Based on malignant biological behaviours, LGD was defined as benign MCN in 36 cases (75%), while HGD and MCN-AIC were classified as malignant MCN in 12 cases (25%). Univariate analysis revealed that age ≥ 50 years [8 (66.7%) vs 8 (22.2%), $P = 0.013$], tumour size ≥ 4 cm [10 (83.3%) vs 13 (36.1%), $P = 0.010$], pancreatic duct dilatation [8 (66.7%) vs 10 (27.8%), $P = 0.039$], and presence of a solid component or mural nodule [8 (66.7%) vs 10 (27.8%), $P = 0.039$] were associated with malignant MCN. However, sex, clinical symptoms, serum CA19-9 Level, tumour location, septations and calcification did not correlate with malignancy ($P < 0.05$) (Table 1).

Further multivariate analysis demonstrated that all four statistically significant indicators were independent risk factors for the preoperative diagnosis of malignant MCNs ($P < 0.05$) (Figure 3). The prediction probability of each indicator for malignancy risk in a cohort of patients was then explored. The results of the analysis showed that age, tumour size, duct dilatation, and solid component/mural nodule all had good performance in predicting malignancy risk, as evidenced by the area under the curve (AUC) values of 0.722 (95%CI: 0.546-0.898, $P = 0.220$), 0.736 (95%CI: 0.578-0.894, $P = 0.015$), 0.694 (95%CI: 0.517-0.872, $P = 0.046$), and 0.694 (95%CI: 0.517-0.872, $P = 0.046$), respectively. Furthermore, when the four indicators were combined into a total predictor, the AUC value increased to 0.903 (95%CI: 0.814-0.992, $P < 0.010$), improving the accuracy of the prediction model.

Survival analysis and prognostic variables of MCN-AIC

The follow-up period ranged from 12 mo to 120 mo with a mean of 58.2 mo \pm 32.7 mo. Of the 36 patients with benign MCNs, 6 were lost to follow-up, and 1 died of an abrupt cerebral infarction. The remaining 29 patients had an excellent prognosis; their 5-year disease-specific survival rate was 100%. Of the 12 patients with malignant MCNs, 3 died at 8, 14, and 46 mo after surgery; the 5-year disease-specific survival rate was 70.1%. All deaths occurred in MCN-AIC patients.

Consequently, the clinicopathological characteristics of the 11 MCN-AIC patients were further explored (Table 2). The tumours examined in this study did not display any signs of lymph node involvement, distant metastasis, or nerve invasion. In addition, all the tumours were successfully resected, and the margins were negative. Based on the AJCC cancer staging system[6], all 11 cases of MCN-AIC were categorized as stage I, with 7 patients having stage IA cancers and 4 having stage IB cancers, depending on the tumour size. The encapsulated invasion of MCN-AIC was defined as infiltrating components not exceeding the outermost layer of the capsule, with or without infiltration into the subepithelial stroma or cystic septa[7]. Using this definition, 9 tumours were encapsulated, while 3 were extracapsular (Cases 1-3). In Case 1 and Case 2, the cancerous tissue extended into the capsule and intersected with the surrounding pancreatic parenchyma. The tumour in Case 3 was located in the head of the pancreas and showed infiltration into the adjacent duodenal muscular layer. There was no significant difference in age ($P = 0.301$), tumour size ($P = 0.109$), sex ($P = 0.402$), postoperative adjuvant therapy ($P = 0.952$) or TNM stage ($P = 0.400$). However, the difference in infiltration of the capsule was

Table 1 Clinicopathologic and radiological features in 48 patients

Variable	Benign group (n = 36)	Malignant group (n = 12)	P value
Sex			0.142
Male	8 (22.2)	6 (50.0)	
Female	28 (77.8)	6 (50.0)	
Age, yr			0.013
≥ 50	8 (22.2)	8 (66.7)	
< 50	28 (77.8)	4 (33.3)	
Clinical symptoms			0.499
Yes	20 (55.6)	8 (66.7)	
No	16 (44.4)	4 (33.3)	
Serum CA19-9 level			0.077
Elevate	9 (25)	7 (58.3)	
Normal	27 (75)	5 (41.7)	
Tumor size, cm			0.005
≥ 4	13 (36.1)	10 (83.3)	
< 4	23 (63.9)	2 (16.7)	
Location			0.348
Head and neck	8 (22.2)	5 (41.7)	
Body and tail	28 (77.8)	7 (58.3)	
Duct dilatation			0.039
Yes	10 (27.8)	8 (66.7)	
No	26 (72.2)	4 (33.3)	
Solid component/mural nodule			0.039
Yes	10 (27.8)	8 (66.7)	
No	26 (72.2)	4 (33.3)	
Septations			0.867
Yes	16 (44.4)	5 (41.7)	
No	20 (55.6)	7 (58.3)	
Calcification			0.851
Yes	9 (25)	4 (33.3)	
No	27 (75)	8 (66.7)	

Significant *P* in bold. Data presented in parentheses represent percentages. CA19-9: Carbohydrate antigen 19-9.

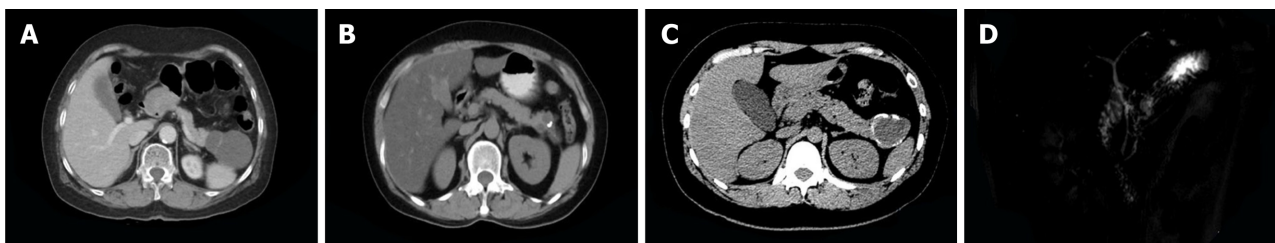
statistically significant ($P < 0.001$) (Figure 4).

DISCUSSION

The advancements and widespread use of imaging technology have led to an apparent rise in the prevalence of PCLs[1]. PCLs encompass both neoplastic and nonneoplastic lesions, with pancreatic cystic neoplasms (PCNs) representing a substantial subset. PCNs comprise serous cystic neoplasms (SCNs), solid pseudopapillary neoplasms (SPNs), IPMNs and mucinous cystic neoplasms. SCNs and SPNs are nearly benign and low-grade malignant tumours, respectively. IPMNs and MCNs, also known as pancreatic mucinous neoplasms, produce viscid mucin and have the potential to progress to PDAC. Notably, they are easier to detect by preoperative imaging than Pan IN due to the particular hypodensity of the cystic tumour.

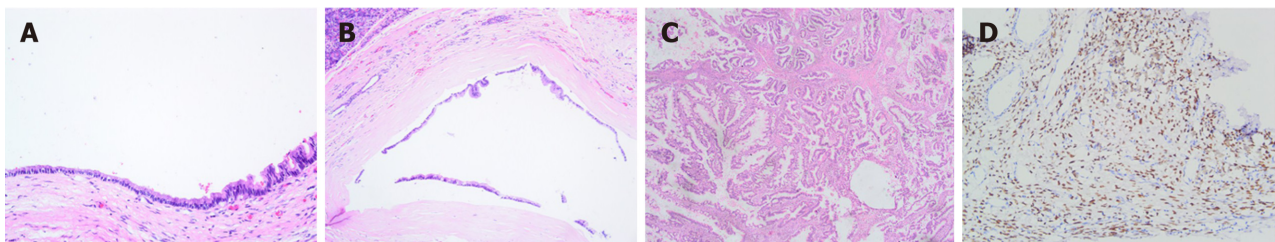
Table 2 Characteristics of 11 patients with mucinous cystic neoplasm/associated invasive carcinoma

Case	Age (yr)	Sex	Tumor size (cm)	Largest dimension (cm)	Invasion pattern	pT stage	pTNM stage	Status	Overall survival (mo)	Adjuvant chemotherapy
1	72	Female	8.0	3.0	Extracapsular	T2	IB	Death	8	Yes
2	60	Male	14.0	1.2	Extracapsular	T1	IA	Death	14	Yes
3	57	Male	7.2	4.0	Extracapsular	T2	IB	Death	46	No
4	64	Female	5.0	< 0.1	Encapsulated	T1	IA	Alive	56	Yes
5	56	Male	6.4	2.0	Encapsulated	T1	IA	Alive	53	Yes
6	43	Female	5.0	< 0.1	Encapsulated	T1	IA	Alive	38	No
7	52	Female	4.5	3.0	Encapsulated	T2	IB	Alive	47	No
8	28	Male	11.0	2.0	Encapsulated	T1	IA	Alive	104	Yes
9	34	Female	3.0	< 0.2	Encapsulated	T1	IA	Alive	75	No
10	45	Male	4.0	1.5	Encapsulated	T1	IA	Alive	24	No
11	63	Female	6.0	< 0.2	Encapsulated	T1	IA	Alive	94	Yes



DOI: 10.3748/wjg.v29.i20.3119 Copyright ©The Author(s) 2023.

Figure 1 Representative radiographic images showing the mucinous cystic neoplasms. A: Computed tomography (CT) scan showing a cystic neoplasm in the pancreatic tail with a clear boundary and linear separation within the lesion; B: CT scan showing multilocular cysts with a slightly high-density solid component, thickened septa, and punctate calcifications; C: CT scan showing a cyst with a slightly thickened cyst wall and multiple calcification foci; D: Magnetic resonance cholangiopancreatography showing mixed signals of the mass and the dilatation of the nearby pancreatic duct.



DOI: 10.3748/wjg.v29.i20.3119 Copyright ©The Author(s) 2023.

Figure 2 Representative micrographs showing the mucinous cystic neoplasm. A: The epithelium exhibits mild to moderate cellular and structural dysplasia, and there is subepithelial ovarian-type stroma (OTS), haematoxylin-eosin staining (H&E) × 200; B: The epithelium demonstrates papillary hyperplasia with some cells shedding into the lumen, and the stroma is partially replaced by fibrous collagen, H&E × 100; C: MCN-associated invasive carcinoma extended into the adjacent pancreatic tissue, and the epithelium exhibited severe dysplasia, H&E × 100; D: The OTS was positive for PR-staining, EnVision × 200.

Compagno and Oertel[8] initially distinguished MCN from SCN in 1978, citing its higher potential for malignancy. However, confusion between IPMNs and MCNs persisted until the International Association of Pancreatology designated OTS as the diagnostic criterion for MCN in 2006[9]. Earlier reports on MCNs inevitably included IPMN cases, leading to a high reported incidence of malignant transformation ranging from 6% to 39% over the last few decades[10-13]. In our sample, 25% of MCN cases were malignant, a rate nearly consistent with the findings of Höhn *et al*[14]. Loss of OTS was reported after the malignant transformation of MCNs[15]. In our study, although some cases showed this particular phenomenon following malignant transformation, with replacement by interstitial fibrous collagen, the remaining OTS was still visible. Once OTS cannot be recognized, detection of positive PR is recommended for a definitive diagnosis[16]. All cases in our study exhibited positive

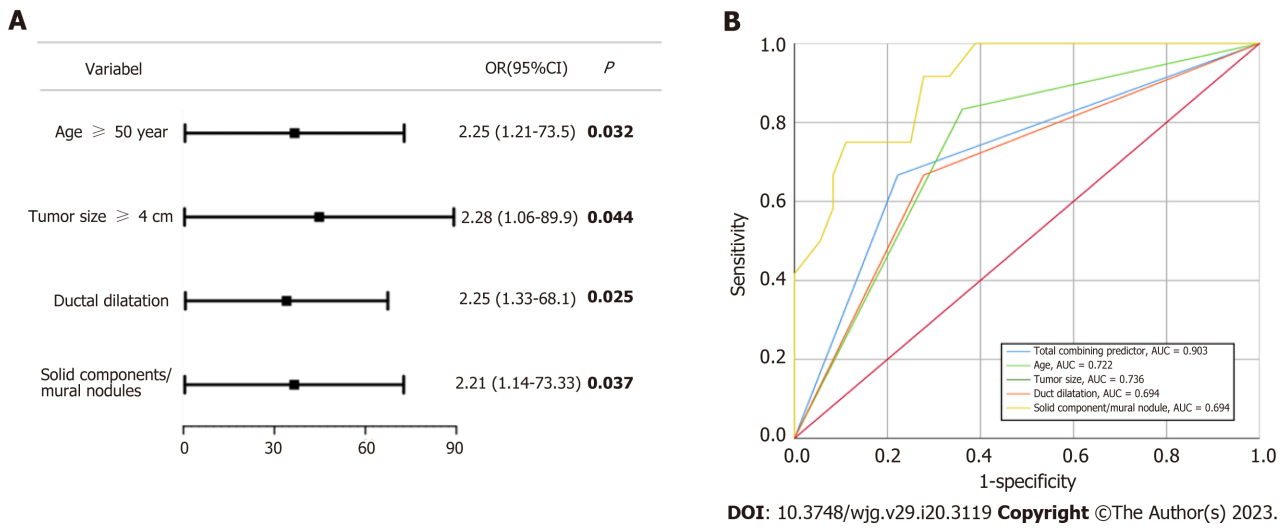


Figure 3 Risk factors of malignant mucinous cystic neoplasm. A: Binary logistic regression analysis of preoperative risk factors for malignancy; B: Receiver operating characteristic curve analysis of the combined predictors and individual indicators. 95%CI: 95% confidence interval; AUC: Area under the curve.

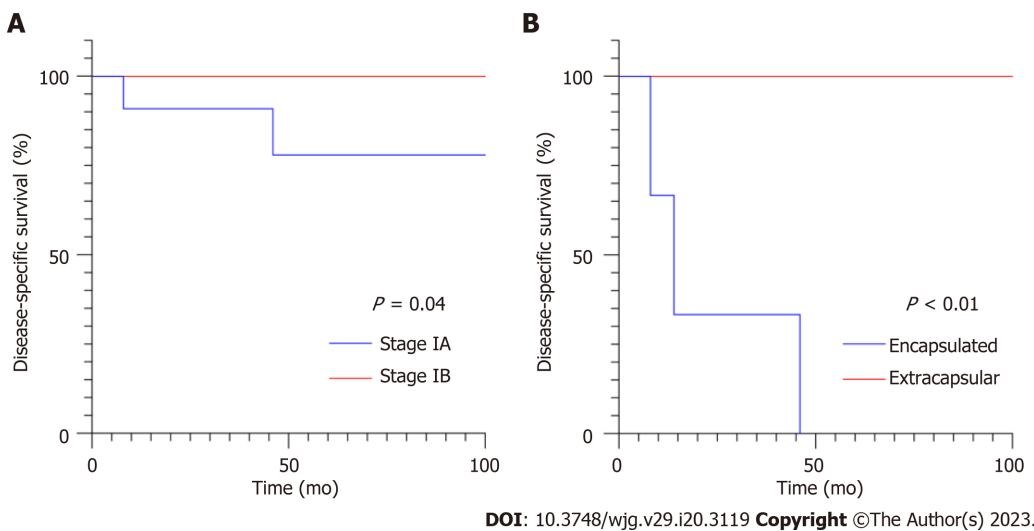


Figure 4 Prognostic factors for mucinous cystic neoplasm with associated invasive carcinoma. A: There was no significant difference in prognosis between stage IA and stage IB mucinous cystic neoplasm with associated invasive carcinoma (MCN-AIC) ($P = 0.400$); B: Encapsulated MCN-AIC is associated with a significantly better prognosis ($P < 0.001$).

staining, ensuring accurate diagnosis.

Currently, there are no reliable preoperative variables that can be used to accurately predict the malignant potential of PCNs.

As one of the most frequently utilized preoperative assessment modalities, imaging has garnered considerable attention in the field of radiomics research for identifying certain subtypes of PCNs and stratifying the risk of IPMNs[17]. Conversely, MCNs have received far less attention than IPMNs, mainly owing to their less substantial incidence and malignancy rate. The management criteria for MCNs remain ambiguous and differ from those of IPMNs. Due to the inability to accurately predict the malignant potential of MCNs through preoperative inspection, it was formerly recommended that all MCNs amenable to surgery be removed regardless of lesion size[13]. Fortunately, the latest guidelines recommend monitoring for eligible MCNs[4,18], although the inclusion criteria are similar to those for IPMNs. This parallelism with IPMN criteria may warrant further consideration. A substantial proportion of patients diagnosed with pancreatic mucinous cysts prior to surgery are subsequently found to have benign disease and do not need surgery[19], highlighting the need for improved identification of those cases with malignant potential. Therefore, given the limitations of current risk stratification schemes in predicting malignant transformation of MCNs, further investigation regarding potential risk factors is essential. While a variety of clinicopathological features and imaging findings have been proposed as potential risk factors for malignancy, their importance remains controversial across different studies[12,14,20-23]. In addition to the variables included in current guidelines, such as

tumour size, wall nodule, and duct dilation, other factors, including sex, location, wall thickening/enhancement, weight, and serum CA19-9 Level, have also been reported to be relevant. Our own research identified age, tumour size, solid component or mural nodule, and duct dilation as independent risk indicators.

To the best of our knowledge, age has not been widely recognized in the literature as a significant risk factor for malignant transformation of MCNs. The mean ages of patients with benign and malignant MCNs were 45.2 years \pm 12.7 years and 52.2 years \pm 13.4 years, respectively, which were comparable to those previously described in the literature[24]. Age has been shown to be related to malignancy in a cohort of pancreatic mucinous neoplasms[25]. Crippa *et al*[12] suggested that age was statistically significant in univariate analysis but did not emerge as a significant factor in multivariate analysis for malignant MCNs. Whether age is an independent risk factor for malignant MCNs needs further study. The occurrence of malignant MCNs appears to increase with age and seems to represent a dynamic pathological transition from adenoma to adenocarcinoma over time.

The average diameter of MCN masses in our investigation was found to be 5.8 cm, which is consistent with the previously reported average diameter of 6-11 cm. It has been emphasized that MCNs should be stratified into surveillance and surgery groups based on a diameter threshold of 4.0 cm, as stated in current guidelines[18]. Tumour size \geq 4 cm was confirmed to be an independent risk for malignant MCNs in our study. In our research, we further identified that the presence of a solid component or mural nodule in MCNs is an independent risk factor for malignancy; it even ranks first in the likelihood of malignancy in certain studies[23]. The combination of solid component or mural nodule and tumour size has been utilized as a tool for identifying malignancy in some studies. In one cohort, it was reported that all malignant MCNs were either larger than 4 cm in diameter or had nodules[12]. Consistent with this, guidelines recommend surgical intervention for MCNs larger than 4 cm in diameter or for those with a mural nodule.

The majority of patients with MCNs are typically asymptomatic. In our analysis, while the percentage of malignant patients with clinical symptoms was higher than that of benign patients, the difference was not statistically significant. The relationship between clinical symptoms and malignancy in MCNs is still debatable[14,25], although surgical excision is advised if symptoms are present[18]. During follow-up, the increase in mass size can often result in nonspecific mass-related clinical complaints. In one case from our cohort, surgical intervention was advised after the tumour became larger than 4 cm and clinical symptoms appeared in the sixth year of imaging surveillance.

Unlike IPMNs, MCNs typically do not communicate with the pancreatic duct, which is one of their distinguishing features. Duct dilatation is a high-risk factor for malignant transformation in IPMNs, with dilatation greater than 10 mm being an unequivocal indication for surgery[18,26]. Similarly, our study found that pancreatic duct dilatation is a concerning imaging finding in MCNs, as verified by other investigations[23].

The management of malignant pancreatic tumours is predominantly centred on postoperative follow-up, whereas the management of MCNs places greater emphasis on the potential risks associated with preoperative monitoring and misdiagnosis. The management plan for IPMN is relatively mature, considering that dedicated management guidelines for IPMN have been published[1]. However, despite MCN being a precursor lesion of pancreatic cancer, similar to IPMN, the management plan for MCN remains unclear, particularly in identifying high-risk factors. Although the risk factors and surgical indications for IPMN and MCN are not differentiated in some guidelines[4], the demographic, cystic, histological and other characteristics of these two tumours differ, so they should be managed differently, particularly with respect to exploring risk factors. Unfortunately, our findings suggest that the risk factors for malignant MCNs are quite similar to those for IPMNs. The size of the lesion and the presence of solid components/wall nodules have been widely recognized as high-risk factors for malignant transformation of MCNs and IPMNs in various guidelines and publications, including our study. While various other malignant risk factors for MCN reported in the literature are statistically significant, they require further confirmation. In the case of IPMNs, the characteristic risk factor is main pancreatic duct dilation, especially when the diameter exceeds 10 mm, given that IPMNs grow within the pancreatic ducts. However, MCNs lack their own characteristic risk factors. Based on their relationship with the pancreatic ducts, IPMNs are classified into the main duct type, mixed duct type, and branch duct type, and direct surgical resection is recommended for the first two types due to a high risk of malignant transformation[18]. However, immediate surgical intervention for MCNs with risk factors remains controversial. Höhn *et al*[14] conducted a retrospective analysis exploring the risk factors for malignant transformation of MCNs, similar to our own analysis. They recommended radical resection surgery for all eligible patients suspected of having MCNs due to concerns about the potential risk of malignant progression and the level of expertise of pancreatic surgeons in low-volume centres. However, this view seems too radical, and the decision for MCN patients to undergo surgery should be more cautious, as the incidence and malignant transformation rate of MCNs are much lower than those of IPMNs[27]. The main argument for surgical resection in all MCN patients based on eliminating the risk of future malignancy seems invalid. It is essential to increase awareness and continuously conduct research on this rare tumour, especially in terms of preoperative malignant risk factors. Based on the above premise, a multidisciplinary team with expertise in pancreatic cysts and surgery can combine various reported risk factors, patient comorbidities, surgery-related complications, and mortality rates

to comprehensively evaluate the potential risks and benefits of surgery and monitoring, thereby making the best treatment decision for the patient.

In addition, preoperative imaging evaluation of various risk indicators for MCNs seems to require the use of different modalities. No single test can accurately diagnose all cases, and in fact, most patients undergo more than one diagnostic procedure[28]. Therefore, the comprehensive use of different detection methods is more conducive to preoperative diagnosis. In our study, this may be attributed to the preference of imaging doctors at our hospital. CT is the preferred initial test for patients undergoing physical examination or with symptoms, and if the CT results are inconclusive or require further confirmation, MRI or EUS will be performed. Unfortunately, there was no significant difference between these three detection methods in our study; nevertheless, combining CT with MRI/EUS increased the preoperative diagnosis rate of our patients from 64.4% to 72.9%. A review of the literature suggests that MRI has slightly higher accuracy in distinguishing between malignant PCNs and benign lesions than CT[29]. MRI was found to be more effective than EUS in distinguishing malignant MCNs [30]. CT combined with MRI was shown to be better than CT alone in the preoperative diagnosis of pancreatic cysts[31]. Moreover, patients with MCNs who have a certain risk of malignant transformation need long-term monitoring or even lifelong monitoring until surgery is no longer a suitable treatment option. For long-term follow-up of MCNs, MRI is the preferred method[18]. This may be because MRI has high contrast resolution and does not involve the use of radiation, which may increase the risk of developing malignant tumours in patients with long-term exposure to CT. EUS is an invasive procedure that highly depends on the operator's skills, especially when combined with aspiration for cyst fluid analysis. EUS is recommended for cysts with significant risk characteristics or when a more accurate diagnosis may change the patient's treatment plan[32].

Complete surgical resection of noninvasive MCNs is a curable treatment, resulting in a 5-year disease-specific survival rate of 100%, as previously reported[33], indicating that postoperative surveillance may not be necessary. As in PDAC patients, prognosis in cases of MCN-AIC was formerly believed to be dismal[34]. However, a series of recent studies have shown that the tumour behaviour and biological characteristics of MCN-AIC are entirely distinct from those of PDAC[23,35,36]. MCN-AIC is often diagnosed at an early stage, and surgical resection is the primary treatment. A study based on SEER research data showed that early-stage MCN-AIC (stage I-II) accounted for 82.9% of cases[37]. All 12 MCN-AIC cases in our study were at stage I, and the 5-year disease-specific survival rate was 70.1%, which was higher than the range of 20%-60% reported in previous literature[12,13,38]. Currently, there is a paucity of studies in which the biological behaviour of invasive MCNs is explored. Previous research indicates that patients with early-stage tumours (stages I and II) have better survival rates than those with high-grade tumours (stages III and IV)[37]. The prognostic variables for patients with MCN-AIC, such as pT grade and capsular invasion, have gained considerable attention. In PDAC, stage I is divided into stages IA and IB, which correspond to stages T1 and T2, respectively, without lymph node metastases and distant metastases[6]. A large cohort study has shown that the survival rate of patients with stage IA PDAC is much higher than that of patients with stage IB PDAC[39]. However, survival disparities between stage IA and IB invasive PDAC derived from MCN-AIC are rarely observed. Our findings, consistent with those of another study[7], demonstrate that there is no significant difference between the two stages. The invasion pattern of the capsule may provide a more accurate prediction of prognosis in MCN-AIC patients than stage classification. The notion of encapsulated invasion is not included in the MCN-AIC classification and guidelines, and the terminology varies somewhat across various research efforts. We adopted the term from the most recent publication[7]. The results of multiple studies have demonstrated that the prognosis is favourable when the invasion is confined to the capsule, and patients with encapsulated invasion exhibit a better survival rate than those with extracapsular invasion. Recurrence has been reported in one of sixteen cases of MCN-AIC confined to the OTS, and the probability of widespread invasion cannot be ruled out because of the minimal quantity of tumour sampled in this case[35]. It has been claimed that encapsulated MCN-AIC has a tumour-free survival rate that is comparable to that of noninvasive MCNs[7]. Our findings revealed that all patients with encapsulated invasion survived, while those with extracapsular invasion died regardless of whether MCN-AIC was stage IA or stage IB. It is recommended that MCN-AIC patients undergo standardized surveillance based on pancreatic cancer guidelines for 5 years after surgery[4]. During monitoring for stage I MCN-AIC, it seems that patients with extracapsular infiltration should be prioritized.

For patients with resected pancreatic cancer, the current standard of care mandates the administration of either a modified FOLFIRINOX (mFOLFIRINOX) or a gemcitabine-based regimen, provided that no contraindications are present[40]. However, limited research has been conducted on the benefits and risks of adjuvant treatment for stage I PDAC, which represents a small proportion of all resectable cases[41]. A study based on the NCDB database indicated that none of the patients with stage IA PDAC had to receive adjuvant treatment following resection, as the side effects and economic costs substantially outweighed the benefits[42]. Despite inadequate data to support this approach, current guidelines advocate adjuvant treatment for MCN-AIC patients comparable to that for patients with PDAC[18]. The role of adjuvant treatment in treating MCN-AIC patients after surgery, particularly for stage I tumours, remains unclear. Two of three patients with stage IA MCN-AIC did not receive adjuvant treatment after surgery, and none of them experienced disease recurrence or death[43]. Of the patients with tumours

who did not receive adjuvant therapy, seven recovered from stage IA and 1 died from stage IB MCN-AIC[7]. These reported cases could be defined as “encapsulated invasion” based on the definition. Patients with stage IA MCN-AIC (T1a and T1b) seem to have the same favourable prognosis as those with LGD or HGD, particularly in the absence of extracapsular invasion. In our research, three IA patients and one IB patient with tumours confined to the capsule did not receive adjuvant treatment and survived, while those with extracapsular infiltration died regardless of whether adjuvant therapy was offered. Diligent monitoring might be preferred over intensive systemic therapy for stage I MCN-AIC with encapsulated invasion.

MCNs are known to harbour gene mutations associated with PDAC, as they are precursor lesions of cancer[17]. However, the genetic pathways underlying IPMNs and MCNs are distinct from one another. The most prevalent and early genetic event in IPMN and MCN carcinogenesis is the *KRAS* mutation [44], which is present in 30% of MCNs, whereas the *GNAS* mutation is almost nonexistent[45,46]. In contrast, the combined detection of *KRAS* and *GNAS* mutations exhibits 100% sensitivity for IPMNs [46]. The decreased frequency of genetic mutations in MCNs compared to IPMNs partly explains why MCNs have a lower probability of malignant transformation. Other mutations, including *TP53*, *PIK3CA*, *PTEN*, *CDKN2A*, and *SMAD4*, have also been described in MCNs but only in advanced stages[47,48]. *KRAS* mutation could be detected in all phases of MCNs and increased with the degree of dysplasia. Sawai *et al*[49] discovered *KRAS* mutations in 19% of LGD and 100% of HGD cases, whereas *TP53* and *CDKN2A* mutations were exclusively observed only in HGD cases. Gene sequencing may aid in the early identification and tailored treatment of MCNs.

This study was subject to several limitations. First, it was a retrospective study that only included patients who underwent surgical resection and were pathologically confirmed to have MCNs, which may result in selection bias. Second, the rarity of MCNs limited the sample size, leading to a large confidence interval that may have hindered statistical analysis. Third, the MRI/EUS results were based on previous CT information, potentially affecting the interpretation of imaging results. Therefore, further multicentre and large-scale studies are needed to explore the clinical, pathological, imaging, and biological behaviours of MCNs.

CONCLUSION

In conclusion, this study involved analysing data from 48 patients who underwent complete resection of MCNs. The incidence of malignant MCNs was low, and the specific risk factors for malignancy were age, tumour size, presence of solid components or mural nodules, and duct dilatation. The prognosis of stage I MCN-AIC was closely related to encapsulated invasion, and complete surgical excision alone or in combination with postoperative treatment may be a viable option for invasive masses confined within the capsule.

ARTICLE HIGHLIGHTS

Research background

Mucinous cystic neoplasms (MCNs) are recognized as precursor lesions of pancreatic cancer. Despite their rarity, the detection of MCNs is on the rise due to advancements in preoperative imaging techniques. Thus, there is a pressing need to increase our knowledge of MCNs to ensure that patients receive the most appropriate treatment decisions.

Research motivation

An inadequate understanding of MCNs can hinder the treatment of patients, underscoring the importance of research on MCNs.

Research objectives

To investigate the risk factors for malignancy in MCNs and the prognostic factors associated with MCN-associated invasive carcinoma (MCN-AIC) to advance our comprehension of this uncommon tumour.

Research methods

This study involved a retrospective analysis of clinical and pathological data, imaging records, and outcomes of patients diagnosed with MCNs at our research centre over a 10-year period. We then investigated the risk factors for malignancy in MCNs and the prognostic factors associated with MCN-AIC.

Research results

A total of 48 patients with MCNs, accounting for 2.8% of pancreatic lesions resected during the study

period, were included in this study. Among these patients, 36 had benign MCNs, while 12 had malignant MCNs. We conducted a comparative analysis of clinical and imaging features and discovered that age, tumour size, solid components or wall nodules, and pancreatic duct dilation were significantly associated with malignancy. Subsequently, we performed a prognostic analysis of malignant MCNs and observed that all malignant MCNs in our study were at stage I, and extracapsular invasion was identified as a significant prognostic factor for poor outcomes.

Research conclusions

Age, tumour size, solid components or wall nodules, and pancreatic duct dilation were independent risk factors associated with malignancy in MCN. In addition, extracapsular invasion was indicative of poor prognosis of MCN-AIC.

Research perspectives

The aim of this study was to enhance the management of MCN, a rare disease, by utilizing patient information from our research centre and conducting research from both preoperative and postoperative perspectives. We hope that this study can provide valuable insights into the management of MCNs.

ACKNOWLEDGEMENTS

We would like to thank Dr. Xian-Jie Jia for significant contributions to data analysis.

FOOTNOTES

Author contributions: Xia Q collected the clinical data and prepared the manuscript; Xia Q and Li F designed the study and supervised the statistical data; Xia Q and Min R designed the research and contributed to the analyses; Sun S, Han YX, and Feng ZZ provided clinical advice; Li N made the pathologic diagnosis and supervised the report; and all authors read and approved the final version.

Supported by the Natural Science Key Project in Universities of Anhui Province, No. KJ2021A0701; Natural Science Key Project of Bengbu Medical College, No. 2020byzd030; and Postgraduate Scientific Research Innovation Program of the Bengbu Medical College, No. Byycx22016.

Institutional review board statement: This study was reviewed and approved by the Ethics Committee of the First Affiliated Hospital of Bengbu Medical College (approval No. 2021085).

Informed consent statement: All study participants, or their legal guardian, provided informed written consent prior to study enrollment.

Conflict-of-interest statement: We have no financial relationships to disclose.

Data sharing statement: No additional data are available.

Open-Access: This article is an open-access article that was selected by an in-house editor and fully peer-reviewed by external reviewers. It is distributed in accordance with the Creative Commons Attribution NonCommercial (CC BY-NC 4.0) license, which permits others to distribute, remix, adapt, build upon this work non-commercially, and license their derivative works on different terms, provided the original work is properly cited and the use is non-commercial. See: <https://creativecommons.org/licenses/by-nc/4.0/>

Country/Territory of origin: China

ORCID number: Qing Xia 0009-0009-9528-5347; Fan Li 0009-0009-0410-963X; Rui Min 0000-0003-3835-1167; Shuai Sun 0000-0001-5838-9424; Yue-Xin Han 0000-0002-2111-7430; Zhen-Zhong Feng 0000-0002-9610-495X; Nan Li 0000-0002-5622-4252.

S-Editor: Chen YL

L-Editor: A

P-Editor: Zhang YL

REFERENCES

- 1 **Tanaka M**, Fernández-Del Castillo C, Kamisawa T, Jang JY, Levy P, Ohtsuka T, Salvia R, Shimizu Y, Tada M, Wolfgang CL. Revisions of international consensus Fukuoka guidelines for the management of IPMN of the pancreas. *Pancreatology* 2017; **17**: 738-753 [PMID: 28735806 DOI: 10.1016/j.pan.2017.07.007]
- 2 **Ketwaroo GA**, Mortelet KJ, Sawhney MS. Pancreatic Cystic Neoplasms: An Update. *Gastroenterol Clin North Am* 2016; **45**: 67-81 [PMID: 26895681 DOI: 10.1016/j.gtc.2015.10.006]
- 3 **Klein AP**. Pancreatic cancer epidemiology: understanding the role of lifestyle and inherited risk factors. *Nat Rev Gastroenterol Hepatol* 2021; **18**: 493-502 [PMID: 34002083 DOI: 10.1038/s41575-021-00457-x]
- 4 **Elta GH**, Enestvedt BK, Sauer BG, Lennon AM. ACG Clinical Guideline: Diagnosis and Management of Pancreatic Cysts. *Am J Gastroenterol* 2018; **113**: 464-479 [PMID: 29485131 DOI: 10.1038/ajg.2018.14]
- 5 **Nagtegaal ID**, Odze RD, Klimstra D, Paradis V, Rugge M, Schirmacher P, Washington KM, Carneiro F, Cree IA; WHO Classification of Tumours Editorial Board. The 2019 WHO classification of tumours of the digestive system. *Histopathology* 2020; **76**: 182-188 [PMID: 31433515 DOI: 10.1111/his.13975]
- 6 **Shi S**, Hua J, Liang C, Meng Q, Liang D, Xu J, Ni Q, Yu X. Proposed Modification of the 8th Edition of the AJCC Staging System for Pancreatic Ductal Adenocarcinoma. *Ann Surg* 2019; **269**: 944-950 [PMID: 29334560 DOI: 10.1097/SLA.0000000000002668]
- 7 **Liang H**, Xie W, Lin X, Wang T, Xie J, Wang C, Xiao SY, Guo Y. Pathologic T1 and T2 encapsulated invasive carcinomas arising from mucinous cystic neoplasms of the pancreas have favorable prognosis and might be treated conservatively. *J Pathol Clin Res* 2021; **7**: 507-516 [PMID: 34062050 DOI: 10.1002/cjp.2.225]
- 8 **Compagno J**, Oertel JE. Microcystic adenomas of the pancreas (glycogen-rich cystadenomas): a clinicopathologic study of 34 cases. *Am J Clin Pathol* 1978; **69**: 289-298 [PMID: 637043 DOI: 10.1093/ajcp/69.1.289]
- 9 **Tanaka M**, Chari S, Adsay V, Fernandez-del Castillo C, Falconi M, Shimizu M, Yamaguchi K, Yamao K, Matsuno S; International Association of Pancreatology. International consensus guidelines for management of intraductal papillary mucinous neoplasms and mucinous cystic neoplasms of the pancreas. *Pancreatology* 2006; **6**: 17-32 [PMID: 16327281 DOI: 10.1159/000090023]
- 10 **Suzuki Y**, Atomi Y, Sugiyama M, Isaji S, Inui K, Kimura W, Sunamura M, Furukawa T, Yanagisawa A, Ariyama J, Takada T, Watanabe H, Suda K; Japanese multiinstitutional study of intraductal papillary mucinous tumor and mucinous cystic tumor. Cystic neoplasm of the pancreas: a Japanese multiinstitutional study of intraductal papillary mucinous tumor and mucinous cystic tumor. *Pancreas* 2004; **28**: 241-246 [PMID: 15084964 DOI: 10.1097/00006676-200404000-00005]
- 11 **Yamao K**, Yanagisawa A, Takahashi K, Kimura W, Doi R, Fukushima N, Ohike N, Shimizu M, Hatori T, Nobukawa B, Hifumi M, Kobayashi Y, Tobita K, Tanno S, Sugiyama M, Miyasaka Y, Nakagohri T, Yamaguchi T, Hanada K, Abe H, Tada M, Fujita N, Tanaka M. Clinicopathological features and prognosis of mucinous cystic neoplasm with ovarian-type stroma: a multi-institutional study of the Japan pancreas society. *Pancreas* 2011; **40**: 67-71 [PMID: 20924309 DOI: 10.1097/MPA.0b013e3181f749d3]
- 12 **Crippa S**, Salvia R, Warshaw AL, Domínguez I, Bassi C, Falconi M, Thayer SP, Zamboni G, Lauwers GY, Mino-Kenudson M, Capelli P, Pederzoli P, Castillo CF. Mucinous cystic neoplasm of the pancreas is not an aggressive entity: lessons from 163 resected patients. *Ann Surg* 2008; **247**: 571-579 [PMID: 18362619 DOI: 10.1097/SLA.0b013e31811f4449]
- 13 **Testini M**, Gurrado A, Lissidini G, Venezia P, Greco L, Piccinni G. Management of mucinous cystic neoplasms of the pancreas. *World J Gastroenterol* 2010; **16**: 5682-5692 [PMID: 21128317 DOI: 10.3748/wjg.v16.i45.5682]
- 14 **Höhn P**, Soydemir MA, Luu AM, Janot-Matuschek M, Tannapfel A, Uhl W, Belyaev O. It's not all about the size—characteristics and risk factors for malignancy of mucinous cystic neoplasms of the pancreas. *Ann Transl Med* 2020; **8**: 1572-1572 [DOI: 10.21037/atm-20-4774]
- 15 **Lam MM**, Swanson PE, Upton MP, Yeh MM. Ovarian-type stroma in hepatobiliary cystadenomas and pancreatic mucinous cystic neoplasms: an immunohistochemical study. *Am J Clin Pathol* 2008; **129**: 211-218 [PMID: 18208800 DOI: 10.1309/U2BBP4EMBAHCM6E6]
- 16 **Izumo A**, Yamaguchi K, Eguchi T, Nishiyama K, Yamamoto H, Yonemasu H, Yao T, Tanaka M, Tsuneyoshi M. Mucinous cystic tumor of the pancreas: immunohistochemical assessment of "ovarian-type stroma". *Oncol Rep* 2003; **10**: 515-525 [PMID: 12684617]
- 17 **Ardeshna DR**, Cao T, Rodgers B, Onongaya C, Jones D, Chen W, Koay EJ, Krishna SG. Recent advances in the diagnostic evaluation of pancreatic cystic lesions. *World J Gastroenterol* 2022; **28**: 624-634 [PMID: 35317424 DOI: 10.3748/wjg.v28.i6.624]
- 18 **The European Study Group on Cystic Tumours of the Pancreas**. European evidence-based guidelines on pancreatic cystic neoplasms. *Gut* 2018; **67**: 789-804 [DOI: 10.1136/gutjnl-2018-316027]
- 19 **Valsangkar NP**, Morales-Oyarvide V, Thayer SP, Ferrone CR, Wargo JA, Warshaw AL, Fernández-del Castillo C. 851 resected cystic tumors of the pancreas: a 33-year experience at the Massachusetts General Hospital. *Surgery* 2012; **152**: S4-12 [PMID: 22770958 DOI: 10.1016/j.surg.2012.05.033]
- 20 **Chang YT**, Tien YW, Jeng YM, Yang CY, Liang PC, Wong JM, Chang MC. Overweight increases the risk of malignancy in patients with pancreatic mucinous cystic neoplasms. *Medicine (Baltimore)* 2015; **94**: e797 [PMID: 25997051 DOI: 10.1097/MD.0000000000000797]
- 21 **Jang KT**, Park SM, Basturk O, Bagci P, Bandyopadhyay S, Stelow EB, Walters DM, Choi DW, Choi SH, Heo JS, Sarmiento JM, Reid MD, Adsay V. Clinicopathologic characteristics of 29 invasive carcinomas arising in 178 pancreatic mucinous cystic neoplasms with ovarian-type stroma: implications for management and prognosis. *Am J Surg Pathol* 2015; **39**: 179-187 [PMID: 25517958 DOI: 10.1097/PAS.0000000000000357]
- 22 **Kim GH**, Choi K, Paik N, Lee KT, Lee JK, Lee KH, Han IW, Kang SH, Heo JS, Park JK. Diagnostic Concordance and Preoperative Risk Factors for Malignancy in Pancreatic Mucinous Cystic Neoplasms. *Gut Liver* 2022; **16**: 637-644 [PMID: 34933278 DOI: 10.5009/gnl210231]
- 23 **Postlewait LM**, Ethun CG, McInnis MR, Merchant N, Parikh A, Idrees K, Isom CA, Hawkins W, Fields RC, Strand M,

- Weber SM, Cho CS, Salem A, Martin RC, Scoggins C, Bentrem D, Kim HJ, Carr J, Ahmad S, Abbott DE, Wilson GC, Kooby DA, Maithel SK. Association of Preoperative Risk Factors With Malignancy in Pancreatic Mucinous Cystic Neoplasms: A Multicenter Study. *JAMA Surg* 2017; **152**: 19-25 [PMID: 27760255 DOI: 10.1001/jamasurg.2016.3598]
- 24 **Riva G**, Pea A, Pilati C, Fiadone G, Lawlor RT, Scarpa A, Luchini C. Histo-molecular oncogenesis of pancreatic cancer: From precancerous lesions to invasive ductal adenocarcinoma. *World J Gastrointest Oncol* 2018; **10**: 317-327 [PMID: 30364837 DOI: 10.4251/wjgo.v10.i10.317]
- 25 **Lee CJ**, Scheiman J, Anderson MA, Hines OJ, Reber HA, Farrell J, Kochman ML, Foley PJ, Drebin J, Oh YS, Ginsberg G, Ahmad N, Merchant NB, Isbell J, Parikh AA, Stokes JB, Bauer T, Adams RB, Simeone DM. Risk of malignancy in resected cystic tumors of the pancreas ≤ 3 cm in size: is it safe to observe asymptomatic patients? A multi-institutional report. *J Gastrointest Surg* 2008; **12**: 234-242 [PMID: 18040749 DOI: 10.1007/s11605-007-0381-y]
- 26 **Megibow AJ**, Baker ME, Morgan DE, Kamel IR, Sahani DV, Newman E, Brugge WR, Berland LL, Pandharipande PV. Management of Incidental Pancreatic Cysts: A White Paper of the ACR Incidental Findings Committee. *J Am Coll Radiol* 2017; **14**: 911-923 [DOI: 10.1016/j.jacr.2017.03.010]
- 27 **Stark A**, Donahue TR, Reber HA, Hines OJ. Pancreatic Cyst Disease: A Review. *JAMA* 2016; **315**: 1882-1893 [PMID: 27139061 DOI: 10.1001/jama.2016.4690]
- 28 **Del Chiaro M**, Segersvärd R, Pozzi Mucelli R, Rangelova E, Kartalis N, Ansoorge C, Arnelo U, Blomberg J, Löhr M, Verbeke C. Comparison of preoperative conference-based diagnosis with histology of cystic tumors of the pancreas. *Ann Surg Oncol* 2014; **21**: 1539-1544 [PMID: 24385209 DOI: 10.1245/s10434-013-3465-9]
- 29 **Mohamed E**, Jackson R, Halloran CM, Ghaneh P. Role of Radiological Imaging in the Diagnosis and Characterization of Pancreatic Cystic Lesions: A Systematic Review. *Pancreas* 2018; **47**: 1055-1064 [PMID: 30199486 DOI: 10.1097/MPA.0000000000001134]
- 30 **Hwang J**, Kim YK, Min JH, Jeong WK, Hong SS, Kim HJ. Comparison between MRI with MR cholangiopancreatography and endoscopic ultrasonography for differentiating malignant from benign mucinous neoplasms of the pancreas. *Eur Radiol* 2018; **28**: 179-187 [PMID: 28779397 DOI: 10.1007/s00330-017-4926-5]
- 31 **Jang DK**, Song BJ, Ryu JK, Chung KH, Lee BS, Park JK, Lee SH, Kim YT, Lee JY. Preoperative Diagnosis of Pancreatic Cystic Lesions: The Accuracy of Endoscopic Ultrasound and Cross-Sectional Imaging. *Pancreas* 2015; **44**: 1329-1333 [PMID: 26465956 DOI: 10.1097/MPA.0000000000000396]
- 32 **van Huijgevoort NCM**, Del Chiaro M, Wolfgang CL, van Hooft JE, Besselink MG. Diagnosis and management of pancreatic cystic neoplasms: current evidence and guidelines. *Nat Rev Gastroenterol Hepatol* 2019; **16**: 676-689 [PMID: 31527862 DOI: 10.1038/s41575-019-0195-x]
- 33 **Xourafas D**, Tavakkoli A, Clancy TE, Ashley SW. Noninvasive intraductal papillary mucinous neoplasms and mucinous cystic neoplasms: recurrence rates and postoperative imaging follow-up. *Surgery* 2015; **157**: 473-483 [PMID: 25596773 DOI: 10.1016/j.surg.2014.09.028]
- 34 **Sarr MG**, Carpenter HA, Prabhakar LP, Orchard TF, Hughes S, van Heerden JA, DiMaggio EP. Clinical and pathologic correlation of 84 mucinous cystic neoplasms of the pancreas: can one reliably differentiate benign from malignant (or premalignant) neoplasms? *Ann Surg* 2000; **231**: 205-212 [PMID: 10674612 DOI: 10.1097/0000658-200002000-00009]
- 35 **Lewis GH**, Wang H, Bellizzi AM, Klein AP, Askin FB, Schwartz LE, Schulick RD, Wolfgang CL, Cameron JL, O'Reilly EM, Yu KH, Hruban RH. Prognosis of minimally invasive carcinoma arising in mucinous cystic neoplasms of the pancreas. *Am J Surg Pathol* 2013; **37**: 601-605 [PMID: 23388125 DOI: 10.1097/PAS.0b013e318273f3b0]
- 36 **Park JW**, Jang JY, Kang MJ, Kwon W, Chang YR, Kim SW. Mucinous cystic neoplasm of the pancreas: is surgical resection recommended for all surgically fit patients? *Pancreatol* 2014; **14**: 131-136 [PMID: 24650968 DOI: 10.1016/j.pan.2013.12.006]
- 37 **Doulamis IP**, Mylonas KS, Kalifountzos CE, Mou D, Haj-Ibrahim H, Nasioudis D. Pancreatic mucinous cystadenocarcinoma: Epidemiology and outcomes. *Int J Surg* 2016; **35**: 76-82 [PMID: 27638187 DOI: 10.1016/j.ijssu.2016.09.017]
- 38 **Nilsson LN**, Keane MG, Shamali A, Millastre Bocos J, Marijijnissen van Zanten M, Antila A, Verdejo Gil C, Del Chiaro M, Laukkarinen J. Nature and management of pancreatic mucinous cystic neoplasm (MCN): A systematic review of the literature. *Pancreatol* 2016; **16**: 1028-1036 [PMID: 27681503 DOI: 10.1016/j.pan.2016.09.011]
- 39 **Muralidhar V**, Nipp RD, Mamon HJ, Punglia RS, Hong TS, Ferrone C, Fernandez-Del Castillo C, Parikh A, Nguyen PL, Wo JY. Association Between Very Small Tumor Size and Decreased Overall Survival in Node-Positive Pancreatic Cancer. *Ann Surg Oncol* 2018; **25**: 4027-4034 [PMID: 30298331 DOI: 10.1245/s10434-018-6832-8]
- 40 **NCCN**. Pancreatic Adenocarcinoma, Version 2. 2022, NCCN Clinical Practice Guidelines in Oncology. [DOI: 10.1111/j.1759-7714.2010.00016.x]
- 41 **Gong J**, Tuli R, Shinde A, Hendifar AE. Meta-analyses of treatment standards for pancreatic cancer. *Mol Clin Oncol* 2016; **4**: 315-325 [PMID: 26998283 DOI: 10.3892/mco.2015.716]
- 42 **Shaib WL**, Narayan AS, Switchenko JM, Kane SR, Wu C, Akce M, Alese OB, Patel PR, Maithel SK, Sarmiento JM, Kooby DA, El-Rayes BF. Role of adjuvant therapy in resected stage IA subcentimeter (T1a/T1b) pancreatic cancer. *Cancer* 2019; **125**: 57-67 [PMID: 30457666 DOI: 10.1002/cncr.31787]
- 43 **Hui L**, Rashid A, Foo WC, Katz MH, Chatterjee D, Wang H, Fleming JB, Tamm EP. Significance of T1a and T1b Carcinoma Arising in Mucinous Cystic Neoplasm of Pancreas. *Am J Surg Pathol* 2018; **42**: 578-586 [PMID: 29462092 DOI: 10.1097/PAS.0000000000001040]
- 44 **Wu J**, Jiao Y, Dal Molin M, Maitra A, de Wilde RF, Wood LD, Eshleman JR, Goggins MG, Wolfgang CL, Canto MI, Schulick RD, Edil BH, Choti MA, Adsay V, Klimstra DS, Offerhaus GJ, Klein AP, Kopelovich L, Carter H, Karchin R, Allen PJ, Schmidt CM, Naito Y, Diaz LA Jr, Kinzler KW, Papadopoulos N, Hruban RH, Vogelstein B. Whole-exome sequencing of neoplastic cysts of the pancreas reveals recurrent mutations in components of ubiquitin-dependent pathways. *Proc Natl Acad Sci U S A* 2011; **108**: 21188-21193 [PMID: 22158988 DOI: 10.1073/pnas.1118046108]
- 45 **Reid MD**, Saka B, Balci S, Goldblum AS, Adsay NV. Molecular genetics of pancreatic neoplasms and their morphologic correlates: an update on recent advances and potential diagnostic applications. *Am J Clin Pathol* 2014; **141**: 168-180 [PMID: 24436263 DOI: 10.1309/AJCP0FKDP7ENVKEV]

- 46 **Singhi AD**, McGrath K, Brand RE, Khalid A, Zeh HJ, Chennat JS, Fasanella KE, Papachristou GI, Slivka A, Bartlett DL, Dasyam AK, Hogg M, Lee KK, Marsh JW, Monaco SE, Ohori NP, Pingpank JF, Tsung A, Zureikat AH, Wald AI, Nikiforova MN. Preoperative next-generation sequencing of pancreatic cyst fluid is highly accurate in cyst classification and detection of advanced neoplasia. *Gut* 2018; **67**: 2131-2141 [PMID: 28970292 DOI: 10.1136/gutjnl-2016-313586]
- 47 **Singhi AD**, Wood LD. Early detection of pancreatic cancer using DNA-based molecular approaches. *Nat Rev Gastroenterol Hepatol* 2021; **18**: 457-468 [PMID: 34099908 DOI: 10.1038/s41575-021-00470-0]
- 48 **Theisen BK**, Wald AI, Singhi AD. Molecular Diagnostics in the Evaluation of Pancreatic Cysts. *Surg Pathol Clin* 2016; **9**: 441-456 [PMID: 27523971 DOI: 10.1016/j.path.2016.04.008]
- 49 **Sawai H**, Kurimoto M, Koide S, Kiriya Y, Haba S, Matsuo Y, Morimoto M, Koide H, Kamiya A, Yamao K. Invasive Ductal Carcinoma Arising in Mucinous Cystic Neoplasm of Pancreas: A Case Report. *Am J Case Rep* 2019; **20**: 242-247 [PMID: 30798329 DOI: 10.12659/AJCR.914092]

Clinical Trials Study

Safety and effectiveness of vonoprazan-based rescue therapy for *Helicobacter pylori* infection

Jing Yu, Yi-Ming Lv, Peng Yang, Yi-Zhou Jiang, Xiang-Rong Qin, Xiao-Yong Wang

Specialty type: Gastroenterology and hepatology**Provenance and peer review:**

Unsolicited article; Externally peer reviewed.

Peer-review model: Single blind**Peer-review report's scientific quality classification**Grade A (Excellent): 0
Grade B (Very good): 0
Grade C (Good): C, C, C
Grade D (Fair): 0
Grade E (Poor): 0**P-Reviewer:** Keikha M, Iran;
Krzyzek P, Poland; Nishida T,
Japan**Received:** February 27, 2023**Peer-review started:** February 27,
2023**First decision:** March 13, 2023**Revised:** March 25, 2023**Accepted:** April 23, 2023**Article in press:** April 23, 2023**Published online:** May 28, 2023**Jing Yu, Yi-Ming Lv, Peng Yang, Yi-Zhou Jiang, Xiang-Rong Qin, Xiao-Yong Wang**, Department of Gastroenterology, The Affiliated Changzhou No. 2 People's Hospital of Nanjing Medical University, Changzhou 213000, Jiangsu Province, China**Corresponding author:** Xiao-Yong Wang, MD, Assistant Professor, Chief Physician, Postdoc, Department of Gastroenterology, The Affiliated Changzhou No. 2 People's Hospital of Nanjing Medical University, No. 29 Xinglong Lane, Tianning District, Changzhou 213000, Jiangsu Province, China. wxy20009@126.com**Abstract****BACKGROUND**Vonoprazan (VPZ)-based regimens are an effective first-line therapy for *Helicobacter pylori* (*H. pylori*) infection. However, their value as a rescue therapy needs to be explored.**AIM**To assess a VPZ-based regimen as *H. pylori* rescue therapy.**METHODS**This prospective, single-center, clinical trial was conducted between January and August 2022. Patients with a history of *H. pylori* treatment failure were administered 20 mg VPZ twice daily, 750 mg amoxicillin 3 times daily, and 250 mg *Saccharomyces boulardii* (*S. boulardii*) twice daily for 14 d (14-d VAS regimen). VPZ and *S. boulardii* were taken before meals, while amoxicillin was taken after meals. Within 3 d after the end of eradication therapy, all patients were asked to fill in a questionnaire to assess any adverse events they may have experienced. At least 4-6 wk after the end of eradication therapy, eradication success was assessed using a ¹³C-urea breath test, and factors associated with eradication success were explored.**RESULTS**Herein, 103 patients were assessed, and 68 patients were finally included. All included patients had 1-3 previous eradication failures. The overall eradication rates calculated using intention-to-treat and per-protocol analyses were 92.6% (63/68) and 92.3% (60/65), respectively. The eradication rate did not differ with the number of treatment failures ($P = 0.433$). The rates of clarithromycin, metronidazole, and levofloxacin resistance were 91.3% (21/23), 100.0% (23/23), and 60.9% (14/23), respectively. There were no cases of resistance to tetracycline,

amoxicillin, or furazolidone. In 60.9% (14/23) patients, the *H. pylori* isolate was resistant to all 3 antibiotics (clarithromycin, metronidazole, and levofloxacin); however, eradication was achieved in 92.9% (13/14) patients. All patients showed metronidazole resistance, and had an eradication rate of 91.3% (21/23). The eradication rate was higher among patients without anxiety (96.8%) than among patients with anxiety (60.0%, $P = 0.025$). No severe adverse events occurred; most adverse events were mild and disappeared without intervention. Good compliance was seen in 95.6% (65/68) patients. Serological examination showed no significant changes in liver and kidney function.

CONCLUSION

VAS is a safe and effective rescue therapy, with an acceptable eradication rate (> 90%), regardless of the number of prior treatment failures. Anxiety may be associated with eradication failure.

Key Words: Vonoprazan; *Saccharomyces boulardii*; Rescue therapy; *Helicobacter pylori*; Eradication; Anxiety

©The Author(s) 2023. Published by Baishideng Publishing Group Inc. All rights reserved.

Core Tip: Vonoprazan (VPZ)-containing triple therapies have been shown to contribute to global antimicrobial resistance, while *Saccharomyces boulardii* (*S. boulardii*) supplementation has significantly improved *Helicobacter pylori* eradication rates and decreased adverse events. This study revealed that the VPZ and amoxicillin dual regimen with *S. boulardii* supplementation is safe and effective *H. pylori* rescue therapy, regardless of the number of prior treatment failures. Acceptable eradication rates (> 90%) were achieved in patients with resistance to clarithromycin, metronidazole, and levofloxacin. However, the regimen may need to be adjusted for patients with anxiety.

Citation: Yu J, Lv YM, Yang P, Jiang YZ, Qin XR, Wang XY. Safety and effectiveness of vonoprazan-based rescue therapy for *Helicobacter pylori* infection. *World J Gastroenterol* 2023; 29(20): 3133-3144

URL: <https://www.wjgnet.com/1007-9327/full/v29/i20/3133.htm>

DOI: <https://dx.doi.org/10.3748/wjg.v29.i20.3133>

INTRODUCTION

Helicobacter pylori (*H. pylori*), which infects over 50% of the global population, is a leading cause of chronic gastritis, peptic ulcer disease, and gastric cancer. The eradication of *H. pylori* can effectively prevent peptic ulcer recurrence and lower gastric cancer incidence[1,2]. In regions with high antibiotic resistance, such as China, 14-d bismuth-containing quadruple therapy (BQT) is the recommended first-line treatment for *H. pylori* infection[3-5]. However, as the rates of resistance to clarithromycin, metronidazole, and levofloxacin have markedly increased worldwide, BQT fails to eradicate *H. pylori* infection in approximately 15%-20% patients[6,7]. Multiple failed attempts at eradication therapy tend to increase the prevalence of multidrug-resistant strains, making rescue treatment more difficult[8,9]. Unlike the above antibiotics, the rates of primary and secondary resistance of *H. pylori* to amoxicillin have remained low and stable[10]. Amoxicillin shows a pH- and time-dependent bactericidal effect. Recently, high-dose, high-frequency dual therapy with amoxicillin and a proton pump inhibitor (PPI) was reported to show promising outcomes when used as a first-line or rescue treatment for the eradication of *H. pylori*[11,12]. The Maastricht VI/Florence Consensus Report recommends high-dose dual therapy with a PPI plus amoxicillin as a rescue therapy for *H. pylori* infection[5].

Vonoprazan (VPZ), the first clinically available potassium-competing acid blocker (P-CAB), produces a more rapid and sustained acid inhibition effect than PPIs[13]. Therefore, VPZ-amoxicillin dual therapy (VA-dual) is expected to be more effective than PPI-amoxicillin dual therapy. In recent years, first-line treatment with VA-dual, consisting of amoxicillin (3 g/d or less) and VPZ (40 mg/d), has been reported to achieve eradication rates of 78.5%-93.5% [14-17]. However, limited reports are available on the success rate of VA-dual as a rescue treatment for *H. pylori* infection; only one retrospective study conducted in China has reported a successful eradication rate of 92.5% after VA-dual[18]. However, the regimens were not consistent, and the frequencies of the amoxicillin and VPZ doses varied. Therefore, further optimization of VA-dual as a rescue treatment is warranted.

Some recent consensus guidelines for the management of *H. pylori* infection have proposed that certain probiotics can effectively decrease the gastrointestinal side effects of *H. pylori* eradication therapies[3-5]. A recent meta-analysis demonstrated that *Saccharomyces boulardii* (*S. boulardii*) supple-

mentation during standard eradication therapy (triple regimen, sequential regimen, or quadruple regimen) significantly improved eradication rates and decreased the overall incidence of adverse events [19]. However, few studies have evaluated the effects of *S. boulardii* as a supplement to the VA-dual regimen in terms of the eradication rate of *H. pylori* and treatment-related adverse events.

Therefore, the aim of this prospective study was to determine the safety and efficacy of VA-dual plus *S. boulardii* supplementation as a rescue treatment for patients with *H. pylori* infection. We additionally explored potential factors influencing eradication rates, and put forward our recommendations to improve *H. pylori* eradication rates in clinical practice.

MATERIALS AND METHODS

Statement of ethics and trial registration

Ethical approval for this pilot study was obtained from Affiliated Changzhou No. 2 People's Hospital of Nanjing Medical University [No. (2021) YLJSD004]. The study adhered to the tenets of the Declaration of Helsinki. Written informed consent was obtained from all patients prior to their enrollment in this study. The study has been registered in the Chinese Clinical Trial Registry (No. ChiCTR2200055125).

Study participants

Patients who attended our center between January and August 2022 were screened for their eligibility to participate in this study. The detailed inclusion criteria were as follows: (1) Patients aged over 18 years; (2) patients with a history of at least one failed *H. pylori* eradication treatment; and (3) a minimum 6-mo interval after the end of the last treatment. The following exclusion criteria were applied: (1) A history of gastric surgery; (2) severe concomitant diseases such as hepatic or renal dysfunction; (3) allergy or contraindication to the drugs used in the study regimen; (4) pregnancy or lactation; (5) treatment with a PPI, bismuth, or an antibiotic within 4 wk before the study treatment; (6) alcohol abuse or drug addiction; and (7) lack of informed consent.

Study design and outcomes

Before enrollment, the patients' demographic data, clinical characteristics, and any concomitant diseases were recorded through medical records and physician interviews. The diagnosis of *H. pylori* infection was based on a positive result of at least one of the following tests: ¹³C-urea breath test (¹³C-UBT), rapid urease test, and histological examination. Some patients also underwent gastroscopy, and *H. pylori* culture and antimicrobial susceptibility testing before treatment. Serum chemistry tests were performed before and after treatment.

All patients were administered VPZ (20 mg twice daily; Takeda Pharmaceutical, Tokyo, Japan), amoxicillin (750 mg 3 times daily; Federal Pharmaceutical, Hong Kong, China), and *S. boulardii* (250 mg twice daily; Laboratoires BIOCDEX, France) for 14 d (14-d VAS regimen). VPZ and *S. boulardii* were taken before meals, while amoxicillin was taken after meals. Patients who felt unwell during treatment or forgot to take their medication were advised to contact the investigators immediately.

All patients were asked to keep the remaining drugs after treatment and fill out the relevant questions in the questionnaire within 3 d after the end of eradication therapy. Adverse events and patient compliance were assessed using the questionnaires and the patients' medication diaries. The intensity of the adverse events was graded as follows: None; mild, causing discomfort but not interfering with daily life; moderate, causing discomfort and interfering with daily life; and severe, causing discomfort requiring cessation of treatment. Patient compliance was rated as good if the patient had taken > 80% of all medications prescribed, and as poor, if not [20]. All patients underwent repeat ¹³C-UBT for the assessment of *H. pylori* infection 4-6 wk after the end of eradication therapy. The *H. pylori* status was interpreted as positive when the δ value was greater than the baseline value of 4, and as negative when the δ value was less than the baseline value of 4. If the δ value exceeded the baseline value, which was between 4 and 6, the test was repeated 1 mo later.

The primary endpoint of this study was the *H. pylori* eradication rate, as confirmed by a negative ¹³C-UBT. All patients were included in the intention-to-treat (ITT) analysis. Patients who did not undergo a ¹³C-UBT during follow-up were considered to have treatment failure in the ITT analysis. Patients who failed to attend follow-up assessments and those with poor compliance were excluded from the per protocol (PP) analysis. The secondary endpoints were the rate of adverse events, patient compliance, resistance to antibiotics, and factors related to the eradication rate.

H. pylori culture and antimicrobial susceptibility testing

From patients who underwent gastroscopy, we collected 2 biopsy specimens for *H. pylori* culture, one from the gastric antrum and another from the gastric corpus. Both specimens were stored at -80 °C in brain-heart infusion broth (Oxoid, Basingstoke, United Kingdom) and immediately transported to Zhiyuan Medical Laboratory Institute (Hangzhou, Zhejiang Province, China) for testing. Fully ground specimens were cultured and maintained for 3-7 d in brain-heart infusion agar medium (Oxoid,

Basingstoke, United Kingdom) supplemented with 5% defibrinated sheep blood at 37 °C in a low-oxygen environment (85% N₂, 10% CO₂, and 5% O₂). *H. pylori* isolates were identified on the basis of colony morphology and urease, catalase, and oxidase positivity.

The standard agar plate dilution method was used to assess *H. pylori* susceptibility to commonly used antibiotics. Minimum inhibitory concentrations (MICs) were calculated after 72 h of culture at 37 °C in a low-oxygen environment. We used *H. pylori* ATCC43504 (NCTC11637) for quality control. Antibiotic resistance was defined at the following MIC values: ≥ 1 µg/mL for clarithromycin, ≥ 8 µg/mL for metronidazole, and ≥ 2 µg/mL each for amoxicillin, furazolidone, levofloxacin, and tetracycline. The MIC values for antibiotic resistance were obtained from the fourth edition of the National Guide to Clinical Laboratory Procedures[21].

Sample-size calculation and statistical analysis

We assumed a 93% eradication rate with VPZ-based rescue therapy[22]. The 95% confidence interval was 86.6%-99.4%, and the sample size was 64 patients. Assuming a 5% follow-up loss, at least 68 patients would be required. Continuous variables were expressed as mean ± SD, and compared between groups by using the *t* test or Mann-Whitney *U* test. Categorical variables were expressed as numbers with percentages, and compared between groups by using the Fisher exact test or Pearson χ^2 test. Statistical significance was inferred at *P* values < 0.05. All statistical analyses were conducted using Statistical Package for the Social Sciences v23.0 (IBM, Armonk, NY, United States) and Power Analysis and Sample Size software v15.0.5 (NCSS LLC, Kaysville, UT, United States).

RESULTS

Patient characteristics

We screened a total of 103 patients for eligibility, and excluded 35 patients who did not meet the inclusion criteria. Thus, finally, 68 patients were enrolled in this study, of whom 62 patients underwent endoscopy, 41 patients underwent serological testing before and after treatment, and 24 patients underwent antimicrobial susceptibility testing. Three patients were excluded from the PP analysis due to poor compliance despite a negative ¹³C-UBT during follow-up (Figure 1).

Of the 68 patients, 20 were men and 48 were women (Table 1). Prior to the present treatment, 47 patients had undergone treatment once, 15 patients had undergone treatment twice, and 6 patients had undergone treatment 3 times. Most patients were asymptomatic (*n* = 37, 54.4%). The most common concomitant diseases were hypertension (*n* = 14, 20.6%) and diabetes (*n* = 9, 13.2%); 4 patients (5.9%) had anxiety disorder. The most common previous treatment regimen was BQT, and the most commonly used antibiotics were amoxicillin, levofloxacin, clarithromycin, and metronidazole, with a few patients using furazolidone.

H. pylori culture and antimicrobial susceptibility testing

Of the 68 patients, 24 (35.3%) underwent *H. pylori* culture and antimicrobial susceptibility testing. *H. pylori* was successfully isolated in 95.8% (23/24) of patients. The rates of resistance to metronidazole, clarithromycin, and levofloxacin were 100% (23/23), 91.3% (21/23), and 60.0% (14/23), respectively. There were no cases of resistance to tetracycline, amoxicillin, or furazolidone. The triple drug-resistance rate (to metronidazole, levofloxacin, and clarithromycin) was 56.3% (9/16) among patients with one prior treatment failure, which increased to 71.4% (5/7) among patients with 2 or more prior treatment failures.

Eradication rate and factors influencing efficacy

The overall eradication rates of 14-d VAS calculated using the ITT and PP analyses were 92.6% (63/68) and 92.3% (60/65), respectively. In 2 of the 5 patients in whom eradication failed, further treatment with VPZ 20 mg twice daily, amoxicillin 1000 mg 3 times daily, and *S. boulardii* 250 mg twice daily for 14 d successfully eradicated the infection. The remaining 3 patients had not yet received additional rescue therapy at the time of writing as less than 6 mo had passed since the end of the previous treatment.

We stratified the *H. pylori* eradication rate by the number of prior treatment failures (Figure 2). The ITT analysis showed that the eradication rates were 93.6%, 93.3%, and 83.3% (*P* = 0.433) among patients with 1, 2, and 3 prior treatment failures, respectively. The corresponding eradication rates according to the PP analysis were 93.2%, 93.3%, and 83.3% (*P* = 0.585). We found that the eradication rate did not significantly differ with the number of previous treatment failures. In addition, eradication rates did not differ between patients who had previously received amoxicillin and those who had not (85.0% *vs* 95.8%, *P* = 0.433).

Among the 23 patients who successfully underwent *H. pylori* culture and antimicrobial susceptibility testing, the ITT analysis showed that similar eradication rates were achieved in the clarithromycin-resistant (90.4%) and clarithromycin-sensitive groups (100%; *P* = 1.00). PP analysis also showed that the eradication rate did not differ between the clarithromycin-resistant and clarithromycin-sensitive groups

Table 1 Clinicodemographic characteristics of the study patients, *n* (%)

Characteristic	Total No. of patients (<i>n</i> = 68)	Number of prior eradication failures		
		1 (<i>n</i> = 47)	2 (<i>n</i> = 15)	3 (<i>n</i> = 6)
Sex (male)	20 (29.4)	10 (21.3)	6 (4.0)	4 (66.7)
Age (yr), mean ± SD	49.60 ± 10.57	49.94 ± 10.00	48.87 ± 12.65	48.83 ± 11.27
Height (m), mean ± SD	1.63 ± 0.07	1.62 ± 0.09	1.64 ± 0.08	1.68 ± 0.10
Weight (kg), mean ± SD	59.52 ± 12.30	56.83 ± 12.19	63.80 ± 9.94	69.92 ± 11.50
BMI (kg/m ²), mean ± SD	22.31 ± 3.64	21.59 ± 3.98	23.63 ± 2.04	24.63 ± 1.80
Lifestyle factors				
Smoking	5 (7.3)	4 (8.5)	0 (0)	1 (16.7)
Drinking	4 (5.9)	0 (0)	1 (6.7)	3 (50.0)
Symptom				
Abdominal pain	7 (10.3)	5 (10.6)	2 (13.3)	0 (0)
Bloating	6 (8.8)	4 (8.5)	2 (13.3)	0 (0)
Diarrhea	1 (1.5)	0 (0)	1 (6.7)	0 (0)
Halitosis	1 (1.5)	1 (2.1)	0 (0)	0 (0)
Belching	13 (19.1)	8 (17.0)	3 (20.0)	2 (33.4)
Nausea	2 (2.9)	2 (4.3)	0 (0)	0 (0)
Bitter taste	1 (1.5)	1 (2.1)	0 (0)	0 (0)
Asymptomatic	37 (54.4)	26 (55.3)	7 (46.7)	4 (66.7)
Concomitant disease				
Diabetes mellitus	9 (13.2)	8 (17.0)	1 (6.7)	0 (0)
Hypertension	14 (20.6)	7 (14.9)	5 (33.3)	2 (33.4)
Anxiety disorder	4 (5.9)	1 (2.1)	2 (13.3)	1 (16.7)
Gastroscopy findings				
Atrophic gastritis	33 (48.6)	27 (57.4)	4 (26.7)	2 (33.4)
Non-atrophic gastritis	24 (35.3)	14 (29.8)	8 (53.3)	2 (33.4)
Peptic ulcer	4 (5.9)	1 (2.1)	1 (6.7)	2 (33.4)
Polyp	1 (1.5)	0 (0)	1 (6.7)	0 (0)
Not applicable (no gastroscopy done)	6 (8.9)	5 (10.6)	1 (13.3)	0 (0)

BMI: Body mass index.

(90.0% vs 100%, respectively, $P = 1.00$). Similarly, we found no significant difference in the *H. pylori* eradication rate between the levofloxacin-resistant and levofloxacin-sensitive groups (ITT: 92.8% vs 88.8%, respectively, $P = 1.00$; PP: 92.3% vs 88.8%, respectively, $P = 1.00$; Figure 3). All patients showed metronidazole resistance, and had an eradication rate of 91.3% (21/23). Notably, eradication was achieved in 92.9% (13/14) patients who showed triple drug resistance (clarithromycin, metronidazole, and levofloxacin).

Anxiety disorder was found to be a risk factor for eradication failure (40.0% vs 3.2%, $P = 0.025$; Table 2). No significant differences in age, sex, height, weight, body mass index, concomitant diseases, gastroscopy findings, and number of prior treatment failures were found between patients with successful and failed rescue therapy.

Adverse events and compliance

A total of 10 patients (14.7%) developed adverse events, including diarrhea (4 patients), skin rash (3 patients), and dry mouth, bloating, and abdominal pain (1 patient each). Most adverse events were mild and disappeared without intervention, except in 2 patients who developed rashes on day 9 and 11, refused continued rescue treatment, and finally recovered after anti-allergy therapy. Another patient

Table 2 Factors potentially influencing *Helicobacter pylori* eradication, *n* (%)

Factor	Eradication failure (<i>n</i> = 5)	Successful eradication (<i>n</i> = 63)	<i>P</i> value
Sex (male)	2 (40.0)	18 (28.6)	0.627
Age (yr), mean ± SD	54.40 ± 5.86	49.22 ± 10.80	0.295
Height (m), mean ± SD	1.62 ± 0.10	1.62 ± 0.07	0.778
Weight (kg), mean ± SD	64.60 ± 11.42	59.12 ± 12.37	0.129
BMI (kg/m ²), mean ± SD	24.43 ± 1.88	22.14 ± 3.70	0.112
Concomitant disease			
Diabetes mellitus	1 (20.0)	8 (12.7)	0.520
Hypertension	1 (20.0)	13 (20.6)	1.000
Anxiety disorder	2 (40.0)	2 (3.2)	0.025
Gastroscopy findings			
Atrophic gastritis	2 (40.0)	31 (49.2)	1.000
Non-atrophic gastritis	3 (60.0)	21 (33.3)	0.337
Peptic ulcer	0 (0.0)	4 (6.3)	1.000
Polyp	0 (0.0)	1 (1.6)	1.000
No. of prior treatments			
1	3 (60.0)	44 (69.8)	0.641
≥ 2	2 (40.0)	19 (30.2)	

BMI: body mass index.

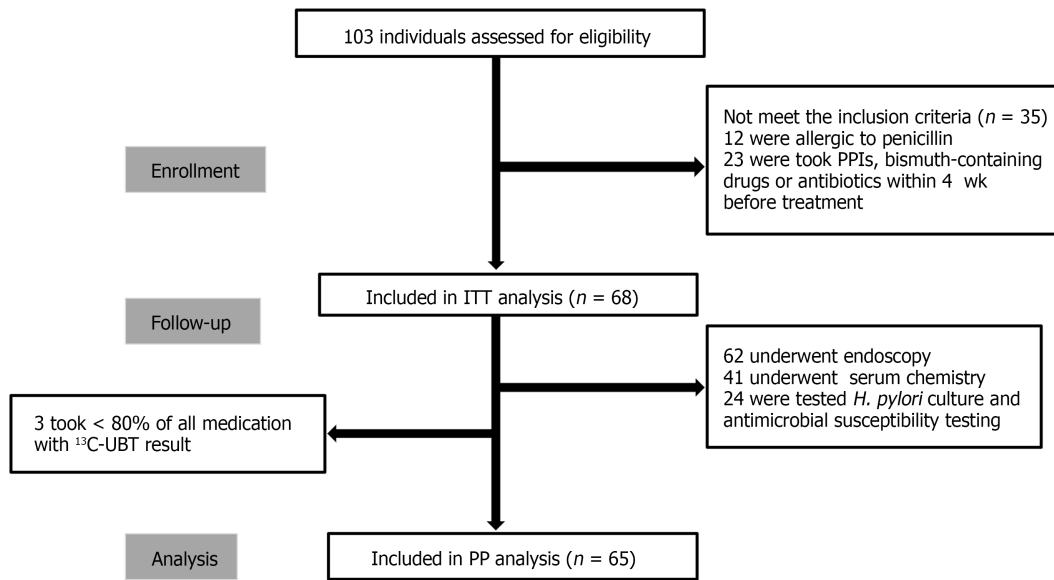


Figure 1 Flow chart of the study. PPI: Proton pump inhibitor; ITT: Intention-to-treat analysis; PP: Per-protocol analysis; UBT: Urea breath test; *H. pylori*: *Helicobacter pylori*.

discontinued treatment on day 7 because of diarrhea, which improved without intervention. The remaining patients took > 80% of all medications prescribed (compliance rate, 95.6%, 65/68; Table 3). Serum chemistry tests revealed no significant differences in liver and kidney function before and after treatment (Table 4). Among the 10 patients who developed adverse events, only 1 patient (with a rash) had eradication failure.

Table 3 Adverse events and patient compliance

Variable	%
Adverse events	
Total adverse events	14.7% (10/68)
Dry mouth	1.5% (1/68)
Skin rash	4.4% (3/68)
Bloating	1.5% (1/68)
Diarrhea	5.9% (4/68)
Abdominal pain	1.5% (1/68)
Grade of adverse event	
Mild	70.0% (7/10)
Moderate	30.0% (3/10)
Severe	0% (0/10)
¹ Compliance	
Good	95.6% (65/68)
Poor	4.4% (3/68)

¹Compliance was rated as good if the patient had taken > 80% of all medications prescribed, and as poor, if not.

Table 4 Comparison of liver and kidney function before and after treatment

Characteristic	Before (n = 41)	After (n = 41)	P value
Total bilirubin (μmol/L), mean ± SD	13.68 ± 4.82	14.96 ± 5.22	0.252
ALT (U/L), mean ± SD	16.92 ± 8.33	21.46 ± 16.03	0.270
AST (U/L), mean ± SD	18.99 ± 7.61	21.03 ± 10.67	0.670
Creatinine (μmol/L), mean ± SD	60.105 ± 12.060	60.53 ± 11.35	0.974

AST: Aspartate transaminase; ALT: Alanine transaminase.

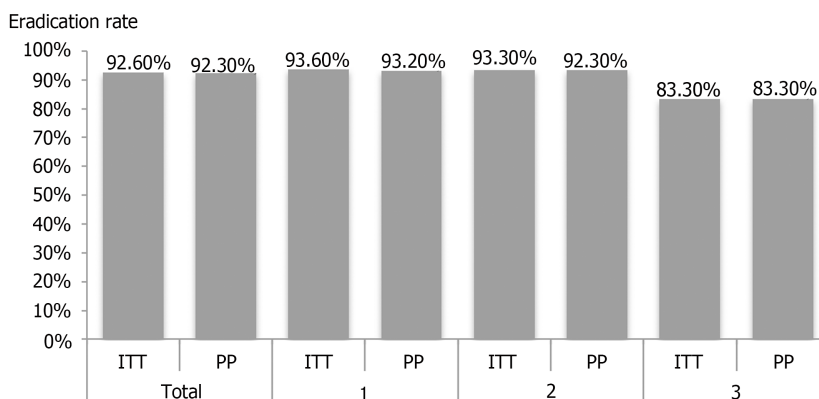


Figure 2 Eradication rates stratified by number of prior treatment failures. ITT: 93.6% vs 93.3% vs 83.3%, *P* = 0.433; PP: 93.2% vs 93.3% vs 83.3%, *P* = 0.585). ITT: Intention-to-treat analysis; PP: Per-protocol analysis.

DISCUSSION

To our knowledge, this study is the first to determine the safety and efficacy of 14-d VA-dual plus *S. boulardii* supplementation as a rescue therapy for *H. pylori* infection. This VAS regimen achieved an

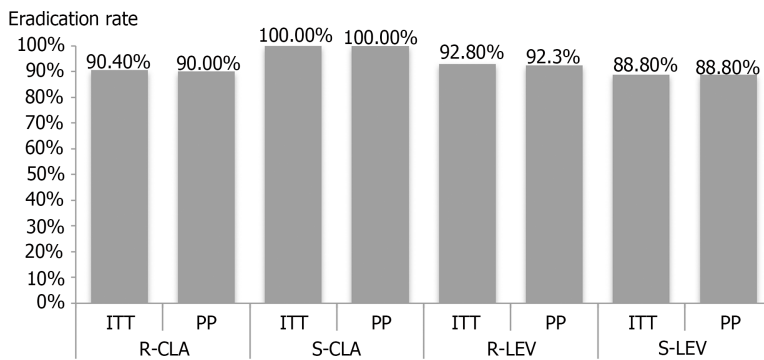


Figure 3 Impact of bacterial antibiotic resistance on eradication rate. ITT: Clarithromycin resistant vs clarithromycin sensitive, $P = 1.00$; levofloxacin resistant vs levofloxacin sensitive, $P = 1.00$; PP: Clarithromycin resistant vs clarithromycin sensitive, $P = 1.00$; levofloxacin resistant vs levofloxacin sensitive, $P = 1.00$. R-CLA: Clarithromycin resistant; S-CLA: Clarithromycin sensitive; R-LEV: Levofloxacin resistant; S-LEV: Levofloxacin sensitive; ITT: Intention-to-treat analysis; PP: Per-protocol analysis.

acceptable eradication rate (92.6% by ITT and 92.3% by PP), regardless of the number of prior treatment failures. Most patients could tolerate this regimen, and compliance was good in this Chinese patient population. Except for anxiety disorder, no other factors were observed to be associated with treatment failure. Notably, eradication was successful in 92.9% (13/14) of patients with multiple antibiotic resistance. Therefore, the 14-d VAS regimen is a safe and effective rescue therapy for *H. pylori* infection.

Currently, *H. pylori* culture-guided therapy is recommended by most consensus guidelines as a rescue therapy for *H. pylori* infection. However, culture-guided therapy is not widely used in routine clinical practice[3-5]. Until recently, susceptibility tests still required the microbiological examination of samples obtained through endoscopy, which is invasive and expensive. In addition, many hospitals lack the facilities required to perform *H. pylori* culture and antimicrobial susceptibility testing, which limits the clinical use of culture-guided therapy in many countries[3,5,20]. Furthermore, *H. pylori* culture is technically challenging. Several studies have reported culture success rates of < 80% among patients with failure of at least one prior *H. pylori* eradication treatment[23]. It should be emphasized that in our study, culture was performed in only 35.3% of the patients. This reflects the current state of routine clinical practice in China. Culture-guided therapy has not yet become a routine clinical practice, and rescue therapy is mainly prescribed on an empirical basis in China.

Compared with PPIs, VPZ, the first clinically applied P-CAB, has a faster and stronger acid-inhibition effect[13]. This provides an opportunity to potentially improve *H. pylori* eradication therapy by simplifying complex regimens and possibly helping to develop effective therapies[5]. In one study, a PP analysis showed that a 7-d VPZ-based regimen (VPZ 20 mg twice daily, sitafloxacin 100 mg twice daily, and amoxicillin 750 mg twice daily) as a third-line therapy resulted in a significantly higher eradication rate than a PPI-based regimen (83.3% vs 57.1%, $P = 0.043$)[24]. In a small study, a 10-d triple therapy regimen consisting of VPZ 20 mg twice daily, rifabutin 150 mg twice daily, and amoxicillin 750 mg twice daily yielded a 100% eradication rate in 19 patients with ≥ 3 prior treatment attempts[25]. Similarly, in 57 patients administered a 7-d rifabutin-containing triple therapy regimen (VPZ 20 mg twice daily, amoxicillin 500 mg 4 times daily, and 150 mg rifabutin 150 mg once daily) as a third- or later-line *H. pylori* eradication regimen, the eradication rate was 91.2%[26]. It should be emphasized that all the above studies were conducted in Japan, and they all used triple regimens containing VPZ and amoxicillin. Although the use of 2 antibiotics may lead to higher eradication rates, this practice promotes the use of an unnecessary second antibiotic[27]. Hence, optimization of VPZ-based rescue therapy needs to be further explored. However, the relevant research in China is limited. Only one retrospective study has reported that the 14-d VA-dual regimen (VPZ 20 mg/d or 40 mg/d and amoxicillin 3000 mg/d) was safe and effective as a rescue therapy (92.5%, 172/186); however, the frequencies and doses of VA-dual therapy varied among the patients[18].

The 14-d VAS regimen used in this study offers certain advantages over previous rescue therapies. First, it minimizes the use of antibiotics, which is especially important in the light of the global increase in *H. pylori* antibiotic resistance. Indeed, VPZ-containing triple therapies have been shown to contribute to global antimicrobial resistance[27]. The 14-d VAS regimen eliminated the need for a second antibiotic while providing remarkable *H. pylori* eradication efficacy. Second, the optimal amoxicillin dose for dual therapy remains uncertain. Available evidence suggests that a dose of 2 g/d is insufficient, and 3 g or 2.25-3.00 g in split doses (every 6 h or 8 h) may be optimal[27]. Therefore, amoxicillin was administered at a dose of 750 mg 3 times daily in the 14-d VAS regimen. Third, for the first time, we supplemented *S. boulardii* to VA-dual as a rescue therapy for *H. pylori* eradication. Several potential mechanisms by which *S. boulardii* acts as an adjunct to *H. pylori* eradication therapy have been elucidated: (1) It inhibits the growth and proliferation of *H. pylori* by upregulating short-chain fatty acids and other antimicrobial substances[28]; (2) it expresses a neuraminidase that reduces the expression of $\alpha(2-3)$ -linked sialic acid

on the epithelial cell surface, which prevents the adhesion of *H. pylori* to the duodenal epithelium[29]; and (3) it reduces the incidence of adverse events and indirectly improves patient compliance, thereby increasing the eradication rate of *H. pylori*[19].

Poor patient compliance is a main cause of treatment failure, and adverse events are a key factor affecting patient compliance[30]. Our 14-d VAS regimen was well tolerated, and all adverse events were mild or moderate, with diarrhea (5.9%) and rash (4.4%) being the most common. Patient compliance was also good, which may be attributable to the low rate of adverse events and the simplicity of the regimen.

We analyzed the factors potentially influencing the eradication rate of the 14-d VAS regimen. Only anxiety disorder was significantly associated with eradication failure; other factors such as gender, age, smoking, and alcohol consumption were not associated with treatment failure. There is evidence that state anxiety and trait anxiety are related to *H. pylori* infection. Anxiety appears to heighten the intensity and perception of gastrointestinal signals, which gives patients more reasons to worry about their health, leading to a higher anxiety response, and making patients more inclined to seek medical advice [31]. Thus, identifying patients with anxiety prior to the treatment of *H. pylori* infection and management by a professional team including a gastroenterologist and a psychologist to improve anxiety may be necessary to improve eradication rates and reduce the costs associated with frequent medical consultations.

This study has some limitations. First, it is impossible to compare the safety and effectiveness of the VA-dual regimen and the VAS regimen because this study is a single-arm pilot study. Large-scale, multicenter randomized controlled trials in areas with different patterns of antibiotic resistance are needed to confirm our results. Second, the number of patients with anxiety disorder in this study was small, and the relevant conclusions and potential mechanisms need to be further explored in future studies. Third, *H. pylori* culture and antimicrobial susceptibility testing were performed in only 35.3% of our patients, and no resistance was detected to amoxicillin. So, it was impossible to determine whether amoxicillin resistance affected the eradication rate of the 14-d VAS regimen. However, considering that the rates of primary and secondary resistance to amoxicillin are low and stable[10], we believe that the 14-d VAS regimen is an effective rescue therapy. Fourth, this study was underpowered to analyze the association between eradication rate and prior eradication regimens because the study patients had previously been treated with multiple different regimens.

CONCLUSION

In conclusion, the 14-d VAS regimen is safe and effective *H. pylori* rescue therapy, with an acceptable eradication rate (> 90%), regardless of the number of prior treatment failures. This regimen avoids the use of additional antibiotics, but may need to be adjusted for patients with anxiety. Large-scale, multicenter randomized controlled trials are needed to confirm our results.

ARTICLE HIGHLIGHTS

Research background

Vonoprazan (VPZ)-containing triple therapies have been shown to contribute to global antimicrobial resistance. Hence, the value of VPZ-based regimens as rescue therapies needs to be explored.

Research motivation

Saccharomyces boulardii (*S. boulardii*) supplementation significantly improved *H. pylori* eradication rates and decreased the incidence of adverse events. We are the first to combine *S. boulardii* supplementation with VPZ-amoxicillin dual therapy (VAS regimen) as a rescue therapy for *H. pylori* eradication.

Research objectives

To determine the safety and efficacy of the VAS regimen as a rescue treatment for *H. pylori* infection.

Research methods

We performed a prospective, single-center, clinical trial with the VAS regimen.

Research results

The overall eradication rates calculated using intention-to-treat and per-protocol analyses were 92.6% and 92.3%, respectively. The eradication rate did not differ with the number of treatment failures ($P = 0.433$). Acceptable eradication rates (> 90%) were achieved in patients with resistance to clarithromycin, metronidazole, and levofloxacin. Most adverse events were mild, and 95.6% patients showed good compliance.

Research conclusions

The VAS regimen is a safe and effective rescue therapy, with an acceptable eradication rate (> 90%), regardless of the number of prior treatment failures.

Research perspectives

Large-scale, multicenter randomized controlled trials in areas with different patterns of antibiotic resistance are needed to confirm our results. It will be necessary to compare the safety and effectiveness of the VPZ-amoxicillin dual therapy regimen with the VAS regimen in the future.

ACKNOWLEDGEMENTS

The authors are grateful to Dr. Liu-Lan Qian for her help in the statistical analysis of this paper.

FOOTNOTES

Author contributions: Wang XY contributed to conception and design of the study, critical revision, analysis and interpretation of data, drafting the article, revising the article; Yu J and Lv YM contributed to acquisition of data, analysis and interpretation of data, and drafting the article; Yang P, Jiang YZ, and Qin XR contributed to acquisition of data, analysis and interpretation of data; and all authors approved the final version of the manuscript.

Supported by the Changzhou Special Fund for Introducing Foreign Talents, No. CQ20204037; and the Changzhou High-Level Medical Talents Training Project, No. 2022CZBJ051.

Institutional review board statement: The study was reviewed and approved by the Clinical Medical Technical Ethics Committee of the Affiliated Changzhou No. 2 People's Hospital of Nanjing Medical University [approval. No. (2021) YLJSD004].

Clinical trial registration statement: This study is registered at Chinese Clinical trial Registry. The registration identification number is ChiCTR2200055125.

Informed consent statement: All study participants provided informed written consent prior to the study enrollment and declare that they have no conflict of interest.

Conflict-of-interest statement: The authors declare that they have no conflict of interest.

Data sharing statement: The data that support the findings of this study are available from the corresponding author upon reasonable request.

CONSORT 2010 statement: The authors have read the CONSORT 2010 statement, and the manuscript was prepared and revised according to the CONSORT 2010 statement.

Open-Access: This article is an open-access article that was selected by an in-house editor and fully peer-reviewed by external reviewers. It is distributed in accordance with the Creative Commons Attribution NonCommercial (CC BY-NC 4.0) license, which permits others to distribute, remix, adapt, build upon this work non-commercially, and license their derivative works on different terms, provided the original work is properly cited and the use is non-commercial. See: <https://creativecommons.org/licenses/by-nc/4.0/>

Country/Territory of origin: China

ORCID number: Jing Yu 0000-0002-4132-3944; Yi-Ming Lv 0000-0002-1546-0339; Peng Yang 0000-0002-5501-0244; Yi-Zhou Jiang 0000-0002-8274-9327; Xiang-Rong Qin 0000-0001-8135-473X; Xiao-Yong Wang 0000-0001-8401-4888.

S-Editor: Chen YL

L-Editor: A

P-Editor: Cai YX

REFERENCES

- Zamani M**, Ebrahimitabar F, Zamani V, Miller WH, Alizadeh-Navaei R, Shokri-Shirvani J, Derakhshan MH. Systematic review with meta-analysis: the worldwide prevalence of Helicobacter pylori infection. *Aliment Pharmacol Ther* 2018; **47**: 868-876 [PMID: 29430669 DOI: 10.1111/apt.14561]
- Chiang TH**, Chang WJ, Chen SL, Yen AM, Fann JC, Chiu SY, Chen YR, Chuang SL, Shieh CF, Liu CY, Chiu HM,

- Chiang H, Shun CT, Lin MW, Wu MS, Lin JT, Chan CC, Graham DY, Chen HH, Lee YC. Mass eradication of Helicobacter pylori to reduce gastric cancer incidence and mortality: a long-term cohort study on Matsu Islands. *Gut* 2021; **70**: 243-250 [PMID: 32792335 DOI: 10.1136/gutjnl-2020-322200]
- 3 **Liu WZ**, Xie Y, Lu H, Cheng H, Zeng ZR, Zhou LY, Chen Y, Wang JB, Du YQ, Lu NH; Chinese Society of Gastroenterology, Chinese Study Group on Helicobacter pylori and Peptic Ulcer. Fifth Chinese National Consensus Report on the management of Helicobacter pylori infection. *Helicobacter* 2018; **23**: e12475 [PMID: 29512258 DOI: 10.1111/hel.12475]
 - 4 **Chey WD**, Leontiadis GI, Howden CW, Moss SF. ACG Clinical Guideline: Treatment of Helicobacter pylori Infection. *Am J Gastroenterol* 2017; **112**: 212-239 [PMID: 28071659 DOI: 10.1038/ajg.2016.563]
 - 5 **Malfertheiner P**, Megraud F, Rokkas T, Gisbert JP, Liou JM, Schulz C, Gasbarrini A, Hunt RH, Leja M, O'Morain C, Ruge M, Suerbaum S, Tilg H, Sugano K, El-Omar EM; European Helicobacter and Microbiota Study group. Management of Helicobacter pylori infection: the Maastricht VI/Florence consensus report. *Gut* 2022 [PMID: 35944925 DOI: 10.1136/gutjnl-2022-327745]
 - 6 **Koroglu M**, Ayvaz MA, Ozturk MA. The efficacy of bismuth quadruple therapy, sequential therapy, and hybrid therapy as a first-line regimen for Helicobacter pylori infection compared with standard triple therapy. *Niger J Clin Pract* 2022; **25**: 1535-1541 [PMID: 36149216 DOI: 10.4103/njcp.njcp_89_22]
 - 7 **Song Z**, Suo B, Zhang L, Zhou L. Rabeprazole, Minocycline, Amoxicillin, and Bismuth as First-Line and Second-Line Regimens for Helicobacter pylori Eradication. *Helicobacter* 2016; **21**: 462-470 [PMID: 27060292 DOI: 10.1111/hel.12313]
 - 8 **Cortés P**, Nelson AD, Bi Y, Stancampiano FF, Murray LP, Pujalte GGA, Gomez V, Harris DM. Treatment Approach of Refractory Helicobacter pylori Infection: A Comprehensive Review. *J Prim Care Community Health* 2021; **12**: 21501327211014087 [PMID: 33949229 DOI: 10.1177/21501327211014087]
 - 9 **Graham DY**, Fischbach L. Helicobacter pylori treatment in the era of increasing antibiotic resistance. *Gut* 2010; **59**: 1143-1153 [PMID: 20525969 DOI: 10.1136/gut.2009.192757]
 - 10 **Li SY**, Li J, Dong XH, Teng GG, Zhang W, Cheng H, Gao W, Dai Y, Zhang XH, Wang WH. The effect of previous eradication failure on antibiotic resistance of Helicobacter pylori: A retrospective study over 8 years in Beijing. *Helicobacter* 2021; **26**: e12804 [PMID: 33860967 DOI: 10.1111/hel.12804]
 - 11 **Bi H**, Chen X, Chen Y, Zhao X, Wang S, Wang J, Lyu T, Han S, Lin T, Li M, Yuan D, Liu J, Shi Y. Efficacy and safety of high-dose esomeprazole-amoxicillin dual therapy for Helicobacter pylori rescue treatment: a multicenter, prospective, randomized, controlled trial. *Chin Med J (Engl)* 2022; **135**: 1707-1715 [PMID: 36193978 DOI: 10.1097/CM9.0000000000002289]
 - 12 **Guan JL**, Hu YL, An P, He Q, Long H, Zhou L, Chen ZF, Xiong JG, Wu SS, Ding XW, Luo HS, Li PY. Comparison of high-dose dual therapy with bismuth-containing quadruple therapy in Helicobacter pylori-infected treatment-naïve patients: An open-label, multicenter, randomized controlled trial. *Pharmacotherapy* 2022; **42**: 224-232 [PMID: 35075679 DOI: 10.1002/phar.2662]
 - 13 **Sakurai Y**, Mori Y, Okamoto H, Nishimura A, Komura E, Araki T, Shiramoto M. Acid-inhibitory effects of vonoprazan 20 mg compared with esomeprazole 20 mg or rabeprazole 10 mg in healthy adult male subjects—a randomised open-label cross-over study. *Aliment Pharmacol Ther* 2015; **42**: 719-730 [PMID: 26193978 DOI: 10.1111/apt.13325]
 - 14 **Zuberi BF**, Ali FS, Rasheed T, Bader N, Hussain SM, Saleem A. Comparison of Vonoprazan and Amoxicillin Dual Therapy with Standard Triple Therapy with Proton Pump Inhibitor for Helicobacter Pylori eradication: A Randomized Control Trial. *Pak J Med Sci* 2022; **38**: 965-969 [PMID: 35634610 DOI: 10.12669/pjms.38.4.5436]
 - 15 **Chey WD**, Mégraud F, Laine L, López LJ, Hunt BJ, Howden CW. Vonoprazan Triple and Dual Therapy for Helicobacter pylori Infection in the United States and Europe: Randomized Clinical Trial. *Gastroenterology* 2022; **163**: 608-619 [PMID: 35679950 DOI: 10.1053/j.gastro.2022.05.055]
 - 16 **Suzuki S**, Gotoda T, Kusano C, Ikehara H, Ichijima R, Ohyauchi M, Ito H, Kawamura M, Ogata Y, Ohtaka M, Nakahara M, Kawabe K. Seven-day vonoprazan and low-dose amoxicillin dual therapy as first-line Helicobacter pylori treatment: a multicentre randomised trial in Japan. *Gut* 2020; **69**: 1019-1026 [PMID: 31915235 DOI: 10.1136/gutjnl-2019-319954]
 - 17 **Gotoda T**, Kusano C, Suzuki S, Horii T, Ichijima R, Ikehara H. Clinical impact of vonoprazan-based dual therapy with amoxicillin for *H. pylori* infection in a treatment-naïve cohort of junior high school students in Japan. *J Gastroenterol* 2020; **55**: 969-976 [PMID: 32666199 DOI: 10.1007/s00535-020-01709-4]
 - 18 **Gao W**, Teng G, Wang C, Xu Y, Li Y, Cheng H. Eradication rate and safety of a "simplified rescue therapy": 14-day vonoprazan and amoxicillin dual regimen as rescue therapy on treatment of Helicobacter pylori infection previously failed in eradication: A real-world, retrospective clinical study in China. *Helicobacter* 2022; **27**: e12918 [PMID: 35877765 DOI: 10.1111/hel.12918]
 - 19 **Zhou BG**, Chen LX, Li B, Wan LY, Ai YW. Saccharomyces boulardii as an adjuvant therapy for Helicobacter pylori eradication: A systematic review and meta-analysis with trial sequential analysis. *Helicobacter* 2019; **24**: e12651 [PMID: 31414551 DOI: 10.1111/hel.12651]
 - 20 **Wang JW**, Hsu PI, Lin MH, Kao J, Tsay FW, Wu IT, Shie CB, Wu DC. The efficacy of culture-guided versus empirical therapy with high-dose proton pump inhibitor as third-line treatment of Helicobacter pylori infection: A real-world clinical experience. *J Gastroenterol Hepatol* 2022; **37**: 1928-1934 [PMID: 35816187 DOI: 10.1111/jgh.15942]
 - 21 **Shang H**, Wang YS, Shen ZY. National Guide to Clinical Laboratory Procedures. 4th ed. Beijing: People's medical Publishing House, 2014: 574-628
 - 22 **Saito Y**, Konno K, Sato M, Nakano M, Kato Y, Saito H, Serizawa H. Vonoprazan-Based Third-Line Therapy Has a Higher Eradication Rate against Sitafloxacin-Resistant Helicobacter pylori. *Cancers (Basel)* 2019; **11** [PMID: 30669474 DOI: 10.3390/cancers11010116]
 - 23 **Gisbert JP**. Empirical or susceptibility-guided treatment for Helicobacter pylori infection? *Therap Adv Gastroenterol* 2020; **13**: 1756284820968736 [PMID: 33240392 DOI: 10.1177/1756284820968736]
 - 24 **Sue S**, Shibata W, Sasaki T, Kaneko H, Irie K, Kondo M, Maeda S. Randomized trial of vonoprazan-based versus proton-pump inhibitor-based third-line triple therapy with sitafloxacin for Helicobacter pylori. *J Gastroenterol Hepatol* 2019; **34**:

- 686-692 [PMID: 30151994 DOI: 10.1111/jgh.14456]
- 25 **Hirata Y**, Yamada A, Niikura R, Shichijo S, Hayakawa Y, Koike K. Efficacy and safety of a new rifabutin-based triple therapy with vonoprazan for refractory *Helicobacter pylori* infection: A prospective single-arm study. *Helicobacter* 2020; **25**: e12719 [PMID: 32602161 DOI: 10.1111/hel.12719]
 - 26 **Inokuchi K**, Mori H, Matsuzaki J, Hirata K, Harada Y, Saito Y, Suzuki H, Kanai T, Masaoka T. Efficacy and safety of low-dose rifabutin-based 7-day triple therapy as a third- or later-line *Helicobacter pylori* eradication regimen. *Helicobacter* 2022; **27**: e12900 [PMID: 35644041 DOI: 10.1111/hel.12900]
 - 27 **Graham DY**, Lu H, Shiotani A. Vonoprazan-containing *Helicobacter pylori* triple therapies contribution to global antimicrobial resistance. *J Gastroenterol Hepatol* 2021; **36**: 1159-1163 [PMID: 32918832 DOI: 10.1111/jgh.15252]
 - 28 **McFarland LV**. Systematic review and meta-analysis of *Saccharomyces boulardii* in adult patients. *World J Gastroenterol* 2010; **16**: 2202-2222 [PMID: 20458757 DOI: 10.3748/wjg.v16.i18.2202]
 - 29 **Sakarya S**, Gunay N. *Saccharomyces boulardii* expresses neuraminidase activity selective for α 2,3-linked sialic acid that decreases *Helicobacter pylori* adhesion to host cells. *APMIS* 2014; **122**: 941-950 [PMID: 24628732 DOI: 10.1111/apm.12237]
 - 30 **Li H**, Liang X, Chen Q, Zhang W, Lu H. Inappropriate treatment in *Helicobacter pylori* eradication failure: a retrospective study. *Scand J Gastroenterol* 2018; **53**: 130-133 [PMID: 29214879 DOI: 10.1080/00365521.2017.1413132]
 - 31 **Addolorato G**, Mirijello A, D'Angelo C, Leggio L, Ferrulli A, Abenavoli L, Vonghia L, Cardone S, Leso V, Cossari A, Capristo E, Gasbarrini G. State and trait anxiety and depression in patients affected by gastrointestinal diseases: psychometric evaluation of 1641 patients referred to an internal medicine outpatient setting. *Int J Clin Pract* 2008; **62**: 1063-1069 [PMID: 18422970 DOI: 10.1111/j.1742-1241.2008.01763.x]

Observational Study

Determination of esophageal squamous cell carcinoma and gastric adenocarcinoma on raw tissue using Raman spectroscopy

Hiroaki Ito, Naoyuki Uragami, Tomokazu Miyazaki, Yuto Shimamura, Haruo Ikeda, Yohei Nishikawa, Manabu Onimaru, Kai Matsuo, Masayuki Isozaki, William Yang, Kenji Issha, Satoshi Kimura, Machiko Kawamura, Noboru Yokoyama, Miki Kushima, Haruhiro Inoue

Specialty type: Gastroenterology and hepatology

Provenance and peer review: Invited article; Externally peer reviewed.

Peer-review model: Single blind

Peer-review report's scientific quality classification

Grade A (Excellent): 0
Grade B (Very good): 0
Grade C (Good): C
Grade D (Fair): 0
Grade E (Poor): 0

P-Reviewer: Gao SG, China

Received: December 12, 2022

Peer-review started: December 12, 2022

First decision: March 9, 2023

Revised: April 10, 2023

Accepted: April 27, 2023

Article in press: April 27, 2023

Published online: May 28, 2023



Hiroaki Ito, Naoyuki Uragami, Yuto Shimamura, Haruo Ikeda, Yohei Nishikawa, Manabu Onimaru, Kai Matsuo, Masayuki Isozaki, Noboru Yokoyama, Haruhiro Inoue, Digestive Disease Center, Showa University Koto Toyosu Hospital, Tokyo 135-8577, Japan

Tomokazu Miyazaki, JSR Corporation, Tokyo 105-0021, Japan

William Yang, Bay Spec Inc., San Jose, CA 95131, United States

Kenji Issha, Fuji Technical Research Inc., Yokohama 220-6215, Japan

Satoshi Kimura, Department of Laboratory Medicine and Central Clinical Laboratory, Showa University Northern Yokohama Hospital, Yokohama 224-8503, Japan

Machiko Kawamura, Department of Hematology, Saitama Cancer Center, Inamachi 362-0806, Japan

Miki Kushima, Department of Pathology, Showa University Koto Toyosu Hospital, Tokyo 135-8577, Japan

Corresponding author: Hiroaki Ito, MD, PhD, Associate Professor, Digestive Disease Center, Showa University Koto Toyosu Hospital, 5-1-38 Toyosu, Koto-ku, Tokyo 135-8577, Japan. h.ito@med.showa-u.ac.jp

Abstract**BACKGROUND**

Cancer detection is a global research focus, and novel, rapid, and label-free techniques are being developed for routine clinical practice. This has led to the development of new tools and techniques from the bench side to routine clinical practice. In this study, we present a method that uses Raman spectroscopy (RS) to detect cancer in unstained formalin-fixed, resected specimens of the esophagus and stomach. Our method can record a clear Raman-scattered light spectrum in these specimens, confirming that the Raman-scattered light spectrum changes because of the histological differences in the mucosal tissue.

AIM

To evaluate the use of Raman-scattered light spectrum for detecting endoscop-

ically resected specimens of esophageal squamous cell carcinoma (SCC) and gastric adenocarcinoma (AC).

METHODS

We created a Raman device that is suitable for observing living tissues, and attempted to acquire Raman-scattered light spectra in endoscopically resected specimens of six esophageal tissues and 12 gastric tissues. We evaluated formalin-fixed tissues using this technique and captured shifts at multiple locations based on feasibility, ranging from six to 19 locations 200 microns apart in the vertical and horizontal directions. Furthermore, a correlation between the obtained Raman scattered light spectra and histopathological diagnosis was performed.

RESULTS

We successfully obtained Raman scattered light spectra from all six esophageal and 12 gastric specimens. After data capture, the tissue specimens were sent for histopathological analysis for further processing because RS is a label-free methodology that does not cause tissue destruction or alterations. Based on data analysis of molecular-level substrates, we established cut-off values for the diagnosis of esophageal SCC and gastric AC. By analyzing specific Raman shifts, we developed an algorithm to identify the range of esophageal SCC and gastric AC with an accuracy close to that of histopathological diagnoses.

CONCLUSION

Our technique provides qualitative information for real-time morphological diagnosis. However, further *in vivo* evaluations require an excitation light source with low human toxicity and large amounts of data for validation.

Key Words: Raman spectroscopy; Squamous cell carcinoma; Adenocarcinoma; Esophagus; Stomach; Label-free cancer detection; Real-time diagnosis

©The Author(s) 2023. Published by Baishideng Publishing Group Inc. All rights reserved.

Core Tip: Cancer diagnosis is a critical step in patient management, and involves a combination of diagnostic modalities or a single investigation. Diagnostic techniques that provide comprehensive data on the disease process can be particularly valuable, and Raman spectroscopy (RS) is one such modality that offers detailed molecular-level information. In this study, we utilized RS to rapidly detect cancer in resected esophageal and stomach specimens, providing information beyond morphology. By providing detailed molecular-level data, RS can provide a more comprehensive understanding of disease processes and aid in accurate diagnosis.

Citation: Ito H, Uragami N, Miyazaki T, Shimamura Y, Ikeda H, Nishikawa Y, Onimaru M, Matsuo K, Isozaki M, Yang W, Issha K, Kimura S, Kawamura M, Yokoyama N, Kushima M, Inoue H. Determination of esophageal squamous cell carcinoma and gastric adenocarcinoma on raw tissue using Raman spectroscopy. *World J Gastroenterol* 2023; 29(20): 3145-3156

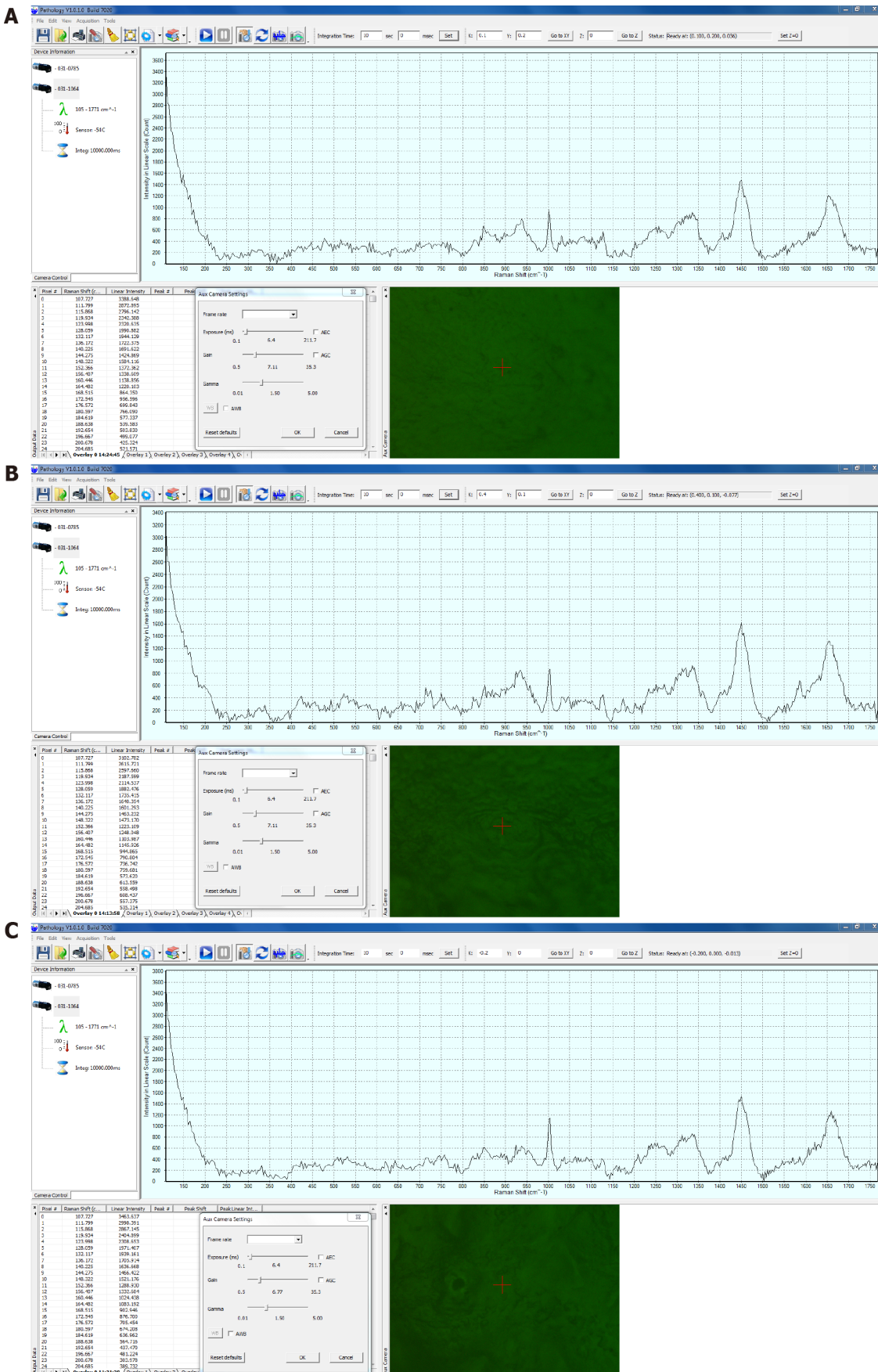
URL: <https://www.wjgnet.com/1007-9327/full/v29/i20/3145.htm>

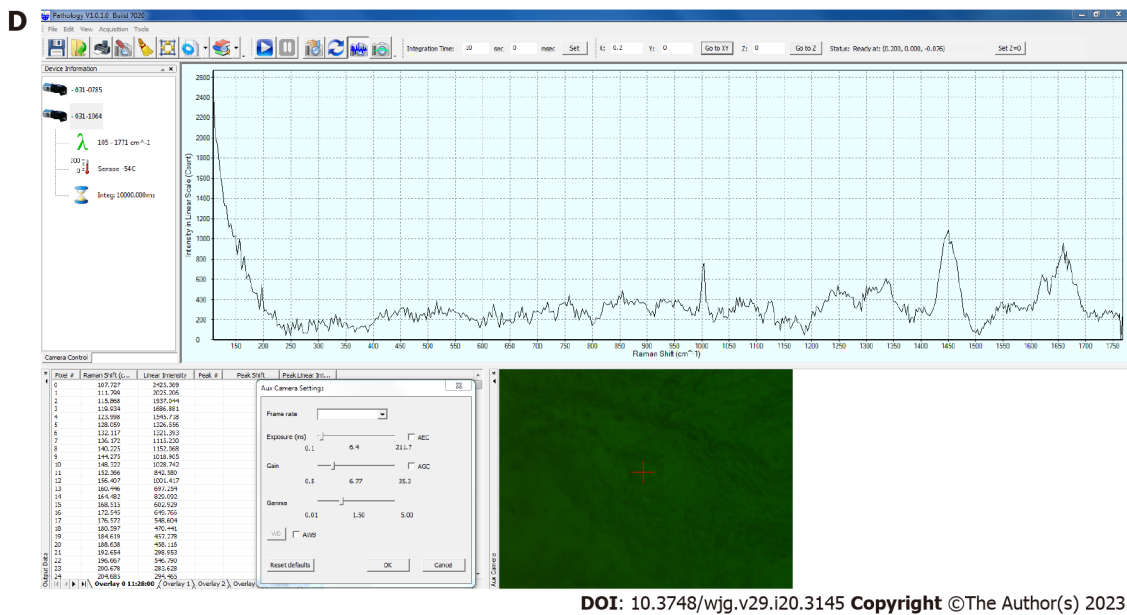
DOI: <https://dx.doi.org/10.3748/wjg.v29.i20.3145>

INTRODUCTION

Gastrointestinal cancers are typically evaluated using various investigative modalities, like radiological imaging, endoscopy, and histopathology[1,2]. Although tissue diagnosis through histopathological evaluation remains the gold standard for diagnosis, it is primarily based on morphological interpretation, even in current molecular-level evaluation practices[3]. In addition to morphology, many other such modalities are rapidly making inroads into practice[3,4]. Unlike morphology alone, immunohistochemistry, which has become almost synonymous with objective histopathological evaluation, is further aided by fluorescence *in situ* hybridization and sequencing. At the other end of the spectrum lies non-invasive/minimally invasive, non-label-based evaluation options, such as near-infrared spectroscopy and Raman spectroscopy (RS)[5].

Endoscopic biopsy is the preferred diagnostic method for gastrointestinal cancer[6]. Recent technological advances in endoscopy have enabled reliable diagnoses based on endoscopic findings alone, which have been further improved by the incorporation of artificial intelligence[5-7]. However, these





DOI: 10.3748/wjg.v29.i20.3145 Copyright ©The Author(s) 2023.

Figure 1 Example of Raman spectra. Screenshots from the software window illustrating the Raman shift plotted against the intensity on a linear scale. A: Normal esophageal mucosa; B: Esophageal squamous cell carcinoma; C: Normal stomach mucosa; D: Stomach adenocarcinoma.

methodologies rely primarily on morphological assessments and do not consider molecular biological information. Tumor tissues contain abnormal molecules and proteins that are absent in normal tissues. The addition of molecular biological information to existing highly evolved morphological diagnostic methods may become an epoch-making technique with higher diagnostic accuracy[5,8,9].

Hence, we evaluated the biological samples using RS to obtain molecular information[8,10]. RS is a nondestructive inspection method that identifies a substance by measuring the type and amount of molecules contained in the substance by analyzing the wavelength of the reflected light obtained by irradiating the target substance with light, such as a laser[11-13]. Furthermore, RS can be used to evaluate substances with all types of properties, including solids[14-16], liquids[9,11], and gases[17], without sample pretreatment. Therefore, RS is an excellent inspection method for evaluating substances within a short time.

Therefore, attempts have been made to evaluate tissue samples using RS. Bergholt *et al*[4] presented a diagnostic technique for esophageal disease in the gastrointestinal tract using RS and published diagnostic techniques for gastric cancer. Moreover, Duraipandian *et al*[3] reported a diagnostic technique for gastric cancer using RS. However, a standard method for biological evaluations using RS has not yet been established.

A major challenge in using RS to evaluate biological samples is interference of autofluorescence[18]. To address this issue, we developed a novel micro-Raman device with unique features that enables effective evaluation of biological samples using RS.

We selected a near-infrared laser, which is not easily affected by autofluorescence, as the excitation light source. Because the Raman-scattered light intensity is inversely proportional to the square of the excitation light wavelength, the scattered light intensity of a long-wavelength near-infrared laser is low [18]. We developed a highly sensitive circuit to detect this weakly scattered light. We attempted to record the Raman-scattered light wavelengths from living esophageal tissues using a micro-Raman device with these characteristics.

MATERIALS AND METHODS

Study population and data collection

Sixteen patients aged 80 years or younger who underwent endoscopic submucosal dissection of the esophagus or stomach at the Digestive Disease Center of Showa University Koto Toyosu Hospital were recruited for this study. Written consent was obtained from all participants. Eleven participants were male and five were female, with an age range of 38-80 years. Eighteen specimens (esophagus, $n = 6$; stomach, $n = 12$) were analyzed (Table 1). This study was approved by the in-hospital clinical research review board (approval number: 18T5009) and conducted in accordance with the Declaration of Helsinki.

Table 1 Patients' background

Patient number	Patient	Clinical diagnosis	Number of lesions	Treatment date
1	50-year-old, female	Esophageal cancer	1	December 20, 2018
2	65-year-old, male	Esophageal cancer	1	December 20, 2018
3	61-year-old, male	Esophageal cancer	1	January 11, 2019
4	61-year-old, male	Esophageal cancer	2	January 18, 2019
5	78-year-old, female	Esophageal cancer	1	April 18, 2019
6	72-year-old, female	Stomach cancer	1	January 8, 2019
7	63-year-old, male	Stomach cancer	1	January 18, 2019
8	56-year-old, male	Stomach cancer	1	January 24, 2019
9	58-year-old, male	Stomach cancer	1	February 3, 2019
10	79-year-old, male	Stomach cancer	1	February 4, 2019
11	77-year-old, male	Stomach cancer	1	February 17, 2019
12	80-year-old, male	Stomach cancer	2	February 28, 2019
13	65-year-old, male	Stomach cancer	1	February 28, 2019
14	68-year-old, male	Stomach cancer	1	April 8, 2019
15	66-year-old, female	Stomach adenoma	1	May 19, 2019
16	38-year-old, female	Stomach submucosal tumor	1	April 9, 2019

Measurement protocol and data capture

Esophageal and stomach tissue samples (including mucosal and submucosal tissues) were collected immediately after endoscopic resection. The tissue was attached to a black rubber plate with a metal pin, and a 0.02 mm thick aluminum foil was sandwiched between the rubber plate and the esophageal tissue to prevent Raman scattered light from the rubber plate from being included in the measurements.

A linear or grid-like measurement grid was set up to include endoscopically diagnosed lesions in the mucosa and the surrounding normal mucosa. Multiple measurement points were selected at 5 mm or 10 mm intervals depending on the shape of the clinically determined lesion. Raman scattered light wavelengths were recorded from 19 or 6 locations at intervals of 200 μm in the vertical and horizontal directions for each selected point depending on the feasibility. To prevent the sample from drying out, distilled water was sprayed on the sample as necessary during the measurement.

A RS device (BaySpec Inc., San Jose, CA, United States) was used, with a computer-controlled stage, an objective lens of 20 \times magnification, a correction collar for near-infrared microscopy (LCPLN20XIR, Olympus Corporation, Tokyo, Japan), and an excitation laser wavelength of 1064 nm. The measurements were captured with a laser power of 200 mW and an exposure time of 10 s per point. Pathologic System Software Version 1.0.1.0 (BaySpec, Inc., San Jose CA, United States) was used and baseline correction was performed without smoothing the waveform. Examples of the Raman spectra of the esophageal and gastric mucosa are shown in [Figure 1](#).

Analysis

Fifteen types of Raman shifts corresponding to the constituent molecules of living tissues ([Table 2](#)) were selected for the analysis. From the recorded Raman-scattered light waveforms, the scattered light intensities of 15 types of Raman shifts were extracted, and the optimum combination matching the range of squamous cell carcinoma (SCC) of the esophagus and gastric adenocarcinoma (AC) by histopathological diagnosis was determined.

RESULTS

The study involved 16 patients, and 18 specimens were resected for histopathological analysis. The results showed that five of the specimens were SCC of the esophagus, 10 were well-differentiated tubular AC of the stomach, one was a gastric adenoma, and one was a gastric carcinoid tumor (NET G1) ([Table 3](#)).

Raman spectra were recorded for all six esophageal and 12 gastric specimens. All combinations of the scattered light intensities of the 15 Raman shifts were calculated to determine the combination that best matched the range of cancer by histopathological diagnosis. In esophageal squamous cell cancer, the

Table 2 Fifteen Raman shift parameters obtained from the raw tissues and the range of the shifts[7,9]

Number	Assigned peak	Shift start (cm ⁻¹)	Shift end (cm ⁻¹)
RS 1	Phenylalanine C-C twist	611	631
RS 2	Cholesterol	700	720
RS 3	Tryptophane ring breath	751	771
RS 4	Tyrosine ring breath	830	850
RS 5	Phenylalanine ring breath	993	1013
RS 6	Skeletal C-C	1060	1080
RS 7	Nucleotide O-P-O	1091	1111
RS 8	Skeletal C-C stretch	1123	1143
RS 9	Amide III beta-sheet	1244	1264
RS 10	Amide III delta (CH) ₂	1275	1295
RS 11	Amide III alpha-helix	1322	1342
RS 12	CH ₂ stretch	1408	1428
RS 13	CH ₃ deformation	1448	1468
RS 14	Phenylalanine C=C	1596	1616
RS 15	Amide I alpha-helix	1647	1667

Table 3 Esophageal and gastric samples and histopathological diagnosis along with TNM classification

Sample number	Patient	Pathological diagnosis (UICC TNM classification)
Eso-1	50-year-old, female	SCC, pT1a (LPM)
Eso-2	65-year-old, male	SCC, pT1a (LPM)
Eso-3	61-year-old, male	SCC, pT1a (MM)
Eso-4	61-year-old, male	SCC, pTis
Eso-5	61-year-old, male	SCC, pTis
Eso-6	78-year-old, female	SCC, pT1b (SM)
Sto-1	72-year-old, female	Tub1, pT1a
Sto-2	63-year-old, male	Tub1>tub2, pT1b2
Sto-3	56-year-old, male	Tub1, pT1b1
Sto-4	58-year-old, male	Tub1, pT1b1
Sto-5	79-year-old, male	Tub1, pT1b1
Sto-6	77-year-old, male	Tub1, pT1a
Sto-7	80-year-old, male	Tub1, pT1b1
Sto-8	80-year-old, male	Tub1, pT1a
Sto-9	65-year-old, male	Tub1, pT1a
Sto-10	68-year-old, male	Tub1, pT1a
Sto-11	66-year-old, female	Tubular adenoma
Sto-12	38-year-old, female	Carcinoid tumor (NET G1), pT1b

Tub1: Well differentiated tubular adenocarcinoma. UICC: Union for International Cancer Control; SCC: Squamous cell carcinoma; TNM: Tumor node metastasis.

Table 4 Raman shift peaks observed in the esophageal and the gastric samples

	Peak 1	Peak 2	Peak 3
Esophagus	RS 8	RS 1	RS 13
Stomach	RS12	RS 5	RS 15

Table 5 Cut-off ratios obtained from the esophagus and stomach samples

	Cut-off 1 (peak 2/peak 1)	Cut-off 2 (peak 3/peak 1)
Esophagus	0.65	2.0
Stomach	1.85	2.0

scattered light intensity of Skeletal C-C stretch was Peak 1, the scattered light intensity of Phenylalanine C-C twist was Peak 2, the scattered light intensity of CH₃ deformation was Peak 3 (Table 4), and Peak 2/Peak 1 was defined as Cut-off 1. Peak 3/Peak 1 was defined as Cut-off 2 (Table 5). The site with more than half of the measurement points having Cut-off 1 greater than 0.65 and Cut-off 2 greater than 2.0 was determined to be the best match for histopathological SCC of the esophagus (Figure 2).

For gastric AC, the scattered light intensity of the CH₂ stretch was Peak 1, Phenylalanine ring breadth was Peak 2, and Amide I alpha helix was Peak 3 (Table 4). The ratio of Peak 2/Peak 1 was defined as Cut-off 1 and Peak 3/Peak 1 was defined as Cut-off 2 (Table 5). The site with more than half of the measurement points with Cut-off 1 greater than 1.85 and Cut-off 2 greater than 2.0 was determined to be the best match for the histopathological diagnosis of gastric AC (Figure 3).

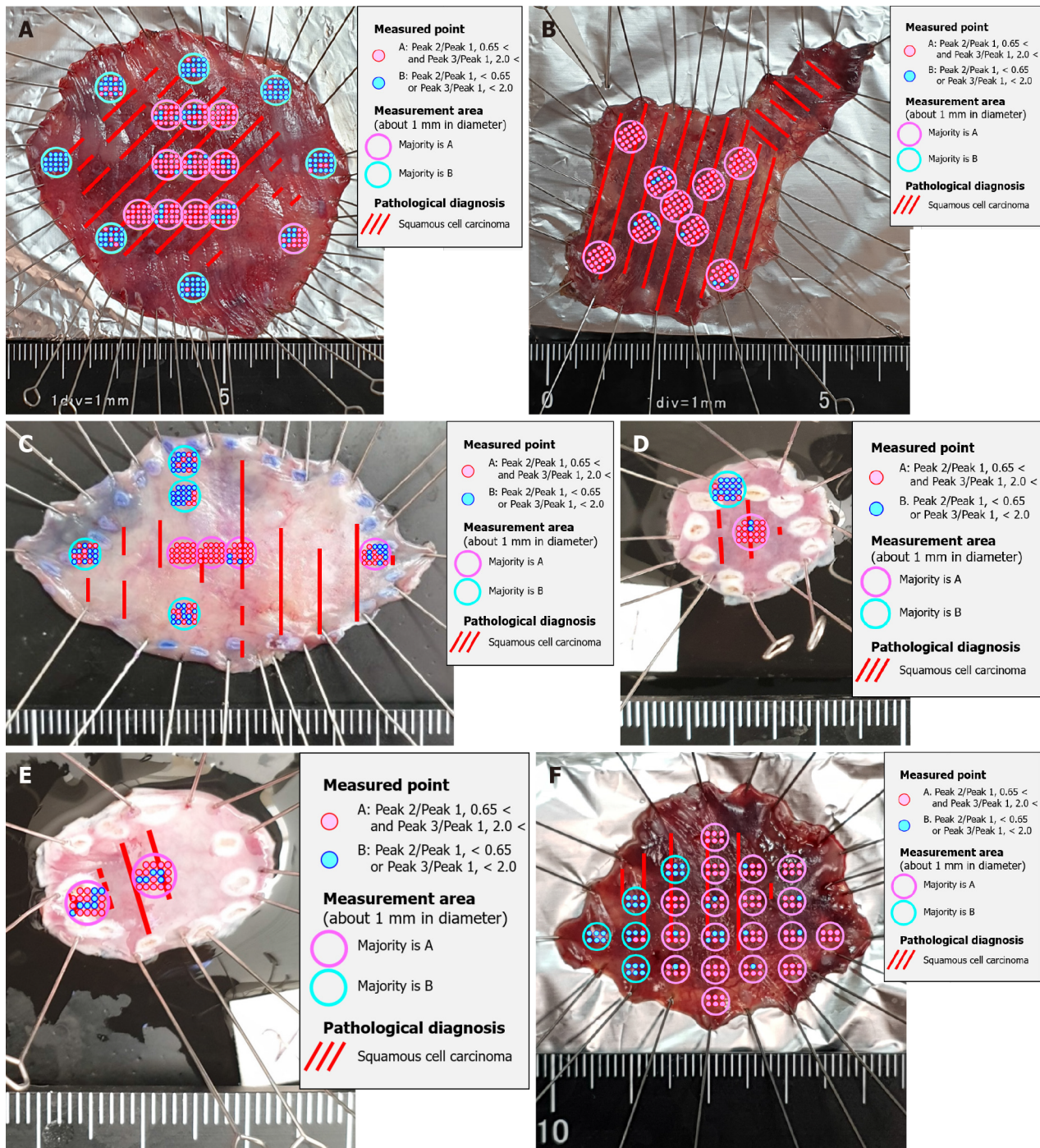
DISCUSSION

Patients with gastrointestinal cancers affecting the esophagus and stomach have symptoms, such as difficulty in swallowing, heartburn, and fullness[6]. Contrast examination or endoscopy is often performed in patients with a clinical evaluation suggestive of esophageal or gastric cancer[6]. Histopathological evaluation of the tissues obtained *via* endoscopic biopsy can be used to confirm the diagnosis[3, 4,6]. In recent years, the accuracy of endoscopic finding-based diagnoses has dramatically improved. One of the reasons for this is the better quality of images obtained through high-resolution camera optics[3,6].

It is highly possible that the ability to diagnose cancer will improve further if it is feasible to depict what cannot be delineated using conventional equipment by making the image richer in features. Another reason is the use of image classification algorithms based on artificial intelligence[13,16,19]. By recognizing and patterning endoscopic images using artificial intelligence, the existence of lesions is clarified, and diagnosis by doctors is supported. Since the diagnosis using artificial intelligence evaluates endoscopic images morphologically, it is possible to prevent the lesion from being overlooked [13,16]. However, its diagnostic ability is not higher than that of an experienced doctor. Another drawback is that diagnostic ability is greatly affected by the quality of the endoscopic image[5,9,14].

As mentioned above, the accuracy of endoscopic diagnosis of lesions in the gastrointestinal tract has greatly improved; however, it is still at the morphological interpretation level[6,7]. Histopathological diagnosis, which is the current definitive diagnostic method, is a form of morphological evaluation; moreover, qualitative information that assists in morphological evaluation is required to improve diagnostic accuracy beyond the existing practice. RS can be used to add qualitative information to the morphological information[2,20]. Short *et al*[1] published a technique for diagnosing lung cancer using bronchoscopy combined with RS. Lui *et al*[21] reported a method for diagnosing skin cancer using RS. Krishna *et al*[22] reported a method for diagnosing oral cancer using RS. Jermyn *et al*[20] reported that RS can be used to identify lesion areas during brain surgery. Furthermore, Bergholt *et al*[6] presented a diagnostic technique for esophageal disease in the gastrointestinal tract using RS, and published diagnostic techniques for gastric cancer[4]. Duraipandian *et al*[3] reported a diagnostic technique for gastric cancer using RS. Molckovsky *et al*[2] reported a diagnostic technique for colon cancer using RS. However, a standard method for analyzing living organisms and biological samples using RS is yet to be developed.

In this study, we selected 15 Raman shifts corresponding to constituent molecules in living tissues. The analysis results of the scattered light intensity of Raman shift of Skeletal C-C stretch, Phenylalanine C-C twist, and CH₃ deformation in SCC of the esophagus, and Raman shift of CH₂ stretch, Phenylalanine ring breadth, and Amide I alpha-helix in gastric AC. The results of the analysis of the scattered light intensity of the shift were in good agreement with the range of morphological cancer

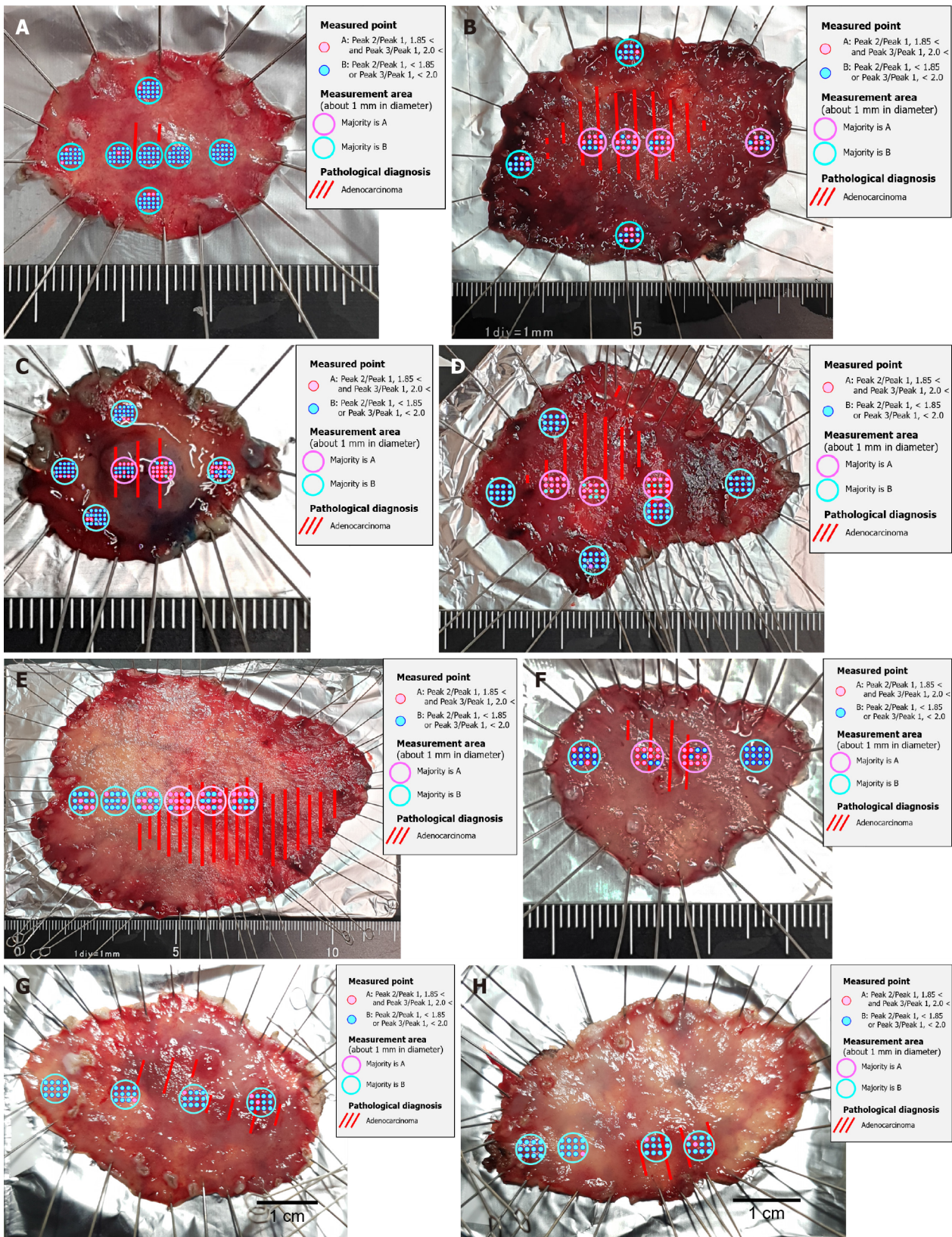


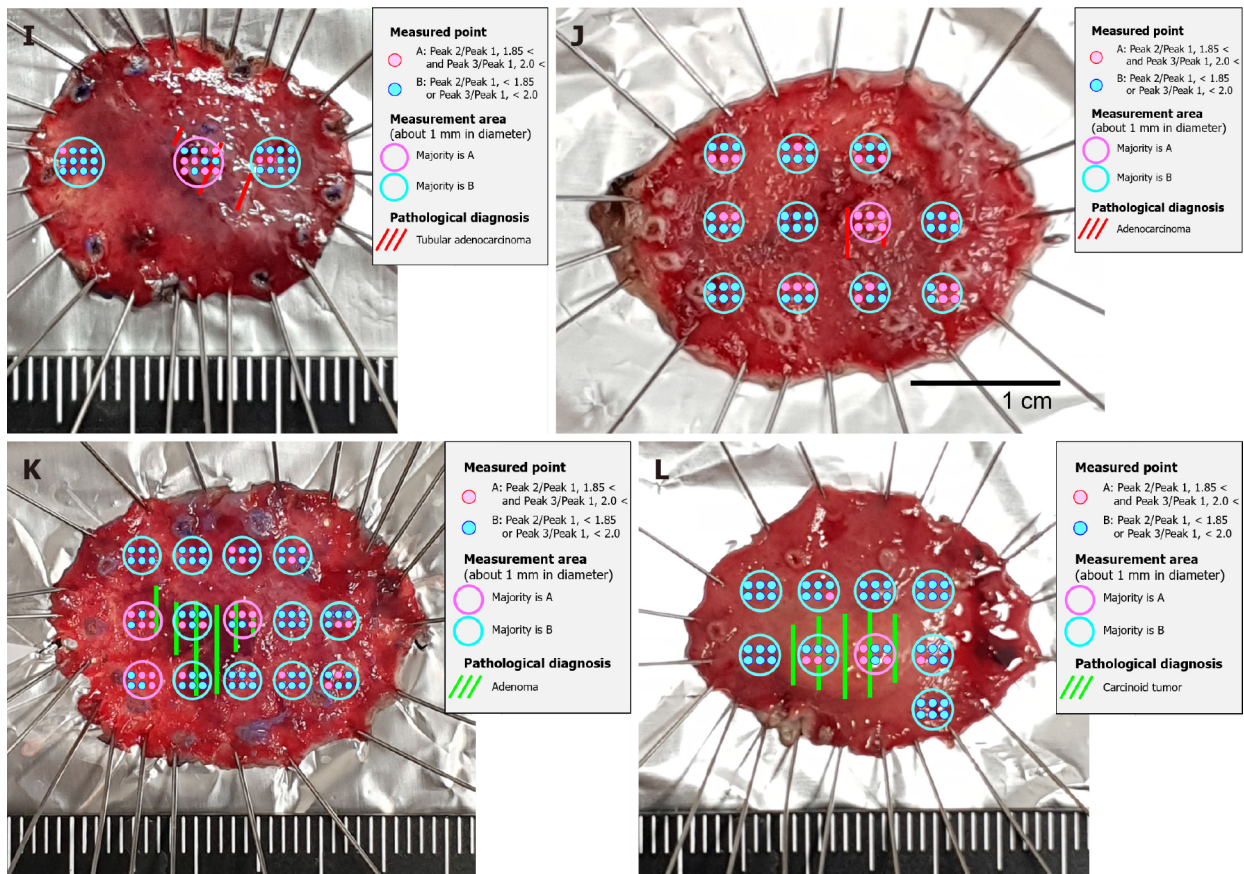
DOI: 10.3748/wjg.v29.i20.3145 Copyright ©The Author(s) 2023.

Figure 2 Comparison of Raman spectroscopic analysis and pathological diagnosis of sample Eso [squamous cell carcinoma, pT1a(LPM)-pT1b(SM)]. A: Eso-1; B: Eso-2; C: Eso-3; D: Eso-4; E: Eso-5; F: Eso-6.

diagnoses offered by histopathological evaluation. SCC of the esophagus and gastric AC are distinct types of cancers with different biological characteristics. Therefore, a significant Raman shift is expected to differ in the analysis conducted using RS. The technique presented in this study has the potential to provide qualitative evaluation in addition to the morphological evaluation currently used. In particular, it may offer valuable information regarding lesions that are challenging to assess using endoscopic or histopathological diagnoses alone.

However, at some sites, the results of this technique did not match the histopathological diagnoses. The limitations of this study include the small number of samples analyzed ($n = 18$), which included both the esophagus and stomach. Hence, there is no doubt that more samples must be analyzed in the future to confirm the accuracy of this technique. Using this technique, molecular information not solely dependent on morphological interpretation can be obtained. Furthermore, it may indicate the degree of mucosal abnormality from normal to cancerous. Evaluation of precancerous tissues may enable highly





DOI: 10.3748/wjg.v29.i20.3145 Copyright ©The Author(s) 2023.

Figure 3 Comparison of Raman spectroscopic analysis and pathological diagnosis of sample Sto (well-differentiated tubular adenocarcinoma, pT1a-pT1b1; tubular adenoma; carcinoid tumor, NET G1). A: Sto-1; B: Sto-2; C: Sto-3; D: Sto-4; E: Sto-5; F: Sto-6; G: Sto-7; H: Sto-8; I: Sto-9; J: Sto-10; K: Sto-11; L: Sto-12.

accurate preventive medicine. We aim to further advance this research and establish a method for predicting the current and future states of the gastrointestinal mucosa with high accuracy by clarifying the correlation between the Raman-scattered light intensity and the tissue state at each Raman shift.

CONCLUSION

Based on the results, it was concluded that RS could accurately identify esophageal SCC and gastric AC by analyzing the scattered light intensities of the 15 types of Raman shifts. The optimum combinations of Raman shifts were identified as Peak 1, Peak 2, and Peak 3 for both cancer types, with specific cut-off values for each peak. Although it is currently used in endoscopic treatment, the qualitative diagnosis of lesions, risk of residual lesions, *etc.*, can be confirmed in a short time by analyzing excised specimens, and treatment can be provided as necessary.

ARTICLE HIGHLIGHTS

Research background

Cancer diagnosis plays an important role in patient management, many researchers focused on the cancer detection, and novel, rapid, and label-free techniques are being developed for routine clinical practice.

Research motivation

To address the issue of using Raman spectroscopy (RS) to evaluate biological samples is interference of autofluorescence.

Research objectives

Our study is to evaluate the use of Raman-scattered light spectrum for detecting endoscopically resected specimens of esophageal squamous cell carcinoma (SCC) and gastric adenocarcinoma (AC).

Research methods

We created a Raman device, which is suitable for observing living tissues, and we attempted to acquire Raman-scattered light spectra in endoscopically resected specimens of six esophageal tissues and 12 gastric tissues. Furthermore, we performed a correlation between the obtained Raman scattered light spectra and histopathological diagnosis.

Research results

We obtained Raman scattered light spectra from all six esophageal and 12 gastric specimens successfully, and developed an algorithm to identify the range of esophageal SCC and gastric AC with an accuracy close to that of histopathological diagnoses.

Research conclusions

In this study, we utilized RS to rapidly detect cancer in resected esophageal and stomach specimens, providing information beyond morphology.

Research perspectives

By providing detailed molecular level data, RS can provide a more comprehensive understanding of disease processes and aid in accurate diagnosis.

FOOTNOTES

Author contributions: Ito H and Miyazaki T designed the study; Ito H was the guarantor, performed measurement, analysis, and interpretation of the data, and drafted the initial manuscript; Uragami N and Miyazaki T contributed to the acquisition, analysis, and interpretation of the data; Uragami N, Shimamura Y, Ikeda H, Nishikawa Y, Onimaru M, Matsuo K, and Isozaki M participated in the collection of the sample; Yang W designed and produced the Raman spectroscopy; Issha K continued importing the Raman spectroscopy; Kimura S, Kawamura M, Yokoyama N, Kushima M, and Inoue H revised the article critically for important intellectual content; Kushima M performed histopathological diagnosis of samples.

Supported by MEXT KAKENHI, JP17K09022 and JP20K07643.

Institutional review board statement: The study protocol was reviewed and approved (No. 18T5009) by the Institutional Review Board of Showa University Koto Toyosu Hospital.

Informed consent statement: All the participants provided written informed consent to participate in the study.

Conflict-of-interest statement: All the authors report no relevant conflicts of interest for this article.

Data sharing statement: No additional data are available.

STROBE statement: The authors read the STROBE Statement checklist of items and the manuscript was prepared and revised according to the STROBE guidelines.

Open-Access: This article is an open-access article that was selected by an in-house editor and fully peer-reviewed by external reviewers. It is distributed in accordance with the Creative Commons Attribution NonCommercial (CC BY-NC 4.0) license, which permits others to distribute, remix, adapt, build upon this work non-commercially, and license their derivative works on different terms, provided the original work is properly cited and the use is non-commercial. See: <https://creativecommons.org/licenses/by-nc/4.0/>

Country/Territory of origin: Japan

ORCID number: Hiroaki Ito 0000-0002-0761-0632; Naoyuki Uragami 0000-0003-2974-8250; Tomokazu Miyazaki 0000-0002-6108-8945; Yuto Shimamura 0000-0002-3831-8327; Haruo Ikeda 0000-0002-1690-8422; Manabu Onimaru 0000-0002-5368-8377; Kai Matsuo 0000-0001-7951-2444; William Yang 0000-0002-8476-3026; Satoshi Kimura 0000-0002-6843-8127; Machiko Kawamura 0000-0002-6138-1690; Noboru Yokoyama 0000-0003-1882-0018; Miki Kushima 0000-0002-1642-0478; Haruhiro Inoue 0000-0002-0551-7274.

S-Editor: Wang JJ

L-Editor: A

P-Editor: Liu JH

REFERENCES

- 1 **Short MA**, Lam S, McWilliams A, Zhao J, Lui H, Zeng H. Development and preliminary results of an endoscopic Raman probe for potential *in vivo* diagnosis of lung cancers. *Opt Lett* 2008; **33**: 711-713 [PMID: 18382526 DOI: 10.1364/OL.33.000711]
- 2 **Molckovsky A**, Song LM, Shim MG, Marcon NE, Wilson BC. Diagnostic potential of near-infrared Raman spectroscopy in the colon: differentiating adenomatous from hyperplastic polyps. *Gastrointest Endosc* 2003; **57**: 396-402 [PMID: 12612529 DOI: 10.1067/mge.2003.105]
- 3 **Duraipandian S**, Sylvest Bergholt M, Zheng W, Yu Ho K, Teh M, Guan Yeoh K, Bok Yan So J, Shabbir A, Huang Z. Real-time Raman spectroscopy for *in vivo*, online gastric cancer diagnosis during clinical endoscopic examination. *J Biomed Opt* 2012; **17**: 081418 [PMID: 23224179 DOI: 10.1117/1.JBO.17.8.081418]
- 4 **Bergholt MS**, Zheng W, Lin K, Ho KY, Teh M, Yeoh KG, So JB, Huang Z. Raman endoscopy for *in vivo* differentiation between benign and malignant ulcers in the stomach. *Analyst* 2010; **135**: 3162-3168 [PMID: 20941419 DOI: 10.1039/c0an00336k]
- 5 **Chakraborty A**, Ghosh A, Barui A. Advances in surface-enhanced Raman spectroscopy for cancer diagnosis and staging. *J Raman Spectrosc* 2020; **51**: 7-36 [DOI: 10.1002/jrs.5726]
- 6 **Bergholt MS**, Zheng W, Ho KY, Yeoh KG, Teh M, So JBY, Huang Z. Real-time depth-resolved Raman endoscopy for *in vivo* diagnosis of dysplasia in Barrett's esophagus. Proceedings of the SPIE BiOS; 2013 Mar 20; San Francisco, California, United States: Society of Photo-Optical Instrumentation Engineers, 2003
- 7 **Ito H**, Urugami N, Miyazaki T, Yang W, Issha K, Matsuo K, Kimura S, Arai Y, Tokunaga H, Okada S, Kawamura M, Yokoyama N, Kushima M, Inoue H, Fukagai T, Kamijo Y. Highly accurate colorectal cancer prediction model based on Raman spectroscopy using patient serum. *World J Gastrointest Oncol* 2020; **12**: 1311-1324 [PMID: 33250963 DOI: 10.4251/wjgo.v12.i11.1311]
- 8 **Wang K**, Qiu Y, Wu C, Wen ZN, Li Y. Surface-enhanced Raman spectroscopy and multivariate analysis for the diagnosis of oral squamous cell carcinoma. *J Raman Spectrosc* 2023; **54**: 355-362 [DOI: 10.1002/jrs.6495]
- 9 **Lei J**, Yang D, Li R, Dai Z, Zhang C, Yu Z, Wu S, Pang L, Liang S, Zhang Y. Label-free surface-enhanced Raman spectroscopy for diagnosis and analysis of serum samples with different types lung cancer. *Spectrochim Acta A Mol Biomol Spectrosc* 2021; **261**: 120021 [PMID: 34116414 DOI: 10.1016/j.saa.2021.120021]
- 10 **Yue X**, Wang Y, Guo D, He G, Sui C, Qu Z, Zhao Y, Liu X. Surface-enhanced Raman spectroscopy is an accurate technique in diagnosis of breast cancer: A meta-analysis. *J Raman Spectrosc* 2022; **53**: 2058-2067 [DOI: 10.1002/jrs.6437]
- 11 **Falamas A**, Faur CI, Baciut M, Rotaru H, Chirila M, Cinta Pinzaru S, Hedesiu M. Raman spectroscopic characterization of saliva for the discrimination of oral squamous cell carcinoma. *Anal Lett* 2020; **54** [DOI: 10.1080/00032719.2020.1719129]
- 12 **Zhang H**, Cheng C, Gao R, Yan Z, Zhu Z, Yang B, Chen C, Lv X, Li H, Huang Z. Rapid identification of cervical adenocarcinoma and cervical squamous cell carcinoma tissue based on Raman spectroscopy combined with multiple machine learning algorithms. *Photodiagnosis Photodyn Ther* 2021; **33**: 102104 [PMID: 33212265 DOI: 10.1016/j.pdpdt.2020.102104]
- 13 **Zhang L**, Wu Y, Zheng B, Su L, Chen Y, Ma S, Hu Q, Zou X, Yao L, Yang Y, Chen L, Mao Y, Ji M. Rapid histology of laryngeal squamous cell carcinoma with deep-learning based stimulated Raman scattering microscopy. *Theranostics* 2019; **9**: 2541-2554 [PMID: 31131052 DOI: 10.7150/thno.32655]
- 14 **Zhan Q**, Li Y, Yuan Y, Liu J. The accuracy of Raman spectroscopy in the detection and diagnosis of oral cancer: A systematic review and meta-analysis. *J Raman Spectrosc* 2020; **51**: 2377-2397 [DOI: 10.1002/jrs.5940]
- 15 **Zheng C**, Qing S, Wang J, Lü G, Li H, Lü X, Ma C, Tang J, Yue X. Diagnosis of cervical squamous cell carcinoma and cervical adenocarcinoma based on Raman spectroscopy and support vector machine. *Photodiagnosis Photodyn Ther* 2019; **27**: 156-161 [PMID: 31136828 DOI: 10.1016/j.pdpdt.2019.05.029]
- 16 **Yu M**, Yan H, Xia J, Zhu L, Zhang T, Zhu Z, Lou X, Sun G, Dong M. Deep convolutional neural networks for tongue squamous cell carcinoma classification using Raman spectroscopy. *Photodiagnosis Photodyn Ther* 2019; **26**: 430-435 [PMID: 31082525 DOI: 10.1016/j.pdpdt.2019.05.008]
- 17 **Böğözi T**, Popp J, Frosch T. Fiber-enhanced Raman multi-gas spectroscopy: what is the potential of its application to breath analysis? *Bioanalysis* 2015; **7**: 281-284 [PMID: 25697186 DOI: 10.4155/bio.14.299]
- 18 **Wachsmann-Hogiu S**, Weeks T, Huser T. Chemical analysis *in vivo* and *in vitro* by Raman spectroscopy--from single cells to humans. *Curr Opin Biotechnol* 2009; **20**: 63-73 [PMID: 19268566 DOI: 10.1016/j.copbio.2009.02.006]
- 19 **Xia J**, Zhu L, Yu M, Zhang T, Zhu Z, Lou X, Sun G, Dong M. Analysis and classification of oral tongue squamous cell carcinoma based on Raman spectroscopy and convolutional neural networks. *J Mod Opt* 2020; **67**: 481-489 [DOI: 10.1080/09500340.2020.1742395]
- 20 **Jermyn M**, Mok K, Mercier J, Desroches J, Pichette J, Saint-Arnaud K, Bernstein L, Guiot MC, Petrecca K, Leblond F. Intraoperative brain cancer detection with Raman spectroscopy in humans. *Sci Transl Med* 2015; **7**: 274ra19 [PMID: 25673764 DOI: 10.1126/scitranslmed.aaa2384]
- 21 **Lui H**, Zhao J, McLean D, Zeng H. Real-time Raman spectroscopy for *in vivo* skin cancer diagnosis. *Cancer Res* 2012; **72**: 2491-2500 [PMID: 22434431 DOI: 10.1158/0008-5472.CAN-11-4061]
- 22 **Krishna H**, Majumder SK, Chaturvedi P, Sidramesh M, Gupta PK. *In vivo* Raman spectroscopy for detection of oral neoplasia: a pilot clinical study. *J Biophotonics* 2014; **7**: 690-702 [PMID: 23821433 DOI: 10.1002/jbio.201300030]

Observational Study

Real-time continuous image guidance for endoscopic retrograde cholangiopancreatography based on 3D/2D registration and respiratory compensation

Da-Ya Zhang, Shuo Yang, Hai-Xiao Geng, Yu-Jia Yuan, Chi-Jiao Ding, Jian Yang, Ming-Yang Li

Specialty type: Surgery**Provenance and peer review:**

Unsolicited article; Externally peer reviewed.

Peer-review model: Single blind**Peer-review report's scientific quality classification**

Grade A (Excellent): 0

Grade B (Very good): B, B

Grade C (Good): C

Grade D (Fair): 0

Grade E (Poor): 0

P-Reviewer: Donato G, Italy;
Lucke-Wold B, United States**Received:** February 27, 2023**Peer-review started:** February 27, 2023**First decision:** March 28, 2023**Revised:** April 7, 2023**Accepted:** April 18, 2023**Article in press:** April 18, 2023**Published online:** May 28, 2023**Da-Ya Zhang, Ming-Yang Li**, Department of Gastroenterology, The First Medical Center, Chinese PLA General Hospital, Beijing 100853, China**Shuo Yang, Hai-Xiao Geng, Yu-Jia Yuan, Chi-Jiao Ding, Jian Yang**, School of Optics and Photonics, Beijing Institute of Technology, Beijing 100081, China**Corresponding author:** Ming-Yang Li, PhD, Chief Physician, Doctor, Department of Gastroenterology, The First Medical Center, Chinese PLA General Hospital, No. 28 Fuxing Road, Haidian District, Beijing 100853, China. mingyangli_pla@163.com

Abstract

BACKGROUND

It has been confirmed that three-dimensional (3D) imaging allows easier identification of bile duct anatomy and intraoperative guidance of endoscopic retrograde cholangiopancreatography (ERCP), which reduces the radiation dose and procedure time with improved safety. However, current 3D biliary imaging does not have good real-time fusion with intraoperative imaging, a process meant to overcome the influence of intraoperative respiratory motion and guide navigation. The present study explored the feasibility of real-time continuous image-guided ERCP.

AIM

To explore the feasibility of real-time continuous image-guided ERCP.

METHODS

We selected 2 3D-printed abdominal biliary tract models with different structures to simulate different patients. The ERCP environment was simulated for the biliary phantom experiment to create a navigation system, which was further tested in patients. In addition, based on the estimation of the patient's respiratory motion, preoperative 3D biliary imaging from computed tomography of 18 patients with cholelithiasis was registered and fused in real-time with 2D fluoroscopic sequence generated by the C-arm unit during ERCP.

RESULTS

Continuous image-guided ERCP was applied in the biliary phantom with a registration error of $0.46 \text{ mm} \pm 0.13 \text{ mm}$ and a tracking error of $0.64 \text{ mm} \pm 0.24$

mm. After estimating the respiratory motion, 3D/2D registration accurately transformed preoperative 3D biliary images to each image in the X-ray image sequence in real-time in 18 patients, with an average fusion rate of 88%.

CONCLUSION

Continuous image-guided ERCP may be an effective approach to assist the operator and reduce the use of X-ray and contrast agents.

Key Words: Endoscopic retrograde cholangiopancreatography; Three-dimensional images; Registration; Cholelithiasis; Hilar cholangiocarcinoma

©The Author(s) 2023. Published by Baishideng Publishing Group Inc. All rights reserved.

Core Tip: Three-dimensional imaging allows easier identification of bile duct anatomy and intraoperative guidance of endoscopic retrograde cholangiopancreatography (ERCP). Continuous image-guided ERCP may be an effective means to assist the operator and reduce the use of X-ray and contrast agents.

Citation: Zhang DY, Yang S, Geng HX, Yuan YJ, Ding CJ, Yang J, Li MY. Real-time continuous image guidance for endoscopic retrograde cholangiopancreatography based on 3D/2D registration and respiratory compensation. *World J Gastroenterol* 2023; 29(20): 3157-3167

URL: <https://www.wjgnet.com/1007-9327/full/v29/i20/3157.htm>

DOI: <https://dx.doi.org/10.3748/wjg.v29.i20.3157>

INTRODUCTION

Endoscopic retrograde cholangiopancreatography (ERCP) was first described by McCune *et al*[1] at George Washington University in 1968. Superselection of difficult bile ducts contributes to a higher incidence of adverse events, as well as increased radiation exposure for patients and endoscopists[2,3]. Recent studies have shown that even low doses of radiation may induce carcinogenic effects[4]. The radiation dose is one of the recommended quality indicators for ERCP[5,6]. Furthermore, injection of a contrast medium is considered a risk factor for post-ERCP pancreatitis and cholangitis[7]. Therefore, developing new technologies to enhance the efficacy and safety of ERCP is urgent.

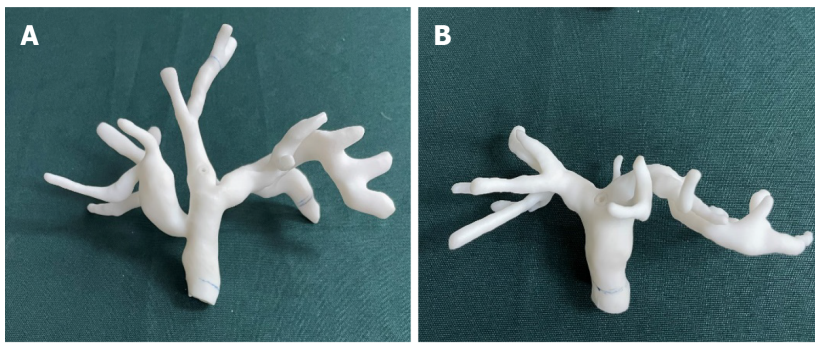
Preoperative three-dimensional (3D) imaging is widely used for planning in interventional radiosurgery. Three-dimensional computed tomography (3D-CT) has been utilized in transcatheter arterial chemoembolization (TACE), and allows for better visualization of small vessels[8,9]. Transjugular intrahepatic portosystemic shunt (TIPS) combines preoperative 3D-CT images with images taken at the time of intervention, and has demonstrated a significant reduction in operation times and radiation doses[10]. Three-dimensional imaging is also beneficial in guiding therapeutic ERCP[11], as it allows easier identification of bile duct anatomy and guides intraoperative navigation, reducing necessary radiation dose and operation time with improved safety[11]. For example, biliary stent placement *via* ERCP in the setting of indeterminate biliary stricture, the X-ray exposure time was reduced from 8.1 min to 35.1 min. However, current 3D biliary imaging does not have good real-time fusion with intraoperative images.

Here, we explored the feasibility of real-time continuous image-guided ERCP, which overcomes the influence of intraoperative respiratory motion and provides an accurate navigation method. Preoperative 3D-CT bile duct sequences were registered and fused with real-time 2D images from the C-arm taken during ERCP; this strategy may improve the quality of ERCP.

MATERIALS AND METHODS

Study population

This was a single-centered prospective observational study of patients receiving ERCP at a tertiary care hospital between July 2021 and March 2022. Twenty patients with cholelithiasis undergoing therapeutic ERCP were recruited. Only patients with a preoperative 3D-CT sequence of the bile duct were eligible. Dynamic 2D images of the bile duct generated by the fluoroscopic C-arm were obtained. Exclusion criteria were: age < 18 y, poor general health, inability to tolerate basic or intravenous anesthesia, uncontrollable coagulation disorder, anticoagulation therapy that could not be discontinued, altered anatomy (*e.g.*, Billroth II gastrectomy or Roux-en-Y anastomosis), pregnancy, and intraoperative



DOI: 10.3748/wjg.v29.i20.3157 Copyright ©The Author(s) 2023.

Figure 1 Biliary phantom setup. A: Biliary model based on patient A; B: Biliary model based on patient B.



DOI: 10.3748/wjg.v29.i20.3157 Copyright ©The Author(s) 2023.

Figure 2 Surgical environment for endoscopic retrograde cholangiopancreatography phantom. A: Respiratory motion simulator; B: X-ray fluoroscopy guidance in navigation.

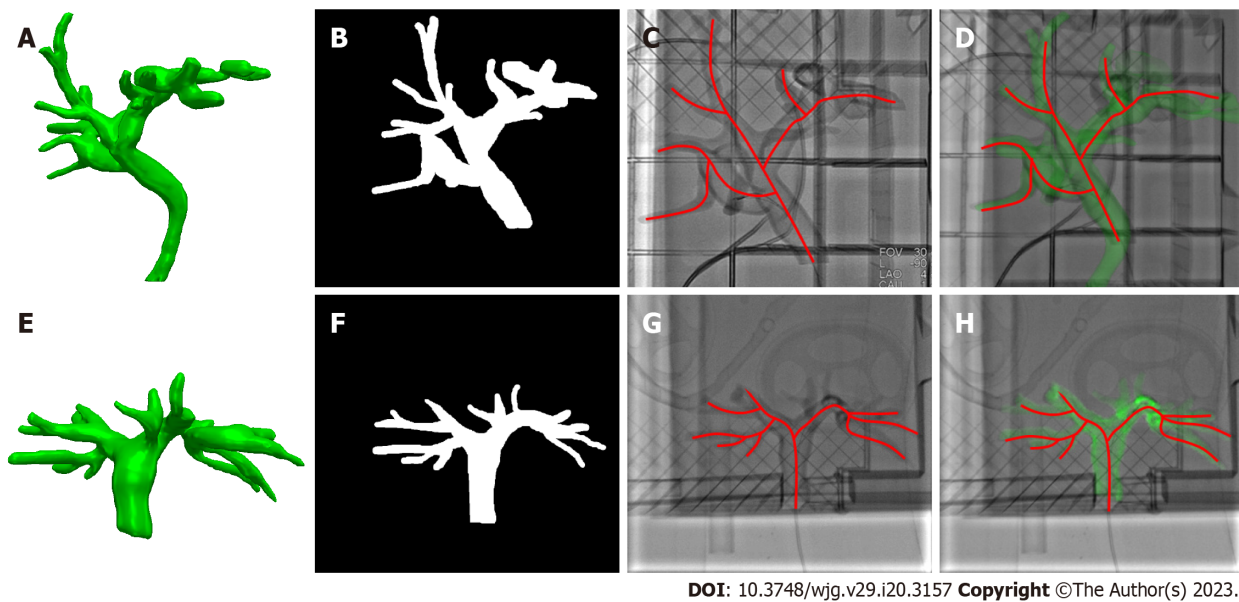
placement of a biliopancreatic stent. Written informed consent was obtained from all patients. The study was approved by the Ethics Committee of the Chinese People's Liberation Army (PLA) General Hospital (No. S2021-415-01) and was conducted per the Declaration of Helsinki.

Human biliary phantom

To verify the accuracy of our 3D/2D registration algorithm, we created 2 3D-printed biliary tract models with different structures to simulate different patients. Enhanced CT scan data of 2 patients with biliary dilatation were inputted into a 3D biomechanics research software tool (Visual 3D, Beijing, China). The operator manually segmented the contours of the biliary tract to acquire surface models. The acquired surface models were inputted into a Stratasys J750 3D printer (Markforged, Watertown, Massachusetts) and printed using resin (Figure 1). The printed phantom was life-sized and hollow, allowing sphincterotomes to enter. The phantom experiment was carried out in the PLA General Hospital operating room (Figure 2). Unlike in clinical experiments, model experiments could be repeated many times to simulate real intraoperative conditions to adjust the algorithm parameters.

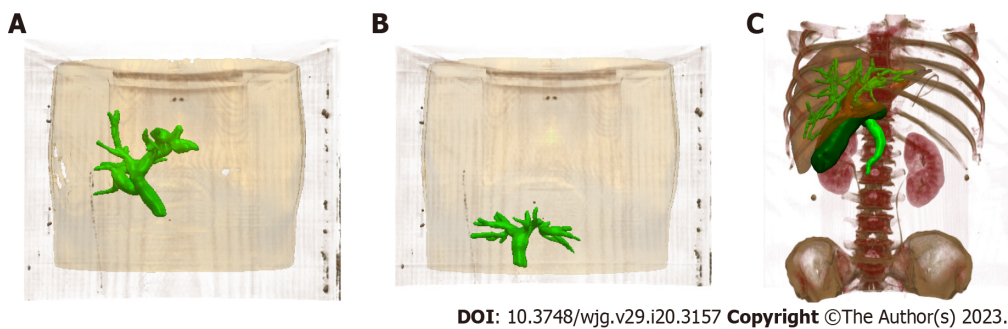
CT and fluoroscopic imaging

An iopromide contrast medium (Ultravist 370; Bayer Healthcare, Leverkusen, Germany) was diluted to visualize the biliary tract. All CT scans were performed in the Imaging Department of PLA General Hospital (uCT 510; United Imaging Healthcare, Shanghai, China) with a slice thickness of 1.25 mm and a tube voltage of 120 kV. Patients were asked to remain in the end-inspiratory state for CT scan. To acquire the best alignment transformation, patients were asked to maintain the same pre-operative state at the beginning of surgery. Then, fluoroscopy was performed and the image was defined as the best matching frame. On the day of the ERCP procedure, the acquired CT scan data were imported into Mimics (Materialise, Belgium) to reconstruct the 3D volume-render models of the biliary tract, liver, gallbladder, and bone. All patients received intraoperative deep sedation. ERCP was performed using a standard endoscope (Olympus Duodenoscope TJF260). When the guidewire was successfully superselected in the bile duct and the contrast agent was injected into the duct, the C-arm system performed 1 consecutive respiratory cycle of fluoroscopy around the patient, producing approximately 20 images which were transmitted in real time to our image navigation system.



DOI: 10.3748/wjg.v29.i20.3157 Copyright ©The Author(s) 2023.

Figure 3 Phantom study of registration and fusion. A and E: Biliary phantom segmentation using computed tomography images; B and F: Biliary phantom segmentation using X-ray fluoroscopy; C and G: Biliary lumen centerline extraction; D and H: Three-dimensional biliary model registered with the best matching frame using X-ray fluoroscopy.



DOI: 10.3748/wjg.v29.i20.3157 Copyright ©The Author(s) 2023.

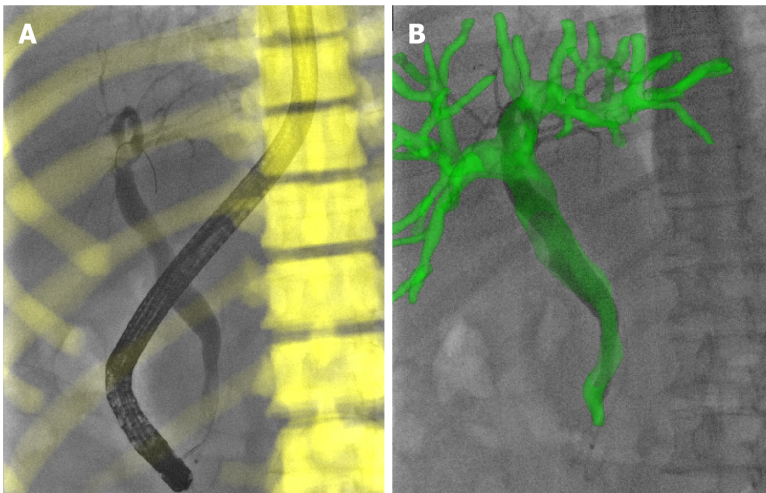
Figure 4 Automatic segmentation of structures based on preoperative computed tomography. A and B: Biliary and skin phantoms of different patients; C: Bone, liver, biliary tract, and gallbladder segmented by a three-dimensional UNet network based on preoperative computed tomography data.

CT co-registration and fusion with the fluoroscopic image

During the registration between CT and X-ray fluoroscopic images, the CT image was aligned with X-ray fluoroscopy through common features. For the biliary phantom, the registration fiducials were extracted from the CT and X-ray images, respectively, to get rigid transformation, by which the 3D biliary model segmented from CT was projected onto the X-ray fluoroscopic image to finish the overlap of biliary roadmapping. The biliary ducts were observed with X-ray images without contrast agents during model experimentation (Figure 3). After the 3D/2D registration was completed, the biliary ducts segmented from CT were projected onto the X-ray image, and the validity of the registration was judged according to the edge blending effect.

The bone, liver, gallbladder, and biliary tract were segmented by a 3D-UNet model based on preoperative CT data (Figure 4). Afterward, the Medical Imaging Interaction Toolkit was used to extract 2D bone structures. Mimics software (Materialise, Leuven, Belgium) was used to extract 3D and 2D biliary centerlines for analysis. Finally, 3D/2D registration based on bone structures was performed to achieve effective fusion of the 3D biliary model and the best matching frame (Figure 3).

The respiratory motion of the patient during the operation affects fusion accuracy. Some researchers have estimated the patient's respiratory state by extracting diaphragm data in real time[12-15]. The diaphragm-based method not only requires manual annotation, but also cannot guarantee real-time performance, thus prolonging the operation time and increasing X-ray radiation exposure. The method based on X-ray image centroid extraction was used in the current study to estimate the respiratory state [9] and monitor the motion change between frames through X-ray image gray distribution. The respiratory motion curve was acquired and used to complete continuous compensation for the fluoroscopy sequence, and real-time biliary roadmapping projected onto X-ray fluoroscopy was completed. This 3D/2D image registration technology is available in the current intraoperative imaging



DOI: 10.3748/wjg.v29.i20.3157 Copyright ©The Author(s) 2023.

Figure 5 Registration and fusion on the best matching frame of the patient. A: Three-dimensional/two-dimensional registration based on bone during endoscopic retrograde cholangiopancreatography; B: Overlay the biliary model on X-ray fluoroscopy through the transformation from bone registration.

system takes approximately 60 s. Our method has a fast calculation speed and is convenient to operate, features that aid in real-time navigation.

Data collection

Quantitative data included the registration error and the tracking error (TE). The registration error was calculated as the mean square error (MSE) between the projection of the 3D and 2D centerline. After finishing respiratory compensation and projecting, the mean MSE was set as the TE. Qualitative parameters included image quality and real-time fusion rates for both preoperative and intraoperative images.

Definitions

Image-guided ERCP: Image quality was defined as “good” if the 3D-CT and fluoroscopic images of the bile duct filled by a contrast medium were visible. The outcome of real-time fusion rates was assessed by the degree to which the bile duct in the fluoroscopic mode matched perfectly with the 3D-CT biliary imaging.

Statistical analysis

Data were assessed for normality, and appropriate descriptive statistics were calculated and expressed as mean \pm standard deviation (SD) and frequency (percentages). Data were analyzed using SPSS version 22 (IBM Corp., Armonk, NY, United States).

RESULTS

Image-guided ERCP had a mean registration error of $0.46 \text{ mm} \pm 0.13 \text{ mm}$ and a TE of $0.64 \text{ mm} \pm 0.24 \text{ mm}$. For patients, the biliary model was projected onto the X-ray based on 3D/2D registration (Figure 5), and the respiratory motion curve was estimated through a continuous X-ray fluoroscopy sequence (Figure 6). Continuous biliary roadmapping guidance was acquired (Figure 7). Our navigation system was performed in the operating room (Figure 8), and it provided image-based guidance in multiple patients (Figure 9). Image quality was good in all 18 cases and CT to X-ray fluoroscopic image registration and fusion were technically feasible, with an average fusion rate of 88% (Supplementary material).

DISCUSSION

In the current study, continuous image guidance for ERCP based on 3D/2D registration was evaluated, and we found that this strategy may be an effective means of real-time localization of the bile duct.

The prognosis of hilar cholangiocarcinoma (HCCA) is extremely poor, and surgery is the only radical treatment modality. However, most patients present with an unresectable tumor or cholangitis, high bilirubin, and insufficient volume of the residual liver; as such, biliary drainage by ERCP is often best

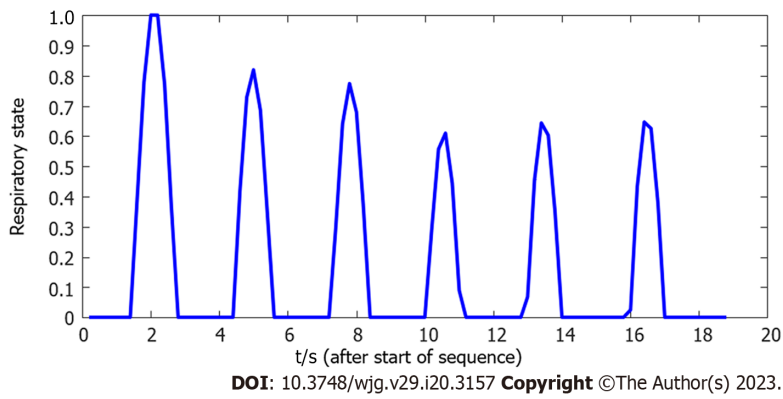


Figure 6 Example of the estimated respiratory state over an 18.8 s X-ray fluoroscopic image sequence.

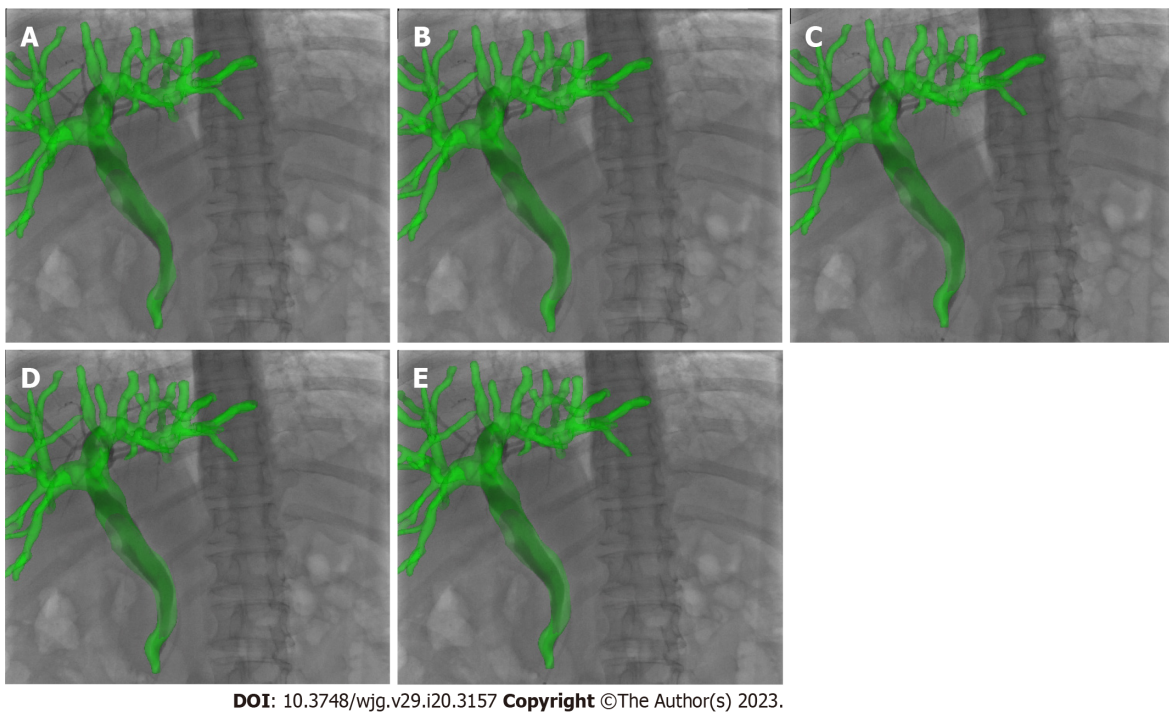
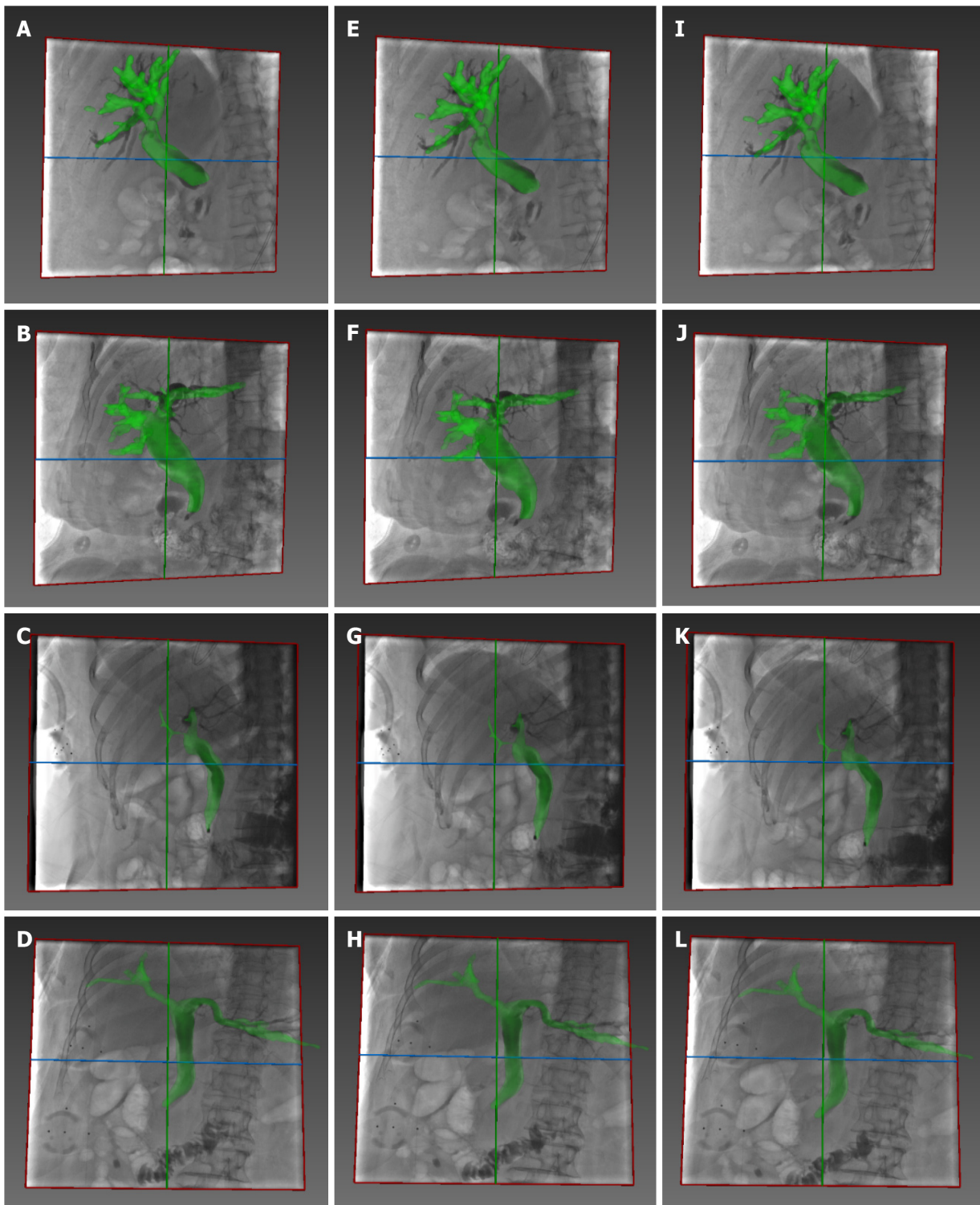


Figure 7 Real-time navigation of image-guided endoscopic retrograde cholangiopancreatography. A: Beginning of inhalation; B: During inhalation; C: End of inhalation; D: During exhalation; E: End of exhalation.



Figure 8 Image-guided endoscopic retrograde cholangiopancreatography navigation system.

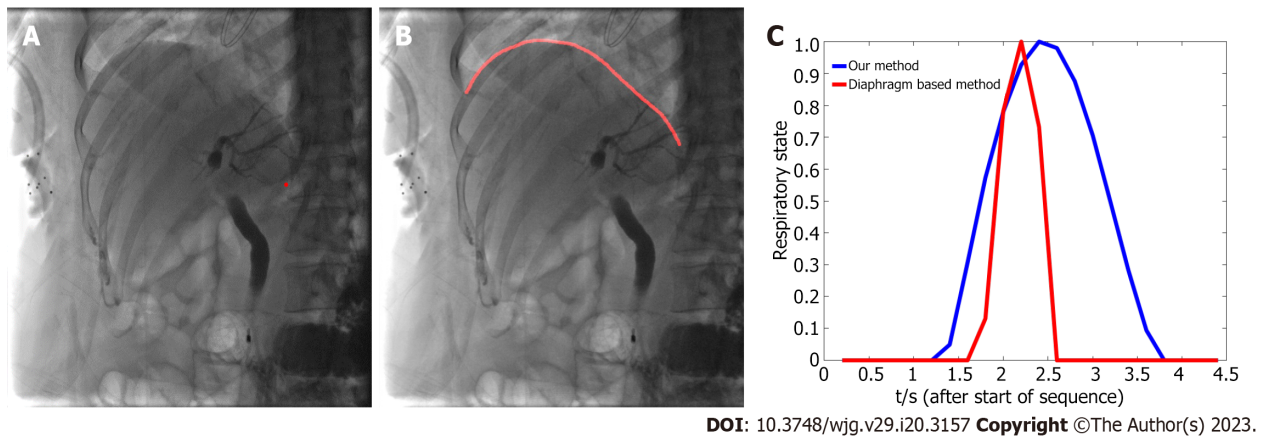
available treatment. Previous studies have shown the benefit of 3D imaging in guiding difficult ERCP procedures[11]. Preoperative 3D-CT, magnetic resonance cholangiopancreatography, magnetic resonance virtual endoscopy, or intraoperative 3D-CT of the cone beam have all provided adequate



DOI: 10.3748/wjg.v29.i20.3157 Copyright ©The Author(s) 2023.

Figure 9 Additional examples of real-time image guidance navigation. A-D: Beginning of the inhalation; E-H: During the inhalation; I-L: End of the inhalation.

guidance for biliary stenting in patients with HCCA, but do not achieve real-time fusion of 3D images with 2D fluoroscopic images or display guidewire or sphincterotomes in three dimensions[16-19]. Our technology can obtain 3D models of the biliary duct, tumor, and hilar vessels through preoperative magnetic resonance imaging/CT segmentation. The registration between preoperative 3D models and intraoperative 2D X-ray images was completed based on the centerlines of the biliary ducts, and 3D models were projected onto X-ray images for display. Meanwhile, based on the respiratory compensation method, a continuous fusion between 3D models and the X-ray image sequences was achieved, and real-time guidance was realized through graphics processing unit acceleration. We believe that our method may provide physicians with more visual information during surgery and



DOI: 10.3748/wjg.v29.i20.3157 Copyright ©The Author(s) 2023.

Figure 10 Comparison between two methods with respect to respiratory state estimation. A: Centroid of the X-ray image; B: Diaphragm of the X-ray image; C: Example of the estimated respiratory state over a 4.4 s X-ray image sequence.

effectively improve the operability of the intervention.

The present study reports real-time fusion of preoperative 3D-CT images with the 2D fluoroscopic images during ERCP. The radiation dose required for the registration between 3D-CT and fluoroscopic image can be considered negligible compared with the total radiation dose for difficult ERCP procedures. In addition, image registration was completed in an average time of 1 min, with a minimal overall increase in total operation time. Therefore, with the real-time visual aid during ERCP, it is likely that less radiation, contrast medium, and operative time may be required during the navigation.

Furthermore, our methods estimated the respiratory state better than the classical diaphragm extraction method[17]. Since the diaphragm is incomplete or invisible during ERCP in some patients, the applicability and robustness of our method are better based on image gray distribution. Furthermore, this method can achieve a more accurate estimation of the respiratory state of the biliary tract, thus ensuring better fusion of 3D-CT and 2D X-ray images. The main reason for this is that the respiratory motion of the diaphragm can reflect well upon the upper edge of the liver, but cannot directly represent the motion of the biliary tract. Experimental results also proved that our method is more accurate for biliary motion estimation of patients under free breathing. Compared with the TE of the diaphragm-based method, based on our cholangiography image fusion results, TE was relatively low ($1.68 \text{ mm} \pm 0.34 \text{ mm}$ vs $0.64 \text{ mm} \pm 0.24 \text{ mm}$), providing more accurate guidance. As shown in Figure 10, the respiratory state estimation based on our method was smoother and closer to the true breathing curve, which ensures the stability of image-guided navigation. Moreover, our method is simpler and faster to compute and process intraoperative X-ray fluoroscopic image sequences in real-time. Conversely, the diaphragm-based method requires real-time segmentation of the diaphragm whether manual or network methods are used, which represents a complex task and ultimately leads to an increase in operation time and radiation dose.

There are further implications of our technology in the context of other minimally invasive procedures such as TACE, TIPS, and spine surgery[8-10,20]. Coronavirus disease-2019 (COVID-19) had devastating impacts on healthcare system operations. The pandemic disrupted normal workflow of spine surgeries, restricting and postponing elective procedures[20]. This disruption may have resulted in the prolonged impairment of patients who were forced to postpone their procedures. Minimally invasive surgery and perioperative telemedicine are inevitable trends in spine surgery after COVID-19. Spine surgery is usually completed under the guidance of X-ray images, and physicians need to conceive the 3D structure of the patient's spine based on clinical experience. The spine is different from the soft liver and there is no respiratory interference; however, the similarity of the structure between the joints and the overall length makes surgery more difficult to perform only under the guidance of X-ray images. Meanwhile, the increase in operation time has also caused longer waiting periods for treatment. Our method can extract the 3D spine structure from preoperative CT and complete 3D/2D registration through the bone structure line, achieving the fusion of 3D information with intraoperative X-ray images. This technology could help physicians better localize lesions and enhance visual perception of depth. Fusion of 3D/2D imaging could also help physicians, especially those with insufficient clinical experience, to observe the patient's spine structure more intuitively and improve surgical efficiency. In summary, the number of spinal surgeries increased following COVID-19 and has continued to rise; our technology may help the hospital to perform more operations and allow patients to receive timely and effective treatment.

COVID-19 has also been associated with an increased risk for ischemic and hemorrhagic strokes[21], conditions often treated with a vascular intervention procedure very similar to TACE that is achieved by embolizing the vessels connected to the aneurysm. Unlike liver vessels, intracranial vessels are not affected by respiratory motion and remain static with the use of X-ray images for guidance. However,

intracranial vessels are generally thin and have multiple branching structures, and thus the risks associated with intracranial surgery are high. Surgeons require more clinical experience to ensure the accuracy of the surgery; otherwise, they may injure other blood vessels or tissues and cause secondary harm to the patient. Our technology can extract data regarding blood vessels connected to the lesion (*e.g.*, aneurysm) before the surgery and guide the surgeon intraoperatively through high-precision registration and fusion. Given the risk of intracranial vascular intervention procedures, our technology could display the vessels around the catheter and render them in different colors to remind the surgeon to be cautious, thus benefiting the safety of the procedure. We believe that our technology may have potential clinical value in treating cerebrovascular diseases and could precisely treat ischemic and hemorrhagic strokes associated COVID-19.

CONCLUSION

Our image-guided ERCP strategy was fully validated in models that may be useful in cannulating specific biliary ducts in patients with complex biliopancreatic diseases such as HCCA. However, clinical studies are still needed to determine if this new approach could improve technical success while reducing radiation exposure and contrast agent administration during ERCP.

ARTICLE HIGHLIGHTS

Research background

Three-dimensional (3D) imaging is beneficial in guiding therapeutic endoscopic retrograde cholangiopancreatography (ERCP), reducing the radiation dose and procedure time while increasing overall procedure safety. However, current 3D biliary imaging does not have good real-time fusion with intraoperative images.

Research motivation

We explored the feasibility of real-time continuous image-guided ERCP, which was shown to overcome the influence of intraoperative respiratory motion and provides an accurate navigation method.

Research objectives

To explore the feasibility of real-time continuous image-guided ERCP.

Research methods

We simulated an ERCP environment using an experimental biliary phantom with the aim of designing a navigation system; this system was further tested in patients undergoing ERCP.

Research results

Continuous image-guided ERCP was applied in the biliary phantom with low registration and tracking errors. This 3D/2D registration accurately transformed preoperative 3D biliary images to each image in the X-ray sequence in real-time.

Research conclusions

Continuous image-guided ERCP may be an effective approach to assist the operator and reduce the use of X-ray and contrast agents.

Research perspectives

Clinical studies are needed to determine if this image-guided ERCP strategy could improve technical success while reducing radiation exposure and contrast agent administration during ERCP.

FOOTNOTES

Author contributions: Yang S and Zhang DY designed the registration algorithm and finished the manuscript; Geng HX designed the experiment and revised the manuscript; Ding CJ and Yuan YJ collected the data; Yang J and Li MY made corrections to the article. Zhang DY and Yang S contributed equally to this work, and they are co-first authors; Li MY and Yang J contributed equally to this work, and they are co-corresponding authors.

Institutional review board statement: The study was reviewed and approved by the Ethics Committee of the General Hospital of the Chinese People's Liberation Army (approval No. S2021-415-01).

Informed consent statement: All study participants or their legal guardian(s) provided informed written consent prior to study enrollment.

Conflict-of-interest statement: The authors declare that they have no conflicts of interest.

Data sharing statement: All data and materials involved in the manuscript are available upon request.

STROBE statement: The authors have read the STROBE Statement – checklist of items, and the manuscript was prepared and revised according to the STROBE Statement – checklist of items.

Open-Access: This article is an open-access article that was selected by an in-house editor and fully peer-reviewed by external reviewers. It is distributed in accordance with the Creative Commons Attribution NonCommercial (CC BY-NC 4.0) license, which permits others to distribute, remix, adapt, build upon this work non-commercially, and license their derivative works on different terms, provided the original work is properly cited and the use is non-commercial. See: <https://creativecommons.org/licenses/by-nc/4.0/>

Country/Territory of origin: China

ORCID number: Da-Ya Zhang 0000-0001-6133-8919; Ming-Yang Li 0000-0003-1567-7121.

S-Editor: Chen YL

L-Editor: Filipodia

P-Editor: Chen YX

REFERENCES

- 1 **McCune WS**, Shorb PE, Moscovitz H. Endoscopic cannulation of the ampulla of Vater: a preliminary report. *Ann Surg* 1968; **167**: 752-756 [PMID: 5646296 DOI: 10.1097/0000658-196805000-00013]
- 2 **Weiser R**, Pencovich N, Mlynarsky L, Berliner-Senderey A, Lahat G, Santo E, Klausner JM, Nachmany I. Management of endoscopic retrograde cholangiopancreatography-related perforations: Experience of a tertiary center. *Surgery* 2017; **161**: 920-929 [PMID: 28027817 DOI: 10.1016/j.surg.2016.10.029]
- 3 **Fung BM**, Pitea TC, Tabibian JH. Difficult Biliary Cannulation in Endoscopic Retrograde Cholangiopancreatography: Definitions, Risk Factors, and Implications. *Eur Med J Hepatol* 2021; **9**: 64-72 [PMID: 34621527]
- 4 **Hong JY**, Han K, Jung JH, Kim JS. Association of Exposure to Diagnostic Low-Dose Ionizing Radiation With Risk of Cancer Among Youths in South Korea. *JAMA Netw Open* 2019; **2**: e1910584 [PMID: 31483470 DOI: 10.1001/jamanetworkopen.2019.10584]
- 5 **Adler DG**, Lieb JG 2nd, Cohen J, Pike IM, Park WG, Rizk MK, Sawhney MS, Scheiman JM, Shaheen NJ, Sherman S, Wani S. Quality indicators for ERCP. *Gastrointest Endosc* 2015; **81**: 54-66 [PMID: 25480099 DOI: 10.1016/j.gie.2014.07.056]
- 6 **Hayashi S**, Takenaka M, Hosono M, Nishida T. Radiation exposure during image-guided endoscopic procedures: The next quality indicator for endoscopic retrograde cholangiopancreatography. *World J Clin Cases* 2018; **6**: 1087-1093 [PMID: 30613666 DOI: 10.12998/wjcc.v6.i16.1087]
- 7 **Dumonceau JM**, Tringali A, Papanikolaou IS, Blero D, Mangiavillano B, Schmidt A, Vanbiervliet G, Costamagna G, Devière J, Garcia-Cano J, Gyökeres T, Hassan C, Prat F, Siersema PD, van Hooft JE. Endoscopic biliary stenting: indications, choice of stents, and results: European Society of Gastrointestinal Endoscopy (ESGE) Clinical Guideline - Updated October 2017. *Endoscopy* 2018; **50**: 910-930 [PMID: 30086596 DOI: 10.1055/a-0659-9864]
- 8 **Hammami H**, Lalys F, Rolland Y, Petit A, Haigron P. Catheter navigation support for liver radioembolization guidance: feasibility of structure-driven intensity-based registration. *Int J Comput Assist Radiol Surg* 2020; **15**: 1881-1894 [PMID: 32870445 DOI: 10.1007/s11548-020-02250-8]
- 9 **Wagner MG**, Periyasamy S, Longhurst C, McLachlan MJ, Whitehead JF, Speidel MA, Laeseke PF. Real-time respiratory motion compensated roadmaps for hepatic arterial interventions. *Med Phys* 2021; **48**: 5661-5673 [PMID: 34431111 DOI: 10.1002/mp.15187]
- 10 **Meine TC**, Dewald CLA, Becker LS, Mähringer-Kunz A, Maasoumy B, Maschke SK, Kirstein MM, Werncke T, Wacker FK, Meyer BC, Hinrichs JB. Correction to: Transjugular intrahepatic portosystemic shunt placement: portal vein puncture guided by 3D/2D image registration of contrast-enhanced multi-detector computed tomography and fluoroscopy. *Abdom Radiol (NY)* 2021; **46**: 398 [PMID: 32642854 DOI: 10.1007/s00261-020-02617-0]
- 11 **Wang Y**, Cao D, Chen SL, Li YM, Zheng YW, Ohkohchi N. Current trends in three-dimensional visualization and real-time navigation as well as robot-assisted technologies in hepatobiliary surgery. *World J Gastrointest Surg* 2021; **13**: 904-922 [PMID: 34621469 DOI: 10.4240/wjgs.v13.i9.904]
- 12 **Timinger H**, Krueger S, Dietmayer K, Borgert J. Motion compensated coronary interventional navigation by means of diaphragm tracking and elastic motion models. *Phys Med Biol* 2005; **50**: 491-503 [PMID: 15773725 DOI: 10.1088/0031-9155/50/3/007]
- 13 **Chen PY**. A novel network module for medical devices. *Annu Int Conf IEEE Eng Med Biol Soc* 2008; **2008**: 1553-1556 [PMID: 19162969 DOI: 10.1109/IEMBS.2008.4649466]
- 14 **King AP**, Boubertakh R, Rhode KS, Ma YL, Chinchapatnam P, Gao G, Tangcharoen T, Ginks M, Cooklin M, Gill JS, Hawkes DJ, Razavi RS, Schaeffter T. A subject-specific technique for respiratory motion correction in image-guided

- cardiac catheterisation procedures. *Med Image Anal* 2009; **13**: 419-431 [PMID: 19223220 DOI: 10.1016/j.media.2009.01.003]
- 15 **Shahshahani A**, Laverdiere C, Bhadra S, Zilic Z. Ultrasound Sensors for Diaphragm Motion Tracking: An Application in Non-Invasive Respiratory Monitoring. *Sensors (Basel)* 2018; **18** [PMID: 30096945 DOI: 10.3390/s18082617]
 - 16 **Toki M**, Tateishi H, Yoshida T, Gondo K, Watanabe S, Hisamatsu T. Utilization of a new technology of 3D biliary CT for ERCP-related procedures: a case report. *BMC Gastroenterol* 2020; **20**: 158 [PMID: 32448154 DOI: 10.1186/s12876-020-01304-0]
 - 17 **Reuterwall M**, Waldthaler A, Lubbe J, Kadesjö N, Pozzi Mucelli R, Del Chiaro M, Lohr M, Arnelo U. Bimodal ERCP, a new way of seeing things. *Endosc Int Open* 2020; **8**: E368-E376 [PMID: 32118109 DOI: 10.1055/a-1070-8749]
 - 18 **Azuma T**, Yamaguchi K, Iida T, Ouhida J, Suzuki M. MR virtual endoscopy for biliary tract and pancreatic duct. *Magn Reson Med Sci* 2007; **6**: 249-257 [PMID: 18239363 DOI: 10.2463/mrms.6.249]
 - 19 **Weigt J**, Pech M, Kandulski A, Malfertheiner P. Cone-beam computed tomography - adding a new dimension to ERCP. *Endoscopy* 2015; **47**: 654-657 [PMID: 25675173 DOI: 10.1055/s-0034-1391483]
 - 20 **Lucke-Wold B**, Cerillo JL, Becsey AN, Chernicki BP, Root KT. Minimally Invasive Procedures, Perioperative Telemedicine, and Decreased Hospital Stays Following Covid-19 Surgical Restrictions: Spinal Surgery. *Arch Med Case Rep Case Study* 2022; **6** [PMID: 36844926]
 - 21 **Small C**, Mehkri Y, Panther E, Felisma P, Lucke-Wold B. Coronavirus Disease-2019 and Stroke: Pathophysiology and Management. *Can J Neurol Sci* 2022; 1-8 [PMID: 35762309 DOI: 10.1017/cjn.2022.267]

Observational Study

Inflammation-related nomogram for predicting survival of patients with unresectable hepatocellular carcinoma received conversion therapy

Jia-Lin Wu, Jun-Yang Luo, Zai-Bo Jiang, Si-Bo Huang, Ge-Run Chen, Hui-Ying Ran, Qi-Yue Liang, Ming-Sheng Huang, Li-Sha Lai, Jun-Wei Chen

Specialty type: Oncology

Provenance and peer review:

Unsolicited article; Externally peer reviewed.

Peer-review model: Single blind

Peer-review report's scientific quality classification

Grade A (Excellent): 0
Grade B (Very good): B, B
Grade C (Good): 0
Grade D (Fair): 0
Grade E (Poor): 0

P-Reviewer: Li YW, China; Yang M, United States

Received: March 3, 2023

Peer-review started: March 3, 2023

First decision: March 24, 2023

Revised: April 2, 2023

Accepted: April 24, 2023

Article in press: April 24, 2023

Published online: May 28, 2023



Jia-Lin Wu, Jun-Yang Luo, Zai-Bo Jiang, Ming-Sheng Huang, Jun-Wei Chen, Department of Interventional Radiology, The Third Affiliated Hospital of Sun Yat-sen University, Guangzhou 510630, Guangdong Province, China

Si-Bo Huang, Ge-Run Chen, The First Clinical Medical College, Guangdong Medical University, Zhanjiang 524000, Guangdong Province, China

Hui-Ying Ran, Qi-Yue Liang, Zhongshan School of Medicine, Sun Yat-sen University, Guangzhou 510080, Guangdong Province, China

Li-Sha Lai, Department of Radiology, Guangzhou First People's Hospital, School of Medicine, South China University of Technology, Guangzhou 510010, Guangdong Province, China

Corresponding author: Jun-Wei Chen, MD, Professor, Interventional Radiologist, Department of Interventional Radiology, The Third Affiliated Hospital of Sun Yat-sen University, No. 600 Tianhe Road, Guangzhou 510630, Guangdong Province, China. chenjw53@mail.sysu.edu.cn

Abstract

BACKGROUND

The efficacy of conversion therapy for patients with unresectable hepatocellular carcinoma (HCC) is a common clinical concern.

AIM

To analyse the prognostic factors of overall survival (OS) in patients with unresectable HCC who received conversion therapy.

METHODS

One hundred and fifty patients who met the inclusion criteria were enrolled and divided into a training cohort ($n = 120$) and a validation cohort ($n = 30$). Using the independent risk factors in the training cohort, a nomogram model was constructed to predict OS for patients treated with transarterial chemoembolization following hepatic resection. The nomogram was internally validated with the bootstrapping method. The predictive performance of nomogram was assessed by Harrell's concordance index (C-index), calibration plot and time-dependent receiver operating characteristic curves and compared with six other

conventional HCC staging systems.

RESULTS

Multivariate Cox analysis identified that albumin, blood urea nitrogen, gamma-glutamyl transpeptidase to platelet ratio, platelet to lymphocyte ratio, macrovascular invasion and tumour number were the six independent prognostic factors correlated with OS in nomogram model. The C-index in the training cohort and validation cohort were 0.752 and 0.807 for predicting OS, which were higher than those of the six conventional HCC staging systems (0.563 to 0.715 for the training cohort and 0.458 to 0.571 for the validation cohort). The calibration plots showed good consistency between the nomogram prediction of OS and the actual observations of OS. Decision curve analyses indicated satisfactory clinical utility. With a total nomogram score of 196, patients were accurately classified into low-risk and high-risk groups. Furthermore, we have deployed the model into online calculators that can be accessed for free at <https://ctmodelforunresectablehcc.shinyapps.io/DynNomapp/>.

CONCLUSION

The nomogram achieved optimal individualized prognostication of OS in HCC patients who received conversion therapy, which could be a useful clinical tool to help guide postoperative personalized interventions and prognosis judgement.

Key Words: Hepatocellular carcinoma; Conversion therapy; Nomogram; Inflammation; Transarterial chemoembolization

©The Author(s) 2023. Published by Baishideng Publishing Group Inc. All rights reserved.

Core Tip: We developed and validated a prognostic nomogram based on inflammation-related biomarkers for patients with unresectable hepatocellular carcinoma after conversion therapy. The proposed conversion therapy model shows increased accuracy, good clinical utility, and better prognostic performance compared with conventional staging systems. Based on the total predictive risk scores, the patients were classified into two groups: low-risk (score < 196) and high-risk group (score ≥ 196), to guide postoperative adjuvant interventions and follow-ups. Furthermore, we have made this prognostic nomogram online for free use (<https://ctmodelforunresectablehcc.shinyapps.io/DynNomapp/>).

Citation: Wu JL, Luo JY, Jiang ZB, Huang SB, Chen GR, Ran HY, Liang QY, Huang MS, Lai LS, Chen JW. Inflammation-related nomogram for predicting survival of patients with unresectable hepatocellular carcinoma received conversion therapy. *World J Gastroenterol* 2023; 29(20): 3168-3184

URL: <https://www.wjgnet.com/1007-9327/full/v29/i20/3168.htm>

DOI: <https://dx.doi.org/10.3748/wjg.v29.i20.3168>

INTRODUCTION

Hepatocellular carcinoma (HCC), the most common type of primary liver cancer, ranks as the sixth most prevalent malignancy and third leading cause of cancer-related deaths worldwide[1]. More so than other cancers, hepatitis B virus (HBV) infection is a hallmark of HCC, with 70%-90% of diagnoses occurring with a background of cirrhosis in highly prevalent Asian countries[2]. Hepatic resection (HR) is deemed the most efficacious therapeutic option for patients diagnosed with early to intermediate stages of HCC. Unfortunately, the majority of Chinese patients with HCC are diagnosed at intermediate or advanced stages with massive or multifocal lesions. Nevertheless, HR is possible for a minority of carefully selected patients with the help of a “conversion therapy” strategy, which refers to conversion of an unresectable HCC to achieve adequate tumour shrinkage and downstaging to undergo HR. However, only a limited number of meticulously screened patients with intermediate or advanced stage HCC qualify for HR.

As per the Barcelona Clinic Liver Cancer (BCLC) staging system, transarterial chemoembolization (TACE) is recommended as the first-line treatment for intermediate stage HCC and has been extensively investigated and widely acknowledged as an effective approach for conversion therapy[3]. Previous studies have demonstrated that HR after local treatments, such as TACE, hepatic artery infusion chemotherapy and radiotherapy with or without other systemic therapeutic measures, can improve tumour shrinkage as well as downstaging. Moreover, these treatments have been shown to enhance patient survival rates without causing significant complications[4-7]. While TACE could potentially

provide surgical options to previously ineligible HCC patients, its high incidence of short-term recurrence remains a significant challenge for conversion therapy. Meanwhile, active conversion strategies to increase the volume of future liver remnant and planning for patients who cannot achieve R0 resection are worth greater consideration. Thus, the development of a validated clinical risk score based on preoperative indices to assess those at high risk of recurrence and death may help formulate optimal management strategies and prevent disease progression.

Links between inflammation and the development of cancer are well established, and HCC is one of the most classic inflammation-linked tumours. During liver inflammation, inflammatory cells and mediators are present before hepatocarcinogenesis and prompt the malignant activity of cancer cells. Additionally, a persistent cancer-related inflammatory microenvironment leads to immune suppression, which promotes the development of HCC[8]. Recently, numerous previous studies have indicated that preoperative inflammatory biomarkers can be capable of predicting HCC prognosis after HR[9,10]. A previous study by Wang *et al*[9] assessed the prognostic value of inflammation-related markers prior to surgery and demonstrated their high effectiveness in predicting survival after surgical resection of HCC. In addition, the researchers concluded that two inflammation-related markers, gamma-glutamyl transpeptidase (GGT) to platelet ratio (GPR) and neutrophil to lymphocyte ratio (NLR), were independently associated with prognosis. However, it is unclear whether preoperative inflammatory biomarkers have a high efficacy in predicting the overall survival (OS) of unresectable HCC patients following conversion therapy.

Nomograms have recently been used as an easy-to-operate predictive tool in HCC and have compared favorably to traditional tumour staging systems[10,11]. However, studies focusing on inflammatory biomarkers for the prognosis of HCC treated with TACE following HR are rare. Therefore, the aim of this study was to develop a conversion therapy model (CT model) that combined clinical factors, tumour radiologic features, inflammation biomarkers and TACE strategy for prognosis in patients with unresectable HCC successfully treated with conversion therapy. A browser-based calculator was developed to conveniently help guide individualized follow-up. A precise estimation of OS prognosis can assist clinical surgeons in selecting more appropriate therapeutic measures for recurrent patients through risk-benefit analysis.

MATERIALS AND METHODS

Study population and design

This study was conducted in accordance with the Declaration of Helsinki and approved by the Institutional Review Board of Ethical Committee of the Third Affiliated Hospital of Sun Yat-sen University (No. II2023-027). Due to the retrospective design of this study, written informed consent from patients was waived. Consecutive Chinese adult individuals with pathologically confirmed primary unresectable HCC who were treated with TACE following HR in our institution from January 2011 to July 2020 were enrolled. The inclusion criteria were as follows: (1) Age between 18 years and 80 years; (2) pathologically proven HCC; and (3) unresectable HCC according to the Chinese expert consensus and acceptance of TACE as the conventional therapy following HR[3]. The exclusion criteria were as follows: (1) Extrahepatic metastasis; (2) history of other malignancies; (3) previous anticancer therapy; (4) current or recent system infection disease and incomplete clinical data; and (5) death or loss to follow-up within 30 d after resection. One hundred fifty patients from our center were included in this study and randomly assigned to a training cohort ($n = 120$) and a validation cohort ($n = 30$). The flow chart of patient selection is shown in [Supplementary Figure 1](#).

Data collection and preoperative examination

For each patient, the following clinical parameters were collected: (1) Preoperative patient characteristics (age, sex, factor of HCC, aetiology of HCC, ascites, and Child-Pugh class); (2) TACE technique [conventional-TACE (cTACE) or drug eluting bead-TACE (DEB-TACE)] and number of TACE treatments; (3) baseline laboratory data, including alpha fetoprotein (AFP) level, white blood cell count, haemoglobin level, platelet count, neutrophil count, lymphocyte ratio, monocyte ratio, neutrophil ratio, aspartate aminotransferase (AST) level, alanine aminotransferase level, GGT level, albumin (ALB) level, total bilirubin level, blood urea nitrogen (BUN) level, serum creatinine level, urea level and prothrombin time (PT); (4) inflammation biomarkers, including GPR, NLR, lymphocyte to monocyte ratio, prognostic nutritional index, platelet to lymphocyte ratio (PLR), systemic immune inflammation index, neutrophil times GGT-to-lymphocyte ratio, AST to platelet ratio index, AST to neutrophil ratio index, and AST (the detailed formulas of inflammation biomarkers are summarized in [Supplementary Table 1](#)); (5) baseline tumour radiologic features [tumour number, largest tumour diameter, tumour capsule, macrovascular invasion (MVI)]; and (6) surgical factors (resection margin and blood transfusion).

TACE procedure and HR

The cTACE or DEB-TACE procedure was performed according to our previously reported protocol[12]. Repeated TACE was implemented according to a multidisciplinary treatment board (consisting of

interventional radiologists, liver surgeons, and medical oncologists) during the follow-up periods and after in-depth discussion with the patient. HR was performed according to the liver surgeons' assessment that the unresectable HCC had transformed into radically operable HCC. HR was performed by clinicians who possessed more than ten years of experience in hepatectomy. Under general anesthesia, HR was conducted through an L-shaped laparotomy or bilateral subcostal incision with a midline extension. Intraoperative ultrasound (US) was performed as standard practice to assess tumor burden, liver remnant, and resection margin[13]. Curative resection was defined as complete remove of all tumor nodules with no residual tumor margin (R0 resection), which was confirmed through pathological examination.

Follow-up and assessment

All patients were monitored in the first month post HR, then at three-month intervals for the first two years, and bi-annual assessments thereafter. During each follow-up, routine blood tests, liver function tests, AFP and imaging examinations (abdominal contrast-enhanced magnetic resonance imaging and computed tomography) were performed. Follow-up ended in July 2022. OS was described as the period from the initial TACE treatment to death attributable to any cause, and patients alive at the end of follow-up were recorded as censored.

Statistical analysis

The statistical analyses were conducted using R software (Version 4.2.1, <http://www.r-project.org>). Categorical variables are presented as *n* (%) and were compared using the chi-square test or Fisher's exact test. Continuous variables are reported as the mean \pm SD, compared by Student's *t* test, or median (interquartile range, IQR), compared by the Mann-Whitney *U* test. We determined the optimal cut-off value for continuous variables and inflammation biomarkers, except AFP and tumour diameter, based on the outcome of OS among all patients, using the "surv_cutpoint" function from the "survminer" R package. OS was calculated using the Kaplan-Meier method, and the log-rank test was used to construct survival curves. Univariate and multivariate Cox proportional hazard regression were conducted to select the independent factors of OS. All factors with *P* < 0.1 in univariate Cox regression were selected for multivariate Cox regression. The nomograms were created using multivariate analysis in the training cohort. The final model selection for the nomograms was determined by a backwards step-down process with the Akaike information criterion.

The predictive performance was measured by the concordance index (C-index) and time-dependent area under the curve (AUC). To assess the clinical utility of the nomogram, decision curve analysis (DCA) was performed by quantifying the net benefits relative to six other conventional HCC staging systems (including BCLC[14], American Joint Committee on Cancer Tumour-Node-Metastasis eighth edition (AJCC TNM 8th)[15], China liver cancer staging (CNLC)[16], Japan integrated staging (JIS)[17], Cancer of the Liver Italian Program (CLIP)[18] and Okuda staging system[19]). The total score of nomogram was used to categorize patients into low-risk and high-risk groups using X-tile[20]. A 2-sided *P* value of less than 0.05 in multivariate Cox regression was considered statistically significant.

RESULTS

Baseline characteristics

A total of 150 patients were recruited in this study and randomly divided into training (*n* = 120) and validation (*n* = 30) cohorts in an 8:2 ratio. The baseline characteristics of patients in the training and validation cohorts are summarized in Table 1. Among all patients, the mean age was 52.1 years (SD: 11.9), 128 (85.3%) patients were male, and 134 (89.3%) patients were HBsAg positive. Regarding TACE techniques, a total of 100 (66.7%) patients received cTACE therapy. In terms of surgical aspects, a resection margin larger than 1 cm was present in 133 patients (88.7%). Fifty-two patients (34.7%) required a blood transfusion during the perioperative period. The median size of the largest intrahepatic tumours was 62.5 mm (range: 10.0-191.0), and 100 (66.7%) were larger than 5.0 cm. More than half of the patients (*n* = 96, 64.0%) were with solitary tumour. Tumour radiologic features showed that well-defined tumour capsule, satellite nodules, and MVI were observed in 110 (73.3%), 36 (24.0%) and 68 (45.3%) patients, respectively. There were no statistically significant differences in baseline clinicopathological features between the training and validation cohorts.

Overall survival

In this study, the median follow-up was 31.5 (range: 4.0-112.0) months. The median survival of the entire cohort was 54 [95% confidence interval (CI): 42-95] mo (Figure 1A). The 1-, 2-, and 3-year OS rates for the training and validation cohorts were 87.5%, 49.3%, 44.2%, and 83.3%, 66.7%, 53.3%, respectively (Figure 1B and C). There was no significant difference observed in OS between the training and validation cohorts [mean OS 37.9 (range, 4-112) mo *vs* 38.0 (range, 5-93 mo, *P* = 0.7].

Table 1 Demographics and clinical characteristics of hepatocellular carcinoma patients

Variables	Training cohort (n = 120)	Validation cohort (n = 30)	Overall cohort (n = 150)	P value
Patient factors				
Age [yr, mean (SD)]	51.5 (12.1)	54.4 (10.9)	52.1 (11.9)	0.419
Sex, male/female	104/16 (86.7%/13.3%)	24/6 (80.0%/20.0%)	128/22 (85.3%/14.7%)	0.526
Etiology, HBV/other	109/11 (90.8%/9.2%)	25/5 (83.3%/16.7%)	134/16 (89.3%/10.7%)	0.39
Ascites, yes/no	20/100 (16.7%/83.3%)	7/23 (23.3%/76.7%)	27/123 (18.0%/82.0%)	0.559
Child-Pugh, A/B	114/6 (95.0%/5.0%)	29/1 (96.7%/3.3%)	143/7 (95.3%/4.7%)	1
Laboratory parameters				
AFP (ng/mL, ≤ 200/> 200)	68/52 (56.7%/43.3%)	15/15 (50.0%/50.0%)	83/67 (55.3%/44.7%)	0.652
HGB [g/dL, median (min, max)]	139 (72, 838)	139 (100, 162)	139 (72, 838)	0.714
PLT [count, × 10 ⁹ /L, median (min, max)]	197 (70, 950)	189 (97, 370)	192 (70, 950)	0.873
AST [U/L, median (min, max)]	36.0 (2, 471)	33.0 (16, 251)	35.0 (2, 471)	0.925
ALT [U/L, median (min, max)]	34.0 (9, 423)	29.0 (12, 329)	34.0 (9, 423)	0.541
ALB (g/L, ≤ 35/> 35)	18/102 (15.0%/85.0%)	2/28 (6.7%/93.3%)	20/130 (13.3%/86.7%)	0.368
TB [μmol/L, median (min, max)]	12.5 (3.2, 28.2)	12.9 (4.3, 30.9)	12.7 (3.2, 30.9)	0.996
GGT [U/L, median (min, max)]	59.5 (15, 435)	57.0 (22, 375)	59.0 (15, 435)	0.987
BUN (mmol/L, ≤ 6.7/> 6.7)	109/11 (90.8%/9.2%)	26/4 (86.7%/13.3%)	135/15 (90.0%/10.0%)	0.734
Creatinine [μmol/L, median (min, max)]	77.6 (23, 218)	74.0 (43, 110)	77.0 (23, 218)	0.263
UA [μmol/L, median (min, max)]	335 (172, 680)	329 (143, 572)	334 (143, 680)	0.899
PT [s, median (min, max)]	13.6 (11.1, 16.5)	13.6 (12.1, 15.6)	13.6 (11.1, 16.5)	0.212
Tumor factors				
Tumor number (1/2/≥ 3)	80/22/18 (66.7%/18.3%/15.0%)	16/7/7 (53.3%/23.3%/23.3%)	96/29/25 (64.0%/19.3%/16.7%)	
Tumor size (cm, ≤ 5/> 5)	39/81 (32.5%/67.5%)	11/19 (36.7%/63.3%)	50/100 (33.3%/66.7%)	0.829
MVI, yes/no	55/65 (45.8%/54.2%)	13/17 (43.3%/56.7%)	68/82 (45.3%/54.7%)	1
Tumor capsule, ill-defined/well-defined	29/91 (24.2%/75.8%)	11/19 (36.7%/63.3%)	40/110 (26.7%/73.3%)	0.249
Satellite nodules, yes/no	26/94 (21.7%/78.3%)	10/20 (33.3%/66.7%)	36/114 (24.0%/76.0%)	0.272
Surgical factors				

TACE (c-TACE/DEB-TACE)	79/41 (65.8%/34.2%)	21/9 (70.0%/30.0%)	100/50 (66.7%/33.3%)	0.829
Resection Margin (cm, < 1/≥ 1)	13/107 (10.8%/89.2%)	4/26 (13.3%/86.7%)	17/133 (11.3%/88.7%)	0.949
Blood transfusion, yes/no	38/82 (31.7%/68.3%)	14/16 (46.7%/53.3%)	52/98 (34.7%/65.3%)	0.184
Conventional staging system				
AJCC (I/II/III)	42/20/58 (35.0%/16.7%/48.3%)	10/4/16 (33.3%/13.3%/53.3%)	52/24/74 (34.7%/16.0%/49.3%)	0.889
BCLC (A/B/C)	31/35/54 (25.8%/29.2%/45.0%)	10/7/13 (33.3%/23.3%/43.3%)	41/42/67 (27.3%/28.0%/44.7%)	0.678
CNLC (I/II/III)	47/19/54 (39.2%/15.8%/45.0%)	12/5/13 (40.0%/16.7%/43.3%)	59/24/67 (39.3%/16.0%/44.7%)	1
Okuda (I/II/III)	65/54/1 (54.2%/45.0%/0.8%)	15/15/0 (50.0%/50.0%/0%)	80/69/1 (53.3%/46.0%/0.7%)	0.749
JIS (0/1/2/3/4)	1/42/55/21/1 (0.8%/35.0%/45.8%/17.5%/0.8%)	0/10/12/8/0 (0%/33.3%/40.0%/26.7%/0%)	1/52/67/29/1 (0.7%/34.7%/44.7%/19.3%/0.7%)	0.716
CLIP (0/1/2/3/4)	27/28/35/21/9 (22.5%/23.3%/29.2%/17.5%/7.5%)	7/7/9/4/3 (23.3%/23.3%/30.0%/13.3%/10.0%)	34/35/44/25/12 (22.7%/23.3%/29.3%/16.7%/8.0%)	0.962
Inflammation index				
GPR (≤ 0.38/> 0.38)	66/54 (55.0%/45.0%)	18/12 (60.0%/40.0%)	84/66 (56.0%/44.0%)	0.773
LMR (≤ 2.39/> 2.39)	26/94 (21.7%/78.3%)	6/24 (20.0%/80.0%)	32/118 (21.3%/78.7%)	1
NLR (≤ 2.00/> 2.00)	60/60 (50.0%/50.0%)	16/14 (53.3%/46.7%)	76/74 (50.7%/49.3%)	0.903
PLR (≤ 84.38/> 84.38)	35/85 (29.2%/70.8%)	13/17 (43.3%/56.7%)	48/102 (32.0%/68.0%)	0.204
NrLR (≤ 644.61/> 644.61)	106/14 (88.3%/11.7%)	28/2 (93.3%/6.7%)	134/16 (89.3%/10.7%)	0.643
APRI (≤ 0.30/> 0.30)	91/29 (75.8%/24.2%)	20/10 (66.7%/33.3%)	111/39 (74.0%/26.0%)	0.429
ANRI (≤ 4.76/> 4.76)	10/110 (8.3%/91.7%)	4/26 (13.3%/86.7%)	14/136 (9.3%/90.7%)	0.623
ALRI (≤ 41.96/> 41.96)	97/23 (80.8%/19.2%)	24/6 (80.0%/20.0%)	121/29 (80.7%/19.3%)	1
PNI (≤ 52.62/> 52.62)	93/27 (77.5%/22.5%)	22/8 (73.3%/26.7%)	115/35 (76.7%/23.3%)	0.809
SII (≤ 336.22/> 336.22)	48/72 (40.0%/60.0%)	13/17 (43.3%/56.7%)	61/89 (40.7%/59.3%)	0.901

AFP: An alpha fetoprotein; HGB: Hemoglobin; PLT: Platelet; AST: Aspartate aminotransferase; ALT: Alanine aminotransferase; GGT: Gamma-glutamyl transpeptidase; ALB: Albumin; TBIL: Total bilirubin; BUN: Blood urea nitrogen; UA: Uric acid; PT: Prothrombin time; MVI: Microvascular invasion; TACE: Transarterial chemoembolization; cTACE: Conventional TACE; DEB-TACE: Drug-eluting beads TACE; GPR: Gamma-glutamyl transpeptidase to platelet ratio; LMR: Lymphocyte to monocyte ratio; NLR: Neutrophil to lymphocyte ratio; PLR: Platelet to lymphocyte ratio; NrLR: Neutrophil times GGT-to-lymphocyte ratio; APRI: Aspartate aminotransferase to platelet ratio index; ANRI: AST to neutrophil ratio index; ALRI: AST to lymphocyte ratio index; PNI: Prognostic nutritional index; SII: Systemic immune-inflammation index.

Independent risk factors and development of the prognostic nomogram

Univariate and multivariate Cox regression analyses were performed in 120 patients from the training cohort to determine the risk factors associated with OS (Supplementary Table 2). As previously described, the optimal cutoff values for inflammation biomarkers were recorded (Supplementary Table 3). Briefly, multivariate analysis identified that preoperative ALB level, BUN level, GPR, PLR, MVI and tumour number were independent risk factors associated with OS (Figure 2). All of these significant independent factors of OS were incorporated into the nomogram (Figure 3A). In addition, a mobile online tool was built to facilitate clinical application, available at <https://ctmodelforunresectablehcc.shinyapps.io/DynNomapp/> (Figure 3B).

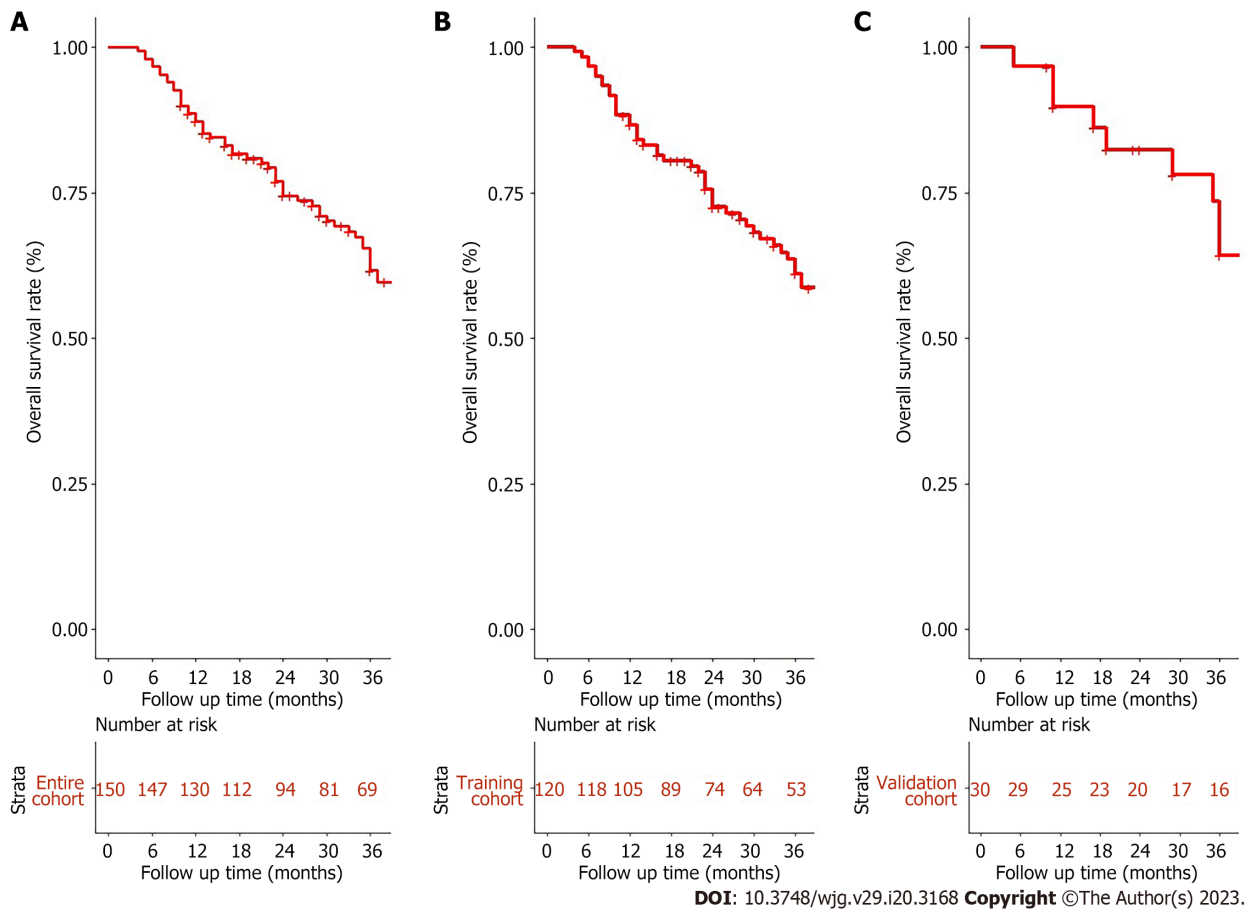


Figure 1 Overall survival for unresectable hepatocellular carcinoma patients accepted conversion therapy. A: Entire cohort; B: Training cohort; C: Validation cohort.

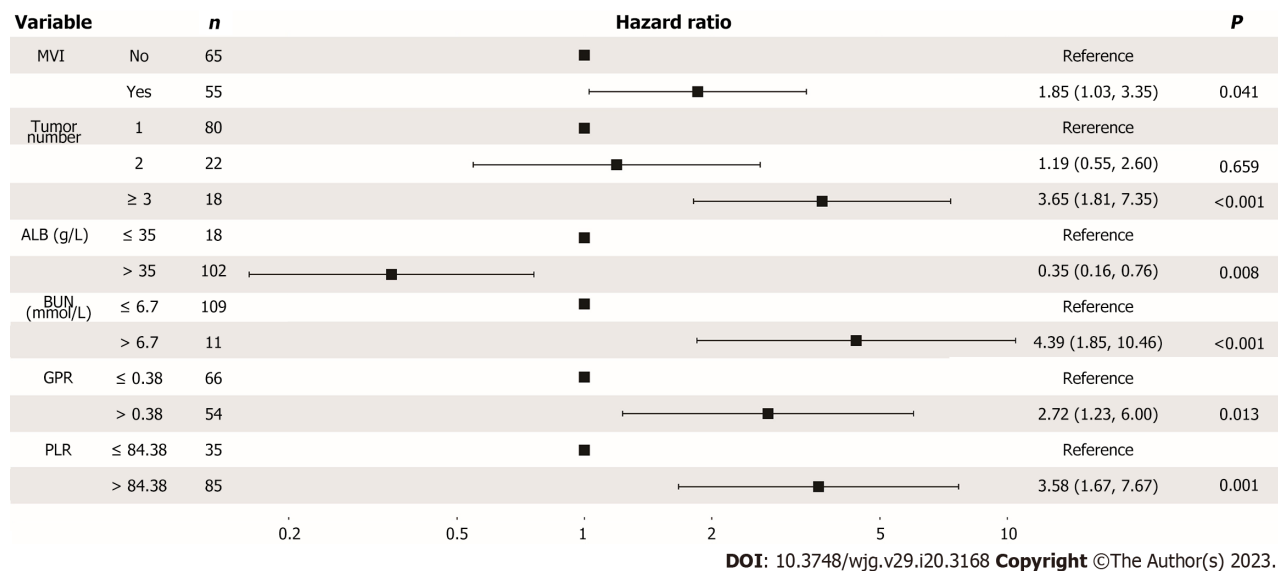
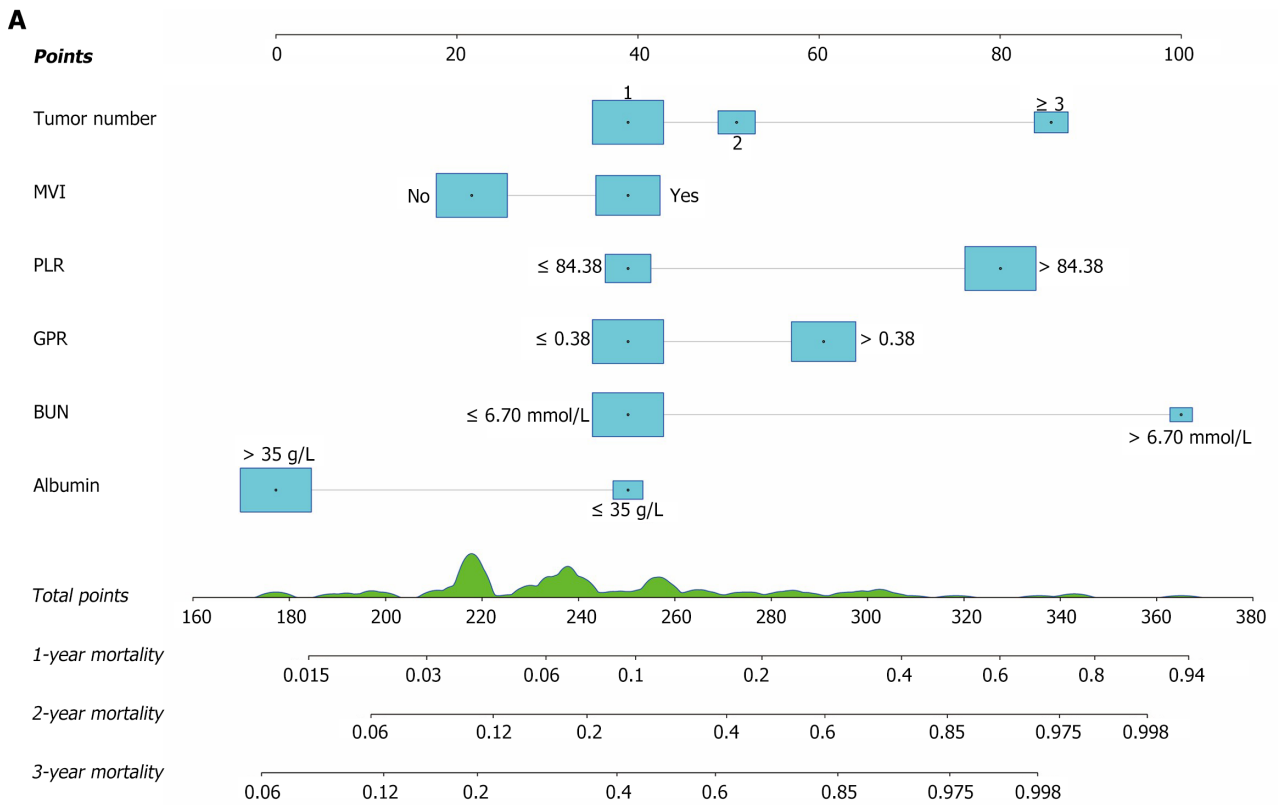


Figure 2 Forest plot for multivariate cox analysis of overall survival in the training cohort. CI: Confident interval; MVI: Macrovascular invasion; ALB: Albumin; BUN: Blood urea nitrogen; GPR: Gamma-glutamyl transpeptidase to platelet ratio; PLR: Platelet to lymphocyte ratio.

Validation of the prediction CT model

Bootstrapping with 1000 resamples in the primary training cohort revealed good predictive performance for OS, resulting in a C-index of 0.752 (95%CI: 0.688-0.815). The AUC in predicting the 1-, 2-, and 3-year OS rates were 0.779 (95%CI: 0.646-0.912), 0.801 (95%CI: 0.693-0.908) and 0.839 (95%CI: 0.748-0.931) in the training cohort and 0.872 (95%CI: 0.682-0.951), 0.892 (95%CI: 0.753-0.974) and 0.876



B

Input preoperative parameters

Albumin: >35 g/L

BUN: ≤6.70 mmol/L

GPR: ≤0.38

PLR: >84.38

MVI: Yes

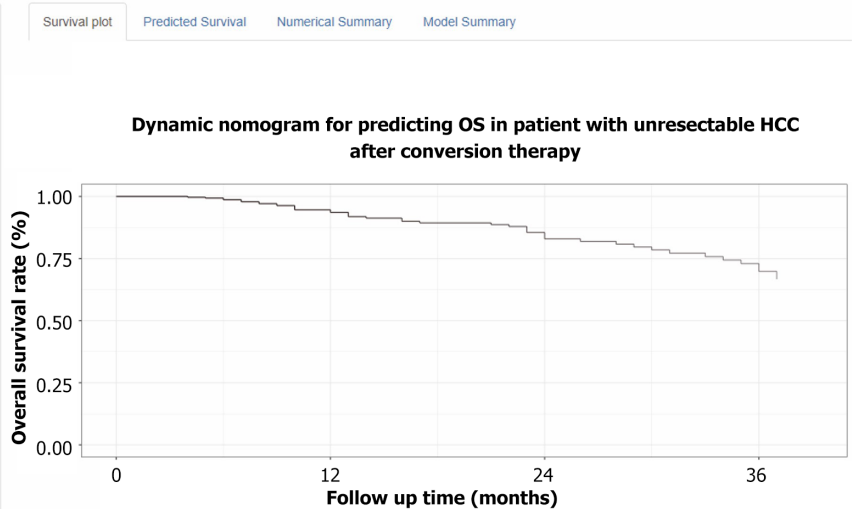
Tumor_number: 1

Predicted Survival at this Follow Up:
 Alpha blending (transparency)

Predict

Press Quit to exit the application

Quit



DOI: 10.3748/wjg.v29.i20.3168 Copyright ©The Author(s) 2023.

Figure 3 Conversion therapy model for unresectable hepatocellular carcinoma patients accepted conversion therapy. A: A constructed nomogram for predicting 1-, 2-, 3-year overall survival; B: Screenshot of the online individualized prediction tool based on the overall survival nomogram model. OS: Overall survival; MVI: Macrovascular invasion; BUN: Blood urea nitrogen; GPR: Gamma-glutamyl transpeptidase to platelet ratio; PLR: Platelet to lymphocyte ratio.

(95%CI: 0.727-0.962) in the validation cohort, respectively (Figure 4A and B). Accordingly, the C-index in the validation cohort reached 0.807 (95%CI: 0.705-0.908), while the calibration plot for the probability of OS at 1, 2, and 3 years depicted a favorable concordance between the predicted and actual outcomes (Figure 4C).

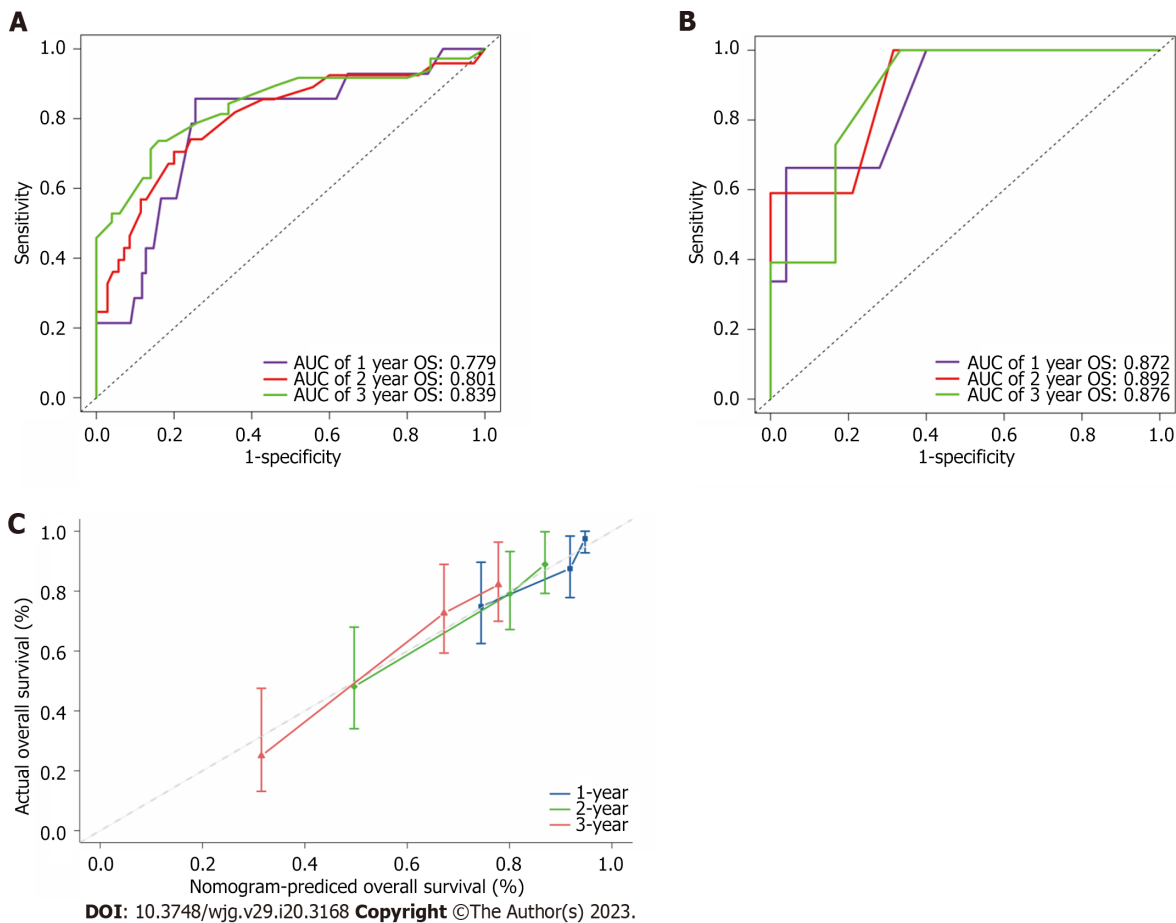


Figure 4 The receiver operating characteristic curves, calibration curve and decision curve analysis curves of the model. A and B: Receiver operating characteristic for overall survival in the training (A) and validation cohort (B), respectively; C: Calibration curve plots of nomogram for predicting 1-year, 2-year and 3-year probability of survival in the training cohort. OS: Overall survival; AUC: Area under the curve.

Comparison of model predictive performance

The discrimination power of the nomogram and common staging systems were compared by the C-index and time-dependent AUC (1, 2, and 3 years). In both the training and validation cohorts, the predictive performance of the CT model was superior to that of the other six conventional HCC staging systems ($P < 0.01$, Figure 5A and B, Supplementary Table 4). DCA indicated a good net benefit compared with six other conventional HCC staging systems at 1, 2 and 3 years after conversion therapy in the training cohort (Figure 5C-E).

Risk stratification based on nomogram scores and prognostic assessment

The patients were categorized into two groups based on their overall predictive risk score: Low risk (score < 196) and high risk (score ≥ 196). The distribution of clinical features and corresponding risk scores in each patient are presented in Figure 6A. The OS curves exhibited significant discrimination between the low-risk and high-risk groups among the entire ($P < 0.001$), training ($P < 0.001$) and validation ($P = 0.041$) cohorts (Figure 6B-D). Additionally, given that inflammation biomarkers are associated with postoperative prognosis, we found that high values of both GPR and PLR were significantly correlated with worse prognostic outcomes in patients after conversion therapy. The low-GPR group exhibited higher 1-, 2-, and 3-year OS rates compared to the high-GPR group (0.93, 0.69, and 0.54 *vs* 0.79, 0.55, and 0.36, $P = 0.038$). Similarly, the low-PLR group demonstrated greater 1-, 2-, and 3-year OS rates in contrast to the high-PLR group (0.92, 0.73, and 0.58 *vs* 0.84, 0.58, and 0.40, $P = 0.01$) (Figure 7A and B). Besides, individuals who exhibited MVI demonstrated an inferior prognosis in contrast to those without vascular invasion (Figure 7C).

DISCUSSION

Conversion therapy is a new therapeutic strategy for individuals diagnosed with HCC at an advanced stage and who may not initially be suitable for radical surgery. Several studies have shown that patients with unresectable HCC who underwent conversion following surgical excision have a much longer OS

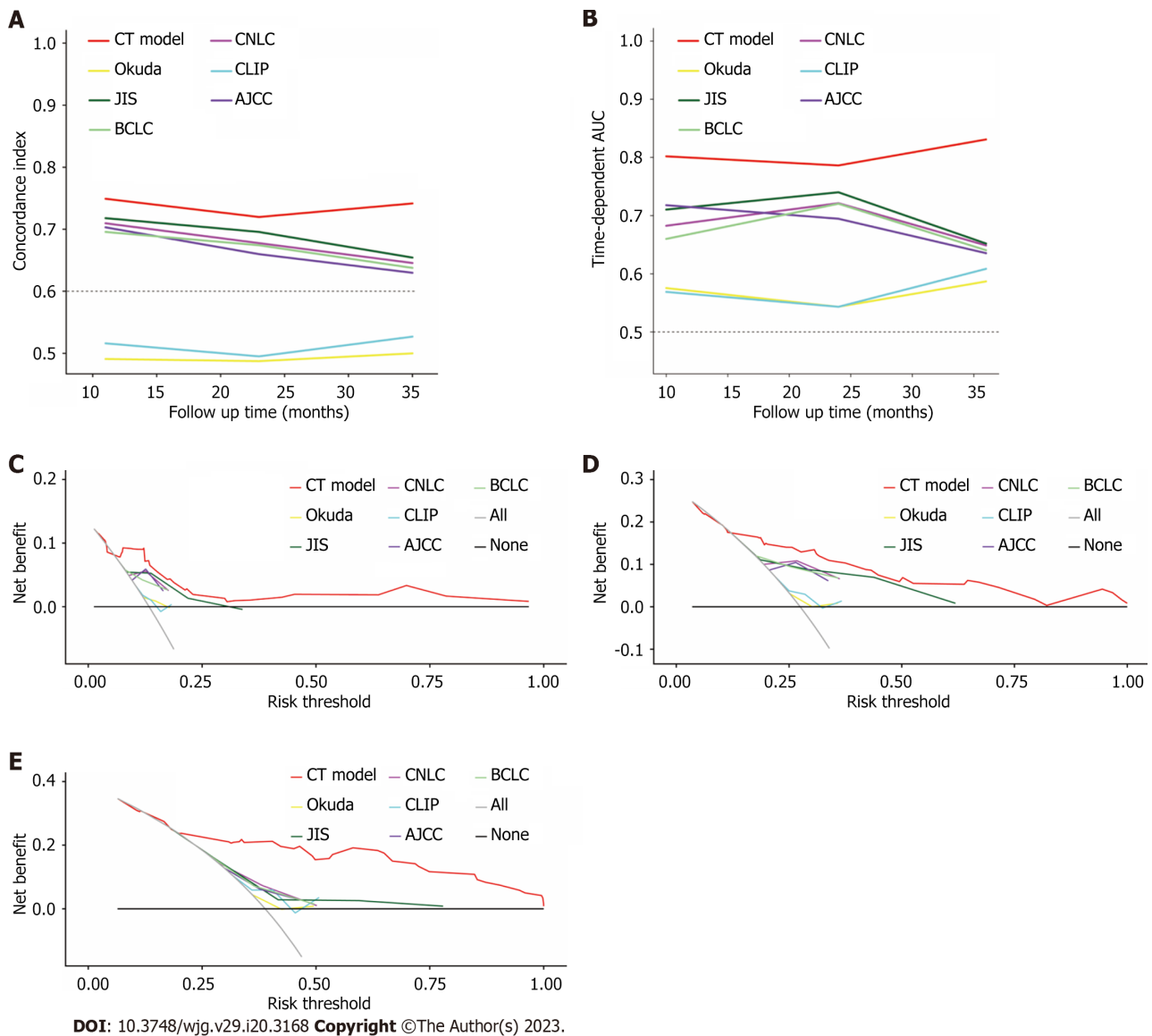
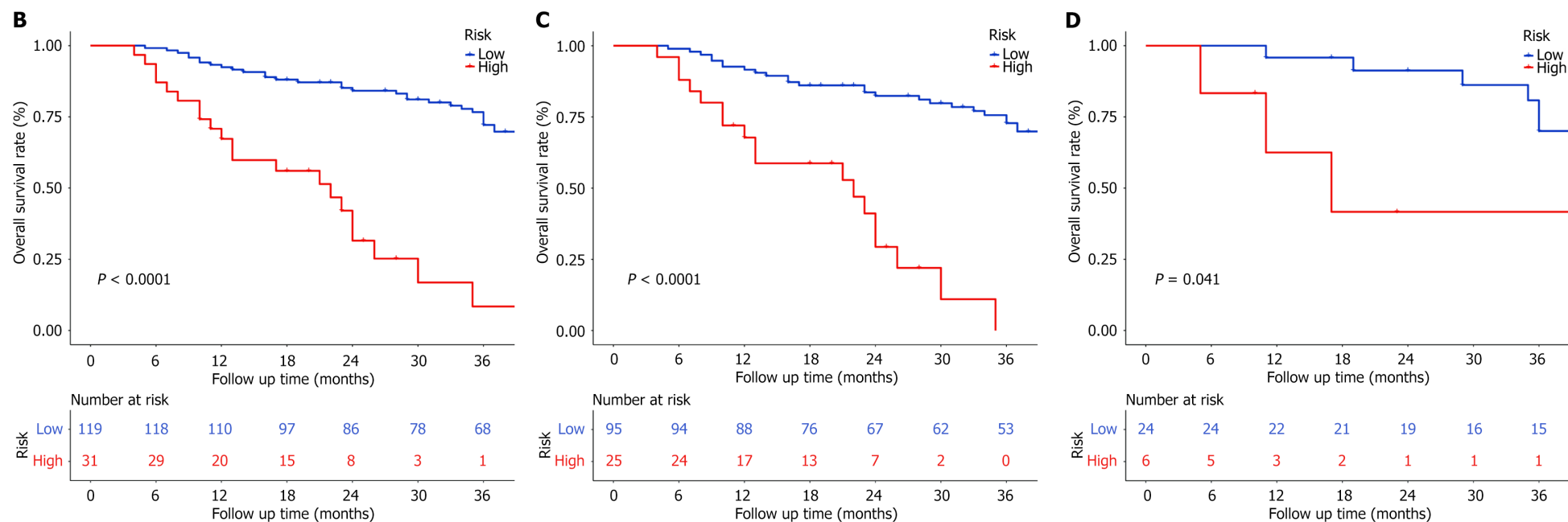


Figure 5 Comparison of model predictive performance in predicting overall survival. A: Comparison of concordance index between conversion therapy (CT) model and traditional staging systems in the training cohort; B: Comparison of time-dependent areas under receiver operating characteristic curve between CT model and other staging systems in the training cohort; the decision curve analysis curve compared the clinical practicability of the CT model and other six conventional hepatocellular carcinoma staging systems; C-E: 1-year (C), 2-year (D) and 3-year (E) survival benefit in the training cohort. AUC: Areas under receiver operating characteristic curve; CT: Conversion therapy; CNLC: China liver cancer staging; CLIP: Cancer of the Liver Italian Program; JIS: Japan integrated staging; BCLC: Barcelona Clinic Liver Cancer; AJCC: American Joint Committee on Cancer.

than those who received palliative treatments such as TACE[3,6,21]. Furthermore, 5-year survival rates for patients with unresectable HCC after conversion therapy (25%-57%) are comparable to those for patients with resectable HCC (30%-60%)[22]. Previous studies have developed prognostic models using preoperative factors to predict postoperative outcomes of early-stage HCC patients after curative resection that achieved good results[9-11], but it remains unclear in the CT model. In this study, we developed and validated a CT model that could accurately predicts prognosis for patients with unresectable HCC treated with TACE following HR.

The nomogram demonstrated great accuracy in predicting conversion therapy outcomes of patients with unresectable HCC. The nomogram developed in our study achieved AUC of 0.779, 0.801, and 0.839 in the training cohort and 0.872, 0.892 and 0.876 in the validation cohort, which were superior to those of the other six conventional HCC staging systems. DCA was also performed and revealed that the nomograms have good clinical utility in patients with unresectable HCC who received the CT model.

Using the nomogram score, clinicians can classify unresectable HCC patients into low- and high-risk groups. Effective postoperative therapeutic management and intensive clinical follow-up can be guided for high-risk individuals following this strategy. Additionally, a web-based dynamic nomogram provides a well-calibrated tool for predicting future clinical outcomes.

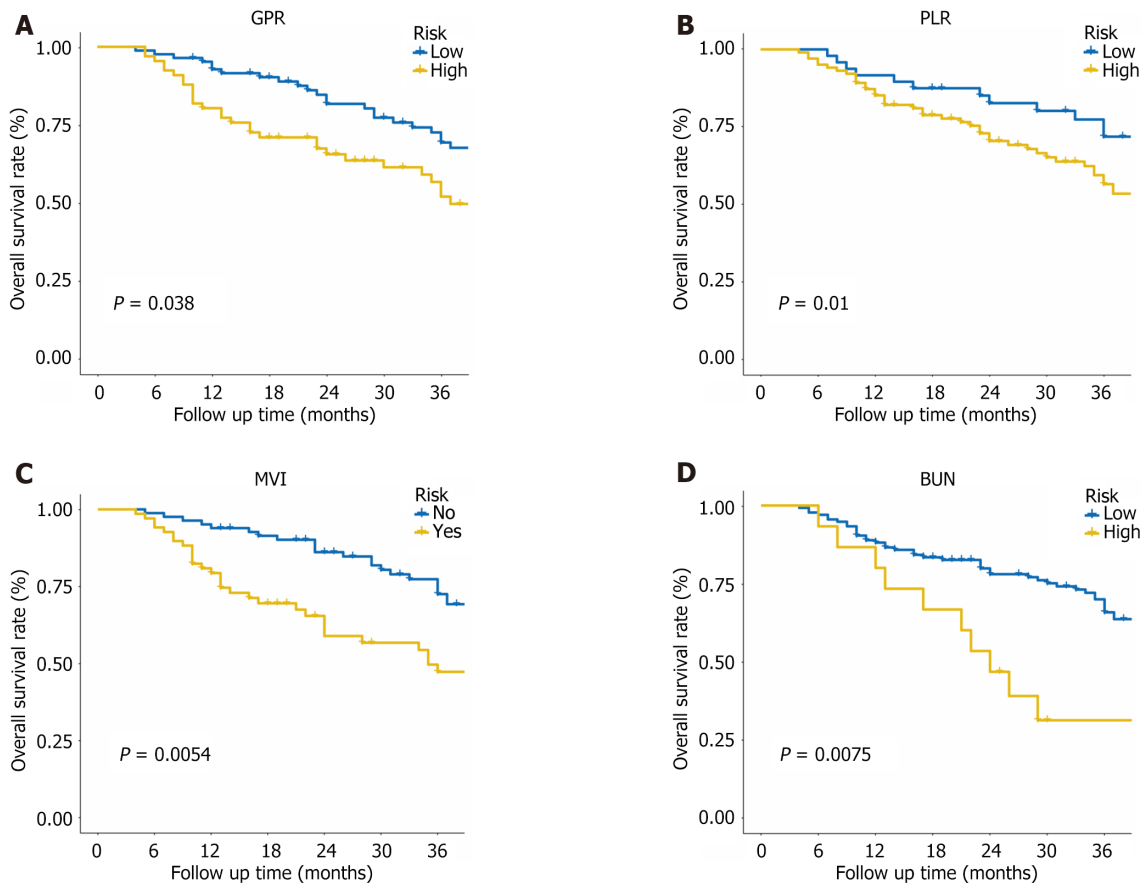


DOI: 10.3748/wjg.v29.i20.3168 Copyright ©The Author(s) 2023.

Figure 6 A Heatmap presents the distribution of corresponding risk score and clinical feature in each patient within high and low risk groups. A: It shows that the patients in low-risk group have more favourable prognosis; B-D: Kaplan-Meier survival curves for patients with low and high risk stratified by the total nomogram score in the entire cohort (B), training cohort (C), and validation cohort (D). ^a $P < 0.05$, ^b $P < 0.01$, ^c $P < 0.001$ was considered significant. ALB: Albumin; MVI: Macrovascular invasion; BUN: Blood urea nitrogen; GPR: Gamma-glutamyl transpeptidase to platelet ratio; PLR: Platelet to lymphocyte ratio; CNLC: China liver cancer staging; CLIP: Cancer of the Liver Italian Program; JIS: Japan integrated staging; BCLC: Barcelona Clinic Liver Cancer; AJCC: American Joint Committee on Cancer.

The present study combined liver and renal function factors, tumour burden and inflammation biomarkers (six significantly independent predictors: ALB, BUN, MVI, tumour number, GPR, and PLR) to establish a more comprehensive model and construct a nomogram CT model that could accurately predict the prognosis for patients with unresectable HCC after conversion therapy. Our findings are consistent with research in previous HCC populations that lower ALB level, MVI presence and multiple tumours were risk factors for long-term survival in patients with unresectable HCC with the CT model [10,23-26].

In terms of clinical utility, the prediction ability of the CT model was significantly improved compared with that of six conventional staging systems (AJCC TNM 8th, CNLC, JIS, CLIP, Okuda, and BCLC staging systems) in both the training and validation cohorts (Figure 5). The conventional staging systems mainly contain factors that may only take certain aspects of the tumour into consideration. Previous studies have noted that inflammatory biomarker combination scores have promising prognostic values in predicting patient survival for different HCC stages in various therapeutic



DOI: 10.3748/wjg.v29.i20.3168 Copyright ©The Author(s) 2023.

Figure 7 Kaplan-Meier survival curves for patients with different level of gamma-glutamyl transpeptidase to platelet ratio, platelet to lymphocyte ratio, macrovascular invasion, and blood urea nitrogen in the entire cohort. A: Gamma-glutamyl transpeptidase to platelet ratio; B: Platelet to lymphocyte ratio; C: Macrovascular invasion; D: Blood urea nitrogen.

modalities[27,28], indicating that combining these potential indicators would greatly improve the model's predictive abilities. Meanwhile, the AUC for the prediction of the 1-, 2-, and 3-year OS rates reached 0.755, 0.750, and 0.838 in the training cohort when we only used clinical information (MVI, ALB, tumour number and BUN) to develop a model, and they were unable to perform robustly in the validation cohort (Supplementary Figure 2). Hence, we constructed a nomogram CT model with clinical information (ALB, BUN, MVI, tumour number) and inflammation biomarkers (PLR and GPR).

PLR and GPR have been reported to be risk indicators of prognosis for OS in previous studies[10,29]. Meanwhile, high GPR was also proven to be an independent risk factor for HCC development and recurrence[30-32]. Our findings indicate that the high-PLR (> 84.38) and high-GPR (> 0.38) groups had significantly lower 12-, 24-, and 36-mo survival rates. Since inflammatory factors in the tumor microenvironment are crucial for HCC therapies, this information can assist clinicians in devising follow-up regimens and postoperative therapies for HCC patients at high or low risk of tumor recurrence after hepatectomy.

We also found that BUN was an independent prognostic factor in this study. Renal function impairment represents a clinically significant event in cirrhosis patients[33]. Preoperative renal dysfunction with high levels of BUN may lead to the development of major complications such as intractable ascites and spontaneous bacterial peritonitis (SBP). Moreover, the development of hepatorenal impairment is strongly associated with circulatory dysfunction, which can lead to various complications such as complicated or refractory ascites, SBP, hyponatremia and hepatorenal syndrome, and a high risk of mortality[34]. In clinical practice, serum creatinine concentration is generally used to assess kidney function in patients with liver diseases, which is also a major prognostic factor of cirrhosis included in the Model for End-Stage Liver Disease. However, several reports have shown that BUN levels have greater prognostic accuracy than serum creatinine concentrations[35-37]. In this study, our findings also showed that high BUN levels were related to worse liver function stage and poor OS outcomes (Figure 7D). Further research is needed to better understand this factor in advanced HCC and better classify and manage patients after conversion therapy.

While this nomogram CT model performed well, we do acknowledge a few potential limitations to this study. First, the nomogram was formulated based on a relatively small sample size obtained from

our single institution, which unavoidably led to selection bias. Further prospective and multicenter cohorts are required to evaluate its performance. Second, statistical power may be limited because several routine clinical variables were not included in our study. Because our study was retrospective, there were variations in performance score, body mass index, dosage and type of injected drugs during TACE, as well as postoperative treatments, among patients. To further bolster our findings, it is necessary to conduct larger and multicenter prospective cohorts. Hence, we will undertake additional research that incorporates more complete clinicopathological information, treatment details, and postoperative treatment modalities to improve the predictive performance of our model. Third, this study was mainly based on HBV-infected patients. Our results may not be applicable in different geographic regions and aetiologies. Fourth, systematic bioinformatic analyses were not included in this nomogram, which showed excellent predictive ability for early-stage HCC patients[38,39]. We will therefore develop a robust prognostic model that integrates both clinical parameters and multi-omics biomarkers to facilitate an understanding of HCC from a biological perspective and contribute to tailoring therapeutic strategies. Despite these limitations, we believe that our work is meaningful for individualized management in HCC patients following conversion therapy.

CONCLUSION

We developed and validated a prognostic nomogram combined with inflammation biomarkers for patients with unresectable HCC after conversion therapy. The proposed CT model shows increased accuracy, good clinical utility, and better prognostic performance than conventional staging systems. Furthermore, we have uploaded this prognostic nomogram online for free use (<https://ctmodelforunresectablehcc.shinyapps.io/DynNomapp/>).

ARTICLE HIGHLIGHTS

Research perspectives

Larger and multicentre prospective cohorts were required to further strengthen our results. We will conduct further investigation that incorporates more complete clinicopathological information, treatment details, and postoperative treatment modalities to improve the predictive performance of our model.

Research conclusions

The nomogram achieved optimal individualized prognostication of OS in HCC patients who received conversion therapy. It could be a useful clinical tool to help guide postoperative personalized interventions and prognosis judgement.

Research results

Multivariate Cox analysis identified that albumin, blood urea nitrogen, gamma-glutamyl transpeptidase to platelet ratio, platelet to lymphocyte ratio, macrovascular invasion and tumour number were the six independent prognostic factors correlated with OS in nomogram model. The C-indices in the training cohort and validation cohort were 0.752 and 0.807 for predicting OS, which were higher than those of the six conventional HCC staging systems (0.563 to 0.715 for the training cohort and 0.458 to 0.571 for the validation cohort). We have deployed the model into online calculators that are freely available at <https://ctmodelforunresectablehcc.shinyapps.io/DynNomapp/>.

Research methods

All patients met the inclusion criteria were enrolled and divided into training and a validation cohort. Using the independent risk factors in the training cohort, nomogram models were constructed to predict OS for patients treated with transarterial chemoembolization following HR. The nomograms were internally validated with the bootstrapping method. The predictive performance of the nomograms was assessed by Harrell's concordance index, calibration plot and time-dependent receiver operating characteristic curves and compared with six other conventional HCC staging systems.

Research objectives

To develop a nomogram to help guide postoperative personalized interventions and prognosis judgement.

Research motivation

To investigate the prognostic factors of overall survival (OS) in patients with unresectable HCC who received conversion therapy.

Research background

Hepatocellular carcinoma (HCC) is the sixth most common malignancy and the third leading cause of cancer-related mortality worldwide. Hepatic resection (HR) is the best therapeutic option for patients with early- and some intermediate-stage HCC. Unfortunately, the majority of Chinese patients with HCC are diagnosed at intermediate or advanced stages with massive or multifocal lesions. HR is possible for a minority of carefully selected patients with the help of a “conversion therapy” strategy, which refers to conversion of an unresectable HCC to achieve adequate tumour shrinkage and downstaging to undergo HR.

FOOTNOTES

Author contributions: Jiang ZB, Chen JW, and Huang MS contributed to conceptualization; Wu JL, Huang SB, Chen GR, Ran HY, and Liang QY contributed to acquisition of data, formal analysis (statistics), and visualization; Wu JL and Luo JY contributed to writing-original draft; Chen JW contributed to writing-review and editing; Huang MS, Jiang ZB, Lai LS, and Chen JW contributed to supervision; and all authors read and approved the final version of the manuscript.

Supported by the National Natural Science Foundation of China, No. 82072035; and Science and Guangzhou Planned Project of Science and Technology, No. 202102010028.

Institutional review board statement: This study was reviewed and approved by the Institutional Review Board of Ethical Committee of the Third Affiliated Hospital of Sun Yat-sen University (approval No. II2023-027-11).

Informed consent statement: Written informed consent of the patients was waived because of the retrospective nature of this study.

Conflict-of-interest statement: The authors declare that they have no known competing financial interests or personal relationships that could have appeared to influence the work reported in this paper.

Data sharing statement: The datasets used and/or analysed during the current study are available from the corresponding author on reasonable request.

STROBE statement: The authors have read the STROBE Statement – checklist of items, and the manuscript was prepared and revised according to the STROBE Statement – checklist of items.

Open-Access: This article is an open-access article that was selected by an in-house editor and fully peer-reviewed by external reviewers. It is distributed in accordance with the Creative Commons Attribution NonCommercial (CC BY-NC 4.0) license, which permits others to distribute, remix, adapt, build upon this work non-commercially, and license their derivative works on different terms, provided the original work is properly cited and the use is non-commercial. See: <https://creativecommons.org/licenses/by-nc/4.0/>

Country/Territory of origin: China

ORCID number: Jia-Lin Wu 0000-0002-8877-8348; Jun-Yang Luo 0000-0002-2665-1608; Zai-Bo Jiang 0000-0003-0523-6488; Si-Bo Huang 0000-0002-2366-6599; Ge-Run Chen 0000-0002-0871-6623; Hui-Ying Ran 0000-0003-4022-9937; Qi-Yue Liang 0000-0001-9926-2622; Ming-Sheng Huang 0000-0003-4749-4231; Jun-Wei Chen 0000-0002-4227-0944.

S-Editor: Chen YL

L-Editor: A

P-Editor: Chen YX

REFERENCES

- 1 Villanueva A. Hepatocellular Carcinoma. *N Engl J Med* 2019; **380**: 1450-1462 [PMID: 30970190 DOI: 10.1056/NEJMra1713263]
- 2 Lavanchy D. Hepatitis B virus epidemiology, disease burden, treatment, and current and emerging prevention and control measures. *J Viral Hepat* 2004; **11**: 97-107 [PMID: 14996343 DOI: 10.1046/j.1365-2893.2003.00487.x]
- 3 Sun HC, Zhou J, Wang Z, Liu X, Xie Q, Jia W, Zhao M, Bi X, Li G, Bai X, Ji Y, Xu L, Zhu XD, Bai D, Chen Y, Dai C, Guo R, Guo W, Hao C, Huang T, Huang Z, Li D, Li T, Li X, Liang X, Liu J, Liu F, Lu S, Lu Z, Lv W, Mao Y, Shao G, Shi Y, Song T, Tan G, Tang Y, Tao K, Wan C, Wang G, Wang L, Wang S, Wen T, Xing B, Xiang B, Yan S, Yang D, Yin G, Yin T, Yin Z, Yu Z, Zhang B, Zhang J, Zhang S, Zhang T, Zhang Y, Zhang A, Zhao H, Zhou L, Zhang W, Zhu Z, Qin S, Shen F, Cai X, Teng G, Cai J, Chen M, Li Q, Liu L, Wang W, Liang T, Dong J, Chen X, Wang X, Zheng S, Fan J; Alliance of Liver Cancer Conversion Therapy, Committee of Liver Cancer of the Chinese Anti-Cancer Association. Chinese expert consensus on conversion therapy for hepatocellular carcinoma (2021 edition). *Hepatobiliary Surg Nutr*

- 2022; **11**: 227-252 [PMID: 35464283 DOI: 10.21037/hbsn-21-328]
- 4 **Hamaoka M**, Kobayashi T, Kuroda S, Iwako H, Okimoto S, Kimura T, Aikata H, Nagata Y, Chayama K, Ohdan H. Hepatectomy after down-staging of hepatocellular carcinoma with portal vein tumor thrombus using chemoradiotherapy: A retrospective cohort study. *Int J Surg* 2017; **44**: 223-228 [PMID: 28676383 DOI: 10.1016/j.ijssu.2017.06.082]
 - 5 **Zhao HT**, Cai JQ. Chinese expert consensus on neoadjuvant and conversion therapies for hepatocellular carcinoma. *World J Gastroenterol* 2021; **27**: 8069-8080 [PMID: 35068855 DOI: 10.3748/wjg.v27.i47.8069]
 - 6 **Fan J**, Tang ZY, Yu YQ, Wu ZQ, Ma ZC, Zhou XD, Zhou J, Qiu SJ, Lu JZ. Improved survival with resection after transcatheter arterial chemoembolization (TACE) for unresectable hepatocellular carcinoma. *Dig Surg* 1998; **15**: 674-678 [PMID: 9845635 DOI: 10.1159/000018676]
 - 7 **Lau WY**, Lai EC. Salvage surgery following downstaging of unresectable hepatocellular carcinoma--a strategy to increase resectability. *Ann Surg Oncol* 2007; **14**: 3301-3309 [PMID: 17891443 DOI: 10.1245/s10434-007-9549-7]
 - 8 **Mantovani A**, Allavena P, Sica A, Balkwill F. Cancer-related inflammation. *Nature* 2008; **454**: 436-444 [PMID: 18650914 DOI: 10.1038/nature07205]
 - 9 **Wang Y**, Sun K, Shen J, Li B, Kuang M, Cao Q, Peng S. Novel Prognostic Nomograms Based on Inflammation-Related Markers for Patients with Hepatocellular Carcinoma Underwent Hepatectomy. *Cancer Res Treat* 2019; **51**: 1464-1478 [PMID: 30913869 DOI: 10.4143/crt.2018.657]
 - 10 **Zeng J**, Zeng J, Liu J. Development of pre and post-operative nomograms to predict individual survival for ideal liver resection candidates with hepatocellular carcinoma. *Liver Int* 2021; **41**: 2974-2985 [PMID: 34416088 DOI: 10.1111/liv.15042]
 - 11 **Wang JC**, Hou JY, Chen JC, Xiang CL, Mao XH, Yang B, Li Q, Liu QB, Chen J, Ye ZW, Peng W, Sun XQ, Chen MS, Zhou QF, Zhang YJ. Development and validation of prognostic nomograms for single large and huge hepatocellular carcinoma after curative resection. *Eur J Cancer* 2021; **155**: 85-96 [PMID: 34371445 DOI: 10.1016/j.ejca.2021.07.009]
 - 12 **Chen J**, Lai L, Luo J, Wang H, Li M, Huang M. DEM-TACE as the initial treatment could improve the clinical efficacy of the hepatocellular carcinoma with portal vein tumor thrombus: a retrospective controlled study. *BMC Cancer* 2022; **22**: 1242 [PMID: 36451104 DOI: 10.1186/s12885-022-10361-5]
 - 13 **Chen J**, Lai L, Lin Q, Huang W, Cai M, Zhu K, Huang M. Hepatic resection after transarterial chemoembolization increases overall survival in large/multifocal hepatocellular carcinoma: a retrospective cohort study. *Oncotarget* 2017; **8**: 408-417 [PMID: 27880724 DOI: 10.18632/oncotarget.13427]
 - 14 **Llovet JM**, Brú C, Bruix J. Prognosis of hepatocellular carcinoma: the BCLC staging classification. *Semin Liver Dis* 1999; **19**: 329-338 [PMID: 10518312 DOI: 10.1055/s-2007-1007122]
 - 15 **Amin MB**, Greene FL, Edge SB, Compton CC, Gershenwald JE, Brookland RK, Meyer L, Gress DM, Byrd DR, Winchester DP. The Eighth Edition AJCC Cancer Staging Manual: Continuing to build a bridge from a population-based to a more "personalized" approach to cancer staging. *CA Cancer J Clin* 2017; **67**: 93-99 [PMID: 28094848 DOI: 10.3322/caac.21388]
 - 16 **Zhou J**, Sun H, Wang Z, Cong W, Wang J, Zeng M, Zhou W, Bie P, Liu L, Wen T, Han G, Wang M, Liu R, Lu L, Ren Z, Chen M, Zeng Z, Liang P, Liang C, Yan F, Wang W, Ji Y, Yun J, Cai D, Chen Y, Cheng W, Cheng S, Dai C, Guo W, Hua B, Huang X, Jia W, Li Y, Liang J, Liu T, Lv G, Mao Y, Peng T, Ren W, Shi H, Shi G, Tao K, Wang X, Xiang B, Xing B, Xu J, Yang J, Yang Y, Ye S, Yin Z, Zhang B, Zhang L, Zhang S, Zhang T, Zhao Y, Zheng H, Zhu J, Zhu K, Shi Y, Xiao Y, Dai Z, Teng G, Cai J, Cai X, Li Q, Shen F, Qin S, Dong J, Fan J. Guidelines for the Diagnosis and Treatment of Hepatocellular Carcinoma (2019 Edition). *Liver Cancer* 2020; **9**: 682-720 [PMID: 33442540 DOI: 10.1159/000509424]
 - 17 **Kudo M**, Chung H, Osaki Y. Prognostic staging system for hepatocellular carcinoma (CLIP score): its value and limitations, and a proposal for a new staging system, the Japan Integrated Staging Score (JIS score). *J Gastroenterol* 2003; **38**: 207-215 [PMID: 12673442 DOI: 10.1007/s005350300038]
 - 18 A new prognostic system for hepatocellular carcinoma: a retrospective study of 435 patients: the Cancer of the Liver Italian Program (CLIP) investigators. *Hepatology* 1998; **28**: 751-755 [PMID: 9731568 DOI: 10.1002/hep.510280322]
 - 19 **Okuda K**, Ohtsuki T, Obata H, Tomimatsu M, Okazaki N, Hasegawa H, Nakajima Y, Ohnishi K. Natural history of hepatocellular carcinoma and prognosis in relation to treatment. Study of 850 patients. *Cancer* 1985; **56**: 918-928 [PMID: 2990661 DOI: 10.1002/1097-0142(19850815)56:4<918::AID-CNCR2820560437>3.0.CO;2-E]
 - 20 **Camp RL**, Dolled-Filhart M, Rimm DL. X-tile: a new bio-informatics tool for biomarker assessment and outcome-based cut-point optimization. *Clin Cancer Res* 2004; **10**: 7252-7259 [PMID: 15534099 DOI: 10.1158/1078-0432.CCR-04-0713]
 - 21 **Lewandowski RJ**, Kulik LM, Riaz A, Senthilnathan S, Mulcahy MF, Ryu RK, Ibrahim SM, Sato KT, Baker T, Miller FH, Omary R, Abecassis M, Salem R. A comparative analysis of transarterial downstaging for hepatocellular carcinoma: chemoembolization vs radioembolization. *Am J Transplant* 2009; **9**: 1920-1928 [PMID: 19552767 DOI: 10.1111/j.1600-6143.2009.02695.x]
 - 22 **Zhang T**, Merle P, Wang H, Zhao H, Kudo M. Combination therapy for advanced hepatocellular carcinoma: do we see the light at the end of the tunnel? *Hepatobiliary Surg Nutr* 2021; **10**: 180-192 [PMID: 33898559 DOI: 10.21037/hbsn-2021-7]
 - 23 **Wang YY**, Xiang BD, Ma L, Zhong JH, Ye JZ, Wang K, Xing BC, Li LQ. Development and Validation of a Nomogram to Preoperatively Estimate Post-hepatectomy Liver Dysfunction Risk and Long-term Survival in Patients With Hepatocellular Carcinoma. *Ann Surg* 2021; **274**: e1209-e1217 [PMID: 32097166 DOI: 10.1097/SLA.0000000000003803]
 - 24 **Zhang B**, Zhang B, Zhang Z, Huang Z, Chen Y, Chen M, Bie P, Peng B, Wu L, Wang Z, Li B, Fan J, Qin L, Chen P, Liu J, Tang Z, Niu J, Yin X, Li D, He S, Jiang B, Mao Y, Zhou W, Chen X. 42,573 cases of hepatectomy in China: a multicenter retrospective investigation. *Sci China Life Sci* 2018; **61**: 660-670 [PMID: 29417360 DOI: 10.1007/s11427-017-9259-9]
 - 25 **Zeng J**, Zeng J, Lin K, Lin H, Wu Q, Guo P, Zhou W, Liu J. Development of a machine learning model to predict early recurrence for hepatocellular carcinoma after curative resection. *Hepatobiliary Surg Nutr* 2022; **11**: 176-187 [PMID: 35464276 DOI: 10.21037/hbsn-20-466]
 - 26 **Wang X**, Mao M, He Z, Zhang L, Li H, Lin J, He Y, Dai S, Hu W, Liu W. Development and Validation of a Prognostic Nomogram in AFP-negative hepatocellular carcinoma. *Int J Biol Sci* 2019; **15**: 221-228 [PMID: 30662361 DOI: 10.7150/ijbs.28720]

- 27 **Nakano M**, Kuromatsu R, Niizeki T, Okamura S, Iwamoto H, Shimose S, Shirono T, Noda Y, Kamachi N, Koga H, Torimura T; Kurume Liver Cancer Study Group of Japan. Immunological inflammatory biomarkers as prognostic predictors for advanced hepatocellular carcinoma. *ESMO Open* 2021; **6**: 100020 [PMID: 33399083 DOI: 10.1016/j.esmoop.2020.100020]
- 28 **Wang C**, He W, Yuan Y, Zhang Y, Li K, Zou R, Liao Y, Liu W, Yang Z, Zuo D, Qiu J, Zheng Y, Li B. Comparison of the prognostic value of inflammation-based scores in early recurrent hepatocellular carcinoma after hepatectomy. *Liver Int* 2020; **40**: 229-239 [PMID: 31652394 DOI: 10.1111/liv.14281]
- 29 **Li J**, Liao Y, Suo L, Zhu P, Chen X, Dang W, Liao M, Qin L, Liao W. A novel prognostic index-neutrophil times γ -glutamyl transpeptidase to lymphocyte ratio (N γ LR) predicts outcome for patients with hepatocellular carcinoma. *Sci Rep* 2017; **7**: 9229 [PMID: 28835713 DOI: 10.1038/s41598-017-09696-y]
- 30 **Zhu YF**, Tan YF, Xu X, Zheng JL, Zhang BH, Tang HR, Yang JY. Gamma-glutamyl transpeptidase-to-platelet ratio and the fibrosis-4 index in predicting hepatitis B virus-related hepatocellular carcinoma development in elderly chronic hepatitis B patients in China: A single-center retrospective study. *Medicine (Baltimore)* 2019; **98**: e18319 [PMID: 31852119]
- 31 **Lemoine M**, Shimakawa Y, Nayagam S, Khalil M, Suso P, Lloyd J, Goldin R, Njai HF, Ndow G, Taal M, Cooke G, D'Alessandro U, Vray M, Mbaye PS, Njie R, Mallet V, Thursz M. The gamma-glutamyl transpeptidase to platelet ratio (GPR) predicts significant liver fibrosis and cirrhosis in patients with chronic HBV infection in West Africa. *Gut* 2016; **65**: 1369-1376 [PMID: 26109530 DOI: 10.1136/gutjnl-2015-309260]
- 32 **Wang WL**, Zheng XL, Zhang ZY, Zhou Y, Hao J, Tang G, Li O, Xiang JX, Wu Z, Wang B. Preoperative γ -glutamyl transpeptidase to platelet ratio (GPR) is an independent prognostic factor for HBV-related hepatocellular carcinoma after curative hepatic resection. *Medicine (Baltimore)* 2016; **95**: e4087 [PMID: 27399101 DOI: 10.1097/MD.0000000000004087]
- 33 **Sort P**, Navasa M, Arroyo V, Aldeguer X, Planas R, Ruiz-del-Arbol L, Castells L, Vargas V, Soriano G, Guevara M, Ginès P, Rodés J. Effect of intravenous albumin on renal impairment and mortality in patients with cirrhosis and spontaneous bacterial peritonitis. *N Engl J Med* 1999; **341**: 403-409 [PMID: 10432325 DOI: 10.1056/NEJM199908053410603]
- 34 **Piano S**, Tonon M, Angeli P. Management of ascites and hepatorenal syndrome. *Hepatol Int* 2018; **12**: 122-134 [PMID: 28836115 DOI: 10.1007/s12072-017-9815-0]
- 35 **Shimada M**, Takenaka K, Fujiwara Y, Gion T, Shirabe K, Yanaga K, Sugimachi K. Risk factors linked to postoperative morbidity in patients with hepatocellular carcinoma. *Br J Surg* 1998; **85**: 195-198 [PMID: 9501814 DOI: 10.1046/j.1365-2168.1998.00567.x]
- 36 **Wang Q**, Ma L, Li J, Yuan C, Sun J, Li K, Qin L, Zang C, Zhao Y, Zhang Y. A Novel Scoring System for Patients with Recurrence of Hepatocellular Carcinoma After Undergoing Minimal Invasive Therapies. *Cancer Manag Res* 2019; **11**: 10641-10649 [PMID: 31908536 DOI: 10.2147/CMAR.S224711]
- 37 **Yoneyama K**, Taniguchi H, Kiuchi Y, Shibata M, Mitamura K. Prognostic index of liver cirrhosis with ascites with and without hepatocellular carcinoma. *Scand J Gastroenterol* 2004; **39**: 1272-1279 [PMID: 15743006 DOI: 10.1080/00365520410008042]
- 38 **Liu F**, Liu D, Wang K, Xie X, Su L, Kuang M, Huang G, Peng B, Wang Y, Lin M, Tian J. Deep Learning Radiomics Based on Contrast-Enhanced Ultrasound Might Optimize Curative Treatments for Very-Early or Early-Stage Hepatocellular Carcinoma Patients. *Liver Cancer* 2020; **9**: 397-413 [PMID: 32999867 DOI: 10.1159/000505694]
- 39 **Wan S**, Lei Y, Li M, Wu B. A prognostic model for hepatocellular carcinoma patients based on signature ferroptosis-related genes. *Hepatol Int* 2022; **16**: 112-124 [PMID: 34449009 DOI: 10.1007/s12072-021-10248-w]

Fecal microbiota transplantation for the treatment of irritable bowel syndrome: A systematic review and meta-analysis

Sofie Ingdam Halkjær, Bobby Lo, Frederik Cold, Alice Højer Christensen, Savanne Holster, Julia König, Robert Jan Brummer, Olga C Aroniadis, Perttu Lahtinen, Tom Holvoet, Lise Lotte Gluud, Andreas Munk Petersen

Specialty type: Gastroenterology and hepatology

Provenance and peer review: Unsolicited article; Externally peer reviewed.

Peer-review model: Single blind

Peer-review report's scientific quality classification

Grade A (Excellent): A
Grade B (Very good): B
Grade C (Good): C, C
Grade D (Fair): D
Grade E (Poor): E

P-Reviewer: Bao CH, China; Rahmati M, Iran; Wu LH, China

Received: February 22, 2023

Peer-review started: February 22, 2023

First decision: March 18, 2023

Revised: April 6, 2023

Accepted: April 18, 2023

Article in press: April 18, 2023

Published online: May 28, 2023



Sofie Ingdam Halkjær, Bobby Lo, Frederik Cold, Lise Lotte Gluud, Andreas Munk Petersen, Gastro Unit, Medical Division, Copenhagen University Hospital Hvidovre, Hvidovre 2650, Denmark

Sofie Ingdam Halkjær, Bobby Lo, Frederik Cold, Andreas Munk Petersen, Copenhagen IBD Center, Copenhagen University Hospital Hvidovre, Hvidovre 2650, Denmark

Alice Højer Christensen, Department of Gastroenterology, Aleris-Hamlet Hospitals Copenhagen, Søborg 2860, Denmark

Savanne Holster, Julia König, Robert Jan Brummer, Nutrition-Gut-Brain Interactions Research Centre, Faculty of Medicine and Health, School of Medical Sciences, Örebro University, Örebro 70362, Sweden

Olga C Aroniadis, Department of Internal Medicine, Division of Gastroenterology, Renaissance School of Medicine, Stony Brook University Hospital, New York, NY 11794-8434, United States

Perttu Lahtinen, Department of Internal Medicine, Päijät-Häme Central Hospital, Lahti 15850, Finland

Perttu Lahtinen, Department of Medicine, University of Helsinki, Helsinki 00014, Finland

Tom Holvoet, Department of Gastroenterology, University Hospital Ghent, Ghent 9000, Belgium

Lise Lotte Gluud, Andreas Munk Petersen, Department of Clinical Medicine, University of Copenhagen, Copenhagen 2200, Denmark

Andreas Munk Petersen, Department of Clinical Microbiology, Copenhagen University Hospital Hvidovre, Hvidovre 2650, Denmark

Corresponding author: Sofie Ingdam Halkjær, MSc, PhD, Senior Researcher, Gastro Unit, Medical Division, Copenhagen University Hospital Hvidovre, Kettegård Alle 30, Hvidovre 2650, Denmark. sofie.ingdam.halkjaer@regionh.dk

Abstract

BACKGROUND

Irritable bowel syndrome (IBS) is the most prevalent gastrointestinal disorder in

developed countries and reduces patients' quality of life, hinders their ability to work, and increases health care costs. A growing number of trials have demonstrated an aberrant gut microbiota composition in IBS, also known as 'gut dysbiosis'. Fecal microbiota transplantation (FMT) has been suggested as a treatment for IBS.

AIM

To assess the efficacy and safety of FMT for the treatment of IBS.

METHODS

We searched Cochrane Central, MEDLINE, EMBASE and Web of Science up to 24 October 2022 for randomised controlled trials (RCTs) investigating the effectiveness of FMT compared to placebo (including autologous FMT) in treating IBS. The primary outcome was the number of patients with improvements of symptoms measured using a validated, global IBS symptoms score. Secondary outcomes were changes in quality-of-life scores, non-serious and serious adverse events. Risk ratios (RR) and corresponding 95%CI were calculated for dichotomous outcomes, as were the mean differences (MD) and 95%CI for continuous outcomes. The Cochrane risk of bias tool was used to assess the quality of the trials. GRADE criteria were used to assess the overall quality of the evidence.

RESULTS

Eight RCTs (484 participants) were included in the review. FMT resulted in no significant benefit in IBS symptoms three months after treatment compared to placebo (RR 1.19, 95%CI: 0.68-2.10). Adverse events were reported in 97 participants in the FMT group and in 45 participants in the placebo group (RR 1.17, 95%CI: 0.63-2.15). One serious adverse event occurred in the FMT group and two in the placebo group (RR 0.42, 95%CI: 0.07-2.60). Endoscopic FMT delivery resulted in a significant improvement in symptoms, while capsules did not. FMT did not improve the quality of life of IBS patients but, instead, appeared to reduce it, albeit non significantly (MD -6.30, 95%CI: -13.39-0.79). The overall quality of the evidence was low due to moderate-high inconsistency, the small number of patients in the studies, and imprecision.

CONCLUSION

We found insufficient evidence to support or refute the use of FMT for IBS. Larger trials are needed.

Key Words: Fecal microbiota transplantation; Irritable bowel syndrome; Meta-analysis; Systematic review

©The Author(s) 2023. Published by Baishideng Publishing Group Inc. All rights reserved.

Core Tip: We did not find evidence to support the use of fecal microbiota transplantation (FMT) for irritable bowel syndrome (IBS) patients outside of clinical trials in this systematic review and meta-analysis. We report possible beneficial effects when FMT is delivered by endoscopy (colonoscopy or gastroscopy). FMT appears to be safe compared to placebo in patients with IBS, regardless of route of administration. Further randomised clinical trials are necessary to clarify the effect, if any, of FMT in IBS.

Citation: Halkjær SI, Lo B, Cold F, Højer Christensen A, Holster S, König J, Brummer RJ, Aroniadis OC, Lahtinen P, Holvoet T, Gluud LL, Petersen AM. Fecal microbiota transplantation for the treatment of irritable bowel syndrome: A systematic review and meta-analysis. *World J Gastroenterol* 2023; 29(20): 3185-3202

URL: <https://www.wjgnet.com/1007-9327/full/v29/i20/3185.htm>

DOI: <https://dx.doi.org/10.3748/wjg.v29.i20.3185>

INTRODUCTION

Irritable bowel syndrome (IBS) is the most prevalent gastrointestinal disorder in developed countries, affecting around 11% of the adult population[1]. The condition reduces patients' quality of life, hinders their ability to work, and increases health care costs[2,3]. A diagnosis of IBS is based on symptoms, assessed using the Rome criteria, that include abdominal pain and altered bowel habits combined with the absence of organic or structural causes[4]. The criteria have changed over time and the most recent are the Rome IV criteria[5]. IBS can be sub-categorised as diarrhoea-predominant, constipation-predominant, mixed, or unclassified[5]. In most patients, IBS is chronic, with symptoms that fluctuate

over time.

The pathogenic mechanisms underlying IBS remain more or less unknown. Genetics[6,7], dietary habits[8], post-infectious conditions[9] and psychological mechanisms[10] are all suspected to be involved. In recent years an increasing number of trials have demonstrated an aberrant gut microbiota composition in IBS[11-14], although not all trials report this aberration and descriptions of it vary between studies[15]. The microbial pathophysiology of IBS remains unknown.

Treating IBS poses a challenge; the syndrome probably represents a heterogeneity of disease mechanisms, which makes it difficult to develop effective therapeutic strategies[16]. Understanding the causes of gut dysbiosis in IBS is crucial[17]. Some trials indicate that probiotics and prebiotics can reduce the symptoms of IBS[18,19]. Fecal microbiota transplantation (FMT) might be an effective therapeutic intervention in IBS[16,20].

FMT is the transfer of stool from a healthy donor to a patient[21]. FMT has been described as far back as the fourth century in China[22]. In modern times, the first published FMT treatment is from 1958, when it was used successfully in four patients with pseudomembranous colitis[23]. Pseudomembranous colitis is now known to be caused by *Clostridioides difficile* infection (CDI). Based on subsequent placebo-controlled studies, FMT is now accepted in daily clinical practice for the treatment of recurrent CDI[24]. In addition, FMT is being investigated as a treatment option in a range of other diseases, *e.g.*, metabolic syndrome, inflammatory bowel diseases, hepatic encephalopathy and multiple sclerosis[25]. The most promising results with FMT, apart from treating recurrent CDI, are for the treatment of inflammatory bowel disease[26-28].

FMT donors can be healthy relatives or anonymous donors. The advantages of the latter are the possibility of selecting donors with a high microbiota diversity and to store screened donor stool in freezers, to be made use of for multiple patients[29]. A European consensus report recommends that donors are chosen based on detailed information about illnesses with a presumed link to intestinal dysbiosis and rigorous testing of faecal and blood samples to avoid the transfer of infectious diseases [30].

FMT can be delivered in several ways, including through upper or lower endoscopic procedures, or by a gastro-duodenal or a rectal tube[31]. Additionally, capsules can release the stool in the small intestines and have been used successfully for the treatment of CDI[32-34]. In the treatment of recurrent CDI, the highest cure rates have been reported with repeated treatments delivered through lower endoscopy[35]; FMT has proven highly effective and patients are willing to undergo the treatment[36].

The microbial pathophysiology of IBS is not clearly understood, as microbiota alterations in IBS could either be a cause of the disease or a consequence of intestinal secretion and motility altered by IBS[37]. The prevailing hypothesis is that FMT might correct the dysbiosis associated with IBS[38,39], leading to a reversal or improvement of symptoms. Gut dysbiosis in IBS is characterised by a lower diversity of bacteria in the microbiota and abnormal proportions of specific bacteria as compared to the microbiota of healthy individuals[37,40]. In IBS and in other patient groups, FMT has resulted in increased bacterial diversity[41,42] and the coexistence of donor and recipient microbiota strains up to one year after treatment[43-45]. However, this is a new and developing field of study and the long-term effects of FMT on the microbiota remain largely unknown, not least of all because donor stools contain many things other than bacteria.

There is increasing evidence for a connection between gut dysbiosis and IBS[46,47]. The administration of FMT by various methods has been described in published case reports and abstracts, as compiled in an earlier review[48]. A number of smaller trials have examined the effect of FMT on IBS specifically[49-57], and several randomised controlled trials (RCTs), using different methods of administration, have been published with mixed results[43,44,58-63]. The effect of FMT can be difficult to assess due to the absence of reliable outcome measures and high placebo response rates[64]. The short- and long-term safety of FMT in patients with IBS is currently unclear.

The objectives of this systematic review were to examine the benefits and harms of FMT *vs* placebo (including autologous FMT, *i.e.*, a participant's own faecal material) for the treatment of patients with IBS.

MATERIALS AND METHODS

We conducted a systematic review and meta-analysis following the recommendations from the Cochrane Handbook for Systematic Reviews of Interventions[65]. The systematic review was registered *a priori* as a protocol[66].

We included RCTs comparing FMT to placebo for the treatment of IBS, regardless of publication status and language of publication. For cross-over trials only data from the first intervention were used. For multi-arm trials only the data from intervention groups relevant to the review were used. We excluded trials with quasi-random designs and cluster RCTs. Trials with mixed disease populations were excluded.

Trials were included if their participants were diagnosed with IBS by a physician or according to accepted, symptom-based diagnostic criteria, such as the Rome III or IV criteria[67] (Supple-

[mentary Table 1](#)). We only included trials that had follow-up after FMT for one week or more. Participants were included regardless of their gender and age.

FMT could be administered in different ways and at different frequencies as there was no standardised procedure. Therefore, we included trials irrespective of FMT procedure, in terms of the quantity of faeces used, the form of faeces (fresh or frozen), the route of administration, the frequency of treatment (*i.e.*, single *vs* multiple infusions) and donor selection (relatives or not). Only trials that used the whole gut microbiome from the donor were included. Trials that used a placebo, or autologous FMT as a placebo, were included. Trials that used selective microbial communities were excluded.

Primary outcomes

The primary outcome was the proportion of patients experiencing an improvement of symptoms (patient-reported), as measured by a validated, global IBS symptoms score (*e.g.*, IBS severity scoring system), as defined by each trial's organisers.

Secondary outcomes

Secondary outcomes were the change in quality of life, as measured by a validated quality of life assessment, *e.g.*, IBS-specific quality-of-life (IBS-QoL), the proportion of patients with non-serious adverse events and serious adverse events according to International Conference on Harmonization-Good Clinical Practice, and dropouts due to adverse events. Outcomes were measured after three and six months.

Literature search

We searched Cochrane Central, MEDLINE, EMBASE and Web of Science. No language or publication date restrictions were applied to the searches. The detailed search strategy is provided in [Supplementary Table 2](#).

We searched the following sources from the inception of each database up until 24 October 2022 and placed no restrictions on the language of publication ([Supplementary Table 2](#)): Cochrane Central (*via* the Ovid Evidence-Based Medicine Reviews Database, from inception); MEDLINE (*via* Ovid from 1946); and EMBASE (*via* Ovid from 1974).

We also searched for ongoing trials on ClinicalTrials.gov (<https://clinicaltrials.gov/>) and the World Health Organisation International Clinical Trials Registry Platform (<https://trialsearch.who.int/>).

The reference lists of all trials identified were then scanned for additional relevant trials. We also contacted the first authors of published and ongoing trials to request recent data or additional data, as needed.

Data collection and analysis

Two independent authors performed the study selection (BL, SIH). Disagreements were resolved by consensus using a third author (AMP). The search results were first screened by title and abstract and subsequently excluded if found non-relevant; the remaining results were screened by full text. Data were extracted independently by two investigators (BL, SIH). Any discrepancies were resolved by consensus using a third author (LLG). An attempt to contact the corresponding author by e-mail was made if data were not available.

A data extraction protocol was developed based on the Cochrane Consumers and Communication Review Group's data and results template and refined accordingly[68]. The following information was extracted from each trial: (1) Author, year of publication, trial design, and study site (country); (2) the mean or median (SD or IQR) change in symptoms, as measured by IBS scoring systems, at the end of the trial; (3) the mean or median (SD or IQR) change in quality of life, as measured by IBS quality of life scoring systems; (4) treatment description (including route of administration, mixed or single donor and fresh or frozen transplant); (5) reported non-serious adverse events and serious adverse events; and (6) dropouts due to adverse events.

Assessment of risk of bias in the studies

The risk of bias was independently assessed by two investigators (BL, FC) using the Cochrane risk of bias tool[69] and the following seven domains were assessed: random sequence generation, allocation concealment, blinding of participants and personnel, blinding of outcome assessment, incomplete outcome data, selective reporting, and other sources of bias ([Supplementary Table 3](#)).

The risk of bias for each domain was rated as either 'high', 'unclear' or 'low'. We classified the overall risk of bias in the trials as low if all the bias domains were classified as being at low risk of bias; we classified the overall risk as high if one or more of the bias domains were classified as having an unclear or high risk of bias. Any disagreement was solved by consensus using a third author (LLG).

Data synthesis

We compared the fixed-effects and random-effects estimates of the intervention effect. If the estimates were similar, we assumed that any small-study effects had a minimal impact on the intervention effect estimate. If the random-effects estimate showed a larger statistical effect, we re-evaluated whether it

was reasonable to conclude that the intervention was more effective in the smaller trials. If the larger trials appeared to be conducted with greater methodological rigour, or were conducted in circumstances more typical of the use of the intervention in practice, we reported the results of meta-analyses only from the larger trials.

Based on predictable clinical heterogeneity, we expected that several analyses would show, at a minimum, moderate heterogeneity ($I^2 > 30\%$). For random-effects models precision decreases, and confidence intervals widen, with increasing heterogeneity. We therefore expected the random-effects model would provide the most conservative (and thus a more accurate) estimate of the intervention effect. As such, we planned to report the results of our analyses based on meta-analyses of random-effects models.

Subgroup and sensitivity analysis

We conducted a number of subgroup analyses: fresh *vs* frozen FMT; quantity of FMT; route of administration (upper gastrointestinal tract (*e.g.*, capsulated, nasogastric, nasoduodenal, gastric tube) *vs* colonic (*e.g.*, rectal)); type of donor (single *vs* mixed); frequency of administration (single *vs* multiple); IBS subtypes (diarrhoea-predominant, constipation-predominant, or mixed type).

Statistical analyses

We combined data from individual trials for meta-analysis when the interventions, patient groups, and outcomes were sufficiently similar, using the Review Manager version 5.4.1. Risk ratios (RR) were calculated for dichotomous outcomes with 95%CI. For continuous outcomes, we calculated the mean difference (MD) if all studies reported their outcomes using the same scale, and standardised MD with 95%CI if the studies used different scales to report their outcomes. We extracted data for all randomised participants and all participants with missing outcome data. Missing data were described, including dropouts and reasons for dropout, as reported by the authors.

Heterogeneity was assessed through a systematic examination of forest plots and quantified by calculating I^2 values. The classification of heterogeneity levels was established using the subsequent thresholds: 0%-40% (insignificant), 40%-60% (moderate), 60%-80% (substantial), and > 80% (considerable). Additionally, the P value for the chi-squared test was included in the evaluation[66].

The outcomes reported in protocols were compared with published trial reports. In addition, for direct meta-analyses with at least 10 randomised clinical trials, we assessed reporting biases through regression analyses and visual inspection of funnel plots from the pairwise meta-analyses.

Assessing the certainty of the evidence

We used the GRADE approach to evaluate the overall certainty of the evidence and we followed the recommendations of the Cochrane Handbook for Systematic Reviews of Interventions[65]. We classified the certainty of evidence as 'high', 'moderate', 'low', or 'very low'.

High certainty: We are very confident that the true effect lies close to that of the estimate of the effect.

Moderate certainty: We are moderately confident in the effect estimate; the true effect is likely to be close to the estimate of the effect, but there is a possibility that it is substantially different.

Low certainty: Our confidence in the effect estimate is limited; the true effect may be substantially different from the estimate of the effect.

Very low certainty: We have very little confidence in the effect estimate; the true effect is likely to be substantially different from the estimate of the effect.

RESULTS

Trial selection

A search conducted on 24 October 2022 identified 2067 records, which were imported for screening into the computer program Covidence (<https://www.covidence.org/>). Of these records, 840 were removed as duplicates. We screened the titles and abstracts of the remaining 1227. We excluded 1160 reports as non-relevant. In total, 67 records met the criteria for full-text review.

After reading the full texts, we excluded 45 as they did not fulfil our eligibility criteria. The remaining 22 texts, originating from eight different trials, were included in our systematic review (Figure 1)[43,44, 58-63].

Supplementary Table 2 contains the complete set of search terms used in each electronic database.

A summary of the trials can be found in Table 1; a full description of them is provided in Supplementary Table 4.

Table 1 Characteristics of randomised controlled trials of faecal microbiota transplantation for treating irritable bowel syndrome

Ref.	Trial design	Country	Sample size	IBS subtypes	Inclusion criteria	Frequency and route of administration	FMT-content	Placebo content	Pretreatment	Number of donors
Aroniadis <i>et al</i> [59], 2019	RCT, crossover	United States	48 (25 FMT vs 23 placebo)	IBS-D	Moderate-to-severe IBS symptoms (IBS-SSS > 175)	3 d of 25 oral capsules	3 × 25 frozen capsules (0.38 g donor stool/capsule) (Openbiome)	Non-toxic brown pigment	PPI for three days	One donor for one patient (four different donors)
El-Salhy <i>et al</i> [60], 2020	RCT, 3 parallel groups	Norway	164 (54/30 gram FMT, 55/60 gram FMT, 55 placebo)	All subtypes	Moderate-to-severe IBS symptoms (IBS-SSS > 175)	Single treatment <i>via</i> gastroscopie to distal duodenum	Once 30 g or 60 gram of frozen feces in sterile saline solution	Autologous faeces	None	One donor
Halkjær <i>et al</i> [43], 2018	RCT, 2 parallel groups	Denmark	51 (25 FMT, 26 placebo)	All subtypes	Moderate-to-severe IBS symptoms (IBS-SSS > 175)	12 d of 25 oral capsules	25 FMT capsules (one daily dose containing approximately 12 g frozen faecal material)	Saline, glycerol and food colouring E150	Bowel cleansing	Donor mix from four donors
Holster <i>et al</i> [61], 2019	RCT, 2 parallel groups	Sweden	16 (8 FMT, 8 placebo)	All subtypes	IBS with small amounts of butyrate-producing bacteria	Single treatment <i>via</i> colonoscopy to the caecum	30 g frozen stool in sterile saline and glycerol	Autologous feces	Bowel cleansing and 4 mg loperamide	Two donors (three patients received stool from donor 1, the remaining five from donor 2)
Holvoet <i>et al</i> [44], 2021	RCT, 2 parallel groups	Belgium	62 (43 FMT, 19 placebo)	IBS-D and IBS-M	Refractory IBS with failure of at least three conventional IBS therapies	Single treatment <i>via</i> nasojejunal administration	Fresh feces mixed with saline	Autologous feces	Bowel cleansing	Two donors
Johnsen <i>et al</i> [62], 2018	RCT, 3 parallel groups	Norway	83 (26 fresh FMT, 29 frozen FMT, 28 placebo)	IBS-D and IBS-M	Moderate-to-severe IBS symptoms (IBS-SSS > 175)	Single treatment administered into the caecum <i>via</i> colonoscopy	50–80 g fresh or frozen feces mixed with saline and glycerol	Autologous feces	Bowel cleansing and 8 mg loperamid	Donor mix from two donors
Lahtinen <i>et al</i> [58], 2020	RCT, 2 parallel groups	Finland	51 (25 FMT, 26 placebo)	IBS-D, IBS-M and IBS-U	Patients who remained symptomatic despite receiving conventional treatment	Single treatment administered into the caecum <i>via</i> colonoscopy	30 g frozen suspension	Autologous feces	Bowel cleansing	One donor
Singh <i>et al</i> [63], 2022	RCT, 4 parallel groups	United States	23 (11 FMT, 12 placebo)	IBS-D	IBS-SSS > 150 or > 175	Single treatment with 19 oral capsules	Capsule contain 0.75 frozen fecal filtrate) (Openbiome)	Glycerol with brown coloring agent	Bowel cleansing	Six donors (unknown if donors were mixed)

FMT: Faecal microbiota transplantation; IBS: Irritable bowel syndrome; IBS-C: Constipation-predominant irritable bowel syndrome; IBS-D: Diarrhoea-predominant irritable bowel syndrome; IBS-M: Mixed irritable bowel syndrome; IBS-U: Unclassified irritable bowel syndrome; RCT: Randomised controlled trials; PPI: Proton pump inhibitors.

Study design and setting

We included eight trials that were published between 2018 and 2022[43,44,58-63]. These were either single-centre trials[44,60-63] or multicentre trials[43,58,59] and were conducted in Belgium[44], Denmark[43], Finland[58], Norway[60,62], Sweden[61] and the United States[59,63].

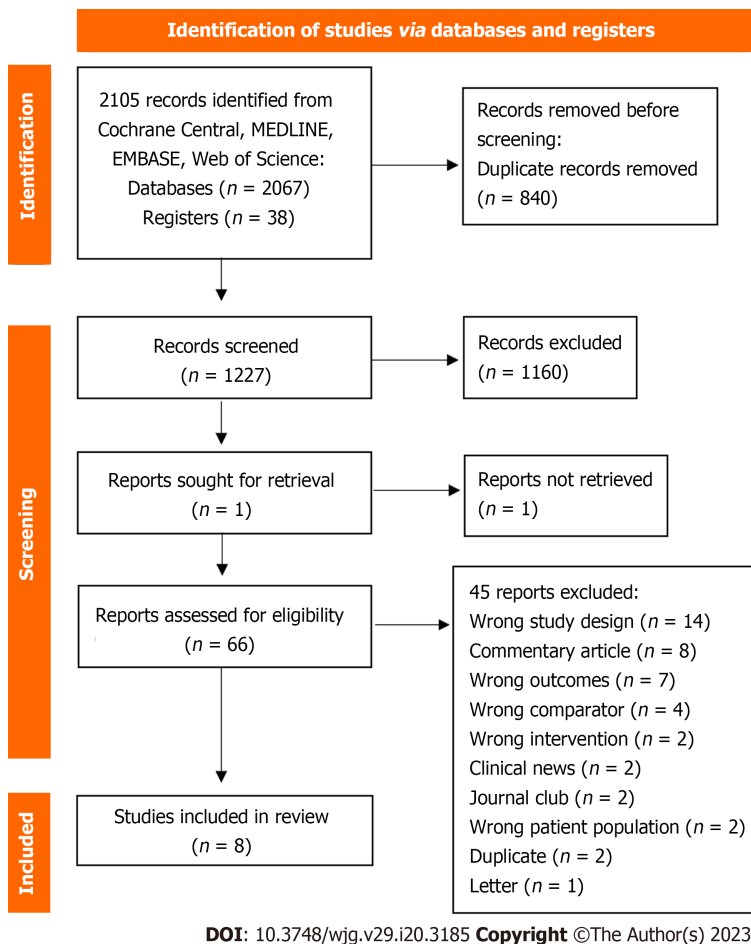


Figure 1 PRISMA flow diagram for the literature search.

All participants in the trials were diagnosed with IBS by a physician and according to accepted, symptom-based diagnostic criteria (*e.g.*, the Rome criteria)[5]. Participants in the Lahtinen *et al*[58] trial were diagnosed by a gastroenterologist, Aroniadis *et al*[59], Halkjær *et al*[43], Holster *et al*[61], Holvoet *et al*[44], Johnsen *et al*[62] and Singh *et al*[63] all used the Rome III criteria; El-Salhy *et al*[60] used the Rome IV criteria.

Four trials included participants with moderate-to-severe IBS symptoms, indicated by a score of 175 or more on the IBS severity scoring system (IBS-SSS)[43,59,60,62]. We are unsure whether Singh *et al*[63] used a score of 150 or 175 or more on the IBS-SSS, as both are referred to in their article. The remaining three trials used other criteria: Holster *et al*[61] only included participants with small amounts of butyrate-producing bacteria in faecal samples, Holvoet *et al*[44] included participants with refractory IBS who had experienced failure of at least three conventional IBS therapies, and Lahtinen *et al*[58] included participants who remained symptomatic despite receiving conventional treatment.

The trials differed in the IBS subtypes they investigated. All subtypes were included in the trials conducted by El-Salhy *et al*[60], Halkjær *et al*[43] and Holster *et al*[61]. Aroniadis *et al*[59] and Singh *et al*[63] included only diarrhoea-predominant participants. Holvoet *et al*[44] and Johnsen *et al*[62] included diarrhoea-predominant or mixed participants. Lahtinen *et al*[58] included diarrhoea-predominant, mixed or un-subtyped participants.

Characteristics of the interventions

All eight trials used faeces from healthy donors for the FMT. Supplementary Table 5 describes their inclusion and exclusion criteria for donors.

The route of administration varied between the trials. Three trials used colonoscopy[58,61,62], one used gastroscopy[60], one used the nasojejunal route[44] and three used oral capsules[43,59,63].

The frequency of administration varied between trials. El Salhy *et al*[60], Holster *et al*[61], Holvoet *et al*[44], Johnsen *et al*[62], Lahtinen *et al*[58] and Singh *et al*[63] administered FMT just once. Aroniadis *et al*[59] administered a total of three doses across three consecutive days. Halkjær *et al*[43] administered a total of 12 doses across 12 consecutive days.

The volume of FMT administered ranged from approximately 100 mL in the El-Salhy *et al*[60] trial to 300 mL in the Holvoet *et al*[44] trial. The faecal quantity varied from 30 g[58,61] to 50-80 g[62]. The

capsule trials used approximately 28.5 g of minimally processed faecal matter[59], 14.25 frozen faecal filtrate[63] and faecal matter derived from approximately 600 g of faeces[43]. Holvoet *et al*[44] used fresh FMT transplant, Johnsen *et al*[62] used both fresh and frozen FMT transplant, while the remaining trials used frozen FMT transplants[43,58-61,63].

Two trials used a single donor for all FMT treatments[58,60]. Holster *et al*[61], Holvoet *et al*[44] and Johnsen *et al*[62] used two donors. Aroniadis *et al*[59] used four donors, where each participant received a FMT from one donor. Singh *et al*[63] used six donors, where each participant received a FMT from one donor. Halkjær *et al*[43] used a FMT donor mix from four donors.

Six trials included bowel cleansing before transplantation[43,44,58,61-63]. Two trials used loperamide before endoscopy to retain the transplant[61,62]. One trial used proton pump inhibitors (PPI) for the three days prior to the transplantation[59].

Five trials used autologous faeces as an alternative to placebo for the comparison group[44,58,60-62]. In the capsule trials, Aroniadis *et al*[59] and Singh *et al*[63] used placebo capsules with a non-toxic, brown pigment and Halkjær *et al*[43] used placebo capsules made from saline, glycerol and food colouring E150.

Risk of bias in the studies

A summary of the risk of bias assessments is reported in [Figure 2](#) and bias assessments for the individual trials are reported in [Supplementary Table 4](#).

Overall, none of the studies had a high risk of bias in any of the seven dimensions considered. However, five of the eight trials[44,58,60,62,63] had an unclear bias for the blinding of outcomes, and four out of eight[43,58,60,61] had a similarly unclear bias in terms of how they reported the handling of incomplete data. In both cases this unclear bias was primarily due to a lack of information.

Effects of the interventions

A summary of the findings is provided in [Table 2](#) for comparing FMT and placebo in treating IBS. We did not assess publication bias as this review only consisted of eight trials. Furthermore, we chose to report the random-effect models' results despite some of the fixed-effect models being found significant as we did not find any larger trial that was more methodologically rigorous. The significant outcomes of the fixed-effect models were most likely due to the small number of trials available in each analysis and their high heterogeneity.

The GRADE rating for the certainty of the evidence examined was low due to moderate-high inconsistency, small numbers of patients and imprecision.

Primary outcomes

Improvement of symptoms: Eight randomised trials, comprising 484 participants, examined whether IBS symptoms improved after three months. Six trials defined improvement of symptoms as a decrease in IBS-SSS of 50 or more[43,44,59,60,63], while Johnson *et al*[62] defined it as a decrease of more than 75 points. Holster *et al*[61] used the gastrointestinal symptom rating scale-IBS and defined improvement as a change of more than 30%. Sixty-four percent (185/290) of FMT participants experienced an improvement of symptoms after three months compared to 42% (82/194) in the placebo group. A meta-analysis showed there was no significant difference between FMT and placebo (RR 1.19, 95%CI: 0.68-2.10, $P = 0.54$, $I^2 = 82\%$; [Figure 3](#)).

Three trials (99 participants) reported on the improvement of symptoms after six months. Thirty per cent (14/47) of FMT participants saw an improvement of their symptoms after six months compared to 38% (20/52) of the placebo group (RR 0.88, 95%CI: 0.33-12.39, $P = 0.8$, $I^2 = 51\%$; [Figure 3](#)).

Secondary outcomes

Adverse events: Seven trials, comprising 450 participants, reported on the proportion of participants who experienced adverse events. Thirty-five per cent (97/274) of the FMT group experienced an adverse event compared to 26% (45/176) of the placebo group (RR 1.17, 95%CI: 0.63-2.15, $P = 0.62$, $I^2 = 69\%$; [Figure 4](#)).

The most frequent adverse events reported in the trials were mild and transient symptoms of the gastrointestinal system.

Serious adverse events: All eight trials, comprising 501 participants, provided data for serious adverse events. A serious adverse event was reported once in a FMT group and twice in placebo groups. In the FMT group, 0.33 per cent (1/302) reported a serious adverse event, compared to 1% (2/199) in the placebo group (RR 0.42, 95%CI: 0.07-2.60, $P = 0.35$, $I^2 = 0\%$; [Supplementary Figure 1](#)).

Holvoet *et al*[44] reported that one participant from the placebo group committed suicide 10 d after the transplantation procedure. Aroniadis *et al*[59] reported one participant from the placebo group was admitted to hospital during week 20 of the trial with acute cholecystitis. Johnsen *et al*[62] reported that one participant from the FMT group was admitted to hospital after the FMT procedure due to transient vertigo and nausea.

Table 2 Summarised findings for comparing fecal microbiota transplantation with placebo for the treatment of irritable bowel syndrome

Outcomes and timeframe	Anticipated absolute effects		Relative effect (95%CI)	Number of participants (trials)	Certainty of the evidence (GRADE)	Comments
	Effect in placebo	Effect difference with FMT (95%CI)				
Improvement of symptoms after three months	42 per 100	8 or more per 100 (from 13 or fewer to 46 or more)	RR 1.19 (0.68-2.10)	484 (8 RCTs)	++- ¹ Low	Improvement of symptoms as measured by a validated global IBS symptoms score (<i>e.g.</i> , IBS-SSS scale from 0, no symptoms, to 500, maximum symptoms) (as defined by each trial)
Improvement of symptoms after six months	38 per 100	5 or fewer per 100 (from 25 or fewer to 52 or more)	RR 0.88 (0.33-2.39)	99 (3 RCTs)	++- ² Low	Improvement of symptoms as measured by a validated global IBS symptoms score (<i>e.g.</i> , IBS-SSS scale from 0, no symptoms, to 500, maximum symptoms) (as defined by each trial)
Adverse events prior to end of trial	26 per 100	4 or more per 100 (from 10 or fewer to 30 or more)	RR 1.17 (0.63-2.15)	450 (7 RCTs)	++- ³ Low	Common adverse events were mild and self-limiting gastrointestinal symptoms
Serious adverse events prior to end of trial	1 per 100	1 or fewer per 100 (from 1 or fewer to 2 or more)	RR 0.42 (0.07-2.60)	501 (8 RCTs)	++- ⁴ Low	Serious adverse events included one suicide (placebo), cholecystitis (placebo), and one admission to the hospital due to discomfort after the FMT procedure
Dropouts due to adverse events prior to end of trial	1 per 100	1 or fewer per 100 (from 1 or fewer to 1 or more)	RR 0.24 (0.03-2.17)	502 (8 RCTs)	++- ⁵ Low	Dropouts due to adverse events include one suicide (placebo) and one for discomfort after the FMT procedure (placebo)
Improvement in QoL scores after three months	NA	NA	MD -6.30 (-13.39 to 0.79)	406 (7 RCTs)	++- ⁶ Low	Improvement of quality of life as measured by a validated scale IBS-QoL, where 34 items are summed and averaged for a total score and then transformed to a 0-100 scale for interpretation (high scores indicate better IBS-QoL)

¹Downgraded two levels due to considerable inconsistency ($I^2 = 82%$) and imprecision (267 events).

²Downgraded two levels due to moderate inconsistency ($I^2 = 51%$) and serious imprecision (34 events).

³Downgraded two levels due to substantial inconsistency ($I^2 = 69%$) and imprecision (142 events).

⁴Downgraded two levels due to serious imprecision (three events) and wide confidence interval.

⁵Downgraded two levels due to serious imprecision (two events) and wide confidence interval.

⁶Downgraded two levels due to moderate inconsistency ($I^2 = 45%$), heterogeneous method, and a small number of participants.

Patients or population: Participants diagnosed with irritable bowel syndrome according to a physician's opinion or an accepted, symptom-based diagnostic criteria. Settings: Inpatient and outpatient. Intervention: Fecal microbiota transplantation. Comparison: Placebo (or autologous feces). FMT: Fecal microbiota transplantation; IBS: Irritable bowel syndrome; SSS: Symptom severity score; QoL: Quality of life measure; MD: mean difference; NA: Not available; RR: Risk ratio.

Dropouts due to adverse events: Eight trials, comprising 502 participants, reported on dropouts due to adverse events; there were none in the FMT groups, but two instances in the placebo groups. None (0/302) of the FMT groups had dropouts due to adverse events compared to 1% (2/200) in the placebo group (RR 0.24, 95%CI: 0.03-2.17, $P = 0.2$, $I^2 = 0%$; [Supplementary Figure 2](#)).

Holster *et al*[61] reported that one participant from the placebo group discontinued the trial after the FMT procedure due to discomfort. The dropout due to an adverse event in Holvoet *et al*[44] was the suicide occurring 10 d after the transplantation procedure in the placebo group.

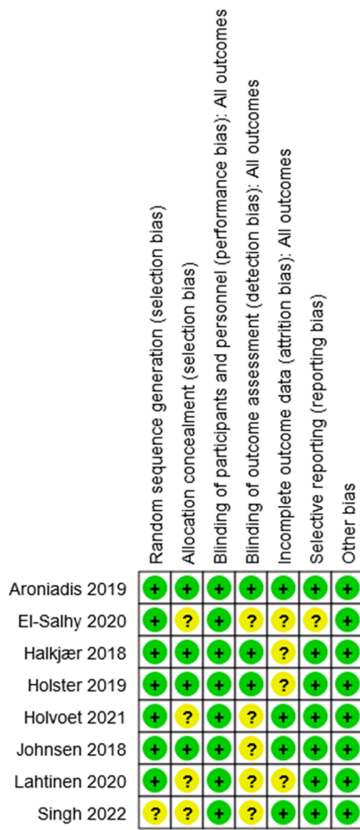
QoL measurements

Seven trials, comprising 406 participants, reported on QoL outcomes. There were no significant differences between the FMT and placebo treatment groups; however, there was a slightly favorable effect seen in the placebo groups (MD -6.30, 95%CI: -13.39 to 0.79, $P = 0.08$, $I^2 = 45%$; [Figure 5](#)).

Subgroup analyses

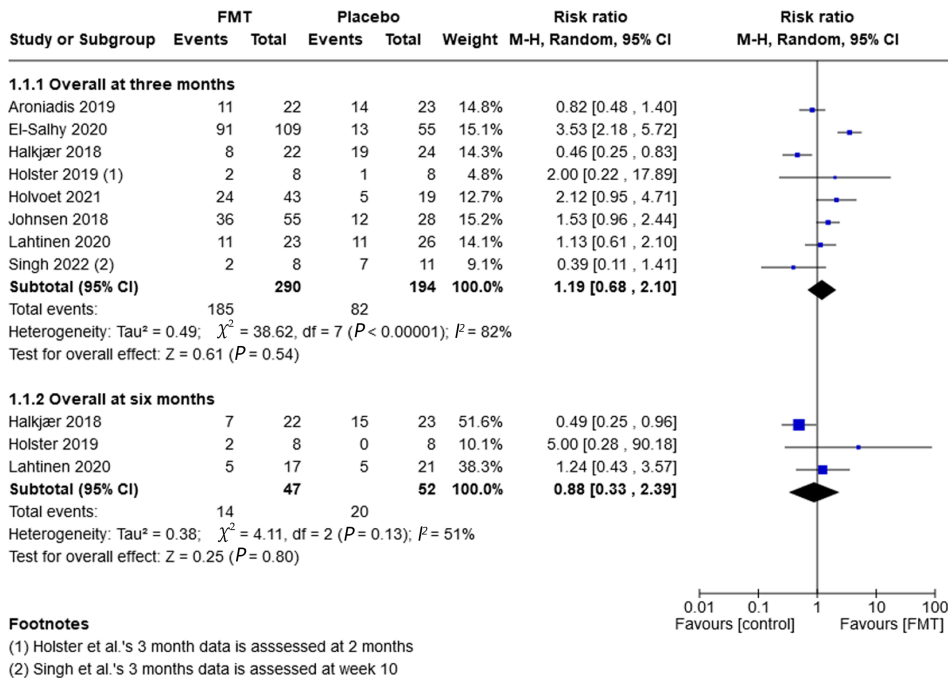
Planned subgroup analyses included fresh *vs* frozen transplant, quantity of transplant, route of administration, type of donor (single *vs* mixed donor), frequency of administration and subtype of IBS ([Supplementary Figures 3-8](#), [Figure 6](#)).

Overall, we found that endoscopic delivery (colonoscopy and upper endoscopy) of the FMT improved IBS-SSS after three months (RR 1.56, 95%CI: 1.04-2.34, $P = 0.03$, $I^2 = 0%$ and RR 3.03, 95%CI: 1.92-4.80, $P \leq 0.00001$, $I^2 = 13%$; [Figure 6](#)). Furthermore, administering a single, large dose of FMT resulted in a greater improvement of the IBS-SSS, while increasing the dose across several treatments was comparable to a placebo ([Supplementary Figures 4 and 6](#)). None of the other subgroup analyses



DOI: 10.3748/wjg.v29.i20.3185 Copyright ©The Author(s) 2023.

Figure 2 Risk of bias assessments for the trials reviewed.



DOI: 10.3748/wjg.v29.i20.3185 Copyright ©The Author(s) 2023.

Figure 3 Forest plot of randomised controlled trials of fecal microbiota transplantation for treating irritable bowel syndrome: Improvement of symptoms after three and six months. FMT: Fecal microbiota transplantation.

demonstrated an effect of FMT over placebo.

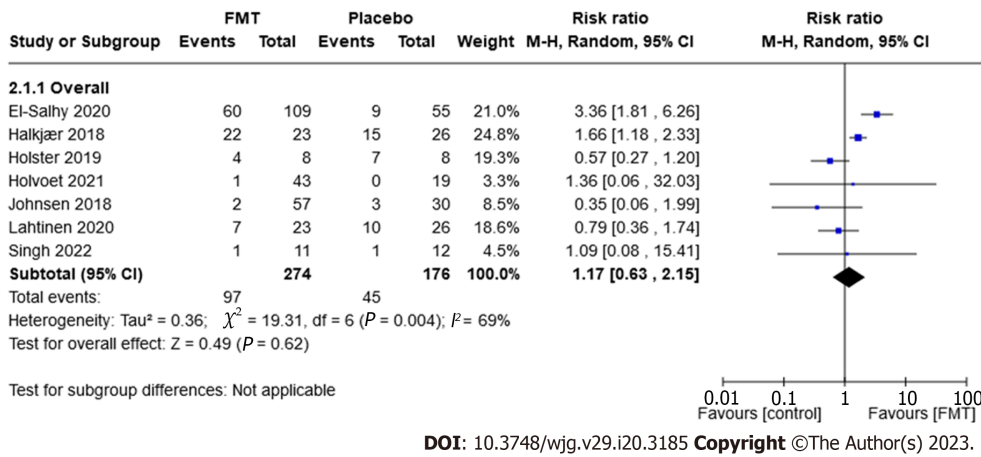


Figure 4 Forest plot of randomised controlled trials of fecal microbiota transplantation for treating irritable bowel syndrome: Adverse events. FMT: Fecal microbiota transplantation.

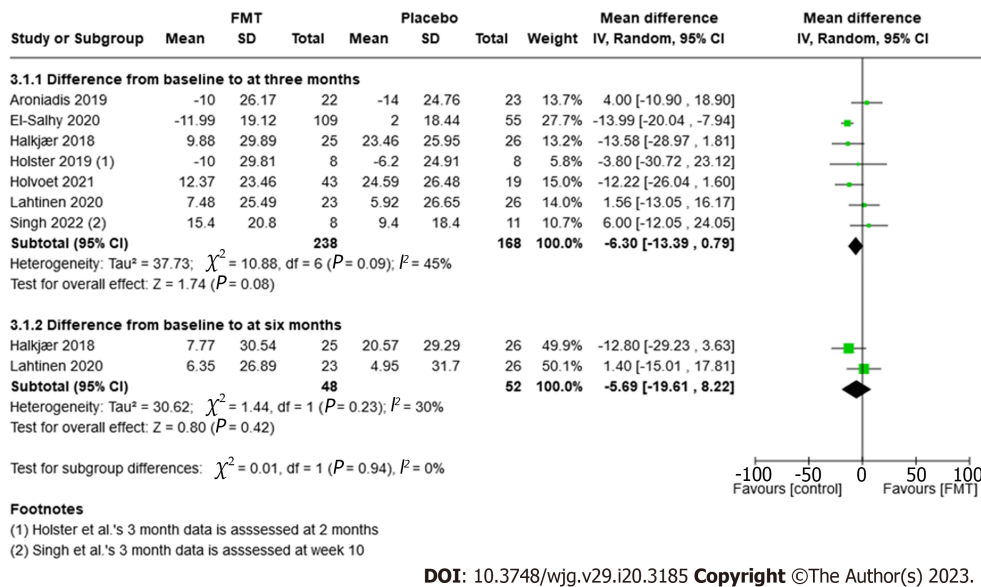


Figure 5 Forest plot of randomised controlled trials of fecal microbiota transplantation for treating irritable bowel syndrome: Quality-of-life scores after three and six months.

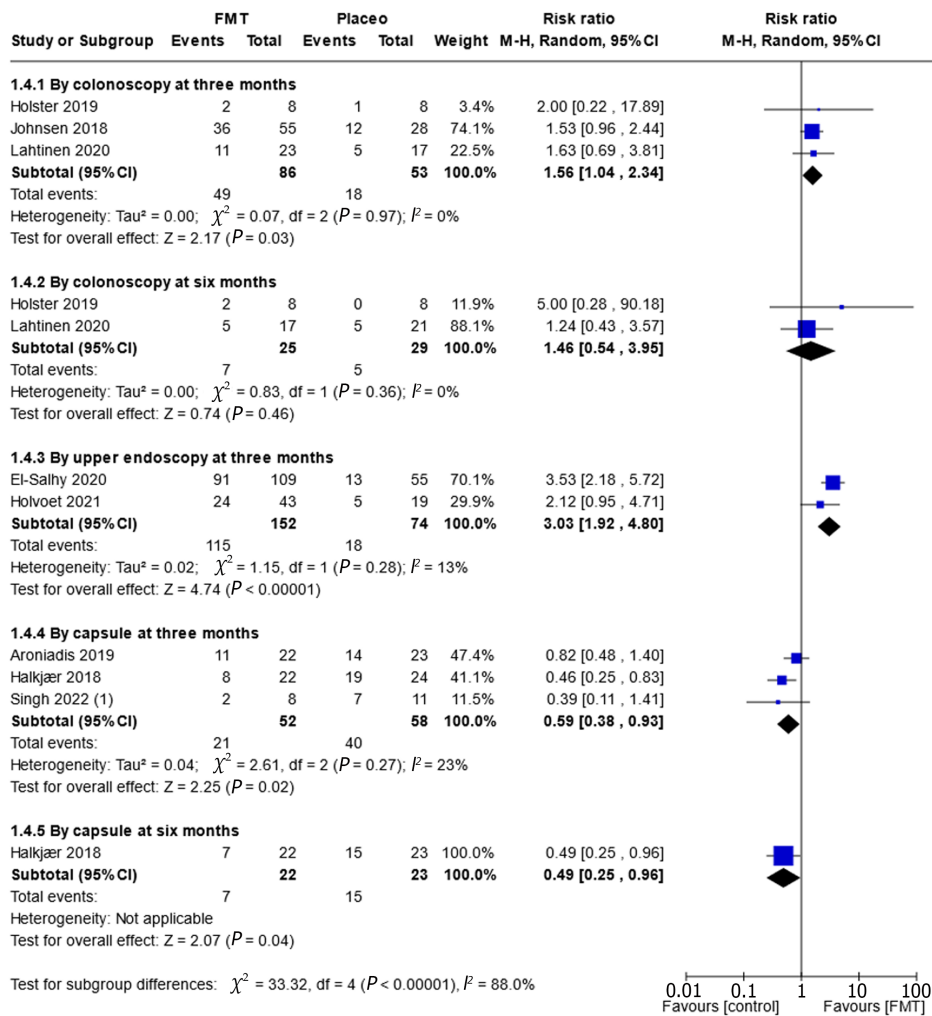
DISCUSSION

This review systematically examined the benefits and harms of FMT *vs* placebo or autologous FMT for the treatment of patients with IBS. Our main objective was to assess the efficacy of FMT for the improvement of symptoms in patients with IBS.

This review combined findings from eight randomised clinical trials that assessed the efficacy of FMT in 465 IBS patients. We found no significant difference in the improvement of symptoms in the FMT groups compared to the placebo groups (*P* = 0.54). The meta-analysis suggests a favorable, but non-significant, effect on quality of life in patients treated with placebo.

In general, placebo response rates are high in IBS patients. Placebo response estimates in prior meta-analyses range from 16% to 72% [64,70]. Likewise, bowel cleansing might contribute to symptom improvement; however, its effects on the microbiota seem to be transient [71,72].

FMT appears to be safe, with mild and self-limiting gastrointestinal symptoms like nausea, constipation, diarrhoea, and stomach pain - all of which are common IBS symptoms. This conclusion was also reached in a previous review assessing FMT for the treatment of inflammatory bowel disease [73]. FMT was not associated with serious adverse events in the treatment of IBS; three such events were reported in total (two in the placebo group and one in the FMT group) and none were considered to be related to the treatment.



Footnotes

(1) Singh *et al.*'s 3 months data is assessed at week 10

DOI: 10.3748/wjg.v29.i20.3185 Copyright ©The Author(s) 2023.

Figure 6 Forest plot of randomised controlled trials of fecal microbiota transplantation for treating irritable bowel syndrome: Improvement of symptoms after three and six months (route of administration subgroup analysis). FMT: Fecal microbiota transplantation.

In general, the results from the trials used for this review were highly heterogeneous. Therefore, it is possible that the absence of a positive overall effect is simply the result of how different the trials were from one another. The trials had pronounced differences in their selection processes for participants and donors, the routes of administration, the transplant quantities, and the frequency of administration. These differences make it difficult to draw conclusions about FMT as a treatment for IBS.

There is scientific evidence to support the hypothesis that FMT may be beneficial for patients with IBS. Observational trials have reported that IBS patients have reduced diversity or aberrant microbiota composition when compared to healthy controls[74]. Altered gut microbiota is also referred to as ‘microbiota dysbiosis’ and has been connected with disturbances in the microbiota gut-brain axis signaling[75]. Furthermore, other modulating agents targeting the microbiota, such as specific probiotic strains and antibiotics, have had demonstrable effects in IBS patients[76]. However, the underlying causes and mechanisms of dysbiosis in IBS and other diseases remain largely unknown. It has yet to be determined whether dysbiosis is a cause or a consequence of IBS, and even a ‘healthy’ microbiome has yet to be satisfactorily defined.

All eight trials included in this review reported on changes in gut microbiota after FMT. Aroniadis *et al*[59], El-Salhy *et al*[60], Halkjær *et al*[43], Lahtinen *et al*[58] and Singh *et al*[63] reported that participants receiving FMT saw changes in their gut microbiota that made their profiles more like the donors, when compared to placebo participants. Johnsen *et al*[62] reported these data in a later publication with the same outcome[77]. Holster *et al*[61] reported that microbiota diversity was not significantly affected by either FMT or placebo (autologous FMT). Holvoet *et al*[44] reported that responders to FMT had a higher baseline microbial diversity compared to those whose FMT treatment failed.

The possible effects, both positive and negative, of autologous FMT as placebo should be borne in mind.

In the treatment of recurrent CDI, the highest cure rates have been reported with repeated treatments delivered through lower endoscopy, but delivery through capsules is also highly effective[35,78]. In contrast, in IBS, FMT administered *via* upper or lower endoscopy, rather than capsules, has resulted in significant improvements in IBS-SSS. While much research has focused on FMT capsules[79], it is possible that the engraftment of the donor microbiota is better accomplished through endoscopic methods in IBS patients. Future RCTs in IBS patients that examines the combination of different routes of delivery for strain engraftment could be very interesting. Such studies would also contribute towards a more comprehensive understanding of microbial engraftment dynamics, which is currently lacking. A recent, systematic meta-analysis with shotgun metagenomic results showed that receiving FMT from multiple routes (for example, both *via* colonoscopy and capsules during the same treatment) resulted in increased engraftment[80]. Likewise, El-Salhy *et al*[81] present additional data from their trial and argue for using super donors since the efficacy of FMT appears to be donor-dependent. This argument needs further corroboration. Finally, data about patient and donor diets could prove relevant when determining the optimal patient-donor match[82].

The findings of this review have limited applicability and generalisability. More trials are needed to investigate whether FMT is a beneficial treatment strategy for IBS. Several aspects of the methods used in these trials could have influenced the effect of FMT, such as the route of administration, duration and interval between treatments, and the quantity of faecal microbiota transplanted to the patient. Despite the subgroup analyses we conducted as part of this review, firm conclusions cannot be drawn due to the small number of events and participants in the trials. Nonetheless, the results do suggest a possible beneficial effect in delivering FMT by endoscopy (colonoscopy or gastroscopy) over other routes.

Most of the patients in the trials we reviewed had moderate-to-severe IBS and were diagnosed according to the Rome III criteria. The newest, Rome IV criteria are more rigorous and it is not clear whether the greater homogeneity of IBS study populations they encourage will affect the efficacy of FMT. We recommend that future trials use the Rome IV criteria.

Additional investigations of microbiota, both when selecting patients of interest and after interventions, are needed in order to establish the precise mechanism of action of FMT as a potential treatment for IBS.

CONCLUSION

We did not find evidence to support the use of FMT for IBS patients outside of clinical trials in this systematic review and meta-analysis. We report a possible beneficial effect when delivering FMT by endoscopy (colonoscopy or gastroscopy). FMT appears to be safe, when compared to placebo, in patients with IBS, regardless of route of administration. Further randomised clinical trials are necessary in order to determine the effect of FMT in IBS.

ARTICLE HIGHLIGHTS

Research background

Irritable bowel syndrome (IBS) is a widespread gastrointestinal disorder accompanied by chronic abdominal pain and altered bowel habits. Gut microbiota disturbances have been linked to the pathophysiology of IBS, with fecal microbiota transplantation (FMT) emerging as a potential treatment strategy.

Research motivation

Manipulating gut microbiota composition *via* FMT could offer a promising avenue for IBS treatment, warranting further investigation into its efficacy and safety.

Research objectives

This review and meta-analysis aimed to evaluate the effectiveness and safety of FMT for treating IBS.

Research methods

A comprehensive search of Cochrane Central, MEDLINE, EMBASE, and Web of Science to identify randomised controlled trials (RCT) comparing FMT to placebo or autologous FMT in IBS patients. Primary outcome was improvement of symptoms, while secondary outcomes were quality-of-life scores and adverse events.

Research results

Our analysis incorporated data from eight RCTs with 484 participants. FMT did not result in significant improvement of symptoms when compared to placebo after three months, and no significant

improvement in quality of life was observed. Subgroup analysis indicated that endoscopic FMT delivery led to symptom improvement, whereas FMT capsules did not. FMT was found to be safe.

Research conclusions

This systematic review and meta-analysis do not support FMT as a treatment for IBS outside of clinical trials. Nevertheless, FMT was found to be safe.

Research perspectives

Large-scale, RCTs are needed to confirm or refute these findings. Investigating the potential significance of combining different FMT delivery routes for strain engraftment could provide a more comprehensive understanding of microbial engraftment dynamics in IBS patients.

FOOTNOTES

Author contributions: Halkjær SI, Gluud LL and Petersen AM conceived the review; Halkjær SI, Lo B, Cold F, Højer Christensen A, Gluud LL and Petersen AM wrote the protocol for the review; Halkjær SI and Lo B searched and selected studies for the review; Halkjær SI, Lo B, Holster S, König J, Brummer RJ, Aroniadis OC, Holvoet T and Lahtinen P collected data for the review; Lo B, Cold F and Gluud LL assessed the risk of bias in the studies used; Halkjær SI, Lo B, Gluud LL and Petersen AM assessed the certainty of the evidence; Halkjær SI and Lo B interpreted the data; Halkjær SI and Lo B wrote the review; Halkjær SI, Lo B, Cold F, Højer Christensen A, Petersen AM, Holster S, König J, Brummer RJ, Aroniadis OC, Holvoet T, Lahtinen P and Gluud LL commented on the review. All authors have read and approved the final manuscript. None of the authors have extracted data from, or assessed the risk of bias in, trials they carried out themselves.

Conflict-of-interest statement: None of the authors report relevant conflicts of interest for this article.

PRISMA 2009 Checklist statement: The authors have read the PRISMA 2009 Checklist, and the manuscript was prepared and revised according to the PRISMA 2009 Checklist.

Open-Access: This article is an open-access article that was selected by an in-house editor and fully peer-reviewed by external reviewers. It is distributed in accordance with the Creative Commons Attribution NonCommercial (CC BY-NC 4.0) license, which permits others to distribute, remix, adapt, build upon this work non-commercially, and license their derivative works on different terms, provided the original work is properly cited and the use is non-commercial. See: <https://creativecommons.org/licenses/by-nc/4.0/>

Country/Territory of origin: Denmark

ORCID number: Sofie Ingdam Halkjær 0000-0001-7518-4252; Bobby Lo 0000-0002-0252-9341; Julia König 0000-0003-0466-1861; Robert Jan Brummer 0000-0002-0362-0008; Perttu Lahtinen 0000-0001-6430-4642; Tom Holvoet 0000-0002-4540-4012; Lise Lotte Gluud 0000-0002-9462-4468; Andreas Munk Petersen 0000-0003-0531-0553.

S-Editor: Zhang H

L-Editor: A

P-Editor: Cai YX

REFERENCES

- 1 Lovell RM, Ford AC. Global prevalence of and risk factors for irritable bowel syndrome: a meta-analysis. *Clin Gastroenterol Hepatol* 2012; **10**: 712-721.e4 [PMID: 22426087 DOI: 10.1016/j.cgh.2012.02.029]
- 2 Spiegel BM. The burden of IBS: looking at metrics. *Curr Gastroenterol Rep* 2009; **11**: 265-269 [PMID: 19615301 DOI: 10.1007/s11894-009-0039-x]
- 3 Canavan C, West J, Card T. Review article: the economic impact of the irritable bowel syndrome. *Aliment Pharmacol Ther* 2014; **40**: 1023-1034 [PMID: 25199904 DOI: 10.1111/apt.12938]
- 4 Saha L. Irritable bowel syndrome: pathogenesis, diagnosis, treatment, and evidence-based medicine. *World J Gastroenterol* 2014; **20**: 6759-6773 [PMID: 24944467 DOI: 10.3748/wjg.v20.i22.6759]
- 5 Drossman DA. Functional gastrointestinal disorders: what's new for Rome IV? *Lancet Gastroenterol Hepatol* 2016; **1**: 6-8 [PMID: 28404114 DOI: 10.1016/S2468-1253(16)30022-X]
- 6 Choi HH, Cho YS. Fecal Microbiota Transplantation: Current Applications, Effectiveness, and Future Perspectives. *Clin Endosc* 2016; **49**: 257-265 [PMID: 26956193 DOI: 10.5946/ce.2015.117]
- 7 Kelly CR, Kahn S, Kashyap P, Laine L, Rubin D, Atreja A, Moore T, Wu G. Update on Fecal Microbiota Transplantation 2015: Indications, Methodologies, Mechanisms, and Outlook. *Gastroenterology* 2015; **149**: 223-237 [PMID: 25982290 DOI: 10.1053/j.gastro.2015.05.008]
- 8 Khanna S, Tosh PK. A clinician's primer on the role of the microbiome in human health and disease. *Mayo Clin Proc* 2014; **89**: 107-114 [PMID: 24388028 DOI: 10.1016/j.mayocp.2013.10.011]

- 9 **Spiller R**, Garsed K. Postinfectious irritable bowel syndrome. *Gastroenterology* 2009; **136**: 1979-1988 [PMID: 19457422 DOI: 10.1053/j.gastro.2009.02.074]
- 10 **Pinn DM**, Aroniadis OC, Brandt LJ. Is fecal microbiota transplantation (FMT) an effective treatment for patients with functional gastrointestinal disorders (FGID)? *Neurogastroenterol Motil* 2015; **27**: 19-29 [PMID: 25424663 DOI: 10.1111/nmo.12479]
- 11 **Kassinen A**, Krogius-Kurikka L, Mäkivuokko H, Rintilä T, Paulin L, Corander J, Malinen E, Apajalahti J, Palva A. The fecal microbiota of irritable bowel syndrome patients differs significantly from that of healthy subjects. *Gastroenterology* 2007; **133**: 24-33 [PMID: 17631127 DOI: 10.1053/j.gastro.2007.04.005]
- 12 **King TS**, Elia M, Hunter JO. Abnormal colonic fermentation in irritable bowel syndrome. *Lancet* 1998; **352**: 1187-1189 [PMID: 9777836 DOI: 10.1016/s0140-6736(98)02146-1]
- 13 **Malinen E**, Rintilä T, Kajander K, Mättö J, Kassinen A, Krogius L, Saarela M, Korpela R, Palva A. Analysis of the fecal microbiota of irritable bowel syndrome patients and healthy controls with real-time PCR. *Am J Gastroenterol* 2005; **100**: 373-382 [PMID: 15667495 DOI: 10.1111/j.1572-0241.2005.40312.x]
- 14 **Mättö J**, Maunuksela L, Kajander K, Palva A, Korpela R, Kassinen A, Saarela M. Composition and temporal stability of gastrointestinal microbiota in irritable bowel syndrome--a longitudinal study in IBS and control subjects. *FEMS Immunol Med Microbiol* 2005; **43**: 213-222 [PMID: 15747442 DOI: 10.1016/j.femsim.2004.08.009]
- 15 **Hugerth LW**, Andreasson A, Talley NJ, Forsberg AM, Kjellström L, Schmidt PT, Agreus L, Engstrand L. No distinct microbiome signature of irritable bowel syndrome found in a Swedish random population. *Gut* 2020; **69**: 1076-1084 [PMID: 31601615 DOI: 10.1136/gutjnl-2019-318717]
- 16 **Rodiño-Janeiro BK**, Vicario M, Alonso-Cotoner C, Pascua-García R, Santos J. A Review of Microbiota and Irritable Bowel Syndrome: Future in Therapies. *Adv Ther* 2018; **35**: 289-310 [PMID: 29498019 DOI: 10.1007/s12325-018-0673-5]
- 17 **Chong PP**, Chin VK, Looi CY, Wong WF, Madhavan P, Yong VC. The Microbiome and Irritable Bowel Syndrome - A Review on the Pathophysiology, Current Research and Future Therapy. *Front Microbiol* 2019; **10**: 1136 [PMID: 31244784 DOI: 10.3389/fmicb.2019.01136]
- 18 **Didari T**, Mozaffari S, Nikfar S, Abdollahi M. Effectiveness of probiotics in irritable bowel syndrome: Updated systematic review with meta-analysis. *World J Gastroenterol* 2015; **21**: 3072-3084 [PMID: 25780308 DOI: 10.3748/wjg.v21.i10.3072]
- 19 **Hungin AP**, Mulligan C, Pot B, Whorwell P, Agréus L, Fracasso P, Lionis C, Mendive J, Philippart de Foy JM, Rubin G, Winchester C, de Wit N; European Society for Primary Care Gastroenterology. Systematic review: probiotics in the management of lower gastrointestinal symptoms in clinical practice -- an evidence-based international guide. *Aliment Pharmacol Ther* 2013; **38**: 864-886 [PMID: 23981066 DOI: 10.1111/apt.12460]
- 20 **El-Salhy M**, Mazzawi T. Fecal microbiota transplantation for managing irritable bowel syndrome. *Expert Rev Gastroenterol Hepatol* 2018; **12**: 439-445 [PMID: 29493330 DOI: 10.1080/17474124.2018.1447380]
- 21 **Cammarota G**, Ianiro G, Tilg H, Rajilić-Stojanović M, Kump P, Satokari R, Sokol H, Arkkila P, Pintus C, Hart A, Segal J, Aloï M, Masucci L, Molinaro A, Scaldaferrì F, Gasbarrini G, Lopez-Sanroman A, Link A, de Groot P, de Vos WM, Högenauer C, Malfertheiner P, Mattila E, Milosavljević T, Nieuwdorp M, Sanguinetti M, Simren M, Gasbarrini A; European FMT Working Group. European consensus conference on faecal microbiota transplantation in clinical practice. *Gut* 2017; **66**: 569-580 [PMID: 28087657 DOI: 10.1136/gutjnl-2016-313017]
- 22 **Zhang F**, Luo W, Shi Y, Fan Z, Ji G. Should we standardize the 1,700-year-old fecal microbiota transplantation? *Am J Gastroenterol* 2012; **107**: 1755; author reply p.1755-1755; author reply p.1756 [PMID: 23160295 DOI: 10.1038/ajg.2012.251]
- 23 **Sha S**, Liang J, Chen M, Xu B, Liang C, Wei N, Wu K. Systematic review: faecal microbiota transplantation therapy for digestive and nondigestive disorders in adults and children. *Aliment Pharmacol Ther* 2014; **39**: 1003-1032 [PMID: 24641570 DOI: 10.1111/apt.12699]
- 24 **van Nood E**, Vrieze A, Nieuwdorp M, Fuentes S, Zoetendal EG, de Vos WM, Visser CE, Kuijper EJ, Bartelsman JF, Tijssen JG, Speelman P, Dijkgraaf MG, Keller JJ. Duodenal infusion of donor feces for recurrent *Clostridium difficile*. *N Engl J Med* 2013; **368**: 407-415 [PMID: 23323867 DOI: 10.1056/NEJMoa1205037]
- 25 **Wortelboer K**, Nieuwdorp M, Herrema H. Fecal microbiota transplantation beyond *Clostridioides difficile* infections. *EBioMedicine* 2019; **44**: 716-729 [PMID: 31201141 DOI: 10.1016/j.ebiom.2019.05.066]
- 26 **Sokol H**, Landman C, Seksik P, Berard L, Montil M, Nion-Larmurier I, Bourrier A, Le Gall G, Lalande V, De Rougemont A, Kirchgessner J, Dagueneil A, Cachanado M, Rousseau A, Drouet É, Rosenzweig M, Hagege H, Dray X, Klatzman D, Marteau P; Saint-Antoine IBD Network, Beaugerie L, Simon T. Fecal microbiota transplantation to maintain remission in Crohn's disease: a pilot randomized controlled study. *Microbiome* 2020; **8**: 12 [PMID: 32014035 DOI: 10.1186/s40168-020-0792-5]
- 27 **Stojek M**, Jabłońska A, Adrych K. The Role of Fecal Microbiota Transplantation in the Treatment of Inflammatory Bowel Disease. *J Clin Med* 2021; **10** [PMID: 34575166 DOI: 10.3390/jcm10184055]
- 28 **Costello SP**, Soo W, Bryant RV, Jairath V, Hart AL, Andrews JM. Systematic review with meta-analysis: faecal microbiota transplantation for the induction of remission for active ulcerative colitis. *Aliment Pharmacol Ther* 2017; **46**: 213-224 [PMID: 28612983 DOI: 10.1111/apt.14173]
- 29 **Cammarota G**, Ianiro G, Kelly CR, Mullish BH, Allegretti JR, Kassam Z, Putignani L, Fischer M, Keller JJ, Costello SP, Sokol H, Kump P, Satokari R, Kahn SA, Kao D, Arkkila P, Kuijper EJ, Vehreschild MJG, Pintus C, Lopetuso L, Masucci L, Scaldaferrì F, Terveer EM, Nieuwdorp M, López-Sanromán A, Kupcinkas J, Hart A, Tilg H, Gasbarrini A. International consensus conference on stool banking for faecal microbiota transplantation in clinical practice. *Gut* 2019; **68**: 2111-2121 [PMID: 31563878 DOI: 10.1136/gutjnl-2019-319548]
- 30 **Keller JJ**, Ooijselaar RE, Hvas CL, Terveer EM, Lieberknecht SC, Högenauer C, Arkkila P, Sokol H, Gridnyev O, Mégraud F, Kump PK, Nakov R, Goldenberg SD, Satokari R, Tkatch S, Sanguinetti M, Cammarota G, Dorofeev A, Gubska O, Ianiro G, Mattila E, Arasaradnam RP, Sarin SK, Sood A, Putignani L, Alric L, Baunwall SMD, Kupcinkas J, Link A, Goorhuis AG, Verspaget HW, Ponsioen C, Hold GL, Tilg H, Kassam Z, Kuijper EJ, Gasbarrini A, Mulder CJJ, Williams HRT, Vehreschild MJGT. A standardised model for stool banking for faecal microbiota transplantation: a

- consensus report from a multidisciplinary UEG working group. *United European Gastroenterol J* 2021; **9**: 229-247 [PMID: 33151137 DOI: 10.1177/2050640620967898]
- 31 **König J**, Siebenhaar A, Högenauer C, Arkkila P, Nieuwdorp M, Norén T, Ponsioen CY, Rosien U, Rossen NG, Satokari R, Stallmach A, de Vos W, Keller J, Brummer RJ. Consensus report: faecal microbiota transfer - clinical applications and procedures. *Aliment Pharmacol Ther* 2017; **45**: 222-239 [PMID: 27891639 DOI: 10.1111/apt.13868]
 - 32 **Lee CH**, Steiner T, Petrof EO, Smieja M, Roscoe D, Nematallah A, Weese JS, Collins S, Moayyedi P, Crowther M, Ropeleski MJ, Jayaratne P, Higgins D, Li Y, Rau NV, Kim PT. Frozen vs Fresh Fecal Microbiota Transplantation and Clinical Resolution of Diarrhea in Patients With Recurrent *Clostridium difficile* Infection: A Randomized Clinical Trial. *JAMA* 2016; **315**: 142-149 [PMID: 26757463 DOI: 10.1001/jama.2015.18098]
 - 33 **Youngster I**, Russell GH, Pindar C, Ziv-Baran T, Sauk J, Hohmann EL. Oral, capsulized, frozen fecal microbiota transplantation for relapsing *Clostridium difficile* infection. *JAMA* 2014; **312**: 1772-1778 [PMID: 25322359 DOI: 10.1001/jama.2014.13875]
 - 34 **Satokari R**, Mattila E, Kainulainen V, Arkkila PE. Simple faecal preparation and efficacy of frozen inoculum in faecal microbiota transplantation for recurrent *Clostridium difficile* infection--an observational cohort study. *Aliment Pharmacol Ther* 2015; **41**: 46-53 [PMID: 25355279 DOI: 10.1111/apt.13009]
 - 35 **Baunwall SMD**, Lee MM, Eriksen MK, Mullish BH, Marchesi JR, Dahlerup JF, Hvas CL. Faecal microbiota transplantation for recurrent *Clostridioides difficile* infection: An updated systematic review and meta-analysis. *EClinicalMedicine* 2020; **29-30**: 100642 [PMID: 33437951 DOI: 10.1016/j.eclinm.2020.100642]
 - 36 **Zellmer C**, De Wolfe TJ, Van Hoof S, Blakney R, Safdar N. Patient Perspectives on Fecal Microbiota Transplantation for *Clostridium Difficile* Infection. *Infect Dis Ther* 2016; **5**: 155-164 [PMID: 27048199 DOI: 10.1007/s40121-016-0106-1]
 - 37 **Lee KN**, Lee OY. Intestinal microbiota in pathophysiology and management of irritable bowel syndrome. *World J Gastroenterol* 2014; **20**: 8886-8897 [PMID: 25083061 DOI: 10.3748/wjg.v20.i27.8886]
 - 38 **Fan WT**, Ding C, Xu NN, Zong S, Ma P, Gu B. Close association between intestinal microbiota and irritable bowel syndrome. *Eur J Clin Microbiol Infect Dis* 2017; **36**: 2303-2317 [PMID: 28785822 DOI: 10.1007/s10096-017-3060-2]
 - 39 **Ringel-Kulka T**, Benson AK, Carroll IM, Kim J, Legge RM, Ringel Y. Molecular characterization of the intestinal microbiota in patients with and without abdominal bloating. *Am J Physiol Gastrointest Liver Physiol* 2016; **310**: G417-G426 [PMID: 26702134 DOI: 10.1152/ajpgi.00044.2015]
 - 40 **Jeffery IB**, O'Toole PW, Öhman L, Claesson MJ, Deane J, Quigley EM, Simrén M. An irritable bowel syndrome subtype defined by species-specific alterations in faecal microbiota. *Gut* 2012; **61**: 997-1006 [PMID: 22180058 DOI: 10.1136/gutjnl-2011-301501]
 - 41 **Mizuno S**, Masaoka T, Naganuma M, Kishimoto T, Kitazawa M, Kurokawa S, Nakashima M, Takeshita K, Suda W, Mimura M, Hattori M, Kanai T. Bifidobacterium-Rich Fecal Donor May Be a Positive Predictor for Successful Fecal Microbiota Transplantation in Patients with Irritable Bowel Syndrome. *Digestion* 2017; **96**: 29-38 [PMID: 28628918 DOI: 10.1159/000471919]
 - 42 **Vaughn BP**, Vatanen T, Allegretti JR, Bai A, Xavier RJ, Korzenik J, Gevers D, Ting A, Robson SC, Moss AC. Increased Intestinal Microbial Diversity Following Fecal Microbiota Transplant for Active Crohn's Disease. *Inflamm Bowel Dis* 2016; **22**: 2182-2190 [PMID: 27542133 DOI: 10.1097/MIB.0000000000000893]
 - 43 **Halkjær SI**, Christensen AH, Lo BZS, Browne PD, Günther S, Hansen LH, Petersen AM. Faecal microbiota transplantation alters gut microbiota in patients with irritable bowel syndrome: results from a randomised, double-blind placebo-controlled study. *Gut* 2018; **67**: 2107-2115 [PMID: 29980607 DOI: 10.1136/gutjnl-2018-316434]
 - 44 **Holvoet T**, Joossens M, Vázquez-Castellanos JF, Christiaens E, Heyerick L, Boelens J, Verhasselt B, van Vlierberghe H, De Vos M, Raes J, De Looze D. Fecal Microbiota Transplantation Reduces Symptoms in Some Patients With Irritable Bowel Syndrome With Predominant Abdominal Bloating: Short- and Long-term Results From a Placebo-Controlled Randomized Trial. *Gastroenterology* 2021; **160**: 145-157.e8 [PMID: 32681922 DOI: 10.1053/j.gastro.2020.07.013]
 - 45 **Li SS**, Zhu A, Benes V, Costea PI, Hercog R, Hildebrand F, Huerta-Cepas J, Nieuwdorp M, Salojärvi J, Voigt AY, Zeller G, Sunagawa S, de Vos WM, Bork P. Durable coexistence of donor and recipient strains after fecal microbiota transplantation. *Science* 2016; **352**: 586-589 [PMID: 27126044 DOI: 10.1126/science.aad8852]
 - 46 **Pimentel M**, Lembo A. Microbiome and Its Role in Irritable Bowel Syndrome. *Dig Dis Sci* 2020; **65**: 829-839 [PMID: 32026278 DOI: 10.1007/s10620-020-06109-5]
 - 47 **Wang L**, Alamar N, Singh R, Nanavati J, Song Y, Chaudhary R, Mullin GE. Gut Microbial Dysbiosis in the Irritable Bowel Syndrome: A Systematic Review and Meta-Analysis of Case-Control Studies. *J Acad Nutr Diet* 2020; **120**: 565-586 [PMID: 31473156 DOI: 10.1016/j.jand.2019.05.015]
 - 48 **Halkjær SI**, Boelsen AW, Günther S, Christensen AH, Petersen AM. Can fecal microbiota transplantation cure irritable bowel syndrome? *World J Gastroenterol* 2017; **23**: 4112-4120 [PMID: 28652664 DOI: 10.3748/wjg.v23.i22.4112]
 - 49 **Andrews P**, Barnes P, Borody T. Chronic constipation reversed by restoration of bowel flora. A case and a hypothesis. *Eur J Gastroenterol Hepatol* 1992; **4**: 245-247
 - 50 **Borody TJ**, George L, Andrews P, Brandl S, Noonan S, Cole P, Hyland L, Morgan A, Maysey J, Moore-Jones D. Bowel-flora alteration: a potential cure for inflammatory bowel disease and irritable bowel syndrome? *Med J Aust* 1989; **150**: 604 [PMID: 2783214 DOI: 10.5694/j.1326-5377.1989.tb136704.x]
 - 51 **Borody TJ**, Warren EF, Leis SM, Surace R, Ashman O, Siarakas S. Bacteriotherapy using fecal flora: toying with human motions. *J Clin Gastroenterol* 2004; **38**: 475-483 [PMID: 15220681 DOI: 10.1097/01.mcg.0000128988.13808.dc]
 - 52 **Cruz Aguilar R**, Buch T, Bajbouj. Fecal microbiota transplantation as a novel therapy for irritable bowel syndrome with predominant diarrhea. *Neurogastroenterol Motil* 2015; **110** [DOI: 10.1111/nmo.14353]
 - 53 **Holvoet T**, Boelens J, Joossens M, Raes J, De Vos M, De Looze D. Fecal Microbiota Transplantation in Irritable Bowel Syndrome With Bloating: Results From a Prospective Pilot Study. *Gastroenterology* 2015; **148**: S963-S964 [DOI: 10.1016/s0016-5085(15)33291-1]
 - 54 **Hong J**, Bang B, Shin Y, Kim H, Kwon K. Treatment of Irritable Bowel Syndrome with Fecal Microbiota Transplantation: A case series of 10 patients. *United European Gastroenterol J* 2016; **A102** [DOI: 10.1177/2050640619866990]

- 55 **Mazzawi T**, El-Salhy M, Lied GA, Hausken T. The Effects of Fecal Microbiota Transplantation on the Symptoms and the Duodenal Neurogenin 3, Musashi 1, and Enteroendocrine Cells in Patients With Diarrhea-Predominant Irritable Bowel Syndrome. *Front Cell Infect Microbiol* 2021; **11**: 524851 [PMID: 34055657 DOI: 10.3389/fcimb.2021.524851]
- 56 **Pinn D**, Aroniadis O, Brandt L. Follow-up Study of Fecal Microbiota Transplantation (FMT) for the Treatment of Refractory Irritable Bowel Syndrome (IBS) 1862. *Am J Gastroenterol* 2013; **108**: S563 [DOI: 10.14309/00000434-201310001-01862]
- 57 **Syzenko G**, Budovska L, Puchkov K. P0397 Efficiency of FMT in cases of ‘Treatment-resistant’ IBS. *United European Gastroenterol J* 2016; **2**: A294
- 58 **Lahtinen P**, Jalanka J, Hartikainen A, Mattila E, Hillilä M, Punkkinen J, Koskenpato J, Anttila VJ, Tillonen J, Satokari R, Arkkila P. Randomised clinical trial: faecal microbiota transplantation versus autologous placebo administered *via* colonoscopy in irritable bowel syndrome. *Aliment Pharmacol Ther* 2020; **51**: 1321-1331 [PMID: 32343000 DOI: 10.1111/apt.15740]
- 59 **Aroniadis OC**, Brandt LJ, Oneto C, Feuerstadt P, Sherman A, Wolkoff AW, Kassam Z, Sadovsky RG, Elliott RJ, Budree S, Kim M, Keller MJ. Faecal microbiota transplantation for diarrhoea-predominant irritable bowel syndrome: a double-blind, randomised, placebo-controlled trial. *Lancet Gastroenterol Hepatol* 2019; **4**: 675-685 [PMID: 31326345 DOI: 10.1016/S2468-1253(19)30198-0]
- 60 **El-Salhy M**, Hatlebakk JG, Gilja OH, Bråthen Kristoffersen A, Hausken T. Efficacy of faecal microbiota transplantation for patients with irritable bowel syndrome in a randomised, double-blind, placebo-controlled study. *Gut* 2020; **69**: 859-867 [PMID: 31852769 DOI: 10.1136/gutjnl-2019-319630]
- 61 **Holster S**, Lindqvist CM, Repsilber D, Salonen A, de Vos WM, König J, Brummer RJ. The Effect of Allogenic Versus Autologous Fecal Microbiota Transfer on Symptoms, Visceral Perception and Fecal and Mucosal Microbiota in Irritable Bowel Syndrome: A Randomized Controlled Study. *Clin Transl Gastroenterol* 2019; **10**: e00034 [PMID: 31009405 DOI: 10.14309/ctg.0000000000000034]
- 62 **Johnsen PH**, Hilpüsch F, Cavanagh JP, Leikanger IS, Kolstad C, Valle PC, Goll R. Faecal microbiota transplantation versus placebo for moderate-to-severe irritable bowel syndrome: a double-blind, randomised, placebo-controlled, parallel-group, single-centre trial. *Lancet Gastroenterol Hepatol* 2018; **3**: 17-24 [PMID: 29100842 DOI: 10.1016/S2468-1253(17)30338-2]
- 63 **Singh P**, Alm EJ, Kelley JM, Cheng V, Smith M, Kassam Z, Nee J, Iturrino J, Lembo A. Effect of antibiotic pretreatment on bacterial engraftment after Fecal Microbiota Transplant (FMT) in IBS-D. *Gut Microbes* 2022; **14**: 2020067 [PMID: 35014601 DOI: 10.1080/19490976.2021.2020067]
- 64 **Ford AC**, Moayyedi P. Meta-analysis: factors affecting placebo response rate in the irritable bowel syndrome. *Aliment Pharmacol Ther* 2010; **32**: 144-158 [PMID: 20412064 DOI: 10.1111/j.1365-2036.2010.04328.x]
- 65 **Higgins JPT**, Green S (editors). *Cochrane Handbook for Systematic Reviews of Interventions* Version 5.1.0 [updated March 2011]. The Cochrane Collaboration, 2011
- 66 **Halkjær SI**, Lo B, Cold F, Christensen AHH, Gluud LL, Petersen AM. Fecal microbiota transplantation for treatment of irritable bowel syndrome (Protocol). *Cochrane Database Syst Rev* 2020 [DOI: 10.1002/14651858.CD013602]
- 67 **Simren M**, Palsson OS, Whitehead WE. Update on Rome IV Criteria for Colorectal Disorders: Implications for Clinical Practice. *Curr Gastroenterol Rep* 2017; **19**: 15 [PMID: 28374308 DOI: 10.1007/s11894-017-0554-0]
- 68 **Cochrane Consumers and Communication La Trobe University**, Ryan R, Synnot A, M P, Hill S. Data extraction template. 2018 [DOI: 10.26181/5b57cfd711743]
- 69 **Higgins JP**, Altman DG, Gøtzsche PC, Jüni P, Moher D, Oxman AD, Savovic J, Schulz KF, Weeks L, Sterne JA; Cochrane Bias Methods Group; Cochrane Statistical Methods Group. The Cochrane Collaboration's tool for assessing risk of bias in randomised trials. *BMJ* 2011; **343**: d5928 [PMID: 22008217 DOI: 10.1136/bmj.d5928]
- 70 **Patel SM**, Stason WB, Legedza A, Ock SM, Kaptchuk TJ, Conboy L, Canenguez K, Park JK, Kelly E, Jacobson E, Kerr CE, Lembo AJ. The placebo effect in irritable bowel syndrome trials: a meta-analysis. *Neurogastroenterol Motil* 2005; **17**: 332-340 [PMID: 15916620 DOI: 10.1111/j.1365-2982.2005.00650.x]
- 71 **Li M**, Qian W, Yu L, Tian F, Zhang H, Chen W, Xue Y, Zhai Q. Multi-Time-Point Fecal Sampling in Human and Mouse Reveals the Formation of New Homeostasis in Gut Microbiota after Bowel Cleansing. *Microorganisms* 2022; **10** [PMID: 36557570 DOI: 10.3390/microorganisms10122317]
- 72 **Jalanka J**, Hillamaa A, Satokari R, Mattila E, Anttila VJ, Arkkila P. The long-term effects of faecal microbiota transplantation for gastrointestinal symptoms and general health in patients with recurrent *Clostridium difficile* infection. *Aliment Pharmacol Ther* 2018; **47**: 371-379 [PMID: 29226561 DOI: 10.1111/apt.14443]
- 73 **Imdad A**, Nicholson MR, Tanner-Smith EE, Zackular JP, Gomez-Duarte OG, Beaulieu DB, Acra S. Fecal transplantation for treatment of inflammatory bowel disease. *Cochrane Database Syst Rev* 2018; **11**: CD012774 [PMID: 30480772 DOI: 10.1002/14651858.CD012774.pub2]
- 74 **Liu HN**, Wu H, Chen YZ, Chen YJ, Shen XZ, Liu TT. Altered molecular signature of intestinal microbiota in irritable bowel syndrome patients compared with healthy controls: A systematic review and meta-analysis. *Dig Liver Dis* 2017; **49**: 331-337 [PMID: 28179092 DOI: 10.1016/j.dld.2017.01.142]
- 75 **Mayer EA**, Knight R, Mazmanian SK, Cryan JF, Tillisch K. Gut microbes and the brain: paradigm shift in neuroscience. *J Neurosci* 2014; **34**: 15490-15496 [PMID: 25392516 DOI: 10.1523/JNEUROSCI.3299-14.2014]
- 76 **Ford AC**, Harris LA, Lacy BE, Quigley EMM, Moayyedi P. Systematic review with meta-analysis: the efficacy of prebiotics, probiotics, synbiotics and antibiotics in irritable bowel syndrome. *Aliment Pharmacol Ther* 2018; **48**: 1044-1060 [PMID: 30294792 DOI: 10.1111/apt.15001]
- 77 **Goll R**, Johnsen PH, Hjerde E, Diab J, Valle PC, Hilpüsch F, Cavanagh JP. Effects of fecal microbiota transplantation in subjects with irritable bowel syndrome are mirrored by changes in gut microbiome. *Gut Microbes* 2020; **12**: 1794263 [PMID: 32991818 DOI: 10.1080/19490976.2020.1794263]
- 78 **Cold F**, Baunwall SMD, Dahlerup JF, Petersen AM, Hvas CL, Hansen LH. Systematic review with meta-analysis: encapsulated faecal microbiota transplantation - evidence for clinical efficacy. *Therap Adv Gastroenterol* 2021; **14**: 17562848211041004 [PMID: 34484424 DOI: 10.1177/17562848211041004]

- 79 **Franc A**, Vetchý D, Fülöpová N. Commercially Available Enteric Empty Hard Capsules, Production Technology and Application. *Pharmaceuticals (Basel)* 2022; **15** [PMID: 36422528 DOI: 10.3390/ph15111398]
- 80 **Ianiro G**, Punčochář M, Karcher N, Porcari S, Armanini F, Asnicar F, Beghini F, Blanco-Míguez A, Cumbo F, Manghi P, Pinto F, Masucci L, Quaranta G, De Giorgi S, Sciumè GD, Bibbò S, Del Chierico F, Putignani L, Sanguinetti M, Gasbarrini A, Valles-Colomer M, Cammarota G, Segata N. Variability of strain engraftment and predictability of microbiome composition after fecal microbiota transplantation across different diseases. *Nat Med* 2022; **28**: 1913-1923 [PMID: 36109637 DOI: 10.1038/s41591-022-01964-3]
- 81 **El-Salhy M**, Hausken T, Hatlebakk JG. Current status of fecal microbiota transplantation for irritable bowel syndrome. *Neurogastroenterol Motil* 2021; **33**: e14157 [PMID: 34236740 DOI: 10.1111/nmo.14157]
- 82 **Orr MR**. The biodiversity dose-response curve translates theory and practice from ecological restoration into research and clinical priorities for fecal microbiota transplantation. *Front Med (Lausanne)* 2022; **9**: 1059148 [PMID: 36438048 DOI: 10.3389/fmed.2022.1059148]

Global research trends on diet and nutrition in Crohn's disease

Muna Shakhshir, Sa'ed H Zyoud

Specialty type: Nutrition and dietetics

Provenance and peer review: Invited article; Externally peer reviewed.

Peer-review model: Single blind

Peer-review report's scientific quality classification

Grade A (Excellent): 0
Grade B (Very good): B, B
Grade C (Good): C
Grade D (Fair): 0
Grade E (Poor): 0

P-Reviewer: Bukhari SM, Saudi Arabia; Leowattana W, Thailand; Valek V, Czech Republic

Received: January 9, 2023

Peer-review started: January 9, 2023

First decision: March 8, 2023

Revised: March 20, 2023

Accepted: May 4, 2023

Article in press: May 4, 2023

Published online: May 28, 2023



Muna Shakhshir, Department of Nutrition, An-Najah National University Hospital, Nablus 44839, Palestine

Sa'ed H Zyoud, Department of Clinical and Community Pharmacy, College of Medicine and Health Sciences, An-Najah National University, Nablus 44839, Palestine

Sa'ed H Zyoud, Poison Control and Drug Information Center (PCDIC), College of Medicine and Health Sciences, An-Najah National University, Nablus 44839, Palestine

Sa'ed H Zyoud, Clinical Research Centre, An-Najah National University Hospital, Nablus 44839, Palestine

Corresponding author: Sa'ed H Zyoud, PhD, Full Professor, Department of Clinical and Community Pharmacy, College of Medicine and Health Sciences, An-Najah National University, Academic Street, Nablus 44839, Palestine. saedzyoud@yahoo.com

Abstract

BACKGROUND

Crohn's disease represents a challenge for patients concerned with the modified diet regimen as well as practitioners who seek the best nutritional therapy. Crohn's disease can alter the body's ability to digest food and to absorb nutrients, resulting in severe vitamin deficiencies, malnutrition and sometimes life-threatening complications. However, a comprehensive bibliometric analysis is lacking to map the current links between nutrition and Crohn's disease in terms of the number of citations, geographic distribution and growth trends of publications.

AIM

To introduce the current state of research as well as hotspots in the field of nutrition and Crohn's disease from a bibliometric standpoint.

METHODS

We searched the Scopus database and selected the relevant literature on nutrition and Crohn's disease that met the inclusion criteria. We analyzed the publication trends and research hotspots by using video object segmentation viewer software.

RESULTS

We included 1237 publications. The number of documents published each year has increased steadily. The United States and the University of Otago, Christchurch, have had the highest productivity, with 208 (16.81%) and 29 (2.34%) documents, respectively. The "role of exclusive enteral nutrition for complicated Crohn's disease" and "manipulation of the gut microbiota as a key target for

Crohn's disease" were the major research areas in 2016-2021, and they could be extensively investigated in the future. Meanwhile, research on "malnutrition in patients with Crohn's disease" appeared to be an area that attracted more research attention before 2016.

CONCLUSION

This is the first bibliometric analysis to map the knowledge structure and trends regarding nutrition in Crohn's disease research over the past two decades. The results provide a comprehensive summary and identification of the frontiers of nutrition and Crohn's disease-related research, which may be used as a resource by researchers in the field.

Key Words: Nutrition; Diet; Crohn's disease; Bibliometric; Microbiota; Malnutrition

©The Author(s) 2023. Published by Baishideng Publishing Group Inc. All rights reserved.

Core Tip: There is much interest in using nutrition therapy approaches to treat Crohn's disease, while the current state of knowledge is still inadequate to make general recommendations. Therefore, a bibliometric analysis of the global trend in research on nutrition and Crohn's disease was conducted. This study outlines the current state of research themes and hotspots in nutrition and Crohn's disease research because no bibliometric research has been conducted to determine worldwide trends in nutrition and Crohn's disease. This facilitates researchers and healthcare providers in identifying potential future research directions.

Citation: Shakhshir M, Zyoud SH. Global research trends on diet and nutrition in Crohn's disease. *World J Gastroenterol* 2023; 29(20): 3203-3215

URL: <https://www.wjgnet.com/1007-9327/full/v29/i20/3203.htm>

DOI: <https://dx.doi.org/10.3748/wjg.v29.i20.3203>

INTRODUCTION

Crohn's disease is a relapsing transmural inflammatory disease of the gut with an unclear etiology; it involves acute attacks followed by periods of remission[1,2]. Crohn's disease can affect the entire gastrointestinal tract, from the mouth to the anus[3]. However, the disease affects the terminal ileum and the colon in most cases, which can result in complications such as stenosis, abscesses and fistula[4]. The prevalence rate of Crohn's disease ranges from 0.6 to 322 per 100000 people[5].

Malnutrition is frequently visible in approximately 65%-75% of patients with Crohn's disease[6]. Malabsorption, gut dysbiosis, small intestinal bacterial overgrowth and symptoms such as weight loss, reduced dietary intake, deficiency of individual nutrients or many nutrients are just a few of the mechanisms that can be related to Crohn's disease-related malnutrition[7,8]. In this case, nutrition, which may take the form of dietary adjustments, parenteral nutrition, or enteral nutrition, plays an important role in treating Crohn's disease[7,9,10]. Parenteral nutrition is a type of nutrition support that is given through an intravenous line. It is used when the digestive tract cannot properly absorb nutrients. In severe cases of Crohn's disease, where the digestive tract is severely damaged, parenteral nutrition may be necessary[7,11]. Furthermore, enteral nutrition is a type of nutrition support that is given through a feeding tube. It can help reduce inflammation and promote healing of the digestive tract. Enteral nutrition may be used as a primary treatment for Crohn's disease or as a supplement to other treatments[7,11].

There is much interest in using nutritional approaches to control and reduce the symptoms of Crohn's disease and to increase the remission time. Nevertheless, there is insufficient scientific support to give health care providers more options regarding dietary therapies. As a result, we performed a bibliometric analysis of the global trends in research on nutrition and Crohn's disease. We summarize the current state of research themes and hotspots in nutrition and Crohn's disease to look for global trends. Our findings will make it easier for researchers and newcomers to understand the current state of the field, to strategize future goals in research and to identify potential future research directions.

MATERIALS AND METHODS

Data sources

We conducted a shortlisted quantitative analysis with an approach based on previously published

scientific outputs to characterize the development of research on nutrition and Crohn's disease over the past two decades. On December 30, 2022, we searched the Scopus database for studies that had been published between 2002 and 2021. The Scopus database is often an essential source of information for bibliometric research and evaluations of scientific publications[12]. Numerous successful bibliometric studies have been performed using the Scopus database as a data source[13-17].

Search strategy

We used relevant publications on nutrition[18,19] and Crohn's disease[20] to choose keywords to search the Scopus database and to identify studies. Each of the chosen keywords relates to nutrition, and we used them as an entry for the "Article Title" field. Due to the possibility that the title/abstract/keyword search would retrieve unnecessary papers, we searched the titles with specific limits to reduce false-positive results[21-24]. When writing the keywords, we used asterisks (*) and quote marks to narrow and broaden the search scope. The keywords we used were *nutrit** or *nutrient** or *diet** or *eat** or *feeding-pertain to nutrition* or *diet per se* rather than other related terminology such as specific names or classes of dietary compounds. Furthermore, we searched all terms related to Crohn's disease in the "Article Title" and/or "Abstract" fields.

Bibliometric indicators

We imported the retrieved data into Microsoft Excel so that we could analyze and tabulate it. We retrieved relevant bibliometric data (such as the number of articles published per year, the types of documents retrieved, countries/regions, institutions, funding agencies, journals and their impact factors (*IF*), citation patterns and the *h-index*) for research publications related to nutrition and Crohn's disease. We used descriptive statistics to analyze our findings. The *Impact Index Per Article* that is being shown refers to the top 10 papers with the highest number of citations, which were obtained from the *Reference Citation Analysis (RCA)*, (<https://referencecitationanalysis.com/>). RCA is a citation analysis database that is open and covers multiple disciplines. The company is located in Pleasanton, CA 94566, United States [25-27].

Data visualization

We analyzed and visualized the data by using VOSviewer software version 1.6.8, a free online tool[28-30]. The software generated visualization maps that displayed the most commonly occurring keywords in the retrieved publications. The size of the node in each map represented the frequency of a particular keyword, indicating the relevance and popularity of the corresponding topic in the field. Based on these maps, the hot topics in the field were identified, revealing the areas that received the most attention and research focus. This analysis provided valuable insights into the current trends and research directions in the field, which can be used to guide future research and inform the decision-making processes. In addition, visualization maps were used to determine international collaboration. VOSviewer can determine the extent of the collaboration between two countries by considering the width of the connecting line and the total number of publications.

RESULTS

Analysis of publication trends

There were 1237 publications on nutrition and Crohn's disease published between 2002 and 2021. The documents recovered were of 9 types, mainly research articles ($n = 791$; 63.95%), followed by reviews ($n = 285$; 23.04%). The total number of publications by year is shown in Figure 1. The number of publications per year increased from 28 in 2002 to 123 in 2021.

Analysis of the country distribution

The publications were from authors representing 108 countries/regions. The top 10 active countries are shown in Table 1. The top 10 countries contributed 905 (73.16%) of the recovered documents. Among the eligible countries, the United States had the highest number of publications ($n = 208$, 16.81%), followed by the United Kingdom ($n = 192$, 15.52%), China ($n = 109$, 8.81%), Japan ($n = 98$, 7.92%), and Canada ($n = 88$, 7.11%). Furthermore, we analyzed countries that had more than 20 publications on nutrition and Crohn's disease. Based on our findings from 18 eligible countries, the United States, the United Kingdom, and Canada are the central countries with links to other countries (Figure 2).

Contributions of institutions

Based on the number of publications, Table 2 includes the top 10 institutions that have produced publications on nutrition and Crohn's disease. The University of Otago, Christchurch (New Zealand), has had the highest scientific production ($n = 29$, 2.34%), followed by Tel Aviv University (Israel), with 25 publications (2.02%). Massachusetts General Hospital (United States) and Jinling Hospital (China) have the third highest production ($n = 22$, 1.78%).

Table 1 Top 10 productive countries/regions involved in nutrition and Crohn's disease from 2002 to 2021

Ranking	Country	No. of documents	%
1 st	United States	208	16.81
2 nd	United Kingdom	192	15.52
3 rd	China	109	8.81
4 th	Japan	98	7.92
5 th	Canada	88	7.11
6 th	Germany	73	5.90
7 th	Spain	71	5.74
8 th	Italy	70	5.66
9 th	France	67	5.42
10 th	Poland	61	4.93

Table 2 Top 10 productive institutions ranked by the number of publications

Ranking	Institute	Country	No. of documents	%
1 st	University of Otago, Christchurch	New Zealand	29	2.34
2 nd	Tel Aviv University	Israel	25	2.02
3 rd	Massachusetts General Hospital	United States	22	1.78
3 rd	Jinling Hospital	China	22	1.78
5 th	UNSW Sydney	Australia	21	1.70
6 th	Harvard Medical School	United States	20	1.62
7 th	University of Glasgow	United Kingdom	19	1.54
7 th	Sydney Children's Hospital, Randwick	Australia	19	1.54
9 th	Medical School of Nanjing University	China	18	1.46
9 th	University of Washington	United States	18	1.46

Analysis of funding agencies

We identified 274 (22.15%) articles that were part of financed projects. The United States funding agencies were the most active in this field, with the National Institute of Diabetes and Digestive and Kidney Diseases ($n = 34$, 2.75%) being the most active. This was followed by the National Institutes of Health ($n = 30$, 2.43%), the National Natural Science Foundation for China Diseases ($n = 30$, 2.43%) and the Crohn's and Colitis Foundation ($n = 20$, 1.62%) (Table 3).

Journal analysis

The top 10 journals that have published the most articles concerning nutrition and Crohn's disease are listed in Table 4 with their *IF* in 2022. Nutrients was the most productive journal, with 57 documents contributing to 4.61% of the total publications, followed by *Inflammatory Bowel Diseases* ($n = 55$, 4.45%), *Alimentary Pharmacology and Therapeutics* ($n = 39$, 3.15%), *Clinical Nutrition* ($n = 29$, 2.34%), and the *Journal of Pediatric Gastroenterology and Nutrition* ($n = 29$, 2.34%).

Citation analysis

There was an average of 29.46 citations per document, for a total of 36444 citations. The h-index of the retrieved documents was 93. A total of 183 (14.8%) of the retrieved documents did not have citations, but 83 had been cited ≥ 100 times. The top 10 articles were cited 3912 times[31-40]. There was a wide range in the total number of citations for these publications, from 310 to 603 (Table 5). The impact index per article for the top 10 most cited articles varied between 10.4 and 70.6 (Table 5).

Keyword analysis of research hotspots

The co-occurrence network map of author keywords with at least 10 occurrences is displayed in Figure 3. Of the 1589 keywords, 43 met the threshold and were mainly concentrated in three aspects: (1)

Table 3 Top 10 funding agencies involved in nutrition and Crohn's disease from 2002 to 2021

Ranking	Funding agencies	Country	No. of publication	%
1 st	National Institute of Diabetes and Digestive and Kidney Diseases	United States	34	2.75
2 nd	National Institutes of Health	United States	30	2.43
2 nd	The National Natural Science Foundation of China	China	30	2.43
4 th	Crohn's and Colitis Foundation	United States	20	1.62
5 th	Medical Research Council	United Kingdom	16	1.29
6 th	AbbVie	United States	12	0.97
6 th	National Cancer Institute	United States	12	0.97
8 th	Canadian Institutes of Health Research	Canada	10	0.81
9 th	Japan Society for the Promotion of Science	Japan	10	0.81
8 th	National Center for Research Resources	United States	10	0.81
8 th	Nestlé Health Science	Switzerland	10	0.81
8 th	Pfizer	United States	10	0.81

Table 4 Ten most productive journals involved in nutrition and Crohn's disease from 2002 to 2021

Ranking	Journal/source title	No. of documents	%	IF ¹
1 st	<i>Nutrients</i>	57	4.61	6.706
2 nd	<i>Inflammatory Bowel Diseases</i>	55	4.45	7.290
3 rd	<i>Alimentary Pharmacology and Therapeutics</i>	39	3.15	9.524
4 th	<i>Clinical Nutrition</i>	29	2.34	7.643
4 th	<i>Journal of Pediatric Gastroenterology and Nutrition</i>	29	2.34	3.288
6 th	<i>Digestive Diseases and Sciences</i>	24	1.94	3.487
7 th	<i>Journal of Crohns and Colitis</i>	22	1.78	10.020
7 th	<i>World Journal of Gastroenterology</i>	22	1.78	5.374
9 th	<i>Gastroenterology</i>	17	1.37	33.883
9 th	<i>Nutrition in Clinical Practice</i>	17	1.37	3.204

¹Journal Citation Reports (Clarivate, 2022). IF: Impact index.

The “role of exclusive enteral nutrition (EEN) for complicated Crohn's disease” (red cluster); (2) “manipulation of the gut microbiota as a key target for Crohn's disease” (green cluster); and (3) “malnutrition in patients with Crohn's disease” (blue group).

We then divided the keywords by specific colors based on the average number of times they appeared in all publications (Figure 4). The blue color represents prior research (before 2016), while more recent studies are indicated by the yellow color (after 2018). Keywords in the groups of “role of EEN for complicated Crohn's disease”; and “manipulation of the gut microbiota as a key target for Crohn's disease” were the major areas in 2016-2021, and they could be extensively considered in the future. Meanwhile, research on “malnutrition in patients with Crohn's disease” appeared to be a research area that attracted more attention before 2016.

DISCUSSION

This bibliometric analysis represents a comprehensive shortlisted overview of nutrition and Crohn's disease research. In the last decade, there has been significant growth in worldwide research interest in this topic. The steady scientific progress over time shows that “manipulation of the gut microbiota as a key target for Crohn's disease” and “EEN for complicated Crohn's disease” are promising clinical approaches that should receive more investigation.

Table 5 Top 10 articles on total citations

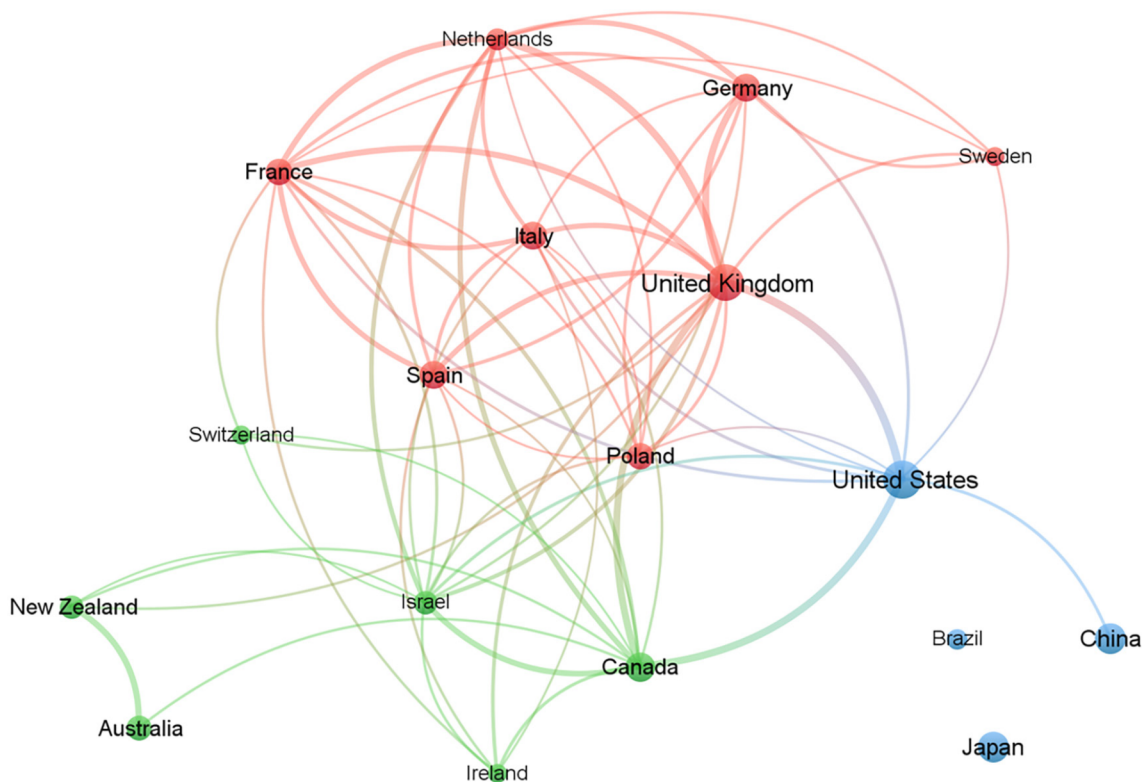
Ranking	Title	Source title	Cited by	Impact index per article ¹	Ref.
1 st	"Dietary intake and risk of developing inflammatory bowel disease: A systematic review of the literature"	<i>American Journal of Gastroenterology</i>	603	29.2	Hou <i>et al</i> [31], 2011
2 nd	"Inflammation, Antibiotics, and Diet as Environmental Stressors of the Gut Microbiome in Pediatric Crohn's Disease"	<i>Cell Host and Microbe</i>	449	70.6	Lewis <i>et al</i> [37], 2015
3 rd	"Diet-induced dysbiosis of the intestinal microbiota and the effects on immunity and disease"	<i>Nutrients</i>	425	36.5	Brown <i>et al</i> [32], 2012
4 th	"Differentiating ulcerative colitis from Crohn disease in children and young adults: Report of a Working Group of the North American Society for Pediatric Gastroenterology, Hepatology, and Nutrition and the Crohn's and Colitis Foundation of America"	<i>Journal of Pediatric Gastroenterology and Nutrition</i>	377	21.3	North American Society for Pediatric Gastroenterology, Hepatology, and Nutrition[33], 2007
5 th	"Enteral nutritional therapy for induction of remission in Crohn's disease"	<i>Cochrane Database of Systematic Reviews</i>	371	10.4	Zachos <i>et al</i> [34], 2007
6 th	"A prospective study of long-term intake of dietary fiber and risk of Crohn's disease and ulcerative colitis"	<i>Gastroenterology</i>	358	38.1	Ananthakrishnan <i>et al</i> [39], 2013
7 th	"Polymeric Diet Alone Versus Corticosteroids in the Treatment of Active Pediatric Crohn's Disease: A Randomized Controlled Open-Label Trial"	<i>Clinical Gastroenterology and Hepatology</i>	342	18.4	Borrelli <i>et al</i> [38], 2006
8 th	"ESPEN guideline: Clinical nutrition in inflammatory bowel disease"	<i>Clinical Nutrition</i>	341	48.9	Forbes <i>et al</i> [35], 2017
9 th	"Western diet induces dysbiosis with increased e coli in CEABAC10 mice, alters host barrier function favouring AIEC colonization"	<i>Gut</i>	336	38.4	Martinez-Medina <i>et al</i> [40], 2014
10 th	"Fine and ultrafine particles of the diet: Influence on the mucosal immune response and association with Crohn's disease"	<i>Proceedings of the Nutrition Society</i>	310	13.3	Lomer <i>et al</i> [36], 2002

¹The impact index per article is presented based on *Reference Citation Analysis* (<https://referencecitationanalysis.com/>).



Figure 1 Growth trends of publications on nutrition and Crohn's disease from 2002 to 2021.

The research found that the United States is the dominant country in this field, potentially due to various factors. These factors could include a higher prevalence of Crohn's disease in Western Europe and North America, where the disease affects 100 to 300 per 100000 people[5]. Other reasons may



DOI: 10.3748/wjg.v29.i20.3203 Copyright ©The Author(s) 2023.

Figure 2 Network visualization map depicting international collaboration in research related to nutrition and Crohn's disease during 2002-2021.

involve the country's investment in research, a diverse range of researchers in the field, access to well-resourced research environments, and a well-trained workforce. Researchers may profit from their country's economic success, which may provide financial assistance and travel chances. This finding is consistent with past studies that have shown the United States to be the top in research productivity[41-43]. Nonetheless, it is critical to remember that research productivity is only one component of scientific research. Other elements, such as research impact and societal ramifications, should be included when assessing the overall success of a research field or country.

Studying collaboration networks can offer useful insights into research partnerships and help pinpoint essential collaborators in a particular field. The United States and the United Kingdom have a distinct advantage in this regard because of their greater economic resources and scientific investments. Both countries have invested significantly in research and development, establishing world-class research institutions and universities. Additionally, they have implemented policies to foster global scientific and technological collaboration, leading to the formation of robust networks of researchers and institutions worldwide. Furthermore, these countries' substantial funding and resources enable them to attract the best talent globally, which has facilitated scientific progress and innovation. The extensive cooperation and collaboration among researchers in these countries have resulted in diverse and strong networks that are crucial in addressing complex scientific challenges[44-47].

We may gain insight into the areas of interest and potential future research directions in this field by analyzing the cooccurrence of the keywords. Its key terms often refer to the most important aspects of a publication; the threshold was met by 43 of the 1589 keywords retrieved from the authors' keywords. Therefore, it is helpful to define important concepts and create a framework for nutrition and Crohn's disease studies by analyzing the associated keywords.

One of the main research hotspots in our study was the role of EEN for complicated Crohn's disease. Enteral nutrition is the preferred feeding route in the induction of remission of active Crohn's disease, as it is a minimally invasive procedure with low risk. On the other hand, enteral nutrition has a beneficial effect on the gut microbiota and intestinal inflammation. Therefore, enteral nutrition has several advantages over parenteral nutrition: It can maintain enterohepatic circulation, reduce the inflammatory response, decrease bacterial overgrowth and translocation and avoid intravenous access complications [4]. EEN was first used in the 1970s and has been established over the last 20 years as an effective nutritional therapy that induces mucosal healing in approximately 80% of patients and provides 100% of daily nutrition requirements from high-energy artificial supplements and modified feeds with probiotics, amino acids, and fatty acids[48]. On the other hand, a prospective study showed that 3 mo of

negative results could have been included. Nevertheless, we believe that the use of title searches significantly reduces research errors. Third, regarding the credibility of the data gathered for our study, the precision and completeness of the keywords we used have a considerable impact. Hence, certain significant and influential articles could have been left off the representative list because the titles of those articles could contain specific types of nutrition or diet.

CONCLUSION

We employed bibliometric techniques to gather 1237 articles on nutrition and Crohn's disease that were published from January 2002 to December 2021. Our findings highlight a network of collaboration among countries, institutions, journals and funding agencies, shedding light on the latest trends and areas of interest in the field of emerging nutrition and Crohn's disease. Research in this area has been increasing steadily over the past decade. The United States and the United Kingdom are the leading contributors to this field, with the highest number of publications and a strong emphasis on international cooperation. The "role of EEN for complicated Crohn's disease" and "manipulation of the gut microbiota as a key target for Crohn's disease" are the current research hotspots. This bibliometric study provides a detailed analysis of nutrition and Crohn's disease research, which can serve as a resource for academics and policymakers in this field.

ARTICLE HIGHLIGHTS

Research background

Crohn's disease symptoms can include abdominal pain, diarrhea, fatigue, and weight loss. While Crohn's disease has no cure, there are techniques to control symptoms, including food and nutrition.

Research motivation

Assessing the current status of research and hotspots in nutrition and Crohn's disease is critical for identifying knowledge gaps and informing future research paths.

Research objectives

Using bibliometric analysis, the purpose of this study is to provide an overview of the current state of nutrition and Crohn's disease research.

Research methods

We conducted a thorough and rigorous analysis utilizing SciVerse Scopus to identify relevant material on nutrition and Crohn's disease. Next, we used VOSviewer software to examine prevalent areas of study and publishing patterns in related domains.

Research results

Over the past 20 years, there has been a rise in cross-border partnerships and interdisciplinary studies concerning the relationship between nutrition and Crohn's disease. Currently, the key areas of research in this field are the use of exclusive enteral nutrition for complicated cases of Crohn's disease and the manipulation of the gastrointestinal microbiome.

Research conclusions

There has been no bibliometric analysis of nutrition and Crohn's disease research in the last two decades. This study provides a complete assessment of the knowledge structure and developments in this topic. As such, the findings are a helpful resource for academics because they provide a detailed assessment and emphasize the frontiers of nutrition and Crohn's disease research.

Research perspectives

The purpose of this research is to identify current trends and focus areas in the field of nutrition and Crohn's disease to guide future research and treatment practice. Using bibliometric analysis, this study provides a comprehensive assessment of the relevant literature, assisting researchers and clinicians in staying up to date on the most recent advances in this field.

ACKNOWLEDGEMENTS

The author thanks An-Najah National University Hospital for all administrative assistance during the

implementation of the project.

FOOTNOTES

Author contributions: Zyoud SH designed the study, collected the data, analyzed the data, made major contributions to the manuscript's literature search and interpretation, and drafted the manuscript; Shakhshir M made major contributions to the manuscript's literature search and interpretation and made revisions to the initial draft; all authors provided a critical review and approved the final manuscript before submission.

Conflict-of-interest statement: The authors have no financial disclosures or conflicts of interest to declare.

PRISMA 2009 Checklist statement: The authors have read the PRISMA 2009 Checklist, and the manuscript was prepared and revised according to the PRISMA 2009 Checklist.

Open-Access: This article is an open-access article that was selected by an in-house editor and fully peer-reviewed by external reviewers. It is distributed in accordance with the Creative Commons Attribution NonCommercial (CC BY-NC 4.0) license, which permits others to distribute, remix, adapt, build upon this work non-commercially, and license their derivative works on different terms, provided the original work is properly cited and the use is non-commercial. See: <https://creativecommons.org/licenses/by-nc/4.0/>

Country/Territory of origin: Palestine

ORCID number: Muna Shakhshir 0000-0002-6213-8457; Sa'ed H Zyoud 0000-0002-7369-2058.

S-Editor: Chen YL

L-Editor: Filipodia

P-Editor: Yu HG

REFERENCES

- GBD 2017 Inflammatory Bowel Disease Collaborators.** The global, regional, and national burden of inflammatory bowel disease in 195 countries and territories, 1990-2017: a systematic analysis for the Global Burden of Disease Study 2017. *Lancet Gastroenterol Hepatol* 2020; **5**: 17-30 [PMID: 31648971 DOI: 10.1016/S2468-1253(19)30333-4]
- Danese S, Parigi TL, Peyrin-Biroulet L, Ghosh S.** Defining difficult-to-treat inflammatory bowel disease: why and how. *Lancet Gastroenterol Hepatol* 2021; **6**: 520-522 [PMID: 34019799 DOI: 10.1016/S2468-1253(21)00141-2]
- Jairath V, Feagan BG.** Global burden of inflammatory bowel disease. *Lancet Gastroenterol Hepatol* 2020; **5**: 2-3 [PMID: 31648974 DOI: 10.1016/S2468-1253(19)30358-9]
- Adamji M, Day AS.** An overview of the role of exclusive enteral nutrition for complicated Crohn's disease. *Intest Res* 2019; **17**: 171-176 [PMID: 30508476 DOI: 10.5217/ir.2018.00079]
- Ng SC, Shi HY, Hamidi N, Underwood FE, Tang W, Benchimol EI, Panaccione R, Ghosh S, Wu JCY, Chan FKL, Sung JJY, Kaplan GG.** Worldwide incidence and prevalence of inflammatory bowel disease in the 21st century: a systematic review of population-based studies. *Lancet* 2017; **390**: 2769-2778 [PMID: 29050646 DOI: 10.1016/S0140-6736(17)32448-0]
- Scaldaferri F, Pizzoferrato M, Lopetuso LR, Musca T, Ingravalle F, Sicignano LL, Mentella M, Miggiano G, Mele MC, Gaetani E, Graziani C, Petito V, Cammarota G, Marzetti E, Martone A, Landi F, Gasbarrini A.** Nutrition and IBD: Malnutrition and/or Sarcopenia? A Practical Guide. *Gastroenterol Res Pract* 2017; **2017**: 8646495 [PMID: 28127306 DOI: 10.1155/2017/8646495]
- Caio G, Lungaro L, Caputo F, Zoli E, Giancola F, Chiarioni G, De Giorgio R, Zoli G.** Nutritional Treatment in Crohn's Disease. *Nutrients* 2021; **13** [PMID: 34066229 DOI: 10.3390/nu13051628]
- Mentella MC, Scaldaferri F, Pizzoferrato M, Gasbarrini A, Miggiano GAD.** Nutrition, IBD and Gut Microbiota: A Review. *Nutrients* 2020; **12** [PMID: 32235316 DOI: 10.3390/nu12040944]
- de Castro MM, Pascoal LB, Steigleder KM, Siqueira BP, Corona LP, Ayrizono MLS, Milanski M, Leal RF.** Role of diet and nutrition in inflammatory bowel disease. *World J Exp Med* 2021; **11**: 1-16 [PMID: 33585174 DOI: 10.5493/wjem.v11.i1.1]
- Verburgt CM, Ghiboub M, Benninga MA, de Jonge WJ, Van Limbergen JE.** Nutritional Therapy Strategies in Pediatric Crohn's Disease. *Nutrients* 2021; **13** [PMID: 33450982 DOI: 10.3390/nu13010212]
- Roncoroni L, Gori R, Elli L, Tontini GE, Doneda L, Norsa L, Cuomo M, Lombardo V, Scricciolo A, Caprioli F, Costantino A, Scaramella L, Vecchi M.** Nutrition in Patients with Inflammatory Bowel Diseases: A Narrative Review. *Nutrients* 2022; **14** [PMID: 35215401 DOI: 10.3390/nu14040751]
- Baas J, Schotten M, Plume A, Cote G, Karimi R.** Scopus as a curated, high-quality bibliometric data source for academic research in quantitative science studies. *Quantitative Science Studies* 2020; **1**: 377-386 [DOI: 10.1162/qss_a_00019]
- Keighobadi M, Nakhaei M, Sharifpour A, Khasseh AA, Safanavaei S, Tabaripour R, Aliyali M, Abedi S, Mehravaran H, Banimostafavi ES, Fakhar M.** A Bibliometric Analysis of Global Research on *Lophomonas* Spp. in Scopus (1933-2019). *Infect Disord Drug Targets* 2021; **21**: 230-237 [PMID: 32718299 DOI: 10.2174/1871526520666200727153142]
- Beovich B, Olausson A, Williams B.** A bibliometric analysis of paramedicine publications using the Scopus database:

- 2010-2019. *Int Emerg Nurs* 2021; **59**: 101077 [PMID: 34571451 DOI: 10.1016/j.ienj.2021.101077]
- 15 **Morandi G**, Guido D, Tagliabue A. A bibliometric study of scientific literature on the dietary therapies for epilepsy in Scopus. *Nutr Neurosci* 2015; **18**: 201-209 [PMID: 24628043 DOI: 10.1179/1476830514Y.0000000118]
 - 16 **Zahri KNM**, Zulkharnain A, Sabri S, Gomez-Fuentes C, Ahmad SA. Research Trends of Biodegradation of Cooking Oil in Antarctica from 2001 to 2021: A Bibliometric Analysis Based on the Scopus Database. *Int J Environ Res Public Health* 2021; **18** [PMID: 33669826 DOI: 10.3390/ijerph18042050]
 - 17 **Kanmodi KK**, Nwafor JN, Salami AA, Egbedina EA, Nnyanzi LA, Ojo TO, Duckworth RM, Zohoori FV. A Scopus-Based Bibliometric Analysis of Global Research Contributions on Milk Fluoridation. *Int J Environ Res Public Health* 2022; **19** [PMID: 35886086 DOI: 10.3390/ijerph19148233]
 - 18 **Zyoud SH**, Shakhshir M, Abushanab AS, Al-Jabi SW, Koni A, Shahwan M, Jairoun AA, Abu Taha A. Mapping the global research landscape on nutrition and the gut microbiota: Visualization and bibliometric analysis. *World J Gastroenterol* 2022; **28**: 2981-2993 [PMID: 35978868 DOI: 10.3748/wjg.v28.i25.2981]
 - 19 **Zyoud SH**, Al-Jabi SW, Koni A, Shakhshir M, Shahwan M, Jairoun AA. Mapping the landscape and structure of global research on nutrition and COVID-19: visualization analysis. *J Health Popul Nutr* 2022; **41**: 25 [PMID: 35689295 DOI: 10.1186/s41043-022-00304-y]
 - 20 **Shen JL**, Zhou Z, Cao JS, Zhang B, Hu JH, Li JY, Liu XM, Juengpanich S, Li MS, Feng X. Biologic therapy for Crohn's disease over the last 3 decades. *World J Clin Cases* 2022; **10**: 594-606 [PMID: 35097085 DOI: 10.12998/wjcc.v10.i2.594]
 - 21 **Sweileh WM**. Analysis and mapping of global research publications on shift work (2012-2021). *J Occup Med Toxicol* 2022; **17**: 22 [PMID: 36514070 DOI: 10.1186/s12995-022-00364-0]
 - 22 **Sweileh WM**. Global research activity on mathematical modeling of transmission and control of 23 selected infectious disease outbreak. *Global Health* 2022; **18**: 4 [PMID: 35062966 DOI: 10.1186/s12992-022-00803-x]
 - 23 **Sweileh WM**. Global research publications on irrational use of antimicrobials: call for more research to contain antimicrobial resistance. *Global Health* 2021; **17**: 94 [PMID: 34429128 DOI: 10.1186/s12992-021-00754-9]
 - 24 **Sweileh WM**. Substandard and falsified medical products: bibliometric analysis and mapping of scientific research. *Global Health* 2021; **17**: 114 [PMID: 34556126 DOI: 10.1186/s12992-021-00766-5]
 - 25 **Wang JL**, Ma YJ, Ma L, Ma N, Guo DM, Ma LS. Baishideng's Reference Citation Analysis database announces the first Article Influence Index of multidisciplinary scholars. *World J Clin Cases* 2022; **10**: 10391-10398 [PMID: 36312463 DOI: 10.12998/wjcc.v10.i29.10391]
 - 26 **Wang JL**, Ma YJ, Ma L, Ma N, Guo DM, Ma LS. Baishideng's Reference Citation Analysis database announces the first Journal Article Influence Index of 101 core journals and a list of high-quality academic journals in gastroenterology and hepatology. *World J Gastroenterol* 2022; **28**: 5383-5394 [PMID: 36312837 DOI: 10.3748/wjg.v28.i37.5383]
 - 27 **Wang JL**, Ma YJ, Ma L, Ma N, Guo DM, Ma LS. Baishideng's Reference Citation Analysis database announces the first Journal Article Influence Index of 104 core journals and a list of high-quality academic journals in orthopedics. *World J Orthop* 2022; **13**: 891-902 [PMID: 36312521 DOI: 10.5312/wjo.v13.i10.891]
 - 28 **Van Eck NJ**, Waltman L. Text mining and visualization using VOSviewer. 2011. [cited 21 March 2023]. Available from: <https://arxiv.org/ftp/arxiv/papers/1109/1109.2058.pdf>
 - 29 **van Eck NJ**, Waltman L. VOSviewer manual. 2013. [cited 21 March 2023]. Available from: https://www.researchgate.net/publication/265012369_VOSviewer_Manual
 - 30 **van Eck NJ**, Waltman L. Software survey: VOSviewer, a computer program for bibliometric mapping. *Scientometrics* 2010; **84**: 523-538 [PMID: 20585380 DOI: 10.1007/s11192-009-0146-3]
 - 31 **Hou JK**, Abraham B, El-Serag H. Dietary intake and risk of developing inflammatory bowel disease: a systematic review of the literature. *Am J Gastroenterol* 2011; **106**: 563-573 [PMID: 21468064 DOI: 10.1038/ajg.2011.44]
 - 32 **Brown K**, DeCoffe D, Molcan E, Gibson DL. Diet-induced dysbiosis of the intestinal microbiota and the effects on immunity and disease. *Nutrients* 2012; **4**: 1095-1119 [PMID: 23016134 DOI: 10.3390/nu4081095]
 - 33 **North American Society for Pediatric Gastroenterology Hepatology and Nutrition**; Colitis Foundation of America, Bousvaros A, Antonioli DA, Colletti RB, Dubinsky MC, Glickman JN, Gold BD, Griffiths AM, Jevon GP, Higuchi LM, Hyams JS, Kirschner BS, Kugathasan S, Baldassano RN, Russo PA. Differentiating ulcerative colitis from Crohn disease in children and young adults: report of a working group of the North American Society for Pediatric Gastroenterology, Hepatology, and Nutrition and the Crohn's and Colitis Foundation of America. *J Pediatr Gastroenterol Nutr* 2007; **44**: 653-674 [PMID: 17460505 DOI: 10.1097/MPG.0b013e31805563f3]
 - 34 **Zachos M**, Tondeur M, Griffiths AM. Enteral nutritional therapy for induction of remission in Crohn's disease. *Cochrane Database Syst Rev* 2007; CD000542 [PMID: 17253452 DOI: 10.1002/14651858.CD000542.pub2]
 - 35 **Forbes A**, Escher J, Hébuterne X, Kłęk S, Krznaric Z, Schneider S, Shamir R, Stardelova K, Wierdsma N, Wiskin AE, Bischoff SC. ESPEN guideline: Clinical nutrition in inflammatory bowel disease. *Clin Nutr* 2017; **36**: 321-347 [PMID: 28131521 DOI: 10.1016/j.clnu.2016.12.027]
 - 36 **Lomer MC**, Thompson RP, Powell JJ. Fine and ultrafine particles of the diet: influence on the mucosal immune response and association with Crohn's disease. *Proc Nutr Soc* 2002; **61**: 123-130 [PMID: 12002786 DOI: 10.1079/pns2001134]
 - 37 **Lewis JD**, Chen EZ, Baldassano RN, Otley AR, Griffiths AM, Lee D, Bittinger K, Bailey A, Friedman ES, Hoffmann C, Albenberg L, Sinha R, Compher C, Gilroy E, Nessel L, Grant A, Chehoud C, Li H, Wu GD, Bushman FD. Inflammation, Antibiotics, and Diet as Environmental Stressors of the Gut Microbiome in Pediatric Crohn's Disease. *Cell Host Microbe* 2015; **18**: 489-500 [PMID: 26468751 DOI: 10.1016/j.chom.2015.09.008]
 - 38 **Borrelli O**, Cordischi L, Cirulli M, Paganelli M, Labalestra V, Uccini S, Russo PM, Cucchiara S. Polymeric diet alone vs corticosteroids in the treatment of active pediatric Crohn's disease: a randomized controlled open-label trial. *Clin Gastroenterol Hepatol* 2006; **4**: 744-753 [PMID: 16682258 DOI: 10.1016/j.cgh.2006.03.010]
 - 39 **Ananthakrishnan AN**, Khalili H, Konijeti GG, Higuchi LM, de Silva P, Korzenik JR, Fuchs CS, Willett WC, Richter JM, Chan AT. A prospective study of long-term intake of dietary fiber and risk of Crohn's disease and ulcerative colitis. *Gastroenterology* 2013; **145**: 970-977 [PMID: 23912083 DOI: 10.1053/j.gastro.2013.07.050]
 - 40 **Martinez-Medina M**, Denizot J, Dreux N, Robin F, Billard E, Bonnet R, Darfeuille-Michaud A, Barnich N. Western diet

- induces dysbiosis with increased E coli in CEABAC10 mice, alters host barrier function favouring AIEC colonisation. *Gut* 2014; **63**: 116-124 [PMID: 23598352 DOI: 10.1136/gutjnl-2012-304119]
- 41 **Zyoud SeH**, Shakhshir M, Abushanab AS, Koni A, Shahwan M, Jairoun AA, Al-Jabi SW. Global research trends on the links between insulin resistance and obesity: a visualization analysis. *Translational Medicine Communications* 2022; **7**: 18 [DOI: 10.1186/s41231-022-00124-6]
- 42 **Zyoud SH**, Al-Jabi SW, Amer R, Shakhshir M, Shahwan M, Jairoun AA, Akkawi M, Abu Taha A. Global research trends on the links between the gut microbiome and cancer: a visualization analysis. *J Transl Med* 2022; **20**: 83 [PMID: 35148757 DOI: 10.1186/s12967-022-03293-y]
- 43 **Yang J**, Deng Y, Cai Y, Liu Y, Peng L, Luo Z, Li D. Mapping trends and hotspot regarding gastrointestinal microbiome and neuroscience: A bibliometric analysis of global research (2002-2022). *Front Neurosci* 2022; **16**: 1048565 [PMID: 36466165 DOI: 10.3389/fnins.2022.1048565]
- 44 **Dusdal J**, Powell JJW. Benefits, Motivations, and Challenges of International Collaborative Research: A Sociology of Science Case Study. *Science and Public Policy* 2021; **48**: 235-245 [DOI: 10.1093/scipol/scab010]
- 45 **Widmer RJ**, Widmer JM, Lerman A. International collaboration: promises and challenges. *Rambam Maimonides Med J* 2015; **6**: e0012 [PMID: 25973264 DOI: 10.5041/RMMJ.10196]
- 46 **Moradi R**, Zargham-Boroujeni A, Soleymani MR. Factors related to the international research collaboration in the health area: A qualitative study. *J Educ Health Promot* 2020; **9**: 267 [PMID: 33282972 DOI: 10.4103/jehp.jehp_497_20]
- 47 **Meißner F**, Weinmann C, Vowe G. Understanding and Addressing Problems in Research Collaboration: A Qualitative Interview Study From a Self-Governance Perspective. *Front Res Metr Anal* 2021; **6**: 778176 [PMID: 35224422 DOI: 10.3389/frma.2021.778176]
- 48 **Ashton JJ**, Gavin J, Beattie RM. Exclusive enteral nutrition in Crohn's disease: Evidence and practicalities. *Clin Nutr* 2019; **38**: 80-89 [PMID: 29398336 DOI: 10.1016/j.clnu.2018.01.020]
- 49 **Fuchigami T**, Ohgushi H, Imamura K, Yao T, Omae T, Watanabe H, Nakano H. Effects of total parenteral nutrition on colonic lesions in Crohn's disease: radiographic and endoscopic study. *Gastroenterol Jpn* 1982; **17**: 521-529 [PMID: 6819178 DOI: 10.1007/BF02779129]
- 50 **Viani K**. Parenteral and enteral nutrition for pediatric oncology in low- and middle-income countries. *Indian J Cancer* 2015; **52**: 182-184 [PMID: 26853395 DOI: 10.4103/0019-509X.175837]
- 51 **Di Caro S**, Fragkos KC, Keetarut K, Koo HF, Sebeos-Rogers G, Saravanapavan H, Barragry J, Rogers J, Mehta SJ, Rahman F. Enteral Nutrition in Adult Crohn's Disease: Toward a Paradigm Shift. *Nutrients* 2019; **11** [PMID: 31540038 DOI: 10.3390/nu11092222]
- 52 **Wu L**, Estrada O, Zaborina O, Bains M, Shen L, Kohler JE, Patel N, Musch MW, Chang EB, Fu YX, Jacobs MA, Nishimura MI, Hancock RE, Turner JR, Alverdy JC. Recognition of host immune activation by *Pseudomonas aeruginosa*. *Science* 2005; **309**: 774-777 [PMID: 16051797 DOI: 10.1126/science.1112422]
- 53 **Spitz J**, Hecht G, Taveras M, Aoyo E, Alverdy J. The effect of dexamethasone administration on rat intestinal permeability: the role of bacterial adherence. *Gastroenterology* 1994; **106**: 35-41 [PMID: 8276206 DOI: 10.1016/s0016-5085(94)94155-6]
- 54 **Lochs H**, Dejong C, Hammarqvist F, Hebuterne X, Leon-Sanz M, Schütz T, van Gemert W, van Gossum A, Valentini L; DGEM (German Society for Nutritional Medicine), Lübke H, Bischoff S, Engelmann N, Thul P; ESPEN (European Society for Parenteral and Enteral Nutrition). ESPEN Guidelines on Enteral Nutrition: *Gastroenterology*. *Clin Nutr* 2006; **25**: 260-274 [PMID: 16698129 DOI: 10.1016/j.clnu.2006.01.007]
- 55 **Han PD**, Burke A, Baldassano RN, Rombeau JL, Lichtenstein GR. Nutrition and inflammatory bowel disease. *Gastroenterol Clin North Am* 1999; **28**: 423-443, ix [PMID: 10372275 DOI: 10.1016/s0889-8553(05)70063-7]
- 56 **Moed HF**. Citation analysis in research evaluation. Springer Science & Business Media. 2006. [cited 21 March 2023]. Available from: <https://link.springer.com/book/10.1007/1-4020-3714-7#book-header>
- 57 **Aksnes DW**, Langfeldt L, Wouters P. Citations, Citation Indicators, and Research Quality: An Overview of Basic Concepts and Theories. *SAGE Open* 2019; **9**: 21582440198 [DOI: 10.1177/2158244019829575]

Inflammatory myofibroblastic tumor of the pancreatic neck misdiagnosed as neuroendocrine tumor: A case report

Jia-Bei Liu, Qian-Biao Gu, Peng Liu

Specialty type: Gastroenterology and hepatology

Provenance and peer review: Unsolicited article; Externally peer reviewed.

Peer-review model: Single blind

Peer-review report's scientific quality classification

Grade A (Excellent): 0
Grade B (Very good): B, B
Grade C (Good): C
Grade D (Fair): 0
Grade E (Poor): 0

P-Reviewer: Kamer E, Turkey; Kumar M, India; Yarmahmoodi F, Iran

Received: March 10, 2023

Peer-review started: March 10, 2023

First decision: April 14, 2023

Revised: April 21, 2023

Accepted: May 4, 2023

Article in press: May 4, 2023

Published online: May 28, 2023



Jia-Bei Liu, Department of Radiology, The First Affiliated Hospital of Hunan Normal University, Hunan Provincial People's Hospital, Changsha 410005, Hunan Province, China

Qian-Biao Gu, Peng Liu, Department of Radiology, The First Affiliated Hospital of Hunan Normal University (Hunan Provincial People's Hospital), Changsha 410005, Hunan Province, China

Corresponding author: Peng Liu, MD, Chief Doctor, Department of Radiology, The First Affiliated Hospital of Hunan Normal University (Hunan Provincial People's Hospital), No. 61 Jiefang West Road, Changsha 410005, Hunan Province, China. lp radiology@163.com

Abstract

BACKGROUND

Inflammatory myofibroblastic tumor (IMT) is a relatively rare tumor. The global incidence of IMT is less than 1%. There is no specific clinical manifestation. It usually occurs in the lungs, but the pancreas is not the predilection site.

CASE SUMMARY

We present a case of a male patient, 51 years old, who was diagnosed with a pancreatic neck small mass on ultrasound one year ago during a physical examination. As he had no clinical symptoms and the mass was relatively small, he did not undergo treatment. However, the mass was found to be larger on review, and he was referred to our hospital. Since the primal clinical diagnosis was pancreatic neuroendocrine tumor, the patient underwent surgical treatment. However, the case was confirmed as pancreatic IMT by postoperative pathology.

CONCLUSION

Pancreatic IMT is relatively rare and easily misdiagnosed. We can better understand and correctly diagnose this disease by this case report.

Key Words: Inflammatory myofibroblastic tumor; Diagnosis; Imaging; Pancreas; Case report

©The Author(s) 2023. Published by Baishideng Publishing Group Inc. All rights reserved.

Core Tip: Inflammatory myofibroblastic tumor (IMT) is a rare mesenchymal tumor composed of spindle-shaped myofibroblasts accompanied by a mixed inflammatory infiltrate, and is particularly rare in the pancreas. The diagnosis of pancreatic IMT is made on the basis of histopathology and immunohistochemistry. Different lesions exhibit diverse biological characteristics, and there are several surgical treatment protocols. This case emphasizes the importance of correct preoperative diagnosis of IMT and reminds us to broaden our thinking in relation to the diagnosis of pancreatic lesions.

Citation: Liu JB, Gu QB, Liu P. Inflammatory myofibroblastic tumor of the pancreatic neck misdiagnosed as neuroendocrine tumor: A case report. *World J Gastroenterol* 2023; 29(20): 3216-3221

URL: <https://www.wjgnet.com/1007-9327/full/v29/i20/3216.htm>

DOI: <https://dx.doi.org/10.3748/wjg.v29.i20.3216>

INTRODUCTION

Inflammatory myofibroblastic tumor (IMT) is a rare mesenchymal tumor. This concept of IMT was first put forward by Pettinato *et al*[1] in 1990. According to the current World Health Organisation (WHO) guidelines, IMTs are typically low-grade neoplasms with occasional malignant potential[2]. An IMT can occur anywhere at any age. This report describes a case of pancreatic IMT.

CASE PRESENTATION

Chief complaints

A 51-year-old male patient was found to have a pancreatic mass more than one year ago.

History of present illness

The patient found a small pancreatic tumor in a physical examination one year ago. However, two months ago, the follow-up of the physical examination center found that the tumor became bigger, then he was referred to our hospital. There were no clinical symptoms throughout the course of the disease.

History of past illness

The patient had a history of hypertension, hyperglycemia, hyperlipidemia, thyroid nodule, prediabetes, and urticaria.

Personal and family history

The patient had no family history of malignant tumors, psychological, or genetic disorders.

Physical examination

The physical examination did not reveal any obvious abnormalities.

Laboratory examinations

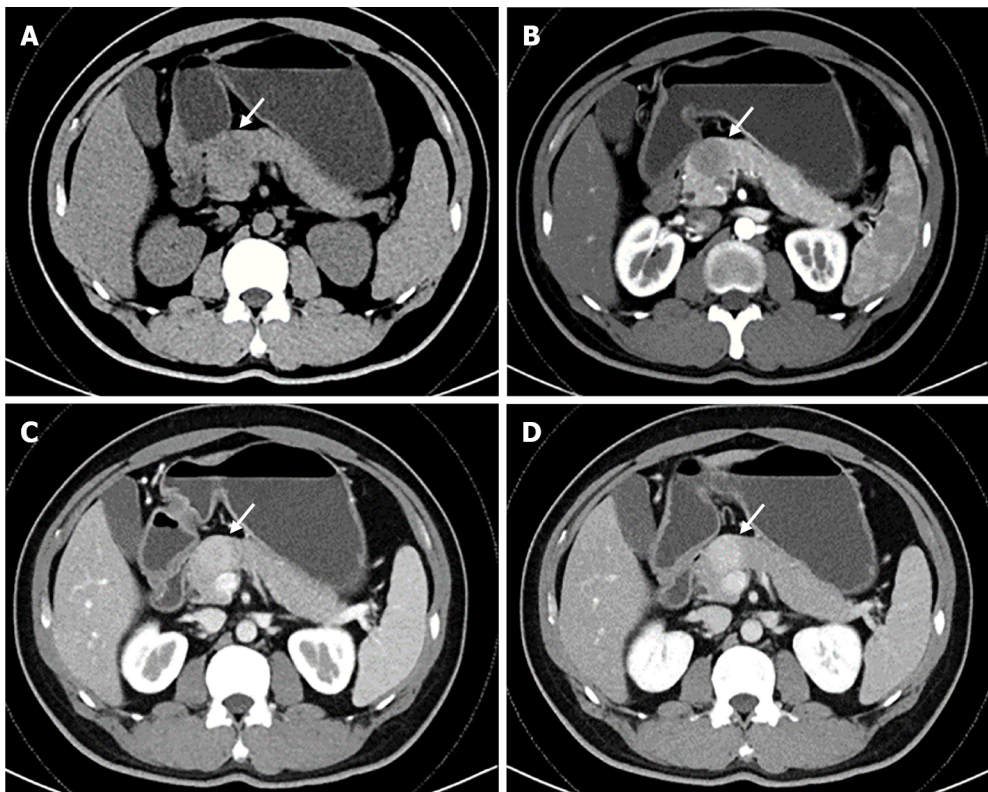
Uric acid and triglyceride levels were elevated. Other blood parameters and tumor markers (carcinoembryonic antigen and cancer antigen 19-9) levels were within the normal range.

Imaging examinations

An abdominal contrast-enhanced computed tomography (CECT) scan showed a round, well-defined, low-density mass 3.5 cm in diameter in the neck of the pancreas. On the CECT scan, the mass showed lower attenuation than the normal pancreatic parenchyma in the pre-contrast phase and arterial phase, and heterogeneous hyperenhancement in the portal venous phase (Figure 1). A pancreatic neuroendocrine tumour was strongly suspected.

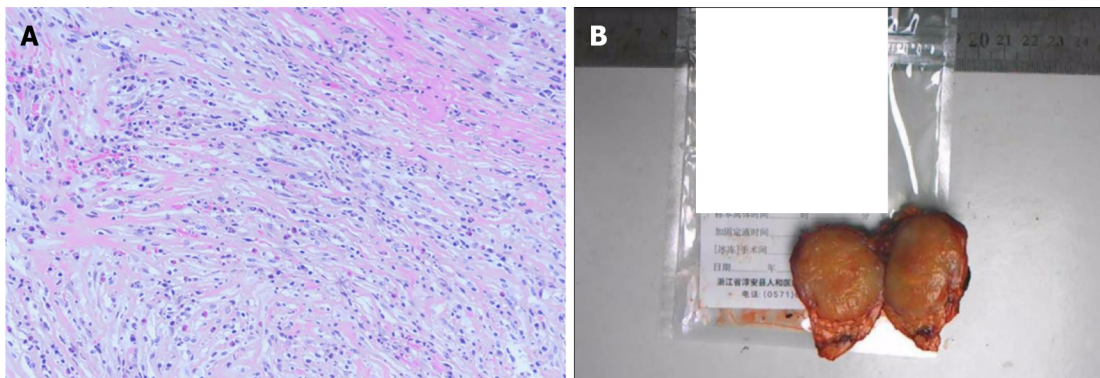
FINAL DIAGNOSIS

The patient was diagnosed with IMT of the pancreas by postoperative pathology (Figure 2).



DOI: 10.3748/wjg.v29.i20.3216 Copyright ©The Author(s) 2023.

Figure 1 Abdominal contrast-enhanced computed tomography. A: Axial non-contrast showed a low-density mass in the neck of the pancreas; B: Arterial phase indicated a distinct hypoattenuating mass; C and D: Venous phase revealed persistent hyperenhancement of the mass (magnetic resonance imaging is similar to computed tomography in enhancement mode and characteristics).



DOI: 10.3748/wjg.v29.i20.3216 Copyright ©The Author(s) 2023.

Figure 2 Histopathological image and resected tumor specimen. A: Spindle-shaped myofibroblasts accompanied by large amounts of plasma cells. B: The resected specimen showing a well-defined neoplasm (some information has been excluded due to patient privacy).

TREATMENT

After completion of preoperative investigations, a laparoscopic middle pancreatectomy was performed.

OUTCOME AND FOLLOW-UP

Postoperative pancreatic leakage occurred in the patient. However, he was discharged in good clinical condition after 40 d. No apparent events were observed at the 2-mo postoperative follow-up.

DISCUSSION

IMT is a rare mesenchymal tumor. Due to its rarity and the fact that the etiology is unknown, there are only a few cases reported. It has been revealed that IMT may have gene rearrangement with anaplastic lymphoma kinase (ALK)[3], and ALK positivity was also associated with a higher recurrence and less chance of distant metastasis[4]. A recent literature review by Chen *et al*[5] in 2021, included 30 patients with IMT occurring in the pancreas. The reported mean age of the patients was 40 years (range, 0-82 years) with an obvious male preponderance. The tumor was mostly located in the head of the pancreas (21/30 patients). In this series, abdominal pain was the most frequent symptom followed by jaundice. Only five cases of asymptomatic pancreatic IMT have been reported in the medical literature[5-9]. Our patient had no clinical symptoms and the pancreatic mass was found on physical examination. Among the previously reported cases of pancreatic IMT, many were initially misdiagnosed as pancreatic cancer, while the present case was misdiagnosed as pancreatic neuroendocrine tumor. Therefore, it is meaningful to collect more cases and information to obtain reliable diagnosis and treatment methods for IMT.

As the low incidence of pancreatic IMT, there is no specific clinical manifestations has been established. It commonly manifests as abdominal pain or jaundice, and can sometimes be asymptomatic. Although IMT is considered a low-grade tumor, one case of pulmonary metastasis has been reported[10].

At present, pancreatic IMT is mainly diagnosed by histopathology and immunohistochemistry[11]. Under the light microscope, the tumour tissue in this case consisted mainly of spindle-shaped myofibroblasts accompanied by a mixed inflammatory infiltrate. The histopathological findings of this case were consistent with previous reports. Myofibroblasts in IMT stain positive for alpha-smooth muscle antigen (SMA), vimentin, and fibronectin, and stain negative for desmin and caldesmon[12]. In this case, immunohistochemistry report showed positive for IgG4, SMA and actin, and negative for desmin, ALK, CD30, S-100, and Catenin B, similar to those in the literature.

To date, pancreatic IMT is easily misdiagnosed as pancreatic neuroendocrine tumour and pancreatic cancer due to the lack of specific imaging features, and its diagnosis is unclear in clinical practice. A circular low-density mass was observed in the pancreatic IMT reported here. After enhancement, the arterial mass is mildly enhanced, the venous phase is significantly enhanced, and the density is progressively higher than that of the surrounding normal pancreas.

However, in some cases, CECT did not show an enhancing mass and was suspected to be ductal adenocarcinoma, which was ultimately confirmed by pathology to be pancreatic IMT. Hence, the radiologic features of pancreatic IMT require further data.

Pancreatic IMT needs to be differentiated from pancreatic neuroendocrine tumor, pancreatic cancer, and solid-pseudopapillary neoplasm. Pancreatic neuroendocrine tumor is uncommon and has no gender predilection[13]. Additionally, the mass shows high enhancement in the arterial or portal phases due to the rich capillary network in the stroma. Pancreatic cancer is typically seen in patients over 60 years old, with a slight male predominance. It is a hypovascular mass with extensive fibrosis on histopathologic examination[14]. Typical ductal adenocarcinomas appear as poorly defined masses with extensive surrounding desmoplastic reaction and they enhance poorly compared to adjacent normal pancreatic tissue. The presence of abrupt pancreatic duct cutoff, upstream pancreatic duct dilatation, upstream pancreatic parenchymal atrophy, and decreased enhancement in the distal pancreatic parenchyma favors a diagnosis of malignancy[15]. Solid-pseudopapillary neoplasms of the pancreas are cystic-solid masses with a complete capsule. They are prone to bleeding, necrosis and calcification. The solid portion shows enhancement in the arterial phase and can continue to enhance in the delayed phase. However, the imaging features of pancreatic IMT from some pancreatic lesions overlap.

In the present case, a wrong diagnosis was made for several reasons. First, the patient had no clinical manifestations, and the clinical history and laboratory indices are unremarkable. Second, the preoperative imaging findings were difficult to distinguish from a pancreatic neuroendocrine tumour. The border of the lesion was distinct, with persistent hyperenhancement of the mass, and typical double duct sign and vascular involvement were not observed. Accordingly, preliminary diagnosis of imaging was limited to benign mass. In general, IMT of the pancreas is lack of characteristic in terms of clinic-radiological features. Therefore, for more accurate diagnosis and treatment of pancreatic IMT, there is a need to obtain more meaningful information.

CONCLUSION

Given the rarity of pancreatic IMT, this case can contribute to further understanding of the etiology, mechanism, imaging characteristics of this disease. Obtaining a better understanding of all aspects of this disease will help provide a more precise diagnosis.

ACKNOWLEDGEMENTS

We are very grateful to Dr. Liu Yu (Hunan Provincial People's Hospital, First Affiliated Hospital of Hunan Normal University) for providing professional guidance to the pathological analysis.

FOOTNOTES

Author contributions: Liu JB contributed to manuscript writing and editing, and data collection; Liu P and Gu QB contributed to conceptualization and supervision; and all authors have read and approved the final manuscript.

Supported by the Clinical Medical Technology Innovation Guiding Project of Hunan Province, No. 2021SK50911; and Scientific Research Project of Hunan Health Commission, No. 202209010030.

Informed consent statement: Informed written consent was obtained from the patient for publication of this report and any accompanying images.

Conflict-of-interest statement: The authors declare that they have no conflict of interest to disclose.

CARE Checklist (2016) statement: The authors have read the CARE Checklist (2016), and the manuscript was prepared and revised according to the CARE Checklist (2016).

Open-Access: This article is an open-access article that was selected by an in-house editor and fully peer-reviewed by external reviewers. It is distributed in accordance with the Creative Commons Attribution NonCommercial (CC BY-NC 4.0) license, which permits others to distribute, remix, adapt, build upon this work non-commercially, and license their derivative works on different terms, provided the original work is properly cited and the use is non-commercial. See: <https://creativecommons.org/licenses/by-nc/4.0/>

Country/Territory of origin: China

ORCID number: Jia-Bei Liu 0009-0007-7049-2484; Qian-Biao Gu 0000-0002-2545-3175; Peng Liu 0000-0002-9023-2344.

S-Editor: Chen YL

L-Editor: A

P-Editor: Chen YL

REFERENCES

- Pettinato G**, Manivel JC, De Rosa N, Dehner LP. Inflammatory myofibroblastic tumor (plasma cell granuloma). Clinicopathologic study of 20 cases with immunohistochemical and ultrastructural observations. *Am J Clin Pathol* 1990; **94**: 538-546 [PMID: 2239820 DOI: 10.1093/ajcp/94.5.538]
- Choi JH**, Ro JY. The 2020 WHO Classification of Tumors of Soft Tissue: Selected Changes and New Entities. *Adv Anat Pathol* 2021; **28**: 44-58 [PMID: 32960834 DOI: 10.1097/PAP.0000000000000284]
- Zhu L**, Li J, Liu C, Ding W, Lin F, Guo C, Liu L. Pulmonary inflammatory myofibroblastic tumor vs IgG4-related inflammatory pseudotumor: differential diagnosis based on a case series. *J Thorac Dis* 2017; **9**: 598-609 [PMID: 28449468 DOI: 10.21037/jtd.2017.02.89]
- Coffin CM**, Hornick JL, Fletcher CD. Inflammatory myofibroblastic tumor: comparison of clinicopathologic, histologic, and immunohistochemical features including ALK expression in atypical and aggressive cases. *Am J Surg Pathol* 2007; **31**: 509-520 [PMID: 17414097 DOI: 10.1097/01.pas.0000213393.57322.c7]
- Chen ZT**, Lin YX, Li MX, Zhang T, Wan DL, Lin SZ. Inflammatory myofibroblastic tumor of the pancreatic neck: A case report and review of literature. *World J Clin Cases* 2021; **9**: 6418-6427 [PMID: 34435007 DOI: 10.12998/wjcc.v9.i22.6418]
- Pungpapong S**, Geiger XJ, Raimondo M. Inflammatory myofibroblastic tumor presenting as a pancreatic mass: a case report and review of the literature. *JOP* 2004; **5**: 360-367 [PMID: 15365204]
- Yamamoto H**, Watanabe K, Nagata M, Tasaki K, Honda I, Watanabe S, Soda H, Takenouti T. Inflammatory myofibroblastic tumor (IMT) of the pancreas. *J Hepatobiliary Pancreat Surg* 2002; **9**: 116-119 [PMID: 12021906 DOI: 10.1007/s005340200013]
- Dulundu E**, Sugawara Y, Makuuchi M. Inflammatory myofibroblastic tumor of the pancreas--a case report. *Biosci Trends* 2007; **1**: 167-169 [PMID: 20103888]
- Berhe S**, Goldstein S, Thompson E, Hackam D, Rhee DS, Nasr IW. Challenges in Diagnosis and Management of Pancreatic Inflammatory Myofibroblastic Tumors in Children. *Pancreas* 2019; **48**: e27-e29 [PMID: 30973469 DOI: 10.1097/MPA.0000000000001290]
- Walsh SV**, Evangelista F, Khettry U. Inflammatory myofibroblastic tumor of the pancreaticobiliary region: morphologic and immunocytochemical study of three cases. *Am J Surg Pathol* 1998; **22**: 412-418 [PMID: 9537467 DOI: 10.1097/0000478-199804000-00004]
- A G H**, Kumar S, Singla S, Kurian N. Aggressive Inflammatory Myofibroblastic Tumor of Distal Pancreas: A Diagnostic

- and Surgical Challenge. *Cureus* 2022; **14**: e22820 [PMID: 35399449 DOI: 10.7759/cureus.22820]
- 12 **Chan JK**, Cheuk W, Shimizu M. Anaplastic lymphoma kinase expression in inflammatory pseudotumors. *Am J Surg Pathol* 2001; **25**: 761-768 [PMID: 11395553 DOI: 10.1097/00000478-200106000-00007]
 - 13 **Lewis RB**, Lattin GE Jr, Paal E. Pancreatic endocrine tumors: radiologic-clinicopathologic correlation. *Radiographics* 2010; **30**: 1445-1464 [PMID: 21071369 DOI: 10.1148/rg.306105523]
 - 14 **Frapas E**, Morla O, Regenet N, Eugène T, Dupas B, Meurette G. A solid pancreatic mass: tumour or inflammation? *Diagn Interv Imaging* 2013; **94**: 741-755 [PMID: 23751230 DOI: 10.1016/j.diii.2013.03.013]
 - 15 **Tamada T**, Ito K, Kanomata N, Sone T, Kanki A, Higaki A, Hayashida M, Yamamoto A. Pancreatic adenocarcinomas without secondary signs on multiphasic multidetector CT: association with clinical and histopathologic features. *Eur Radiol* 2016; **26**: 646-655 [PMID: 26084602 DOI: 10.1007/s00330-015-3880-3]



Published by **Baishideng Publishing Group Inc**
7041 Koll Center Parkway, Suite 160, Pleasanton, CA 94566, USA
Telephone: +1-925-3991568
E-mail: bpgoffice@wjgnet.com
Help Desk: <https://www.f6publishing.com/helpdesk>
<https://www.wjgnet.com>

